Qualitative analysis of functional differential-algebraic systems with applications in control

Islam Boussaada

MÉMOIRE

Présenté pour obtenir

L'HABILITATION A DIRIGER DES RECHERCHES

DE L'ECOLE DOCTORALE STIC, UNIVERSITÉ PARIS SACLAY

LABORATOIRE DES SIGNAUX ET SYSTÈMES

DISCIPLINE : SCIENCES PHYSIQUES

par

Islam BOUSSAADA

ANALYSE QUALITATIVE DE SYSTÈMES ALGÉBRO-DIFFÉRENTIELS
FONCTIONNELS ET SON APPLICATION EN CONTRÔLE

QUALITATIVE ANALYSIS OF FUNCTIONAL DIFFERENTIAL-ALGEBRAIC
SYSTEMS WITH APPLICATIONS IN CONTROL

Soutenue le 17 juin 2016 devant la Commission d'examen (ordre alphabétique) :

Moulay BARKATOU	Professeur, Université de Limoges (Rapporteur)
Gábor STÉPÁN	Professeur, Budapest BME University (Rapporteur)
Eva ZERZ	Professeur, RWTH Aachen University (Rapporteur)
Jean-Michel CORON	Professeur, Université Pierre et Marie Curie (Examinateur)
Silviu-Iulian NICULESCU	Directeur de Recherche, CNRS (Examinateur)
Dorothée NORMAND-CYROT	Directeur de Recherche, CNRS (Examinateur)
Emmanuel TRÉLAT	Professeur, Université Pierre et Marie Curie (Examinateur)
Yacine CHITOUR	Professeur, Université Paris Sud (Invité)
Jean-Marie STRELCYN	Professeur à la retraite, Université Paris Nord (Invité)

Remerciements

Je tiens à remercier vivement les membres du Jury de m'avoir fait l'honneur d'évaluer mes travaux de recherches.

Je tiens à remercier chaleureusement mes trois rapporteurs, Moulay Barkatou, Gábor Stépán et Eva Zerz, pour le temps consacré à la lecture de ce manuscrit.

Ma sincère gratitude va aux autres membres, Yacine Chitour, Jean-Michel Coron, Silviu-Iulian Niculescu, Dorothée Normand-Cyrot, Emmanuel Trélat et Jean-Marie Strelcyn, pour avoir accepté d'évaluer mes travaux de recherches.

J'éprouve une reconnaissance spéciale envers Silviu Niculescu pour m'avoir si chaleureusement accueilli au sein du L2S, pour ses encouragements et son soutien dans la prise de responsabilités et pour avoir été une source continue de conseils et d'intuitions qu'il m'a confiées, et qui sont toujours d'actualité.

Mes remerciements vont également à Jean-Marie Strelcyn pour m'avoir fait bénéficier tout au long de ces années de sa grande culture mathématique et humaine.

Mes sincères remerciements vont aussi à Karim Trabelsi pour son enthousiasme, pour m'avoir toujours soutenu au sein de l'IPSA, d'avoir toujours chaleureusement accepté des dicussions et de m'avoir souvent apporté ses conseils constructifs.

Je remercie enfin toutes les personnes qui ont contribué, souvent de manière cruciale, aux résultats présentés ici ; Azgal Abichou, Magali Bardet, Fazia Bedouhene, Azzedine Benchettah, Catherine Bonnet, Arben Cela, Jie Chen, Raouf Chouikha, Sette Diop, Keqin Gu, Chaker Jammazi, Juan Escareno, Torsten Knüppel, Antonio Loria, Fréderic Mazenc, Wim Michiels, Sabine Mondié, Constantin Morarescu, Hugues Mounier, Elena Panteley, Alban Quadrat, Paul Raynaud de Fitte, Alexandre Renaux, Marc Roussel, Belem Saldivar, Rifat Sipahi, Sami Tliba, Hakki Unal, Tomas Vyhlidal et Frank Woittenek. Sans oublier de remercier mes autres collègues chercheurs de la DRI de l'IPSA pour leur aide et soutien.

Une tendre pensée pour mon épouse Ouerdia et mes trois enfants Alissa, Rayan et Yani, pour leur patience, leur amour et leur encouragement continuels. Last but not least, je remercie chaleureusement mes parents Mohamed et Jamila, mes frères Issam et Khoubeb pour leur soutien infaillible, à mes beaux parents Ameur et Ghenima pour leur aide précieuse.

Merci infiniment.

Table des matières

Contexte général de la thèse et son fil conducteur

"... Douter de tout ou tout croire, ce sont deux solutions également commodes, qui l'une et l'autre nous dispensent de réfléchir."
Henri Poincaré, *La Science et l'Hypothèse, 1902.*

Les recherches présentées dans ce manuscrit s'inscrivent dans le domaine des systèmes dynamiques, de dimensions finie et infinie, et de l'application de la théorie qualitative des systèmes dynamiques aux problèmes de contrôle. Elles s'articulent essentiellement autour de différentes versions du théorème de la variété du centre (en dimension finie et infinie) et de différentes théories des formes normales (avec ou sans contrôle), voir [47, 111, 43, 134]. L'objectif commun à ces recherches est, d'une part, de prouver l'efficacité de ces méthodes dans des applications émanantes des problèmes de contrôle, et d'autre part, d'étendre leur applicabilité à des systèmes algébro-différentiels non-linéaires à retard et dépendant de paramètres. Ces deux théories permettent de réduire, localement (au voisinage d'un point d'équilibre), la structure, ainsi que la dimension des systèmes, sans toutefois perdre l'essentiel des dynamiques. Plus précisément, le théorème de la variété du centre réduit la dimension du système à celle de l'espace propre généralisé associé aux valeurs spectrales imaginaires pures. La théorie des formes normales permet de simplifier la structure du sytème, dans le cas d'un système de commande, en découplant l'état des entrées et en réduisant ses non-linéarités, voir [111, 25]. Il est commode de signaler que cette approche se base sur une succession de changements de variables proches de l'identité, ce qui présente un aspect symbolique permettant de conserver (localement) l'information sur les dynamiques importantes. Ces méthodes symboliques/formelles ont prouvé leur efficacité dans divers problèmes dans l'analyse qualitative des solutions de systèmes dynamiques, voir [17, 16, 3, 182]. En particulier, il est aussi intéressant de rappeler que ces méthodologies apportent un outil complémentaire aux méthodes numériques, surtout lorsqu'il s'agit de systèmes de grande dimension ou même en dimension infinie (équations aux dérivées partielles et systèmes à retard), voir [180, 181, 224].

Le fil conducteur des problèmes et sujets abordés dans ce projet est l'analyse qualitative de systèmes dynamiques au voisinage de points d'équilibre non hyperboliques, ce qui exclut le cadre du théorème de Hartman-Grobman. Ce dernier théorème est aussi connu sous le nom du théorème de linéarisation assurant, lorsqu'il

s'agit de point d'équilibre hyperbolique, une équivalence topologique entre les flots du champs de vecteur (non linéaire) et son jacobien au point d'équilibre en question. Ainsi, il est question, soit (à travers le théorème de la variété du centre) d'exploiter ces valeurs spectrales à partie réelle nulle (lorsqu'elles existent, et lorsqu'il est techniquement possible de les identifier précisément avec leurs multiplicités), soit de caractériser ce type de valeurs spectrales (par caractériser on sous-entend les identifier ainsi que leurs multiplicités algébriques/géométriques respectives). Il en sort alors l'intérêt de préviliger des approches symboliques plus adaptées que les méthodes numériques pour mener à bien ce dernier objectif.

Ces travaux/projet de recherche présente(nt) deux volets. Le premier concerne les systèmes dynamiques en dimension finie, qui est dans la lignée naturelle des sujets traités pendant ma thèse, période pendant laquelle j'ai été guidé par Jean-Marie Strelcyn (Université de Rouen) et Raouf Chouikha (Université Paris Nord) dans la caractérisation (analytique/algébrique) de solutions périodiques des systèmes dynamiques en dimension finie. J'avais fait le choix, en particulier, de me consacrer au problème du centre et plus précisément celui de la propriété d'isochronie (solutions périodiques de période constante, indépendamment des conditions initiales confinées dans la région centrale) pour les systèmes bidimensionnels d'équations différentielles ordinaires. La caractéristique de ces derniers systèmes (2D) est un linéarisé au voisinage du point d'équilibre (souvent considéré, sans perte de généralité, l'origine de $\mathbb{R}^2$) admettant deux valeurs spectrales $\pm j\omega$, ce qu'on appelle souvent un point de Hopf. Ainsi, ces systèmes plans, peuvent être perçus comme une projection spectrale sur une variété invariante/attractive (variété du centre) d'un système de plus grande dimension ayant un point d'équilibre non hyperbolique dont la partie critique de son spectre ne comporte que ces deux valeurs spectrales ($\pm j\omega$ chacune de multiplicité algébrique/géométrique identiquement égale à 1). Si de plus, le reste des valeurs spectrales du système étudié admet des parties réelles négatives alors les dynamiques d'un système 2D de ce type reflèteront (qualitativement) les dynamiques du système initial (de plus grande dimension). Toutefois, mon évolution dans cette thématique (d'analyse qualitative des systèmes de dimension finie) s'est également orientée vers des problématiques telles que le contrôle des systèmes en grande dimension (dépendant de paramétres) et la synchronisation de fréquence pour des systèmes non linéaires couplés.

Les résultats de ce volet sont présentés dans la Sous-partie A. Dans les deux premiers chapitres, il s'agit des résultats des travaux [30] (en collaboration avec Raouf Chouikha et Jean-Marie Strelcyn) et [15] (en collaboration avec Magali Bardet, Raouf Chouikha et Jean-Marie Strelcyn), où une caractérisation/génération des conditions d'isochronie du centre à l'origine pour les systèmes plans de l'équation différentielle ordinaire de type Liénard est établie. Grâce à l'usage de la méthode itérative due à R. Chouikha [62], fondée sur un théorème de Minuro Urabe (1961), nous déterminons de nouveaux cas de centre linéaire perturbé par une non-linéarité non homogène. En particulier, dans [30] pour un centre linéaire perturbé par une

non-linéarité homogène

$$\begin{cases} \dot{x} = y + P_n(x,y) \\ \dot{y} = -x + Q_n(x,y) \end{cases},$$ (1.1)

de **degré n arbitraire** réductible à l'équation de type Liénard, nous avons identifié trois familles toujours linéarisables indépendamment du degré. Dans [15], nous présentons aussi une étude comparative d'efficacité dans le calcul des conditions d'isochronie pour des systèmes de type Liénard (Formes Normales VS C-Algorithme modifié). Nous exhibons également, une famille de systèmes avec un centre isochrone admettant une fonction d'Urabe non standard et une formule explicite de linéarisation est établie.

Enfin, nous contribuons à un problème ouvert posé par Evgenii Volokitin (Académie des Sciences Russe, Institut Sobolev, Novosibirsk) portant sur les systèmes d'Abel

$$\begin{cases} \dot{x} = -y \\ \dot{y} = x(1 + P(y)), \end{cases}$$ (1.2)

avec $P(y) = a_1 y + a_2 y^2 + a_3 y^3 + ... + a_n y^n$.

Dans le chapitre **??**, les résultats de [14] sont repris. En collaboration avec Magali Bardet (Université de Rouen), nous obtenons une réduction de complexité de l'algorithme de Chouikha qu'on appelle par la suite CAR, avantageuse à plus d'un titre lorsqu'elle est comparée aux algorithmes des formes normales dans la caractérisation des systèmes linéarisables au voisinage du centre (dont l'existence est certifiée par un thérème de M. Sabatini) pour les systèmes de type Liénard plan :
— en coût de calcul,
— en fournissant une condition suffisante,
— en indiquant dans certains cas la linéarisation explicite.
L'algorithme présenté prouve son efficacité surtout s'agissant de données rationnelles (ce qui est toujours le cas pour les systèmes polynomiaux plans). Le tableau suivant, dans lequel le temps de calcul est exprimé en secondes, témoigne de l'efficacité de l'algorithme proposé comparé à l'algorithme classique des formes normales dans la caractérisation de la linéarisabilité pour le système (1.2) en variant le degré n :

Par ailleurs, ce même problème d'isochronie peut être considéré comme étant un problème de synchronisation de fréquence indépendamment des conditions initiales (confinées dans l'anneau du centre). Ainsi, dans le chapitre 4, qui reprend les résultats de [28], une synchronisation de fréquence par un retour d'état monomial affectant une seule équation d'un système cubique plan initialement non linéarisable (donnant lieu à une dynamique linéaire) est établie. Les conditions nécessaires sont obtenues grâce au calcul explicite des formes normales.

Ensuite, une application directe de ces approches qualitatives/symboliques (formes normales et variété du centre) nous ont permis d'aborder les problèmes d'analyse et de contrôle d'un véhicule aérien équipé de quatre moteurs, "Quadrotor". Les résultats de [216] en collaboration avec Jing Wang (L2S), Silviu-Iulian Niculescu, Hugues Mounier et Arben Cela (ESIEE) sont repris dans le chapitre 5.

TABLE 1.1 – Temps CPU sur un Pentium cadencé à 1,46 GHz 4Go

n	CAR	Formes Normales
2	~ 0 s	0,060 s
3	0,001 s	0,160 s
4	0,004 s	0,784 s
5	0,008 s	4,728 s
6	0,016 s	31,430 s
7	0,052 s	263,033 s
8	0,116 s	2335,962 s
9	0,284 s	A court de mémoire
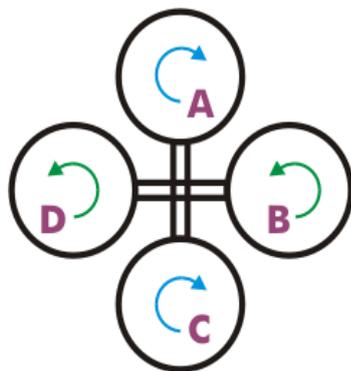
Plus précisément, un modèle dynamique 12- dimensionnel a été réduit à un système dynamique plan.

Les résultats du deuxième volet sont présentés dans la Sous-partie B. Il reprend les sujets et résultats que j'aborde depuis octobre 2010 essentiellement avec Silviu-Iulian Niculescu et Hugues Mounier. Au début dans le cadre de mon activité post-doctorale en automatique au L2S (2010-2011), puis en tant que chercheur associé au L2S (depuis 2011). Il s'agit de la modélisation, de l'analyse et du contrôle des équations algébro-différentielles ainsi que l'étude des systèmes dynamiques en dimension infinie ; plus précisément, les sytèmes non linéaires à retard et les équations aux dérivées partielles hyperboliques. En effet, les systèmes de commande évoluent souvent en présence de retards, voir [147]. Ces retards sont souvent justifiés par les latences entre l'acquisition de l'information et la prise de décision et entre la prise de décision et l'exécusion de cette décision. Le retard peut aussi être perçu comme un paramètre intrinsèque au système, et ce, typiquement dans des applications évoquant des phénomènes de propagation (propagation de vibrations en torsion et en traction-compression le long d'un train de tiges d'un système de forage pétrolier), ou des retards intentionnellement incorporés dans les lois de commandes afin d'éviter la démultiplication des capteurs, ou encore en raison de contraintes technologiques

empêchant l'aquisition instantanée des informations sur l'état du système (telle la stabilisation d'un pendule inversé par des lois de commande retardées dispensant ainsi de l'usage d'un capteur de vitesse angulaire).

Dans ce contexte, trois pistes ont été essentiellement explorées. La première, consiste à exploiter des approches et résultats de l'analyse des équations différentielles fonctionnelles dans des problèmes concrets de contrôle. En effet, dans le chapitre 6, nous reprenons les résultats obtenus dans [34] ainsi que dans [35], deux travaux en collaboration avec Silviu-Iulian Niculescu et Constantin Morarescu (CRAN, Université de Lorraine), il s'agit de l'analyse des dynamiques induites par la commande retardée. Un système d'équations différentielles ordinaires non linéaires modélisant un pendule inversé sur un chariot est étudié. Suite à l'usage de commande de type proportionnel à plusieurs retards nous mettons en évidence l'apparition de dynamiques inhabituelles pour des systèmes en dimension finie. Nous identifions une bifurcation de co-dimension 3 au voisinage d'une valeur propre triple en zéro. Cette multiplicité dépasse la dimension du système initial (système plan). Nous élaborons une analyse non-linéaire basée sur le théorème de la variété du centre pour les systèmes en dimension infinie puis la forme normale des dynamiques centrales est analysée. L'étude se réduit à l'analyse d'un système tri-dimensionnel. Les bifurcations de Hopf et de fourche (Pitchfork) sont étudiées pour plusieurs lois de commandes retardées [35]. La stabilisation du pendule est ensuite obtenue grâce à l'éclatement du paramètre de perturbation. Nous mettons également en évidence que la connaissance de l'état à deux instants τ_1 et τ_2 suffisamment proches permet d'éviter l'estimation de la vitesse souvent indispensable pour de bonnes performances de la loi de commande [10].

D'autre part, en collaboration avec Silviu-Iulian Niculescu, Hugues Mounier et Arben Cela, Belem Saldivar et Sabine Mondié (Conacyt, Mexique) nous nous intéressons à une application issue de l'industrie pétrolière. Cette partie est présentée dans les chapitres 7-9 qui reprennent des résultats de [36, 29, 146, 42]. Il s'agit de la modélisation, de l'analyse et du contrôle des vibrations d'un système de forage. L'industrie de forage pétrolier localise des poches d'hydrocarbure de plus en plus profondes (actuellement de 3 à 7 km) ; de ce fait les vibrations de rotation (torsionnelles) et celles de traction-compression peuvent causer une fatigue et une usure prématurées du train de tiges. Notre travail porte sur l'analyse et le contrôle d'un modèle qui prend en considération les deux types de vibrations, et comporte deux équations d'ondes couplées (chacune décrit un type de vibration). En plus, le couplage de ces deux types de vibrations est pris en compte dans les conditions aux bord et il est considéré comme non linéaire. Tous ces éléments de modélisation permettent d'obtenir une description assez élaborée des dynamiques induites le long du train de tiges. Dans la modélisation qu'on considère, les vibrations en traction-compression $U(t, s)$ et les vibrations torsionnelles $\Phi(t, s)$ sont gouvernées par les
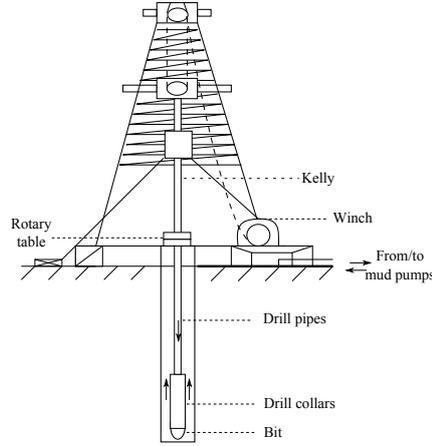
FIGURE 1.1 – Système de forage rotatif
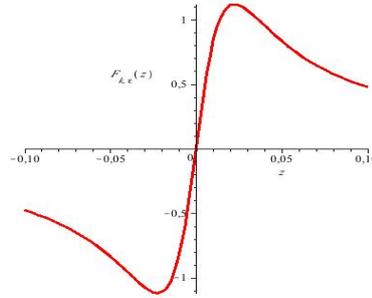
FIGURE 1.2 – Modèle de frottement

equations d'ondes suivantes :

$$
\begin{cases}
\ddot{U}(t,s) = c^2\, U''(t,s), \\
U'(t,0) = \dfrac{\alpha}{E\,\Gamma}(\dot{U}(t,0) - H(t)), \\
M\,\ddot{U}(t,L) = -E\,\Gamma U'(t,L) + F(\dot{U}(t,L)), \\
\ddot{\Phi}(t,s) = \tilde{c}^2\, \Phi''(t,s), \\
\Phi'(t,0) = \dfrac{\beta}{G\,\Gamma}(\dot{\Phi}(t,0) - \Omega(t)), \\
J\,\ddot{\Phi}(t,L) = -G\,\Gamma\,\Phi'(t,L) + \tilde{F}(\dot{U}(t,L)).
\end{cases}
\tag{1.3}
$$

où G est le module de Young de l'acier des tiges, E est le module de Young d'élasticité, J est l'inertie de rotation du système, M est masse du système, L est longueur des tiges, Γ est la section moyenne et ρ est la densité volumique, ainsi les vitesses d'onde s'écrivent : $c = \sqrt{\frac{E}{\rho}}$ et $\tilde{c} = \sqrt{\frac{G}{\rho}}$. Notons que les profils de frottement F et $\tilde{F}$ ont été modélisés par : $z \mapsto \frac{k\,z}{k^2\,z^2+\zeta}$ avec $0 < \zeta << 1$ et $k \in \mathbb{N}^*$, voir figure 1.2. Le

modèle d'EDP établi se ramène au système à retard de type neutre

$$\begin{cases} \dot{x}(t) - a\,\dot{x}(t-\tau) & = f(x(t), x(t-\tau)) \\ \dot{y}(t) - b\,\dot{y}(t-\tilde{\tau}) & = g(x(t), x(t-\tau), y(t), y(t-\tilde{\tau})) \end{cases} \qquad (1.4)$$

où g et f sont des fonctions non linéaires. En particulier, une analyse basée sur le théorème de la variété du centre et sur l'utilisation des formes normales est établie. Le choix de transformer le modèle d'EDP en DDE est justifié par le fait que le modèle physique sera accompagné d'un modèle de transmission (usage de technologie wifi qui induit naturellement un retard) permettant de recueillir des informations sur l'état de l'outil au fond du puits. Ces informations sont précieuses pour la tâche de contrôle. Afin d'éviter que les dynamiques des vibrations ne présentent des cycles limite, nous travaillons sur l'élaboration d'un contrôle qui dépend de la vitesse de rotation à l'extérieur du puits et de la force élévatrice appliquée sur les tiges en haut du puits également. Un travail de synthèse dans cette thématique est présenté dans [146], il comporte de nouveaux modèles distinguant les différentes parties du système de forage, il inclut des modèles de transmission et les différentes lois de commandes connues pour stabiliser les vibrations le long du système de forage.

Une des contributions essentielles de cette thèse, rentrant dans le cadre de l'étude des racines de quasipolynômes, est présentée dans les chapitres 10 et 11, elle reprend les résultats de [41, 31, 37, 40].

Les résultats obtenus consolident les connaissances actuelles dans la caractérisation des valeurs spectrales imaginaires pures des systèmes à retard. En effet, des approches efficaces existent pour l'identification de telles valeurs spectrales (par exemple, l'approche des faisceaux matriciels, la transformée de Rekasius et d'autres encore), mais à notre connaissance, aucune d'entre elles ne permet d'établir la multiplicité de celles-ci. Ceci s'explique par l'apparition du retard dans les polynômes définissant les dérivées d'un quasipolynôme. L'intérêt de cette piste réside dans le fait que la dimension du projeté de l'état dans cette variété n'est autre que la dimension de l'espace propre généralisé associé aux valeurs spectrales imaginaires pures, d'où une caractérisation de la variété centrale associée à ces valeurs spectrales. En premier lieu, dans [31] nous mettons en évidence l'aspect algébrique du problème de caractérisation de la multiplicité de la valeur spectrale en zéro. Dans ce travail nous avons obtenu une description, en terme de variétés et d'idéaux, des conditions (sur les paramètres d'un quasipolynôme) assurant une multiplicité admissible pour une valeur spectrale en zéro. Ce constat nous a permis dans [37], d'établir un lien entre la multiplicité de zéro en tant que racine d'un quasipolynôme générique et le problème d'interpolation d'Hermite et ainsi les matrices Confluents de Vandermonde. Nous montrons par ce biais, que la borne de multiplicté de la singularité en zéro peut atteindre la borne de Polya-Szegö [176] qui n'est autre que le degré du quasipolynôme considéré [1] et nous établissons explicitement les valeurs des paramètres du quasipolynôme assurant toute multiplicité admissible (inférieure ou égale à la borne

---

1. Le degré d'un quasipolynôme n'est autre que la somme des degrés des polynômes impliqués plus leur nombre moins un.

de Polya-Szegö). Nous démontrons également que la borne de multiplicité d'une valeur spectrale en zéro dépend de la structure du quasipolynôme plutôt que de son degré. Cela nous a permis de caractériser la structure d'un quasipolynôme par une matrice d'incidence de Birkhoff (mettant en évidence l'aspect creux des polynômes impliqués). Un travail de synthèse de ces résultats est présenté dans [40], voir le chapitre 10.

Ce travail a été généralisé dans l'exploration de la multiplicité des valeurs spectrales imaginaires pûres. D'abord, la limitation d'autres approches dans la caractérisation de la multiplicité a été soulignée dans [41]. En effet, au travers d'un exemple explicite il a été démontré que la substitution de Rekasius, par exemple, échoue dans de telles investigations. D'autre part, il est prouvé que la multiplicité d'une valeur spectrale de fréquence non nulle ne peut atteindre la multiplicité de Polya-Szegö. Une approche basée sur des matrices fonctionnelles confluentes de Vandermonde est proposée, une nouvelle borne plus fine pour la multiplicité de telles valeurs spectrales est établie ; voir le chapitre 11.

Toujours dans ce contexte de l'exploration des multiplicités admissibles d'une valeur spectrale et de leur incidence sur les dynamiques des systèmes à retard, cette étude nous a permis d'identifier des propriétés intéressantes. En premier lieu, dans [41], pour une équation scalaire à retard discret, il a été démontré que la borne de multiplicité de Polya-Szegö peut être atteinte pour les valeurs spectrales réelles. En plus, une fois cette borne atteinte, alors le point d'equilibre est asymptotiquement stable. En terminologie algébrique (dans l'espace des paramètres), cela revient à dire que la sous variété définissant cette valeur spectrale multiple correspond à une sous variété stable du point d'équilibre. Cette propriété a été étendue pour des systèmes (à retard) plans dans [122]. Ce résultat a été exploité dans le cadre de l'analyse du modèle de croissance du tournesol (Sunflower equation)

$$\ddot{x} + \frac{a}{\tau}\dot{x} + \frac{b}{\tau}\sin(x(t-\tau)) = 0, \tag{1.5}$$

deux valeurs spectrales réelles doubles ont été retrouvées. Leur existence guaranti, localement et sous des conditions appropriées, la stabilité asymptotique du point d'équilibre à l'origine.

Dans le cadre d'une collaboration en cours avec Silviu Niculescu, Tomas Vyhlidal (Prague University) et Hakki Unal (Inria Saclay), ayant pour objectif d'élaborer une approche de stabilisation basée sur cette propriété, les premières simulations de l'analyse de certains systèmes mécaniques motive l'intérêt de systèmatiser ce critère sous forme d'une procédure informatique.

Dans l'optique de proposer une approche d'analyse qualitative unifiée pour des systèmes comportant des équations différentielles fonctionnelles couplées à des équations algébriques, nous nous sommes proposé d'étendre l'applicabilité du théorème de la variété du centre à une classe de systèmes algébro-différentiels connue sous le nom de systèmes de propagation sans perte, ce qui fait l'objet du Chapitre 13, reproduisant les résultats obtenus dans [32] mais sous une forme étendue de ce travail en collaboration avec Silviu-Iulian Niculescu et Wim Michiels (CU Leuven, Belgique).

Ces systèmes sont souvent utilisés pour modéliser des systèmes complexes dont ils est difficile de mesurer une partie de l'état, nécessitant ainsi des observateurs pour les approcher. Pour ce faire, nous élaborons d'abord une projection spectrale pour un système de propagation sans perte (équation différentielle à retard couplée avec une équation aux différences à retard) dont une forme simplifiée et linéarisée est la suivante :

$$\begin{cases} \dot{x}(t) & = A\,x(t) + B\,y(t-\tau) \\ y(t) & = C\,x(t) + D\,y(t-\tau) \end{cases} \tag{1.6}$$

avec $(x,y)^T \in C_{\tau,n+m}$ où $C_{\tau,n+m}$ est l'espace de Banach des fonctions continues de $[-\tau,0]$ dans $\mathbb{R}^{m+n}$. Etant donné qu'aucun retard n'est appliqué à x, cette variable peut être vue comme $x \in \mathbb{R}^n$.

Ce type de systèmes apparait de manière naturelle dans les problèmes de commande, voir [151]. Ce problème est en général contourné en dérivant la deuxième equation de (1.6) pour obtenir le système à retard de type neutre comme dans [1]

$$\begin{cases} \dot{x}(t) = A\,x(t) + B\,y(t-\tau) \\ \dot{y}(t) - D\,\dot{y}(t-\tau) = C\,A\,x(t) + C\,B\,y(t-\tau). \end{cases} \tag{1.7}$$

Cette manipulation permet de donner une idée des valeurs spectrales certes, mais malheureusement ne permet pas au système de propagation sans perte de bénéficier des conditions de stabilité et de stabilisation du système de type neutre. En effet, la projection spectrale sur la variété centrale du système neutre ne correspond pas à celle du système (1.6) puisqu'une valeur spectrale supplémentaire (en zéro) d'ordre k apparait dans (1.7). A titre d'exemple, il est possible d'avoir un système de propagation sans perte ayant un point d'équilibre asymptotiquement stable contrairement au système neutre. La contribution de [32] consiste à élaborer une projection spectrale associé à (1.6) sans passer par une équation de type neutre, pour ainsi établir une méthode fournissant une approximation en dimension finie (élimination du retard).
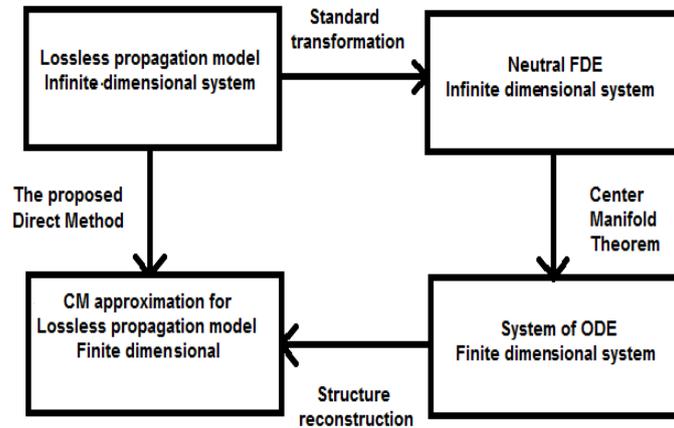
Nous exhibons également dans ce travail des conditions suffisantes pour la convergence du développement en série des solutions de ce type de système.

Pour conclure, cette section a succintement mis en évidence le fil conducteur des sujets abordés dans les chapitres qui suivent. L'ordre de présentation des chapitres n'est pas que chronologique ; il reflète l'enchènement du questionnement qui a conduit à ces travaux. La motivation principale est d'établir une méthdologie unifiée et effective dans la caractérisation de propriétés qualitatives des systèmes dynamiques (comportant certaines complexités). Les perspectives correspondant à ces recherches feront l'objet du chapitre 14.

Première partie

Analysis of finite dimensional dynamical systems and its applications

Analyse de systèmes dynamiques de dimension finie et ses applications

"... D'ailleurs, ce qui nous rend ces solutions périodiques si précieuses,
c'est qu'elles sont, pour ainsi dire, la seule brèche par où nous puissions
essayer de pénétrer dans une place jusqu'ici réputée inabordable."
Henri Poincaré, *Les méthodes nouvelles de la mécanique céleste, 1892.*

Characterizing isochronous centers of Liénard-type planar systems

A classical dynamical system is called isochronous if it features in its phase space an open, fully-dimensional, region where all of its solutions are periodic in all their degrees of freedom with the same, fixed period-independently from the initial data, provided they are inside the isochrony region (the center annulus) [44]. As emphasized in the historical note given in [188], the interest in the isochronicity property is an old problem which started with the history of clocks based on some sort of periodic motion, such as the swinging of a pendulum. Based on his knowledge that the cycloid is a tautochrone (a frictionless particle sliding down a wire in the shape of a cycloid reaches the lowest point in the same amount of time, regardless of its starting position). In the 17th century Huygens designed and built a pendulumclock. This is probably the earliest example of a nonlinear isochronous system. Since the last century, the interest in characterizing of such a property becomes a prolific literature topic, for instance, the number of 7571 publications listed in the data base of elsevier etitions contains the word "isochronous" (in different contexts).

Of course, in the real world the examples of purely isochronous behavior are rather rare, otherwise life would be pretty dull, see [44].

In this chapter, we are concerned with planar systems of ordinary differential equations. The proofs of the results given in this chapter can be found in [30]. We study the isochronicity of centers at $O \in \mathbb{R}^2$ for systems $\dot{x} = -y + A(x,y), \ \dot{y} = x + B(x,y)$, where $A, \ B \in \mathbb{R}[x,y]$, which can be reduced to the Liénard-type equation. Several new families of isochronous centers are provided. All these results are established using intensive computer algebra and Gröbner basis computations.

2.1 Introduction

2.1.1 Generalities

The hunting of isochronous centers is now a flourishing activity. By this chapter we would like to contribute to it.

Let us consider the system of real differential equations of the form

$$\frac{dx}{dt} = \dot{x} = -y + A(x,y), \qquad \frac{dy}{dt} = \dot{y} = x + B(x,y), \qquad (2.1)$$

where (x, y) belongs to an open connected subset $U \subset \mathbb{R}^2$, $A, B \in C^\infty(U, \mathbb{R})$, where A and B as well as their first derivatives vanish at $(0, 0)$. An isolated singular point $p \in U$ of system (2.1) is a *center* if there exists a punctured neighborhood $V \subset U$ of p such that every orbit of (2.1) lying in V is a closed orbit surrounding p. A center p is *isochronous* if the period is constant for all closed orbits in some neighborhood of p.

The simplest example is the linear isochronous center at the origin $O = (0, 0)$ given by the system

$$\dot{x} = -y, \ \dot{y} = x. \tag{2.2}$$

The problem of caracterization of couples (A, B) such that O is an isochronous center (even a center) for the system (2.1) is largely open.

An overview of J. Chavarriga and M. Sabatini [52] present the basic results concerning the problem of the isochronicity, see also [7, 60, 188].

The well known Poincaré Theorem assert that when A and B are real analytic, a center of (2.1) is isochronous if and only if in some analytic coordinate system it take the form of the linear center (2.2). Let us formulate now another theorem of the same vein (see for example [7], Th.13.1 and [188], Th.4.2.1).

Theorem A ([145], Th.3.3) *Let us suppose that the origin O is an isochronous center of system* (2.1)*. Let $F(x, y) = x^2 + y^2 + o(|(x, y)|^2)$ be an analytic first integral defined in some neighborhood of O. Then there exists an analytic change of coordinates $u(x, y) = x + o(|(x, y)|)$, $v(x, y) = x + o(|(x, y)|)$ bringing the system* (2.1) *to the linear system $\dot{u} = -v$, $\dot{v} = u$ and such that $F(x, y) = u^2(x, y) + v^2(x, y)$.*

We pass now to the heart of the matter. To make this chapter more accessible, we report all strictly technical remarks to Appendix, Section 7.

In some circumstances a system (2.1) can be reduced to *the Liénard type equation*

$$\ddot{x} + f(x)\dot{x}^2 + g(x) = 0 \tag{2.3}$$

with $f, g \in C^1(J, \mathbb{R})$, where J is some neighborhood of $0 \in \mathbb{R}$ and $g(0) = 0$. If this is so, the system (2.1) is called *reducible*. To the equation (2.3) one associate the two dimentional (planar) Liénard type system

$$\left. \begin{array}{l} \dot{x} = y \\ \dot{y} = -g(x) - f(x)y^2 \end{array} \right\} \tag{2.4}$$

For reducible systems considered in this chapter, the nature of singular point O for both system (2.1) and (2.4) is the same (see Appendix, Sec.2.7) ; in particular this concerns the centers and isochronous centers.

Let us return now to the Liénard type equation (2.3). Let us define the following functions

$$F(x) := \int_0^x f(s)ds, \quad \phi(x) := \int_0^x e^{F(s)}ds. \tag{2.5}$$

When $xg(x) > 0$ for $x \neq 0$, define the function X by

$$\frac{1}{2}X(x)^2 = \int_0^x g(s)e^{2F(s)}ds \tag{2.6}$$

such that $xX(x) > 0$ for $x \neq 0$.

Let us formulate now the following Theorems which are the departure point of this chapter.

Theorem B ([194], Th.1) *Let $f, g \in C^1(J, \mathbb{R})$. If $xg(x) > 0$ for $x \neq 0$, then the system (2.4) has a center at the origin O. When f, g are analytic , this condition is also necessary.*

When $f, g \in C^1(J, \mathbb{R})$, the first integral of the system (2.4) is given by the formula

$$I(x, \dot{x}) = 2 \int_0^x g(s)e^{2F(s)}ds + (\dot{x}e^{F(x)})^2 \tag{2.7}$$

Theorem C ([62], Th.2.1) *Let f, g be real analytic functions defined in a neighborhood J of $0 \in \mathbb{R}$, and let $xg(x) > 0$ for $x \neq 0$. Then system (2.4) has an isochronous center at O if and only if there exists an odd function h which satisfies the following conditions*

$$\frac{X(x)}{1 + h(X(x))} = g(x)e^{F(x)}, \tag{2.8}$$

the function $\phi(x)$ satisfies

$$\phi(x) = X(x) + \int_0^{X(x)} h(t)dt, \tag{2.9}$$

and $X(x)\phi(x) > 0$ for $x \neq 0$.

In particular, when f and g are odd, then O is an isochronous center if and only if $g(x) = e^{-F(x)}\phi(x)$, or equivalently $h = 0$.

The function h is called *Urabe function*. The above Theorem implies

Corollary A ([62], Cor.2.4) *Let f, g be functions analytic in a neighborhood of $0 \in \mathbb{R}$, and $xg(x) > 0$ for $x \neq 0$. The origin O is isochronous center of system (2.4) with Urabe function $h = 0$ if and only if*

$$g'(x) + g(x)f(x) = 1 \tag{2.10}$$

In [62] the second author described how the use of Theorem C allows to an algorithm (C-algorithm, see Sec.2.7 Appendix for more details) for searching the cases when O is an isochronous center for reducible system (2.1), with application to the case when A and B are polynomials of degree 3. This work was continued in [63].

The main results obtained in the two last cited chapters are the necessary and sufficient conditions for isochronicity of the center at O in term of parameters for the cubic system

$$\left.\begin{array}{l} \dot{x} = -y + axy + bx^2y \\ \dot{y} = x + a_1x^2 + a_3y^2 + a_4x^3 + a_6xy^2 \end{array}\right\} \tag{2.11}$$

The aim of this chapter is to extend investigations made in [62, 63] for systems with higher order perturbations of the linear center $\dot{x} = -y$, $\dot{y} = x$.

Like in [62], our main tool to investigate the isochronous centers for multiparameters systems reducible to Liénard type equation is C-algorithm. Nevertheless when searching only the isochronous centers with zero Urabe function the Corollary A give a much simpler method which is widely used in this chapter. It consists to identify the parameters values for which identity (3.10) is satisfied.

In all cases considered in [63] as well as in the present chapter the Urabe function is of the form $h(X) = \frac{k_1 X^s}{\sqrt{k_2 + k_3 X^{2s}}}$ where s is an odd natural number and $k_2 > 0$. Like in [63], we ask if the Urabe function of corresponding Lienard type equation (called in the future also the Urabe function of the isochronous center under consideration) is always of the above form.

The complexity of many examples of isochronous centers described in this chapter clearly indicate the end of purely enumerative study in this field.

In our investigations we have used *Maple* in its version 10. To compute the Gröbner basis (with DRL order) of the obtained systems of polynomial equations, we have used *Salsa Software* more precisely the implementation *FGb* [93].

2.1.2   Beyond the degree 3

We present now the list of reducible systems for which we study the isochronous centers at the origin.

1. In Section 2.2 we study the most general homogeneous perturbation of arbitrary degree $n \geq 3$ of the linear center which belongs to the Case 1 from the Appendix, Sec.2.7 :

$$\left.\begin{array}{rl} \dot{x} &= -y + ayx^{n-1} \\ \dot{y} &= x + bx^{n-2}y^2 + cx^n \end{array}\right\} \tag{2.12}$$

   Here we found 3 isochronous centers for even $n \geq 4$ and 2 isochronous centers for odd $n \geq 3$ which seems to be new.

2. In Sections 2.3 and 2.4 we study the most general polynomial perturbation of degree four of the linear center which belongs to the Case 1 from the Appendix Sec. 2.7 :

$$\left.\begin{array}{l} \dot{x} = -y + a_{11}yx + a_{21}yx^2 + a_{31}yx^3 \\ \dot{y} = x + b_{20}x^2 + b_{30}x^3 + b_{02}y^2 + b_{12}xy^2 + b_{22}x^2y^2 + b_{40}x^4 \end{array}\right\} \tag{2.13}$$

   First using Corollary A we identify all isochronous centers with zero Urabe function. Here we found 6 isochronous centers which seems to be new. The study of this system by C-algorithm can not be performed by our actual computer facilities. Thus, we select for investigation two sub-families; the first one when $a_{1,1} = b_{3,0} = 0$ and the second one when $a_{1,1} = a_{2,1} = 0$. Here we found 8 isochronous centers which seems to be new.

3. In Section 2.5 we study the most general polynomial perturbation of degree five of the linear center which belongs to the Case 1 from the Appendix

Sec.2.7 :

$$
\left.\begin{aligned}
\dot{x} &= -y + a_{11}yx + a_{21}yx^2 + a_{31}yx^3 + a_{41}yx^4 \\
\dot{y} &= x + b_{20}x^2 + b_{30}x^3 + b_{02}y^2 + b_{12}xy^2 + b_{22}x^2y^2 + b_{32}x^3y^2 + b_{40}x^4 + b_{50}x^5
\end{aligned}\right\}
$$
(2.14)

Using Corollary A we identify all isochronous centers with zero Urabe function where $b_{50} = 0$. Here we found eight isochronous centers which seems to be new.

4. In Section 2.6 we study the following Abel system of arbitrary degree $n \geq 2$ which belongs to the Case 2 from the Appendix Sec. 2.7 :

$$
\left.\begin{aligned}
\dot{x} &= -y \\
\dot{y} &= \sum_{k=0}^{n} a_k xy^k,
\end{aligned}\right\}
$$
(2.15)

where $a_k \in \mathbb{R}$, for $k = 0, \ldots, n$. Here we verify that up to $n = 9$ there are not other isochronous centers from the one found by Volokitin and Ivanov in [83].

Let us stress that by Theorem B, in all the above cases the origin O is always a center (indeed, the condition $xg(x) > 0$ for $x \neq 0$ is satisfied for sufficiently small $|x|$; see Appendix Sec. 2.7).

When describing in Sec.2.3-2.6 the identified isochronous centers, all parameters intervaining in the formulas are arbitrary, except that one always suppose that the polynomials at the denominators are non zero. To avoid the misprints all formulas are written exactly in the form produced by *Maple*. All fractions which appear in the formulas are irreducible. In all cases when we was able to write down first integrals and linearizing changes of variables, the explicit formulas are reported.

2.2 Homogeneous perturbation of arbitrary degree

As it will be proven in Theorem 1, from Corollary A it easily follows that for arbitrary $n \geq 2$, the system (2.12) admit exactly two isochronous centers with zero Urabe function.

Moreover, following Theorem C when $n \geq 3$ is odd, other isochronous centers does not exist.

When $n \geq 4$ is even the preliminary investigation of the system (2.12) performed by C-algorithm strongly suggest that for such n there exists exactly one additional isochronous center with non zero Urabe function. Its existence is proved in Theorem 2. Unfortunately, its uniqueness is not yet proved for arbitrary even $n \geq 4$. For $n = 4, 6, 8$ the uniqueness was proved using *Maple* and Gröbner Basis technique.

Let us underline that our final proofs are done by the hand computations, without use of computer algebra.

Taking into account the condition $g'(x) + f(x)g(x) = 1$ from Corollary A, one obtain easily the following Theorem

Theorem 1. *For $n \geq 2$ the system (2.12) has an isochronous center at the origin O with zero Urabe function only in one of the following two cases*

$$\left.\begin{array}{rl} \dot{x} & = -y + ax^{n-1}y \\ \dot{y} & = x + ax^{n-2}y^2 \end{array}\right\} \tag{2.16}$$

$$\left.\begin{array}{rl} \dot{x} & = y + \frac{b}{n}x^{n-1}y \\ \dot{y} & = x + bx^{n-2}y^2 - \frac{b(n-1)}{n^2}x^n \end{array}\right\} \tag{2.17}$$

Moreover, for odd $n \geq 3$ there are no other isochronous centers.

System (2.12) is reducible to the system (2.4) with

$$f(x) = \frac{x^{n-2}(b + an - a)}{1 - ax^{n-1}} \quad \text{and} \quad g(x) = \left(1 - ax^{n-1}\right)(x + cx^n)$$

(see Appendix, Sec.7.1)

The condition $g'(x) + f(x)g(x) = 1$ allows directly to the following two cases :

1. $\{a = b, c = 0\}$ which gives the system (2.16).

2. $\left\{c = -\frac{b(n-1)}{n^2}, a = \frac{b}{n}\right\}$ which gives the system (2.17).

Applying Sabatini formula (2.7) using *Maple*, one see that for $n = 4..8$ the first integral of system (2.16) takes the form

$$H_{(2.16)} = \frac{\left(x^2 + y^2\right)}{\left(-1 + a\,x^{n-1}\right)^{\frac{2}{n-1}}}$$

Then Theorem A suggest that the linearizing change of coordinates is

$$u = \frac{x}{\sqrt[n-1]{1 - a\,x^{n-1}}}, \quad v = \frac{y}{\sqrt[n-1]{1 - a\,x^{n-1}}} \tag{2.18}$$

Now by hand computations one verify that $H_{(2.16)}$ is always a first integral of system (2.16) and using *Maple* one easily check that (2.18) is a linearizing change of coordinates.

Exactly the same arguments work for the system (2.17). Its first integral is

$$H_{(2.17)} = \frac{x^2\left(1 + cx^{n-1}\right)^2 + y^2}{(n-1)^2\left(n - 1 + ncx^{n-1}\right)^{\frac{2n}{n-1}}}$$

and its linearizing change of coordinates is

$$u = \frac{x\left(1 + cx^{n-1}\right)}{(n-1)\left(\left(n - 1 + ncx^{n-1}\right)^{\frac{n}{n-1}}\right)}, \quad v = \frac{y}{(n-1)\left(\left(n - 1 + ncx^{n-1}\right)^{\frac{n}{n-1}}\right)}$$

Theorem 2. *The system (2.12) with arbitrary even $n \geq 2$ and $a = 2b$, $c = -b$, $b \neq 0$, has an isochronous center at the origin with non zero Urabe function*

$$h(X) = \frac{bX^{n-1}}{\sqrt{1 + b^2 X^{2n-2}}} \tag{2.19}$$

Indeed, when $a = 2b$ and $c = -b$ the system (2.12) writes

$$\left.\begin{array}{ll} \dot{x} & = -y + 2byx^{n-1} \\ \dot{y} & = x + bx^{n-2}y^2 - bx^n \end{array}\right\}. \tag{2.20}$$

To simplify the formulas let us perform the following change of variables $(x, y) \longmapsto (x/b, y/b)$ the system (2.20) takes the form

$$\left.\begin{array}{ll} \dot{x} & = -y + 2yx^{n-1} \\ \dot{y} & = x + x^{n-2}y^2 - x^n \end{array}\right\} \tag{2.21}$$

Which is reducible to the Liénard type equation (2.3) with

$$f(x) = \frac{(-1 + 2n)x^{n-2}}{1 - 2x^{n-1}} \quad \text{and} \quad g(x) = \left(1 - 2x^{n-1}\right)(x - x^n)$$

Then

$$F(x) = \int_0^x f(s)ds = \frac{1 - 2n}{2n - 2}\ln\left(1 - 2x^{n-1}\right)$$

which gives the right hand side of the equality (2.8)

$$g(x)e^{F(x)} = \frac{x(1 - x^{n-1})}{\left(1 - 2x^{n-1}\right)^{\frac{1}{2n-2}}}.$$

On the other hand, $e^{2F(x)} = \left(1 - 2x^{n-1}\right)^{\frac{1-2n}{n-1}}$.

From the equation (2.6) we compute

$$X(x) = \sqrt{2\int_0^x g(s)e^{2F(s)}ds} = \frac{x}{\left(1 - 2x^{n-1}\right)^{\frac{1}{2n-2}}}$$

and

$$h(X(x)) = \frac{X(x)^{n-1}}{\sqrt{1 + X(x)^{2n-2}}} = \frac{x^{n-1}}{1 - x^{n-1}}$$

Then we compute the left hand side of the equality (2.8) :

$$\frac{X(x)}{1 + h(X(x))} = \frac{\frac{x}{(1-2x^{n-1})^{\frac{1}{2n-2}}}}{1 + \frac{x^{n-1}}{1-x^{n-1}}} = \frac{x(1 - x^{n-1})}{\left(1 - 2x^{n-1}\right)^{\frac{1}{2n-2}}}$$

Which proves that the equality (2.8) is satisfied. Let us stress that the above computations remains valid for every $n \geq 2$. Nevertheless, for n odd h is not an odd function and thus it is not an Urabe function which is odd by definition.

Theorem 3. *For arbitrary $n \geq 2$, the system (2.20) has the following first integral*

$$H_{(2.20)} = \frac{\left(x^2 + y^2\right)^{n-1}}{2bx^{n-1} - 1}.$$

Using formula (2.7), one easily compute by *Maple* the first integral for $n = 4, 6, 8$. The obtained results strongly suggest the veracity of formula for $H_{(2.20)}$. Now one easily verify by hand computations that $H_{(2.20)}$ is a first integral.

Let us return to system (2.12). It is well known that for $n = 2$, this system has an isochronous center in exactly four cases, so called Loud isochronous centers (see [140, 62]). They correspond to $(a = b, c = 0)$, $(a = \frac{b}{2}, c = -\frac{b}{4})$, $(a = 2b, c = -b)$ and $(b = \frac{a}{4}, c = 0)$. The first two are those from Theorem 1 , the third is the one from Theorem 2. Let us note the Taylor expansion of the Urabe function $h(X) = c_1 X + c_3 X^3 + \ldots$. As noted at the begining of the Section, for $n = 4$ one has exactly 3 cases of isochronous centers. Why such a difference ? The difference is in the algebraic structure of the equations generated by C-algorithm. For $n = 2$, the second of such equations is $-3 c_1 + a - 2 c - b = 0$ and c_1 can be non zero, while for $n \geq 3$, the second such equation is always $c_1 = 0$. Thus the freedom for existence of non zero Urabe function is greater for $n = 2$ then for $n \geq 3$.

2.3 Non homogeneous perturbation of degree four with zero Urabe function

Taking into account the condition $g'(x) + f(x)g(x) = 1$ from Corollary A, using *Maple* one obtain easily the following Theorem.

Theorem 4. *The system (2.13) has an isochronous center at the origin O with zero Urabe function only in one of the following six cases, where one suppose that all denominators are non zero polynomials.*

$\boxed{22I}$

$$\left.\begin{array}{rl} \dot{x} &= -y + b_{02}xy + a_{21}x^2y + a_{31}x^3y \\ \dot{y} &= x + b_{02}y^2 + a_{21}xy^2 + a_{31}x^2y^2 \end{array}\right\}$$

$\boxed{II}$

$$\left.\begin{array}{rl} \dot{x} &= -y + b_{02}xy - 3/2\,b_{30}x^2y + b_{02}b_{30}x^3y \\ \dot{y} &= x + b_{02}y^2 + b_{30}x^3 - 9/2\,b_{30}xy^2 + 3\,b_{02}b_{30}x^2y^2 \end{array}\right\}$$

$\boxed{III}$

$$\left.\begin{array}{rl} \dot{x} &= -y + (b_{02} + 2\,b_{20})\,xy + a_{21}x^2y + \left(b_{20}a_{21} - b_{02}b_{20}{}^2 - 4\,b_{20}{}^3\right)x^3y \\[2mm] \dot{y} &= x + b_{20}x^2 + b_{02}y^2 + \left(a_{21} + b_{02}b_{20} + 4\,b_{20}{}^2\right)xy^2 \\ &\quad + \left(2\,b_{20}a_{21} - 2\,b_{02}b_{20}{}^2 - 8\,b_{20}{}^3\right)x^2y^2 \end{array}\right\}$$

$\boxed{IV}$

$$\dot{x} \;=\; -y + \frac{\left(-9\,b_{30}b_{20}{}^2 - b_{20}{}^2 a_{21} + 2\,b_{20}{}^4 + 4\,b_{30}a_{21} + 6\,b_{30}{}^2\right)}{b_{20}\left(-b_{20}{}^2 + 4\,b_{30}\right)}\,xy$$
$$+\,a_{21}x^2 y + \frac{b_{30}\left(-2\,b_{30}b_{20}{}^2 - b_{20}{}^2 a_{21} + 4\,b_{30}a_{21} + 6\,b_{30}{}^2\right)}{b_{20}\left(-b_{20}{}^2 + 4\,b_{30}\right)}\,x^3 y$$

$$\dot{y} \;=\; x + b_{20}x^2 + \frac{\left(-17\,b_{30}b_{20}{}^2 - b_{20}{}^2 a_{21} + 4\,b_{20}{}^4 + 4\,b_{30}a_{21} + 6\,b_{30}{}^2\right)}{b_{20}\left(-b_{20}{}^2 + 4\,b_{30}\right)}\,y^2$$
$$+\,b_{30}x^3 + 2\,\frac{\left(-b_{20}{}^2 a_{21} + 4\,b_{30}a_{21} + b_{30}b_{20}{}^2 - 3\,b_{30}{}^2\right)}{-b_{20}{}^2 + 4\,b_{30}}\,xy^2$$
$$+\,3\,\frac{b_{30}\left(-2\,b_{3,0}b_{20}{}^2 - b_{20}{}^2 a_{21} + 4\,b_{30}a_{21} + 6\,b_{30}{}^2\right)}{b_{20}\left(-b_{20}{}^2 + 4\,b_{30}\right)}\,x^2 y^2$$

$\boxed{V}$

$$\dot{x} \;=\; -y - \frac{\left(-32\,b_{40}b_{30}b_{20}{}^2 + 42\,b_{40}{}^2 b_{20} + 8\,b_{40}b_{20}{}^4 + b_{40}b_{30}{}^2 - 2\,b_{30}{}^2 b_{20}{}^3 + 7\,b_{30}{}^3 b_{20}\right)}{-b_{30}{}^2 b_{20}{}^2 + 4\,a_{2,4,0}b_{20}{}^3 - 18\,b_{40}b_{30}b_{20} + 27\,b_{40}{}^2 + 4\,b_{30}{}^3}\,xy$$
$$-\,\frac{\left(6\,b_{30}{}^4 - 2\,b_{20}{}^2 b_{30}{}^3 - 27\,b_{40}b_{20}b_{30}{}^2 + 8\,b_{30}b_{40}b_{20}{}^3 + 39\,b_{30}b_{40}{}^2 - 4\,b_{40}{}^2 b_{20}{}^2\right)}{-b_{30}{}^2 b_{20}{}^2 + 4\,b_{40}b_{20}{}^3 - 18\,b_{40}b_{30}b_{20} + 27\,b_{40}{}^2 + 4\,b_{30}{}^3}\,x^2 y$$
$$-\,2\,\frac{b_{40}\left(-b_{30}{}^2 b_{20}{}^2 - 14\,b_{40}b_{30}b_{20} + 18\,b_{40}{}^2 + 4\,b_{40}b_{20}{}^3 + 3\,b_{30}{}^3\right)}{-b_{30}{}^2 b_{20}{}^2 + 4\,b_{40}b_{20}{}^3 - 18\,b_{40}b_{30}b_{20} + 27\,b_{40}{}^2 + 4\,b_{30}{}^3}\,x^3 y$$

$$\dot{y} \;=\; x + b_{20}x^2 - \frac{\left(-68\,b_{40}b_{30}b_{20}{}^2 + 96\,b_{40}{}^2 b_{20} + 16\,b_{40}b_{20}{}^4 + b_{40}b_{30}{}^2 - 4\,b_{30}{}^2 b_{20}{}^3 + 15\,b_{30}{}^3 b_{20}\right)}{-b_{30}{}^2 b_{20}{}^2 + 4\,b_{40}b_{20}{}^3 - 18\,b_{40}b_{30}b_{20} + 27\,b_{40}{}^2 + 4\,b_{30}{}^3}\,y^2$$
$$+\,b_{30}x^3 - 2\,\frac{\left(9\,b_{30}{}^4 - 3\,b_{20}{}^2 b_{30}{}^3 - 40\,b_{40}b_{20}b_{30}{}^2 + 12\,b_{30}b_{40}b_{20}{}^3 + 60\,b_{30}b_{40}{}^2 - 8\,b_{40}{}^2 b_{20}{}^2\right)}{-b_{30}{}^2 b_{20}{}^2 + 4\,b_{40}b_{20}{}^3 - 18\,b_{40}b_{30}b_{20} + 27\,b_{40}{}^2 + 4\,b_{30}{}^3}\,xy^2$$
$$-\,8\,\frac{b_{40}\left(-b_{30}{}^2 b_{20}{}^2 - 14\,b_{40}b_{30}b_{20} + 18\,b_{40}{}^2 + 4\,b_{40}b_{20}{}^3 + 3\,b_{30}{}^3\right)}{-b_{30}{}^2 b_{20}{}^2 + 4\,b_{40}b_{20}{}^3 - 18\,b_{40}b_{30}b_{20} + 27\,b_{40}{}^2 + 4\,b_{30}{}^3}\,x^2 y^2 + b_{40}x^4$$

$\boxed{VI}$

$$\dot{x} \;=\; -y + \left(2\,b_{20} + b_{02}\right)xy - \frac{b_{20}{}^2}{32}\left(567\,Z^2 b_{20} + 24\,Z b_{02} - 804\,Z b_{20} + 113\,b_{20} - 8\,b_{02}\right)x^3 y$$
$$+\,\frac{b_{20}\left(13032\,Z^2 b_{02} - 4488\,Z b_{02} + 68719\,Z^2 b_{20} - 22970\,Z b_{20} + 384\,b_2 + 1943\,b_{20}\right)}{24(387\,Z^2 - 144\,Z + 13)}\,x^2 y$$

$$\dot{y} \;=\; x + b_{20}x^2 + b_{02}y^2 - \frac{Z b_{20}{}^2(27\,Z - 17)}{4 + 12\,Z}\,x^3$$
$$-\,\frac{b_{20}}{32}\left(-108\,Z^2 b_{02} + 1053\,Z^2 b_{20} + 152\,Z b_{02} - 1964\,Z b_{20} - 76\,b_{02} + 155\,b_{20}\right)xy^2$$
$$-\,\frac{b_{20}{}^2}{8}\left(567\,Z^2 b_{20} + 24\,Z b_{02} - 804\,Z b_{20} + 113\,b_{20} - 8\,b_{02}\right)x^2 y^2 + 1/4\,Z b_{20}{}^3 x^4$$

where Z is the only real root of the equation $27\,s^3 - 47\,s^2 + 13\,s - 1 = 0$, which is equal to

$$Z = \frac{1}{81}\sqrt[3]{39428 + 324\sqrt{93}} + \frac{1156}{81}\frac{1}{\sqrt[3]{39428 + 324\sqrt{93}}} + \frac{47}{81}$$

2.4 Non homogeneous perturbations of degree four

Let us consider system (2.13)

$$\begin{aligned}
\dot{x} &= -y + a_{11}yx + a_{21}yx^2 + a_{31}yx^3 \\
\dot{y} &= x + b_{20}x^2 + b_{30}x^3 + b_{02}y^2 + b_{12}xy^2 + b_{22}x^2 y^2 + b_{40}x^4
\end{aligned}\Bigg\}$$

We would like to identify all its isochronous centers by C-algorithm, without taking into account the nature of its Urabe function. In full generality this problem is unattainable today for our actual computer possiblities. Indeed, we do not succeed to compute a Gröbner basis for the nine C-algorithm generated polynomials on 9 unknown $\{a_{ij}\}$ and $\{b_{sr}\}$ of all even degrees between 2 and 18.

Inspecting the system under consideration one sees that when annulations of some parameters $\{a_{ij}\}$ and $\{b_{rs}\}$ allows to substantial simplification of the system. This is the reason of our choice of two families presented below which have the codimension two in the parameters space.

2.4.1 First family

Let us assume $a_{11} = b_{30} = 0$, in this case (2.13) reduces to the system

$$\left.\begin{array}{rl} \dot{x} & = -y + a_{21}x^2y + a_{31}yx^3 \\ \dot{y} & = x + b_{20}x^2 + b_{02}y^2 + b_{12}xy^2 + b_{22}x^2y^2 + b_{40}x^4 \end{array}\right\} \qquad (2.22)$$

For this system having a center at the origin O, we give isochronicity necessary and sufficient conditions depending only on the following seven real parameters $a_{21}, a_{31}, b_{20}, b_{02}, b_{12}, b_{22}, b_{40}$.

Theorem 5. *The system* (2.22) *has an isochronous center at O if and only if its parameters satisfy one of the folowing six conditions :*

$\boxed{22I}$

$$\left.\begin{array}{rl} \dot{x} & = y + \frac{b_{22}}{4}x^3y \\ \dot{y} & = x + b_{22}x^2y^2 - \frac{3b_{22}}{16}x^4 \end{array}\right\}$$

$\boxed{II}$

$$\left.\begin{array}{rl} \dot{x} & = -y + 2b_{22}yx^3 \\ \dot{y} & = x + b_{22}x^2y^2 - b_{22}x^4 \end{array}\right\}.$$

$\boxed{III}$

$$\left.\begin{array}{rl} \dot{x} & = -y + a_{21}x^2y + a_{31}x^3y \\ \dot{y} & = x + a_{21}xy^2 + a_{31}x^2y^2 \end{array}\right\}$$

$\boxed{IV}$

$$\left.\begin{array}{rl} \dot{x} & = -y + 2/3\,b_{20}{}^2x^2y - 4/3\,b_{20}{}^3x^3y \\ \dot{y} & = x + b_{20}x^2 - 2\,b_{20}y^2 + 8/3\,b_{20}{}^2xy^2 - 8/3\,b_{20}{}^3x^2y^2 \end{array}\right\}$$

$\boxed{V}$

$$\left.\begin{array}{rl} \dot{x} & = -y + 2/3\,b_{20}{}^2x^2y - 4/3\,b_{20}{}^3x^3y \\ \dot{y} & = x + b_{20}x^2 - 2\,b_{20}y^2 + 8/3\,b_{20}{}^2xy^2 - 8/3\,b_{20}{}^3x^2y^2 \end{array}\right\}$$

$\boxed{VI}$

$$
\left.
\begin{aligned}
\dot{x} &= -y + b_{20}{}^2 \left(2 + \frac{a_{31}}{b_{20}{}^3}\right) x^2 y + a_{31} x^3 y \\
\dot{y} &= x + b_{20} x^2 - 2\, b_{20} y^2 + b_{20}{}^2 \left(4 + \frac{a_{31}}{b_{20}{}^3}\right) x y^2 + 2\, a_{31} x^2 y^2
\end{aligned}
\right\}
$$

where $b_{20} \neq 0$.

C-algorithm gives the six candidates to be isochronous centers. 19 derivatives was essential to obtain the necessary conditions of isochronicity. For the sake of brevity we omit all computer algebra details.

To perform the succesful application of C-algorithm, we add the two tricks explained in Appendix, Sec.2.7 : homogenization and reduction of the dimension of the parameters space by one. This allows to the proof that the cases I-VI of Theorem 5 satisfy the necessary conditions of isochronicity. We check that the necessary conditions are also sufficient by direct application of Corollary A to the cases I, III-VI. Indeed, in all those four cases $g'(x) + f(x)g(x) = 1$. The case II is a particular case of the system (2.20) when $n = 4$, studied in Theorem 2.

Let us note that among the above six cases only the cases I, II and III with $a_{21} = 0$ represent the homogeneous perturbations. All other cases are non-homogeneous.

Note also that the above three homogeneous cases was already identified by Theorems 2 and 1. But at the difference of the quoted Theorems, here we have the exhaustive list of isochronous centers for $n = 4$.

2.4.2 Second family

Consider system (2.13), with $a_{11} = a_{21} = 0$. We obtain the seven parameter real system of degree 4.

$$
\left.
\begin{aligned}
\dot{x} &= -y + a_{31} y x^3 \\
\dot{y} &= x + b_{20} x^2 + b_{02} y^2 + b_{30} x^3 + b_{12} x y^2 + b_{22} x^2 y^2 + b_{40} x^4
\end{aligned}
\right\}
\tag{2.23}
$$

For this system having a center at the origin O, we give isochronicity necessary and sufficient conditions depending only on these seven real parameters $b_{30}, a_{31}, b_{20}, b_{02}, b_{12}, b_{22}, b_{40}$.

System (2.23) reduces to the equation (2.3) with

$$
\left.
\begin{aligned}
f(x) &= \frac{b_{02} + b_{12} x + (b_{22} + 3 a_{31}) x^2}{1 - a_{31} x^3}, \\
g(x) &= (x + b_{20} x^2 + b_{30} x^3 + b_{40} x^4)(1 - a_{31} x^3)
\end{aligned}
\right\}
$$

Theorem 6. *The system* (2.23) *has an isochronous center at O if and only if its parameters satisfy one of the folowing seven cases :*

The three cases I, II and III with $a_{21} = 0$ from Theorem 5 given by homogeneous perturbations and the following four cases whose correspend to the non-homogeneous perturbations

$\boxed{IV}$

$$\left.\begin{aligned}
\dot{x} &= -y + 1/4\,b_{02}{}^3 x^3 y \\
\dot{y} &= x - 1/2\,b_{02}x^2 + b_{02}y^2 + 1/2\,b_{02}{}^2 xy^2 + 1/2\,b_{02}{}^3 x^2 y^2
\end{aligned}\right\}$$

$\boxed{V}$

$$\left.\begin{aligned}
\dot{x} &= -y + \tfrac{1}{192}\,b_{02}{}^3 \left(-21 + 5\sqrt{33}\right) x^3 y \\
\dot{y} &= x - 1/2\,b_{02}x^2 + b_{02}y^2 + 1/48\,b_{02}{}^2 \left(9 - \sqrt{33}\right) x^3 \\
&\quad + 1/16\,b_{02}{}^2 \left(-1 + \sqrt{33}\right) xy^2 + \tfrac{1}{64}\,b_{02}{}^3 \left(-21 + 5\sqrt{33}\right) x^2 y^2
\end{aligned}\right\}$$

$\boxed{VI}$

$$\left.\begin{aligned}
\dot{x} &= -y - \tfrac{1}{192}\,b_{02}{}^3 \left(21 + 5\sqrt{33}\right) x^3 y \\
\dot{y} &= x - 1/2\,b_{02}x^2 + b_{02}y^2 + 1/48\,b_{02}{}^2 \left(9 + \sqrt{33}\right) x^3 \\
&\quad - 1/16\,b_{02}{}^2 \left(1 + \sqrt{33}\right) xy^2 - \tfrac{1}{64}\,b_{02}{}^3 \left(21 + 5\sqrt{33}\right) x^2 y^2
\end{aligned}\right\}$$

$\boxed{VII}$

$$\left.\begin{aligned}
\dot{x} &= -y + \frac{2}{3549}\,\frac{b_{20}{}^3\left(-43\,t^{2/3} - 7670\sqrt{3297} + 12112\,\sqrt[3]{t} + 52\,\sqrt[3]{t}\sqrt{3297} - 336886\right)}{t^{2/3}}\,x^3 y \\[2mm]
\dot{y} &= x - 2\,b_{2,0}y^2 - \frac{1}{10647}\,\frac{b_{2,0}\left(-3822\,b_{2,0}t^{2/3} - 6242964\,b_{2,0} - 127764\,b_{2,0}\sqrt{3297} + 159432\,b_{2,0}\sqrt[3]{t}\right)}{t^{2/3}}\,xy^2 \\
&\quad - \frac{1}{10647}\,\frac{b_{2,0}\left(1032\,b_{2,0}{}^2 t^{2/3} + 184080\,b_{2,0}{}^2\sqrt{3297} - 290688\,b_{2,0}{}^2\sqrt[3]{t} - 1248\,b_{2,0}{}^2\sqrt{3297}\sqrt[3]{t} + 8085264\,b_{2,0}{}^2\right)}{t^{2/3}}\,y^2 x^2 \\
&\quad + b_{2,0}x^2 - \frac{1}{10647}\,\frac{b_{2,0}\left(-53144\,b_{2,0}\sqrt[3]{t} + 2080988\,b_{2,0} + 42588\,b_{2,0}\sqrt{3297} - 5824\,b_{2,0}t^{2/3}\right)}{t^{2/3}}\,x^3 \\
&\quad - \frac{1}{10647}\,\frac{b_{2,0}\left(-2150\,b_{2,0}{}^2 t^{2/3} - 11926\,b_{2,0}{}^2\sqrt[3]{t} + 234\,b_{2,0}{}^2\sqrt{3297}\sqrt[3]{t} + 1085248\,b_{2,0}{}^2 + 18720\,b_{2,0}{}^2\sqrt{3297}\right)}{t^{2/3}}\,x^4
\end{aligned}\right\}$$

where $t = 22868 + 468\sqrt{3297}$

The necessary conditions of the isochronicity of the center at the origin for system (2.23) are the seven cases given in the theorem and can are obtained using C-algorithm. One easily checks that the obtained necessary conditions are also sufficient by direct application of Corollary A to the cases IV-VII. Indeed, in all those four cases $g'(x) + f(x)g(x) = 1$.

The centers $I - III$ of Theorem 2 have been already identified in [55].

2.5   Non homogeneous perturbation of degree five with zero Urabe function

By Corollary A the problem is reduced to solve the equation $g'(x) + f(x)g(x) = 1$, with f and g defined in Appendix, Sec.7.1 with respect to the system (2.14). In this case the equation $g'(x) + f(x)g(x) = 1$ is equivalent to some system of 8 polynomials depending on 12 unknown $\{a_{ij}\}$ and $\{b_{sr}\}$ of degree $2, 2, 2, 1, 2, 2, 2, 2$. Applying the

Gröbner basis method one obtain a basis of 90 polynomials whose degrees varies between 1 and 8. This system is too hard to handle. Inspecting the system under consideration one sees that when $b_{50} = 0$ a great simplification of the system appears. This is the reason of our choice $b_{50} = 0$.

Theorem 7. *The system* (2.14) *where* $b_{50} = 0$ *has an isochronous center at the origin* O *with zero Urabe function only in one of the following eight cases, where one suppose that all denominators are non zero polynomials.*

$\boxed{22I}$

$$\left.\begin{aligned}
\dot{x} &= -y + a_{11}xy + b_{12}x^2y + a_{31}x^3y + b_{32}x^4y \\
\dot{y} &= x + a_{11}y^2 + b_{12}xy^2 + a_{31}x^2y^2 + b_{32}x^3y^2
\end{aligned}\right\}$$

$\boxed{II}$

$$\left.\begin{aligned}
\dot{x} &= -y + a_{11}xy + a_{31}x^3y - 3/4\, a_{11}a_{31}x^4y \\
\dot{y} &= x + a_{11}y^2 + 4\, a_{31}x^2y^2 - 3/4\, x^4a_{31} - 3\, a_{11}a_{31}x^3y^2
\end{aligned}\right\}$$

$\boxed{III}$

$$\left.\begin{aligned}
\dot{x} &= -y + \tfrac{a_{31}}{b_{30}}xy + \left(3\, b_{30} + b_{12}\right)x^2y + a_{31}x^3y + \left(9/2\, b_{30}{}^2 + b_{12}b_{30}\right)x^4y \\
\dot{y} &= x + \tfrac{a_{31}}{b_{30}}y^2 + b_{30}x^3 + b_{12}xy^2 + 3\, a_{31}x^2y^2 + \left(\tfrac{27}{2}\, b_{30}{}^2 + 3\, b_{12}b_{30}\right)x^3y^2
\end{aligned}\right\}$$

$\boxed{IV}$

$$\left.\begin{aligned}
\dot{x} &= -y + a_{11}xy + \left(b_{12} - 2\, b_{20}{}^2 - a_{11}b_{20}\right)x^2y + a_{31}x^3y + \\
&\quad \left(-b_{12}b_{20}{}^2 + 4\, b_{20}{}^4 + 2\, a_{11}b_{20}{}^3 + a_{31}b_{20}\right)x^4y \\[2mm]
\dot{y} &= x + b_{20}x^2 + \left(-2\, b_{20} + a_{11}\right)y^2 + b_{12}xy^2 + \left(b_{12}b_{20} - 4\, b_{20}{}^3 - 2\, a_{11}b_{20}{}^2 + a_{31}\right)x^2y^2 \\
&\quad + \left(-2\, b_{12}b_{20}{}^2 + 8\, b_{20}{}^4 + 4\, a_{11}b_{20}{}^3 + 2\, a_{31}b_{20}\right)x^3y^2
\end{aligned}\right\}$$

$\boxed{V}$

$$\left.\begin{aligned}
\dot{x} &= -y + a_{11}xy + a_{31}x^3y \\
&\quad - \frac{\left(13\, b_{30}{}^2b_{20} - 11\, b_{30}b_{20}{}^3 - 5\, b_{30}a_{11}b_{20}{}^2 + 2\, b_{20}{}^5 + a_{11}b_{20}{}^4 + a_{31}b_{20}{}^2 - 4\, a_{31}b_{30} + 4\, a_{11}b_{30}{}^2\right)}{b_{20}\left(4\, b_{30} - b_{20}{}^2\right)}x^2y \\
&\quad - \frac{b_{30}\left(-b_{30}a_{11}b_{20}{}^2 + 7\, b_{30}{}^2b_{20} - 2\, b_{30}b_{20}{}^3 - 4\, a_{31}b_{30} + 4\, a_{11}b_{30}{}^2 + a_{31}b_{20}{}^2\right)}{b_{20}\left(4\, b_{30} - b_{20}{}^2\right)}x^4y \\[3mm]
\dot{y} &= x + b_{20}x^2 + \left(-2\, b_{20} + a_{11}\right)y^2 + b_{30}x^3 \\
&\quad - \frac{\left(25\, b_{30}{}^2b_{20} - 22\, b_{30}b_{20}{}^3 - 9\, b_{30}a_{11}b_{20}{}^2 + 4\, b_{20}{}^5 + 2\, a_{11}b_{20}{}^4 + a_{31}b_{20}{}^2 - 4\, a_{31}b_{30} + 4\, a_{11}b_{30}{}^2\right)}{b_{20}\left(4\, b_{30} - b_{20}{}^2\right)}xy^2 \\
&\quad + \frac{\left(7\, b_{30}{}^2b_{20} - 2\, b_{30}b_{20}{}^3 - b_{30}a_{11}b_{20}{}^2 - 2\, a_{31}b_{20}{}^2 + 8\, a_{31}b_{30} + 4\, a_{11}b_{30}{}^2\right)}{4\, b_{30} - b_{20}{}^2}x^2y^2 \\
&\quad - 3\, \frac{b_{30}\left(-b_{30}a_{11}b_{20}{}^2 + 7\, b_{30}{}^2b_{20} - 2\, b_{30}b_{20}{}^3 - 4\, a_{31}b_{30} + 4\, a_{11}b_{30}{}^2 + a_{31}b_{20}{}^2\right)}{b_{20}\left(4\, b_{30} - b_{20}{}^2\right)}x^3y^2
\end{aligned}\right\}$$

$\boxed{VI}$

$$
\begin{aligned}
\dot{x} &= -y + \frac{\left(108\,b_{40}{}^2 - 42\,b_{40}b_{20}{}^3 + 81\,a_{31}b_{40} + b_{20}{}^6 - 3\,b_{20}{}^3 a_{31}\right)}{b_{20}{}^2\left(-b_{20}{}^3 + 27\,b_{40}\right)}\,xy \\
&\quad + 3\,\frac{\left(-3\,b_{40}b_{20}{}^3 - b_{20}{}^3 a_{31} + 27\,a_{31}b_{40} + 36\,b_{40}{}^2\right)}{b_{20}\left(-b_{20}{}^3 + 27\,b_{40}\right)}\,x^2 y + a_{31}x^3 y \\
&\quad + 3\,\frac{b_{40}\left(-b_{20}{}^3 a_{31} + 36\,b_{40}{}^2 + 27\,a_{31}b_{40}\right)}{b_{20}{}^2\left(-b_{20}{}^3 + 27\,b_{40}\right)}\,x^4 y \\[2mm]
\dot{y} &= x + b_{20}x^2 + 3\,\frac{\left(b_{20}{}^6 - 32\,b_{40}b_{20}{}^3 + 36\,b_{40}{}^2 + 27\,a_{31}b_{40} - b_{20}{}^3 a_{31}\right)}{b_{20}{}^2\left(-b_{20}{}^3 + 27\,b_{40}\right)}\,y^2 \\
&\quad + 1/3\,b_{20}{}^2 x^3 + 6\,\frac{\left(-4\,b_{40}b_{20}{}^3 - b_{20}{}^3 a_{31} + 27\,a_{31}b_{40} + 36\,b_{40}{}^2\right)}{b_{20}\left(-b_{20}{}^3 + 27\,b_{40}\right)}\,xy^2 \\
&\quad - 3\,\frac{\left(b_{20}{}^3 a_{31} - 27\,a_{31}b_{40} + 12\,b_{40}{}^2\right)}{-b_{20}{}^3 + 27\,b_{40}}\,x^2 y^2 \\
&\quad + b_{40}x^4 + 12\,\frac{b_{40}\left(-b_{20}{}^3 a_{31} + 36\,b_{40}{}^2 + 27\,a_{31}b_{40}\right)}{b_{20}{}^2\left(-b_{20}{}^3 + 27\,b_{40}\right)}\,x^3 y^2
\end{aligned}
\Biggr\}
$$

$\boxed{VII}$

$$
\begin{aligned}
\dot{x} &= -y + a_{11}xy - 3\,\frac{b_{30}\left(13\,b_{40}{}^2 + 2\,b_{30}{}^3\right)}{27\,b_{40}{}^2 + 4\,b_{30}{}^3}\,x^2 y \\
&\quad - \frac{\left(5\,b_{30}{}^3 b_{40} + 36\,b_{40}{}^3 - 27\,a_{11}b_{30}b_{40}{}^2 - 4\,a_{11}b_{30}{}^4\right)}{27\,b_{40}{}^2 + 4\,b_{30}{}^3}\,x^3 y \\
&\quad + \frac{b_{40}\left(b_{40}b_{30}{}^2 + 27\,a_{11}b_{40}{}^2 + 4\,a_{11}b_{30}{}^3\right)}{27\,b_{40}{}^2 + 4\,b_{30}{}^3}\,x^4 y \\[2mm]
\dot{y} &= x + a_{11}y^2 + b_{30}x^3 - 6\,\frac{b_{30}\left(3\,b_{30}{}^3 + 20\,b_{40}{}^2\right)}{27\,b_{40}{}^2 + 4\,b_{30}{}^3}\,xy^2 \\
&\quad - 3\,\frac{\left(-27\,a_{11}b_{30}b_{40}{}^2 - 4\,a_{11}b_{30}{}^4 + 7\,b_{30}{}^3 b_{40} + 48\,b_{40}{}^3\right)}{27\,b_{40}{}^2 + 4\,b_{30}{}^3}\,x^2 y^2 \\
&\quad + b_{40}x^4 + 4\,\frac{b_{40}\left(b_{40}b_{30}{}^2 + 27\,a_{11}b_{40}{}^2 + 4\,a_{11}b_{30}{}^3\right)}{27\,b_{40}{}^2 + 4\,b_{30}{}^3}\,x^3 y^2
\end{aligned}
\Biggr\}
$$

$\boxed{VIII}$

$$
\left.
\begin{aligned}
\dot{x} &= -y + a_{11}yx + a_{21}yx^2 + a_{31}yx^3 + a_{41}yx^4 \\
\dot{y} &= x + b_{20}x^2 + b_{30}x^3 + b_{02}y^2 + b_{12}xy^2 + b_{22}x^2 y^2 + b_{32}x^3 y^2 + b_{40}x^4 + b_{50}x^5
\end{aligned}
\right\}
$$
$$(2.24)$$

where

$$
a_{31} = \frac{P_{31}}{Q},\ a_{21} = \frac{b_{20}P_{21}}{Q},\ a_{41} = \frac{P_{41}}{Q},\ b_{32} = \frac{P_{32}}{Q},\ b_{02} = \frac{P_{02}}{Q},\ a_{11} = \frac{P_{11}}{Q},\ b_{22} = \frac{P_{22}}{Q}
$$

such that

$$
\begin{aligned}
P_{31} ={}& 9\,b_{30}{}^5 + 2\,b_{30}{}^4 b_{12} - 3\,b_{30}{}^4 b_{20}{}^2 - 46\,b_{40}b_{20}b_{30}{}^3 - 1/2\,b_{30}{}^3 b_{12}b_{20}{}^2 \\
&+ 14\,b_{30}{}^2 b_{20}{}^3 b_{40} - 9\,b_{30}{}^2 b_{40}b_{12}b_{20} + 60\,b_{30}{}^2 b_{40}{}^2 + 2\,b_{30}b_{40}b_{12}b_{20}{}^3 \\
&+ \tfrac{27}{2}\,b_{30}b_{12}b_{40}{}^2 + 20\,b_{30}b_{20}{}^2 b_{40}{}^2 - 36\,b_{40}{}^3 b_{20} - 8\,b_{20}{}^4 b_{40}{}^2
\end{aligned}
$$

$$
\begin{aligned}
P_{21} ={}& -13\,b_{40}b_{30}{}^2 b_{20} + 2\,b_{40}b_{12}b_{20}{}^3 - 9\,b_{40}b_{30}b_{12}b_{20} + 3\,b_{30}{}^4 - 4\,b_{40}{}^2 b_{20}{}^2 \\
&+ \tfrac{27}{2}\,b_{12}b_{40}{}^2 + 21\,b_{40}{}^2 b_{30} - b_{30}{}^3 b_{20}{}^2 - 1/2\,b_{30}{}^2 b_{20}{}^2 b_{12} + 4\,b_{40}b_{30}b_{20}{}^3 + 2\,b_{12}b_{30}{}^3
\end{aligned}
$$

$$
\begin{aligned}
P_{41} ={}& \tfrac{27}{2}\,b_{12}b_{40}{}^3 + 60\,b_{40}{}^3 b_{30} + 2\,b_{40}b_{12}b_{30}{}^3 + 12\,b_{40}{}^2 b_{30}b_{20}{}^3 - 8\,b_{40}{}^3 b_{20}{}^2 \\
&- 1/2\,b_{40}b_{30}{}^2 b_{20}{}^2 b_{12} - 9\,b_{40}{}^2 b_{30}b_{12}b_{20} + 9\,b_{40}b_{30}{}^4 + 2\,b_{40}{}^2 b_{12}b_{20}{}^3 - 3\,b_{40}b_{30}{}^3 b_{20}{}^2 \\
&- 40\,b_{40}{}^2 b_{30}{}^2 b_{20}
\end{aligned}
$$

$$
\begin{aligned}
P_{32} ={}& 54\,b_{12}b_{40}{}^3 + 240\,b_{40}{}^3 b_{30} + 8\,b_{40}b_{12}b_{30}{}^3 + 48\,b_{40}{}^2 b_{30}b_{20}{}^3 - 32\,b_{40}{}^3 b_{20}{}^2 \\
&- 2\,b_{40}b_{30}{}^2 b_{20}{}^2 b_{12} - 36\,b_{40}{}^2 b_{30}b_{12}b_{20} + 36\,b_{40}b_{30}{}^4 + 8\,b_{40}{}^2 b_{12}b_{20}{}^3 \\
&- 12\,b_{40}b_{30}{}^3 b_{20}{}^2 - 160\,b_{40}{}^2 b_{30}{}^2 b_{20}
\end{aligned}
$$

$$
\begin{aligned}
P_{20} ={}& -16\,b_{40}b_{20}{}^5 + 80\,b_{40}b_{30}b_{20}{}^3 - 104\,b_{40}{}^2 b_{20}{}^2 + 4\,b_{30}{}^2 b_{20}{}^4 - 18\,b_{30}{}^3 b_{20}{}^2 \\
&- 41\,b_{40}b_{30}{}^2 b_{20} + 2\,b_{40}b_{12}b_{20}{}^3 - 9\,b_{40}b_{30}b_{12}b_{20} + 9\,b_{30}{}^4 + \tfrac{27}{2}\,b_{12}b_{40}{}^2 \\
&+ 60\,b_{40}{}^2 b_{30} - 1/2\,b_{30}{}^2 b_{20}{}^2 b_{12} + 2\,b_{12}b_{30}{}^3
\end{aligned}
$$

$$
\begin{aligned}
P_{22} ={}& 180\,b_{30}{}^2 b_{40}{}^2 - 144\,b_{40}{}^3 b_{20} - 32\,b_{20}{}^4 b_{40}{}^2 + 6\,b_{30}b_{40}b_{12}b_{20}{}^3 + 27\,b_{30}{}^5 + 6\,b_{30}{}^4 b_{12} \\
&- 9\,b_{30}{}^4 b_{20}{}^2 + \tfrac{81}{2}\,b_{30}b_{12}b_{40}{}^2 - 144\,b_{40}b_{20}b_{30}{}^3 + 44\,b_{30}{}^2 b_{20}{}^3 b_{40} \\
&+ 88\,b_{30}b_{20}{}^2 b_{40}{}^2 - 27\,b_{30}{}^2 b_{40}b_{12}b_{20} - 3/2\,b_{30}{}^3 b_{12}b_{20}{}^2
\end{aligned}
$$

$$
\begin{aligned}
P_{11} ={}& -41\,b_{40}b_{30}{}^2 b_{20} + 2\,b_{40}b_{12}b_{20}{}^3 - 9\,b_{40}b_{30}b_{12}b_{20} + 9\,b_{30}{}^4 - 8\,b_{40}b_{20}{}^5 \\
&- 50\,b_{40}{}^2 b_{20}{}^2 + \tfrac{27}{2}\,b_{12}b_{40}{}^2 + 60\,b_{40}{}^2 b_{30} - 10\,b_{30}{}^3 b_{20}{}^2 + 2\,b_{30}{}^2 b_{20}{}^4 \\
&- 1/2\,b_{30}{}^2 b_{20}{}^2 b_{12} + 44\,b_{40}b_{30}b_{20}{}^3 + 2\,b_{12}b_{30}{}^3
\end{aligned}
$$

$$
Q = 4\,b_{40}b_{20}{}^4 - 18\,b_{40}b_{30}b_{20}{}^2 + 27\,b_{40}{}^2 b_{20} - b_{30}{}^2 b_{20}{}^3 + 4\,b_{20}b_{30}{}^3
$$

2.6 Abel polynomial system

By planar Abel system of order n we understand the system

$$
\left.\begin{aligned}
\dot{x} &= -y \\
\dot{y} &= \sum_{k=0}^{n} P_k(x)y^k
\end{aligned}\right\}
\tag{2.25}
$$

where $\{P_k(x)\}_{0 \le k \le n}$ are smooth functions.

This section is concerned by the following Abel system

$$
\left.\begin{aligned}
\dot{x} &= -y \\
\dot{y} &= x(1 + P(y)),
\end{aligned}\right\}
\tag{2.26}
$$

with $P(y) = a_1y + a_2y^2 + a_3y^3 + ... + a_ny^n$, $a_k \in \mathbb{R}$, for $k = 0, \ldots, n$. This is a particular Abel system (2.25) where $P_k(x) := a_kx$, $0 \le k \le n$.

2.6.1 Characterization of isochronous centers

The system (2.36) is reducible (see Appendix, Sec. 7.1 case 2) to the Liénard type equation (2.3) with

$$\left. \begin{aligned} f(x) &= -\frac{P'(x)}{(1 + P(x))} \\ g(x) &= x(1 + P(x)) \end{aligned} \right\} \tag{2.27}$$

Definitions (2.6),(2.5) and Theorems B and C from Sec. 2.1 remains valid. Applied to the Abel system (2.36) they give :

Theorem 8. *The origin O is a center for the system* (2.36).

The center at O, is isochronous if and only if there exists an odd function h defined in some neighborhood of $0 \in \mathbb{R}$ which satisfies the following conditions

$$\frac{X}{1 + h(X)} = x,$$

$$\phi(x) = X(x) + \int_0^{X(x)} h(t)dt$$

and $X(x)\phi(x) > 0$ for $x \ne 0$.

In particular, when P is an even polynomial then the origin O is isochronous center if and only if $P = 0$.

The above result is obtained as follow. One has, $xg(x) = x^2(1 + P(x)) > 0$ for $x \ne 0$ and $|x|$ small enougth. Then the Theorem B implies that the origin O is a center of the system (2.36).

Now

$$F(x) = \int_0^x f(s)ds = -\ln(1 + P(x)),$$

thus

$$\phi(x) = \int_0^x e^{F(s)}ds = \int_0^x \frac{ds}{1 + P(s)} \tag{2.28}$$

Then we obtain

$$g(x)e^{F(x)} = x(1 + P(x))e^{-\ln(1+P(x))} = x$$

Following Theorem C, one obtain

$$\frac{X(x)}{1 + h(X(x))} = x$$

as well as the identity (2.9).

For the particular case when P is even, it is easy to see that f and g are odd. Theorem C thus implies $h = 0$ and consequently $X(x) = x$. From (2.9) one deduce that $\phi(x) = X$. Then (2.28) implies that $P \equiv 0$.

The following paragraph is devoted to illustrate the last theorem by example.

2.6.2 An application

Let us consider the Abel system (2.36) with $n = 9$:

$$\left.\begin{array}{l} \dot{x} = -y \\ \dot{y} = x + \displaystyle\sum_{i=1}^{9} a_i x y^i \end{array}\right\} \tag{2.29}$$

with $a_k \in \mathbb{R}$, $1 \le k \le 9$. As follows from Theorem 8, the origin O is always a center for (2.29).

Theorem 9. *Only in the case*

$$\left.\begin{array}{l} \dot{x} = -y \\ \dot{y} = x + axy + \dfrac{a^2}{3}xy^2 + \dfrac{a^3}{27}xy^3 \end{array}\right\} \tag{2.30}$$

where $a \in \mathbb{R}$

We apply C-algorithm for

$$f(x) = -\frac{P'(x)}{(1 + P(x))} \text{ and } g(x) = x(1 + P(x)),$$

where $P(x) = \sum_{i=1}^{9} a_i x^i$. We obtain the unique one-parameter family (2.30), and computations gives the Urabe function

$$h(X) = -\frac{a_1 X}{3} = \frac{k_1 X}{\sqrt{k_2^2 + k_3 X^2}}$$

with $k_1 = -a_1/3$, $k_2 = 1$, $k_3 = 0$.

By the evident rescalling $\frac{a}{3}x \mapsto x$ and $\frac{a}{3}y \mapsto y$ the system (2.30) take the form

$$\left.\begin{array}{l} \dot{x} = -y \\ \dot{y} = x(1 + y)^3. \end{array}\right\} \tag{2.31}$$

The isochronous center at the origin O for the system (2.31) was already depisted in [83] by showing that the system (2.31) commutes with some transversal polynomial system, but its first integral nor the linearizing change of coordinates was not provided. We will now compute both of them.

— **First integral** In the variables $u = y$ and $v = x(1 + y)^3$ the system (2.31) is reducible to the Liénard type equation $\ddot{u} + f(u)\dot{u}^2 + g(u) = 0$ where $f(u) = -\frac{3}{1+u}$ and $g(u) = u(1 + u)^3$. By formula (2.7) from Theorem B one easily obtain that $I(u, v) = \frac{u^2}{(1+u)^2} + \frac{v^2}{(1+u)^6}$ is a first integral of the corresponding planar system

$$\left.\begin{array}{l} \dot{u} = v \\ \dot{v} = -g(u) - f(u)v^2. \end{array}\right\}$$

Returning to the variables (x, y) one recover first integral of the system (2.31) :

$$I_{(2.31)}(x, y) = x^2 + \frac{y^2}{(1 + y)^2}.$$

— **Linearization** To this aim we use the method of [101] base on the exitence of vector field Y transversal to the vector field defined by the system (2.31) and commuting with it. *Maple* computations gives such field Y :

$$\left. \begin{aligned} \dot{x} &= x + xy \\ \dot{y} &= -x^2 y^3 + y^2 - 3\,y^2 x^2 + y - 3\,yx^2 - x^2 \end{aligned} \right\} \tag{2.32}$$

Following the method described in [101], we first establish an inverse integrating factor $V(x,y)$ of the system (2.31) :

$$V(x,y) = -\,(y+1)\left(x^2 + 2\,yx^2 + y^2 x^2 + y^2\right)$$

which leads to the first integrals H (already known) and I of the systems (2.31) and (2.32) respectively :

$$\left. \begin{aligned} H(x,y) &= x^2 + \frac{y^2}{(1+y)^2} \\ I(x,y) &= -x + \arctan\left(\frac{(y+1)\,x}{y}\right) \end{aligned} \right\}$$

Let us define $\tilde{f}(z) = z$ and $\tilde{g}(z) = tan(z)$.
By the Theorem 4 of [101] we obtain the linearizing change of coordinates

$$\left. \begin{aligned} u &= \frac{\sqrt{\tilde{f}(H(x,y))}\,\tilde{g}(I(x,y))}{\sqrt{1 + \tilde{g}^2(I(x,y))}} \\[2em] v &= \frac{\sqrt{\tilde{f}(H(x,y))}}{\sqrt{1 + \tilde{g}^2(I(x,y))}} \end{aligned} \right\}$$

Maple produce the following more explicit formulas that we reproduce without any change to avoid the misprints :

$$\left. \begin{aligned} u(x,y) &= \frac{-\sqrt{\frac{x^2 + 2\,yx^2 + y^2 x^2 + y^2}{(y+1)^2}}\,\tan\left(x - \arctan\left(\frac{(y+1)x}{y}\right)\right)}{\sqrt{1 + \left(\tan\left(x - \arctan\left(\frac{(y+1)x}{y}\right)\right)\right)^2}} \\[2em] v(x,y) &= \sqrt{\frac{x^2 + 2\,yx^2 + y^2 x^2 + y^2}{(y+1)^2}}\,\frac{1}{\sqrt{1 + \left(\tan\left(x - \arctan\left(\frac{(y+1)x}{y}\right)\right)\right)^2}}\,. \end{aligned} \right\} \tag{2.33}$$

The fact that this change of variables is really a linearizing one can be easily verified by *Maple* which gives $\dot{u} = -v$, $\dot{v} = u$ as expected.

In the light of Theorem 9, it is natural to ask if the system (2.30) is the unique system with isochronous center at the origin O inside the family (2.25).

Even for the system (2.25) whith $n = 10$, our actual computer possibilies are not sufficient to give an answer.

2.7 Appendix

2.7.1 Reduction to the Liénard type equation

At the present we know two cases when reduction of the system (2.1) to the Liénard type equation (2.3) is possible.

— Case 1 : When $-y + A(x,y) = -y\tilde{A}(x)$ and $x + B(x,y) = \tilde{B}(x) + \tilde{C}(x)y^2$ the system (2.1) can be written

$$\left.\begin{array}{l} \dot{x} = -y\tilde{A}(x) \\ \dot{y} = \tilde{B}(x) + \tilde{C}(x)y^2 \end{array}\right\} \tag{2.34}$$

By the change of coordinates $(u,v) := (x, -y\tilde{A}(x))$ we obtain

$$\left.\begin{array}{l} \dot{u} = v \\ \dot{v} = -\tilde{A}(u)\tilde{B}(u) + \dfrac{(\tilde{A}'(u) - \tilde{C}(u))}{\tilde{A}(u)}v^2 \end{array}\right\}. \tag{2.35}$$

In this way we obtain the reduction to the system (2.3) with $g(x) = \tilde{A}(x)\tilde{B}(x)$ and $f(x) = -\frac{(\tilde{A}'(x) - \tilde{C}(x))}{\tilde{A}(x)}$.

— Case 2 : When $A(x,y) = 0$ and $B(x,y) = xP(y)$ where $P(0) = 0$. In this case the system (2.1) can be written

$$\left.\begin{array}{l} \dot{x} = -y \\ \dot{y} = x(1 + P(y)) \end{array}\right\}. \tag{2.36}$$

By the change of coordinates $(u,v) := (y, x(1 + P(y)))$ we obtain

$$\left.\begin{array}{l} \dot{u} = v \\ \dot{v} = -u(1 + P(u)) + v^2\dfrac{P'(u)}{1 + P(u)} \end{array}\right\}$$

We obtain the system (2.3) with $f(x) = -\frac{P'(x)}{1+P(x)}$ and $g(x) = x(1 + P(x))$.

In both cases the determinant of the Jacobian matrix of coordinate change does not vanish at $(0,0)$. Thus the nature of singular point O is the same for system (2.1) and (2.4).

2.7.2 C-Algorithm

Theorem C from Section 1 leads to an algorithm, first introduced in [62] (see also[63]), in what follow called C-algorithm, which allows to obtain necessary conditions for isochronicity of the center at the origin O for equation (2.3).

Below we recall basic steps of the algorithm.

Let h be the Urabe function defined in the Theorem C, and $u = \phi(x)$. We assume that function ϕ is invertible near the origin O .

$$\tilde{g}(u) := \frac{X}{1 + h(X)}, \tag{2.37}$$

where now X is considered as a function of u. Our further assumption is that functions $f(x)$ and $g(x)$ depend polynomially on certain numbers of parameters $\alpha := (\alpha_1, \ldots, \alpha_p) \in \mathbb{R}^p$.

By Theorem C, if the system (2.3) has isochronous center at the origin O, then the Urabe function h must be odd, so we have

$$h(X) = \sum_{k=0}^{\infty} c_{2k+1} X^{2k+1}, \tag{2.38}$$

and moreover,

$$\tilde{g}(u) = g(x)e^{F(x)}, \quad \text{where} \quad x = \phi^{-1}(u). \tag{2.39}$$

Hence, the right hand sides of (2.37) and (2.39) must be equal. Hence, we expand the both right hand sides into the Taylor series around the origin O and equate the corresponding coefficients. To this end we need to calculate k-th derivatives of (2.37) and (2.39).

For (2.37), by straightforward differentiation, we have

$$\frac{d^k \tilde{g}(u)}{du^k} = \frac{d}{dX}\left(\frac{d^{k-1}\tilde{g}(u)}{du^{k-1}}\right)\frac{dX}{du} \tag{2.40}$$

Using induction, one can show that for (2.39) we obtain

$$\frac{d^k \tilde{g}(u)}{du^k} = e^{(1-k)F(x)}S_k(x), \tag{2.41}$$

where $S_k(x)$ is a function of $f(x), g(x)$ and their derivatives.

Therefore to compute the first m conditions for isochronicity of system (2.3) we proceed as follows.

1. We fix m and write

$$h(X) = \sum_{k=1}^{m} c_{2k-1} X^{2k-1} + O(X^{2m}), \quad c := (c_1, c_3, \ldots, c_{2m-1}).$$

2. Next, we compute

$$v_k := \frac{d^k \tilde{g}}{du^k}(0), \quad w_k = S_k(0)$$

for $k = 1, \ldots, 2m+1$. Note that those quantities are polynomials in α and c.

3. By the Theorem C we obtain the equations $v_k = w_k$ for $k = 1, \ldots, 2m+1$. Let us note that always $v_1 = w_1 = 1$ and thus the first equation is meaningless. It appears that we can always eliminate parameters c from these equations. For every $k \geq 0$, c_{2k+1} appear for the first time, and in a linear way, in the equation $w_{2k+2} = w_{2k+2}$. This allows to the formula $c_{2k+1} = \varphi_{2k+1}(\alpha)$ for some multivariate polynomial φ_{2k+1}. This leads in natural way to the consecutive elimination of $c_1, c_3, \ldots, c_{2m-1}$. Finally, we obtain at most m polynomial equations $s_1 = s_2 = s_3 = \ldots = s_M = 0$ with p unknows α_i. These equations gives M necessary conditions for isochronicity of system (2.3).

For more details see [62, 63].

2.7.3 The choice of an appropriate Gröbner basis

Let us consider the following system

$$\left.\begin{array}{rl} \dot{x} & = -y + a_{11}yx + \ldots + a_{n-1,1}yx^{n-1} \\ \dot{y} & = x + b_{20}x^2 + b_{02}y^2 + \ldots + b_{n-2,2}x^{n-2}y^2 + b_{n,0}x^n \end{array}\right\} \qquad (2.42)$$

which is reducible to the equation (2.3) with

$$f(x) = \frac{b_{02} + a_{11} + \ldots + (b_{n-2,2} + (n-1)a_{n-1,1})x^{n-2}}{1 - a_{11}x - \ldots - a_{n-1,1}x^{n-1}}, \qquad (2.43)$$

$$g(x) = (x + b_{20}x^2 + \ldots + b_{n,0}x^n)(1 - a_{11}x - \ldots - a_{n-1,1}x^{n-1}). \qquad (2.44)$$

In this chapter we have investigated the two types of high degree polynomial perturbations, homogeneous and non-homogeneous ones. It seems that C-algorithm is efficient for computing isochronicity necessary conditions for higher degree homogeneous perturbations. In this case system (2.42) reduces to the following one

$$\left.\begin{array}{rl} \dot{x} & = -y + a_{k-1,1}yx^{k-1} \\ \dot{y} & = x + b_{k-2,2}x^{k-2}y^2 + b_{k,0}x^k \end{array}\right\} \qquad (2.45)$$

where $k \in \{2, \ldots, n\}$.

For this homogeneous polynomial perturbation of the linear center, C-algorithm generate homogeneous polynomial equations in the parameters $b_{k-2,2}, b_{k,0}$ and $a_{k-1,1}$. Solving these polynomials, gives all the parameters values for which the real polynomial differential system (2.45) is isochronous at the origin O.

However, for the non-homogeneous perturbation case, C-algorithm generate non-homogeneous polynomial system. Moreover, non-homogeneous perturbations depend on a bigger number of parameters.

We note that for $n = 3$, C-algorithm succeeds to establish isochronicity criteria, however for $n = 4$ the obtained polynomials from the algorithm are much more involved. For example, for the system (2.42) with $n = 4$ reduces to

$$\left.\begin{array}{l} \dot{x} = -y + a_{11}yx + a_{21}yx^2 + a_{31}yx^3 \\ \dot{y} = x + b_{20}x^2 + b_{30}x^3 + b_{02}y^2 + b_{12}xy^2 + b_{22}x^2y^2 + b_{40}x^4 \end{array}\right\}$$

its associated first two non-zero polynomials obtained by applying C-algorithm are the followings

$$P_2 = 3\,a_{21} - 3\,b_{12} + a_{11}{}^2 - b_{20}a_{11} - 9\,b_{30} + 4\,b_{02}{}^2 - 5\,a_{11}b_{02} + 10\,b_{20}{}^2 + 10\,b_{20}b_{02}, \quad (2.46)$$

$$\begin{aligned}
P_3 = {}& 72\,a_{21}{}^2 + 396\,b_{20}a_{11}b_{12} + 90\,a_{11}b_{02}b_{12} + 36\,a_{11}b_{22} + 324\,a_{31}b_{02} \\
& - 36\,a_{21}b_{12} - 468\,b_{20}a_{11}a_{21} + 612\,b_{20}a_{21}b_{02} - 4116\,a_{11}b_{20}{}^2b_{02} \\
& + 108\,b_{20}a_{31} - 540\,b_{30}a_{21} - 324\,b_{40}a_{11} + 1566\,b_{30}a_{11}b_{02} - 288\,b_{20}b_{22} \\
& - 459\,b_{30}a_{11}{}^2 - 1296\,b_{40}b_{02} - 306\,a_{21}a_{11}b_{02} + 1428\,b_{20}a_{11}{}^2b_{02} \\
& + 153\,a_{21}a_{11}{}^2 - 117\,a_{11}{}^2b_{12} - 191\,b_{20}a_{11}{}^3 + 180\,b_{20}b_{02}b_{12} + 43\,a_{11}{}^4 \\
& - 2319\,b_{20}a_{11}b_{02}{}^2 - 289\,a_{11}{}^3b_{02} - 360\,b_{02}b_{22} - 36\,b_{12}{}^2 - 171\,a_{21}b_{02}{}^2 \\
& + 513\,b_{30}b_{02}{}^2 + 537\,a_{11}{}^2b_{02}{}^2 + 351\,b_{02}{}^2b_{12} - 271\,a_{11}b_{02}{}^3 + 542\,b_{20}b_{02}{}^3 \\
& + 756\,b_{20}b_{30}b_{02} + 2268\,b_{20}b_{30}a_{11} - 20\,b_{02}{}^4 + 1120\,b_{20}{}^4 + 798\,a_{11}{}^2b_{20}{}^2 \\
& - 2240\,a_{11}b_{20}{}^3 - 1512\,b_{20}b_{40} + 1008\,b_{20}{}^2a_{21} - 252\,b_{20}{}^2b_{12} \\
& + 1806\,b_{20}{}^2b_{02}{}^2 + 2240\,b_{20}{}^3b_{02}
\end{aligned}$$

To solve the first nine non-zero obtained polynomials requests high performance computer and the standard accessible computer algebra systems for solving polynomial equations are not able to find a solution.

For solving polynomial equations the Gröbner bases are used. It is well known, see [19], that the form and the size of the Göbner basis of a polynomial ideal depends strongly on a choice of monomial ordering. A bad choice of the monomial ordering can be a main reason why the Gröbner basis cannot be practically determined.

Our basic observation concerning algebraic structure of polynomial equations which give necessary conditions for the isochronicity in a case of non-homogeneous perturbations is the following. Although the polynomials are not homogeneous, a careful analysis shows that they are quasi-homogeneous. In fact, one can notice that polynomial P_2 given by (2.46) is homogeneous if we give weight 2 for a_{21}, b_{12} and b_{30}, and weight 1 for the remaining variables. More importantly we can find such a choice of weights for which all the obtained polynomials are homogeneous.

The above observation shows that our main problem, i.e., finding a Gröbner basis, concerns as a matter of fact, finding a Gröbner basis of a homogeneous ideal. It is well know, see [19, p. 466], that homogeneous Gröbner bases have many 'nice' properties which make them extremely useful for solving large and computationally demanding problems.

In fact, for non-homogeneous case of (2.42), the use of weighted degree gives a homogeneous Gröbner base.

To incorporate our observation into the C-algorithm we choose a new parametrization for the problem. First, we observe that all polynomials which are obtained by means of the C-algorithm are homogeneous if we choose the following weights

1. $i + j - 1$ for parameters a_{ij} and b_{ij}

2. $2i + 1$ for c_{2i+1}.

Knowing this we introduced new parameters A_{ij}, B_{ij}, and C_{2i+1} putting

$$A_{ij}^{i+j-1} = a_{ij} \quad B_{ij}^{i+j-1} = b_{ij}, \quad C_{2i+1}^{2i+1} = c_{2i+1} \tag{2.47}$$

After this reparametrization system (2.42) reads

$$\left.\begin{array}{l} \dot{x} = -y + A_{11}yx + \ldots + A_{n-1,1}^{n-1}yx^{n-1} \\ \dot{y} = x + B_{20}x^2 + B_{02}y^2 + \ldots + B_{n-2,2}^{n-1}x^{n-2}y^2 + B_{n,0}^{n-1}x^n \end{array}\right\} \tag{2.48}$$

As in the case of isochronous center the Urabe function is odd, we search it under the form

$$h(X) = \sum_{k=0}^{\infty} C_{2k+1}^{2k+1} X^{2k+1} = C_1 X + C_3^3 X^3 + C_5^5 X^5 + C_7^7 X^7 + \ldots \tag{2.49}$$

We emphasize that from the isochronicity conditions for (2.48), expressed in terms of its parameters, it is easy to reconstruct the parameters values for which the system (2.42) admits isochronous center at the origin O, by a simply use of (2.47).

The described reparametrization gives rise to homogeneous equations and allows to reduce the number of the parameters appearing in (2.48) by one. First, we assume $B_{20} = 0$, and then solve the isochronicity problem for system (2.48) under this assumption. Next, for $B_{20} \neq 0$, we apply on (2.48) the following change of coordinates

$$(x, y) \mapsto \frac{1}{B_{20}}(x, y) \tag{2.50}$$

We obtain

$$\left.\begin{array}{l} \dot{x} = -y + \left(\frac{A_{11}}{B_{20}}\right)xy + .. + \left(\frac{B_{n-1,1}}{B_{20}}\right)^{n-1}yx^{n-1} \\ \\ \dot{y} = x + x^2 + \left(\frac{B_{02}}{B_{20}}\right)y^2 + .. + \left(\frac{B_{n-2,2}}{B_{2,0}}\right)^{n-1}x^{n-2}y^2 + \left(\frac{B_{n,0}}{B_{20}}\right)^{n-1}x^n \end{array}\right\} \tag{2.51}$$

Hence, without loss of generality we can put $B_{20} = 1$, and find the parameters values for which the center is isochronous.

We note that for an arbitrary $k \in \mathbb{N}$, the problem of the isochonicity of the center for homogeneous perturbations of the form (2.45) reduces to solve a number of polynomial equations with 3 parameters.

Recall that linear center perturbed by homogeneous polynomial, was investigated by W.S. Loud in [140] for the quadratic case, and in [62] Loud results are recovered by the described algorithm, see also [60].

Homogeneous perturbations was also studied by Chavarriga and coworkers. For the fourth and fifth degree homogeneous perturbations, see [50, 51], where the homogeneous perturbations different from those studied in the present chapter are considered.

Note that the polynomials issued from the 19 derivations and associated eliminations for the system (2.13) (with 9 parameters), exceed the authorized memory of ordinary computers (2 Go of Random Access Memory) in computations of the Gröbner basis by the known efficient implementation FGb [93].

Generating linearizable centers for Liénard-type planar systems

In this chapter we explore a wider class of systems reducible to Liénard-type equations, which extends the approach presented in Chapter 2. Furthermore, we establish an explicit formula for linearizing such a class of systems having a constant Urabe function. The proofs of the results given in this chapter can be found in [15]. In this chapter, we study the isochronicity conditions for the center at the origin $O \in \mathbb{R}^2$ for systems

$$\dot{x} = -y + A(x,y), \ \dot{y} = x + B(x,y),$$

where $A, \ B \in \mathbb{R}[x,y]$, which can be reduced to the Liénard-type equation. When $deg(A) \leq 4$ and $deg(B) \leq 4$, the so-called C-algorithm produced 36 new multi-parameter families of isochronous centers. For a large class of isochronous centers we provide an explicit general formula for linearization. This chapter is a direct continuation of the previous one, but it can be read independently.

3.1 Introduction

Let us consider the system of real differential equations of the form

$$\frac{dx}{dt} = \dot{x} = -y + A(x,y), \qquad \frac{dy}{dt} = \dot{y} = x + B(x,y), \tag{3.1}$$

where (x,y) belongs to an open connected subset $U \subset \mathbb{R}^2$ containing the origin $O = (0,0)$, with $A, B \in C^1(U, \mathbb{R})$ such that A and B as well as their first partial derivatives vanish at O. An isolated singular point $p \in U$ of system (3.1) is a *center* if there exists a punctured neighborhood $V \subset U$ of p such that every orbit of (3.1) lying in V is a closed orbit surrounding p. A center p is *isochronous* if the period is constant for all closed orbits in some neighborhood of p.

The simplest example is the linear system with an isochronous center at the origin O :

$$\dot{x} = -y, \ \dot{y} = x. \tag{3.2}$$

The problem of characterization of couples (A, B) such that O is an isochronous center (even for a center) for the system (3.1) is largely open.

The well known Poincaré Theorem asserts that when A and B are real analytic, a center of (3.1) at the origin O is isochronous if and only if in some real analytic

coordinate system it takes the form of the linear center (3.2) (see for example [7], Th.13.1, and [188], Th.4.2.1).

An overview [52] presents the basic results concerning the problem of the isochronicity, see also [7, 60, 188]. As this chapter is a direct continuation of [30], we refer the reader to it for general introduction to the subject. Here we will recall only the strictly necessary facts.

In some circumstances system (3.1) can be reduced to *the Liénard-type equation*

$$\ddot{x} + f(x)\dot{x}^2 + g(x) = 0 \tag{3.3}$$

with $f, g \in C^1(J, \mathbb{R})$, where J is some neighborhood of $0 \in \mathbb{R}$ and $g(0) = 0$. In this case, system (3.1) is called *reducible*. Equation (3.3) is associated to the equivalent, two dimensional, Liénard-type system

$$\left.\begin{aligned} \dot{x} &= y \\ \dot{y} &= -g(x) - f(x)y^2 \end{aligned}\right\}. \tag{3.4}$$

For reducible systems considered in this chapter, the nature (center and isochronicity) of the singular point O for both systems (3.1) and (3.4) is the same.

Let us return now to the Liénard-type equation (3.3). Let us define the following functions

$$F(x) := \int_0^x f(s)ds, \quad \phi(x) := \int_0^x e^{F(s)}ds. \tag{3.5}$$

The first integral of the system (3.4) is given by the formula ([194], Th.1)

$$I(x, \dot{x}) = \frac{1}{2}(\dot{x}e^{F(x)})^2 + \int_0^x g(s)e^{2F(s)}ds. \tag{3.6}$$

When $xg(x) > 0$ for $x \neq 0$, define the function X by

$$\frac{1}{2}\xi(x)^2 = \int_0^x g(s)e^{2F(s)}ds \tag{3.7}$$

and $x\xi(x) > 0$ for $x \neq 0$.

Theorem 10 ([194], Theorem 2)**.** *Let $f, g \in C^1(J, \mathbb{R})$. If $xg(x) > 0$ for $x \neq 0$, then the system (3.4) has a center at the origin O. When f and g are real analytic, this condition is also necessary.*

Theorem 11 ([62], Theorem 2.1)**.** *Let f and g be real analytic functions defined in a neighborhood J of $0 \in \mathbb{R}$, and let $xg(x) > 0$ for $x \neq 0$. Then system (3.4) has an isochronous center at O if and only if there exists an odd function $h \in C^1(J, \mathbb{R})$ which satisfies the following conditions*

$$\frac{\xi(x)}{1 + h(\xi(x))} = g(x)e^{F(x)}, \tag{3.8}$$

the function $\phi(x)$ satisfying

$$\phi(x) = \xi(x) + \int_0^{\xi(x)} h(t)dt, \tag{3.9}$$

and $\xi(x)\phi(x) > 0$ for $x \neq 0$.

In fact by (3.7), it is easy to see that (3.8) and (3.9) are equivalent. When those equivalent conditions are satisfied, then the function h is analytic in the neighborhood J. h is called the *Urabe function* of system (3.4), or of its equivalent (3.3).

Corollary 1 ([62], Corollary 2.4). *Let f and g be real analytic functions defined in a neighborhood of $0 \in \mathbb{R}$, and $xg(x) > 0$ for $x \neq 0$. The origin O is an isochronous center of system (3.4) with Urabe function $h = 0$ if and only if*

$$g'(x) + g(x)f(x) = 1 \tag{3.10}$$

for x in a neighborhood of 0.

In the sequel we shall call the Urabe function of the isochronous center of reducible system (3.1) the Urabe function of the corresponding Liénard-type equation.

In [62] the third author used Theorem 11 in order to build an algorithm (called C-Algorithm, see Appendix of [30] for more details) to look for isochronous centers at the origin for reducible system (3.1). He applied it to the case where A and B are polynomials of degree 3. This work was continued in [63] and in [30].

In this chapter we apply the so called *Rational C-Algorithm* introduced in [14] which is an adaptation of the C-Algorithm for the case of rational function f and g (see (3.3), (3.4)).

The aim of the present chapter is to extend these studies to the following real multiparameter family of polynomial system of differential equations :

$$\left.\begin{array}{l} \dot{x} = -y + a_{1,1}xy + a_{2,0}x^2 + a_{2,1}x^2y + a_{3,0}x^3 + a_{3,1}x^3y + a_{4,0}x^4 \\ \dot{y} = x + b_{0,2}y^2 + b_{1,1}xy + b_{2,0}x^2 + b_{1,2}xy^2 + b_{2,1}x^2y + b_{3,0}x^3 + b_{2,2}x^2y^2 + b_{3,1}x^3y + b_{4,0}x^4 \end{array}\right\}. \tag{3.11}$$

The reported results, which are obtained by Maple computations are reproduced without almost any change to avoid misprints.

The chapter is organized as follows. In Section 3.2 we report the necessary background and describe the investigated subfamilies of system (3.11). In Sections 3.3 and 3.4 we describe the obtained new isochronous centers. In total we provide 36 new families of isochronous centers. Among them two *Monsters* (3.57) and (3.58) of extreme complexity, never encountered before.

Let us stress that when describing the Urabe functions of the isochronous centers from Section 3.3, for the first time we encounter the *non-standard* examples of it. Indeed, up to now all identified Urabe functions was always of the form $h(\xi) = \frac{a\,\xi^{2n+1}}{\sqrt{b+c\,\xi^{4n+2}}}$ where a, b, $c \in \mathbb{R}$, $b > 0$ and n a non negative integer (see for instance[62, 30]).

Finally, in Section 3.5, when Urabe function $h = 0$, we describe the explicit general formula for linearizing change of coordinates whose existence is insured by the Poincaré theorem. We report also 5 examples of such linearization.

3.2 Preliminaries

3.2.1 Choudhury-Guha Reduction

Let us consider the real polynomial system

$$\left.\begin{array}{l} \dot{x} = p_0\left(x\right) + p_1\left(x\right) y \\ \dot{y} = q_0\left(x\right) + q_1\left(x\right) y + q_2\left(x\right) y^2 \end{array}\right\}, \tag{3.12}$$

where $p_0, p_1, q_0, q_1, q_2 \in \mathbb{R}[x]$.

We will always assume that $O = (0,0) \in \mathbb{R}^2$ is a singular point of (3.12), that is $p_0(0) = q_0(0) = 0$. Let us assume also that $p_1(0) \neq 0$.

Let us note that the system (3.11) is a particular case of (3.12) when

$$\left.\begin{array}{l} p_0\left(x\right) = a_{2,0}x^2 + a_{3,0}x^3 + a_{4,0}x^4 \\ p_1\left(x\right) = -1 + a_{1,1}x + a_{2,1}x^2 + a_{3,1}x^3 \\ q_0\left(x\right) = x + b_{2,0}x^2 + b_{3,0}x^3 + b_{4,0}x^4 \\ q_1\left(x\right) = b_{1,1}x + b_{2,1}x^2 + b_{3,1}x^3 \\ q_2\left(x\right) = b_{0,2} + b_{1,2}x + b_{2,2}x^2 \end{array}\right\}. \tag{3.13}$$

The following change of coordinates $x = x$, $z = p_0\left(x\right) + p_1\left(x\right) y$ transforms the system (3.12) to the system

$$\left.\begin{array}{l} \dot{x} = z \\ \dot{z} = \left(\dfrac{q_2\left(x\right)}{p_1\left(x\right)} + \dfrac{p_1'\left(x\right)}{p_1\left(x\right)}\right) z^2 + \left(-\dfrac{\left(p_1'\left(x\right)\right) p_0\left(x\right)}{p_1\left(x\right)} + q_1\left(x\right) + p_0'\left(x\right) - 2\dfrac{q_2\left(x\right) p_0\left(x\right)}{p_1\left(x\right)}\right) z \\ \quad + \dfrac{q_2\left(x\right) \left(p_0\left(x\right)\right)^2}{p_1\left(x\right)} - q_1\left(x\right) p_0\left(x\right) + p_1\left(x\right) q_0\left(x\right) \end{array}\right\}. \tag{3.14}$$

If

$$-\frac{\left(p_1'\left(x\right)\right) p_0\left(x\right)}{p_1\left(x\right)} + q_1\left(x\right) + p_0'\left(x\right) - 2\frac{q_2\left(x\right) p_0\left(x\right)}{p_1\left(x\right)} = 0, \tag{3.15}$$

the system (3.12) is of Liénard-type (3.4),

with

$$\left.\begin{array}{l} f(x) = -\left(\dfrac{q_2\left(x\right)}{p_1\left(x\right)} + \dfrac{p_1'\left(x\right)}{p_1\left(x\right)}\right) \\ g(x) = -\dfrac{q_2\left(x\right) \left(p_0\left(x\right)\right)^2}{p_1\left(x\right)} + q_1\left(x\right) p_0\left(x\right) - p_1\left(x\right) q_0\left(x\right) \end{array}\right\}. \tag{3.16}$$

To the best of our knowledge, the above reduction of the system (3.12) to Liénard-type system (3.4) was proposed for the first time in a preliminary and never published version of [59]. It is then natural to name it Choudhury-Guha reduction.

In all considered cases (see (3.13)) it is easy to see that for $|x|$ small enough $g(x) = x + x^2\, \tilde{g}(x)$ where $\tilde{g}$ is a real analytic function. Thus $x\, g(x) > 0$ for $x \neq 0$, $|x|$ small enough and Theorem 11 insures that the origin O is a center for the system (3.4). Our aim is to decide when this center is isochronous.

When p_0 and q_1 identically vanish, (3.15) is satisfied and we recover the *standard reduction* from [30] (see Case 1 from Sec. 1 of [30]). Many particular cases of system (3.11) where studied, using this standard reduction.

1. In [62] : $a_{1,1} = a_{2,0} = a_{3,0} = a_{3,1} = a_{4,0} = b_{2,2} = b_{4,0} = b_{3,1} = b_{2,1} = b_{1,1} = 0$. That means that $p_0(x) = q_1(x) = 0$, $p_1(x) = -1 + a_{2,1}x^2$ and $\deg(q_0(x)) \leq 3$, $\deg(q_2(x)) \leq 1$.

2. In [63] : $a_{2,0} = a_{3,0} = a_{3,1} = a_{4,0} = b_{2,2} = b_{4,0} = b_{3,1} = b_{2,1} = b_{1,1} = 0$. That means that $p_0(x) = q_1(x) = 0$ and we consider only cubic systems.

3. In [30] three families are studied :

   (a) $a_{2,0} = a_{3,0} = a_{4,0} = b_{3,1} = b_{2,1} = b_{1,1} = 0$ with zero Urabe function.

   (b) $a_{1,1} = b_{3,0} = a_{2,0} = a_{3,0} = a_{4,0} = b_{3,1} = b_{2,1} = b_{1,1} = 0$.

   (c) $a_{1,1} = a_{2,1} = a_{2,0} = a_{3,0} = a_{4,0} = b_{3,1} = b_{2,1} = b_{1,1} = 0$.

3.2.2 Investigated families

The exhaustive study of all isochronous center at the origin for the system (3.11) is hopeless at the present. Even for cubic system when all quartic terms vanish this problem is not yet solved.

Let us note that the condition (3.15) is equivalent to the following system of equations :

$$
\left.
\begin{aligned}
& 2\,a_{2,0} + b_{1,1} = 0, \\
& -b_{2,1} + a_{1,1}b_{1,1} + a_{1,1}a_{2,0} - 2\,b_{0,2}a_{2,0} - 3\,a_{3,0} = 0, \\
& a_{1,1}b_{2,1} - 4\,a_{4,0} - b_{3,1} + 2\,a_{1,1}a_{3,0} - 2\,b_{0,2}a_{3,0} - 2\,b_{1,2}a_{2,0} + a_{2,1}b_{1,1} = 0, \\
& -a_{3,1}a_{2,0} + 3\,a_{1,1}a_{4,0} + a_{2,1}b_{2,1} - 2\,b_{0,2}a_{4,0} - 2\,b_{2,2}a_{2,0} + a_{2,1}a_{3,0} + a_{1,1}b_{3,1} + \\
& -2\,b_{1,2}a_{3,0} + a_{3,1}b_{1,1} = 0, \\
& a_{3,1}b_{2,1} + a_{2,1}b_{3,1} + 2\,a_{2,1}a_{4,0} - 2\,b_{1,2}a_{4,0} - 2\,b_{2,2}a_{3,0} = 0, \\
& a_{3,1}b_{3,1} - 2\,b_{2,2}a_{4,0} + a_{3,1}a_{4,0} = 0.
\end{aligned}
\right\}.
$$

(3.17)

In the present chapter we determine all isochronous centers of the system (3.11) in each of the following three cases.

1. When the standard reduction is possible (i.e. $p_0(x) = 0$ and $q_1(x) = 0$, that is $a_{2,0} = a_{3,0} = a_{4,0} = b_{3,1} = b_{2,1} = b_{1,1} = 0$). We provide all candidates for isochronous centers in the cases where either $a_{1,1} = 0$, or $b_{2,0} = -3\,b_{0,2}$. In all the cases but one (a subcase of $b_{2,0} = -3\,b_{0,2}$), we prove the isochronicity. The general case is not yet completely explored.

2. When Choudhury-Guha reduction for the cubic case is possible (i.e. conditions (3.17) are satisfied and $a_{3,1} = a_{4,0} = b_{3,1} = b_{2,2} = b_{4,0} = 0$). For this case we obtain the exhaustive list of all isochronous centers at the origin.

3. When Choudhury-Guha reduction is possible and the Urabe function is null. That means that condition (3.17) and condition (3.10) for f and g defined by (3.16) are simultaneously satisfied. In this case we provide 25 examples of new isochronous centers and our analysis is not exhaustive.

Moreover, when the Urabe function $h = 0$, we give the explicit formulas for linearizing coordinates from Poincaré Theorem. We report 5 examples where such coordinates are explicitly computed.

3.2.3 Time-reversible systems

The general notion of time-reversible system of ordinary differential equations goes back to [74] where the motivations and general discussion can be found. Here we follow Sec. 1 of [49] (see also Sec. 3.5 [188]).

The planar system (3.1) of ordinary differential equation is *time-reversible* if there exists at least one straight line passing through the origin which is a symmetry axis of the phase portrait of the system under consideration. By appropriate rotation this straight line is mapped on the x-axis and the phase portrait of the rotated system is invariant with respect to symmetry $(x, y) \to (x, -y)$ if only one change time t into $-t$.

Note that a system

$$\dot{x} = P(x, y), \ \dot{y} = Q(x, y),$$

is time-reversible system with respect to x-axis if and only if $P(x, -y) = -P(x, y)$ and $Q(x, -y) = Q(x, y)$. When P and Q are polynomials, this means that the variable y appears in all monomials of P in odd power and in all monomials of Q in even power (0 included).

Consequently, to decide if a polynomial center for system (3.1) is time-reversible or not, we consider the rotated system in coordinates (x_α, y_α), where $x_\alpha = x \cos\alpha - y \sin\alpha$ and $y_\alpha = x \sin\alpha + y \cos\alpha$ and we examine the parity of the powers of the variable y_α for all angles α.

This notion plays an essential role in our topics. Indeed, for system (3.1) the origin is either a center or a focus. Thus, if such system is time-reversible the focus case is excluded and the origin is necessarily a center.

To the best of our knowledge the majority of already known isochronous centers for polynomial system (3.1) are time-reversible. For instance, all systems studied in [213, 49, 62, 63, 30, 56] are time reversible. Moreover, among 27 polynomial isochronous centers presented in tables $3 - 29$ of [52] only 7 are not time-reversible; indeed, those from tables 17 and $23 - 28$. In what concerns the cubic isochronous centers for system (3.1) the complete enumeration of those which are time reversible was obtained in [56]; there are 17 such cases. In [52] one find 4 non time-reversible isochronous centers (tables $25 - 28$) and in the present chapter we present three new such cases which are described in Theorem 14. In [55] a complete list of quartic homogeneous time-reversible isochronous centers is provided, there are 9 such cases. In the present chapter we provide 33 new cases of quartic (non homogeneous) iso-

chronous centers. Among them 8 are time reversible and at least 23 are not time reversible.

3.2.4 Background on Gröbner bases

The use of the Rational C-Algorithm leads to a system of polynomial equations

$$f_1 = 0, \ldots, f_m = 0 \tag{3.18}$$

with $f_i \in \mathbb{R}[x_1, \ldots, x_n]$. To solve this system we consider the ideal $\langle f_1, \ldots, f_m \rangle \subset \mathbb{R}[x_1, \ldots, x_n]$. For this aim, we use Gröbner Bases computations. In this section, we recall the basic facts about Gröbner bases, and refer the reader to [68] for details.

A *monomial ordering* is a total order on monomials that is compatible with the product and such that every nonempty set has a smallest element for the order. The leading term of a polynomial is the greatest monomial appearing in this polynomial.

A *Gröbner basis* of an ideal $\mathcal{I}$ for a given monomial ordering is a set G of generators of $\mathcal{I}$ such that the leading terms of G generate the ideal of leading terms of polynomials in $\mathcal{I}$. A polynomial is *reduced* with respect to the Gröbner basis G when its leading term is not a multiple of those of G. The basis is *reduced* if each element $g \in G$ is reduced with respect to $G \setminus \{g\}$. For a given monomial ordering, the reduced Gröbner basis of a given set of polynomials exists and is unique, and can be computed using one's favorite general computer algebra system, like Maple, Magma or Singular. The most efficient Gröbner basis algorithm is currently F_4 [94], which is implemented in the three above cited systems. For our computations, we use the FGb implementation of F_4 available in Maple [93].

The complexity of a Gröbner basis computation is well known to be generically exponential in the number of variables, and in the worst case doubly exponential in the number of variables. Moreover, the choice of the monomial ordering is crucial for time of the computation.

The *grevlex* ordering is the most suited ordering for the computation of the (reduced) Gröbner basis. The monomials are first ordered by degree, and the order between two monomials of the same degree $x_\alpha = x_1^{\alpha_1} \cdots x_n^{\alpha_n}$ and $x_\beta = x_1^{\beta_1} \cdots x_n^{\beta_n}$ is given by $x_\alpha \succ x_\beta$ when the last nonzero element of $(\alpha_1 - \beta_1, \ldots, \alpha_n - \beta_n)$ is negative. Thus, among the monomials of degree d, the order is

$$x_1^d \succ x_1^{d-1} x_2 \succ x_1^{d-2} x_2^2 \succ \cdots \succ x_2^d \succ x_1^{d-1} x_3 \succ x_1^{d-2} x_2 x_3 \succ x_1^{d-2} x_3^2 \succ \cdots \succ x_n^d.$$

However, a Gröbner basis for the grevlex ordering is not appropriate for the computation of the solutions of the system (3.18). The most suited ordering for this computation is the *lexicographical* ordering (or *lex* ordering for short). The monomials are ordered by comparing the exponents of the variables in lexicographical order. Thus, any monomial containing x_1 is greater than any monomial containing only variables $x_2, \ldots, x_n$.

Under some hypotheses (radical ideal with a finite number of solutions, and up to a linear change of coordinates), the Gröbner Basis of an ideal $\langle f_1, \ldots, f_m \rangle$ for the

lexicographical order $x_1 > \ldots > x_n$ has the shape

$$\{x_1 - g_1(x_n), x_2 - g_2(x_n), \ldots, x_{n-1} - g_{n-1}(x_{n-1}), g_n(x_n)\}, \qquad (3.19)$$

where the g_i's are univariate polynomials. In this case, the computation of the solutions of the system follows easily. In the general case, the shape of the Gröbner basis for the lexicographical ordering is more complicated, but it is equivalent to several triangular systems for which the computation of the solutions are easy.

An important point is that a Gröbner basis for the lex order is in general hard to compute directly. It is much faster to compute first a Gröbner basis for the grevlex order, and then to make a change of ordering to the lex order.

The precise ordering we use to compute the Gröbner bases of the polynomial systems occuring in this chapter is a weighted order : we fix a weight $i + j - 1$ for the variables $a_{i,j}$ and $b_{i,j}$ (see (3.11)), and use the weighted grevlex or lex ordering. For those orderings, the polynomials are `homogeneous`, which simplifies the computation. Indeed, without loss of generality, we can pick a variable $a_{i,j}$ and split the computations into two cases $a_{i,j} = 0$ and $a_{i,j} = 1$ (the same concerns $b_{i,j}$). The entire set of solutions can then be recovered in the standard way. For instance, all solutions with $a_{1,1} \neq 0$ for system (3.11) are obtained from solutions with $a_{1,1} = 1$ by the change of variables $X = a_{1,1} x$ and $Y = a_{1,1} y$. This trick reduces by one the number of variables for the Gröbner basis computation and improves the time of the computations. **In what follows, all results are presented up to such homogenization**.

Finally, we use repeatedly the *Radical Membership Theorem* :

Theorem 12 ([68]). *Let $I = \langle f_1, \ldots, f_s \rangle$ be an ideal of $k[x_1, \ldots, x_n]$, then f belongs to $\sqrt{I}$ if and only if $\langle f_1, \ldots, f_s, 1 - yf \rangle = \langle 1 \rangle = k[x_1, \ldots, x_n, y]$.*

3.3 The standard reduction

In this section we are concerned by system (3.11) with $a_{2,0} = a_{3,0} = a_{4,0} = b_{3,1} = b_{2,1} = b_{1,1} = 0$ which gives :

$$\left.\begin{array}{l} \dot{x} = -y + a_{1,1}xy + a_{2,1}x^2y + a_{3,1}x^3y \\ \dot{y} = x + b_{2,0}x^2 + b_{3,0}x^3 + b_{0,2}y^2 + b_{1,2}xy^2 + b_{2,2}x^2y^2 + b_{4,0}x^4 \end{array}\right\}. \qquad (3.20)$$

Recall that all cases when the origin O is an isochronous center of the system (3.20) with zero Urabe function are described in [30]. In the following theorem we omit all isochronous centers with zero Urabe function, as well as all cubic isochronous centers that where all described in [63, 62].

For each case we prove the isochronicity by determining explicitly its Urabe function. For system (k) we will denote it by $h_{(k)}$.

Theorem 13. *The following particular cases of system* (3.20) *have an isochronous center at the origin O.*

$$\left.\begin{aligned}
\dot{x} &= -y + 3\,x^2 y \pm \sqrt{2} x^3 y \\
\dot{y} &= x \pm \sqrt{2} x^2 \mp \frac{\sqrt{2}}{2} y^2 + x^3 + 4\,x y^2 \pm 2\sqrt{2} x^2 y^2 \pm \frac{\sqrt{2}}{4} x^4
\end{aligned}\right\}, \quad \text{where } h_{(3.21)} = -\frac{\pm\xi}{\sqrt{2 + 9\,\xi^2}}.$$
$$(3.21)$$

$$\left.\begin{aligned}
\dot{x} &= -y + x^3 y \\
\dot{y} &= x + \frac{1}{2} x^2 y^2 - \frac{1}{2} x^4
\end{aligned}\right\}, \quad \text{where } h_{(3.22)} = \frac{\xi^3}{\sqrt{4 + \xi^6}}. \qquad (3.22)$$

$$\left.\begin{aligned}
\dot{x} &= -y - \frac{x^2 y}{2} + \frac{x^3 y}{8} + x y \\
\dot{y} &= x - \frac{3\,x^2}{4} + \frac{y^2}{4} + \frac{5\,x^3}{24} + \frac{3\,x y^2}{8} - \frac{x^2 y^2}{16} - \frac{x^4}{48}
\end{aligned}\right\}, \quad \text{where } h_{(3.23)} = \frac{3\,\xi}{\sqrt{16 + 9\,\xi^2}}.$$
$$(3.23)$$

$$\left.\begin{aligned}
\dot{x} &= -y + 9\,x^2 y + 6\,x^3 y + x y \\
\dot{y} &= x + \frac{3\,x^2}{2} - \frac{y^2}{2} + x^3 + 12\,x y^2 + 12\,x^2 y^2 + \frac{x^4}{2}
\end{aligned}\right\}, \quad \text{where } h_{(3.24)} = -\frac{\xi}{\sqrt{4 + 49\,\xi^2}}.$$
$$(3.24)$$

$$\left.\begin{aligned}
\dot{x} &= -y - \left(3\,a_{3,1} + \frac{2}{9}\right) x^2 y + a_{3,1} x^3 y + x y \\
\dot{y} &= x + \left(-3\,a_{3,1} + \frac{1}{9}\right) x y^2
\end{aligned}\right\}, \quad \text{where } h_{(3.25)} = \frac{\xi}{\sqrt{(1 - 27\,a_{3,1})\xi^2 + 9}}.$$
$$(3.25)$$

$$\left.\begin{aligned}
\dot{x} &= -y + x y \\
\dot{y} &= x - \frac{3\,x^2}{2} + y^2 + x^3 - \frac{x^4}{4}
\end{aligned}\right\}, \quad \text{where } h_{(3.26)} = \frac{\xi}{\sqrt{1 + \xi^2}}. \qquad (3.26)$$

Moreover, all other possible isochronous centers at O for non cubic system (3.20)*, where either $a_{1,1} = 1$ or $b_{2,0} = -3\,b_{0,2}$, and with non vanishing Urabe functions, belong to the family*

$$\left.\begin{aligned}
\dot{x} &= -y + \left(-\frac{3}{8} - 2\,b_{2,2}\right) x^2 y + \left(\frac{1}{16} + b_{2,2}\right) x^3 y + x y \\
\dot{y} &= x - \frac{3\,x^2}{4} + \frac{y^2}{4} + \frac{3\,x^3}{8} - 2\,b_{2,2} x y^2 + b_{2,2} x^2 y^2 - \frac{x^4}{16}
\end{aligned}\right\}. \qquad (3.27)$$

In particular, when $b_{2,2} \in \{-\frac{1}{16}, 0, \frac{1}{16}\}$, the origin O is an isochronous center with non-standard Urabe functions :

$$h_{\{b_{2,2} = -\frac{1}{16}\}} = \frac{\sqrt{2}\sqrt{2\,L\left(\frac{\xi^2}{4}\right) + 8}\sqrt{\frac{\xi^2}{L\left(\frac{\xi^2}{4}\right)}}\left(L\left(\frac{\xi^2}{4}\right) + 3\right) L\left(\frac{\xi^2}{4}\right)}{2\,\xi\left(L\left(\frac{\xi^2}{4}\right) + 4\right)\left(L\left(\frac{\xi^2}{4}\right) + 1\right)},$$

where $L = LambertW$ is the Lambert function (see [89]),

$$h_{\{b_{2,2}=0\}} = \frac{\sqrt{2}\sqrt{\frac{-4+\xi^2+2\sqrt{4+2\xi^2}}{\xi^2}}\,\xi\left(\xi^2 + 2\sqrt{4+2\xi^2} + 2\right)}{(2+\xi^2)\left(\sqrt{4+2\xi^2}+6\right)},$$

$$h_{\{b_{2,2}=\frac{1}{16}\}} = \frac{\sqrt{2}\xi\sqrt{2\xi^2+32}\left(\xi^2+12\right)}{2\left(\xi^2+4\right)\left(\xi^2+16\right)}.$$

Necessary conditions are given by C-Algorithm. Indeed, 19 steps are necessary to find the algebraic conditions of isochronicity (see Appendix A of [30]). We did not succeed in computing the full grevlex Gröbner basis of the corresponding system of polynomial equations. We restricted ourselves to the cases $a_{1,1} = 0$, which gives the cases (3.21)-(3.22), and $\{a_{1,1} = 1, b_{2,0} = -3b_{0,2}\}$ which gives the cases (3.23)-(3.25) and (3.27). We also get case (3.26) as a particular solution.

For each case we determine its Urabe function, which shows that the obtained conditions are also sufficient. For systems (3.21)-(3.26) the procedure in Section 2 of [30] is applied.

The search of the Urabe function for sytem (3.27) is more subtle. Indeed, we verified that for all values of parameters the first 20 necessary conditions of isochronicity given by C-algorithm are satisfied. This strongly suggests that for all values of parameters the system (3.27) has an isochronous center at the origin O. For this system

$$f(x) = -\frac{20 - 96\,xb_{2,2} + 64\,x^2b_{2,2} - 12\,x + 3\,x^2}{-16 - 6\,x^2 - 32\,x^2b_{2,2} + 16\,x^3b_{2,2} + x^3 + 16\,x}$$

and

$$g(x) = \frac{1}{256}\left(-16 - 6\,x^2 - 32\,x^2b_{2,2} + 16\,x^3b_{2,2} + x^3 + 16\,x\right)x\left(-16 + 12\,x - 6\,x^2 + x^3\right).$$

from formula (3.7) one obtains

$$\xi^2(x) = 2\,x^2\,(2-x)^{-2\,(16\,b_{2,2}+1)^{-1}}\left(4\,x^2b_{2,2} + 1/4\,x^2 - x + 2\right)^{-\frac{16\,b_{2,2}-1}{16\,b_{2,2}+1}}. \qquad (3.28)$$

From formula (3.8) one deduces that

$$h(\xi(x)) = -\frac{x\left(12 - 6\,x + x^2\right)}{(x-4)\left(x^2 - 2\,x + 4\right)}.$$

Now the problem is to find the reciprocal function $x = x(\xi)$. Unfortunately we succeeded in finding it only for $b_{2,2} \in \{-\frac{1}{16}, 0, \frac{1}{16}\}$ because in those cases the equation (3.28) takes a sufficiently simple form.

Note that the system (3.22) was already identified in Theorem 2.2 of [30].

3.4 The Choudhury-Guha reduction

3.4.1 Cubic isochronous centers

Choudhury-Guha reduction is more general than the standard one used in preceding chapters [30]. Here we provide the complete enumeration of all cubic systems from (3.11) and we find three new cases of isochronous centers at the origin. The system we consider is :

$$\left.\begin{aligned}
\dot{x} &= -y + a_{1,1}xy + a_{2,0}x^2 + a_{2,1}x^2y + a_{3,0}x^3 \\
\dot{y} &= x + b_{2,0}x^2 + b_{1,1}xy + b_{0,2}y^2 + b_{2,1}yx^2 + b_{1,2}y^2x + b_{3,0}x^3
\end{aligned}\right\}. \tag{3.29}$$

Condition (3.15) is equivalent to the following system of equations :

$$\left.\begin{aligned}
&2\,a_{2,0} + b_{1,1} = 0 \\
&a_{1,1}a_{2,0} - 3\,a_{3,0} - b_{2,1} + a_{1,1}b_{1,1} - 2\,b_{0,2}a_{2,0} = 0 \\
&a_{1,1}b_{2,1} - 2\,b_{0,2}a_{3,0} + 2\,a_{1,1}a_{3,0} + a_{2,1}b_{1,1} - 2\,b_{1,2}a_{2,0} = 0 \\
&a_{2,1}a_{3,0} + a_{2,1}b_{2,1} - 2\,b_{1,2}a_{3,0} = 0
\end{aligned}\right\}. \tag{3.30}$$

Theorem 14. *Under the assumptions* (3.30) *the origin O is an isochronous center of System* (3.29) *only in one of the following cases :*

1. *The standard reduction is possible, that means $a_{3,0} = a_{2,0} = b_{1,1} = b_{2,1} = 0$ and the system is one of those from Theorem 3 of [63].*

2. *We are in one of the following cases :*

$$\left.\begin{aligned}
\dot{x} &= -y - 2\,b_{2,0}xy + x^2 + 2\,b_{2,0}x^3 \\
\dot{y} &= x - 4\,b_{2,0}y^2 - 2\,xy + b_{2,0}x^2 + 4\,b_{2,0}x^2y + 2\,x^3
\end{aligned}\right\}, \tag{3.31}$$

$$\left.\begin{aligned}
\dot{x} &= -y \pm 2\,\sqrt{2}xy + x^2 \mp 2\,\sqrt{2}x^3 \\
\dot{y} &= x \pm 8\,\sqrt{2}y^2 - 2\,xy \mp 3\,\sqrt{2}x^2 \mp 12\,\sqrt{2}x^2y + 10\,x^3
\end{aligned}\right\}, \tag{3.32}$$

$$\left.\begin{aligned}
\dot{x} &= -y - \frac{1}{2}\,b_{2,0}xy + x^2 + \frac{1}{2}\,b_{2,0}x^3 \\
\dot{y} &= x - b_{2,0}y^2 - 2\,xy + b_{2,0}x^2 + b_{2,0}x^2y + \left(2 + \frac{1}{4}\,b_{2,0}^2\right)x^3
\end{aligned}\right\}. \tag{3.33}$$

Démonstration. The necessary conditions are given by the solutions of the polynomial system of equations consisting of equations (3.30) (called $C_1, \ldots, C_4$) and the 8 equations obtained from the Rational C-Algorithm (15 steps), called $C_5, \ldots, C_{12}$. Let us denote by I the ideal generated by $C_1, \ldots, C_{12}$.

We exclude the standard reduction by adding to I the variable T and the polynomial

$$C_{13} = (Ta_{3,0} - 1)(Ta_{2,0} - 1)(Tb_{1,1} - 1)(Tb_{2,1} - 1).$$

For $a_{2,0} = 0$, a Gröbner basis of $\langle C_1, \ldots, C_{12}, C_{13}, a_{2,0}\rangle$ is $\langle 1 \rangle$ (i.e. there is no solution), which implies that we can take $a_{2,0} = 1$. We use the weighted order $b_{1,1} > b_{2,1} > b_{3,0} > b_{1,2} > a_{2,1} > b_{0,2} > a_{1,1} > b_{2,0} > a_{3,0}$.

First, a Gröbner basis of system $\langle C_1, \ldots, C_6 \rangle$ for the weighted lex order contains the polynomial

$$P = (a_{1,1} + 2\, b_{0,2})(a_{2,1} - a_{1,1}a_{3,0} - a_{3,0}^2).$$

We split our problem into two subcases according to this factorization.

— for $a_{1,1} + 2\, b_{0,2} = 0$, we get only one real solution

$$\left.\begin{aligned}
\dot{x} &= -y + x^2 \\
\dot{y} &= x - 2xy + 2x^3
\end{aligned}\right\},$$

which is a particular case of (3.33) with $b_{2,0} = 0$.

— for $a_{2,1} - a_{1,1}a_{3,0} - a_{3,0}^2 = 0$, we eliminate the solutions that are not real by adding to the system the polynomials $P_i \cdot T_i - 1$ for each P_i in

$$\{16\, a_{3,0}^2 + 1,\, 4\, a_{3,0}^2 + 9,\, 4\, a_{3,0}^2 + 1,\, a_{3,0}^2 + 4,\, a_{3,0}^2 + 1,\, a_{3,0}^2 + 16,\, a_{3,0}^2 + 9 - 4\, b_{2,0}\, a_{3,0} + 4\, b_{2,0}^2\}$$

that have no real solution. Then, the solutions of the resulting system are those quoted in the theorem.

Sufficiency. For the cases (3.31) and (3.32) we have $g'(x) + f(x)g(x) = 1$. Hence by Corollary 1 the origin is an isochronous center. Moreover we easily check that $h_{(3.33)}(\xi) = -\frac{1}{2}\, b_{2,0}\xi$. $\qquad\qquad\square$

3.4.2 Quartic isochronous centers

Our first target was to identify all isochronous centers at the origin with zero Urabe function for the system (3.11)

$$\left.\begin{aligned}
\dot{x} &= -y + a_{1,1}xy + a_{2,0}x^2 + a_{2,1}x^2y + a_{3,0}x^3 + a_{3,1}x^3y + a_{4,0}x^4 \\
\dot{y} &= x + b_{0,2}y^2 + b_{1,1}xy + b_{2,0}x^2 + b_{1,2}xy^2 + b_{2,1}x^2y + b_{3,0}x^3 + b_{2,2}x^2y^2 + b_{3,1}x^3y + b_{4,0}x^4
\end{aligned}\right\}$$

under the condition (3.17). That means finding all values of the 15 parameters for which the equation $g'(x) + f(x)\, g(x) = 1$ is satisfied where f and g are defined by (3.16) (see Corollary 1).

When the standard reduction is possible, that means $a_{4,0} = a_{3,0} = a_{2,0} = b_{1,1} = b_{2,1} = b_{3,1} = 0$ all the 6 isochronous centers with zero Urabe function were described in Theorem 3.1 of [30]. Otherwise when the Choudhury-Guha reduction needs to be applied the problem becomes substantially more complicated.

Taking in account the great complexity of the problem we did not succeed in solving it completely. Nevertheless, during our investigations we obtained 25 new isochronous centers for the system (3.11), two of them of extreme complexity, called Monsters. We are convinced that our list is not exhaustive.

The procedure to obtain the isochronous centers listed below consists in solving by Gröbner method the system (3.17) simultaneously with the set of equations on

parameters which corresponds the equation $g'(x) + f(x)\,g(x) = 1$. First, one applies the Solve routine of Maple (based on Gröbner basis technic) which splits the variety of solutions into 37 subvarieties. The cases (3.34)-(3.57) were obtained by detailed inspection of some of them. The remaining 7 isochronous centers (3.51)-(3.58) were obtained by restricting ourselves to $b_{2,2} = a_{3,1} = 0$ and by application of the standard Gröbner basis technique.

We verified also that all above isochronous centers are not time-reversible, except perhaps the two Monsters (3.57) and (3.58).

Theorem 15. *The following quartic systems have an isochronous center at the origin O with zero Urabe function.*

$$\left.\begin{aligned}\dot{x} &= -y + b_{0,2}xy + x^2 - b_{0,2}x^3 \\ \dot{y} &= x + b_{0,2}y^2 - 2\,xy + 2\,x^3 - b_{0,2}x^4\end{aligned}\right\}, \tag{3.34}$$

$$\left.\begin{aligned}\dot{x} &= -y + xy - a_{3,0}x^2 + a_{3,0}x^3 \\ \dot{y} &= x + y^2 + 2\,a_{3,0}xy + 2\,a_{3,0}{}^2x^3 - a_{3,0}{}^2x^4\end{aligned}\right\}, \tag{3.35}$$

$$\left.\begin{aligned}\dot{x} &= -y + xy - a_{3,0}x^2 + a_{3,0}x^3 \\ \dot{y} &= x + 3\,y^2 + 2\,a_{3,0}xy - x^2 + 4\,a_{3,0}x^2y + \left(\frac{1}{3} + 2\,a_{3,0}{}^2\right)x^3 + a_{3,0}{}^2x^4\end{aligned}\right\}, \tag{3.36}$$

$$\left.\begin{aligned}\dot{x} &= -y + xy - a_{3,0}x^2 + a_{3,0}x^3 \\ \dot{y} &= x + 4\,y^2 + 2\,a_{3,0}xy - \frac{3\,x^2}{2} + 6\,a_{3,0}x^2y + \left(1 + 2\,a_{3,0}{}^2\right)x^3 + \left(-\frac{1}{4} + 2\,a_{3,0}{}^2\right)x^4\end{aligned}\right\}, \tag{3.37}$$

$$\left.\begin{aligned}\dot{x} &= -y + \frac{b_{0,2}xy}{3} + x^2 - \frac{b_{0,2}x^3}{3} \\ \dot{y} &= x + b_{0,2}y^2 - 2\,xy - \frac{b_{0,2}x^2}{3} - \frac{4\,b_{0,2}x^2y}{3} + \left(\frac{b_{0,2}{}^2}{27} + 2\right)x^3 + \frac{b_{0,2}x^4}{3}\end{aligned}\right\}, \tag{3.38}$$

$$\left.\begin{aligned}\dot{x} &= -y + \frac{b_{0,2}xy}{4} + x^2 - \frac{b_{0,2}x^3}{4} \\ \dot{y} &= x + b_{0,2}y^2 - 2\,xy - \frac{3\,b_{0,2}x^2}{8} - \frac{3\,b_{0,2}x^2y}{2} + \left(\frac{b_{0,2}{}^2}{16} + 2\right)x^3 + \left(-\frac{1}{256}b_{0,2}{}^3 + \frac{b_{0,2}}{2}\right)x^4\end{aligned}\right\}, \tag{3.39}$$

$$\left.\begin{aligned}
\dot{x} &= -y - \frac{45}{8}\,x^2 y + x^2 + \frac{45}{8}\,x^4 \\
\dot{y} &= x - 2\,xy - \frac{225}{8}\,xy^2 + \frac{19}{2}\,x^3 + 45\,x^3 y
\end{aligned}\right\}, \tag{3.40}$$

$$\left.\begin{aligned}
\dot{x} &= -y + \frac{b_{4,0}{}^2 x^2 y}{2} + x^2 - \frac{b_{4,0}{}^2 x^4}{2} \\
\dot{y} &= x + b_{4,0}y^2 - 2\,xy - \frac{b_{4,0}x^2}{2} + b_{4,0}{}^2 xy^2 - 2\,b_{4,0}x^2 y + 2\,x^3 - b_{4,0}{}^2 x^3 y + b_{4,0}x^4
\end{aligned}\right\}, \tag{3.41}$$

$$\left.\begin{aligned}
\dot{x} &= -y + \left(-2 + 2\sqrt{19}\right)x^2 y + x^2 - \left(-2 + 2\sqrt{19}\right)x^4 \\
\dot{y} &= x \pm \alpha_1 y^2 - 2\,xy \mp \frac{\alpha_1 x^2}{2} + \alpha_2 xy^2 \mp 2\,\alpha_1 x^2 y + \alpha_4 x^3 + \alpha_3 x^3 y \pm 4\,\alpha_1 x^4
\end{aligned}\right\}, \tag{3.42}$$

where
$\alpha_1 = \sqrt{-106 + 34\sqrt{19}}$, $\alpha_2 = -10 + 10\sqrt{19}$, $\alpha_3 = 16 - 16\sqrt{19}$, $\alpha_4 = -13 + 3\sqrt{19}$.

$$\left.\begin{aligned}
\dot{x} &= -y + a_{1,1}xy + \frac{15}{8}\,a_{1,1}{}^2 x^2 y + x^2 - x^3 a_{1,1} - \frac{15}{8}\,x^4 a_{1,1}{}^2 \\
\dot{y} &= x - \frac{a_{1,1}y^2}{2} - 2\,xy + \frac{3\,a_{1,1}x^2}{4} + \frac{15}{4}\,a_{1,1}{}^2 xy^2 + 3\,a_{1,1}x^2 y + 2\,x^3 - \frac{15}{4}\,a_{1,1}{}^2 x^3 y - \frac{5\,a_{1,1}x^4}{2}
\end{aligned}\right\}, \tag{3.43}$$

$$\left.\begin{aligned}
\dot{x} &= -y \mp \frac{2}{35}\,\alpha_5 xy + \alpha_6 x^2 y + x^2 \pm \frac{2}{35}\,\alpha_5 x^3 - \alpha_6 x^4 \\
\dot{y} &= x \pm \frac{\alpha_5 y^2}{35} - 2\,xy \mp \frac{3}{70}\,\alpha_5 x^2 + 5\,\alpha_6 xy^2 \mp \frac{6}{35}\,\alpha_5 x^2 y + \alpha_7 x^3 - 8\,\alpha_6\,x^3 y \pm \frac{38}{35}\,\alpha_5 x^4
\end{aligned}\right\}, \tag{3.44}$$

where
$\alpha_5 = \sqrt{-77798 + 1162\sqrt{4691}}$, $\alpha_6 = -\frac{354}{5} + \frac{6\sqrt{4691}}{5}$, $\alpha_7 = -\frac{2183}{35} + \frac{27}{35}\sqrt{4691}$.

$$\left.\begin{aligned}
\dot{x} &= -y + xy - \frac{3\,a_{3,0}x^2}{4} + a_{3,0}x^3 - \frac{a_{3,0}x^4}{4} \\
\dot{y} &= x + 3\,y^2 + \frac{3\,a_{3,0}xy}{2} - x^2 + \frac{9\,a_{3,0}x^2y}{4} + \left(\frac{1}{3} + \frac{9}{8}\,a_{3,0}{}^2\right)x^3 - \frac{3\,a_{3,0}x^3y}{4} - \frac{3\,a_{3,0}{}^2x^4}{8}
\end{aligned}\right\}, \tag{3.45}$$

$$\left.\begin{aligned}
\dot{x} &= -y + xy \pm \frac{\sqrt{2}}{2}\,x^2 \mp \frac{2\sqrt{2}}{3}\,x^3 \pm \frac{\sqrt{2}}{6}\,x^4 \\
\dot{y} &= x + 6\,y^2 \mp \sqrt{2}xy - \frac{5}{2}\,x^2 \mp \frac{9}{2}\,\sqrt{2}x^2y + \frac{13}{3}\,x^3 \pm \frac{3\sqrt{2}}{2}x^3y - \frac{4}{3}\,x^4
\end{aligned}\right\}, \tag{3.46}$$

$$\left.\begin{aligned}
\dot{x} &= -y \mp 2\,\sqrt{2}xy + x^2 \pm 2\,\sqrt{2}x^3 \\
\dot{y} &= x \mp 6\,\sqrt{2}y^2 - 2\,xy \pm 2\,\sqrt{2}x^2 \pm 8\,\sqrt{2}x^2y + \frac{14}{3}\,x^3 \mp 2\,\sqrt{2}x^4
\end{aligned}\right\}, \tag{3.47}$$

$$\left.\begin{aligned}
\dot{x} &= -y + a_{1,1}xy + a_{1,1}{}^2x^2y + x^2 - a_{1,1}x^3 \\
&\quad - a_{1,1}{}^2x^4 \\
\dot{y} &= x + 3\,a_{1,1}y^2 - 2\,xy - a_{1,1}x^2 + 2\,a_{1,1}{}^2xy^2 \\
&\quad - 4\,a_{1,1}x^2y + 2\,x^3 - 2\,a_{1,1}{}^2x^3y + a_{1,1}x^4
\end{aligned}\right\}, \tag{3.48}$$

$$\left.\begin{aligned}
\dot{x} &= -y + a_{1,1}xy + 3\,a_{1,1}{}^2x^2y + x^2 - a_{1,1}x^3 - 3\,a_{1,1}{}^2x^4 \\
\dot{y} &= x + 4\,a_{1,1}y^2 - 2\,xy - \frac{3}{2}\,a_{1,1}x^2 + 6\,a_{1,1}{}^2xy^2 - 6\,a_{1,1}x^2y + 2\,x^3 - 6\,a_{1,1}{}^2x^3y + 2\,a_{1,1}x^4
\end{aligned}\right\}, \tag{3.49}$$

$$\left.\begin{aligned}
\dot{x} &= -y + a_{1,1}xy + \left(a_{1,1}{}^2 - \frac{3}{2}\,b_{0,2}a_{1,1} + \frac{1}{2}\,b_{0,2}{}^2\right)x^2y \\
&\quad + x^2 - a_{1,1}x^3 - \left(a_{1,1}{}^2 - \frac{3}{2}\,b_{0,2}a_{1,1} + \frac{1}{2}\,b_{0,2}{}^2\right)x^4 \\
\dot{y} &= x + b_{0,2}y^2 - 2\,xy + \left(\frac{1}{2}\,a_{1,1} - \frac{1}{2}\,b_{0,2}\right)x^2 + \left(2\,a_{1,1}{}^2 - 3\,b_{0,2}a_{1,1} + b_{0,2}{}^2\right)xy^2 \\
&\quad + \left(2\left(a_{1,1}{}^2 - \frac{3}{2}\,b_{0,2}a_{1,1} + \frac{1}{2}\,b_{0,2}{}^2\right) - 2\left(2\,a_{1,1}{}^2 - 3\,b_{0,2}a_{1,1} + b_{0,2}{}^2\right)\right)x^3y \\
&\quad + \left(-2\,a_{1,1} + b_{0,2}\right)x^4 + \left(2\,a_{1,1} - 2\,b_{0,2}\right)x^2y + 2\,x^3
\end{aligned}\right\}. \tag{3.50}$$

$$
\left.
\begin{aligned}
\dot{x} &= -y + a_{1,1}xy + x^2 - a_{1,1}x^3 \\
\dot{y} &= x + 4\,a_{1,1}y^2 - 2\,xy - \frac{3}{2}\,a_{1,1}x^2 - 6\,a_{1,1}x^2y + \left(2 + a_{1,1}{}^2\right)x^3 + \left(2\,a_{1,1} - \frac{1}{4}\,a_{1,1}{}^3\right)x^4
\end{aligned}
\right\},
$$
$$(3.51)$$

$$
\left.
\begin{aligned}
\dot{x} &= -y + a_{1,1}xy + x^2 - a_{1,1}x^3 \\
\dot{y} &= x + 3\,a_{1,1}y^2 - 2\,xy - a_{1,1}x^2 - 4\,a_{1,1}x^2y + \left(\frac{1}{3}\,a_{1,1}{}^2 + 2\right)x^3 + a_{1,1}x^4
\end{aligned}
\right\},
$$
$$(3.52)$$

$$
\left.
\begin{aligned}
\dot{x} &= -y + 2\,\beta\,xy + x^2 - 2\,\beta\,x^3 \\
\dot{y} &= x + 8\,\beta\,y^2 - 2\,xy - 3\,\beta\,x^2 - 12\,\beta\,x^2y + 14\,x^3 - 2\,\beta\,x^4
\end{aligned}
\right\},
\qquad (3.53)
$$
where $\beta = \pm\sqrt{3}$.

$$
\left.
\begin{aligned}
\dot{x} &= -y + \alpha\,xy + x^2 - 4/3\,\alpha\,x^3 + 2/3\,x^4 \\
\dot{y} &= x + 6\,\alpha\,y^2 - 2\,xy - 5/2\,\alpha\,x^2 - 9\,\alpha\,x^2y + \frac{26}{3}\,x^3 + 6\,x^3y - 8/3\,\alpha\,x^4
\end{aligned}
\right\},
\quad (3.54)
$$

$$
\left.
\begin{aligned}
\dot{x} &= -y + \alpha\,xy + x^2 - \frac{4}{3}\,\alpha\,x^3 + \frac{2}{3}\,x^4 \\
\dot{y} &= x + 3\,\alpha\,y^2 - 2\,xy - \alpha\,x^2 - 3\,\alpha\,x^2y + \frac{8}{3}\,x^3 + 2\,x^3y - \frac{2}{3}\,\alpha\,x^4
\end{aligned}
\right\},
\quad (3.55)
$$
where $\alpha = \pm\sqrt{2}$.

$$
\left.
\begin{aligned}
\dot{x} &= -y + a_{1,1}xy + x^2 + \left(a_{1,1}{}^2 - \frac{3}{2}\,b_{0,2}a_{1,1} + \frac{1}{2}\,b_{0,2}{}^2\right)x^2y - a_{1,1}x^3 + \left(-a_{1,1}{}^2 + \frac{3}{2}\,b_{0,2}a_{1,1} - \frac{1}{2}\,b_{0,2}{}^2\right)x^4 \\
\dot{y} &= x + b_{0,2}y^2 - 2\,xy + \left(\frac{1}{2}\,a_{1,1} - \frac{1}{2}\,b_{0,2}\right)x^2 + \left(2\,a_{1,1}{}^2 - 3\,b_{0,2}a_{1,1} + b_{0,2}{}^2\right)xy^2 \\
&\quad + \left(2\,a_{1,1} - 2\,b_{0,2}\right)x^2y + 2\,x^3 + \left(-2\,a_{1,1}{}^2 + 3\,b_{0,2}a_{1,1} - b_{0,2}{}^2\right)x^3y + \left(-2\,a_{1,1} + b_{0,2}\right)x^4
\end{aligned}
\right\}
$$
$$(3.56)$$

Finally, the two *Monsters* mentioned in Introduction are of the form

$$
\left.
\begin{aligned}
\dot{x} &= -y + T x y + M x^2 y + x^2 - T x^3 - M x^4 \\
\dot{y} &= x + P y^2 - 2\, x y - \frac{P}{2} x^2 + 5\, M x y^2 - 2\, P x^2 y + S x^3 - 8\, M x^3 y + 4\, P x^4
\end{aligned}
\right\},
$$
$$(3.57)$$

$$
\left.
\begin{aligned}
\dot{x} &= -y + \alpha\, x y + M\, x^2 y + x^2 - \alpha\, x^3 - M\, x^4 \\
\dot{y} &= x + 5\, M x y^2 - 8\, M x^3 y - 2\, x y + \frac{B_{0,2}}{12\left((M+9)\,\alpha\,\beta\right)} y^2 - \frac{\delta}{12\,(M+9)\,\alpha\,\beta} x^2 \\
&\quad - \frac{\delta}{3\,(M+9)\,\alpha\,\beta} x^2 y - \frac{B_{3,0}}{2\,(M+9)\,\beta} x^3 - \frac{B_{4,0}}{12(M+9)\,\alpha\,\beta} x^4
\end{aligned}
\right\},
$$
$$(3.58)$$

The exact description of their coefficients is too cumbersome to be reproduced here. They are written down in arXiv variant of the present chapter (arXiv :1005.5048, isochronous centers (4.23) and (4.30) respectively).

3.5 Explicit Linearization

3.5.1 Linearization formulas

Let us consider the Liénard type system (3.4)

$$
\left.
\begin{aligned}
\dot{x} &= y \\
\dot{y} &= -g(x) - f(x) y^2
\end{aligned}
\right\}
$$

with a center at the origin $(0,0)$ where f and g are real analytic in a neighborhood of zero.

It is known by Sabatini formula (3.6) that the first integral associated to the system (3.4) can be written

$$
I(x, \dot{x}) = \int_0^x g(s) e^{2F(s)} ds + \frac{1}{2}(\dot{x} e^{F(x)})^2 \tag{3.59}
$$

where $F(x) = \int_0^x f(s) ds$.

Following [59] (see also [112]), let us perform the following change of variables

$$
\left.
\begin{aligned}
p(x, \dot{x}) &= \dot{x} e^{F(x)} \\
q(x) &= \int_0^x e^{F(s)} ds
\end{aligned}
\right\}. \tag{3.60}
$$

As $\dfrac{\partial(p,q)}{\partial(x,\dot{x})} = -e^{2F(x)} < 0$ and $p(0,0) = q(0) = 0$ then this is an analytic change of variables preserving the origin and well defined around it. Moreover, $q'(x) = e^{F(x)} > 0$ and thus the function $x \longmapsto q(x)$ is strictly increasing. In the (p,q) coordinates the first integral (3.59) becomes

$$I(x,\dot{x}) = H(p,q) = \frac{1}{2}p^2 + U(q), \tag{3.61}$$

where U is some uniquely defined real analytic function, $U(0) = 0$. Now it is easy to see that the system (3.4) in (p,q) coordinates can be written as

$$\left. \begin{aligned} \dot{q} &= \frac{\partial H}{\partial p} = p \\ \dot{p} &= -\frac{\partial H}{\partial q} = -\frac{d}{dq}U \end{aligned} \right\} \tag{3.62}$$

that is as a Hamiltonian system corresponding to the Hamiltonian (3.61).

The main result of this Section is

Theorem 16. *Let us consider the Liénard-type system* (3.4) *with real analytic functions f and g such that $x\,g(x) > 0$ for $x \neq 0$. Then the origin O is an isochronous center with Urabe function $h = 0$ if and only if $U(q) = \dfrac{q^2}{2}$.*

Démonstration. It is easy to see that O is a center. Now, from Corollary 1, one knows that O is an isochronous center with Urabe function $h = 0$ if and only if $g'(x) + g(x)f(x) = 1$ or equivalently $g'(x)e^{F(x)} + g(x)f(x)e^{F(x)} = e^{F(x)}$. The last equality is nothing else $\left(g(x)e^{F(x)}\right)' = \left(\int_0^x e^{F(s)}ds\right)'$. As $g(0)e^{F(0)} = 0$, when integrating one obtains $g(x)e^{F(x)} = \int_0^x e^{F(s)}ds$ or equivalently $U'(q) = q$ because $(\frac{dU}{dq})(q(x)) = g(x)\,e^{F(x)}$. Since $U(0) = 0$ one has $U(q) = \frac{1}{2}q^2$. $\qquad\qquad\square$

Consequently when the Urabe function h identically vanishes , the system of coordinate (p,q) defined by (3.60) is the linearizing system of coordinates for system (3.4). Indeed,

$$\left. \begin{aligned} \dot{q} &= p \\ \dot{p} &= -q \end{aligned} \right\}. \tag{3.63}$$

It is interesting to compare the theorem 16 with Chalykh-Veselov theorem that we formulate only for potential U without pole at 0.

Theorem 17 ([48], Theorem 1)**.** *Let us consider the Hamiltonian system with the Hamiltonian $H(P,Q) = \frac{1}{2}P^2 + U(Q)$ where U is a rational function without pole at 0. Then O is an isochronous center for the associated Hamiltonian system $\dot{Q} = \dfrac{\partial H}{\partial P},\ \dot{P} = -\dfrac{\partial H}{\partial Q}$ if and only if up to a shift $Q \to Q + a$ and adding a constant, $U(Q) = k\,Q^2$ for some $k \in \mathbb{R} - \{0\}$.*

3.5.2 Examples

Now applying formula (3.60) we provide 5 examples of linearization of isochronous centers with zero Urabe function. The reduction to Liénard-type system (3.4) is always obtained by standard or Choudhury-Guha reduction. To compute variables (p, q) see ((3.60)) we use Maple, and the identity (3.63) was verified in all cases. Our choice is somewhere random, because all reported examples with zero Urabe function are good for such purpose.

Cubic examples

1. Consider the case 6 of Theorem 3 of [63], that is the system

$$
\left.
\begin{aligned}
\dot{x} &= -y + a_{1,1}xy + \left(a_{1,1}{}^2 - \frac{3\,a_{1,1}b_{0,2}}{2} + \frac{b_{0,2}{}^2}{2}\right)x^2y \\
\dot{y} &= x + \left(-\frac{b_{0,2}}{2} + \frac{a_{1,1}}{2}\right)x^2 + b_{0,2}y^2 + \left(2\,a_{1,1}{}^2 - 3\,a_{1,1}b_{0,2} + b_{0,2}{}^2\right)xy^2
\end{aligned}
\right\}.
\tag{3.64}
$$

In this case the functions f and g are

$$
\left.
\begin{aligned}
f(x) &= -\frac{b_{0,2} + \left(2\,a_{1,1}{}^2 - 3\,a_{1,1}b_{0,2} + b_{0,2}{}^2\right)x + a_{1,1} + 2\left(a_{1,1}{}^2 - \frac{3\,a_{1,1}b_{0,2}}{2} + \frac{b_{0,2}{}^2}{2}\right)x}{-1 + a_{1,1}x + \left(a_{1,1}{}^2 - \frac{3\,a_{1,1}b_{0,2}}{2} + \frac{b_{0,2}{}^2}{2}\right)x^2} \\
g(x) &= \left(1 - a_{1,1}x - \left(a_{1,1}{}^2 - \frac{3\,a_{1,1}b_{0,2}}{2} + \frac{b_{0,2}{}^2}{2}\right)x^2\right)\left(x + \left(-\frac{b_{0,2}}{2} + \frac{a_{1,1}}{2}\right)x^2\right)
\end{aligned}
\right\},
\tag{3.65}
$$

for which we obtain the following linearizing change of coordinates

$$
\left.
\begin{aligned}
q(x) &= -\frac{(2 + a_{1,1}x - b_{0,2}x)\,x e^{2\,(a_{1,1}-b_{0,2})\frac{(A(x)-A(0))}{\sqrt{-5\,a_{1,1}{}^2+6\,a_{1,1}b_{0,2}-2\,b_{0,2}{}^2}}}}{\left(-2 + 2\,a_{1,1}x + 2\,a_{1,1}{}^2x^2 - 3\,x^2a_{1,1}b_{0,2} + x^2b_{0,2}{}^2\right)} \\
p(x, y) &= \frac{-2y\,q(x)}{(2 + a_{1,1}x - b_{0,2}x)\,x}
\end{aligned}
\right\}
\tag{3.66}
$$

where

$$
A(x) = \arctan\left(\frac{2\,a_{1,1}{}^2x - 3\,x\,a_{1,1}b_{0,2} + xb_{0,2}{}^2 + a_{1,1}}{\sqrt{-5\,a_{1,1}{}^2 + 6\,a_{1,1}b_{0,2} - 2\,b_{0,2}{}^2}}\right).
\tag{3.67}
$$

2. Consider system (3.31) from Theorem 14. In this case the functions f and g are

$$
\left.
\begin{aligned}
f(x) &= -6\,\frac{b_{2,0}}{1 + 2\,b_{2,0}x} \\
g(x) &= x\left(2\,b_{2,0}{}^2x^2 + 3\,b_{2,0}x + 1\right)
\end{aligned}
\right\},
\tag{3.68}
$$

for which we obtain the following linearizing change of coordinates

$$\left.\begin{aligned} q(x) &= \frac{x\,(b_{2,0}x+1)}{(1+2\,b_{2,0}x)^2} \\ p(x,y) &= \frac{-y+x^2}{(1+2\,b_{2,0}x)^2} \end{aligned}\right\}.$$

(3.69)

Quartic examples

1. As a quartic example we consider the system III of Theorem 3.1 of [30]. We choose the following restrictions on the parameters $a_{21} = -3, b_{0,2} = -4, b_{20} = \frac{1}{2}$ to obtain simple, presentable expressions for linearizing variables.

$$\left.\begin{aligned} \dot{x} &= -y - 3\,xy - 3\,x^2y - x^3y \\ \dot{y} &= x + \frac{1}{2}\,x^2 - 4\,y^2 - 4\,xy^2 - 2\,x^2y^2 \end{aligned}\right\}.$$

(3.70)

In this case the functions f and g are

$$\left.\begin{aligned} f(x) &= -\frac{7 + 10\,x + 5\,x^2}{1 + 3\,x + 3\,x^2 + x^3} \\ g(x) &= \frac{1}{2}\,\left(1 + 3\,x + 3\,x^2 + x^3\right) x\,(2+x) \end{aligned}\right\},$$

(3.71)

for which we obtain the following linearizing change of coordinates

$$\left.\begin{aligned} q(x) &= \frac{1}{2}\,x\,(2+x)\,\mathrm{e}^{-\frac{x(2+x)}{(1+x)^2}}\,(1+x)^{-2} \\ p(x,y) &= -y\mathrm{e}^{-\frac{x(2+x)}{(1+x)^2}}\,(1+x)^{-2} \end{aligned}\right\}.$$

(3.72)

2. We consider the system (3.57) of Theorem 15.

In this case the functions f and g are

$$\left.\begin{aligned} f(x) &= \frac{4\,a_{1,1}{}^2x - 6\,xb_{0,2}a_{1,1} + 2\,xb_{0,2}{}^2 + a_{1,1} + b_{0,2}}{1 - a_{1,1}x - a_{1,1}{}^2x^2 + 3/2\,x^2b_{0,2}a_{1,1} - 1/2\,x^2b_{0,2}{}^2} \\ g(x) &= -1/4\,x\,(a_{1,1}x - xb_{0,2} + 2)\,\left(-2 + 2\,a_{1,1}x + 2\,a_{1,1}{}^2x^2 - 3\,x^2b_{0,2}a_{1,1} + x^2b_{0,2}{}^2\right) \end{aligned}\right\},$$

(3.73)

for which we obtain the following linearizing change of coordinates

$$\left.\begin{aligned} q(x) &= -\frac{x\,(a_{1,1}x - xb_{0,2} + 2)\,S\,(x)}{-2 + 2\,a_{1,1}x + 2\,a_{1,1}{}^2x^2 - 3\,x^2b_{0,2}a_{1,1} + x^2b_{0,2}{}^2} \\ p(x,y) &= 2\,\frac{\left(x^2 - y\right) S\,(x)}{-2 + 2\,a_{1,1}x + 2\,a_{1,1}{}^2x^2 - 3\,x^2b_{0,2}a_{1,1} + x^2b_{0,2}{}^2} \end{aligned}\right\},$$

(3.74)

where

$$S\,(x) = e^{\dfrac{2\,(a_{1,1}-b_{0,2})\,\left(\arctan\left(\dfrac{2\,a_{1,1}{}^2x - 3\,xb_{0,2}a_{1,1} + xb_{0,2}{}^2 + a_{1,1}}{\sqrt{-5\,a_{1,1}{}^2 + 6\,b_{0,2}a_{1,1} - 2\,b_{0,2}{}^2}}\right) - \arctan\left(\dfrac{a_{1,1}}{\sqrt{-5\,a_{1,1}{}^2 + 6\,b_{0,2}a_{1,1} - 2\,b_{0,2}{}^2}}\right)\right)}{\sqrt{-5\,a_{1,1}{}^2 + 6\,b_{0,2}a_{1,1} - 2\,b_{0,2}{}^2}}}.$$

A rational example

Let us consider the system

$$\left.\begin{aligned}\dot{x} &= -y + \frac{yx}{1+x} \\ \dot{y} &= x + \frac{y^2}{1+x}\end{aligned}\right\}. \tag{3.75}$$

In this case the functions f and g are

$$\left.\begin{aligned}f(x) &= \frac{2+x}{1+x} \\ g(x) &= \frac{x}{1+x}\end{aligned}\right\}, \tag{3.76}$$

for which we obtain the following linearizing change of coordinates

$$\left.\begin{aligned}q(x) &= xe^x \\ p(x,y) &= ye^x\,(1+x)\end{aligned}\right\}. \tag{3.77}$$

3.5.3 Comments

It is really astonishing that in all above cases the linearizing variables (p, q) are always expressed in "finite terms". This follows from the fact that if $g'(x) + f(x)\,g(x) = 1$ then $f = \frac{1-g'}{g}$. Moreover, as $g(0) = 0$ and $g'(0) = 1$ the singularity of f at zero is spurious. In all examples considered in this and related chapters [62, 63, 30] f and g always are rational functions. Then $F(x) = \int_0^x f(s)\,ds$ is expressed in "finite terms" and thus also $p(x, \dot{x})$. The problem is slightly more delicate in what concerns $q(x)$. But $\int e^{F(s)}\,ds = \int e^{\int f(s)\,ds}\,ds = \int e^{\int \frac{1-g'(s)}{g(s)}\,ds}\,ds = \int \frac{1}{g(s)}e^{\int \frac{1}{g(s)}\,ds}\,ds = e^{\int \frac{1}{g(s)}\,ds} + const.$ g being a rational function, $\int \frac{ds}{g(s)}$ is obtained in "finite terms" and thus also $\int e^{F(s)}\,ds$.

Amplitude Independent Frequency Synchroniser for a Cubic Planar Polynomial System

This work reproduces the results of [28] in which the isochronicity is seen as a synchronization property. Nonlinear feedbacks (monomials) are used to synchronize a coupled system of two agents. The chapter aim is to provide some insights on the use of (only) nonlinear interconnexions to design a realization qualitatively enabling a desired behavior. The problem of local linearizability of the planar linear center perturbed by a cubic nonlinearity in the whole system of parameters (14 parameters) is far from being solved. Synchronization problem [174, 24] consists in bringing appropriate modifications on a given system to obtain a desired dynamic. The desired phase portrait throughout this paper contains a compact region around a singular point at the origin in which lies periodic orbits with the same period (independently from the chosen initial conditions). In this paper, starting from a 5-parameters non isochronous Chouikha cubic system [62], we identify all possible monomial perturbations of degree $d \in \{2, 3\}$ insuring local linearizability of the perturbed system. The necessary conditions are obtained by the Normal Forms method. These conditions are real algebraic equations (multivariate polynomials) in the parameters of the studied ordinary differential system. The efficient algorithm FGb [93] for computing the Gröbner basis is used. For the family studied in this paper, an exhaustive list of possible parameters values insuring local linearizability is established. All the found cases are already known in the literature but the context is different since our goal is the synchronisation not the classification. This paper can be seen as a direct continuation of several new works concerned with the hinting of cubic isochronous centers in particular [62, 56, 63, 30, 15, 14], as it may also be considered an adaptation of a qualitative theory method to a synchronization problem.

4.1 Problem statement

We consider the planar dynamical system,

$$\frac{dx}{dt} = \dot{x} = X(x, y), \qquad \frac{dy}{dt} = \dot{y} = Y(x, y), \tag{4.1}$$

where (x, y) belongs to an open connected subset $U \subset \mathbb{R}^2$, $X, Y \in C^k(U, \mathbb{R})$, and $k \geq 1$. Due to Poincaré : an isolated singular point $p \in U$ of (4.1) is a center if and only if there exists a punctured neighborhood $V \subset U$ of p such that every orbit in V is a cycle surrounding p. A center is said to be *isochronous* if all the orbits surrounding it have the same period. An overview of J.Chavarriga and M.Sabatini [52] present the methods and basic results concerning the problem of the isochronicity, see also [66, 62, 14, 30, 15].

Synchronization problem consists in bringing appropriate modifications on a given system to obtain a desired dynamic, see [174, 24]. Along this paper, the desired phase portrait contains a compact region around a singular point at the origin in which lies periodic orbits with the same period (independently from the chosen initial conditions which is not always the case). More concretely, in this paper we consider the following problem ; Starting from a non isochronous polynomial planar system, are there any polynomial perturbation which insures the local linearizability of the perturbed system. In this paper we adopt the normal forms method often used in qualitative theory investigations ; center-focus problem, bifurcation problem and local linearizability problem. The problem of local linearizability conditions of of the planar linear center perturbed by cubic nonlinearities (in all generalities on the system parameters 14 parameters) is far from being solved.

In this paper, starting from a 5-parameters non isochronous Chouikha cubic system [62], we identify all possible monomial perturbations of degree $d \in \{2, 3\}$ insuring local linearizability of the perturbed system. Investigations are based on the normal forms Theory.

In the following system as well as in all other considered systems, all parameters are reals.

Consider the real Lièrnard Type equation

$$\ddot{x} + f(x)\dot{x}^2 + g(x) = 0 \tag{4.2}$$

or equivalently its associated two dimensional (planar) system

$$\left. \begin{array}{l} \dot{x} = y \\ \dot{y} = -g(x) - f(x)y^2 \end{array} \right\} \tag{4.3}$$

The study of isochronicity of (4.2) was established first in M. Sabatini paper [194]. The sufficient conditions of the isochronicity of the origin O for system (4.3) with f and g of class C^1 are given. In the analytic case, the necessary and sufficient conditions for isochronicity are given by A.R.Chouikha in [62]. In the same paper, the author implemented a new algorithmic method for computing isochronicity conditions for system (4.3) called C-algorithm. As an application of this algorithm, the author studied the following cubic system

$$\left. \begin{array}{l} \dot{x} = -y + \tilde{a}_{1,2,1}x^2y \\ \dot{y} = x + \tilde{a}_{2,2,0}x^2 + \tilde{a}_{2,0,2}y^2 + \tilde{a}_{2,3,0}x^3 + \tilde{a}_{2,1,2}xy^2 \end{array} \right\} \tag{4.4}$$

where all the parameters values for which system (4.4) has an isochronous center at
the origin are established in the following theorem.

We note that the coefficient $a_{i,j,k}$ denotes the parameter of the monomial per-
turbation of the ith equation of the linear isochronous center ($\dot{x} = -y$, $\dot{y} = x$) of
degree j in x and of degree k in y

Theorem 18 (Chouikha,[62])**.** *System* (4.4) *has an isochronous center at* 0 *if and
only if its parameters satisfy one of the following conditions*

    1. $\tilde{a}_{2,3,0} = -(2/3)\tilde{a}_{1,2,1}$, $\tilde{a}_{2,1,2} = 3\tilde{a}_{1,2,1}$, $\tilde{a}_{2,2,0} = \tilde{a}_{2,0,2} = 0$

    2. $\tilde{a}_{2,1,2} = \tilde{a}_{1,2,1}$, $\tilde{a}_{2,2,0} = \tilde{a}_{2,3,0} = \tilde{a}_{2,0,2} = 0$

    3. $\tilde{a}_{2,3,0} = (1/14)\tilde{a}_{2,0,2}^2$, $\tilde{a}_{2,1,2} = (3/7)\tilde{a}_{2,0,2}^2$, $\tilde{a}_{1,2,1} = (1/7)\tilde{a}_{2,0,2}^2$, $\tilde{a}_{2,2,0} = -(1/2)\tilde{a}_{2,0,2}$

    4. $\tilde{a}_{2,1,2} = \tilde{a}_{2,0,2}^2$, $\tilde{a}_{2,3,0} = 0$, $\tilde{a}_{1,2,1} = (1/2)\tilde{a}_{2,0,2}^2$, $\tilde{a}_{2,2,0} = -(1/2)\tilde{a}_{2,0,2}$.

A 1-parameter perturbation of system (4.4) is studied in [63]. Namely, the follo-
wing system

$$\left.\begin{array}{l} \dot{x} = -y + \underline{a_{1,1,1}xy} + a_{1,2,1}x^2y \\ \dot{y} = x + a_{2,2,0}x^2 + a_{2,0,2}y^2 + a_{2,3,0}x^3 + a_{2,1,2}xy^2 \end{array}\right\} \qquad (4.5)$$

which is system (4.4) perturbed by the underlined term. All the values of the pa-
rameters for which the above system (4.5) has an isochronous center at the origin
were found.
Note that the above system stills reducible to the Liénard type equation for wich
C-algorithm is applicable, see [30].

Section 2 is devoted to recall the head lines of the methodology of the Normal
Forms algorithm, called in the sequel NF algorithm, which will allow us to obtain
isochronicity necessary conditions.

The last section is concerned with the main result, which is an application of the
NF method. Indeed, we consider an unknown 1-directional monomial perturbation
of degree two or three of the system (4.4), namely

$$\left.\begin{array}{l} \dot{x} = -y + a_{1,2,1}x^2y + \underline{\Psi_1(x,y)} \\ \dot{y} = x + a_{2,2,0}x^2 + a_{2,0,2}y^2 + a_{2,3,0}x^3 + a_{2,1,2}xy^2 + \underline{\Psi_2(x,y)} \end{array}\right\}, \qquad (4.6)$$

in which only one of the monomials Ψ_1 or Ψ_2 is non zero monomial ($\Psi_1\Psi_2 = 0$) of
degree $d \in \{2, 3\}$.

The problem turns to study eight polynomial cubic systems which are not re-
ducible by the transformations described in [30] to Liénard type equation. For each
system, we identify the values of the parameters for which the singular point at thea
origin is an isochronous center. Hence it is done for (4.6).

4.2 The normal forms method

The normal form theory which is due essentially to Poincaré, presents a basic
tool in understanding the qualitative behavior of orbit structures of a vector field

near equilibria [111]. It was used for the study of center conditions and the nature of bifurcation of a given vector field. We also recall a pioneer work in this field established by Pleshkan (see[175]), in which the author presented an investigation method of isochronicity in the case of linear center perturbed by homogeneous cubic nonlinearity. The principle of Pleshkan's algorithm is very close to the one presented in Algaba et.al paper [5], where the normal form theory is used in the analysis of isochronicity and gave a recursive method for the isochronicity investigation. In the last cited paper, the autors studied cubic Liénard equation and obtained a characterization of the reversible Liénard equation having an isochronous center at the origin.

Let $x = (x_1, x_2) \in \mathbb{R}^2$ and $f(x_1, x_2) \in \mathbb{R}[x_1, x_2] \times \mathbb{R}[x_1, x_2]$ and consider the general planar system

$$\dot{x} = Lx + f(x) = Lx + f_2(x) + f_3(x) + \ldots + f_k(x) + \ldots, \tag{4.7}$$

where Lx represents the linear part, L the Jacobian matrix associated to system (4.7) and $f_k(x)$ denotes the kth order vector homogeneous polynomials of x. We assume that the system admits an equilibrium at the origin O. The essential idea of the Normal Form theory is to find a near identity transformation

$$x = y + h(y) = y + h_2(y) + h_3(y) + \ldots + h_k(y) + \ldots, \tag{4.8}$$

by which the resulting system

$$\dot{y} = Ly + g(x) = Ly + g_2(y) + g_3(y) + \ldots + g_k(y) + \ldots, \tag{4.9}$$

becomes as simple as possible. In this sense, the terms that are not essential in the local dynamical behavior are removed from the analytical expression of the vector field. Let us denote by $h_k(y)$ and $g_k(y)$ the kth order vectors homogeneous polynomials of y. According to Takens normal form theory, we define an operator as follows :

$$L_k : H_k \to H_k, \quad U_k \in H_k \mapsto L_k(U_k) = [U_k, u_1] \in H_k \tag{4.10}$$

where $u_1 = Ly$ is the linear part of the vector field and H_k denotes a linear vector space containing the kth degree homogeneous vector polynomials of $y = (y_1, y_2)$. The operator $[.,.]$ is called the Lie Bracket, defined by

$$[U_k, u_1] = LU_k - D(U_k)u_1$$

where D denotes the frechet derivative.

Next, we define the spaces R_k and K_k as the range of L_k and the complementary space of R_k respectively. Thus, $H_k = R_k + K_k$ and one can then choose bases for K_k and R_k. The normal form theorem determines how it is possible to reduce the analytic expression of the vector field (see Gukenheimer-Holmes [111]). The authors give explicitly an analysis for the quadratic and the cubic cases. Consequently, a

vector homogeneous polynomial $f_k \in H_k$ can be split into two parts, such that one of them can be spanned in K_k and the remaining part in R_k.

Normal form theory shows that the part belonging to R_k can be eliminated and the remaining part can be retained in the normal form. By the equations (4.7), (4.8) and (4.9), we can obtain algebraic equations one order after another.

Theorem 19 ([222]). *The recursive formula for computing the normal form coefficients and the nonlinear transformation are given by :*

$$g_k = f_k + [h_k, Ly] + \sum_{i=2}^{k-1}(Df_i h_{k-i+1} - Dh_{k-i+1}g_i)$$

$$+ \sum_{i=2}^{[k/2]} \frac{551}{i!} \sum_{j=i}^{k-i} D^i f_j \sum_{\substack{l_1+l_2+\ldots+l_i=k-(j-i) \\ 2 \le l_1,l_2,\ldots,l_i \le k+2-(i+j)}} h_{l_1} h_{l_2} \ldots h_{l_i},$$

for $k = 2, 3, \ldots$

see also [179, 221].

System (4.9) can be transformed to the polar coordinate system with $y_1 = rcos(\theta), y_2 = rsin(\theta)$ so that

$$\dot{r} = \sum_{j=1}^{N} \alpha_{2j+1} r^{2j+1} + O(r^{2N+3}), \ \dot{\theta} = 1 + \sum_{j=1}^{N} \beta_{2j+1} r^{2j} + O(r2N+2). \quad (4.11)$$

Recall that a necessary condition to have a center at the origin is that all the focal values α_{2j+1} vanish. By the Hilbert's basis theorem, the set of focal values has a finite basis in the ring of polynomials in the coefficients of the initial system (4.7). Since the non vanishing of one of the angular component coefficient implies dependency of an associated period constant, a necessary condition for which this center is isochronous is that β_{2j+1} vanish.

Recall that our study is motivated by the interest of describing a synchronizer for a desired dynamic but also to underline the key role that can the classification of centers and isochronous centers of polynomial systems have in applications such that synchronization problems.

4.3 Main results : Applications of the NF algorithm to characterize cubic systems with linearizable center

In our study, we use *Maple*. To compute the Gröbner basis of the obtained polynomial equations in the ring of characteristic 0, we employ the *Salsa Software* [93]. More precisely we use the *FGb* algorithm which is the most efficient algorithm in computing Gröbner basis [19], at least for the polynomial systems studied in this paper. We note also that we have used DRL ordering in all computations established in this paper.

Since our approach in investigation of isochronicity conditions is based on an algorithmic method, then we can guess that every simplification is beneficial in the goal of speeding the computations and reducing the necessary memory size. Solving multivariate algebraic equations (real polynomials) can be a very hard task if we try to manipulate the polynomial equations without tricks. Interested readers can find in the website of *Salsa Software* [93], more precisely the page of J.C.Faugère, some important rules in solving polynomial systems and about Gröbner basis.

Let us consider the more general cubic perturbation of linear center :

$$\left.\begin{array}{l}\dot{x} = y + a_{1,2,0}x^2 + a_{1,0,2}y^2 + a_{1,1,1}xy + a_{1,3,0}x^3 + a_{1,2,1}x^2y + a_{1,1,2}xy^2 + a_{1,0,3}y^3 \\ \dot{y} = -x + a_{2,2,0}x^2 + a_{2,0,2}y^2 + a_{2,1,1}xy + a_{2,30}x^3 + a_{2,2,1}x^2y + a_{2,1,2}xy^2 + a_{2,0,3}y^3\end{array}\right\}$$
$$(4.12)$$

or equivalently the following one :

$$\left.\begin{array}{l}\dot{x} = -y + \tilde{a}_{1,2,0}x^2 + \tilde{a}_{1,0,2}y^2 + \tilde{a}_{1,1,1}xy + \tilde{a}_{1,3,0}x^3 + \tilde{a}_{1,2,1}x^2y + \tilde{a}_{1,1,2}xy^2 + \tilde{a}_{1,0,3}y^3 \\ \dot{y} = x + \tilde{a}_{2,2,0}x^2 + \tilde{a}_{2,0,2}y^2 + \tilde{a}_{2,1,1}xy + \tilde{a}_{2,30}x^3 + \tilde{a}_{2,2,1}x^2y + \tilde{a}_{2,1,2}xy^2 + \tilde{a}_{2,0,3}y^3\end{array}\right\}.$$

Observe that we can easily reconstruct the coefficient $\tilde{a}_{i,j,k}$ from the ones in (4.12) by the change of coordinates $(x, y) \mapsto (-x, y)$.

The classification of all the isochronous centers of the above system is a very hard task. By any recursive method from those quoted in [52], solving the isochronicity problem for system (4.12) is very difficult in the sense of solving multivariate polynomials. Here, the variables are the 14 parameters of the polynomial differential system (4.12). Hence it needs very important computation supports.

With a realistic point of view, several authors have chosen some particular cases of the above system for investigation like the homogeneous cubic perturbations of the linear center [175, 52] and time reversible cubic systems [56, 100].

In our case, we focus on an unknown 1-directional 1-parameter perturbation of the system (4.4) which is system (4.6). Therefore, we ramify our study to all possible cases.

In the sequel, every subsection will be concerned with a possible 1-parameter perturbation of system (4.4).

Recall that $a_{i,j,k}$ denotes the parameter of the monomial perturbation of the ith equation in system (4.4) of degree j in x and of degree k in y.

4.3.1   perturbation $a_{1,1,1}$

As a continuation of the result of [62] on system (4.4), the authors in [63] investigated a 1-parameter perturbation of (4.4) which is (4.5).

Theorem 20 ([63]). *System* (4.5) *has an isochronous center at the origin O if and only if*

$$a_{1,2,1} = \frac{-a_{1,1,1} + a_{1,1,1}a_{2,2,0} - 10a_{2,2,0}^2 + 5a_{1,1,1}a_{2,0,2} - 10a_{2,0,2}a_{2,0,2} - 4a_{2,0,2}^2 + 9a_{2,3,0} + 3a_{2,1,2}}{3} \quad and$$

it's parameters satisfy one of the following sets of conditions

1. $2a_{2,2,0} + a_{2,0,2} - a_{1,1,1} = 0$
   $a_{2,0,2}^2 - 3a_{2,0,2}a_{1,1,1} + 2a_{1,1,1}^2 - 6a_{2,3,0} - \frac{4a_{2,1,2}}{3} = 0$
   $a_{2,0,2}a_{2,3,0} - 3a_{2,3,0}a_{1,1,1} + \frac{a_{2,1,2}a_{1,1,1}}{6} - \frac{a_{2,0,2}a_{2,1,2}}{6} = 0$
   $a_{2,3,0}^2 a_{1,1,1}^2 - 3a_{2,3,0}^2 + \frac{a_{1,1,1}^2 a_{2,3,0}a_{2,1,2}}{6} + \frac{a_{2,3,0}^2 a_{2,1,2}}{3} + \frac{5a_{2,1,2}^2 a_{2,3,0}}{36} - \frac{a_{2,1,2}^3}{5} = 0$
   $a_{2,1,2}a_{1,1,1}a_{2,0,2} + 6a_{2,3,0}a_{1,1,1}^2 - a_{2,1,2}a_{1,1,1}^2 - 18a_{2,3,0}^2 - a_{2,3,0}a_{2,1,2} + \frac{2a_{2,1,2}^2}{3} = 0$

2. $a_{2,1,2} = 0$ *and*

   (a) $a_{2,3,0} = a_{2,0,2} - 1/4a_{1,1,1} = a_{2,2,0} = 0$

   (b) $4a_{2,3,0} - 3a_{1,1,1} = a_{2,2,0} + a_{1,1,1} = a_{1,1,1}^2 - 3a_{2,3,0} = 0$

   (c) $a_{2,0,2} - 2a_{1,1,1} = a_{2,3,0} - a_{1,1,1}^2 = a_{2,2,0} + 2a_{1,1,1} = 0$

   (d) $a_{2,0,2} - 1/3a_{1,1,1} = a_{2,2,0} + 2/3a_{1,1,1} = 9/2a_{2,3,0} - a_{1,1,1}^2 = 0$

3. $a_{2,3,0} = 0$ *and*

   (a) $a_{2,2,0} + 1/2a_{2,0,2} - 1/2a_{1,1,1} = a_{2,0,2}^2 - 3a_{2,0,2}a_{1,1,1} + 2a_{1,1,1}^2 - a_{2,1,2} = 0$

   (b) $2a_{2,0,2} - a_{1,1,1} = 2a_{2,2,0} + a_{1,1,1} = 0$

   (c) $a_{2,0,2} - a_{1,1,1} = a_{2,2,0} = 0$

   (d) $a_{2,0,2} = a_{1,1,1}^2 - 9a_{2,1,2} = a_{2,2,0} = 0$

We contribute by classifying the isochronous centers of all the remaining 1-parameter perturbations of system (4.4). Eight systems are studied to do this. For these perturbations, first, we check if the center (at the origin O) conditions are satisfied and after we give necessary and sufficient isochronicity conditions depending only on the six real parameters.

4.3.2   Perturbation $a_{1,0,3}$

We are concerned by the following system

$$\left.\begin{array}{l} \dot{x} = y + a_{1,2,1}x^2 y + \underline{a_{1,0,3}y^3} \\ \dot{y} = -x + a_{2,2,0}x^2 + a_{2,0,2}y^2 + a_{2,3,0}x^3 + a_{2,1,2}xy^2 \end{array}\right\} \tag{4.13}$$

Lemma 1. *The investigation of isochronicity criteria of system* (4.13) *reduces to the investigation in the following three cases*

1. $a_{1,0,3} = 0$
2. $a_{1,0,3} = 1$
3. $a_{1,0,3} = -1$

For the case $a_{1,0,3} \neq 0$, two cases are to be analyzed.
First we assume that $a_{1,0,3} > 0$. We use on (4.13) the change of coordinates :

$$(x, y) \mapsto a_{1,0,3}^{1/2}(x, y) \tag{4.14}$$

to obtain

$$\left.\begin{aligned}
\dot{x} &= y + \frac{a_{1,2,1}}{a_{1,0,3}}x^2 y + y^3 \\
\dot{y} &= -x + \frac{a_{2,2,0}}{a_{1,0,3}^{1/2}}x^2 + \frac{a_{2,0,2}}{a_{1,0,3}^{1/2}}y^2 + \frac{a_{2,3,0}}{a_{1,0,3}}x^2 + \frac{a_{2,1,2}}{a_{1,0,3}}xy^2
\end{aligned}\right\} . \tag{4.15}$$

When the solutions of the isochronicity problem of system (4.15) are established, we can easily reconstruct those of the original system (4.13) by the transformation

$$(x,y) \mapsto (1/a_{1,0,3}^{1/2})(x,y). \tag{4.16}$$

If $a_{1,0,3} < 0$, then (4.13) can be written as

$$\left.\begin{aligned}
\dot{x} &= y + a_{1,2,1}x^2 y - \tilde{a}_{1,0,3}y^3 \\
\dot{y} &= -x + a_{2,2,0}x^2 + a_{2,0,2}y^2 + a_{2,3,0}x^3 + a_{2,1,2}xy^2
\end{aligned}\right\}$$

with $-a_{1,0,3} = \tilde{a}_{1,0,3} > 0$. Applying the following change of coordinates

$$(x,y) \mapsto \tilde{a}_{1,0,3}^{1/2}(x,y) \tag{4.17}$$

yields

$$\left.\begin{aligned}
\dot{x} &= y + \frac{a_{1,2,1}}{\tilde{a}_{1,0,3}}x^2 y - y^3 \\
\dot{y} &= -x + \frac{a_{2,2,0}}{\tilde{a}_{1,0,3}^{1/2}}x^2 + \frac{a_{2,0,2}}{\tilde{a}_{1,0,3}^{1/2}}y^2 + \frac{a_{2,3,0}}{\tilde{a}_{1,0,3}}x^2 + \frac{a_{2,1,2}}{\tilde{a}_{1,0,3}}xy^2
\end{aligned}\right\} . \tag{4.18}$$

The reconstruction of the solutions of (4.13) can be obtained from those of (4.18), by the change of coordinates

$$(x,y) \mapsto (1/\tilde{a}_{1,0,3}^{1/2})(x,y).$$

Remark 1. If one is concerned with quadratic perturbations of system (4.4) with the parameter $a_{i,j,2-j}$
    we can consider the two cases namely,

    1. $a_{i,j,2-j} = 0$

    2. $a_{i,j,2-j} = 1$

Indeed, when $a_{i,j,2-j} \neq 0$, the change of coordinates

$$(x,y) \mapsto a_{i,j,2-j}(x,y)$$

reduces the problem to the case $a_{i,j,2-j} = 1$.
    Lastly, thanks to the transformation

$$(x,y) \mapsto 1/a_{i,j,2-j}(x,y),$$

we can easily reconstruct the solutions of the problem when $a_{i,j,2-j} \neq 0$.

Theorem 21. *System (4.13) has an isochronous center at O if and only if its parameters satisfy one of the following conditions :*

1. $a_{1,0,3} = 0$

   (a) $a_{1,2,1} = a_{2,1,2}, a_{2,2,0} = a_{2,0,2} = a_{2,3,0} = 0$

   (b) $a_{1,2,1} = -3/2\, a_{2,3,0},\ a_{2,1,2} = -9/2\, a_{2,3,0},\ a_{2,2,0} = a_{2,0,2} = 0$

   (c) $a_{1,2,1} = a_{2,2,0} = -1/2,\ a_{2,0,2} = 1,\ a_{2,1,2} = -1,\ a_{2,3,0} = 0$

   (d) $a_{1,2,1} = -1/7,\ a_{2,2,0} = -1/2,\ a_{2,0,2} = 1,$
      $a_{2,3,0} = -1/14,\ a_{2,1,2} = -3/7$

2. $a_{1,0,3} = 1$

   (a) $a_{1,2,1} = -9/2,\ a_{2,1,2} = -3/2,\ a_{2,2,0} = a_{2,0,2} = a_{2,3,0} = 0$

   (b) $a_{2,3,0} = 1,\ a_{1,2,1} = a_{2,1,2} = -3,\ a_{2,2,0} = a_{2,0,2} = 0$

   (c) $a_{2,0,2} = -3/2,\ a_{2,3,0} = 0,\ a_{2,1,2} = a_{1,2,1} = a_{2,2,0} = 0$

   (d) $a_{2,0,2} = 3/2,\ a_{2,3,0} = 0,\ a_{2,1,2} = a_{1,2,1} = a_{2,2,0} = 0$

   (e) $a_{1,2,1} = -1, a_{2,2,0} = a_{2,0,2} = \pm\frac{\sqrt{2}}{2}, a_{2,1,2} = -2,\ a_{2,3,0} = 0,$

3. $a_{1,0,3} = -1$

   (a) $a_{2,3,0} = -1,\ a_{1,2,1} = a_{2,1,2} = 3,\ a_{2,2,0} = a_{2,0,2} = 0$

   (b) $a_{1,2,1} = 9/2, a_{2,1,2} = 3/2, a_{2,3,0} = a_{2,2,0} = a_{2,0,2} = 0$

In this proof, we do not present the algorithm generated polynomials which are too long.

We use the strategy given in lemma 2. We note also that we investigate only the real values of the parameters for which system (4.13) has an isochronous center at the origin.

1. Assume $a_{1,0,3} = 0$ and then solve the isochronicity problem for system (4.13) under this assumption. We use the following change of coordinates $(x, y) \mapsto (-x, y)$ to obtain system (4.4) studied in [62]. The investigation following the two cases :

   (a) $a_{2,0,2} = 0$

   (b) $a_{2,0,2} = 1$

   covers, (with respect to a linear change of coordinates), all the values of the parameters for which the center at the origin of system (4.4), see Remark 1. In [62], the author used C-algorithm which characterizes isochronicity by establishing associated Urabe function.

2. Consider the case $a_{1,0,3} = 1$. Computations of normal forms of the initial system in polar form give (4.11)

$$\dot{r} = \sum_{j=1}^{N} \alpha_{2j+1} r^{2j+1} + O(r^{2N+3}),\ \dot{\theta} = 1 + \sum_{j=1}^{N} \beta_{2j+1} r^{2j} + O(r^{2N+2})$$

we obtain in the radial component $\alpha_{2j+1} = 0$ until order $N = 6$. So that the first six necessary conditions to have a center are satisfied. Analyzing isochronicity involves the angular component. Using *FGb* for computing the

Gröbner basis of the obtained first six quantities in the angular component, we obtain a Gröbner basis of 27 polynomials denoted G_1 such that it's first element is

$$-a_{2,3,0}\, a_{2,2,0}\left(-a_{2,1,2}^2 + 9\, a_{2,3,0}\right).$$

Then we analyze the isochronicity problem in the following three cases, which are given by the vanishing of one factor of the above expression.

(a) $a_{2,3,0} = 0$, we substitute this condition into G_1 we compute again the associated Gröbner basis, we obtain a basis of 14 polynomials, when we solve it we obtain the following four real solutions to the problem :

   i. $a_{1,0,3} = 1$, $a_{2,1,2} = -3/2$, $a_{1,2,1} = -9/2$, $a_{2,3,0} = a_{2,2,0} = a_{2,0,2} = 0$

   ii. $a_{1,0,3} = 1$, $a_{2,0,2} = 3/2$, $a_{2,3,0} = a_{1,2,1} = a_{2,2,0} = a_{2,1,2} = 0$

   iii. $a_{1,0,3} = 1$, $a_{2,0,2} = -3/2$, $a_{2,3,0} = a_{1,2,1} = a_{2,2,0} = a_{2,1,2} = 0$

   iv. $a_{1,0,3} = 1$, $a_{1,2,1} = -1$, $a_{2,2,0} = a_{2,0,2} = \pm\frac{\sqrt{2}}{2}$, $a_{2,1,2} = -2$

(b) For $a_{2,2,0} = 0$, substituting this assumption in G_1, and computing it's associated Gröbner basis which contains 7 polynomials, after solving it we obtain the solutions :

   i. $a_{1,0,3} = 1$, $a_{2,0,2} = 3/2$, $a_{2,2,0} = a_{1,2,1} = a_{2,3,0} = a_{2,1,2} = 0$

   ii. $a_{1,0,3} = 1$, $a_{2,0,2} = -3/2$, $a_{2,2,0} = a_{1,2,1} = a_{2,3,0} = a_{2,1,2} = 0$

   iii. $a_{1,0,3} = 1$, $a_{2,1,2} = -3/2$, $a_{1,2,1} = -9/2$, $a_{2,2,0} = a_{2,3,0} = a_{2,0,2} = 0$

   iv. $a_{1,0,3} = a_{2,3,0} = 1$, $a_{2,1,2} = a_{1,2,1} = -3$, $a_{2,2,0} = a_{2,0,2} = 0$

(c) Similarly for $a_{2,3,0} = (1/9)a_{2,1,2}^2$, we obtain the solutions

   i. $a_{1,0,3} = 1$, $a_{2,0,2} = -3/2$, $a_{2,2,0} = a_{1,2,1} = a_{2,3,0} = a_{2,1,2} = 0$

   ii. $a_{1,0,3} = 1$, $a_{2,0,2} = 3/2$, $a_{2,2,0} = a_{1,2,1} = a_{2,3,0} = a_{2,1,2} = 0$

   iii. $a_{1,0,3} = a_{2,3,0} = 1$, $a_{2,1,2} = a_{1,2,1} = -3$, $a_{2,2,0} = a_{2,0,2} = 0$

It's easy to see that several solutions are repeated above. For example cases $(10.11 \equiv 2(b)i)$ and $(2(a)iii \equiv 2(b)ii)$. We claim that there are only 5 solutions to the problem when $a_{1,0,3} = 1$ which are given in the theorem.

Analysis of the theorem cases with $a_{1,0,3} = 1$

— 2a- In this case system (4.13) reduces to

$$\left.\begin{aligned} \dot{x} &= y - 9/2yx^2 + y^3 \\ \dot{y} &= -x - 3/2xy^2 \end{aligned}\right\}$$

which is a cubic homogeneous perturbation of linear center with isochronous center at the origin. Indeed, we use the change of coordinates $(x, y) \mapsto (\frac{y}{\sqrt{2}}, \frac{x}{\sqrt{2}})$ we obtain system $\tilde{S}^*_3$ given in [52, 175]. A first integral, a linearizing change of coordinate and a transversal commuting system are established for homogeneous perturbations (see[145, 52]).

— 2b- System (4.13) reduces to

$$\left.\begin{array}{l} \dot{x} = y - 3\,x^2 y + y^3 \\ \dot{y} = -x + x^3 - 3\,xy^2 \end{array}\right\}$$

which is an homogeneous perturbation of linear center, by the change of coordinates $(x, y) \mapsto (y, x)$ reduces to system S^*_1 of [175, 145, 52].

— 2c- and 2d- For these two cases system (4.13) reduces to

$$\left.\begin{array}{l} \dot{x} = y + y^3 \\ \dot{y} = -x \pm 3/2\,y^2 \end{array}\right\}$$

We see that by the change of coordinate $(x, y) \mapsto (y, x)$, we have a Liénard systems $x'' + f(x)x' + g(x) = 0$ satisfying

$$g(x) = g'(0)x + \frac{551}{x^3}(\int_0^x sf(s)ds)^2 \tag{4.19}$$

then the origin is an isochronous center. See [61, 64, 5] for more details about characterization of isochronicity for Liénard equation.

— 2e- In this case system (4.13) is a time- reversible system with an isochronous center at O. Indeed, in polar coordinates it reduces to

$$\left.\begin{array}{l} \dot{r} = -1/2 \sin(\theta)\,r^2\sqrt{2} + 1/2\,r^3 \sin(2\,\theta) \\ \dot{\theta} = 1 + (-1/2 \cos(2\,\theta) + 1/2)\,r^2 - 1/2\,r \cos(\theta)\,\sqrt{2} \end{array}\right\}$$

which belongs to the family ii) (with $R_1 = r_1 = -\frac{\sqrt{2}}{2}$ if $a_{2,2,0} = a_{2,0,2} = \frac{\sqrt{2}}{2}$) and ($R_1 = r_1 = \frac{\sqrt{2}}{2}$ if $a_{2,2,0} = a_{2,0,2} = -\frac{\sqrt{2}}{2}$) of the theorem 8.11 in Garcia thesis, see also system CR_4 of [52].

3. $a_{1,0,3} = -1$. When executing the normal form *Maple* code, there is no change from the case $a_{1,0,3} = 1$: the coefficients of radial component of system (4.11) are such that $\alpha_{2j+1} = 0$ until order $N = 6$. The first six necessary conditions to have a center are satisfied. On a similar way as the case $a_{1,0,3} = 1$, for analyzing isochronicity we are concerned by the angular component. We compute the Gröbner basis ,denoted G_{-1}, of the obtained first six quantities in the angular component. We obtain an ideal of 27 polynomials such that its first element is

$$a_{2,2,0}a_{2,3,0}\left(a_{2,1,2}^2 + 9a_{2,3,0}\right).$$

Then we analyze the isochronicity problem in the following three cases, which are the vanishing of each of the factors of the above expression.

(a) For $a_{2,3,0} = 0$, we substitute this assumption in G_{-1}. We compute again the Gröbner basis associated to this case. We obtain a basis of 14 polynomials. when we solve it we obtain the unique real solution to the problem :

      i. $a_{1,0,3} = -1, a_{1,2,1} = 9/2, a_{2,1,2} = 3/2, a_{2,3,0} = a_{2,2,0} = a_{2,0,2} = 0$

(b) For $a_{2,2,0} = 0$ we do the same as for the last case and obtain the two real solutions

      i. $a_{1,0,3} = a_{2,3,0} = -1,\ a_{1,2,1} = a_{2,1,2} = 3,\ a_{2,2,0} = a_{2,0,2} = 0$

      ii. $a_{1,0,3} = -1, a_{1,2,1} = 9/2, a_{2,1,2} = 3/2, a_{2,3,0} = a_{2,2,0} = a_{2,0,2} = 0$

(c) $a_{2,3,0} = -(1/9)a_{2,1,2}^2$ in the same way as for the first and second cases we obtain

      i. $a_{1,0,3} = a_{2,3,0} = -1,\ a_{1,2,1} = a_{2,1,2} = 3,\ a_{2,2,0} = a_{2,0,2} = 0$

We conclude that in the case $a_{1,0,3} = -1$, we have only two solutions to the isochronicity problem.

Analysis of the theorem cases with $a_{1,0,3} = -1$

These two solutions are cubic homogeneous perturbations of the linear center, which can be found in [52].

— 3a- in this case, system (4.13) can be written

$$\left.\begin{aligned} \dot{x} &= y + 3\,x^2 y - y^3 \\ \dot{y} &= -x - x^3 + 3\,xy^2 \end{aligned}\right\}$$

  by the change of coordinates $(x, y) \mapsto (-x, -y)$, it reduces to system $S^*{}_1$ of [175, 145, 52], which have an isochronous center at the origin.

— 3b- system (4.13) can be written

$$\left.\begin{aligned} \dot{x} &= y + 9/2 yx^2 - y^3 \\ \dot{y} &= -x + 3/2 xy^2 \end{aligned}\right\}$$

  we use the change of coordinates $(x, y) \mapsto (\frac{y}{\sqrt{2}}, \frac{x}{\sqrt{2}})$ we obtain system $S^*{}_3$ with isochronous center at the origin O given in [52, 175].

That ends the proof.

4.3.3   Perturbation $a_{1,3,0}$

Consider the system

$$\left.\begin{aligned} \dot{x} &= y + a_{1,2,1}x^2 y + \underline{a_{1,3,0}x^3} \\ \dot{y} &= -x + a_{2,2,0}x^2 + a_{2,0,2}y^2 + a_{2,3,0}x^3 + a_{2,1,2}xy^2 \end{aligned}\right\} \qquad (4.20)$$

Theorem 22. *System* (4.20) *with $a_{1,3,0} \neq 0$ has no center at the origin. Moreover, system* (4.20) *has an isochronous center at the origin O if and only if it reduces to system* (4.4) *and its parameters satisfy one of isochronicity cases from those of Theorem 18.*

Analogously to lemma 2 we have to analyse $a_{1,3,0} = \pm 1$.

Executing the *Maple* code, which gives the normal form of (4.20) in it's polar form (4.11)

$$\dot{r} = \sum_{j=1}^{N} \alpha_{2j+1} r^{2j+1} + O(r^{2N+3}), \ \dot{\theta} = 1 + \sum_{j=1}^{N} \beta_{2j+1} r^{2j} + O(r^{2N+2})$$

we obtain in the radial component such that $\alpha_3 = \pm\frac{3}{8}$, then in this case, the singular point can not be a center.

4.3.4 Perturbation $a_{2,0,3}$

This perturbation represents system (4.4) perturbed by the additional monomial with the parameter $a_{2,0,3}$

$$\left.\begin{array}{l} \dot{x} = y + a_{1,2,1}x^2 y \\ \dot{y} = -x + a_{2,2,0}x^2 + a_{2,0,2}y^2 + a_{2,3,0}x^3 + a_{2,1,2}xy^2 + \underline{a_{2,0,3}y^3} \end{array}\right\} \tag{4.21}$$

Theorem 23. *System* (4.21) *with* $a_{2,0,3} \neq 0$ *has no center at the origin. Moreover, system* (4.21) *has an isochronous center at O if and only if it reduces to system* (4.4) *and its parameters satisfy one case of isochronicity conditions given in Theorem* (18)*.*

Analogously to lemma 2.

Consider $a_{2,0,3} = \pm 1$.

Executing the *Maple* code, which gives the normal form of (4.21) in it's polar form (4.11)

$$\dot{r} = \sum_{j=1}^{N} \alpha_{2j+1} r^{2j+1} + O(r^{2N+3}), \ \dot{\theta} = 1 + \sum_{j=1}^{N} \beta_{2j+1} r^{2j} + O(r^{2N+2})$$

we obtain in the radial component such that $\alpha_3 = \pm\frac{3}{8}$, then in this case, the singular point cant be a center.

4.3.5 Perturbation $a_{1,1,2}$

This case represents system (4.4) perturbed by the monomial with the parameter $a_{1,1,2}$

$$\left.\begin{array}{l} \dot{x} = y + a_{1,2,1}x^2 y + \underline{a_{1,1,2}xy^2} \\ \dot{y} = -x + a_{2,2,0}x^2 + \underline{a_{2,0,2}y^2} + a_{2,3,0}x^3 + a_{2,1,2}xy^2 \end{array}\right\} \tag{4.22}$$

Theorem 24. *System* (4.22) *with* $a_{1,1,2} \neq 0$ *has no center at the origin. Moreover, system* (4.22) *has an isochronous center at O if and only if it reduces to one case of isochronicity from those of system* (4.4)*.*

when $a_{1,1,2} \neq 0$ we obtain in the radial component $\alpha_3 = \pm\frac{551}{8}$, then in this case, the singular point at the origin cant be a center.

4.3.6   Perturbation $a_{2,2,1}$

This case represents system (4.4) perturbed by the monomial with the parameter $a_{2,2,1}$

$$\left.\begin{array}{l} \dot{x} = y + a_{1,2,1}x^2y \\ \dot{y} = -x + a_{2,2,0}x^2 + a_{2,0,2}y^2 + a_{2,3,0}x^3 + a_{2,1,2}xy^2 + \underline{a_{2,2,1}x^2y} \end{array}\right\} \qquad (4.23)$$

Theorem 25. *System* (4.23) *with* $a_{2,2,1} \neq 0$ *has no center at the origin. Moreover, system* (4.23) *has an isochronous center at* O *if and only if it reduces to one case of isochronicity from those of system* (4.4).

By the same reason from the one of the last case, we substitute $a_{2,2,1} = \pm 1$ in the system, then we obtain in the radial component $\alpha_3 = \pm\frac{551}{8}$, in this case, the singular point at the origin can not be a center.

4.3.7   Perturbation $a_{1,0,2}$

This perturbation represents system (4.4) with an additional monomial $a_{1,0,2}y^2$ in the first equation .

$$\left.\begin{array}{l} \dot{x} = y + a_{1,2,1}x^2y + \underline{a_{1,0,2}y^2} \\ \dot{y} = -x + a_{2,2,0}x^2 + a_{2,0,2}y^2 + a_{2,3,0}x^3 + a_{2,1,2}xy^2 \end{array}\right\} \qquad (4.24)$$

Theorem 26. *System* (4.24) *with* $a_{1,0,2} \neq 0$ *has no isochronous center at the origin. Moreover, system* (4.24) *has an isochronous center at* O *if and only if* $a_{1,0,2} = 0$ *and it reduces (modulo a linear change of coordinates) to system* (4.4) *such as its parameters satisfy one of the four cases given in Theorem* 18.

Démonstration. Since we have a quadratic perturbation of system (4.4), thanks to Remark 1 we study the cases $a_{1,0,2} \in \{0,1\}$. If $a_{1,0,2} = 0$, system (4.24) admit an isochronous center at the origin if and only if it reduces to (4.4) and its parameters satisfy one the isochronicity conditions given by Theorem 18. We assume $a_{1,0,2} = 1$, and we compute first the radial component of the normal form in polar coordinates. The first radial component $\alpha_3 = -a_{2,0,2}/4$, then we substitute the assumption $a_{2,0,2} = 0$ in the remaining five α_{2j+1} and we compute the associated Gröbner base, we find $\alpha_5 = a_{2,2,0}(a_{2,1,2} + a_{1,2,1})$. We continue the analysis in the three cases :

1. $a_{2,2,0} = 0$

2. $(a_{2,1,2} + a_{1,2,1}) = 0$

Unfortunately, we computed in each case the Gröbner base and there are no common roots between the multivariate polynomials β_{2j+1} of the angular component.

□

4.3.8 Perturbation $a_{1,2,0}$

Consider the system

$$\left.\begin{aligned}
\dot{x} &= y + a_{1,2,1}x^2y + \underline{a_{1,2,0}x^2} \\
\dot{y} &= -x + a_{2,2,0}x^2 + a_{2,0,2}y^2 + a_{2,3,0}x^3 + a_{2,1,2}xy^2
\end{aligned}\right\} \qquad (4.25)$$

Theorem 27. *System* (4.25) *with* $a_{1,2,0} \neq 0$ *has an isochronous center at* O *if and only if ,modulo a linear change of coordinates, its parameters satisfy*

$$a_{2,3,0} = -4/9, a_{2,1,2} = 0, a_{1,2,1} = 0, a_{2,2,0} = 0, a_{2,0,2} = 0, a_{1,2,0} = 1$$

Démonstration. Consider the case $a_{1,2,0} = 1$. We compute first, under this assumption, the radial component of the normal form of system (4.25). We obtain $\alpha_3 = a_{2,2,0}/4$. Then the first necessary condition to have a center at the origin is the vanishing of $a_{2,2,0}$. We substitute this additional assumption in the remaining coefficients of the radial component $(\alpha_5 \ldots \alpha_{13})$. A common factor appears which is $a_{2,0,2}$.

Hence we obtain two cases to analyse center conditions $a_{2,0,2} = 0$ and $a_{2,0,2} \neq 0$. For the case $a_{2,0,2} \neq 0$, we divide all the expressions of the coefficients of the radial component by $a_{2,0,2}$. We compute the associated Gröbner basis which is generated by 8 polynomials and gives 3 cases for each one the first six necessary conditions for the center are satisfied. Namely the following

$$\{a_{2,1,2} = 0, a_{1,2,1} = 0, a_{2,2,0} = 0, a_{2,0,2} = 0, a_{1,2,0} = 1, a_{2,3,0} = -3/4\}$$

$$\{a_{2,2,0} = 0, a_{1,2,0} = 1, a_{2,3,0} = 0, a_{2,0,2} = -1, a_{2,1,2} = -a_{1,2,1}\}$$

$$\{a_{2,2,0} = 0, a_{1,2,0} = 1, a_{2,3,0} = 0, a_{2,1,2} = -a_{1,2,1}, a_{2,0,2} = 1\}$$

The first solution is rejected, because we have assumed that $a_{2,0,2} \neq 0$.

For the second and the third solution of center condition investigation, we substitute each of those into the angular component coefficients expressions. We compute the Gröbner bases of the obtained multivariate polynomial systems. Unfortunately in the two cases it gives Gröbner basis $\equiv [1]$ which means that there are not common roots.

We return to the remaining case $a_{1,2,0} = 1$, $a_{2,2,0} = a_{2,0,2} = 0$ which ensures the first six necessary conditions of the singular point at the origin to be a center. Substituting this assumption in the angular component coefficients and computing its associated Gröbner basis which is generated by three polynomials. This gives the unique solution to the problem of isochronicity

$$a_{2,3,0} = -4/9, \ a_{1,2,0} = 1, \ a_{2,1,2} = a_{1,2,1} = a_{2,2,0} = a_{2,0,2} = 0$$

Then system (4.25) reduces to

$$\left.\begin{aligned}
\dot{x} &= y + x^2 \\
\dot{y} &= -x - 4/9\,x^3
\end{aligned}\right\}$$

Which is a Liénard isochronous system with $f(x) = -2\,x$, $g(x) = x + 4/9\,x^3$ satisfying

$$g(x) = g'(0)x + \frac{551}{x^3}\left(\int_0^x sf(s)ds\right)^2$$

$\square$

4.3.9   Perturbation $a_{2,1,1}$

$$\left.\begin{aligned}\dot{x} &= y + a_{1,2,1}x^2y\\ \dot{y} &= -x + a_{2,2,0}x^2 + a_{2,0,2}y^2 + \underline{a_{2,1,1}xy} + a_{2,3,0}x^3 + a_{2,1,2}xy^2\end{aligned}\right\} \tag{4.26}$$

Theorem 28. *System* (4.26) *with* $a_{2,1,1} \neq 0$ *has an isochronous center at O if and only if its parameters satisfy one of the following two cases*

1. $a_{2,1,1} = 1$, $a_{2,3,0} = -1/9$, $a_{2,1,2} = a_{1,2,1} = a_{2,2,0} = a_{2,0,2} = 0$
2. $a_{2,1,1} = 1$, $a_{2,1,2} = -2/9$, $a_{1,2,1} = 1/9$, $a_{2,2,0} = a_{2,0,2} = a_{2,3,0} = 0$

Démonstration. Consider the $a_{2,1,1} = 1$

We compute first, under this assumption, the radial component of the normal form of system (4.26). We obtain $\alpha_3 = (a_{2,0,2} + a_{2,2,0})/8$, then the first necessary condition to have a center at the origin is the vanishing of α_3.

We substitute this additional assumption $a_{2,0,2} = -a_{2,2,0}$ in the following coefficient of the radial component $\alpha_5 = -1/48\,a_{2,0,2}\,(a_{1,2,1} - a_{2,1,2} + a_{2,3,0})$, then it appears two cases to analyze : $\{a_{2,0,2} = a_{2,2,0} = 0\}$ and $\{a_{2,0,2} = -a_{2,2,0},\ a_{1,2,1} - a_{2,1,2} + a_{2,3,0} = 0\}$

1. $a_{2,0,2} = a_{2,2,0} = 0$ We substitute this additional assumption in the remaining coefficients of the radial component $\alpha_7, \ldots, \alpha_{13}$ which gives $\alpha_3 = \alpha_5 \ldots = \alpha_{13} = 0$. Hence, the first six center necessary conditions are satisfied.

    Substituting the assumptions into the angular component coefficients expressions, computing associated Gröbner basis gives the two real solutions. The first one is

    $$\{a_{2,1,1} = 1, a_{2,3,0} = -1/9, a_{2,1,2} = a_{2,2,0} = a_{2,0,2} = a_{1,2,1} = 0\}$$

    under which system (4.26) reduces to

    $$\left.\begin{aligned}\dot{x} &= y\\ \dot{y} &= -x + xy - 1/9\,x^3\end{aligned}\right\}$$

    we have an isochronous Liénard systems with

    $$f(x) = -x \text{ and } g(x) = x + 1/9\,x^3$$

    which satisfy

    $$g(x) = g'(0)x + \frac{551}{x^3}\left(\int_0^x sf(s)ds\right)^2$$

The second one is

$$\{a_{2,2,0} = 0, a_{2,0,2} = 0, a_{2,1,1} = 1, a_{2,3,0} = 0, a_{2,1,2} = -2/9, a_{1,2,1} = 1/9\}$$

under which system (4.26) reduces to

$$\left.\begin{aligned}\dot{x} &= y + 1/9x^2y \\ \dot{y} &= -x + xy - 2/9\,xy^2\end{aligned}\right\}$$

By the change of coordinates $(x,y) \mapsto (y,x)$ we obtain

$$\left.\begin{aligned}\dot{x} &= -y + xy - 2/9\,x^2y \\ \dot{y} &= x + 1/9\,xy^2\end{aligned}\right\}$$

Which belongs to the Liénard Type equation (4.2) with $f(x) = -3\,(2\,x - 3)^{-1}$ and $g(x) = 1/9\,x\,(2\,x - 3)\,(x - 3)$. The isochronicity of this last system is proved since it belongs to the case 9 of the Theorem 3 of Chouikha et.al in [63].

2. $a_{2,0,2} = -a_{2,2,0}$ and $a_{1,2,1} - a_{2,1,2} + a_{2,3,0} = 0$

Unfortunately in this case, after computing Gröbner basis, no real solutions are found.

$\square$

Theorem 29. *System* (4.4) *has an amplitude independent frequency synchronizer at O if and only if its parameters satisfy one of the cases of Theorem 3-Theorem 11.*

4.4 Conclusion

To summarize, for the eight monomial perturbations studied in this paper we have identified all possible amplitude independent frequency synchronizers. Moreover, we claim that all isochronous cases are known in a fragmented literature but our study insures that for the studied family there are no other (necessary conditions). Each of them was found in a classification of a specific family of planar differential systems which are different from the context of the ones studied in this paper (synchronization). For isochronous centers of Liénard systems the reader can see for instance [64, 52]. The papers [62, 63] are concerned with the planar differential Liénard Type equations. For cubic time reversible systems see [52, 100, 56] and for cubic homogeneous perturbations of linear center see [52, 100, 145].

Analysis and control of quadrotor via a Normal Form approach

Arial vehicles are often modeled by high dimensional dynamical systems. This work shows that standard techniques of qualitative theory of differential equations (center manifold/normal forms) may be directly applied to such systems for control aim. The proofs of the results of this chapter can be found in [216].

This paper focuses on the analysis and control of some mathematical models representing the dynamics of a quadrotor. By using a normal form approach, the highly coupled parts in the quadrotor system are eliminated, while all possible properties of the original system are not changed. The bifurcations of the system are then analyzed. A two-dimensional system is deduced at the origin which can determine the stability and possible local bifurcations of the system. Based on the normal form and indirect method of Lyapunov, we propose a state feedback control method which, compared to a standard PID control, has faster response time and less tracking errors especially with wind disturbance.

5.1   Introduction

The quadrotor (see in Figure 5.1) is a mini unmanned aerial vehicle (UVA) with four rotors, which has been widely studied in the last decades [120, 27, 21, 217]. It is a system with four inputs, six outputs and highly coupled states. Due to its simplicity both in mechanical structure and maneuver, it is widely used in surveillance, search and rescue, mobile sensor networks [120]. Many methods have been proposed for controlling quadrotors. For example, Bouabdallah et al.[27] have proposed a backstepping control used separately in two subsystems. Besnard et al.[21] have proposed a sliding mode control driven by a disturbance observer. Wang et al.[217] have presented an event driven model free control which can avoid heavy computation. However, to the best of the authors' knowledge, the bifurcation of the dynamical system have never been studied.

The method of normal forms is an useful approach in studying the dynamical system properties [134]. Its purpose is employing successive coordinate transformations to construct the simplest form of the system. The normal form exhibits all possible properties of the original system. The normal forms of any degree with a single input were obtained by using change of coordinates and feedback [127]. For multi-input systems, the normal forms are deduced from the system with two inputs [208]. Based on the normal forms, the bifurcations and its control were studied by
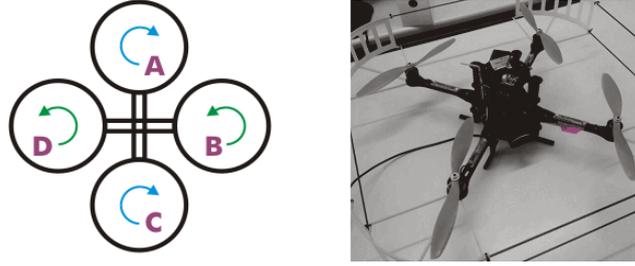
FIGURE 5.1 – The quadrotor(right) from Ascending technologies(Available at ESIEE).

several authors [127, 131]. Center manifold is usually applied with the normal forms. It reduces the system to a center manifold associated with parts of the system with the eigenvalues with zero real parts at a bifurcation point [47].

To the best of our knowledge, the normal form and center manifold theories have never been used in the analysis and control of quadrotor. In this paper, the normal form of the quadrotor system is firstly calculated. By using such a methodology, the highly coupled parts in quadrotor system are eliminated. Under certain control laws, the normal form is reduced into a two dimensional system at the bifurcation point by using center manifold theory. Also, a simple control method based on the normal form using state feedback is proposed. The control laws are proposed to ensure the asymptotical stability of the system by moving all the eigenvalues of the system to the open left half plane. Comparing to PID control, the proposed method has faster response time and less tracking errors especially when there is wind disturbance, as illustrated at the end of the paper. The interest of considering such control laws lies in the simplicity of the controller as well as in its practical implementation facility.

The paper is organized as follows : In Section 5.2, the model of quadrotor is given. In Section 5.3, the normal form of quadrotor is deduced. In Section 5.4, the bifurcation of the system under certain control laws is analyzed. In Section 5.5, simulations with and without wind disturbance using the proposed method and PID control are given.

5.2 The quadrotor model

The chosen model of quadrotor is depicted in equations (5.1). The rotation angles ϕ, θ and ψ are along the world axis x, y and z respectively, namely roll, pitch and yaw. $w_i(i = 1..4)$ are the accelerations caused by four rotors, which are the inputs of the system. ($g = 9.8\text{m/s}^2$ the gravity).

$$\ddot{x} = -w_1 sin\theta, \qquad \ddot{y} = w_1 cos\theta sin\phi, \qquad \ddot{z} = w_1 cos\theta cos\phi - g,$$
$$\ddot{\phi} = w_2, \qquad \ddot{\theta} = w_3, \qquad \ddot{\psi} = w_4. \qquad (5.1)$$

We introduce the variables as $x_1 = x$, $x_2 = \dot{x}$, $x_3 = y$, $x_4 = \dot{y}$, $x_5 = z$, $x_6 = \dot{z}$, $x_7 = \phi$, $x_8 = \dot{\phi}$, $x_9 = \theta$, $x_{10} = \dot{\theta}$, $x_{11} = \psi$, $x_{12} = \dot{\psi}$. Therefore, we can rewrite the system as :

$$\begin{aligned}
\dot{x}_1 &= x_2, & \dot{x}_2 &= -w_1 sin(x_9), & \dot{x}_3 &= x_4, & \dot{x}_4 &= w_1 cos(x_9) sin(x_7), \\
\dot{x}_5 &= x_6, & \dot{x}_6 &= w_1 cos(x_9) cos(x_7) - g, & \dot{x}_7 &= x_8, & \dot{x}_8 &= w_2, & (5.2) \\
\dot{x}_9 &= x_{10}, & \dot{x}_{10} &= w_3, & \dot{x}_{11} &= x_{12}, & \dot{x}_{12} &= w_4.
\end{aligned}$$

5.3 Normal form of the system

It is easy to see that the equilibria of the system (5.2) are $x_e = (c_1, 0, c_2, 0, c_3, 0, k\pi, 0, k\pi, 0, c_4, 0)$, $w = (g, 0, 0, 0)$, where $k = 0, \pm 1, \pm 2, ...$, $c_i(i = 1..4) \in \mathbb{R}$ are constants and g is the gravity. Note in the real control system, $\phi, \theta \in (-\pi/2, \pi/2)$ and $\psi \in [0, \pi)$. Therefore, without losing generality, only the equilibrium $x_0 = (x, w) = (0, 0, 0, 0, 0, 0, 0, 0, 0, 0, 0, 0, g, 0, 0, 0)$ is considered. We move x_0 to the origin by changing the coordinates of the inputs $w_1 = u_1 + g, w_2 = u_2, w_3 = u_3, w_4 = u_4$. Then, using the Taylor series of function $sin(x)$ and $cos(x)$ at $x = 0$. The system (5.2) can be written in polynomial form as follows. Here, O^5 are the polynomials with 5th and higher degree :

$$\begin{aligned}
\dot{x}_1 &= x_2, \quad \dot{x}_2 = -gx_9 - u_1 x_9 + \frac{gx_9^3}{6} + \frac{u_1 x_9^3}{6} + O^5, \\
\dot{x}_3 &= x_4, \quad \dot{x}_4 = gx_7 + u_1 x_7 - \frac{gx_7^3}{6} - \frac{gx_9^2 x_7}{2} - \frac{u_1 x_7^3}{6} - \frac{u_1 x_9^2 x_7}{2} + O^5, \\
\dot{x}_5 &= x_6, \quad \dot{x}_6 = u_1 - \frac{gx_7^2}{2} - \frac{gx_9^2}{2} - \frac{u_1 x_7^2}{2} - \frac{u_1 x_9^2}{2} + \frac{gx_7^4}{24} + \frac{gx_9^2 x_7^2}{4} + \frac{gx_9^4}{24} + O^5, \\
\dot{x}_7 &= x_8, \quad \dot{x}_8 = u_2, \quad \dot{x}_9 = x_{10}, \quad \dot{x}_{10} = u_3, \quad \dot{x}_{11} = x_{12}, \quad \dot{x}_{12} = u_4.
\end{aligned}$$

Using the state and input transformation $y_1 = x_1$, $y_2 = x_2$, $y_3 = x_3$, $y_4 = x_4$, $y_5 = x_5$, $y_6 = x_6$, $y_7 = gx_7$, $y_8 = gx_8$, $y_9 = gx_9$, $y_{10} = gx_{10}$, $y_{11} = x_{11}$, $y_{12} = x_{12}$, $v_1 = u_1$, $v_2 = gu_2$, $v_3 = gu_3$, $v_4 = u_4$, we change the system (5.3) into Brunovsky form :

$$\begin{aligned}
\dot{y}_1 &= y_2, \quad \dot{y}_2 = -y_9 - \frac{v_1 y_9}{g} + \frac{y_9^3}{6g^2} + \frac{v_1 y_9^3}{6g^3} + O^5, \\
\dot{y}_3 &= y_4, \quad \dot{y}_4 = y_7 + \frac{v_1 y_7}{g} - \frac{y_7 y_9^2}{2g^2} - \frac{y_7^3}{6g^2} - \frac{v_1 y_7^3}{6g^3} - \frac{v_1 y_7 y_9^2}{2g^3} + O^5, \quad (5.3) \\
\dot{y}_5 &= y_6, \quad \dot{y}_6 = v_1 - \frac{y_7^2}{2g} - \frac{y_9^2}{2g} - \frac{v_1 y_7^2}{2g^2} - \frac{v_1 y_9^2}{2g^2} + \frac{y_7^4}{24g^3} + \frac{y_7^2 y_9^2}{4g^3} + \frac{y_9^4}{24g^3} + O^5, \\
\dot{y}_7 &= y_8, \quad \dot{y}_8 = v_2, \quad \dot{y}_9 = y_{10}, \quad \dot{y}_{10} = v_3, \quad \dot{y}_{11} = y_{12}, \quad \dot{y}_{12} = v_4.
\end{aligned}$$

The system (5.3) can be written as :

$$\dot{y} = f(y) + g(y)v = Ay + f^{(2)}(y) + f^{(3)}(y) + Bv + g^{(1)}(y)v + g^{(2)}(y)v + O^4 \quad (5.4)$$

where A, B are the coefficients of the linear parts, $f^{(2)}(y)$, $g^{(1)}(y)v$ are the second degree homogeneous polynomials of the system, $f^{(3)}(y)$, $g^{(2)}(y)v$ are the third degree homogeneous polynomials.

We take a third-degree homogeneous transformation for example [132] :

$$y = z + \phi^{(2)}(z) + \phi^{(3)}(z) \tag{5.5}$$

which z are the new states of the system. $\phi^{(2)}(z)$ is a second degree homogeneous polynomial and $\phi^{(3)}(z)$ is a third degree homogeneous polynomial of the states z, whose coefficients will be defined later.

We get the derivative of equation (5.5). Therefore, the derivative of the new states z are :

$$\dot{z} = (I + \frac{d\phi^{(2)}}{dz} + \frac{d\phi^{(3)}}{dz})^{-1}\dot{y} \tag{5.6}$$

where,

$$(I + \frac{d\phi^{(2)}}{dz} + \frac{d\phi^{(3)}}{dz})^{-1} = I - \frac{d\phi^{(2)}}{dz} - \frac{d\phi^{(3)}}{dz} + (\frac{d\phi^{(2)}}{dz})^2 + (\frac{d\phi^{(3)}}{dz})^2 + 2\frac{d\phi^{(2)}}{dz}\frac{d\phi^{(3)}}{dz}...$$

In (5.4), we rewrite the $f(y)$ and $g(y)$ using the new states z.

$$f(y) = A(y) + f^{(2)}(y) + f^{(3)}(y) + O^4 = Az + A\phi^{(2)}(z) + f^{(2)}(z) + A\phi^{(3)}(z) + f^{(3)}(z)...$$
$$g(y) = B + g^{(1)}(y) + g^{(2)}(y) + O^3 = B + g^{(1)}(z) + g^{(1)}(\phi^{(2)}(z)) + g^{(2)}(z)...$$

Therefore, with the help of the equations (5.4), (5.6), by now we have the new system :

$$\dot{z} = Az + Bv + A\phi^{(2)}(z) + f^{(2)}(z) + g^{(1)}(z)v - \frac{d\phi^{(2)}}{dz}Az - \frac{d\phi^{(2)}}{dz}Bv + A\phi^{(3)}(z)$$

$$+ f^{(3)}(z) + g^{(2)}(z)v + g^{(1)}(\phi^{(2)}(z))v - \frac{d\phi^{(2)}}{dz}(A\phi^{(2)}(z) + f^{(2)}(z) + g^{(1)}(z)v)$$

$$- \frac{d\phi^{(3)}}{dz}(Az + Bv) + (\frac{d\phi^{(2)}}{dz})^2(Az + Bv) + O^4$$

For the simplicity of the system, the states z and the inputs v should be separated. In the third degree normal form, the polynomial $g^{(1)}(z)v$, $g^{(2)}(z)v$ should be canceled.

$$g^{(1)}(z) - \frac{d\phi^{(2)}}{dz}B = 0$$

$$g^{(2)}(z) + g^{(1)}(\phi^{(2)}(z)) - \frac{d\phi^{(2)}}{dz}g^{(1)}(z) - \frac{d\phi^{(3)}}{dz}B + (\frac{d\phi^{(2)}}{dz})^2B = 0$$

Therefore, the transformation in equation (5.5) should be :

$$\phi^{(2)}(z) = (0, -\frac{z_6 z_9}{g}, 0, \frac{z_6 z_7}{g}, 0, 0, 0, 0, 0, 0, 0, 0),$$

$$\phi^{(3)}(z) = (0, 0, 0, 0, 0, -\frac{z_6 z_7^2}{2g^2} - \frac{z_6 z_9^2}{2g^2}, 0, 0, 0, 0, 0, 0).$$

Using the same method, we can calculate the normal form of any degree. A Maple package 'QualitativeODE'(Available upon request) has been made for calculating the

normal form of quadrotor. Using this programme, we get the third degree normal form of the system (5.3) as :

$$
\begin{aligned}
\dot{z}_1 &= z_2 - \frac{z_6 z_9}{g}, & \dot{z}_2 &= -z_9 + \frac{z_6 z_{10}}{g} - \frac{z_9^3}{3g^2} - \frac{z_7^2 z_9}{2g^2} + O^4, \\
\dot{z}_3 &= z_4 + \frac{z_6 z_7}{g}, & \dot{z}_4 &= z_7 - \frac{z_6 z_8}{g} + \frac{z_7^3}{3g^2} + O^4, \\
\dot{z}_5 &= z_6 - \frac{z_6 z_7^2}{2g^2} - \frac{z_6 z_9^2}{2g^2}, & \dot{z}_6 &= v_1 - \frac{z_7^2}{2g} - \frac{z_9^2}{2g} + \frac{z_6 z_7 z_8}{g^2} + \frac{z_6 z_9 z_{10}}{g^2} + O^4, \\
\dot{z}_7 &= z_8, \quad \dot{z}_8 = v_2, \quad \dot{z}_9 = z_{10}, & \dot{z}_{10} &= v_3, \quad \dot{z}_{11} = z_{12}, \quad \dot{z}_{12} = v_4.
\end{aligned}
\tag{5.7}
$$

5.4 Bifurcation and simplification of the control system

5.4.1 Bifurcation of the roots

It is easy to see that in the linear part of the equation (5.7), z_1 is related only to z_2, z_9, z_{10}, v_3 ; z_3 is related to z_4, z_7, z_8, v_2 ; z_5 is related to z_6, v_1 ; z_{11} is related to z_{12}, v_4. Therefore, the control laws can be defined as :

$$
\begin{aligned}
v_1 &= K_{11}z_5 + K_{12}z_6, & v_2 &= K_{21}z_3 + K_{22}z_4 + K_{23}z_7 + K_{24}z_8, \\
v_4 &= K_{41}z_{11} + K_{42}z_{12}, & v_3 &= K_{31}z_1 + K_{32}z_2 + K_{33}z_9 + K_{34}z_{10}.
\end{aligned}
$$

In this way, we can move the related eigenvalues in each group separately without changing the eigenvalues in other groups. Here, we define $v_i (i = 1..4)$ as :

$$
\begin{aligned}
v_1 &= -256z_5 + K_{12}z_6, & v_2 &= -100z_3 - 308z_4 - 256z_7 - 32z_8, \\
v_4 &= -1024z_{11} + K_{42}z_{12}, & v_3 &= 100z_1 + 308z_2 - 256z_9 - 32z_{10}.
\end{aligned}
$$

The system has three equilibria $P_1^e = (0,0,0,0,0,0,0,0,0,0,0,0)$, $P_2^e = (0,0,43.45,$
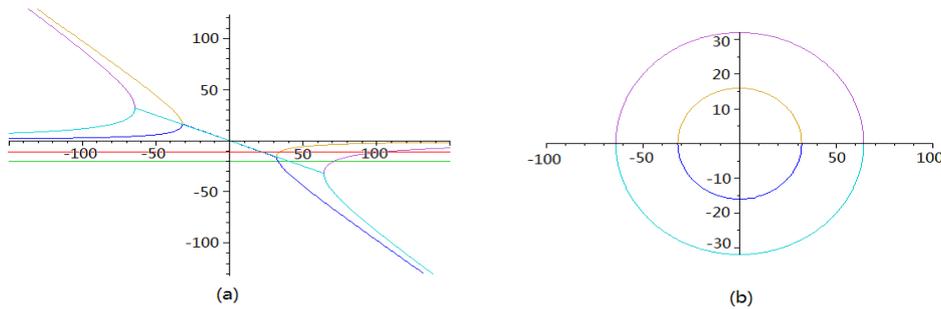

FIGURE 5.2 – The eigenvalues when K_{12} changes from -150 to 150 : (a) the real parts. (b) the imaginary parts.

$0, -0.057, 0, -16.97, 0, 0, 0, 0, 0)$ and $P_3^e = (0, 0, -43.45, 0, -0.057, 0, 16.97, 0, 0, 0, 0, 0)$. However, only the origin P_1^e can be stable when K_{12}, K_{42} change.

At the equilibrium P_1^e, for simplicity $K_{12} = K_{42}$, when K_{12} changes, the real and imaginary parts of the eigenvalues are in Figure 5.2. When $K_{12} < 0$, the system has four eigenvalues with positive real parts, and the system becomes unstable. When $K_{12} > 0$, the system has all eigenvalues with negative real parts, and the system is asymptotically stable. When $K_{12} = 0$, the system has two pairs of pure imaginary eigenvalues $\pm 16i$ and $\pm 32i$, and all other eigenvalues have negative real parts, which is a four dimensional center manifold. The stability cannot be determined by the linear part of the system. It depends on the nonlinearity of the system.

5.4.2   Center manifold : Hopf point

The aim of this part is to get the reduced system which can determine the stability and possible local bifurcations of the system at one bifurcation point [111]. A system can be written as :

$$\dot{x} = A(b)x + F(x), \qquad x \in R^n$$

where b is a free parameter, $b \in R$.

At its origin $x = [0, ..., 0]$, $J(b)$ is the Jordan form of the matrix $A(b)$ and Q is a matrix which enables $Q(b)J(b)Q^{-1}(b) = A(b)$. Therefore, we have :

$$\dot{x} = Q(b)J(b)Q^{-1}(b)x + F(x) \quad \Rightarrow \quad Q^{-1}(b)\dot{x} = J(b)Q^{-1}(b)x + Q^{-1}(b)F(x)$$

we define $y = Q^{-1}(b)x$, then

$$\dot{y} = J(b)y + Q^{-1}(b)F(Q(b)y) = J(b)y + \tilde{F}(y) \tag{5.8}$$

we can separate the Jordan matrix J as matrices B and C whose eigenvalues have zero real parts and negative real parts respectively. Therefore, we can rewrite the system (5.8) at the origin with $x = [0, ..., 0]$.

$$\dot{y}_0 = By_0 + f(y_0, y_-), \qquad \dot{y}_- = Cy_0 + g(y_0, y_-).$$

Since the center manifold is tangent to E^c(the $y_- = 0$ space), we define

$$y_- = h(y_0, b), \quad h(0, 0) = Dh(0, 0) = 0, \quad \dot{b} = 0. \tag{5.9}$$

We can calculate the function $h(y_0, b)$ by using

$$\dot{y}_- = Dh(y_0, b)\dot{y}_0 = Dh(y_0, b)[By_0 + f(y_0, h(y_0, b))] = Cy_0 + g(y_0, h(y_0, b))$$

Therefore, we can get the local evolution equations of y_0 which can determine the stability of the original system.

In quadrotor center manifold analysis, the control laws are defined as :

$$v_1 = -256z_5 - bz_6 - z_5^3, \qquad v_2 = -100z_3 - 308z_4 - 256z_7 - 32z_8,$$
$$v_4 = -10z_{11} - 24z_{12}, \qquad v_3 = 100z_1 + 308z_2 - 256z_9 - 32z_{10}.$$

The bifurcation of the system is like in previous subsection. When $b < 0$, the system has two eigenvalues with positive real parts. When $b > 0$, the system has all eigenvalues with negative real parts. When $b = 0$, the system has two pure imaginary eigenvalues $\pm 16i$, and all other eigenvalues have negative real parts. The stability depends on the nonlinear parts of the system. We can use the center manifold theory to simplify the system, and further simplify the study of the bifurcation of the system. In this control system, $y_0 = [y_1, y_2]^T = [z_5, z_6]^T$ and $y_- = [y_3, y_4, y_5, y_6, y_7, y_8, y_9, y_{10}, y_{11}, y_{12}]^T = [z_1, z_2, z_3, z_4, z_7, z_8, z_9, z_{10}, z_{11}, z_{12}]^T$.

We seek a quadratic center manifold (a are parameters to be defined later) :

$$y_i = a_{i200}y_1^2 + a_{i020}y_2^2 + a_{i002}b^2 + a_{i110}y_1y_2 + a_{i101}y_1b + a_{i011}y_2b, \quad i = 3..12$$

Using the method mentioned before, we get $h(y_0, b) = [-0.62b^2, -0.62b^2, -0.76b^2, -0.76b^2, 0, 0, 0, 0, -0.42b^2, -23.58b^2]$ in equation (5.9).

Therefore, the reduced system on the center manifold can be written :

$$\begin{aligned}
\dot{y}_1 &= 16y_2 - 0.41b^4 - 0.011b^8 - (b + 0.057b^4)y_1 + 0.00024y_2^3 \\
\dot{y}_2 &= -16y_1 + 0.67b^4y_1
\end{aligned} \tag{5.10}$$

In the reduced system, when b is positive (negative), the origin is a stable (unstable) focus. When $b = 0$, the origin is a center. The phase portrait of equation (5.10) when $b = -0.5$, $b = 0$ and $b = 0.5$ are depicted in Figure 5.3.
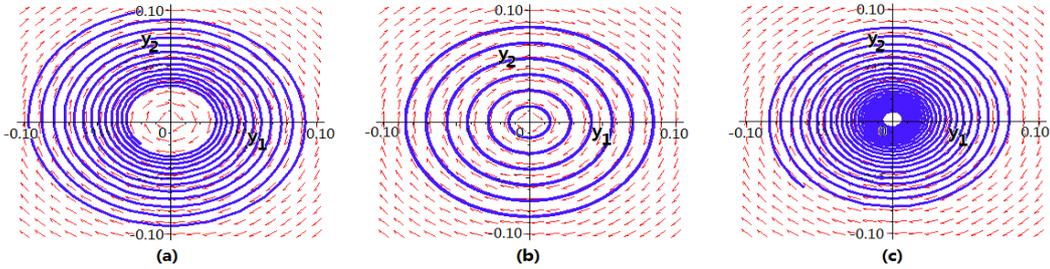
FIGURE 5.3 – The phase portrait of the reduced system : (a) b=-0.5. (b) b=0. (c) b=0.5.

5.5 Quadrotor control

Here we propose a control method based on the normal form and Lyapunov theory. In equation (5.7), the Jacobian matrix of the system can be easily found. If the system is time invariant, the indirect method of Lyapunov says that if the eigenvalues of Jacobian matrix of the system at the origin are in the open left half complex plane, then the origin is asymptotically stable. Therefore, we can define the

state feedback as follows to move all the eigenvalues of the system to the open left half plane. x_r, y_r, z_r, ψ_r are the references.

$$v_1 = -256(z_5 - z_r) - 32z_6, \qquad v_2 = -1700(z_3 - y_r) - 1000z_4 - 256z_7 - 32z_8$$
$$v_4 = -256(z_{11} - \psi_r) - 32z_{12}, \quad v_3 = 1700(z_1 - x_r) + 1000z_2 - 256z_9 - 32z_{10}$$

The simulation task is to let quadrotor follow a square path with the length of 2m while hovering at the altitude of 10m, which is given in Figure 5.4. The totally sample time is 20s. For comparison, the simulations using PID control are also given.
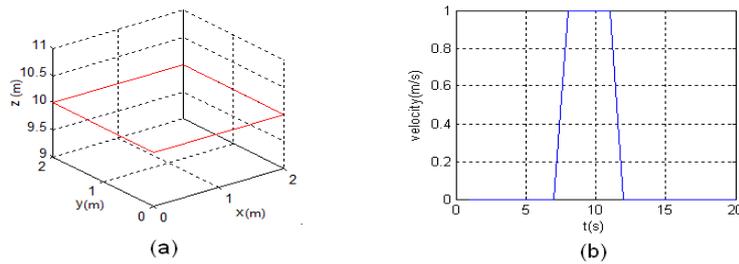

FIGURE 5.4 – (a) Reference trajectory for the quadrotor. (b) Wind disturbance.

5.5.1 Simulation without wind disturbance

The simulation results are given in Figure 5.5. The response time using the proposed method is less than using PID control.

5.5.2 Simulation with wind disturbance

During the trajectory, there may have wind disturbance with velocity 1m/s as in Figure 5.4, which occurs in all x, y and z axis. The simulation results are given in Figure 5.6. Both methods can keep the stability during the wind disturbance. However, using the proposed method, there are less tracking errors.

5.6 Conclusion

In this paper, the normal form of quadrotor is deduced. A Maple package 'QualitativeODE'(Available upon request) has been written for calculating the normal form of any degree of the system. From equation (5.7), we can see that the highly coupled parts in quadrotor system are eliminated. This makes the analysis of the dynamical system easier. Under certain control laws, the system can be further deduced using center manifold theorem. A two dimensional system is deduced which can determine the stability and possible local bifurcations of the control system at the origin. Based on the normal form and indirect method of Lyapunov, we proposed
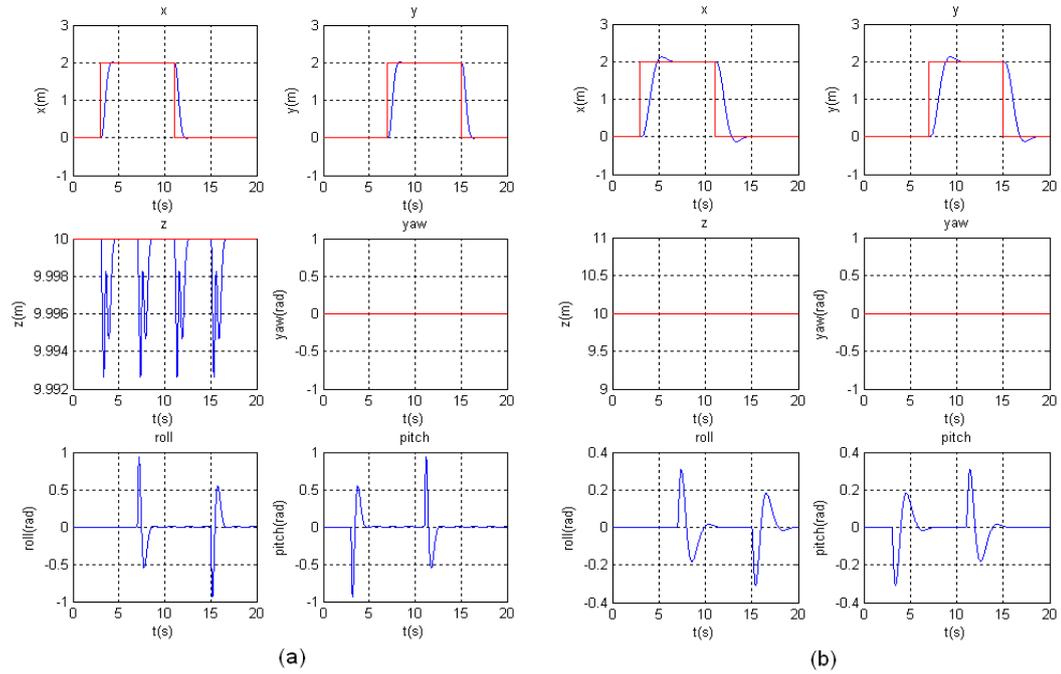
FIGURE 5.5 – The simulation without wind disturbance : (a) the proposed method. (b) PID control.

a state feedback control method with computational simplicity as well as practical implementation facility. This method achieved good results. In the simulations, the system can remain stable with small tracking errors even if there is wind disturbance. Also, this method has faster response time than PID control.
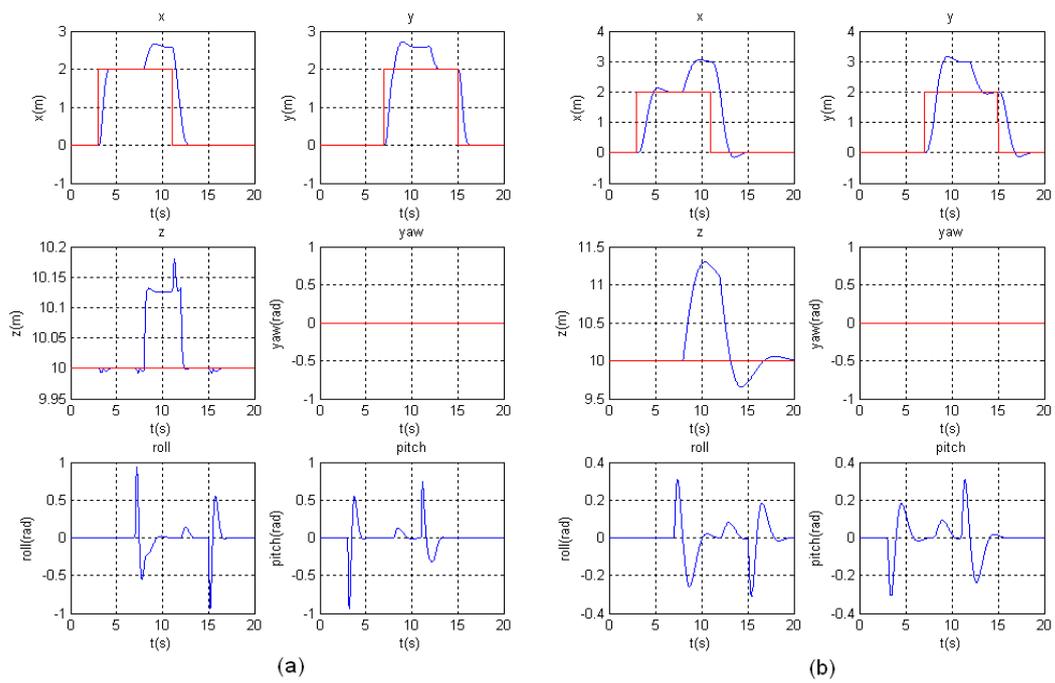
FIGURE 5.6 – The simulation with wind disturbance : (a) the proposed method. (b) PID control.

Deuxième partie

Qualitative analysis of functional Differentia algebraic equations and their applications

Analyse qualitative des équations algébro-differentielles fonctionnelles et leurs applications

"... If the proof starts from axioms, distinguishes several cases, and takes thirteen lines in the text book ... it may give the youngsters the impression that mathematics consists in proving the most obvious things in the least obvious way."

George Pólya, *Mathematical Discovery : on Understanding, Learning, and Teaching Problem Solving, 1981.*

Inverted Pendulum Stabilization : Characterization of Codimension-Three Triple Zero Bifurcation Via Multiple Delayed Proportional Gains

This work reproduces the results from [35] and [34], in which we design a multi-delayed-proportional controllers allowing to stabilize the inverted pendulum by avoiding a relatively high codimension of the zero spectral value. The center manifold theorem for functional differential equations is exploited. The normal form of the projected dynamical equations in the center manifold is then analyzed. Namely, we consider the problem of stabilization of systems possessing a multiple zero eigenvalue at the origin. The controller that we propose, uses multiple delayed measurements instead of derivative terms. Doing so, we increase the performances of the closed loop in presence of system uncertainties and/or noisy measurements. The problem formulation and the analysis is presented through a classical engineering problem which is the stabilization of an inverted pendulum on a cart moving horizontally. On one hand, we perform a nonlinear analysis of the center dynamics described by a three dimensional system of ordinary differential equations with a codimension-three triple zero bifurcation. On the other hand, we present the complementary stability analysis of the corresponding linear time invariant system with two delays describing the behavior around the equilibrium. The aim of this analysis is to characterize the possible local bifurcations. Finally, the announced control scheme is numerically illustrated and discussed.

6.1 Introduction

In this paper, we employ the classical problem of stabilization of a balancing inverted pendulum on a horizontally moving cart (see for instance [10, 85, 135, 157, 199, 200]) to illustrate the control design and performances of delayed proportional controllers. This problem is often used to discuss new ideas in control of nonlinear dynamical systems. This is certainly due to the richness of its dynamics despite the relative simple structure of the physical system. Among possible applications, we

emphasize the modeling of the human balance control [152].

It is well known that the pendulum has two equilibria, one is stable and it corresponds to the pendulum pointing downwards while the other one is unstable and corresponds to the upward position of the pendulum (inverted pendulum). Therefore, the pendulum can be maintained in the upward position only in presence of an appropriate control input. F.M. Atay pointed out (see [10]) that a simple position feedback is not sufficient to obtain satisfactory closed-loop performances. In order to solve the problem one needs additional knowledge such as the rate of change of the position. Thus, a classical controller will contain a derivative feedback term. In [10] the author proposed a proportional minus delay controller (PMD) to obtain asymptotic stability of undamped second-order systems modeling an inverted pendulum. Doing so, the effect of the derivative term is obtained by using a delayed feedback. A proportional controller that locally maintain the pendulum in the upright position was also designed in [135]. In this work it is shown that, when the proportional controller is delayed and the time-delay is not too large, the controller still locally stabilizes the system. Among other results, the authors show the loss of stability when the delay exceeds a critical value, a supercritical Andronov-Hopf Bifurcation [134] occurs generating stable limit cycles.

To the best of the authors' knowledge, PMD controllers were first introduced by I.H. Suh & Z. Bien in [207] where it is shown that the conventional P-controller equipped with an appropriate time-delay performs an averaged derivative action and thus can replace the PD-controller. It was emphasized that this strategy provides quick responses to input changes but also the insensitiveness to high-frequency noise.

More recently ([200]), J. Sieber and & B. Krauskopf designed a delayed Proportional Derivative (PD) controller that stabilizes the inverted pendulum on a horizontally moving cart. Moreover, they complement the nonlinear analysis with the local stability analysis of the linearized system around equilibrium. The later characterizes all the possible local bifurcations and is based on the center manifold theory and normal forms, which are known to be powerful tools for the local qualitative study of the dynamics. The study emphasized the existence of a codimension-three triple zero bifurcation. It is also shown that the stabilization of the inverted pendulum in its upright position cannot be achieved by a delayed PD controller when the delay exceeds some critical value τ_c. In [201], the authors investigate some modifications of the delayed PD scheme that allows extending the range of the admissible delay by taking into account the angular acceleration. An alternative possibility is to introduce an artificial delay in the angular position feedback. It is worth noting that, replacing the derivative with its numerical approximation will not allow to directly apply the results in [200]. Indeed, the behavior of a system (even a linear one) may be different from the behavior of its approximation. In [153], it has been shown that using a polynomial function $(1 - s\frac{\tau}{n})^n$ of arbitrary degree n to approximate an exponential $e^{-s\tau}$ allows finding stabilizing controller gains for the approximated system even when they do not necessarily exist for the original one. Furthermore, introducing a deliberately delay was suggested in [197] to solve the static output feedback sliding mode control problem for a broader class of linear uncertain systems. In-

deed, it is shown that the reduced order sliding mode dynamics are stabilized by the introduced artificial delay.

The use of PD controller needs the knowledge of the velocity history but in some circumstances we are only able to have approximate measurements due to technological constraints. In absence of measurements of the derivative, a classical idea is to use an observer to reconstruct the state, but this might degrade the performance to some extent [10] and it is, in general, computationally involved for delay systems. In fact, when the position measurements are accessible by sensors, one can avoid such degradation by restricting the design to delayed proportional gains. However, it is important to mention that in some circumstances, which can be justified by some technical or technological constraints, it may be more conceivable to use sensors for the velocity and the acceleration rather than a position sensor. The starting idea of our work is a result proposed by W. Michiels & S-I. Niculescu in [166]. As proven there, a chain of n integrators can be stabilized using n distinct delay blocks, where a delay block is described by two parameters : "gain" and "delay". The interest of considering control laws of the form $\sum_{k=1}^{m} \gamma_k \, y(t - \tau_k)$ lies in the simplicity of the controller as well as in its easy practical implementation. The performances of delayed controllers to overcome the challenge of stabilizing the inverted pendulum are emphasized in the following recent works [10, 200, 135].

The main contribution of the paper is the analysis of a proportional controller with artificial delays that is able to stabilize the inverted pendulum without the use of derivative measurements. This type of controllers will be called multi-delayed-proportional controllers (MDP) in the sequel. Our analysis agrees with the claim of F.M. Atay [10] but extends it by proving that the knowledge of the delayed derivative gain considered in the delayed PD controller [200] can be replaced by using two delayed position values. We firstly use MDP controllers to reach the configuration of multiple-zero eigenvalue described in [200] and secondly, we identify the appropriate parameter values that stabilize the inverted pendulum avoiding the singularity. It is worth mentioning that, if the presence of the root at the origin is independent of the delay values, its multiplicity depends on the existing relations between the delays and the other parameters of the system. Moreover, such a root at the origin admits a bounded multiplicity [176].

We show that, on the center manifold, the considered MDP controller achieves the same trajectories as the delayed PD considered in [200]. Moreover, we point out that using the proposed MDP we are able to obtain the critical parameter values associated with a triple zero singularity for the delayed PD (see Remark 3). In some sense, this can be seen as a discretization of the feedback state derivative. By the way, such a constructive approach has been adopted in a different context for the controller design developed in [166, 129]. The stability analysis of the delayed linearized system employs the geometrical interpretation of the corresponding characteristic equation proposed in [155, 110, 154]. An alternative technique for studying the stability of this class of systems is proposed in [202]. For more details on the existing techniques, the reader is referred to [123]. We point out that we are providing stability regions in delay parameter space. Thus, rounding the values due

to numerical implementation does not generate troubles as far as the delays are far enough of the crossing curves. This issue is known in the literature as fragility of the controller and it mainly appears when the design is made for a continuous system but the implementation is done in a digital fashion. A non-fragile controller allows rounding numerical values without loosing stability properties. A methodology to design non-fragile PI, PD or PID controllers has been presented in previous works of the authors (see for instance [150]). The main idea is to chose the controller parameters that maximize the distance to the closest tangent to the crossing stability manifold (i.e. the manifold that separates to regions with different number of unstable roots).

The remaining part of our paper is organized as follows. First, the model of the inverted pendulum on a cart is introduced as well as some mathematical notions used in the analysis. Next, a double delay block control strategy is presented and analyzed. The analysis of the proposed controller includes the linear stability analysis pointing out the Andronov-Hopf bifurcation as well as the multiple-zero singularity, which suggests a central dynamics analysis. Conclusions, comparisons and future work end the paper.

6.2 Settings and useful notions

6.2.1 Friction free model of an Inverted Pendulum on a Cart

In the sequel we consider the friction free model presented in [200] by adopting the same notations. Denote the mass of the cart M, the mass of the pendulum m and let the relative mass be $\varepsilon = m/(m + M)$.

In the dimensionless form, if frictions are neglected, the dynamics of the inverted pendulum on a cart in figure 10.2 is governed by the following ODE, see also [201] :

$$\left(1 - \frac{3\varepsilon}{4}\cos^2(\theta)\right)\ddot{\theta} + \frac{3\varepsilon}{8}\dot{\theta}^2\sin(2\theta) - \sin(\theta) + D\cos(\theta) = 0, \tag{6.1}$$

where D represents the horizontal driving force exerted by the control law.

In the next section, the horizontal control force will be referred to as position feedback. This was suggested in [166, 129] in the context of stabilizing a finite dimensional system consisting of a chain of $2-$ integrators : $D = \sum_{k=1}^{2} a_k\, \theta(t - \tau_k)$.

In the sequel, we explicitly design the controller that avoids the triple zero singularity.

6.2.2 Prerequisites : Space decomposition for time-delay systems

Consider the general discrete delayed autonomous first-order nonlinear system where its linear and nonlinear quantities are separated as follows :

$$\frac{d}{dt}x(t) = \sum_{k=0}^{n} A_k\, x(t - \tau_k) + \mathcal{F}(x(t), \ldots, x(t - \tau_n)), \tag{6.2}$$
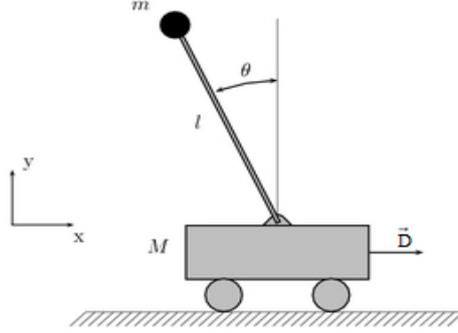
FIGURE 6.1 – Inverted Pendulum on a cart

where A_i are $n \times n$ real valued matrices, the delays τ_k are ordered such that $\tau_i < \tau_j$ when $i < j$, $\tau_n = r$ and $\tau_i \geq 0$.

The latter system can be written as :

$$\frac{d}{dt}x = \mathcal{L}x_t + \mathcal{F}(x_t), \tag{6.3}$$

where $x_t \in C_{r,n} = C([-r,0], \mathbb{R}^n)$, $x_t(\theta) = x(t+\theta)$ denotes the system state, $\mathcal{L}$ is a bounded linear operator such that $\mathcal{L}\phi = \sum_{k=0}^{n} A_k \phi(-\tau_k)$ and $\mathcal{F}$ is assumed to be a sufficiently smooth function mapping $C_{r,n}$ into $\mathbb{R}^n$ with $\mathcal{F}(0) = \mathcal{D}\mathcal{F}(0) = 0$ where $\mathcal{D}$ is the Fréchet derivative. The linear operator $\mathcal{L}$ can be written in the integral form as $\mathcal{L}\phi = \int_{-r}^{0} d\eta(\theta)\phi(\theta)$ where η is a real valued $n \times n$ matrix.

The linearization of (13.56) is given by

$$\frac{d}{dt}x = \mathcal{L}x_t, \tag{6.4}$$

the solution of which is given by the operator $\mathcal{T}(t)$ defined by $\mathcal{T}(t)(\phi) = x_t(.,\phi)$ such that $x_t(.,\phi)(\theta) = x(t+\theta,\phi)$ for $\theta \in [-r,0]$. This is a strongly continuous semigroup, the infinitesimal generator of which is $\mathcal{A} = \frac{d\phi}{d\theta}$ with the domain

$$\mathcal{D}om(\mathcal{A}) = \left\{ \phi \in C_{r,n} : \frac{d\phi}{d\theta} \in C_{r,n}, \dot{\phi}(0) = \frac{d\phi(0)}{d\theta} = \mathcal{L}\phi \right\}.$$

It is also known that the spectrum of $\mathcal{A}$ is $\sigma(\mathcal{A}) = \sigma_p(\mathcal{A})$ (point spectrum) and consists of complex values $\lambda \in \mathbb{C}$ satisfying the characteristic equation $p(\lambda) = 0$, (see [206, 151, 123] for further insights on the stability of delay-differential equations).

In the spirit of [75], let us denote by $\mathcal{M}_\lambda$ the eigenspace associated with $\lambda \in \sigma(\mathcal{A})$. We define $C_{r,n}^* = C([-r,0], \mathbb{R}^{n*})$ where $\mathbb{R}^{n*}$ is the space of n-dimensional row vectors and consider the bilinear form on $C_{r,n}^* \times C_{r,n}$ as proposed in [115] :

$$(\psi, \phi) = \psi(0)\,\phi(0) + \int_{-r}^{0} \int_{0}^{\theta} \psi(\tau - \theta)d\eta(\theta)\phi(\tau)d\tau.$$

Let $\mathcal{A}^T$ be the transposed operator of $\mathcal{A}$, i.e., $(\psi, \mathcal{A}\phi) = (\mathcal{A}^T\psi, \phi)$. The following result enables the decomposition of the space $C_{r,n}$.

Theorem 30 (Banach space decomposition, [115]). *Let Λ be a nonempty finite set of eigenvalues of $\mathcal{A}$, let $P = span\{\mathcal{M}_\lambda(\mathcal{A}), \lambda \in \Lambda\}$ and $P^T = span\{\mathcal{M}_\lambda(\mathcal{A}^T), \lambda \in \Lambda\}$. Then P is invariant under $\mathcal{T}(t), t \geq 0$ and there exists a space $\mathcal{Q}$, also invariant under $\mathcal{T}(t)$, such that $C_{r,n} = P \bigoplus Q$. Furthermore, if $\Phi = (\phi_1, \ldots, \phi_m)$ is a basis of P, and $\Psi = col(\psi_1, \ldots, \psi_m)$ is a basis of P^T in $C^*_{r,n}$ such that $(\Psi, \Phi) = Id$, then*

$$Q = \{\phi \in C_{r,n} \mid (\Psi, \phi) = 0\} \text{ and}$$
$$P = \{\phi \in C_{r,n} \mid \exists b \in \mathbb{R}^m : \phi = \Phi b\}. \tag{6.5}$$

Also, $\mathcal{T}(t)\Phi = \Phi\, e^{Bt}$, where B is an $m \times m$ matrix such that $\sigma(B) = \Lambda$.

Consider the extension of the space $C_{r,n}$ that contains continuous functions on $[-r, 0)$ with a possible jump discontinuity at 0, we denote this Banach space BC (identified to $C_{n,r} \times \mathbb{R}^n$). A given function $\xi \in BC$ can be written as $\xi = \varphi + X_0 \alpha$, where $\varphi \in C_{r,n}$, $\alpha \in \mathbb{R}^n$ and X_0 is defined by $X_0(\theta) = 0$ for $-r \leq \theta < 0$ and $X_0(0) = Id_{n \times n}$. Then the Hale-Verduyn Lunel bilinear form [115] can be extended to the space $C^*_{r,n} \times BC$ by $(\psi, X_0) = \psi(0)$. Under the above consideration one can write equation (13.56) as an abstract ODE :

$$\dot{x} = \tilde{\mathcal{A}}x + X_0 \mathcal{F}(x). \tag{6.6}$$

where

$$\tilde{\mathcal{A}}\phi = \dot{\phi} + X_0[\mathcal{L}\phi - \dot{\phi}(0)], \tag{6.7}$$

with domain $D(\tilde{\mathcal{A}}) = C^1_{n,r}([-r, 0], \mathbb{R}^n)$. Due to the projection $\Pi : BC \to P$ defined by $\Pi(\varphi + X_0\alpha) = \Phi[(\Psi, \varphi) + \Psi(0)\alpha]$ and the state decomposition such that $x = \Phi y + z$ where $y \in \mathbb{R}^m$ and $z \in Q \cap C^1_{r,n} \triangleq Q^1$. Then, the equation (13.56) can be split into two equations. Our interest lies essentially in the evolution equation for the finite dimensional part of the space, i.e., the first equation of the following system :

$$\begin{cases} \dot{y} = By + \Psi(0)\mathcal{F}(\Phi y + z), \\ \dot{z} = \tilde{\mathcal{A}}_{Q^1} z + (I - \Pi)\mathcal{F}(\Phi y + z). \end{cases} \tag{6.8}$$

For more details and insights, see for instance, [115, 92]. Assume now that $\mathcal{F}$ depends on some parameter p, and denote the semiflow generated by (6.8) as $\mathcal{S}(t, y, z, p)$, then $\mathcal{S}$ is equivalent to the semiflow generated by (13.56) :

Theorem 31 (Existence and Properties of the Center Manifold). *Let $k > 0$ and $\mathcal{U}_y \times \mathcal{U}_z \times \mathcal{U}_p$ be a small neighborhood of $(0, 0, p_0) \in \mathbb{R}^n \times Q \times \mathbb{R}^m$. There exists a graph $\omega : \mathcal{U}_y \times \mathcal{U}_p \to Q$ of smoothness C^k such that the following statements hold.*

1. *(Invariance) The manifold $\{(y, z) \in \mathcal{U}_y \times Q : z = \omega(y, p)\}$ is invariant with respect to $\mathcal{S}$ relative to $\mathcal{U}_y \times \mathcal{U}_z$.*

2. *(Exponential attraction) Let (y, z) be such that $\mathcal{S}(y, z, p) \in \mathcal{U}_y \times \mathcal{U}_z$ $\forall t \geq 0$. Then there exists $\tilde{y}$ and $\tilde{t} \geq 0$ such that $\|\mathcal{S}(t + \tilde{t}, y, z, p) - \mathcal{S}(t, \tilde{y}, \omega(\tilde{y}), p)\| \leq K e^{-t\alpha}$ for some positive real number α and for all $t > 0$.*

6.2.3 Multiplicity of the root at the origin : Polya-Szegö Bound

Consider the quasipolynomial function $\Delta : \mathbb{C} \times \mathbb{R}^N_+ \to \mathbb{C}$ of the form :

$$\Delta(\lambda, \tau) = P_0(\lambda) + \sum_{k=1}^{N} P_k(\lambda)\, e^{-\tau_k \lambda}, \tag{6.9}$$

where τ_k, $k = 1, \ldots, N$ are constant delays such that $\tau_1 < \tau_2 \ldots < \tau_N$ and $\tau = (\tau_1, \ldots, \tau_N)$ is the delays vector. Without any loss of generality, assume that the polynomial P_0 is a monic of degree n in λ and the polynomials P_k are such that $\deg(P_k) \leq n - 1$, $\forall 1 \leq k \leq N$. One can prove that the quasipolynomial function (10.4) admits an infinite number of zeros, see for instance [4, 20]. However, the multiplicity of any root is bounded, in particular the root at the origin. The following result, due to Polya-Szegö, gives to such a bound :

Proposition 1 (Pólya-Szegö, [176], pp.144). *Let $\tau_1, \ldots, \tau_N$ denote real numbers such that $\tau_1 < \tau_2 < \ldots < \tau_N$ and $d_1, \ldots, d_N$ positive integers such that $d_1 + d_2 + \ldots + d_N = D$.*

Let $f_{i,j}(s)$ stand for the function $f_{i,j}(s) = s^{i-1}\, e^{\tau_j s}$, for $1 \leq i \leq d_j$ and $1 \leq j \leq N$. Let $\sharp$ be the number of zeros of the function

$$f(s) = \sum_{1 \leq j \leq N, 1 \leq i \leq d_j} c_{i,j}\, f_{i,j}(s),$$

that are contained in the horizontal strip $\alpha \leq \mathcal{I}(z) \leq \beta$.
Assuming that

$$\sum_{1 \leq k \leq d_1} |c_{k,1}| > 0 \quad and \quad \sum_{1 \leq k \leq d_N} |c_{k,N}| > 0,$$

then

$$\frac{(\tau_N - \tau_1)\,(\beta - \alpha)}{2\,\pi} - D + 1 \leq \sharp \leq \frac{(\tau_N - \tau_1)\,(\beta - \alpha)}{2\,\pi} + D - 1.$$

The proof of the mentioned Pólya-Szegö result is mainly based on Rouché's Theorem [4]. It can be generically exploited to establish a bound for the multiplicity of the zero spectral value that we denote by $\sharp_{PS}$. Indeed, setting $\alpha = \beta = 0$ we get $\sharp_{PS} \leq D - 1$. This gives a sharp bound when all the system parameters are left free. Nevertheless, it is obvious that the Pólya-Szegö bound does not change if certain coefficients $c_{i,j}$ vanish without affecting the degree of the quasipolynomial function.

The above result from [38] sets the necessary and sufficient conditions guaranteeing the Pólya-Szegö multiplicity for the zero singularity.

Proposition 2 ([38]). *The multiplicity of the zero singularity reaches the Pólya-Szegö a bound if and only if the parameters of (10.4) satisfy simultaneously :*

$$a_{0,k} = -\sum_{i=1}^{N} \left[a_{i,k} + \sum_{j=0}^{k-1} \frac{(-1)^{j+1}\, a_{i,j}\tau_i^{k-j}}{(k-j)!} \right], \quad 0 \leq k \leq \# - 1. \tag{6.10}$$

where $a_{i,l}$ stands for the coefficient of the monomial λ^l for the polynomial P_i for $1 \leq i \leq N$.

Furthermore, it is shown in [38] that, under the nondegeneracy of an appropriate functional Birkhoff matrix, the multiplicity of the zero root for the quasipolynomial function (10.4) cannot be larger than n plus the number of nonzero coefficients of the polynomial family $(P_k)_{1 \leq k \leq N}$, which is sharper than $\sharp_{PS}$.

Remark 2. Increasing the multiplicity of the zero singularity induces richer (more complex) dynamics in the neighborhood of the steady state. We show in the sequel that the proposed methodology is able to stabilize the solutions around the unstable equilibrium point even when the multiplicity of the zero singularity reaches its maximum value.

6.3   Double Delay Block

Let the horizontal driving force exerted by the control law be $D = a\,\theta(t - \tau_1) + b\,\theta(t - \tau_2)$. Thus, equation (10.36) can be written as a Delay-Differential Equation (DDE) of the form :

$$\dot{x} = f(x(t), x(t - \tau_1), x(t - \tau_2), \lambda), \tag{6.11}$$

where $x = (x_1, x_2)^T = \left(\theta(t), \dot{\theta}(t)\right)^T$ and $\lambda = (a, b, \tau_1, \tau_2)$. The right hand side $f : \mathbb{R}^2 \times \mathbb{R}^2 \times \mathbb{R}^2 \times \mathbb{R}^4 \to \mathbb{R}^2$ is given by :

$$
\begin{aligned}
f_1(x, y, z, \lambda) &= x_2 \\
f_2(x, y, z, \lambda) &= \frac{-\frac{3\varepsilon}{8}\sin(2\,x_1)x_2^2 + \sin(x_1) - \cos(x_1)\,(a\,y_1 + b\,z_1)}{1 - \frac{3\varepsilon}{4}\cos^2(x_1)}.
\end{aligned}
\tag{6.12}
$$

where $y = \left(\theta(t - \tau_1), \dot{\theta}(t - \tau_1)\right)^\top$ and $z = \left(\theta(t - \tau_2), \dot{\theta}(t - \tau_2)\right)^\top$.
The phase space of (6.11)-(6.12) is the space of continuous functions over the delay interval
$[-\max(\tau_1, \tau_2), 0]$ with values in $\mathbb{R}^2$. Obviously $f(-x, -y, -z, \lambda) = -f(x, y, z, \lambda)$, and thus, the origin represents always an equilibrium point.

6.3.1   Linear Stability Analysis

As emphasized in Remark 2, we consider the maximum multiplicity for the zero spectral value (the most complex configuration). Taking the relative mass $\varepsilon = \frac{3}{4}$ guaranties such a maximum multiplicity. Note that, if $\varepsilon \in (0, 1)$, and regardless of the multiplicity of the zero singularity, all the following steps apply albeit in a simpler fashion. One easily checks that the zero multiplicity is less than four (otherwise τ_1 and τ_2 have opposite signs). Indeed, the linearization of f with respect to its three

arguments, x, y and z at the origin is given by :

$$\partial_1 f(0,0,0,\lambda) = \begin{bmatrix} 0 & 1 \\ \frac{16}{7} & 0 \end{bmatrix}, \quad \partial_2 f(0,0,0,\lambda) = \begin{bmatrix} 0 & 0 \\ -\frac{16}{7}a & 0 \end{bmatrix},$$

$$\partial_3 f(0,0,0,\lambda) = \begin{bmatrix} 0 & 0 \\ -\frac{16}{7}b & 0 \end{bmatrix}.$$

Then, the characteristic function reads :

$$\Delta(z) = z^2 + \frac{16}{7}(a\,\mathrm{e}^{-z\,\tau_1} + b\,\mathrm{e}^{-z\,\tau_2} - 1).$$

Several approaches can be used for characterizing imaginary crossing roots of quasipolynomials as well as their crossing directions, see for instance [167, 202]. Here, we follow the idea proposed by [110, 155]. We introduce the *stability crossing curves* **T**, which represents the set of (τ_1, τ_2) such that $\Delta(z)$ has imaginary solutions. As the parameters (τ_1, τ_2) cross the stability crossing curves, some characteristic roots cross the imaginary axis. Introduce also the *crossing set* Ω, which is defined as the collection of all $\omega > 0$ such that there exists a parameter pair (τ_1, τ_2) such that $\Delta(j\omega, \tau_1, \tau_2) = 0$. Using Proposition 3.1 in [110] the following stability characterization can be deduced :

Proposition 3. *For $a + b < 1$, the crossing set Ω is empty so the system is delay independently unstable. When $a + b > 1$, the crossing set Ω reduces to one interval $(0, \omega^r]$ and* **T** *is a series of open-ended curves* $\mathbf{T}_{u,v}^{\pm}$ *where* $\mathbf{T}_{u,v}^{-}$ *and* $\mathbf{T}_{u,v+1}^{+}$ *are connected at ω^r.*

We emphasize that
— when $a + b > 1$, $a > b$ the crossing set Ω contains only simple solution of Δ
— when $a + b > 1$, $a < b$ one has frequencies $\omega \in \Omega$ which are solution of multiplicity 2 for Δ.

The function Δ has a root 0 along the red solid red curve in figure 6.4 given by $a + b = 1$, where the origin undergoes a pitchfork bifurcation.

In a similar way, we can introduce the stability crossing curves **A** in the parameter space (a, b) and the corresponding crossing set Γ. Thus **A** is the set of (a, b) for which $\Delta(z)$ has imaginary solutions while Γ consist of those frequencies ω for which there exists a parameter pair (a, b) such that $\Delta(j\omega, a, b) = 0$. The stability analysis in the (a, b) parameter space is summarized as follows :

Proposition 4. *The crossing set Γ consists of all frequencies satisfying :*

$$0 < \omega < \left| \frac{\pi}{\tau_1 - \tau_2} \right|,$$

and for any given τ_1 and τ_2 the crossing curves are defined by :

$$\begin{cases} a = -\dfrac{\sin(\omega\tau_2)}{\sin(\omega\tau_1)}b, \\[2mm] b = \dfrac{1 + \frac{7}{16}\omega^2}{cos(\omega\tau_2) - \frac{\sin(\omega\tau_2)}{\sin(\omega\tau_1)}\cos(\omega\tau_1)} \end{cases}, \quad \forall \omega \in \Gamma. \tag{6.13}$$
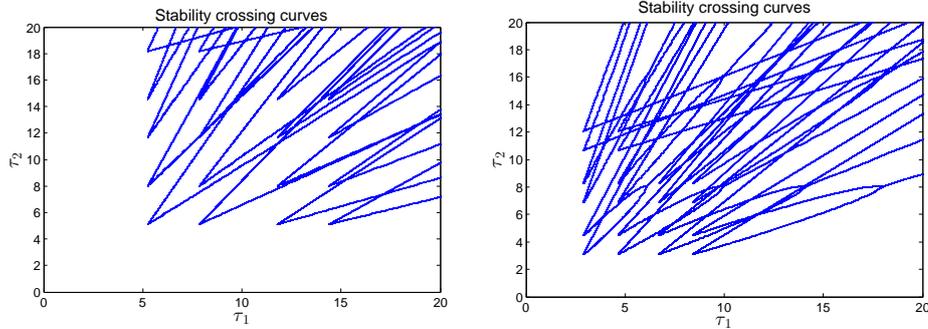
FIGURE 6.2 – Stability in delay parameter space for $a = \frac{4}{5}$, $b = \frac{3}{5}$ on the left and for $a = \frac{4}{5}$, $b = \frac{7}{5}$ on the right
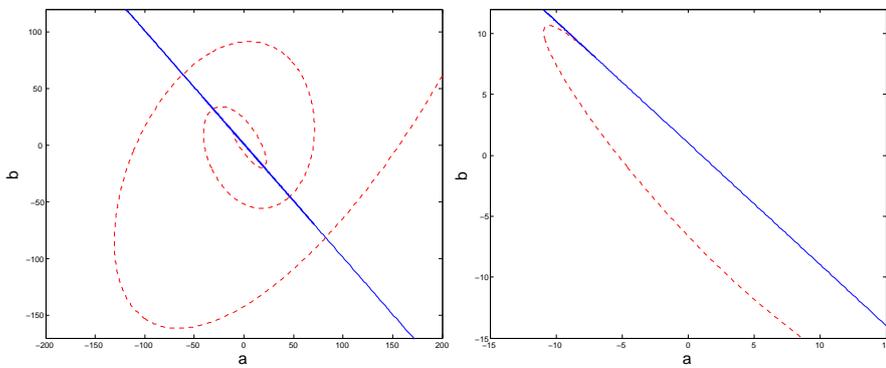
FIGURE 6.3 – Left : Dashed curve represents the stability crossing curve in (a, b) parameter space for $\tau_1 = 1$, $\tau_2 = \frac{7}{8}$ while the solid curve is the line $a + b = 1$. Right : Zoom in the neighborhood of $\omega = 0$.

It is always possible to normalize one of the delays by a simple scaling of time. Without any lack of generality, assume that $\tau_1 = 1$. As can be seen in figure 6.3, when ω approaches 0 the crossing curve approaches the line $a + b = 1$.

The quasipolynomial function Δ has a purely imaginary root $i\,\omega$ if the gains a and b satisfy (6.13). Thus, equation (6.13) defines the curve of Hopf Bifurcation in
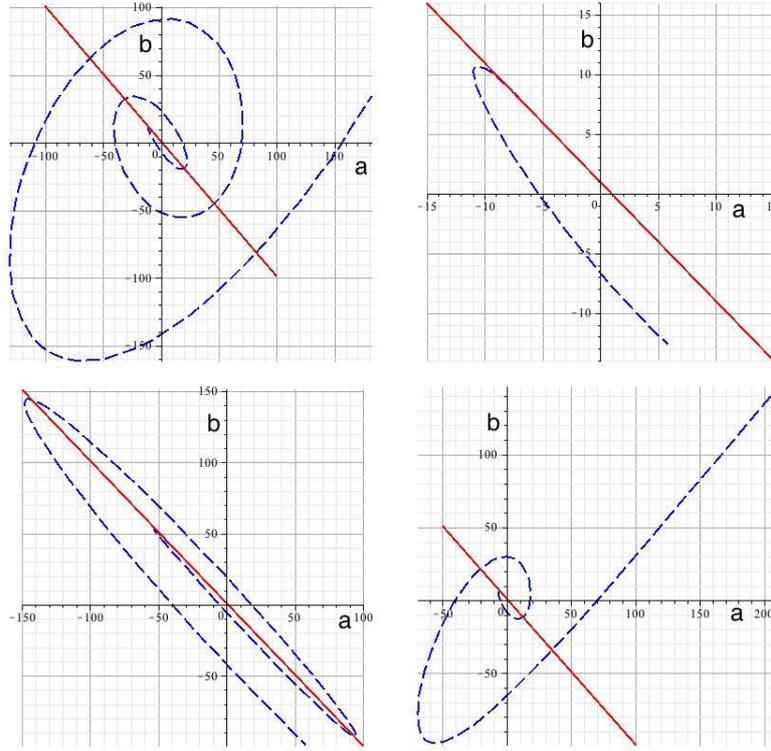
FIGURE 6.4 – Bifurcations curves of (6.11)-(6.12) in the gains (a,b) plan (solid red=Pitchfork, discontinuous blue=Hopf) with $\tau_1 = 1$ and τ_2 such that (top left) $\tau_2 = \frac{7}{8}$ (top right) $\tau_2 = \frac{7}{8}$ the neighborhood of (-7,8) (bottom left) $\tau_2 = \frac{7}{8} + \frac{1}{10}$ (bottom right) $\tau_2 = \frac{7}{8} - \frac{1}{10}$

the (a, b) plane, dashed blue line in figure 6.4. We note also that substituting $\omega = 0$ in the expressions of a and b allows deriving the values of the gain guarateeing an eigenvalue at zero of algebraic multiplicity 2. Substituting these values into the third derivative of characteristic function Δ and replacing $\tau_2 = \tau_1 + \delta$ leads to the control loop latency $\tau_1^* = \frac{1}{2}(\sqrt{\delta^2 + 8 - 6\varepsilon} - \delta)$ already identified in [201] where the linear analysis and a comparative study is made (PMD vs Acceleration-dependent control). It is also shown that the "optimal" value of the control loop latency is reached when $\delta = 0$.

Remark 3. In [200], the authors consider $D = a\,\theta(t - \tau) + b\,\dot{\theta}(t - \tau)$ and prove that the truncated cubic central dynamics reduces to :

$$\dot{u} = \begin{bmatrix} 0 & 1 & 0 \\ 0 & 0 & 1 \\ \alpha & \beta & \gamma \end{bmatrix} u + \begin{bmatrix} 0 \\ 0 \\ u_1^3 \end{bmatrix},$$

where α, β and γ are small parameters, showing that the triple zero singularity can be avoided.
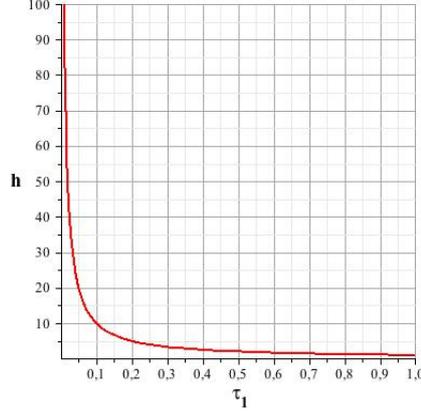
FIGURE 6.5 – The delay difference $h = \tau_2 - \tau_1$ vs τ_1 for conserving a triple eigenvalue at zero

To recover the analysis established in [200], consider a horizontal driving force $D = a\theta(t - \tau_1) + \tilde{b}(\theta(t - \tau_1) - \theta(t - \tau_1 - h))$ where $\tilde{b} = \frac{b}{h}$ and, without loss of generality, assume that $\tau_1 \leq \tau_2$, that is $h \geq 0$. Then $\lim_{h \to 0} D = a\theta(t - \tau_1) + b\dot{\theta}(t - \tau_1)$. Thus, the configuration of a triple zero eigenvalue is ensured by the set of conditions $\left\{ a = 1, b = \tau_1, h = -\frac{-1 + \tau_1{}^2}{\tau_1}, \tau_2 = \tau_1{}^{-1} \right\}$. By imposing h to converge to zero, τ_1 tends to $\tau_1^* = 1$ so that the gain b tends to $b^* = \tau_1^* = 1$ which are, as expected, the identified values in [200]. In Figure 6.5 we represent the delay difference $\tau_2 - \tau_1$.

Remark 4. It is worth noting that the delay normalization (setting $\tau_1 = 1$) does not affect the existence of the triple zero eigenvalue. Indeed, when τ_1 is left free the set of conditions :

$$\left\{ a = \frac{-7}{8\,\tau_1 - 7}, b = \frac{8\tau_1{}^2}{8\,\tau_1{}^2 - 7}, \tau_2 = \frac{7}{8\,\tau_1} \right\}$$

ensures this configuration.

Now, to argue the above normalization, let us consider the simplest demonstrative example ; a scalar equation with two delays : $\dot{x} = a_0 x(t) + a_1 x(t - \tau_1) + a_2 x(t - \tau_2)$. We introduce the following time scaling $t = \zeta \tau_1$ and consider a new variable $v(\zeta) = x(t)$. Thus, the dynamics of the new variable v is governed by

$$v'(\zeta) = \frac{dv(\zeta)}{d\zeta} = \dot{x}(t)\frac{dt}{d\zeta} = \tau_1 \left(a_0\,x(t) + a_1\,x(t - \tau_1) + a_2\,x(t - \tau_2) \right)$$

$$= b_0\,v(\zeta) + b_1\,v(\zeta - 1) + b_2\,v(\zeta - \tau)$$

where $b_i = a_i/\tau_1$ for $i = 0, \ldots, 2$ and $\tau = \tau_2/\tau_1$. Which justifies as expected the adopted normalization.

6.3.2 Normal Form of the Central Dynamics

Several approaches exist to establish the decomposition of the Banach space of continuous functions, see for instance [45, 200, 11]. In the sequel, we follow the elegant approach based on the computation of the spectral projection presented in [200]. It is worth to mention that this spectral projection is mainly based on the bilinear form presented in the previous section justifying the universality of the spectral decomposition modulo the chosen base of the generalized eigenspace associated with pure imaginary spectral values.

The parameter point $\lambda_0 = (a_0, b_0, \tau_1{}^*, \tau_2{}^*) = (-7, 8, 1, \frac{7}{8})$ characterizes a triple zero eigenvalue at the origin. As said above, it is always possible to re-scale the time in order to normalize one of the delays to 1 (τ_1 becomes 1 and τ_2 becomes τ_2/τ_1) so the rescaled system (6.11)-(6.12) reads

$$
\begin{cases}
f_1(x, \lambda) = x_2, \\
f_2(x, \lambda) = \dfrac{\left(-\frac{9}{32} \sin\left(2\,x_1\right) x_2{}^2 + \tau_1{}^2 \, \sin\left(x_1\right) - \tau_1{}^2 \, \cos\left(x_1\right)\left(a y_1 + b z_1\right)\right)}{1 - \frac{9}{16}\left(\cos\left(x_1\right)\right)^2}.
\end{cases}
\quad (6.14)
$$

Let X be the Banach space $\mathbb{R}^2 \times C([-1, 0], \mathbb{R}^2)$. Consider

$$
D(H) := \{(y, \tilde{y}) \in \mathbb{R}^2 \times C^1([-1, 0], \mathbb{R}^2) \ : \ \tilde{y}(0) = y\} \subset X,
$$

and define the linear operator

$$
H : D(H) \subset X \to X,
$$
$$
H \begin{bmatrix} y \\ \tilde{y} \end{bmatrix} = \begin{bmatrix} \partial_1 f(0,0,0,\lambda)\tilde{y}(0) + \partial_2 f(0,0,0,\lambda)\tilde{y}(-1) + \partial_3 f(0,0,0,\lambda)\tilde{y}(-\frac{7}{8}) \\ \partial_s \tilde{y} \end{bmatrix},
$$
$$
(6.15)
$$

where the spatial variable in $C^1([-1, 0], \mathbb{R}^2)$ is denoted by s. The operator H is a closed unbounded operator. It generates a strongly continuous semigroup $T(t)$ of bounded operators in $Y = \{(y, \tilde{y}) \in \mathbb{R}^2 \times C([-1, 0], \mathbb{R}^2) \ : \ \tilde{y}(0) = y\} \subset X$. The semigroup $T(.)$ is compact for $t > 1$.

Let g be the nonlinear part of f i.e.

$$
g\left(\begin{bmatrix} y \\ \tilde{y} \end{bmatrix}, \lambda\right) = \begin{bmatrix} g_0(\tilde{y}(0), \tilde{y}(-1), \tilde{y}(-\frac{7}{8}), \lambda) \\ 0 \end{bmatrix},
\quad (6.16)
$$

where

$$
g_0(\tilde{y}(0), \tilde{y}(-1), \tilde{y}(-\frac{7}{8}), \lambda) = f(\tilde{y}(0), \tilde{y}(-1), \tilde{y}(-\frac{7}{8}), \lambda) -
$$
$$
\left(\partial_1 f(0,0,0,\lambda)\tilde{y}(0) + \partial_2 f(0,0,0,\lambda)\tilde{y}(-1) + \partial_3 f(0,0,0,\lambda)\tilde{y}(-\frac{7}{8})\right).
$$

System (6.11)-(6.12) is equivalent to the autonomous evolution equation :

$$
\dot{x} = Hx + g(x, \lambda).
\quad (6.17)
$$

The decomposition of the Banach space reads $X = P \bigoplus Q$ where P is the H-invariant generalized eigenspace associated to the triple zero singularity and is isomorphic to $\mathbb{R}^3$, and Q is also H-invariant of infinite dimension. Next, we compute Φ a basis of P satisfying $H\Phi = \Phi J$, where :

$$
\Phi(s) = [\phi_1, \phi_2, \phi_3] = \begin{bmatrix} 1 & 0 & 1 \\ 0 & 1 & 0 \\ 1 & s & \frac{s^2}{2}+1 \\ 0 & 1 & s \end{bmatrix}, \text{ and } J = \begin{bmatrix} 0 & 1 & 0 \\ 0 & 0 & 1 \\ 0 & 0 & 0 \end{bmatrix}.
$$

We also compute the invariant spectral projection $\mathcal{P} : X \to P$ satisfying $\mathcal{P}x = Res_{z=0}(z\,I - H)^{-1}$. Thus, $\mathcal{P}x = l_1(x)\phi_1 + l_2(x)\phi_2 + l_3(x)\phi_3$ where :

$$
l_1(x) = \frac{169}{300}\tilde{y}_1(0) - \frac{222179}{144000}\tilde{y}_2(0) - \frac{222179}{9000}\int_0^1 \tilde{y}_1(t-1)dt
$$
$$
+ \frac{222179}{7875}\int_0^{\frac{7}{8}} \tilde{y}_1(t-\frac{7}{8})dt - \frac{676}{75}\int_0^1 t\tilde{y}_1(t-1)dt + \frac{5408}{525}\int_0^{\frac{7}{8}} t\tilde{y}_1(t-\frac{7}{8})dt
$$
$$
+ \frac{64}{5}\int_0^1 t^2\tilde{y}_1(t-1)dt - \frac{512}{35}\int_0^{\frac{7}{8}} t^2\tilde{y}_1(t-\frac{7}{8})dt,
$$
$$
l_2(x) = \frac{8}{5}\tilde{y}_1(0) + \frac{169}{300}\tilde{y}_2(0) + \frac{676}{75}\int_0^1 \tilde{y}_1(t-1)dt - \frac{5408}{525}\int_0^{\frac{7}{8}} \tilde{y}_1(t-\frac{7}{8})dt
$$
$$
- \frac{128}{5}\int_0^1 t\tilde{y}_1(t-1)dt + \frac{1024}{35}\int_0^{\frac{7}{8}} t\tilde{y}_1(t-\frac{7}{8})dt,
$$
$$
l_3(x) = \frac{8}{5}\tilde{y}_2(0) + \frac{128}{5}\int_0^1 \tilde{y}_1(t-1)dt - \frac{1024}{35}\int_0^{\frac{7}{8}} \tilde{y}_1(t-\frac{7}{8})dt,
$$

which allows decomposing (6.17) to :

$$
\dot{v} = Jv + \Psi(0)g_0(\tilde{\Phi}(0)v + \tilde{w}_0, \tilde{\Phi}(-1)v + \tilde{w}(-1), \tilde{\Phi}(-\frac{7}{8})v + \tilde{w}(-\frac{7}{8}))
$$
$$
\dot{w}_0 = \partial_1 f\tilde{w}_0 + \partial_2 f\tilde{w}(-1) + \partial_3 f\tilde{w}(\frac{7}{8})
$$
$$
+ (I - \Phi(0)\Psi(0))g_0(\tilde{\Phi}(0)v + \tilde{w}_0, \tilde{\Phi}(-1)v + \tilde{w}(-1), \tilde{\Phi}(-\frac{7}{8})v + \tilde{w}(-\frac{7}{8}))
$$
$$
\dot{w} = \partial_s\tilde{w} - \tilde{\Phi}\Psi(0)g_0(\tilde{\Phi}(0)v + \tilde{w}_0, \tilde{\Phi}(-1)v + \tilde{w}(-1), \tilde{\Phi}(-\frac{7}{8})v + \tilde{w}(-\frac{7}{8})),
$$

where $\tilde{w}_0 = \tilde{w}(0)$ and :

$$
\Psi(0) = \begin{bmatrix} \frac{169}{300} & -\frac{222179}{144000} \\ \frac{8}{5} & \frac{169}{300} \\ 0 & \frac{8}{5} \end{bmatrix}, \tilde{\Phi}(s) = \begin{bmatrix} 1 & s & 1+\frac{s^2}{2} \\ 0 & 1 & s \end{bmatrix}.
$$

By using the Center Manifold Theorem presented in the previous section and the following changes of coordinates :

$$a = -7 - \frac{35}{128}\,\alpha\,r^6, b = 8 + \frac{5}{16}\,\gamma\,r^2, \tau_1 = 1 - \frac{7}{768}\,\beta\,r^4, \qquad (6.18)$$

$$v_1 = r^3 u_1, v_2 = r^5 u_2, v_3 = r^7 u_3, w = r^3 q, \qquad (6.19)$$

where r is a sufficiently small parameter, we arrive to the expansion of the graph (the center manifold) in power of r which is of order 6, i.e., $q(u, \mu, r) = r^6 q_6(u, \mu, r)$, where $\mu = (\alpha, \beta, \gamma)$ and the expression of the flow on the local center manifold is

$$\dot{u} = \begin{bmatrix} 0 & 1 & 0 \\ 0 & 0 & 1 \\ \alpha & \beta & \gamma \end{bmatrix} u + \begin{bmatrix} 0 \\ 0 \\ u_1^3 \end{bmatrix} + r^2 R(u, \mu, r), \qquad (6.20)$$

where the remainder is a smooth function $R : \mathbb{R}^3 \times \mathbb{R}^3 \times \mathbb{R} \to \mathbb{R}^3$.

6.3.3 Concluding remark

It is important to recall that, in a neighborhood of the origin, the stability of the solution of the normal form (6.20) in the center manifold proves the local stability of the solution of the initial infinite dimensional system (6.11). Moreover, one can easily establish values for α, β and γ so that the matrix associated with the linear part of the normal form (6.20) be Hurwitz (all eigenvalues with negative real part). Thus, choosing a sufficiently small value for the scale parameter r and using (6.18) allow us to establish the values of the gains and the delays guaranteeing the stability of the inverted pendulum.

It is important to note that the global bifurcation diagram is beyond the scope of this paper. Furthermore, it is clear from the literature that the bifurcation diagram for the triple zero singularity (in all generality) is very complicated not only from a theoretical point of view but also from a numerical point of view [80, 81, 96]. However, under the $\mathbb{Z}_2$ symmetry as for the cubic truncation of (6.20), we refer the reader to [6] where such a type of symmetry is identified for the Chua equations. The global analysis established in [200] applies for the present configuration since the same cubic truncated normal form is considered.

Remark 5. We point out that a larger multiplicity for the zero singularity might occur when using a controller consisting in three delay blocks $D = \sum_{k=1}^{3} a_k \theta(t - \tau_k)$, this is a natural consequence of Proposition 2 [1], see also [38] for further details. Indeed, the zero singularity codimension bound is equal to 4 inducing richer dynamics.

---

1. It is obvious that such a controller implies an additional coefficient

Such a configuration is guaranteed by the following values of coefficients :

$$
\begin{cases}
a_1 = \dfrac{7}{8}\,\dfrac{8\,\tau_2{}^2 + 7}{(8\,\tau_2\tau_1{}^2 - 14\,\tau_1 - 7\,\tau_2)\,(-\tau_2 + \tau_1)}, \quad a_2 = -\dfrac{7}{8}\,\dfrac{8\,\tau_1{}^2 + 7}{(-7\,\tau_1 + 8\,\tau_1\tau_2{}^2 - 14\,\tau_2)\,(-\tau_2 + \tau_1)}, \\[3mm]
a_3 = \dfrac{\left(64\,\tau_1{}^2\tau_2{}^2 - 112\,\tau_1\tau_2 + 49\right)\left(8\,\tau_1\tau_2 - 7\right)}{8\left(8\,\tau_2\tau_1{}^2 - 14\,\tau_1 - 7\,\tau_2\right)\left(-7\,\tau_1 + 8\,\tau_1\tau_2{}^2 - 14\,\tau_2\right)}, \quad \tau_3 = 7\,\dfrac{\tau_2 + \tau_1}{8\,\tau_1\tau_2 - 7}, \\[3mm]
\text{where } \ \tau_1 \neq \tau_2, \ \ \tau_1 \neq \dfrac{14\,\tau_2}{-7 + 8\,\tau_2{}^2}, \ \ \tau_2 \neq \dfrac{14\,\tau_2}{-7 + 8\,\tau_1{}^2} \ \ \text{and } \ 8\,\tau_1\tau_2 > 7.
\end{cases}
$$

$$(6.21)$$

6.4   Pyragas-Type controller

By Pyragas controller, we understand a controller of the form

$$u(t) := \alpha(\theta(t) - \theta(t - \tau)).$$

It is worth mentioning that such a controller proved interest in the stabilization of unstable periodic orbits, see for instance, [177, 178]. Furthermore, in Laplace domain, the corresponding characteristic function includes an additional root at the origin.

In this section we consider the control law

$$D(t) = a\,(\theta(t) - \theta(t - \tau_1)) + b\,(\theta(t) - \theta(t - \tau_2)) + c\,\theta(t),$$

and consider the relative mass $\varepsilon = 3/4$. Equation (10.36) can be written as a DDE of the form :

$$\dot{x} = f(x(t), x(t - \tau_1), x(t - \tau_2), \lambda),\qquad(6.22)$$

where $x = (x_1, x_2)^\top = \left(\theta(t), \dot{\theta}(t)\right)^\top$ and $\lambda = (a, b, \tau_1, \tau_2)$. The right hand side $f : \mathbb{R}^2 \times \mathbb{R}^2 \times \mathbb{R}^2 \times \mathbb{R}^4 \to \mathbb{R}^2$ is given by :

$$
\begin{cases}
f_1(.\lambda) = x_2, \\[2mm]
f_2(.,\lambda) = \dfrac{-\frac{9}{32}\,\sin\left(2\,x_1\right) x_2{}^2 + \sin\left(x_1\right)}{1 - \frac{9}{16}\left(\cos\left(x_1\right)\right)^2} \\[4mm]
\qquad - \dfrac{\cos\left(x_1\right)\left(a\left(x_1 - y_1\right) + b\left(x_1 - z_1\right) + cx_1\right)}{1 - \frac{9}{16}\left(\cos\left(x_1\right)\right)^2},
\end{cases}
\qquad(6.23)
$$

where $y = (y_1, y_2)^\top = (\theta(t - \tau_1), \dot{\theta}(t - \tau_1))^\top$ and $z = (z_1, z_2)^\top = (\theta(t - \tau_2), \dot{\theta}(t - \tau_2))^\top$.

6.4.1   Linear Stability Analysis

It is always possible to normalize one of the delays by a simple scaling of time, let $\tau_1 = 1$. The linearization of f with respect to its three arguments, x, y and z at

the origin is given by

$$\partial_1 f(0, \lambda) = \begin{bmatrix} 0 & 1 \\ \frac{16(1-a-b-c)}{7} & 0 \end{bmatrix},$$

$$\partial_2 f(0, \lambda) = \begin{bmatrix} 0 & 0 \\ \frac{16}{7} a & 0 \end{bmatrix}, \ \partial_3 f(0, \lambda) = \begin{bmatrix} 0 & 0 \\ \frac{16}{7} b & 0 \end{bmatrix},$$

where $f(0, \lambda)$ designate $f(0, 0, 0, \lambda)$. Then, the characteristic function is given by

$$\Delta(\lambda) = \lambda^2 + \frac{16(a+b+c-1)}{7} - \frac{16}{7} e^{-\lambda \tau_1} a - \frac{16}{7} e^{-\lambda \tau_2} b. \tag{6.24}$$

The stability analysis follows from Proposition 3.1 in [110].

Remark 6. The crossing set Ω associated to the system described by the characteristic equation (6.24) consists of a finite union of intervals. Moreover, when $c \neq 1$, all the intervals are closed while for $c = 1$ all the intervals are closed excepting the first one which has the left end equals zero i.e. a value that does not belong to the crossing set. The stability crossing curves are either open ended or closed as explained in the classification proposed by [110] (see figure 6.6 for the case $c = 1$ which is relevant for this study).
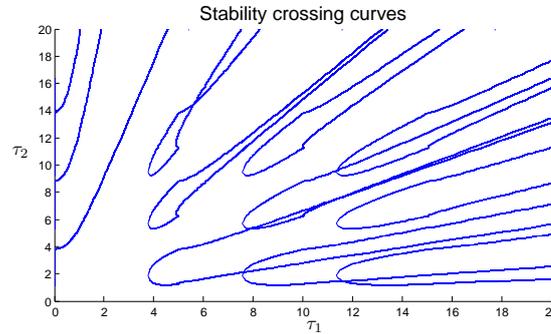
FIGURE 6.6 – The crossing curves associated to the first interval $(0, \omega^r]$ for $a = \frac{6}{5}$, $b = \frac{3}{5}$ and $c = 1$. The curves $\mathbf{T}_{u,v}^-$ and $\mathbf{T}_{u,v+1}^+$ are connected at ω^r.

In the (a, b, c) parameter space instead of crossing curves we have stability crossing surfaces referred to as $\mathbf{A}$. The corresponding crossing set is again dented by Γ. Thus, $\mathbf{A}$ is the set of (a, b, c) such that $\Delta(z)$ has imaginary solutions while Γ consist of those frequencies ω such that there exists a parameter triple (a, b, c) such that $\Delta(j\omega, a, b, c) = 0$. The stability analysis in (a, b, c) parameter space is summarized as follows :

Proposition 5. *The crossing set Γ consist of all frequencies satisfying*

$$0 < \omega < \left| \frac{\pi}{\tau_1 - \tau_2} \right|,$$

and the crossing surfaces are defined $\forall \omega \in \Gamma$ by :

$$\begin{cases} a \in \mathbb{R} \\ b = -\dfrac{\sin(\omega\tau_1)}{\sin(\omega\tau_2)} a \\ c = 1 + \frac{7}{16}\omega^2 - a - b + a\cos(\omega\tau_1) + b\cos(\omega\tau_2) \end{cases} \quad .$$

It is easy to see that as ω approaches 0 the parameter c approaches 1 (for illustration see figure 6.7).
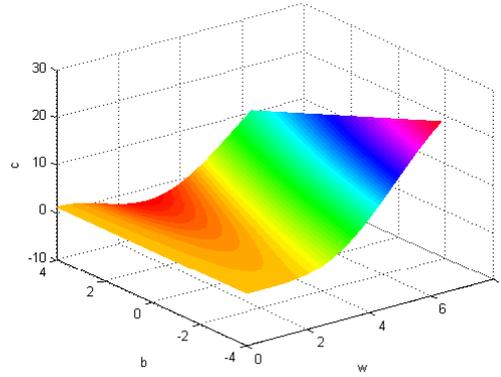
FIGURE 6.7 – The stability crossing surface in the (ω, b, c) parameter space for $\tau_1 = 1$, $\tau_2 = \frac{1}{2}$ and $a = 2$

The function Δ with arbitrary gain c has a purely imaginary root iw if :

$$\begin{cases} a = \dfrac{7\sin(w\tau_2)w^2 + 16\sin(w\tau_2) - 16\sin(w\tau_2)c}{16\sin(w\tau_2) - 16\sin(w\tau_2 - w) - 16\sin(w)}, \\ b = \dfrac{-7\sin(w)w^2 - 16\sin(w) + 16\sin(w)c}{16\sin(w\tau_2) - 16\sin(w\tau_2 - w) - 16\sin(w)}. \end{cases} \tag{6.25}$$

We note that substituting a and b into the second derivative of Δ and by setting $w = 0$ one gets the relation $a\,\tau_1 = -b\,\tau_2$ guarateeing a zero eigenvalue of algebraic multiplicity 2. Finally, a zero eigenvalue of algebraic multiplicity 3 is given by

$$a = \frac{7}{8}\frac{1}{(\tau_1 - \tau_2)\tau_1}, \; b = -\frac{7}{8}\frac{1}{\tau_2\,(\tau_1 - \tau_2)}, \; c = 1.$$

This shows that the configuration of a triple zero eigenvalue can not be achieved when one of the gains a or b vanishes, in other words, two Pyragas controllers are necessary to reach this multiplicity.

Equation (6.25) defines the curve of Hopf Bifurcation in the (a, b) plane in figure 7.2 for $c = 1$ and several values of the delay τ_2, thus there are coexistence of Pitchfork and Hopf bifurcation on this curves.
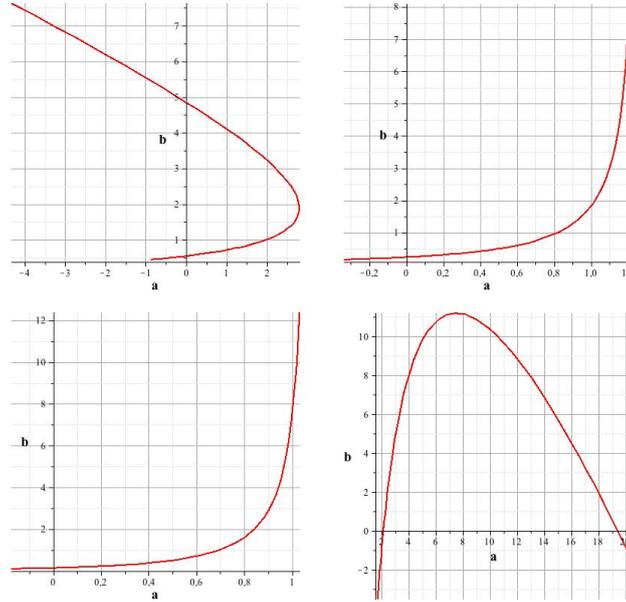
FIGURE 6.8 – Hopf curves for (6.23)-(6.22) in the gains plan (a,b) with $c = \tau_1 = 1$ and τ_2 such that (top left) $\tau_2 = 2$ (top right) $\tau_2 = 3$ (bottom left) $\tau_2 = 4$ (bottom right) $\tau_2 = \frac{1}{2}$

Note also, that when $\tau_1 \tau_2 \neq 0$ a zero eigenvalue of multiplicity 4 is not possible since the fourth derivative at zero gives $2(\tau_1 + \tau_2)$.

6.4.2 Central Dynamics

We show that a triple zero eigenvalue occurs for arbitrary value of the delay τ_2. Then let us restrict to the case of a fixed value for the delay $\tau_2 = 2$, the parameter point $\lambda_0 = (a_0, b_0, c_0, \tau_1{}^*, \tau_2{}^*) = (-\frac{7}{8}, \frac{7}{16}, 1, 1, 2)$ characterize a triple zero eigenvalue at the origin. System (6.23)-(6.22) can be normalized by setting $\tau_1 = 1$ leading to :

$$
\begin{cases}
f_1(.,\lambda) = x_2, \\
f_2(.,\lambda) = \dfrac{-\frac{9}{32} \sin(2\,x_1)\,x_2{}^2 + \tau_1{}^2 \sin(x_1)}{1 - \frac{9}{16}\left(\cos(x_1)\right)^2} \\
\qquad - \dfrac{\tau_1{}^2\,\cos(x_1)\left(a\,(x_1 - y_1) + b\,(x_1 - y_1) + c\,x_1\right)}{1 - \frac{9}{16}\left(\cos(x_1)\right)^2}.
\end{cases}
\tag{6.26}
$$

Let X be the Banach space $\mathbb{R}^2 \times C([-1,0], \mathbb{R}^2)$. Consider

$$
D(H) := \{(y, \tilde{y}) \in \mathbb{R}^2 \times C^1([-1,0], \mathbb{R}^2) \; : \; \tilde{y}(0) = y\} \subset X,
$$

and define the linear operator $H \begin{bmatrix} y \\ \tilde{y} \end{bmatrix}$

$$= \begin{bmatrix} \partial_1 f(0,\lambda)\tilde{y}(0) + \partial_2 f(0,\lambda)\tilde{y}(-1) + \partial_3 f(0,\lambda)\tilde{y}(-2) \\ \partial_s \tilde{y} \end{bmatrix},$$

where the spatial variable in $C^1([-2,0], \mathbb{R}^2)$ is denoted by s. Let g be the nonlinear part of f i.e.

$$g\left(\begin{bmatrix} y \\ \tilde{y} \end{bmatrix}, \lambda \right) = \begin{bmatrix} g_0(\tilde{y}(0), \tilde{y}(-1), \tilde{y}(-2), \lambda) \\ 0 \end{bmatrix}, \tag{6.27}$$

where :

$$g_0(\tilde{y}(0), \tilde{y}(-1), \tilde{y}(-2), \lambda) = f(\tilde{y}(0), \tilde{y}(-1), \tilde{y}(-2), \lambda) - \\ \left(\partial_1 f(0,\lambda)\tilde{y}(0) + \partial_2 f(0,\lambda)\tilde{y}(-1) + \partial_3 f(0,\lambda)\tilde{y}(-2) \right).$$

System (6.22)-(6.23) is equivalent to the autonomous evolution equation :

$$\dot{x} = Hx + g(x, \lambda). \tag{6.28}$$

The decomposition of the Banach space $X = P \bigoplus Q$ such that P is the H-invariant generalized eigenspace associated to triple zero sigularity which is isomorphic to $\mathbb{R}^3$ and Q also H-invariant of infinite dimension. Next, we compute Φ a basis of P satisfying $H\Phi = \Phi J$ where

$$\Phi(s) = [\phi_1, \phi_2, \phi_3] = \begin{bmatrix} 1 & 0 & 1 \\ 0 & 1 & 0 \\ 1 & s & \frac{s^2}{2}+1 \\ 0 & 1 & s \end{bmatrix}, \text{ and } J = \begin{bmatrix} 0 & 1 & 0 \\ 0 & 0 & 1 \\ 0 & 0 & 0 \end{bmatrix}.$$

We compute the invariant spectral projection $\mathcal{P} : X \to P$ such that $\mathcal{P}x = Res_{z=0}(z\,I-$

$H)^{-1}$. In other words, $\mathcal{P}x = l_1(x)\phi_1 + l_2(x)\phi_2 + l_3(x)\phi_3$ where :

$$
\begin{cases}
l_1(x) = \dfrac{7}{12}\,\tilde{y}_1(0) - \dfrac{131}{144}\,\tilde{y}_2(0) + \dfrac{131}{72}\int_0^1 \tilde{y}_1(t-1)\,dt \\[2mm]
\qquad - \dfrac{131}{144}\int_0^2 \tilde{y}_1(t-2)\,dt + 7/6 \int_0^1 t\tilde{y}_1(t-1)\,dt \\[2mm]
\qquad - \dfrac{7}{12}\int_0^2 t\tilde{y}_1(t-2)\,dt - \int_0^1 t^2\tilde{y}_1(t-1)\,dt \\[2mm]
\qquad + 1/2 \int_0^2 t^2\tilde{y}_1(t-2)\,dt, \\[3mm]
l_2(x) = \tilde{y}_1(0) + \dfrac{7}{12}\,\tilde{y}_2(0) - 7/6 \int_0^1 \tilde{y}_1(t-1)\,dt \\[2mm]
\qquad + \dfrac{7}{12}\int_0^2 \tilde{y}_1(t-2)\,dt + 2 \int_0^1 t\tilde{y}_1(t-1)\,dt \\[2mm]
\qquad - \int_0^2 t\tilde{y}_1(t-2)\,dt, \\[3mm]
l_3(x) = \tilde{y}_2(0) - 2 \int_0^1 \tilde{y}_1(t-1)\,dt + \int_0^2 \tilde{y}_1(t-2)\,dt,
\end{cases}
$$

which allows decomposing equation (6.28) to :

$$
\begin{cases}
\dot{v} = Jv + \Psi(0)g_0 \\
\dot{\tilde{w}}_0 = \partial_1 f\tilde{w}_0 + \partial_2 f\tilde{w}(-1) + \partial_3 f\tilde{w}(-2) \\
\qquad + (I - \Phi(0)\Psi(0))g_0 \\
\dot{\tilde{w}} = \partial_s \tilde{w} - \tilde{\Phi}\Psi(0)g_0,
\end{cases}
$$

g_0 designate $g_0(\tilde{\Phi}(0)v + \tilde{w}_0, \tilde{\Phi}(-1)v + \tilde{w}(-1), \tilde{\Phi}(-2)v + \tilde{w}(-2))$ and $\tilde{w}_0 = \tilde{w}(0)$ and

$$
\Psi(0) = \begin{bmatrix} \frac{7}{12} & -\frac{131}{144} \\ 1 & \frac{7}{12} \\ 0 & 1 \end{bmatrix}, \quad \tilde{\Phi}(s) = \begin{bmatrix} 1 & s & 1 + \frac{s^2}{2} \\ 0 & 1 & s \end{bmatrix}.
$$

By using the Center Manifold Theorem presented in the previous section and the following changes of coordinates :

$$
a = -\frac{7}{8} + \frac{7}{8}\,\alpha\,r^2, b = \frac{7}{16} + \frac{7}{16}\,\beta\,r^2, c = 1 + \frac{7}{16}\,\sigma\,r^2,
$$

$$
\tau_1 = 1 + \frac{1}{2}\,\delta\,r^4, v_1 = r^3 u_1, v_2 = r^5 u_2, v_3 = r^7 u_3, w = r^3 q,
$$

we arrive to the expansion of the graph (the center manifold) in power of r which is of order 6 i.e. $q(u, \mu, r) = r^6 q_6(u, \mu, r)$ where $\mu = (\alpha, \beta, \gamma)$ and the expression of the flow on the local center manifold :

$$
\dot{u} = \begin{bmatrix} 0 & 1 & 0 \\ 0 & 0 & 1 \\ -\alpha' & \beta' & \gamma' \end{bmatrix} u + \begin{bmatrix} 0 \\ 0 \\ u_1^3 \end{bmatrix} + r^2 R(u, \mu, r),
$$

where $\alpha' = \delta(\sigma + \beta)$, $\beta' = 3\delta$, $\gamma' = \alpha - \sigma - 3\beta$ and R is the remainder, a smooth function in u, μ and r.

6.5 Notes and comments

The use of multiple delay blocks was suggested in [166, 129] for stabilizing chains of integrators. In this paper, we design such a multi-delayed-proportional controllers allowing to stabilize the inverted pendulum by avoiding a triple zero eigenvalue singularity. This singularity was already identified in [200] through the use of a delayed PD controller. Such a singularity underlines an interesting observation : the multiplicity of the zero spectral value might exceed the dimension of the control-free system [38]. We have shown that a multi-delayed-proportional controller allows to offset the derivative gain while keeping the same performance. These results agree with the claim of [10], that is, the effect of the delay is similar to derivative feedback in modifying the behavior of the system. However, we extend the claim to the nonlinear analysis by proving that the cubic truncated normal form of the center manifold dynamics is the same as the one obtained by using a delayed PD regulator. Thus, the global analysis for the codimension-3 triple zero bifurcation established in [200] applies for the presented configuration.

Delay System Modeling of Rotary Drilling Vibrations

Vibrations in rotary drilling systems are oscillations occurring without being intentionally provoked. They often have detrimental effects on the system performance and are an important source of economic losses ; drill bit wear, pipes disconnection, borehole disruption and prolonged drilling time. By this chapter, we provide an improved modeling for the rotary drilling system. Among others, the proposed modeling takes into account the infinite dimensional settings of problem, as well as, the nonlinear interconnected dynamics. This chapter reproduces mainly the results of [146, 42].

7.1 Introduction

A rotary drilling structure is mainly composed of a rig, a drillstring, and a bit. In oil well drilling operations, one of the most important problem to deal with consists in suppressing harmful vibrations yielding to stick-slip and bit-bouncing oscillations. Indeed, these undesired dynamics can cause various damages such as pipes and bit break. This spoilage has a leaden economical effect. The drilling control failure is mainly due to poor modeling and/or control. This chapter focuses on the modeling task upon which the analysis and control rely on. The modeling must entail two aspects. The first one, "physics dynamics", consists in describing the motions equations of the phenomena occurring during the drilling process. The second, "sensing and transmission model", amounts to write down equations allowing to obtain informations on the bit state, an essential information to overcome the above mentioned problems. Unfortunately, this information is degraded and/or delayed, due to technological constraints. In this chapter, we are concerned solely by physical modeling, yet, we are taking into account transmission in deriving an overall system's model. In the literature, one may find several types of models ranging from partial differential equations to ordinary differential equation ones with one or several degrees of freedom representing the dynamics of drilling systems. This contribution is organized as follows : In the first section, we report the most relevant works concerned by the physical modeling of the drilling vibrations. The second section is devoted to present the PDE model that we build to account for axial and torsional vibrations. The proposed model improves the known models since it addresses several critical

issues that arise when the latter are considered. The chapter is completed by insights on Wireless sensing transmission models, as well as on actuating and related motor types. Finally, we derive a model covering most of the dynamics needed to be taken into account for control purposes. The chapter ends with some comments in wireless-transmission and real-time control methodology.

7.2   State of the Art

To the best of the authors' knowledge, torsional drilling vibrations have received much more attention compared to axial vibrations.

As underlined in [211], the simplest approximation consists in neglecting the effects of the axial and lateral vibrations and in ignoring the finite propagation time of torsional waves along the drillstring. The model turns to be a simple forced torsional pendulum under nonlinear damping at the bit. Thus, the full spectrum of the torsional vibrations is replaced by a simple torsional spring that couples the torque Φ_{top} from the top-drive with the torque Φ_{bit} generated in the bit/rock interface. Such an approximation leads to the following coupled system model

$$\begin{cases} \ddot{\Phi}_{top} + G_{top}(\Phi_{top} - \Phi_{bit}) = T_{motor}(\Phi_{top}, \Phi_{bit}, \dot{\Phi}_{top}, t), \\ \ddot{\Phi}_{bit} + G_{bit}(\Phi_{bit} - \Phi_{top}) = -\mathcal{F}(\dot{\Phi}_{bit}), \end{cases} \quad (7.1)$$

where $\mathcal{F}$ designates the bit-torque friction, G_{bit} G_{top} are the coupling physical constants, $G_{top} = G/\rho$ is some positive constant proportional to the torsional rigidity of the drillstring, $G_{bit} = GJ_{top}/J_{bit}$ and T_{motor} is the top control torque. Here G denotes the shear modulus of drilling steel, ρ is the steel density, J_{top} and J_{bit} are respectively the inertia moment of a pipe section and the inertia moment of the drill collar section.

In [125], the drillstring system is modeled as two coupled masses as shown in Figure 7.1. J_{top} and J_{bit} are two inertial masses locally damped by d_{top} and d_{bit}.
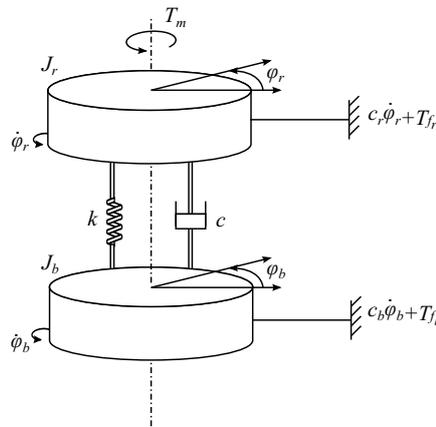

FIGURE 7.1 – Drill string two-coupled masses model.

The inertias are coupled through an elastic shaft of stiffness k and damping c. Let us define Φ_{top}, Φ_{bit} as the angular positions of the rotary and the bit respectively; $\dot{\Phi}_{top}$, $\dot{\Phi}_{bit}$ as their angular velocities, $u(t) = WoB$ is the weight on the bit control signal, $v(t)$ is the rotary table torque control signal used to regulate $\dot{\Phi}_{top}$, μ is the friction coefficient; A, B, H, C_o are model matrices given in (7.4), $\Psi(t) = \Psi(u(t)) = Hu(t)$, x is the state vector and y_o is the output variable. For a more detailed description, see, for instance, [71]. With the above notations, the model is represented as follows :

$$\dot{x}(t) = Ax(t) + Bv(t) + \Psi(t)\mu \tag{7.2}$$
$$y_o = C_o\, x = \dot{\Phi}_{top},$$

where the state $x = [x_1\ x_2\ x_3]^T$ is defined as follows :

$$x_1 = \Phi_{top} - \Phi_{bit}, \quad x_2 = \dot{\Phi}_{top}, \quad x_3 = \dot{\Phi}_{bit} \tag{7.3}$$

and

$$A = \begin{pmatrix} 0 & 1 & -1 \\ -\frac{k}{J_{top}} & -\frac{d_{top}+c}{J_{top}} & \frac{c}{J_{top}} \\ \frac{k}{J_{bit}} & \frac{c}{J_{bit}} & -\frac{c+d_{bit}}{J_{bit}} \end{pmatrix}, \ B = \begin{pmatrix} 0 \\ \frac{1}{J_{top}} \\ 0 \end{pmatrix}$$

$$H = \begin{pmatrix} 0 \\ 0 \\ -\frac{1}{J_{bit}} \end{pmatrix}, \quad C_o = \begin{pmatrix} 0 & 1 & 0 \end{pmatrix} \tag{7.4}$$

In [164], a piecewise-smooth model of three degrees of freedom, which exhibits friction-induced stick-slip oscillations, is considered in order to describe a simplified torsional lumped-parameter model of an oilwell drillstring. In [163] a piecewise finite dimensional multi degree of freedom (multi DOF) model is considered for describing the torsional motion. In [162], a more general nonlinear differential equation-based model of a drillstring is analyzed. The aim of the proposed drillstring model is to avoid simulation problems due to the discontinuities originated by dry friction. Namely, the system of ordinary differential equations

$$\dot{x}(t) = Ax(t) + Bu(t) + T_f(x(t)), \tag{7.5}$$

where $x(t)$ is the state, A and B are constant matrices of appropriate dimension and T_f is the torque on bit. In [163], the authors reproduce stick-slip vibrations under different operating conditions. The model used for the torque on the bit is the main difference with respect to other models proposed in the literature. In [161], a discontinuous lumped parameter torsional model of four degrees of freedom is considered. This model allows to describe drill pipes and drill collars behavior. The closed-loop system has two discontinuity surfaces where one of them gives rise to self-excited bit stick-slip oscillations and bit sticking phenomena.

Several PDE models were introduced in the literature for specific describing torsional vibrations. For instance, in [12], torsional vibrations are modeled by a wave equation and the stick-slip dynamics are numerically characterized. In [189] a similar model is studied and a flatness-based approach that avoids such undesired dynamics is introduced. In [195] and [196], a wave equation model to reproduce torsional drilling dynamics is proposed, this model is coupled to a damped harmonic oscillator model described by an ODE to approximates the longitudinal dynamics of the drilling system. In [187] as well as in [104] a nonlinear analytical study is introduced for the case of simple nonlinearities that occurs for a simplified frictional weight and torque which are proportional to $1 + sign(dU/dt)$ where U denotes the axial vibration. This model corresponds to a simplified torsional lumped-parameter model of an oilwell drillstring. An alternative method to characterize the stick-slip motion and other bit-sticking problems in such a drilling system is proposed. The method is based on the study of the relationships between the different types of system equilibria and the existing sliding motion when the bit velocity is zero. It is shown that such a sliding motion plays a key role in the presence of non-desired bit oscillations and transitions. Furthermore, a proportional-integral-type controller is designed in order to drive the rotary velocities to a desired value. The ranges of the controller and the system parameters which lead to a closed-loop system without bit-sticking phenomena are identified.

Unfortunately, the models considered in [164, 161, 163, 162] are linear ones, a quite crude approximation to the nonlinearities of the drillstring system leading to impoverish the possible dynamics. Moreover, the friction torque is always considered as a piecewise linear function of the state, which can be improved by the friction law that we are discussing in some of the following paragraphs.

7.3   Wave equation modelling

We consider a solid homogeneous metal flexible bar of length L and of section σ_0. We are concerned by axial vibrations. Let $q(x,t)$ be the displacement at time t of a point x of the bar with respect to its equilibrium position. Let $T(x,t)$ be the tension applied on the bar at the point x at time t.

The *fundamental elasticity law* establishes a relation between the elongation $dl := l - l_0$ and the infinitesimal tension $dT := T - T_0$ (where we consider an element of length l_0 under the mean tension T_0) by :

$$\frac{dT}{\sigma_0} = E_0 \frac{dl}{l_0}, \tag{7.6}$$

where E_0 designates the Young modulus, or elasticity factor under the tension T_0. This law can be applied only for a sufficiently small relative elongation dl/l_0. Since at time t, the segment $(x, x + \Delta x)$ is of static length l_0 and occupies the position $(x + q(x,t),\ x + \Delta x + q(x + \Delta x, t))$. The length of the segment passes from $l_0 = \Delta x$

to $l = l_0 + dl = \Delta x + \partial_x q \Delta x$, we then have $\dfrac{dl}{l_0} = \partial_x q$, and the elasticity law implies :

$$T - T_0 = E_0 \sigma_0 \partial_x q. \tag{7.7}$$

Let ρ_0 be the linear density at the equilibrium of the bar (that is the rate of mass
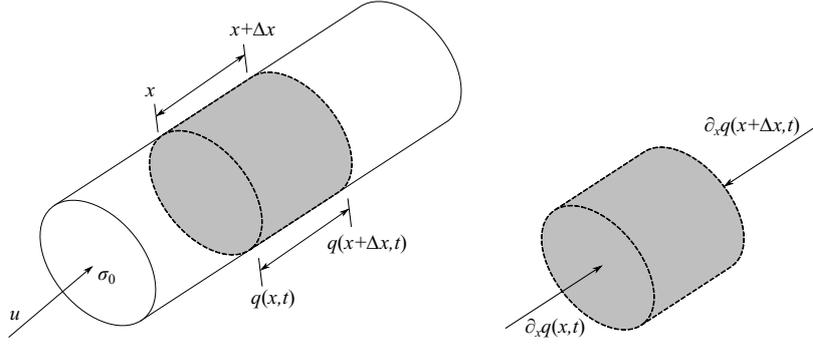
FIGURE 7.2 – (Left) Flexible Bar, (Right) Tension applied in a short segment of the bar

per a length unit). The fundamental principle of dynamics reads $\rho_0 \partial_t^2 q \Delta x = \partial_x T dx$, by using (7.7) we have

$$\rho_0 \partial_t^2 q = E_0 \sigma_0 \partial_x^2 q, \tag{7.8}$$

which is a wave equation with speed $\nu = \sqrt{\dfrac{E_0 \sigma_0}{\rho_0}}$.

The axial vibrations of a solid bar constitute the essential of the sound propagation phenomena. The obtained model can be normalized, yielding to :

$$\partial_t^2 q(x,t) = \partial_x^2 q(x,t) \tag{7.9a}$$

$$\partial_x q(0,t) = -u(t) \qquad \partial_x q(1,t) = 0 \tag{7.9b}$$

$$q(x,0) = q_0(x) \qquad \partial_t q(x,0) = q_{t_0}(x) \tag{7.9c}$$

where $x \in [0,1]$. The equation (7.9a) is the normalized wave equation (7.8) where (7.9b) is the boundary condition and (7.9c) is the initial equation. By Eq.(7.7) and (7.9b), one can see that we apply a control law at the point $x = 0$ and no tension is applied on the free end ($x = 1$).

7.4 PDE models

The lumped parameter model of the drillstring described in [12] consists of an angular pendulum of stiffness C ended with a lumped inertia J and a mass M. The latter two are free to move axially and represent the BHA as a unique rigid body. At the top of the drillstring, an upward force H and a constant angular velocity Ω

are imposed. It is assumed that the weight-on-bit provided by the drillstring to the bit $W_0 = W_s - H$ is constant, which implies that the hook load H is adjusted to compensate for the varying submerged weight of the drillstring W_s. More precisely, the authors describe the torsional motion of a driven drillstring by the following wave equation with boundary conditions :

$$\begin{cases} \partial_t^2 \Phi(t,s) = c^2 \, \partial_s^2 \Phi(t,s), \\ \partial_t \Phi(t,0) = \Omega, \\ J \, \partial_t^2 \Phi(t,L) = -G\,\Gamma\, \partial_s \Phi(t,L) + F(\partial_t \Phi(t,L)), \end{cases} \qquad (7.10)$$

c is a constant wave speed : $c = \sqrt{G/\rho}$, L is the bit position with respect to the s axis, $F(\partial_t \Phi(t,L))$ the reaction frictional torque at the bit and $G\Gamma\,\partial_s \Phi(t,L)$ is the contact torque along the drillstring, (here $\partial_s = \partial()/\partial s$ is the derivation with respect to s). In this work, the authors reduce the study of the model to the study of the associated neutral differential equation for which they establish an analytical linearized stability criterion and give some numerical bifurcation elements. Certainly, the infinite dimensional aspect of the above model is adequate for describing the drilling process, but ignoring the axial vibrations and their influence on the global dynamics is disadvantageous when the aim is to establish a steadfast model.

A similar model but with different boundary conditions was already established in [189] and exploits the flatness property of the wave equation for suppressing the stick-slip undesired dynamics. Indeed, the author proves that the use of the top velocity measures ensures the control and the stabilization of the torsional vibrations.

The contribution [98] is worth mentioning, where a wave equation with different boundary conditions is used to model torsional vibrations for which the authors establish ultimate bounds for a distributed drill pipe model. The result is obtained through an analysis based on a difference equation model and on a wave equation description achieved through the direct Lyapunov method.

Next, in [187] as well as in [105], the authors considered a simplified drillstring model which describes not only the torsional vibration but also the axial one :

$$\begin{cases} I\,\dfrac{d}{dt^2}\Phi(t) + C(\Phi(t) - \Omega\,t) = -T(t), \\ \qquad\qquad M\,\dfrac{d}{dt^2}U(t) = W_0 - W(t). \end{cases} \qquad (7.11)$$

The variables U and Φ denote the vertical and the angular positions of the drag bit, respectively. The reacting weight-on-bit $W(t)$ originates from the process of rock destruction occurring at the bit-rock interface and $T(t)$ is the reacting torque-on-bit. The stick-slip dynamics is numerically studied in [187] and in [105] a nonlinear analytical study is conducted for a simple frictional weight and torque proportional to $1 + sign(dU/dt)$. On the one hand, the model depicted in (7.10) neglects axial vibrations and on the other hand the lumped model (7.11) loses the infinite dimensional character of a PDE model.

In [211], the authors consider a PDE modeling the torsional vibrations and propose a mechanism called torsional rectification and compare it with existing soft-torque devices through a series of mathematical models. Both analytic and numerical simulations indicate that many of the volatilities suffered by existing soft-torque feedback approaches used to avoid slip-stick can be eliminated by their proposed alternative. Ignoring the axial vibrations and their influence on the torsional dynamics is disadvantageous since the study concerns exclusively the control of torsional vibrations.

7.5   A System-Oriented Approach : Interconnected dynamics

We aim at presenting an improved partial differential equations model with more realistic coupled nonlinear boundary conditions. This model takes into account the axial and torsional vibrations along the drilling system. Furthermore, an adjustable three dependent parameters analytic model is taken for the torque on bit. The proposed friction law is a nonlinear function allowing to continuously reproduce classical empirical friction profiles. Moreover, the established physical model can be transformed into a *time-delay system*. This fact is noteworthy since the measurement of the bit state is delayed, due to technological constraints. In our opinion, this is thus a natural way to design a model with unified structure.

The description of the considered model governing the mechanical axial/torsional vibrations follows.

7.5.1   Drillstring mechanics

Denoting by U the axial vibrations and by Φ the torsional vibrations, the improved model is :

$$\begin{cases} \partial_t^2 U(t,s) = c^2\, \partial_s^2 U(t,s), \\ E\,\Gamma\, \partial_s U(t,0) = \alpha_1 \partial_t U(t,0) - \alpha_2 H(t), \\ M\, \partial_t^2 U(t,L) = -E\,\Gamma \partial_s U(t,L) + F(\partial_t U(t,L)), \end{cases} \tag{7.12}$$

and

$$\begin{cases} \partial_t^2 \Phi(t,s) = \tilde{c}^2\, \partial_s^2 \Phi(t,s), \\ G\,\Sigma\, \partial_s \Phi(t,0) = \beta_1 \partial_t \Phi(t,0) - \beta_2 \Omega(t), \\ J\, \partial_t^2 \Phi(t,L) = -G\,\Sigma\, \partial_s \Phi(t,L) + \tilde{F}(\partial_t U(t,L)). \end{cases} \tag{7.13}$$

Here G is the shear modulus of the drillstring steel and E the Young's elasticity modulus. Then, the wave speeds can be expressed by $c = \sqrt{E/\rho}$ and $\tilde{c} = \sqrt{G/\rho}$. The inertia $J = M\,r^2$ where r is taken as the averaged radius of the drill pipes, Γ is the averaged section of the drill pipes and Σ is the quadratic momentum. The nonlinear nature of the model is considered by taking appropriate models of the friction profiles F and $\tilde{F}$ of the form : $z \mapsto pk\, z/(k^2\, z^2 + \zeta)$, where the parameters
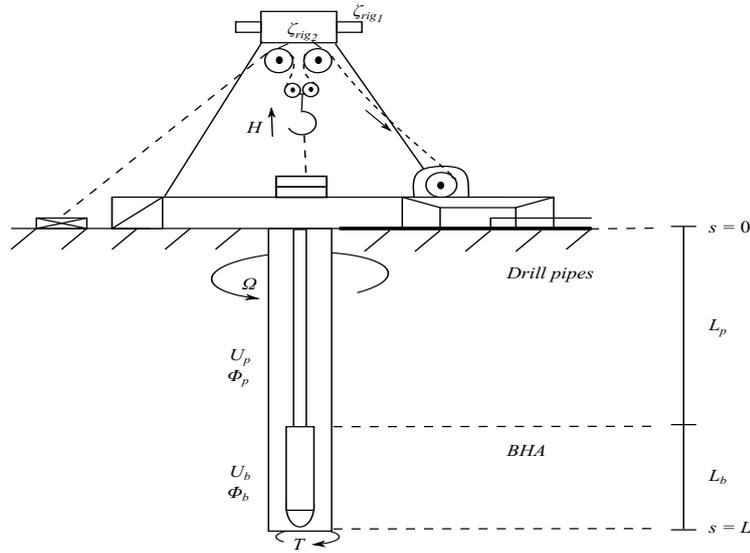
FIGURE 7.3 – Simplified scheme depicting an oilwell rotary drilling system
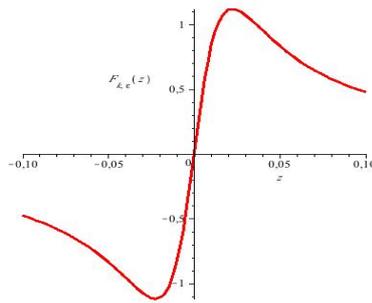
FIGURE 7.4 – The profile of the friction F

k, ζ ($0 < \zeta \ll 1$ and $0 < k < 1$) are positive integers responsible of the sharpness of the friction force function and p is acting on its amplitude, see [36, 29]. Moreover, the behavior of the chosen friction model is close from the empirical model (the white friction force) but its smoothness is very useful in experimental identifications, see Figure 7.4.

The contributions of the proposed model can be summarized as follows :
— **Infinite-dimensional setting for modeling :** As emphasized by (7.12)-(7.13), each type of vibrations is described by a PDE. The first equation of (7.12) means that axial vibrations U are governed by a wave equation with velocity c. In the second equation of (7.12), the reacting force due to the drillstring at the top is seen as the difference between the imposed vertical upward force and the actual drillstring friction force of viscous type at the top $\alpha\partial_t U(t, 0)$. The second equation of (7.12) describes a behavior equation

sampled at the top of the hole. It simply expresses that the difference between the H the brake motor control (upward hook force) and the force generated by the gradient of the axial vibration at the top $\alpha \partial_s U(t,0)$ is nothing else than a friction force of viscous type $\alpha \partial_t U(t,0)$. Furthermore, for equation (7.13), torsional vibrations are also assumed to obey to a wave equation with velocity $\tilde{c}$. In the second equation of (7.13) the right hand side describes the difference between the motor speed and angular velocity of the first pipe. Finally, the third equation of (7.12) and (7.13) are established by applying the Fundamental Laws of Motion [2] at the bit.

— **Coupled dynamics :** The third equation of (7.13) generates the interconnection between the two dynamics. Indeed, it is generally recognized that the torque on bit, which is the main generator for friction in the drilling torsional vibrations, is expressed as a function of the axial vibration (see for instance [104]).

— **Nonlinear dynamics :** Both of the functions F and $\tilde{F}$ are assumed to be nonlinear functions allowing to reproduce continuously the classical empirical friction profile.

7.5.2 Actuating part and motor types

The drilling system includes three motors, which convert electrical energy into mechanical energy : one for the rotary table, one for the drawworks, and one for the mud pump, yielding three control variables. Each machine is modeled by a system of mechatronic equations as follows. The motor types have to be quite resistant, wherefrom the following choices.

DC motor. A first type of motor is the direct current armature control motor. The torque developed by the motor is proportional to the stator's flux and the current in the armature and we have $\Gamma = k_f \, \psi \, K_a \, I$ where Γ is the shaft torque, ψ is the magnetic flux in the stator field, which is assumed to be constant, I is the current in the motor armature. Since the flux is maintained constant, we can also write $\Gamma = k_T \, I$ where $k_T = k_f \, \psi \, K_a$.

When a current carrying conductor passes through a magnetic field, a voltage V_b appears, corresponding to the so-called back electromagnetic force $V_b = k_e \, \omega$ where ω is the rotation speed of the motor shaft. The constant k_T and k_e have the same value. Kirchhoff's law yields the electronic equation of the motor :

$$V - V_{res} - V_{coil} - V_b = 0, \tag{7.14}$$

where V is the input voltage, $V_{res} = -R\,I$ the armature resistor voltage (R being the armature resistor), $V_{coil} = L\,\dot{I}$ the armature inductance voltage (L being the armature inductance). The motor's electrical equation is then

$$L\,\dot{I} = -k_e\,\omega - R\,I + V. \tag{7.15}$$

Induction motor. A second type of motor is the induction machine. When AC current is applied to such a machine, the rotating magnetic field is set up in the

stator. This rotating field is moving with respect to the rotor windings and thus induces a current flow in the rotor. The current flowing in the rotor windings sets up it own magnetic field. In the stationary reference frame ($\omega_S = 0$) the stator voltage vector can be expressed as $v_s{}^S = R_s i_s{}^S + \dot{\psi}_s^S$ where i_S^S and ψ_S^S are the stator current and rotor flux vectors. In the same way the rotor voltage vector can be expressed in the rotor fixed reference frame rotating with $\omega_R : v_r{}^R = R_r i_r{}^R + \dot{\psi}_r^R$, whereas i_r^R and ψ_r^R are the rotor current and rotor flux vectors. The transformation in an arbitrary reference frame rotating with ω_k yields :

$$\begin{cases} v_s^k = R_s i_s^k + \dot{\psi}_s^k + jp\omega_k \psi_s^k \\ v_r^k = R_r i_r^k + \dot{\psi}_r^k + jp(\omega_k - \omega_r)\psi_r^k. \end{cases} \tag{7.16}$$

The flux vectors may be expressed as :

$$\begin{cases} \psi_s^k = L_s i_s^k + L_m i_r^k \\ \psi_r^k = L_r i_r^k + L_m i_s^k. \end{cases} \tag{7.17}$$

In the following the so-called D/Q-reference frame which is aligned to the rotor flux vector will be used and the superscript will be omitted, i.e. $\psi_r = \psi_{rd} + j\psi_{rq} = \psi_r^S e^{-j\rho}$, whereas ρ is the rotor flux angle in the stationary reference frame. Substituting the stator flux and rotor current vectors in (7.16) using (7.17) and introducing $\eta = 1 - (L_m^2/L_s L_r)$, $\chi = L_m^2 R_r / \sigma L_s L_r^2 + R_s / \sigma L_s$, $\zeta = R_r / L_r$ and $\xi = L_m / \sigma L_s L_r$. To further simplify the notations, we shall set : $I_{sd} = I_d$, $I_{sq} = I_q$, the stator current components in the D/Q reference frame, $\psi_{rd} = \psi_d$ the rotor flux D component, $v_{sd} = v_d$, $v_{sq} = v_q$ the stator voltage components in the D/Q reference frame.

We thus obtain conclude with the description of the induction machine model : its electric model and its mechanical model which respectively consist of four and a two dimensional nonlinear system. Indeed, the current/flux equations are given by

$$\begin{cases} \dot{\psi}_d = -\zeta(\psi_d - L_m I_d) \\[4pt] \dot{\rho} = p\omega_R + \zeta L_m \dfrac{I_d}{\psi_d} \\[4pt] \dot{I}_d = -\chi I_d + \zeta\xi\psi_d + p\omega_R I_q + \zeta L_m \dfrac{I_q^2}{\psi_d} + \dfrac{v_d}{\eta L_s} \\[4pt] \dot{I}_q = -\chi I_q - p\xi\omega_R I_d - \zeta L_m \dfrac{I_q I_d}{\psi_d} + \dfrac{v_q}{\eta L_s} \end{cases} \tag{7.18}$$

and the mechanical model is defined by

$$\begin{cases} J\dot{\omega}_R = \mu\psi_{rd} I_{sq} - T_l \\ \dot{\theta}_R = \omega_R, \end{cases} \tag{7.19}$$

whereas $\mu = 3pM/2L_r$ and θ_R is the rotor angle and T_l the load torque.

7.6 Integration into a more complete Traction-Compression/Torsional Model

7.6.1 Step by step description

A more complete model can be established by considering the BHA length and vibrations, neglected in the previous model. Thus, the length of the drillstring L denotes $L_p + L_b$ where L_p is the pipes length and L_b is the BHA length. Here, the vibrations along the pipes will be distinguished from the ones along the BHA. Thus the model for axial vibrations U_p and torsional vibrations Φ_p along the pipes and axial vibrations U_b and torsional vibrations Φ_b along the BHA are governed by the system of PDE (7.20)-(7.27).

Pipe Drillstring The pipe drillstring deformation is modelled through a wave equation with both internal viscoelastic Kelvin-Voigt damping, and simple viscous damping :

$$\begin{cases} \rho A_p \partial_t^2 U_p(t,s) = E A_p\,\partial_s^2 U_p(t,s) + \varepsilon_{U_p}^i \partial_t \partial_s U_p(t,s) + \gamma_{U_p}^v \partial_t U_p(t,s) \\ \rho J_p \partial_t^2 \Phi_p(t,s) = G J_p\,\partial_s^2 \Phi_p(t,s) + \varepsilon_{\Phi_p}^i \partial_t \partial_s \Phi_p(t,s) + \gamma_{\Phi_p}^v \partial_t \Phi_p(t,s), \end{cases} \tag{7.20}$$

where $0 < s < L_p$, the internal damping coefficients are $\varepsilon_{U_p}^i$, $\varepsilon_{\Phi_p}^i$, and the viscous damping coefficients are $\gamma_{U_p}^v$, $\gamma_{\Phi_p}^v$. Additionnally, ρ is the steel density, E (resp. G) denotes Young's (resp. the shear) modulus of drillstring steel, and A_p, J_p are the cross-section and polar inertia moment of one section, given by :

$$A_p = \pi(r_{po}^2 - r_{pi}^2), \qquad J_p = \frac{\pi}{2}\left(r_{po}^4 - r_{pi}^4\right),$$

with r_{pi} and r_{po} the inner and outer pipe radius.

Top Boundary Conditions At $s = 0$, we consider the following boundary condition for Φ_p :

$$J_{top}\partial_t^2 \Phi_p(t,0) = G J_p \partial_s \Phi_p(t,0) + u_T(t), \tag{7.21}$$

with J_{top} the top drive inertia, and u_T the torque produced by the rotary table motor, taken as a *control input.* which is a more realistic boundary condition compared to the one in [104, 12] : $\Phi_p(t,0) = \Omega_0 t$. Note that eq. (7.21) can also be completed by the mechanical equation of an induction machine in place of (7.19).

The upward force H acts in the top hole device composed mainly of the derrick, the crown block and the traveling block. This whole setting is modeled as a two coupled mass spring system, following [173]

$$\begin{cases} M_{rg_1}\ddot{\zeta}_{rg_1}(t) + \gamma_{rg_1}\dot{\zeta}_{rg_1}(t) + M_{rg_1}g = u_F(t) + k_{rg_{12}}(\zeta_{rg_2}(t) - \zeta_{rg_1}(t)) - k_{rg_{01}}\zeta_{rg_{ini}}(t) \\ M_{rg_2}\ddot{\zeta}_{rg_2}(t) + \gamma_{rg_2}\dot{\zeta}_{rg_2}(t) + M_{rg_2}g = -H(t) - k_{rg_{12}}(\zeta_{rg_2}(t) - \zeta_{rg_1}(t)). \end{cases} \tag{7.22}$$

Here, ζ_{rg_1} accounts for vibrations in all drilling rig elements except the drilling string, BHA, cables, drawworks, travelling and crown blocks ; ζ_{rg_2} accounts for elasticity

in cables, crown and travelling blocks; the effort $k_{rg_{01}}\zeta_{rg_{ini}}$ represents the ground reaction force and $u_F(t) = k_{rg_{01}}(\zeta_{rg_1}(t) - \zeta_{rg_0}(t))$ is a tension force in the cable at the drawworks level, taken as a *control input* (being directly related to the drawworks rotation motor). The parameters M_{rg_i}, γ_{rg_1} and $k_{rg_{ij}}$ are equivalent masses, damping coefficients and stiffness coefficients, respectively.

For U_p consider the boundary condition at $s = 0$:

$$M_{top}\partial_t^2 U_p(t, 0) = EA_p\partial_s U_p(t, 0) + H(t). \tag{7.23}$$

with M_{top} the top drive mass. In [104], a simpler boundary condition is adopted : $EA_p\partial_s U_p(t, 0) = H(t)$. The initial conditions are taken such that Φ_p, $\partial_t\Phi_p$, $\partial_s\Phi_p$, U_p, $\partial_t U_p$, $\partial_s U_p$ vanish at $t = 0$.

Drill Collars The BHA equations for axial vibrations U_b and torsional vibrations Φ_b are given by

$$\begin{cases} \rho A_b \partial_t^2 U_b(t, s) = GA_b\,\partial_s^2 U_b(t, s) + \varepsilon_{U_b}^i\,\partial_t\partial_s U_b(t, s) + \gamma_{U_b}^v\,\partial_t U_b(t, s) \\ \rho J_b \partial_t^2 \Phi_b(t, s) = EJ_b\,\partial_s^2 \Phi_b(t, s) + \varepsilon_{\Phi_b}^i\,\partial_t\partial_s \Phi_b(t, s) + \gamma_{\Phi_b}^v\,\partial_t \Phi_b(t, s), \end{cases} \tag{7.24}$$

where $L_p < s < L$, and A_b, J_b are, as above, the cross-section and polar inertia moment of one section, given by

$$A_b = \pi(r_{bo}^2 - r_{bi}^2), \qquad J_b = \frac{\pi}{2}\,(r_{bo}^4 - r_{bi}^4),$$

with r_{bi} and r_{bo} are inner and outer drill collar radius.

Pipe/Drill Collar Continuity Conditions To achieve continuity in speed and effort, Φ_p, Φ_b, U_b and U_p satisfy the connexion conditions :

$$\begin{cases} \partial_t\Phi_b(t, L_p) = \partial_t\Phi_p(t, L_p) \\ \partial_s\Phi_b(t, L_p) = \dfrac{J_p}{J_b}\partial_s\Phi_p(t, L_p) \\ \partial_t U_b(t, L_p) = \partial_t U_p(t, L_p), \\ \partial_s U_b(t, L_p) = \dfrac{A_p}{A_b}\partial_s U_p(t, L_p), \end{cases} \tag{7.25}$$

where J_* and A_* are $J_* = \pi(r_{*o}^4 - r_{*i}^4)/2$ and $A_* = \pi(r_{*o}^2 - r_{*i}^2)$.

Bottom Hole Boundary Conditions The boundary conditions at $s = L$ for torsional vibrations Φ_b are

$$J_{bit}\partial_t^2 \Phi_b(t, L) = -G\,J_b\,\partial_s\Phi_p(t, L) + T_{bit}(t), \tag{7.26}$$

where T_{bit} is the reaction torque at the bit. For axial vibrations, the bottom boundary condition is

$$M_{bit}\partial_t^2 U_b(t, L) = -EA_b\partial_s U_p(t, 0) + W_{bit}(t). \tag{7.27}$$

where M_{bit} is the bit's mass, and $W_{bit}(t)$, the reaction force at the bit due to the so called dynamic weight on bit (DWOB).

Forces/Moments Expressions The bottom hole force and moment can be decomposed into a cutting and a frictional part

$$T_{bit} = T_c + T_f, \qquad W_{bit} = W_c + W_f, \tag{7.28}$$

Friction Force/Moment. The expressions for T_f and W_f are taken as (see for instance [104] and [172]) :

$$T_f(t) = \frac{a^2}{2} \gamma \mu \sigma l \, \mathcal{F}(\|V_b(L,t)\|), \qquad W_f(t) = a l \sigma \, \mathcal{F}(\|V_b(L,t)\|),$$

where a is the bit radius, l the length of the wearflat, σ the contact stress, γ accounts for the distribution and orientation of the frictional forces acting at the wearflat/rock interface, μ the ratio between the horizontal and the vertical components of the frictional force, $V_b = (\partial_t U_p, \partial_t \Phi_p)$ and $\mathrm{sgn}(V_b)$ designate the orientation of V_b with respect to the horizontal plane, and $\mathcal{F}$ is an adimensional friction function. We consider the following expressions for such an $\mathcal{F}$, as for instance in [172]

$$\mathcal{F}(r) = \frac{\alpha r}{\sqrt{r^2 + \varepsilon^2}}, \tag{7.29}$$

or in [212]

$$\mathcal{F}(r) = \beta \left(\tanh(r) + \frac{\gamma_1}{1 + \gamma_2 r^2} \right). \tag{7.30}$$

Cutting Force/Moment. The expressions for T_c and W_c are taken as (see e.g. [104]) :

$$T_c(t) = \frac{a^2}{2} \varepsilon d(t), \qquad W_c(t) = a \zeta \varepsilon d(t),$$

where a is the bit radius, d the depth of cut, ε is the intrinsic specific energy, and ζ the ratio of the vertical to the horizontal force for a sharp cutter. Here the cut depth $d(t)$ is deduced from the relation

$$d(t) = n(U_b(t, L) - U_b(t - t_n, L)), \tag{7.31}$$

where n is the bit number of blades and t_n is implicitly given through the relation

$$\frac{2\pi}{n} = \Phi_b(t, L) - \Phi_b(t - t_n, L). \tag{7.32}$$

The range of t_n is given by $t_{n_0} = 2\pi/(n\Omega_0)$, with Ω_0 a nominal rotating speed at the top. Note that, in [172], T_c is defined by :

$$T_c(t) = -a_4 (\mathcal{F}(\|V_b(L,t)\|)))^2 d(t). \tag{7.33}$$

7.6.2   Full Model Summary

Let us rewrite the previous model in a more compact form.

Pipe Drillstring Pipes wave equation (torsion–traction/compression)

$$\rho A_p \partial_t^2 U_p(t,s) = E A_p \, \partial_s^2 U_p(t,s) + \varepsilon_{U_p}^i \, \partial_t \partial_s U_p(t,s) + \gamma_{U_p}^v \, \partial_t U_p(t,s), \tag{7.34a}$$

$$\rho J_p \partial_t^2 \Phi_p(t,s) = G J_p \, \partial_s^2 \Phi_p(t,s) + \varepsilon_{\Phi_p}^i \, \partial_t \partial_s \Phi_p(t,s) + \gamma_{\Phi_p}^v \, \partial_t \Phi_p(t,s). \tag{7.34b}$$

Top Boundary Conditions Induction motor (torsion) :

$$\dot{\psi}_{\Phi d} = -\zeta_\Phi (\psi_{\Phi d} - L_{\Phi m} I_d) \tag{7.35a}$$

$$\dot{\rho}_\Phi = p\omega_{\Phi R} + \zeta_\Phi L_{\Phi m} \frac{I_{\Phi d}}{\psi_{\Phi d}} \tag{7.35b}$$

$$\dot{I}_{\Phi d} = -\chi_\Phi I_{\Phi d} + \zeta_\Phi \xi_\Phi \psi_{\Phi d} + p_\Phi \omega_{\Phi R} I_{\Phi q} + \zeta_\Phi L_{\Phi m} \frac{I_{\Phi q}^2}{\psi_{\Phi d}} + \frac{v_{\Phi d}}{\eta_\Phi L_{\Phi s}} \tag{7.35c}$$

$$\dot{I}_{\Phi q} = -\chi_\Phi I_{\Phi q} - p_\Phi \xi_\Phi \omega_{\Phi R} I_{\Phi d} - \zeta_\Phi L_{\Phi m} \frac{I_{\Phi q} I_{\Phi d}}{\psi_{\Phi d}} + \frac{v_{\Phi q}}{\eta L_{\Phi s}}. \tag{7.35d}$$

Drill pipes top boundary condition (torsion) :

$$J_{top} \partial_t^2 \Phi_p(t,0) = G J_p \partial_s \Phi_p(t,0) + u_T(t). \tag{7.36}$$

Induction motor (traction/compression) :

$$\dot{\psi}_{Ud} = -\zeta_U (\psi_{Ud} - L_{Um} I_d) \tag{7.37a}$$

$$\dot{\rho}_U = p\omega_{UR} + \zeta_U L_{Um} \frac{I_{Ud}}{\psi_{Ud}} \tag{7.37b}$$

$$\dot{I}_{Ud} = -\chi_U I_{Ud} + \zeta_U \xi_U \psi_{Ud} + p_U \omega_{UR} I_{Uq} + \zeta_U L_{Um} \frac{I_{Uq}^2}{\psi_{Ud}} + \frac{v_{Ud}}{\eta_U L_{Us}} \tag{7.37c}$$

$$\dot{I}_{Uq} = -\chi_U I_{Uq} - p_U \xi_U \omega_{UR} I_{Ud} - \zeta_U L_{Um} \frac{I_{Uq} I_{Ud}}{\psi_{Ud}} + \frac{v_{Uq}}{\eta L_{Us}}. \tag{7.37d}$$

Top hole assembly (traction/compression) :

$$M_{rg_1} \ddot{\zeta}_{rg_1}(t) + \gamma_{rg_1} \dot{\zeta}_{rg_1}(t) + M_{rg_1} g = u_F(t) + k_{rg_{12}}(\zeta_{rg_2}(t) - \zeta_{rg_1}(t)) - k_{rg_{01}} \zeta_{rg_{ini}}(t) \tag{7.38a}$$

$$M_{rg_2} \ddot{\zeta}_{rg_2}(t) + \gamma_{rg_2} \dot{\zeta}_{rg_2}(t) + M_{rg_2} g = -H(t) - k_{rg_{12}}(\zeta_{rg_2}(t) - \zeta_{rg_1}(t)). \tag{7.38b}$$

Drill pipes top boundary condition (traction/compression) :

$$M_{top} \partial_t^2 U_p(t,0) = E A_p \partial_s U_p(t,0) + H(t). \tag{7.39}$$

Drill Collars

$$\rho A_b \partial_t^2 U_b(t,s) = G A_b \, \partial_s^2 U_b(t,s) + \varepsilon_{U_b}^i \, \partial_t \partial_s U_b(t,s) + \gamma_{U_b}^v \, \partial_t U_b(t,s), \tag{7.40a}$$

$$\rho J_b \partial_t^2 \Phi_b(t,s) = E J_b \, \partial_s^2 \Phi_b(t,s) + \varepsilon_{\Phi_b}^i \, \partial_t \partial_s \Phi_b(t,s) + \gamma_{\Phi_b}^v \, \partial_t \Phi_b(t,s). \tag{7.40b}$$

Pipe/Drill Collar Continuity Conditions

$$\partial_t \Phi_b(t, L_p) = \partial_t \Phi_p(t, L_p) \tag{7.41a}$$

$$\partial_s \Phi_b(t, L_p) = \frac{J_p}{J_b} \partial_s \Phi_p(t, L_p) \tag{7.41b}$$

$$\partial_t U_b(t, L_p) = \partial_t U_p(t, L_p) \tag{7.41c}$$

$$\partial_s U_b(t, L_p) = \frac{A_p}{A_b} \partial_s U_p(t, L_p). \tag{7.41d}$$

Bottom Hole Boundary Conditions Drill collar bit boundary condition (torsion) :

$$J_{bit}\partial_t^2 \Phi_b(t, L) = -G\,J_b\,\partial_s \Phi_p(t, L) + T_{bit}(t). \tag{7.42}$$

Drill collar bit boundary condition (traction/compression) :

$$M_{bit}\partial_t^2 U_b(t, L) = -EA_b\partial_s U_p(t, 0) + W_{bit}(t). \tag{7.43}$$

Forces/Moments Expressions Bottom hole force and moment :

$$T_{bit} = T_c + T_f, \qquad W = W_c + W_f. \tag{7.44}$$

Friction Force/Moment :

$$T_f(t) = \frac{a^2}{2}\,\gamma\mu\sigma l\,\mathcal{F}(\|V_b(L, t)\|), \qquad W_f(t) = al\sigma\,\mathcal{F}(\|V_b(L, t)\|).$$

Adimensional friction function expressions :

$$\mathcal{F}(r) = \frac{\alpha r}{\sqrt{r^2 + \varepsilon^2}} \qquad \text{First expression} \tag{7.45}$$

$$\mathcal{F}(r) = \beta \left(\tanh(r) + \frac{\gamma_1}{1 + \gamma_2 r^2} \right) \quad \text{Second expression} \tag{7.46}$$

Cutting Force/Moment :

$$T_c(t) = \frac{a^2}{2}\,\varepsilon d(t), \qquad W_c(t) = a\zeta\varepsilon d(t)$$

Cut depth $d(t)$ defined by $d(t) = n(U_b(t, L) - U_b(t - t_n, L))$.
One revolution duration t_n such that $\frac{2\pi}{n} = \Phi_b(t, L) - \Phi_b(t - t_n, L)$.

7.7 Wireless-transmission and Real-time methodology

In this section, we focus on the way to bring the measurement from downhole to surface so we can use it in order to improve the observer/controller behavior. There are mainly three types of transmission : i) through telemetry signals along

the drilling fluid, often referred to as mud-pressure pulses, ii) through acoustic waves along the drillstring [65], iii) through wired drill pipes.

In most of the literature, electronic equipments are designed for data acquisition and for modulation purpose. It should be implemented as an autonomous system energized either by a mud operated electrical turbine or by a battery pack [209].

Mud-pulse telemetry This technology uses the mud that goes through the drilling system as a transmission media. The data will be represented by pressure pulses. According to [209], the pulser actuator (a stepper-motor-based device) and a main valve restricts the flow and creates some pressure-pulse sequence. A piezoelectric device captures these variations that are then analyzed by a micro-controller. Evidently, due to the irregular nature the mud flow, the low frequency vibrations produced by mud pumps and pulsation dampeners the signals are corrupted by noise. Furthermore, they have an important attenuation. Some characteristics to highlight are [137], [65], [79] its cost-effective data transfer, its very low bite rate (1 or 2 bits per second). Mud-pulse velocity declines with the disturbances of mud density, gas content and mud compressibility. It becomes more difficult with increasing well depth. Pulse waves travel through the borehole at 1200 meters per second [137], hence the measure arrives with some delay that increases up to tmax $\tau_{max} \approx 6.6$ *seconds*.

Acoustic data transmission over a drill string Since the acoustic wave propagation velocity in the string material is at least three times superior to that in the mud of the borehole [65], and a higher transmission rate is possible (typically 6 bps), acoustic transmission seems to be the best way to emit pulses to the surface. These acoustic waves are generated by torsional contractions created by magneto restrictive rings set inside the pipe [78]. In this case $\tau_{max} \approx 2.2$ *secons*. It is useful to note that there exists an attenuation of around 4 $dB/300m$ [77]. However, we can neglect it because there is always a possibility of setting a repeater at any joint at each $10 - 15$ meters of the section. We consider that this fact does not add any extra considerable delay since the repeater's amplification can occur almost instantaneously.

The telemetry system sends signals directly to the surface through the channel. Usually, there is an embedded sensor measuring $\dot{\phi}_b$ downhole. A measurement noise $S(t)$ is added to the data and then coded all together, so that it can be transmitted through the acoustic channel G. At surface, a receiver will read the encoded signal with the noise $N(t)$. Furthermore, a digital algorithm is used to decode this data and make it available for the use for further treatments. Both methods can be modeled by the schematic as shown in Figure 7.5. On the bit state measurement side, there are mainly three types of transmission :
Transmission delay range and friction hypothesis Due to technical considerations we can assume that the transmission media is, as a first approximation, like a pure delay system with delay time $\tau \in [0, \tau_{max}]$. Moreover, the well's depth increases
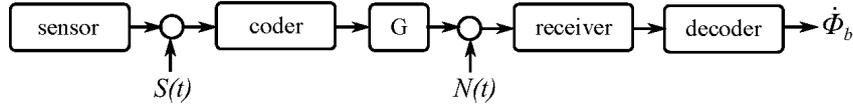
FIGURE 7.5 – Testbed schematics with sonar pulses

at a very slow rate and it stops each $10 - 15$ meters. In this procedure, the delay can be recalculated. Hence, the delay can be defined as a constant, that is $\dot{\tau} = 0$. On the other hand, we will consider that the friction coefficient is constant or at least slow time variant $\dot{\tau} \approx 0$. This approximation is often assumed in the context of adaptive control. This hypothesis means that the rate of variation of the rock friction coefficient does not exhibit substantial changes during drill-operation. Even if the drilled surfaces may have different friction characteristics, the rate of penetration remains small $(\dot{d} \approx 0)$.

Real-time control The general real time control architecture has to handle output signal transmission, state observation under variable delay and signal noises presence as well as the state feedback control calculation and actuation update. A detailed description of a such an architecture is given in [125] where more emphasis is put on observer performance in presence of transmission delay variations, noise perturbation and friction coefficient variation. Due to these parameter variation the overall observer/controller order is increased which has to be considered in the specification of real time control architecture. We will not go further in the specification and the design of overall real time communication and calculation architecture which is out of the scope of this work, but it is important to emphasize the fact that the reliability, bandwidth and signal to noise ratio of data transmission channel is of great importance in the quality of state observation and control.

7.8   Concluding Remarks :

The complete description of a Drilling oilwell machine involves three interconnected systems : i) A mechanical system, more precisely, the drillstring that is the down-hole part of the drilling device, ii) The mechatronic system : composed mainly from two induction machines : the first acting axially and the second acting in rotation, iii) A transmission system that consists from sensors (piezoelectric) and a transmission vector that can be for instance the wireless technology.

Briefly, the interconnection of such components can be summarized as follows : The drilstring and the induction machine are connected via the derrick, the crown and the traveling block for the axial actions and via the rotary table for angular rotation. Moreover, the induction motors are the only actuators leading to the control for guaranteeing a regular drilling process. The success of such a task lies mainly on the bit-data (the mechanical system) furnished by the sensors and transmitted by

wireless to the top. The transmitted data are then responsible on the motor actions.

Finally, it is worthy to note that the preceding model does not take into account the bending vibrations (leading to whirling) of the drilling collar, nor the drilling fluid dynamics.

Appendix : Notations table

Variable	Signification
L_p	Pipe length
L_b	Bor Hole Assemble length
L	$= L_p + L_b$
U_p, U_b	Pipe, drill collar traction/compression deformation
Φ_p, Φ_b	Pipe, drill collar torsional deformation
$\varepsilon_{U_p}^i, \varepsilon_{\Phi_p}^i$	Internal damping coefficients
$\gamma_{U_p}^v, \gamma_{\Phi_p}^v$	Viscous damping coefficients
ρ	Steel density
E , G	Young's, shear modulus of drillstring steel
A_p, J_p	Cross-section and polar inertia moment of one pipe section
A_b, J_b	Cross-section and polar inertia moment of one drill collar section
r_{po}, r_{pi}	Outer, inner pipe radius
r_{bo}, r_{bi}	Outer, inner drill collar radius
$\Psi_{\Phi d}, \Psi_{Ud}$	D component of rotary table (torsion) induction motor flux
$L_{\Phi m}, L_{Um}$	Torsion, traction/compression induction motor mutual inductance
$I_{\Phi d}, I_{\Phi q}$	D, Q component of stator current in torsion induction motor
I_{Ud}, I_{Uq}	D, Q component of stator current in traction/compression induction motor
J_{top}	Top drive inertia
u_T	Rotary table motor torque, taken as a *control input*
H	Force acting in the top hole device
ζ_{rg_1}	accounts for vibrations in all drilling rig elements except the drilling string, BHA, cables, drawworks, travelling and crown blocks
ζ_{rg_2}	accounts for elasticity in cables, crown and travelling blocks
$k_{rg_{01}} \zeta_{rg_{ini}}$	ground reaction force
$u_F(t)$	$= k_{rg_{01}}(\zeta_{rg_1}(t) - \zeta_{rg_0}(t))$, tension force in the cable at the drawworks level, taken as a *control input*
$M_{rg_i}, \gamma_{rg_1}, k_{rg_{ij}}$	equivalent masses, damping coefficients and stiffness coefficients
M_{top}	Top drive mass
U_b, Φ_b	axial, torsional vibrations
T_{bit}	Bit reaction torque
M_{bit}	Bit's mass

$W_{bit}(t)$	Reaction force at the bit
$T_c,\ W_c$	Bottom hole cutting torque and force
$T_f,\ W_f$	Bottom hole friction torque and force
a	Bit radius
l	Length of the wearflat
σ	Contact stress
γ	accounts for the distribution and orientation of the frictional forces acting at the wearflat/rock interface
μ	Ratio between the horizontal and the vertical components of the frictional force
V_b	$= (\partial_t U_p, \partial_t \Phi_p)$
$\text{sgn}(V_b)$	designate the orientation of V_b with respect to the horizontal plane
$\mathcal{F}$	Adimensional friction function
d	Depth of cut
ε	Intrinsic specific energy
ζ	Ratio of the vertical to the horizontal force for a sharp cutter
n	Bit blade number

Bifurcation analysis of the drilling system

On the one hand, Bifurcation theory is concerned with the study of changes in the qualitative structure of the solutions of a given family of differential equations. In dynamical systems, a bifurcation occurs when a small smooth alteration of the parameter values (the bifurcation parameters) causes a sudden qualitative or topological change in its behavior. Bifurcations occur in both continuous systems (described by ODEs, DDEs or PDEs), and discrete systems (described by maps). The term bifurcation was introduced in 1885 by Henri Poincaré [210]. Bifurcations can be classified into two main categories : *global bifurcations*, which occur when larger invariant sets of the system *collide* with each other, or with the equilibrium point of the system ; and *local bifurcations*, which can be analyzed through variations of the local stability properties of the equilibrium point. Some examples of reduced codimension bifurcations' of local type are : Pitchfork bifurcation, Andronov-Hopf bifurcation and Bogdanov-Takens bifurcation. On the other hand, a wide range of applications involve hyperbolic PDEs in modelling interesting and relatively complex dynamical phenomena. These hyperbolic PDEs themselves may be reducible to neutral functional differential equations, see for instance the wave equations modelling of wind instruments given in [69, 70] and the linear density-flow hyperbolic systems studied in [18] or to a non autonomous difference equations as established in [58, 57]. In our context, in order to characterize the qualitative dynamic response of the rotary drilling system, this chapter addresses its local bifurcation analysis. Based on the center manifold theorem [47] and normal forms theory [111], a set of neutral-type time-delay equations that model the coupled axial-torsional drilling vibrations is reduced via spectral projections to a finite-dimensional system described by an ODE which simplifies the analysis and control task. This chapter reproduces mainly the results from [146].

8.1   Local bifurcation analysis

Consider the following system of equations describing the coupled axial-torsional drilling vibrations :

$$\begin{cases} \dfrac{\partial^2 U}{\partial s^2}(s,t) = c^2 \dfrac{\partial^2 U}{\partial t^2}(s,t), \quad c = \sqrt{\dfrac{\rho_a}{E}} \\[2mm] E\Gamma \dfrac{\partial U}{\partial s}(0,t) = \alpha \dfrac{\partial U}{\partial t}(0,t) - u_H(t) \\[2mm] E\Gamma \dfrac{\partial U}{\partial s}(L,t) = -M_B \dfrac{\partial^2 U}{\partial t^2}(L,t) + F\left(\dfrac{\partial U}{\partial t}(L,t)\right) \end{cases}$$

and

$$\begin{cases} \dfrac{\partial^2 \Phi}{\partial s^2}(s,t) = \tilde{c}^2 \dfrac{\partial^2 \Phi}{\partial t^2}(s,t), \quad \tilde{c} = \sqrt{\dfrac{\rho_a}{G}} \\[2mm] GJ \dfrac{\partial \Phi}{\partial s}(0,t) = \beta \dfrac{\partial \Phi}{\partial t}(0,t) - u_T(t) \\[2mm] GJ \dfrac{\partial \Phi}{\partial s}(L,t) = -I_B \dfrac{\partial^2 \Phi}{\partial t^2}(L,t) - \tilde{F}\left(\dfrac{\partial U}{\partial t}(L,t)\right) \end{cases}$$

where $U(s,t)$ and $\Phi(s,t)$ are the rotary angle and the longitudinal position respectively. The system is controlled through the upward hook force u_H and the rotary table motor torque u_T. The nonlinear aspect of the model is considered by taking functions F and $\tilde{F}$ of the form :

$$z \mapsto p\bar{k}\, z/(\bar{k}^2\, z^2 + \zeta),$$

where the parameters $\bar{k}$, ζ ($0 < \zeta \ll 1$ and $0 < \bar{k} < 1$) are positive integers responsible of the sharpness of the friction force function and p is acting on its amplitude.

Using d'Alembert theorem, the above PDE model can be transformed into the following pair of coupled neutral-type time-delay equations :

$$\begin{aligned} \ddot{U}_b(t) - \tilde{\Upsilon}\ddot{U}_b(t - 2\tilde{\tau}) &= -\tilde{\Psi}\dot{U}_b(t) - \tilde{\Upsilon}\tilde{\Psi}\dot{U}_b(t - 2\tilde{\tau}) \\ &\quad + \frac{1}{M_B}F\left(\dot{U}_b(t)\right) - \frac{1}{M_B}\tilde{\Upsilon}F\left(\dot{U}_b(t - 2\tilde{\tau})\right) + \tilde{\Pi}u_H(t - \tilde{\tau}), \end{aligned}$$

$$\begin{aligned} \ddot{\Phi}_b(t) - \Upsilon\ddot{\Phi}_b(t - 2\tau) &= -\Psi\dot{\Phi}_b(t) - \Upsilon\Psi\dot{\Phi}_b(t - 2\tau) \\ &\quad + \frac{1}{I_B}\tilde{F}\left(\dot{U}_b(t)\right) - \frac{1}{I_B}\Upsilon\tilde{F}\left(\dot{U}_b(t - 2\tau)\right) + \Pi u_T(t - \tau), \end{aligned}$$

where

$$\begin{aligned} \tilde{\Pi} &= \frac{2\tilde{\Psi}}{\alpha + cE\Gamma}, \quad \tilde{\Upsilon} = \frac{\alpha - cE\Gamma}{\alpha + cE\Gamma}, \quad \tilde{\Psi} = \frac{cE\Gamma}{M_B}, \quad \tilde{\tau} = cL, \\ \Pi &= \frac{2\Psi}{\beta + \tilde{c}GJ}, \quad \Upsilon = \frac{\beta - \tilde{c}GJ}{\beta + \tilde{c}GJ}, \quad \Psi = \frac{\tilde{c}GJ}{I_B}, \quad \tau = \tilde{c}L, \end{aligned}$$

and $\dot{U}_b(t)$, $\dot{\Phi}_b(t)$ are the the axial and angular velocities at the bottom extremity, respectively.

A normalization of the above model yields the following dimensionless equations :

$$\ddot{U}_b(t) - \tilde{\Upsilon}_n \ddot{U}_b(t-2) = -\tilde{\Psi}_n \dot{U}_b(t) - \tilde{\Upsilon}_n \tilde{\Psi}_n \dot{U}_b(t-2) \tag{8.1}$$
$$+ \frac{1}{M_B} F\left(\dot{U}_b(t)\right) - \frac{1}{M_B} \tilde{\Upsilon}_n F\left(\dot{U}_b(t-2)\right) + \tilde{\Pi}_n u_H(t-1),$$

$$\ddot{\Phi}_b(t) - \Upsilon_n \ddot{\Phi}_b(t-2\tau) = -\Psi_n \dot{\Phi}_b(t) - \Upsilon_n \Psi_n \dot{\Phi}_b(t-2\tau) \tag{8.2}$$
$$+ \frac{1}{I_B} \tilde{F}\left(\dot{U}_b(t)\right) - \frac{1}{I_B} \Upsilon_n \tilde{F}\left(\dot{U}_b(t-2\tau)\right) + \Pi_n u_T(t-\tau),$$

where τ is the ratio of the speeds $\tau = \tilde{c}/c$ and

$$\tilde{\Pi}_n = \frac{2\tilde{\Psi}_n}{\alpha+1}, \quad \tilde{\Upsilon}_n = \frac{\alpha-1}{\alpha+1}, \quad \tilde{\Psi}_n = \frac{1}{M_B},$$
$$\Pi_n = \frac{2\tilde{c}GJ}{I_B\left(cE\Gamma\beta + \tilde{c}GJ\right)}, \quad \Upsilon_n = \frac{cE\Gamma\beta - \tilde{c}GJ}{cE\Gamma\beta + \tilde{c}GJ}, \quad \Psi_n = \frac{\tilde{c}GJ}{cE\Gamma I_B}.$$

First, we analyze the uncontrolled system ($u_H = u_T = 0$). Denote by x_1 and x_2 the axial and angular velocities at the bottom extremity ($\dot{U}_b$ and $\dot{\Phi}_b$ respectively). The state-space matrix representation of the system is written as follows :

$$\begin{cases} \dot{x}(t) = D_1\,\dot{x}(t-2) + D_2\,\dot{x}(t-2\tilde{c}/c) + A_0\,x(t) + A_1\,x(t-2) \\ \qquad + A_2\,x(t-2\tilde{c}/c) + \mathcal{F}(x(t), x(t-2), x(t-2\tilde{c}/c)) \end{cases} \tag{8.3}$$

where $x = (x_1, x_2)^T$, $\mathcal{F} : \mathbb{R}^n \times \mathbb{R}^n \times \mathbb{R}^n \to \mathbb{R}^n$ is a mapping representing the nonlinear part of the system (8.1)-(8.2), and the matrices D_1, D_2, A_0, A_1, A_2 are given by :

$$D_1 = \begin{bmatrix} \tilde{\Upsilon}_n & 0 \\ 0 & 0 \end{bmatrix}, \quad D_2 = \begin{bmatrix} 0 & 0 \\ 0 & \Upsilon_n \end{bmatrix},$$

$$A_0 = \begin{bmatrix} -\frac{\tilde{\Psi}_n(p\bar{k}+\zeta)}{\zeta} & 0 \\ \frac{p\bar{k}}{J\zeta} & -\Psi_n \end{bmatrix}, \quad A_1 = \begin{bmatrix} -\frac{\tilde{\Upsilon}_n\tilde{\Psi}_n(p\bar{k}+\zeta)}{\zeta} & 0 \\ 0 & 0 \end{bmatrix}, \quad A_2 = \begin{bmatrix} 0 & 0 \\ -\frac{\Upsilon_n p\bar{k}}{\zeta I_B} & -\Upsilon_n\Psi_n \end{bmatrix}.$$

The characteristic equation is a powerful tool for analysing stability of the steady state solution of functional differential equation. In what follows we discuss the stability conditions of the drilling system based in the bifurcation parameters p (parameter related to the amplitude of the friction forces F and $\tilde{F}$) and α (viscous friction coefficient at the top extremity) [36]. The numerical values of the model parameters are given in Table 9.4, see also [146] for further discussion the system parameters.

Here the friction force amplitude p as well as the mass at the BHA M_B are left free and are considered as the bifurcation parameters. When $p = p_c$ then zero is an eigenvalue with algebraic and geometric multiplicity 1. Moreover, zero is the only eigenvalue with zero real part and the remaining eigenvalues have negative real parts. Furthermore, there exists a *Pitchfork bifurcation*, which comes from the

$\mathbb{Z}_2$ symmetry structure of the system. When in addition the mass at the BHA M_B reaches some critical value $M_B = M^*$, then zero is an eigenvalue of algebraic multiplicity 2 and of geometric multiplicity 1. Furthermore, under such conditions zero is the only eigenvalue with zero real part and the remaining eigenvalues have negative real parts. The zero eigenvalue is non-semisimple and the singularity is of *Bogdanov-Takens* type. Finally, although there are no characteristic roots with positive real parts, the system (8.3) is formally stable, but not asymptotically stable.

As discussed in [146], the characteristic equation of system (8.3) is given by

$$
\begin{aligned}
det(\Delta) &= F_1(\lambda)\, F_2(\lambda, p) \\
&= \left(\lambda(1 - \mathrm{e}^{-\lambda\,\tau_2} \Upsilon_n) - \Upsilon_n + \mathrm{e}^{-\lambda\,\tau_2} \Upsilon_n \Psi_n \right) \times \\
&\quad \left(\lambda(1 - \mathrm{e}^{-2\lambda} \tilde{\Upsilon}_n) + \frac{\tilde{\Upsilon}_n \tilde{\Psi}_n \left(p\bar{k} + \zeta \right)}{\zeta} \mathrm{e}^{-2\lambda} + \frac{\tilde{\Psi}_n \left(p\bar{k} + \zeta \right)}{\zeta} \right).
\end{aligned}
$$

For the sake of simplicity, let us consider separately the factors $F_1(\lambda)$ and $F_2(\lambda, p)$. The first factor is given by :

$$
F_1(\lambda) = \left(\lambda(1 - \mathrm{e}^{-\lambda\,\tau_2} \Upsilon_n) - \Upsilon_n + \mathrm{e}^{-\lambda\,\tau_2} \Upsilon_n \Psi_n \right).
$$

Notice that $F_1(\lambda)$ is a scalar first order quasi-polynomial of neutral type. It is easy to prove that the associated continuous-time difference equation is asymptotically stable. Indeed, the scalar quasi-polynomial satisfy the conditions of the Pontryagin theorem leading to prove that all spectral values have negative real part (for further insights on the proof see [218]). Thus, one concludes that there are no imaginary crossing roots for the factor F_1. Consider now the second factor $F_2(\lambda, p)$ defined as :

$$
F_2(\lambda, p) = \left(\lambda(1 - \mathrm{e}^{-2\lambda} \tilde{\Upsilon}_n) + \frac{\tilde{\Upsilon}_n \tilde{\Psi}_n \left(p\bar{k} + \zeta \right)}{\zeta} \mathrm{e}^{-2\lambda} + \frac{\tilde{\Psi}_n \left(p\bar{k} + \zeta \right)}{\zeta} \right).
$$

Similarly, it is easy to show that apart from $\omega_0 = 0$, there are no spectral values with zero real part. Moreover, $p = p_c = 6.66749$ is the only possible value of p leading to a spectral value in zero. Considering the parameterization $\mu = \alpha - 30\,p$ and using the model parameters given in Table 9.4 of Section 8.5, F_2 can be written as :

$$
F_2(\lambda, M_B, p) = \left(-M_B + 0.99\, M_B \mathrm{e}^{-2\lambda} \right) \lambda + \left(-29.7\,p - 0.99 \right) \mathrm{e}^{-2\lambda} + 30\,p - 1
$$

A simple substitution of $\lambda = 0$ into F_2 shows that $p = p_c$ leads to a first spectral value on the imaginary axis $\lambda_1 = 0$; a Pitchfork bifurcation comes from the $\mathbb{Z}_2$ symmetry structure of the system. If additionally $(p = p_c)\, M_B = M^*$, then the first derivative of F_2 vanish at $\lambda_2 = 0$. Since the null space $\mathcal{N}(\lambda_0\, Id - A)$ have only one eigenvector :

$$
v_0 = \begin{bmatrix} 1 \\ 4.853 \times 10^{11} \end{bmatrix},
$$

there exists then, a double root of non-semisimple type at zero. Moreover, in such a particular case, and for the same reasons as for the first factor, the remaining roots of F_2 have negative real parts.

In conclusion, the system is formally stable but not asymptotically stable (although there are no characteristic roots with positive real parts) and the singularity is of *Bogdanov-Takens* type [134].

Remark 7. The multiplicity of the root at the origin can not exceed two for the considered parameter values. However, it is worthy of note that, for general second-order systems of neutral type the maximal multiplicity of the characteristic root at the origin is less than the degree of the generic quasipolynomial.

8.2 Model reduction

Generally speaking, Functional Differential Equations (FDE) share some properties with Ordinary Differential Equations (ODE). This section presents a normal form theory-based technique allowing to approximate a Neutral Delay Differential Equation (NDDE) by an ODE. The transformation method, based in the *Center Manifold Theorem*, simplifies the system structure, preserving the qualitative dynamic of the system in a neighborhood of the equilibrium state.

Consider the general form of a discrete time-delay autonomous first-order nonlinear system of neutral-type :

$$\frac{d}{dt}[x(t) + \sum_{k=1}^{n} A_k\, x(t - \tau_k)] = \sum_{k=0}^{n} B_k\, x(t - \tau_k) + \mathcal{F}(x(t), \dots, x(t - \tau_n)), \qquad (8.4)$$

where A_i, B_j are $n \times n$ real valued matrices (there is at least one matrix $A_k \neq 0$ for some $k \in \{1, 2, \dots, n\}$). The time-delays are such that $\tau_0 = 0$, $\tau_i < \tau_j$ for $i < j$ and $\tau_n = r$.

System (13.55) can be written in compact form as follows :

$$\frac{d}{dt}\mathcal{D}x_t = \mathcal{L}x_t + \mathcal{F}(x_t), \qquad (8.5)$$

where $x_t \in C = C([-r, 0], \mathbb{R}^n)$, $x_t(\theta) = x(t + \theta)$. The bounded linear operators $\mathcal{D}$ and $\mathcal{L}$ are such that $\mathcal{D}\phi = \phi(0) + \sum_{k=1}^{n} A_k\, \phi(-\tau_k)$ and $\mathcal{L}\phi = \sum_{k=0}^{n} B_k\, \phi(-\tau_k)$, $\mathcal{F}$ is a sufficiently smooth function mapping C into $\mathbb{R}^n$ with $\mathcal{F}(0) = D\mathcal{F}(0) = 0$. The linear operators $\mathcal{D}$ and $\mathcal{L}$ can be written in the integral form as $\mathcal{L}\phi = \int_{-r}^{0} d\eta(\theta)\phi(\theta)$ and $\mathcal{D}\phi = \phi(0) + \int_{-r}^{0} d\mu(\theta)\phi(\theta)$, where μ and η are two real valued $n \times n$ matrices.

The linear part of system (13.56) is given by :

$$\frac{d}{dt}\mathcal{D}x_t = \mathcal{L}x_t. \qquad (8.6)$$

Let $\mathcal{T}(t)(\phi) = x_t(., \phi)$, with $x_t(., \phi)(\theta) = x(t + \theta, \phi)$ for $\theta \in [-r, 0]$, the solution operator associated with the linear system. $\mathcal{T}(t)$ is a strongly continuous semigroup with the infinitesimal generator given by $\mathcal{A} = \frac{d\phi}{d\theta}$ with the domain

$$\mathcal{D}om(\mathcal{A}) = \{\phi \in C : \frac{d\phi}{d\theta} \in C, \mathcal{D}\frac{d\phi}{d\theta} = \mathcal{L}\phi\} \ .$$

The spectrum of $\mathcal{A}$, $\sigma(\mathcal{A}) = \sigma_p(\mathcal{A})$, consists of complex values $\lambda \in \mathbb{C}$ satisfying the characteristic equation : $p(\lambda) = \det\Delta(\lambda) = 0$. See [206, 151] for further details.

Denote by $\mathcal{M}_\lambda$, the eigenspace associated with $\lambda \in \sigma(\mathcal{A})$. We define $C^* = C([-r, 0], \mathbb{R}^{n*})$, where $\mathbb{R}^{n*}$ is the space of n-dimensional row vectors. Consider the bilinear form on $C^* \times C$, proposed in [115] :

$$
\begin{aligned}
(\psi, \phi) &= \phi(0)\,\psi(0) - \int_{-r}^0 d[\int_0^\theta \psi(\tau - \theta)d\mu(\tau)] \\
&+ \int_{-r}^0 \int_0^\theta \psi(\tau - \theta)d\eta(\theta)\phi(\tau)d\tau
\end{aligned}
\tag{8.7}
$$

Let $\mathcal{A}^T$ be the transposed operator of $\mathcal{A}$, i.e., $(\psi, \mathcal{A}\phi) = (\mathcal{A}^T\psi, \phi)$. The following result leads to an appropriate decomposition of the space C.

Theorem 32. *[115] Let Λ be a nonempty finite set containing the eigenvalues of $\mathcal{A}$ and let $P = span\{\mathcal{M}_\lambda(\mathcal{A}), \lambda \in \Lambda\}$ and $P^T = span\{\mathcal{M}_\lambda(\mathcal{A}^T), \lambda \in \Lambda\}$. Then P is invariant under $\mathcal{T}(t)$, $t \geq 0$ and there exists a space $\mathcal{Q}$, also invariant under $\mathcal{T}(t)$ such that $C = P \bigoplus Q$. Furthermore, if $\Phi = (\phi_1, \ldots, \phi_m)$ forms a basis of P, and $\Psi = col(\psi_1, \ldots, \psi_m)$ is a basis of P^T in C^*, such that $(\Phi, \Psi) = Id$, then*

$$
\begin{aligned}
Q &= \{\phi \in C \setminus (\Psi, \phi) = 0\}, \\
P &= \{\phi \in C \setminus \exists b \in \mathbb{R}^m : \phi = \Phi b\}.
\end{aligned}
\tag{8.8}
$$

Moreover, $\mathcal{T}(t)\Phi = \Phi\,e^{Bt}$, where B is a $m \times m$ matrix such that $\sigma(B) = \Lambda$.

Denote by BC, the extension of the space C containing continuous functions on $[-r, 0)$ with a possible jump discontinuity at 0. A given function $\xi \in BC$ can be written as : $\xi = \varphi + X_0\alpha$, where $\varphi \in C$, $\alpha \in \mathbb{R}^n$ and $X_0(\theta) = 0$ for $-r \leq \theta < 0$, $X_0(0) = Id_{n\times n}$. The Hale-Verduyn Lunel bilinear form (8.7) can be extended to the space $C^* \times BC$ by $(\psi, X_0) = \psi(0)$, and the infinitesimal generator $\mathcal{A}$ is extended to an operator $\tilde{\mathcal{A}}$ (defined in C^1) into the space BC as follows :

$$\tilde{\mathcal{A}}\phi = \mathcal{A}\phi + X_0[\mathcal{L}\phi - \mathcal{D}\phi']. \tag{8.9}$$

On the basis of the above considerations, equation (13.56) can be written as an abstract ODE [91], as follows :

$$\dot{x}_t = \tilde{\mathcal{A}}x_t + X_0\mathcal{F}(x_t). \tag{8.10}$$

The projection $\Pi : BC \to P$, satisfying $\Pi(\varphi + X_0\alpha) = \Phi[(\Psi, \varphi) + \Psi(0)\alpha]$, yields $x_t = \Phi y(t) + z_t$, where $y(t) \in \mathbb{R}^m$. Equation (13.56) can be represented as :

$$
\begin{cases}
\dot{y} = By + \Psi(0)F(\Phi y + z) \\
\dot{z} = \tilde{\mathcal{A}}_Q + (I - \Pi)X_0\mathcal{F}(\Phi y + z).
\end{cases}
\tag{8.11}
$$

After writing z as a function of y, we focus only on the first equation.

The center manifold of a dynamical system is composed by orbits whose behavior around the equilibrium point is not managed by the attraction of the stable manifold (given by the eigenspace of eigenvectors corresponding to eigenvalues with negative real) nor by the repulsion of the unstable manifold. The analysis of the center manifold requires the equilibrium point to be hyperbolic. Center manifolds play an important role in bifurcation theory because interesting system behavior takes place on it.

8.3 Center manifold and normal forms theory

The center manifold is a powerful tool to analyze the dynamic behavior of a given system in a neighborhood of a non-hyperbolic equilibrium point x^*.

Definition 1. Consider a C^1 map $h : \mathbb{R} \mapsto Q$. The graph of h is said to be a local manifold associated with system (13.56), if $h(0) = Dh(0) = 0$.

Remark 8. There exists a neighborhood V of $0 \in \mathbb{R}^n$ such that for each $\xi \in V$, $\delta = \delta(\xi) > 0$. The solution x of system (13.56) with initial data $\Phi\xi + h(\xi)$ exists on the interval $]-\delta - r, \delta[$; it is given by $x_t = \Phi y(t) + h(y(t))$ for $t \in [0, \delta[$, where $y(t)$ is the unique solution of the ODE :

$$
\begin{aligned}
\dot{y} &= By + \Psi(0)F(\Phi y + h(y)), \\
y(0) &= \xi.
\end{aligned}
\tag{8.12}
$$

Only a few works have investigated the center manifold that arise when considering different matrices B; see for instance [11], where the characterization of the function h in equation (8.12) is detailed. On this basis, it is possible to decompose the eigenspace into the subspace containing all imaginary eigenvalues (having real part equal to zero) and the one with the remaining spectral values (that are assumed to have negative real parts).

In what follows, we adopt the formulations introduced in [152] for the study of the center manifold, originally developed for delay differential equations.

It is worthy of note that $y \in \mathbb{R}^2$ for the most common singularities; for instance, the (one-parameter) Andronov-Hopf bifurcation and the (two-parameter) Bogdanov-Takens bifurcation. See for instance [134].

It is well known that, *normal forms theory* is useful in analyzing local dynamics in the neighborhood of singular points. Among other problems, local bifurcation and stability analysis take advantage of it.

Let $x = (x_1, \ldots, x_n) \in \mathbb{R}^n$, and let $f(x_1, \ldots, x_n)$ be a polynomial vector with components in $\mathbb{R}[x_1, \ldots, x_n]$. Consider the general n-dimensional system of ODE :

$$
\dot{x} = Lx + f(x) = Lx + f_2(x) + f_3(x) + \ldots,
\tag{8.13}
$$

where L is the Jacobian matrix associated with system (8.13), Lx represents the linear part of the system, and $f_k(x)$ denotes the kth homogeneous polynomial vector.

We assume that the system admits an equilibrium at the origin "o". The basic idea of the normal form theory is to find a near-identity transformation :

$$x = y + h(y) = y + h_2(y) + h_3(y) + \ldots + h_k(y) + \ldots, \qquad (8.14)$$

so that, the resulting system,

$$\dot{y} = Ly + g(x) = Ly + g_2(y) + g_3(y) + \ldots + g_k(y) + \ldots, \qquad (8.15)$$

be as simple as possible. In that sense, the terms that are not essential in the local dynamic behavior are removed from the analytical expression of the vector field. Let us denote by $h_k(y)$ and $g_k(y)$, the kth homogeneous polynomial vectors of y. According to *Takens normal form theory* [111], we define the following operators :

$$L_k : H_k \to H_k, \quad U_k \in H_k \mapsto L_k(U_k) = [U_k, u_1] \in H_k, \qquad (8.16)$$

where $u_1 = Ly$ is the linear part of the vector field, and H_k denotes a linear vector space containing the kth homogeneous polynomial vector of $y = (y_1, \ldots, y_n)$. The operator $[.,.]$, called *Lie Bracket*, is defined as :

$$[U_k, u_1] = LU_k - D(U_k)u_1,$$

where D denotes the *Frechet derivative*.

The next step is to determine the spaces R_k and K_k ; the range of H_k ; and the complementary space of R_k, so that $H_k = R_k + K_k$. Now, bases for K_k and R_k can be chosen. The normal form theorem establishes a transformation of the analytic expression of the vector field, see for instance [111], where a detailed analysis of the quadratic and cubic cases is given.

Consequently, a homogeneous polynomial vector $f_k \in H_k$ can be divided into two parts ; one of them can be spanned in K_k, and the remaining one in R_k. Normal form theory suggests that the part belonging to R_k can be disregarded and the one of K_k can be retained in normal form. Through this method, algebraic equations are obtained from (8.13), (8.14) and (8.15).

Next, we aim to apply the above ideas to analyze the qualitative behavior of the drilling system.

8.3.1   Drilling system analysis

In [92], a decomposition method to compute the normal form of a singular delay system linearly dependent on one parameter (of the class studied in [114]) is proposed. We aim to extend the proposed techniques to the case of NFDE systems. To this end, system (8.3) is rewritten as :

$$
\begin{aligned}
\frac{d}{dt} \mathcal{D} x_t :&= \mathcal{L}_0 \, x_t + \tilde{\mathcal{F}}_{p, M_B}(x_t) \\
&= \mathcal{L}_0 \, x_t + (\mathcal{L} - \mathcal{L}_0) \, x_t + \mathcal{F}_{\mu, p_\varepsilon}(x_t),
\end{aligned} \qquad (8.17)
$$

where $\tilde{\mathcal{F}}$ is regarded as a perturbation, $\mathcal{L}_0 = \mathcal{L}|_{\{p=p_c,\, M_B=M^*\}}$, and

$$
\mathcal{F}_p = \left[\begin{array}{c} -0.006750\, px_1^3(t) + 0.006682 px_1^3(t-2) \\ -1.875\, px_1^3(t) + 1.874998\, px_1^3(t-3.176) \end{array} \right].
$$

Clearly,

$$
\frac{d}{dt} \mathcal{D}\, x_t = \mathcal{L}_0\, x_t, \tag{8.18}
$$

corresponds to the perturbation-free system.

Following [152], we compute first, the evolution equation associated to the center manifold of system (8.18).

Considering the drilling system parameters given in Table 9.4, the matrix Φ, depending on θ, is defined as :

$$
\Phi(\theta) = \left[\begin{array}{cc} 1 - \theta & 1 \\ 4.853 \times 10^{11} - 4.853 \times 10^{11}\theta & 4.853 \times 10^{11} \end{array} \right],
$$

where $\theta \in [-3.176, 0]$. The adjoint linear equation associated to system (8.3) is given by :

$$
\dot{u}(t) = D_1 \dot{u}(t+2) + D_2 \dot{u}\,(t+2\tilde{c}/c) - A_0 u(t) - A_1 u(t+2) - A_2 u\,(t+2\tilde{c}/c). \tag{8.19}
$$

Consider the following basis for the generalized eigenspace corresponding to the double eigenvalue $\lambda_0 = 0$ evaluated at $\theta = 0$,

$$
\Psi(\theta) = \left[\begin{array}{cc} -86050 & 0 \\ -8.810 \times 10^{12} + 0.4924583\xi & 0 \end{array} \right], \quad \xi \in [0, 3.176].
$$

The associated bilinear form is given by :

$$
\begin{aligned}
(\psi, \varphi) =\ & \psi(0)(\varphi(0) - D_1\varphi(-2) - D_2\varphi(-3.176)) \\
& + \int_{-2}^{0} \psi(\xi+2)A_1\varphi(\xi)d\xi \\
& + \int_{-3.176}^{0} \psi(\xi+3.176)A_2\varphi(\xi)d\xi \\
& - \int_{-2}^{0} \psi'(\xi+2)D_1\varphi(\xi)d\xi \\
& - \int_{-3.176}^{0} \psi'(\xi+3.176)D_2\varphi(\xi)d\xi.
\end{aligned}
$$

Notice that, according to the bilinear form, we have that $(\Psi, \Phi) = Id$. Hence, the space C can be decomposed as $C = P \bigoplus Q$, where $P = \{\varphi = \Phi z;\ z \in \mathbb{R}^2\}$ and $Q = \{\varphi \in C;\ (\Psi, \varphi) = 0\}$. It is important to emphasize that the subspaces P and

Q are invariant under the semigroup $T(t)$. Matrix B (referred in 8.12), satisfying $\mathcal{A}\Phi = \Phi B$, is given by :

$$B = \begin{bmatrix} 0 & 0 \\ -1 & 0 \end{bmatrix}. \tag{8.20}$$

Consider the following decomposition $x_t = \Phi y(t) + z(t)$, where $z(t) \in Q$, $y(t) \in \mathbb{R}^2$, $z(t) = h(y(t))$ and h is some analytic function such that $h : P \to Q$. The explicit solution corresponding to the center manifold is determined by :

$$\dot{y}(t) = By(t) + \Psi(0)\mathcal{F}[\Phi(\theta)y(t) + h(\theta, y(t))], \tag{8.21}$$

$$\frac{\partial h}{dy}\{By + \Psi(0)\mathcal{F}[\Phi(\theta)y + h]\} + \Phi(\theta)\Psi(0)\mathcal{F}[\Phi(\theta)y + h],$$

$$= \begin{cases} \dfrac{\partial h}{d\theta}, & -3.176 \leqslant \theta \leqslant 0, \\ \mathcal{L}(h(\theta, y)) + \mathcal{F}[\Phi(\theta)y + h(\theta, y)], & \theta = 0, \end{cases} \tag{8.22}$$

where $h = h(\theta, y)$, and $\tilde{\mathcal{F}}$ is defined in (8.17). Further details are given in [152].

It is easy to show that, the evolution of the solutions of system (8.18) on the center manifold can be determined by solving (8.22) (subject to $p = p_c$, $M_B = M^*$) for $h(\theta, y)$, and (8.21) for $y(t)$ (considering the truncation order). Notice that $\mathcal{F}$ is an odd function, which implies that it is the computation of h is not required to obtain a cubic truncation.

Based on these assessments, and considering $p = p_c$, $M_B = M^*$, the system of neutral-type time-delay equations (8.1)-(8.2), describing the coupled axial-torsional drilling dynamics, is reduced to the following third-order ODE :

$$\dot{y}(t) = \begin{bmatrix} 0 & 0 \\ -1 & 0 \end{bmatrix} \begin{bmatrix} y_1 \\ y_2 \end{bmatrix}$$
$$+ \begin{bmatrix} \left(\begin{array}{c} 0.65\,{y_1}^3 + 1.025\,{y_1}^2 y_2 \\ -0.140\,y_1 {y_2}^2 + 0.102\,{y_2}^3 \end{array} \right) \\ \left(\begin{array}{c} 2.54\,{y_1}^3 - 1.554\,{y_1}^2 y_2 \\ +0.267\,y_1 {y_2}^2 - 0.0004\,{y_2}^3 \end{array} \right) \end{bmatrix}. \tag{8.23}$$

In order to analyze the parameter bifurcations, we compute the evolution equation of the trajectories of the perturbed system (8.17) on the center manifold. Now, p and M_B are given respectively by $p = p_c + \mu_1$ and $M_B = M^* + \mu_2$ where $\mu_{1,2}$ are small parameters (recall that the approximation associated to the perturbation-free system (8.18) was developed with $p = p_c$ and $M_B = M^*$). The introduction of a time scaling as well as a small scaling parameter (blow-up parameter) allows zooming the neighborhood of the singularity, see for instance [200].

The cubic normal form reduction of system (8.3) :

$$\begin{cases} \dot{z}_1 = \gamma\,z_1 + \delta\,z_2 - z_1 {z_2}^2 \\ \dot{z}_2 = -z_1 \end{cases} \tag{8.24}$$

is obtained by considering the change of coordinates,

$$\mu_1 = 1326.69991\,\gamma\,r^2,\ p = p_c + \mu_1,\ \mu_2 = 17,87\,\delta r,\ M_B = M^* + \mu_2,\ y_1 = r^2 z_1,\ y_2 = rz_2,$$

and the time scaling defined by $t_{old} = r\,t_{new}$.

Figure 8.1 shows phase space portraits of the reduced model (8.24) on the center manifold, in different scenarios : perturbation-free system ($p = p_c$) and system subject to perturbations ($p = p_c + \mu_1$), for $\gamma = -2$ and $\gamma = 2$.

8.4 Notes and references

Bifurcation theory provides a framework for understanding the behavior of dynamical systems, playing a key role in the study of several real-world problems. For instance, in the context of biological systems, the ability of making dramatic changes in the system output is essential for proper body functioning ; bifurcations are therefore ubiquitous in biological networks [8]. A different application example is given in [114], where physiological systems, modeled by delay differential equations with double-zero eigenvalue singularity, are analyzed in the light of Bogdanov-Takens bifurcations. Another application field is presented in [130], where bifurcations arising in mechanical and physical systems, modeled by nonlinear partial differential equations, are investigated.

A wide range of tools and techniques of the qualitative theory of differential equations and bifurcation principles to the study of nonlinear oscillations can be found in [111]. Detailed studies on one and two-parameter bifurcations in continuous and discrete time dynamical systems are presented in [134].

Qualitative analysis of the drilling system presented in this chapter is based on a reduced model. The infinite-dimensional representation of the coupled axial-torsional drilling dynamics, given by the set of neutral-type time-delay equations (8.1)-(8.2), is reduced to an ODE allowing a simplified qualitative system analysis. The model transformation is developed by using normal forms theory concepts. On that basis, the stability of the steady-state of system (8.3) is investigated.

An alternative stability analysis of the drilling system developed in the frequency domain framework is presented in [158] ; it uses the lumped parameter model describing the coupled axial-torsional drilling dynamics described also in [146], coupled to the bit-rock interface model. The steady-state solution of the model is considered and its stability to small perturbations is analyzed. Some stability charts are derived from such analysis, thus deducing the stable operating regime in the WoB-rotary speed parameter plane. It is concluded that large speeds are eventually stable for all weights on bit, but such large speeds may not be practically feasible. As we shall see in subsequent chapters, an increase of the rotary velocity constitutes a well-known empirical practice to avoid drilling oscillations.

A different analysis approach to derive operational guidelines for avoiding the stick-slip phenomenon is presented in [160] ; it uses a n-dimensional lumped parameter model. The model is assumed to be coupled to a frictional torque on bit

approximated by a combination of the switch model (Dry friction plus Karnopp's model). The identification of key drilling parameters ranges for which non-desired torsional oscillations are present is carried out by analyzing Hopf bifurcations in the vicinity of the system equilibrium point when rotary velocities are greater than zero. Changes in drillstring behavior are studied through variations in three parameters : the weight on the bit, the rotary speed at the top-rotary drillstring system and the torque given by the surface motor. The intersection of the region of parameters where no Hopf bifurcations are present with the region where no stuck bit is possible provides a good estimation of the system parameters which provide safe drilling operations. See also [159], where an optimum range of operating parameters with different WOB and revolutions per minute combinations were provided to ensure the highest possible ROP. The underlying idea of avoiding the stick-slip phenomenon is to drive the rotary velocities of drillstring components to specified values. A discontinuous lumped-parameter torsional model of four degrees of freedom, coupled to the torque on bit model is considered.

Bifurcation analysis methods to characterize the system response are carried out through frequency-domain techniques. Alternative strategies to investigate the stability and the dynamic response of the drilling system are developed through the temporal approach. The following chapter addresses a dissipativity analysis of the system without control actions. This analysis, developed within the time-domain framework, allows concluding on the system's practical stability.

8.5 Drilling system parameters

This section presents the numerical values of the drilling system parameters reflecting typical operating conditions in real oilwell drilling platforms.

Symbol	Parameter	Numerical value
L	String length	3000 m
G	Shear modulus	80×10^9 N m^{-2}
E	Young modulus	200×10^9 N m^{-2}
I_B	Moment of inertia of the drill bit	144 kg m^2
ρ_a	Density	8000 Kg/m^3
R_b	Bit radius	6 cm
Γ	Drillstring's cross-section	35 cm^2
J	Drillstring's second moment of area	19 cm^4
M_B	Mass at the BHA	40000 Kg
α	Viscous friction coefficient	200.025 kg/s
β	Angular momentum	2000 Nms
p	Friction force amplitud	35
k	Constant of the friction top angle	0.3
ζ	Constant of the friction top angle	0.01

TABLE 8.1: Numerical values of the drilling system parameters corresponding to the coupled axial-torsional model [36].

(a)

(b)

(c)
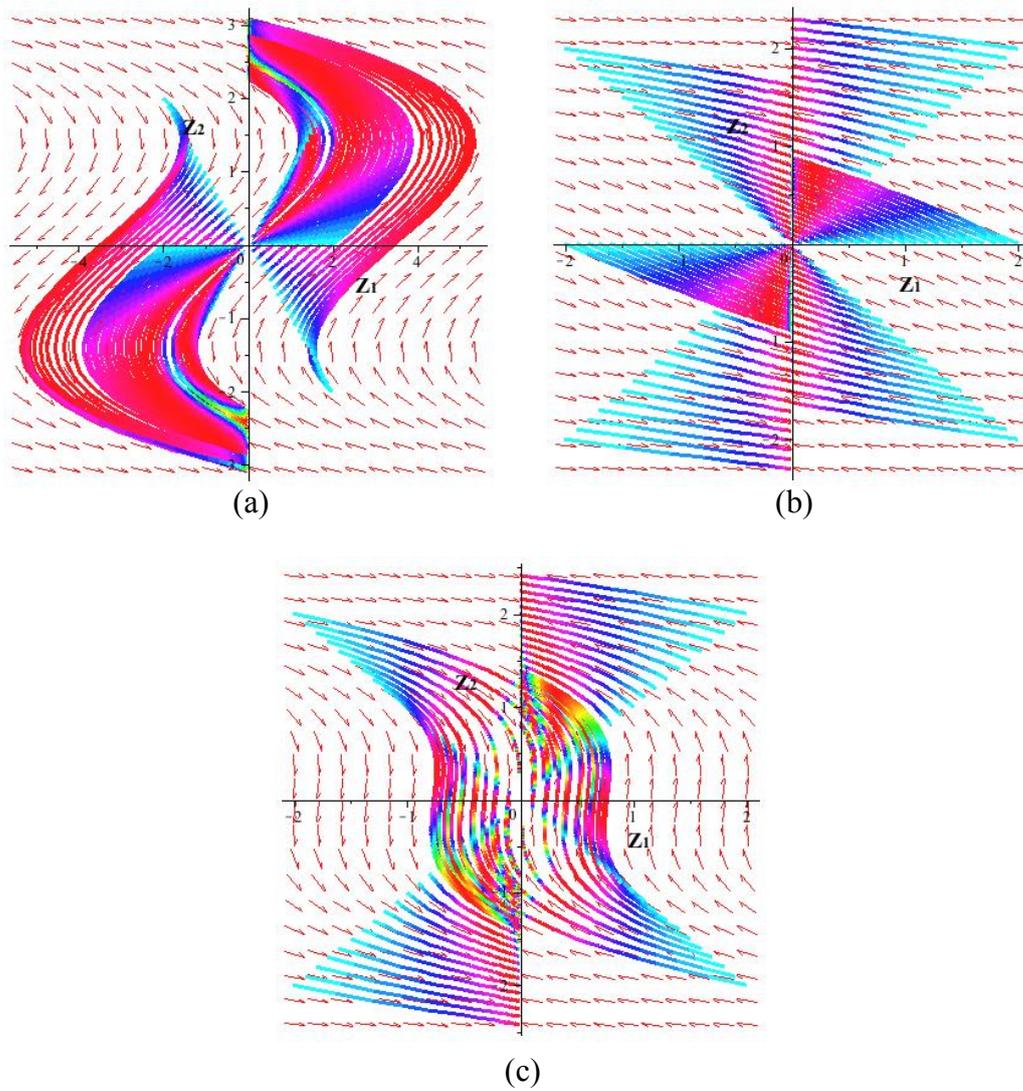
FIGURE 8.1 – Phase portrait of the reduced form of the axial-torsional drilling system model (8.3), given by (8.24). (a) Perturbed system case ($p = p_c + \mu$), $\gamma = -2$. (b) Perturbed system case ($p = p_c + \mu$), $\gamma = 2$. (c) Perturbation-free case ($p = p_c$), $\gamma = 0$.

Low-order controllers

Drillstring platforms usually operate with reduced-order simple control laws which make the drillstring rotate at a constant speed ; only a few of them include controllers to tackle the vibration problem.

This chapter presents some of the most frequently used low-order controllers to regulate the angular velocity and tackle the stick-slip phenomenon.

First, a PI-like control law is derived to maintain a constant rotary speed. The controller is designed under the basis of a two DOF lumped parameter model ; its gains are adjusted by means of the classic two-time-scales separation method [72].

Next, two classic solutions to counteract the stick-slip phenomenon are discussed : the soft torque and the torsional rectification controllers. The torsional rectification control constitutes an improved version of the classical PI speed controller ; it allows the absorption of the energy at the top extremity to avoid the reflection of torsional waves back down to the drillstring. The soft-torque is one of the most popular vibration control methods ; it has the form of a standard speed controller but includes a high-pass filtered torque signal. Both control methods are evaluated in this chapter ; furthermore, an analytic treatment is developed to characterize the torsional energy reflection provided by the torsional rectification controller.

Finally, a novel technique to reduce the stick-slip and bit-bounce is introduced. Based on the bifurcation analysis of the drilling system, a pair of low-order controllers aimed at eliminating axial and torsional coupled vibrations are designed : delayed proportional and delayed PID. The performances of the proposed control techniques are highlighted through simulation of the coupled system. This chapter reproduces mainly the results from [146].

9.1 Angular velocity regulation

A simple technique to overcome the problem of angular speed regulation is proposed in [71]. The low-order controller presented below is designed on the basis of the following two DOF lumped parameter model describing the drillstring torsional dynamics :

$$
\begin{aligned}
I_p \ddot{\Phi}_p + c \left(\dot{\Phi}_p - \dot{\Phi}_b \right) + k \left(\Phi_p - \Phi_b \right) + d_p \dot{\Phi}_p &= u_T \\
I_b \ddot{\Phi}_b - c \left(\dot{\Phi}_p - \dot{\Phi}_b \right) - k \left(\Phi_p - \Phi_b \right) + d_b \dot{\Phi}_b &= -T(\dot{\Phi}_b),
\end{aligned}
\tag{9.1}
$$

where $\dot{\Phi}_p$ and $\dot{\Phi}_b$ denote the angular velocity at the top and bottom extremities, respectively, u_T is the motor torque provided by the rotary table and $T(\dot{\Phi}_b)$ is the frictional torque describing the bit-rock interaction.

The angular velocity regulation control law is defined as :

$$u_T = k_1 \left(\Omega_0 - \dot{\Phi}_p \right) + k_2 \int \left(\Omega_0 - \dot{\Phi}_p \right) dt - k_3 \left(\dot{\Phi}_p - \dot{\Phi}_b \right). \tag{9.2}$$

This reduced-order controller, aimed at regulating the rotational velocity to a certain reference velocity Ω_0.
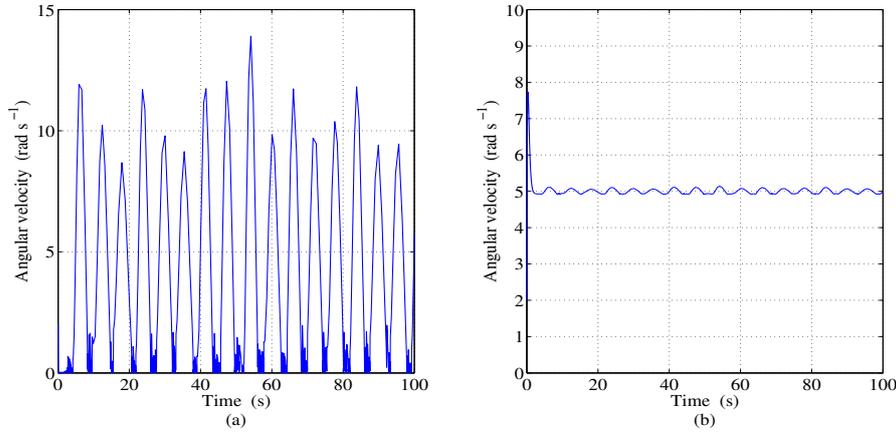
FIGURE 9.1 – Simulation of the lumped parameter model (9.1) coupled to the frictional torque model from [146] Trajectories of the drilling system in closed loop with the speed regulation controller (9.2) with $k_1 = 15725$, $k_2 = 30576$, $k_3 = 194$, for a reference angular velocity $\Omega_0 = 5\mathrm{rad}\ \mathrm{s}^{-1}$. (a) Angular velocity at the bottom extremity. (b) Angular velocity at the upper extremity.

Figures 9.1 and 9.2 show the control performance for $\Omega_0 = 5\mathrm{rad}\ \mathrm{s}^{-1}$ and $\Omega_0 = 10\mathrm{rad}\ \mathrm{s}^{-1}$, respectively. The numerical values of the system parameters are given in [146].

Notice the controller (9.2) is not able to regulate the angular velocity at the bottom end for $\Omega_0 = 5\mathrm{rad}\ \mathrm{s}^{-1}$.

9.1.1 Synthesis of the controller

There are different methods for adjusting the controller gains ; one of them is the classic two-time-scales separation method [72] detailed below.

Following [71], a variable z and a constant κ defined as :

$$z = k \left(\Phi_p - \Phi_b \right), \quad \kappa^2 = \frac{1}{k},$$

are introduced.
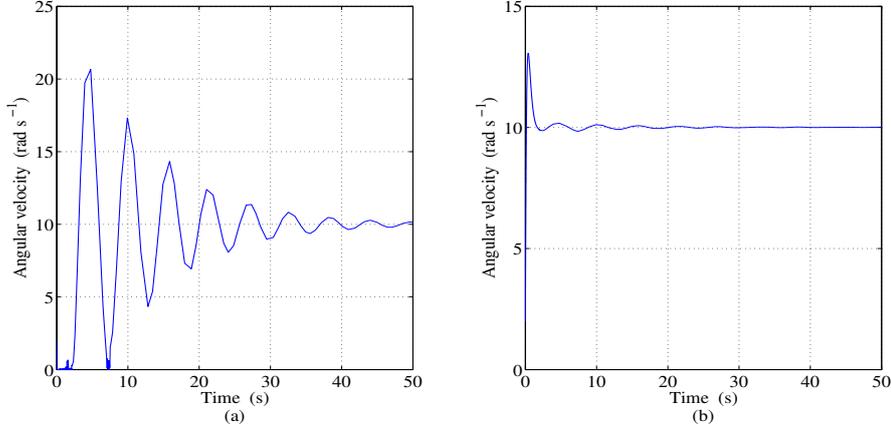
FIGURE 9.2 – Simulation of the lumped parameter model (9.1) coupled to the frictional torque model from [146]. Trajectories of the drilling system in closed loop with the speed regulation controller (9.2) with $k_1 = 15725$, $k_2 = 30576$, $k_3 = 194$, for a reference angular velocity $\Omega_0 = 10\text{rad s}^{-1}$. (a) Angular velocity at the bottom extremity. (b) Angular velocity at the upper extremity.

According to the drilling model (9.1), the dynamics of Φ_p and z are described by :

$$u_T = I_p\ddot{\Phi}_p + c\kappa^2\dot{z} + z + d_p\dot{\Phi}_p$$

$$\kappa^2\ddot{z} = \ddot{\Phi}_p - \ddot{\Phi}_b = -\left(\frac{1}{I_p} + \frac{1}{I_b}\right)z - \kappa^2\left(\frac{c}{I_p} + \frac{c}{I_b}\right)\dot{z}$$

$$-\frac{d_p}{I_p}\dot{\Phi}_p + \frac{d_b}{I_b}\dot{\Phi}_b + \frac{1}{I_p}u_T + \frac{1}{I_b}T(\dot{\Phi}_b),$$

which can be written as :

$$u_T = I_p\ddot{\Phi}_p + c\kappa^2\dot{z} + z + d_p\dot{\Phi}_p$$

$$\kappa^2\ddot{z} = -\frac{z}{I_{eq}} - \kappa^2\left(\frac{c}{I_{eq}} - \frac{d_b}{I_b}\right)\dot{z} + \left(\frac{d_b}{I_b} - \frac{d_p}{I_p}\right)\dot{\Phi}_p + \frac{u_T}{I_p} + \frac{T(\dot{\Phi}_b)}{I_b}, \quad (9.3)$$

with $I_{eq} = \left(\frac{1}{I_p} + \frac{1}{I_b}\right)^{-1}$.

Since the torsional stiffness takes large values, it is assumed that $\kappa^2 \simeq 0$; then it follows that

$$u_{Ts} = I_p\ddot{\Phi}_p + z + d_p\dot{\Phi}_p \quad (9.4)$$

$$0 = -\frac{z}{I_{eq}} + \left(\frac{d_b}{I_b} - \frac{d_p}{I_p}\right)\dot{\Phi}_p + \frac{u_{Ts}}{I_p} + \frac{T(\dot{\Phi}_b)}{I_b}, \quad (9.5)$$

where the rotary torque u_T is split into slow (u_{Ts}) and fast (u_{Tf}) modes :

$$u_T = u_{Ts} + \kappa u_{Tf}. \quad (9.6)$$

From (9.5), we have that

$$z = I_{eq} \left[\left(\frac{d_b}{I_b} - \frac{d_p}{I_p} \right) \dot{\Phi}_p + \frac{u_{Ts}}{I_p} + \frac{T(\dot{\Phi}_b)}{I_b} \right],$$

by substituting the above equation into (9.4) we obtain :

$$\ddot{\Phi}_p + \left(\frac{d_b + d_p}{I_p + I_b} \right) \dot{\Phi}_p = \frac{1}{I_p + I_b} u_{Ts} - \frac{1}{I_p + I_b} T(\dot{\Phi}_b).$$

Assume that u_{Ts} is chosen as :

$$u_{Ts} = \left(k_1 + \frac{k_2}{s} \right) \left(\Omega_0 - \dot{\Phi}_p \right),$$

and define the variable $\tilde{\Phi}_p$ as follows

$$\dot{\tilde{\Phi}}_p = \Omega_0 - \dot{\Phi}_p$$

then, $\tilde{\Phi}_p = \frac{\Omega_0 - \dot{\Phi}_p}{s}$ and $\ddot{\tilde{\Phi}}_p = -\ddot{\Phi}_p$.

For $(d_b + d_p) \ll (I_p + I_b)$, we have that

$$\dddot{\tilde{\Phi}}_p + \left(\frac{k_1}{I_p + I_b} \right) \ddot{\tilde{\Phi}}_p + \left(\frac{k_2}{I_p + I_b} \right) \dot{\tilde{\Phi}}_p = \frac{1}{I_p + I_b} T(\dot{\Phi}_b).$$

Then, by imposing a damping δ_r and natural frequency ω_n in the closed-loop dynamics, the values of k_1 and k_2 can be computed from

$$\begin{aligned} k_1 &= (I_p + I_b) \left(2\delta_r \omega_n - \frac{d_b + d_p}{I_p + I_b} \right) \\ k_2 &= (I_p + I_b) \, \omega_n^2. \end{aligned}$$

Substituting (9.6) into (9.3) gives :

$$\kappa^2 \ddot{z} = -\frac{z}{I_{eq}} - \kappa^2 \left(\frac{c}{I_{eq}} - \frac{d_b}{I_b} \right) \dot{z} + \left(\frac{d_b}{I_b} - \frac{d_p}{I_p} \right) \dot{\Phi}_p + \frac{u_{Ts}}{I_p} + \frac{\kappa}{I_p} u_{Tf} + \frac{T(\dot{\Phi}_b)}{I_b}. \qquad (9.7)$$

Following the two-time scales separation approach, it is assumed that the slow mode has reached its steady state value, thus, equation (9.7) can be rewritten as :

$$\kappa^2 \ddot{z} = -\frac{z}{I_{eq}} - \kappa^2 \left(\frac{c}{I_{eq}} - \frac{d_b}{I_b} \right) \dot{z} + \frac{\kappa}{I_p} u_{Tf} + \frac{T(\dot{\Phi}_b)}{I_b} + \rho_p \left(\dot{\Phi}_p^*, \Phi_p^* \right), \qquad (9.8)$$

where the superscript * denotes the steady-state value and

$$\begin{aligned} \rho_p \left(\dot{\Phi}_p^*, \Phi_p^* \right) &= \left(\frac{d_b}{I_b} - \frac{d_p}{I_p} \right) \dot{\Phi}_p^* + \frac{u_{Ts} \left(\dot{\Phi}_p^*, \Phi_p^* \right)}{I_p} \\ &= \frac{z^*}{I_{eq}} - \frac{T(\dot{\Phi}_b)}{I_b}. \end{aligned}$$

Defining the fast error coordinate as $\zeta = z - z^*$, equation (9.8) can be rewritten as :

$$\ddot{\zeta} + \left(\frac{c}{I_{eq}} + \frac{d_b}{I_b} \right) \dot{\zeta} + \frac{1}{\kappa^2 I_{eq}} \zeta = \frac{1}{I_p \kappa} u_{Tf}.$$

By choosing $u_{Tf} = -k_3 \dot{\zeta}$, we obtain :

$$\ddot{\zeta} + \left(\frac{c}{I_{eq}} + \frac{d_b}{I_b} + \frac{k_3}{I_p \kappa} \right) \dot{\zeta} + \frac{1}{\kappa^2 I_{eq}} \zeta = 0,$$

then, prescribing a damping value for the torsion dynamics δ_{tor}, the value of k_3 can be computed as follows

$$k_3 = \frac{I_p}{\sqrt{k}} \left(2\delta_{tor} \sqrt{k} I_{eq} - \frac{c}{I_{eq}} - \frac{d_b}{I_b} \right).$$

9.2 Drilling vibration control

The control law (9.2) is designed to regulate the drillstring angular velocity, but it does not considers the vibration problem. This section presents a pair of reduced-order torque feedback controllers aimed at maintaining a constant rotary speed while reducing torsional vibrations.

9.2.1 Torsional rectification control

A torsional rectification method to suppress the stick-slip phenomenon is proposed in [184] ; the strategy takes advantage of the fact that the general solution of the wave equation describing torsional drillstring vibrations allows the identification of both "up" and "down" moving components.

The underlying idea consists in maintaining the energy of the "down" traveling wave constant in the presence of the nonlinear boundary conditions describing the bit-rock frictional interface.

Without loss of generality, it is assumed that the speed of torsional waves is one ; the torsional excitations of the drilling system, described by the drillstring angular displacement $\Phi(s,t)$, are modeled by the wave equation :

$$\frac{\partial^2 \Phi}{\partial t^2}(s,t) = \frac{\partial^2 \Phi}{\partial s^2}(s,t), \quad 0 \leqslant s \leqslant 1 \tag{9.9}$$

with boundary conditions

$$\frac{\partial^2 \Phi}{\partial t^2}(0,t) = F_0 \left(\frac{\partial \Phi}{\partial t}(0,t), \frac{\partial \Phi}{\partial s}(0,t), \Phi(0,t), t \right)$$

$$\frac{\partial^2 \Phi}{\partial t^2}(1,t) = F_1 \left(\frac{\partial \Phi}{\partial t}(1,t), \frac{\partial \Phi}{\partial s}(1,t), \Phi(1,t), t \right)$$

where $s = 0$ denotes the connection of the drillstring with the rotary table, and $s = 1$ the bottom extremity. The functions F_0 and F_1 are determined by the top

drive and friction torques at the upper and bottom extremities respectively. The general solution of the wave equation is given by

$$\Phi(s,t) = \phi(t+s) + \psi(t-s),$$

where ϕ and ψ are arbitrary continuously differentiable real-valued functions, with ϕ representing an arbitrary up-traveling wave and ψ an arbitrary down-traveling wave. The time and spatial derivatives of $\Phi(s,t)$ are

$$
\begin{aligned}
\frac{\partial \Phi}{\partial t}(s,t) &= \dot\phi(t+s) + \dot\psi(t-s), \\
\frac{\partial \Phi}{\partial s}(s,t) &= \dot\phi(t+s) - \dot\psi(t-s),
\end{aligned}
$$

respectively. Since the contact torque at any point "s" of the drillstring is proportional to $\frac{\partial \Phi}{\partial s}(s,t)$, $\dot\psi$ represents the transmission of torque to the BHA. In order to drive the angular velocity to a prescribed constant rotary speed, $\dot\psi$ must be maintained close to a constant value. To this end, the quantity $\Psi(t)$ defined by

$$\Psi(t) = \frac{\partial \Phi}{\partial t}(0,t) - \frac{\partial \Phi}{\partial s}(0,t) = 2\dot\psi(t) \tag{9.10}$$

must be monitored.

A Newton-type equation is chosen to describe the top boundary condition :

$$\frac{\partial^2 \Phi}{\partial t^2}(0,t) = G_{top}\frac{\partial \Phi}{\partial s}(0,t) + u_T(t) \tag{9.11}$$

where G_{top} is proportional to the torsional rigidity of the drillstring ($G_{top} = \frac{GJ}{LI_T}$) see [146] for further details.

A commonly used control law to maintain a constant angular velocity Ω_0 is given by :

$$u_T(t) = k_p\dot\xi(t) + k_i\xi(t), \tag{9.12}$$

where $k_p > 0$ and k_i are the proportional and integral gain variables respectively and

$$
\begin{aligned}
\xi(t) &= \Omega_0 t - \Phi(0,t) + \xi_0 \\
\dot\xi(t) &= \Omega_0 - \frac{\partial \Phi}{\partial t}(0,t),
\end{aligned}
$$

where ξ_0 denotes the displacement of the drillstring at the upper extremity from its reference value.

In [184], an improved control strategy is proposed ; the contact torque between the drillstring and the rotary table can be monitored by introducing a compensating drive torque that rectifies the up-travelling torsional waves on the drillstring. The control law is written as :

$$u_T(t) = k_p\dot\xi(t) + k_i\xi(t) - \lambda\Psi(t), \tag{9.13}$$

where $\lambda \geqslant 0$ and $\Psi(t)$ is given in (9.10). The torsional rectification control law (9.13) is evaluated in [184] for different values of the control gains k_p, k_i, and λ; besides, the effect of an incident torsional harmonic wave on the rotary table is explored. By analytical and numerical analyses it is concluded that the reflected torsional energy from the upper extremity can be decreased by increasing the control parameter λ.

9.2.2   Soft-torque control

The soft-torque, introduced in [118], is a control approach widely used in the drilling industry to tackle torsional vibrations. This controller has the form of the standard speed controller (9.12) but it includes a high-pass filtered torque signal, i.e.,

$$u_T(t) = \kappa_p \dot{\tilde{\xi}}(t) + \kappa_i \, \tilde{\xi}(t), \tag{9.14}$$

with

$$\begin{aligned}
\tilde{\xi}(t) &= \Omega_0 \, t - h \int T_f(t) dt - \Phi(0,t) + \xi_0, \\
\dot{\tilde{\xi}}(t) &= \Omega_0 - h T_f(t) - \frac{\partial \Phi}{\partial t}(0,t),
\end{aligned} \tag{9.15}$$

where h is an additional control parameter and T_f is defined as :

$$T_f(t) \equiv T_{\text{contact}}(t) - T_c(t),$$

T_c denotes the output of a low-pass filter applied to the contact torque :

$$T_{\text{contact}}(t) = -G_{top} \, \frac{\partial \Phi}{\partial s}(0,t),$$

measured at the upper extremity. An AC low-pass filter is modeled by :

$$\dot{T}_c(t) = \omega_c \, (T_{\text{contact}}(t) - T_c(t)),$$

where ω_c is the cut-off angular frequency.

By considering that

$$\int T_f(t) \, dt = \frac{1}{\omega_c} \int \dot{T}_c(t) dt = \frac{1}{\omega_c} \, T_c(t),$$

equation (9.15) can be rewritten as :

$$\tilde{\xi}(t) = \Omega_0 \, t - \frac{h}{\omega_c} \, T_c(t) - \Phi(0,t) + \xi_0.$$

9.2.3   Torsional energy reflection and stick-slip reduction

The performance of the torsional rectification controller (9.13) can be evaluated through the analysis of the energy reflection at the top extremity. To this end,

consider the following solution to the equation (9.9) which describes a harmonic wave :

$$\Phi(s,t) = A_{\phi,\omega} \sin\left(\omega\left(t+s\right)\right) + A_{\psi,\omega} \sin\left(\omega\left(t-s\right)+\alpha_\omega\right) + \Omega_0 t + C_0 s$$

where ω is the angular frequency, $A_{\phi,\omega}$ is the amplitude of the wave incident on the rotary from below, and $A_{\psi,\omega}$ is the amplitude of the reflected wave. The constants C_0, α_ω and the ratio $A_{\psi,\omega}/A_{\phi,\omega}$ are determined from equations (9.11)-(9.13) as follows :

$$\begin{aligned}
C_0 &= \frac{\lambda\Omega_0 - k_i\xi_0}{G_{top} + \lambda}, \\
\alpha_\omega &= \tan^{-1}\left(\frac{2\omega\left(k_i - \omega^2\right)\left(G_{top} + \lambda\right)}{\omega^4 - \left(2k_i + \left(G_{top} - k_p\right)\eta\right)\omega^2 + k_i^2}\right) \\
\frac{A_{\psi,\omega}}{A_{\phi,\omega}} &= \frac{k_i - \omega^2}{\left(k_i - \omega^2\right)\cos\left(\alpha_\omega\right) + \omega\eta\sin\left(\alpha_\omega\right)} \\
\eta &= G_{top} + k_p + 2\lambda,
\end{aligned}$$

the reflection coefficient is thus defined as

$$r_\omega = \left|\frac{A_{\psi,\omega}}{A_{\phi,\omega}}\right| = \sqrt{\frac{\omega^4 + a\omega^2 + k_i^2}{\omega^4 + b\omega^2 + k_i^2}}$$

where

$$a = \left(G_{top} - k_p\right)^2 - 2k_i, \quad b = \eta^2 - 2k_i.$$
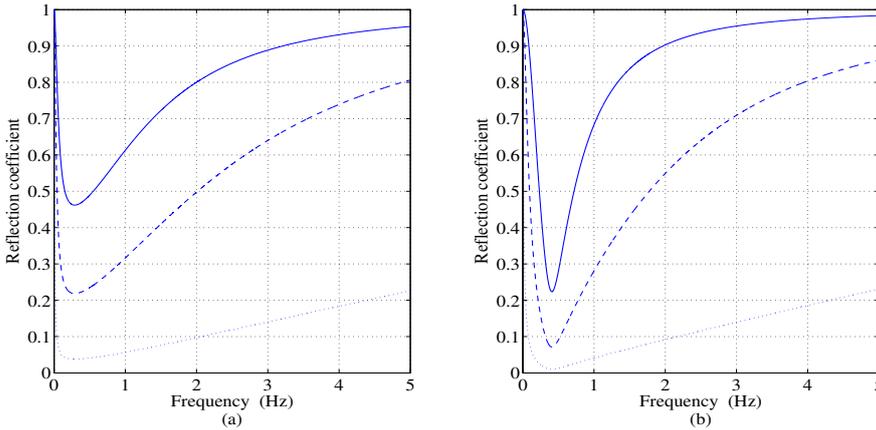

FIGURE 9.3 – Reflection coefficient r_ω as a function of the frequency ω with $\lambda = 0$ (solid line), $\lambda = 1$ (dashed line) and $\lambda = 10$ (dotted line). (a) Shape of r_ω for the parameters $kp = 1.314$, $k_i = 0.08336$, $G_{top} = 0.4836$. (b) Shape of r_ω for the parameters $k_p = 0.3658$, $k_i = 0.1672$, $G_{top} = 0.5765$.

The absorption of vibrational energy is greater when the reflection coefficient takes small values. It is easy to prove that the torsional energy reflected from the rotary table is reduced by increasing the control parameter λ. This is shown in Figure 9.3 which depicts the shape of the reflection coefficient r_ω as a function of the angular frequency ω for different values of λ. Different data sets are considered : Figure 9.3(a) uses the parameters $kp = 1.314$, $k_i = 0.08336$, $G_{top} = 0.4836$, and Figure 9.3(b) the parameters $k_p = 0.3658$, $k_i = 0.1672$, $G_{top} = 0.5765$.

Notice that as the torsional rectification feedback λ is increased, the reflection coefficient r_ω uniformly decreases ; this behavior corresponds to an increase of torsional vibration absorption.

A similar analysis for evaluating the performance of the soft torque controller (9.14) is presented in [184] ; it is concluded that the shape of the reflection coefficient does not varies uniformly with the control parameter h. Besides, it is proven that the torsional rectification controller exhibits an improved performance compared with the soft torque one.

In order to asses the ability of the torque feedback controllers (9.12), (9.13) and (9.14) in eliminating the stick-slip phenomenon, we propose to test them by using two different modeling approaches. A lumped parameter model describing the torsional drilling behavior coupled to the simplified ToB model given in [146] is first considered. Next, we use an a neutral-type time-delay model derived from a distributed parameter representation of the coupled torsional-axial drilling dynamics, subject to the ToB model, which is inspired by the Karnopp friction law.
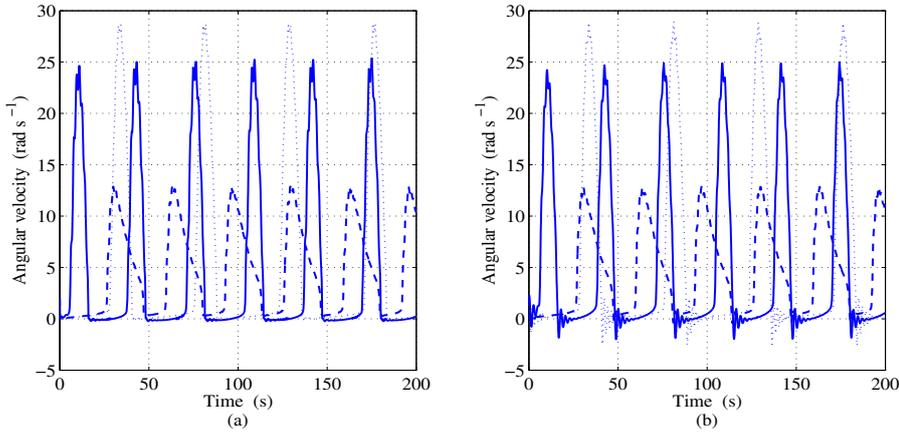
FIGURE 9.4 – Simulation of the simplified model (9.16)-(9.17). Trajectories of the drilling system in closed loop with the standard speed controller (9.12) (dotted line), the torsional rectification control law (9.13) (dashed line), and the soft torque control (9.14) (solid line) with $k_p = 0.3658$, $k_i = 0.1672$, $\lambda = 1$, for a reference angular velocity $\Omega_0 = 5 \text{rad s}^{-1}$. (a) Angular velocity at the bottom extremity. (b) Angular velocity at the upper extremity.

According to the geometrical formulation of elasticity laws established in [9], the boundary conditions of the wave equation can be modeled as follows :

$$\frac{\partial^2 \Phi}{\partial t^2}(0,t) - G_{top}\frac{\partial \Phi}{\partial s}(0,t) - u_T(t) = 0$$

$$\frac{\partial^2 \Phi}{\partial t^2}(1,t) + G_{bit}\frac{\partial \Phi}{\partial s}(1,t) + T\left(\frac{\partial \Phi}{\partial t}(1,t)\right) = 0$$

where T describes the frictional torque at the bit, $u_T(t)$ the motor torque considered as a control input. The top drive and BHA inertias are scaled into the constants $G_{top} = \frac{GJ}{LI_T}$ and $G_{bit} = \frac{GJ}{LI_B}$.
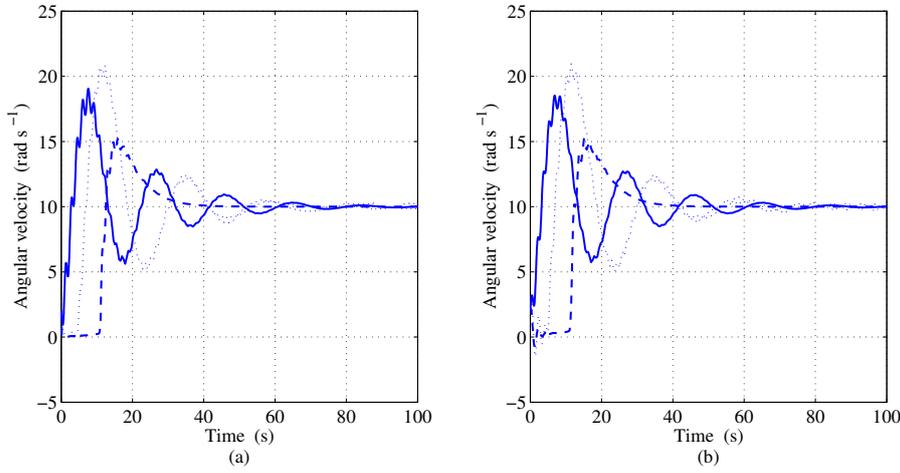

FIGURE 9.5 – Simulation of the simplified model (9.16)-(9.17). Trajectories of the drilling system in closed loop with the standard speed controller (9.12) (dotted line), the torsional rectification control law (9.13) (dashed line), and the soft torque control (9.14) (solid line) with $k_p = 0.3658$, $k_i = 0.1672$, $\lambda = 1$, for a reference angular velocity $\Omega_0 = 10\text{rad s}^{-1}$. (a) Angular velocity at the bottom extremity. (b) Angular velocity at the upper extremity.

An approximation of the drillstring torsional dynamics is obtained by ignoring the infinite-dimensional character of the system and considering it as a torsional pendulum that couples the top drive torque with the frictional torque arising from the bit-rock contact. By defining the torsional displacements at the top and bottom extremities $\Phi(0,t)$, $\Phi(1,t)$ as Φ_p and Φ_b, respectively, and by considering $\frac{\partial \Phi}{\partial s}(1,t) \simeq \Phi_b - \Phi_p$, the equations of motion are given by :

$$\ddot{\Phi}_p + G_{top}(\Phi_p - \Phi_b) - u_T(t) = 0 \qquad (9.16)$$

$$\ddot{\Phi}_b + G_{bit}(\Phi_b - \Phi_p) + T\left(\dot{\Phi}_b\right) = 0.$$

The frictional torque T can be approximated by the following function :

$$T(\dot{\Phi}_b(t)) = \frac{2\bar{k}p\dot{\Phi}_b(t)}{\dot{\Phi}_b^2(t) + \bar{k}^2}, \quad \bar{k} > 0, \; p > 0.$$

(9.17)

Figures 9.4 and 9.5 show the system response to the torque feedback controllers : standard (9.12), torsional rectification (9.13) and soft torque (9.14) for $\Omega_0 = 5$rad s^{-1} and $\Omega_0 = 10$rad s^{-1}, respectively.

Notice that, as remarked in [184], the torsional rectification controller provides superior performance when the simplified model (9.16)-(9.17) is considered.

Consider now, the neutral-type time-delay model of the torsional-axial coupled drilling dynamics given by :

$$
\begin{aligned}
\dot{z}(t) - \Upsilon\dot{z}(t - 2\tau) &= -\Psi z(t) - \Upsilon\Psi z(t - 2\tau) \\
&\quad -\frac{1}{I_{\mathrm{B}}}T(z(t)) + \frac{1}{I_{\mathrm{B}}}\Upsilon T(z(t - 2\tau)) + \Pi\Omega(t - \tau), \quad (9.18)
\end{aligned}
$$

where $z(t)$ is the angular velocity at the bottom extremity, and

$$\Pi = \frac{2\Psi\beta}{\beta + \tilde{c}GJ}, \quad \Upsilon = \frac{\beta - \tilde{c}GJ}{\beta + \tilde{c}GJ}, \quad \Psi = \frac{\tilde{c}GJ}{I_{\mathrm{B}}}, \quad \tau = \sqrt{\frac{I}{GJ}}L, \quad \tilde{c}GJ = \sqrt{IGJ}.$$

(9.19)

Similarly, the wave equation with boundary conditions, corresponding to the axial drilling dynamics is transformed into the following neutral-type equation :

$$
\begin{aligned}
\dot{y}(t) - \tilde{\Upsilon}\dot{y}(t - 2\tilde{\tau}) &= -\tilde{\Psi}y(t) - \tilde{\Upsilon}\tilde{\Psi}y(t - 2\tilde{\tau}) \\
&\quad -\frac{1}{M_{\mathrm{B}}}T(z(t)) + \frac{1}{M_{\mathrm{B}}}\tilde{\Upsilon}T(z(t - 2\tilde{\tau})) + \tilde{\Pi}u_H(t - \tilde{\tau})(9.20)
\end{aligned}
$$

where $y(t)$ is the axial velocity at the bottom extremity, and

$$\tilde{\Pi} = \frac{2\tilde{\Psi}}{\alpha + cE\Gamma}, \quad \tilde{\Upsilon} = \frac{\alpha - cE\Gamma}{\alpha + cE\Gamma}, \quad \tilde{\Psi} = \frac{cE\Gamma}{M_B}, \quad \tilde{\tau} = cL.$$

(9.21)

Also consider the model frictional torque on bit

$$T\left(\dot{\Phi}_b(t)\right) = c_b\dot{\Phi}_b(t) + W_{ob}R_b\mu_b\left(\dot{\Phi}_b(t)\right)\mathrm{sgn}\left(\dot{\Phi}_b(t)\right).$$

(9.22)

The term $c_b\dot{\Phi}_b(t)$ represents the viscous damping torque at the bottom end and the expression $W_{ob}R_b\mu_b\left(\dot{\Phi}_b(t)\right)\mathrm{sgn}\left(\dot{\Phi}_b(t)\right)$ approximates the dry friction torque. Notations R_b and W_{ob} stand for the bit radius and the weight on bit, respectively. The term $c_b\dot{\Phi}_b(t)$ represents the viscous damping torque at the bottom end and the expression $W_{ob}R_b\mu_b\left(\dot{\Phi}_b(t)\right)\mathrm{sgn}\left(\dot{\Phi}_b(t)\right)$ approximates the dry friction torque. Notations R_b and W_{ob} stand for the bit radius and the weight on bit, respectively. The friction coefficient $\mu_b(\dot{\Phi}_b(t))$ is given by :

$$\mu_b\left(\dot{\Phi}_b(t)\right) = \mu_{cb} + (\mu_{sb} - \mu_{cb})\mathrm{e}^{-\gamma_b|\dot{\Phi}_b(t)|},$$

(9.23)

where μ_{cb}, μ_{sb} denote the Coulomb and static friction coefficients, the constant $0 <
\gamma_b < 1$ defines the velocity decrease rate. Consider also the frictional torque on bit
model, derived from the Karnopp friction law, see [42, 146]. Obviously, this system
representation constitutes a more reliable description of the dynamics taking place
during the drilling performance. Figures 9.6 and 9.7 show the system trajectories
in closed loop with the controllers (9.12), (9.13) and (9.14). Observe that, under
this modeling approach, the soft-torque control method performs better than the
standard speed controller and than the torsional rectification one; in fact, these last
ones are unable to eliminate the stick-slip for low angular velocities.
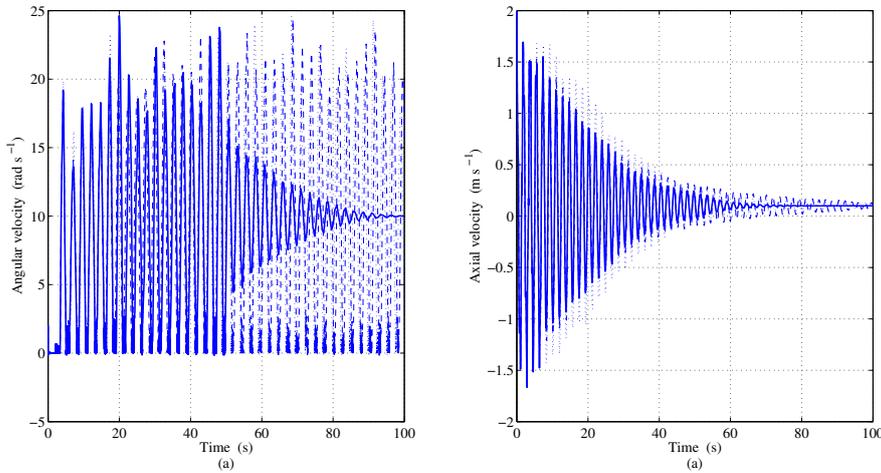
FIGURE 9.6 – Simulation of the neutral-type time-delay model (9.18)-(9.20) coupled
to the frictional torque model (9.22)-(9.23). Trajectories of the drilling system in
closed loop with the standard speed controller (9.12) (dotted line), the torsional
rectification control law (9.13) (dashed line), and the soft torque control (9.14)
(solid line) with $k_p = 0.3658$, $k_i = 0.1672$, $\lambda = 0.01$, for a reference angular velocity
$\Omega_0 = 10\text{rad s}^{-1}$. (a) Angular velocity at the bottom extremity. (b) Axial velocity at
the bottom extremity.

9.3   Bifurcation analysis-based controllers

This section presents a pair of control schemes to tackle both axial and torsional
vibrations occurring along a rotary oilwell drilling system. It will be shown that the
implementation of low-order delayed feedback controllers allows reducing undesired
vibrations leading to an acceptable drilling performance.

Consider the following coupled torsional-axial model :
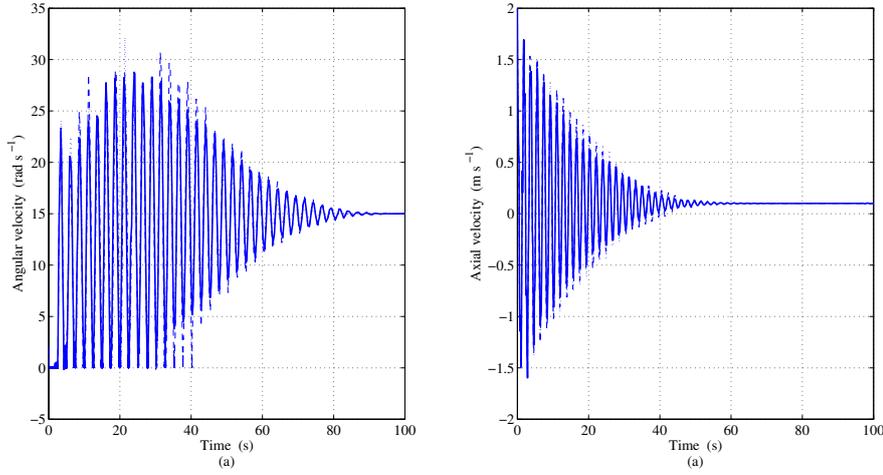
FIGURE 9.7 – Simulation of the neutral-type time-delay model (9.18)-(9.20) coupled to the frictional torque model (9.22)-(9.23). Trajectories of the drilling system in closed loop with the standard speed controller (9.12) (dotted line), the torsional rectification control law (9.13) (dashed line), and the soft torque control (9.14) (solid line) with $k_p = 0.3658$, $k_i = 0.1672$, $\lambda = 0.01$, for a reference angular velocity $\Omega_0 = 15 \text{rad s}^{-1}$. (a) Angular velocity at the bottom extremity. (b) Axial velocity at the bottom extremity.

and

$$
\begin{cases}
\dfrac{\partial^2 U}{\partial s^2}(s,t) = c^2 \dfrac{\partial^2 U}{\partial t^2}(s,t), \quad c = \sqrt{\dfrac{\rho_a}{E}} \\[2mm]
E\Gamma \dfrac{\partial U}{\partial s}(0,t) = \alpha \dfrac{\partial U}{\partial t}(0,t) - u_H(t) \\[2mm]
E\Gamma \dfrac{\partial U}{\partial s}(L,t) = -M_B \dfrac{\partial^2 U}{\partial t^2}(L,t) + F\left(\dfrac{\partial U}{\partial t}(L,t)\right)
\end{cases}
\tag{9.24}
$$

and

$$
\begin{cases}
\dfrac{\partial^2 \Phi}{\partial s^2}(s,t) = \tilde{c}^2 \dfrac{\partial^2 \Phi}{\partial t^2}(s,t), \quad \tilde{c} = \sqrt{\dfrac{\rho_a}{G}} \\[2mm]
GJ \dfrac{\partial \Phi}{\partial s}(0,t) = \beta \dfrac{\partial \Phi}{\partial t}(0,t) - u_T(t) \\[2mm]
GJ \dfrac{\partial \Phi}{\partial s}(L,t) = -I_B \dfrac{\partial^2 \Phi}{\partial t^2}(L,t) - \tilde{F}\left(\dfrac{\partial U}{\partial t}(L,t)\right)
\end{cases}
\tag{9.25}
$$

where U and Φ stand for the axial and the torsional position, and the control inputs u_H and u_T correspond to the brake motor control and the torque provided by the rotary table.

By using the d'Alembert transformation, the system of PDE (9.24)-(9.25) is reduced to the following system of Neutral Delay Differential Equations (NDDE) :

$$\ddot{U}_b(t) - \tilde{\Upsilon}_n \ddot{U}_b(t-2) = -\tilde{\Psi}_n \dot{U}_b(t) - \tilde{\Upsilon}_n \tilde{\Psi}_n \dot{U}_b(t-2) \tag{9.26}$$
$$+ \frac{1}{M_B} F\left(\dot{U}_b(t)\right) - \frac{1}{M_B} \tilde{\Upsilon}_n F\left(\dot{U}_b(t-2)\right) + \tilde{\Pi}_n u_H(t-1),$$

$$\ddot{\Phi}_b(t) - \Upsilon_n \ddot{\Phi}_b(t-2\tau) = -\Psi_n \dot{\Phi}_b(t) - \Upsilon_n \Psi_n \dot{\Phi}_b(t-2\tau) \tag{9.27}$$
$$+ \frac{1}{I_B} \tilde{F}\left(\dot{U}_b(t)\right) - \frac{1}{I_B} \Upsilon_n \tilde{F}\left(\dot{U}_b(t-2\tau)\right) + \Pi_n u_T(t-\tau),$$

with

$$\tilde{\Pi}_n = \frac{2\tilde{\Psi}_n}{\alpha+1}, \quad \tilde{\Upsilon}_n = \frac{\alpha-1}{\alpha+1}, \quad \tilde{\Psi}_n = \frac{1}{M_B},$$

$$\Pi_n = \frac{2\tilde{c}GJ}{I_B\left(cE\Gamma\beta + \tilde{c}GJ\right)}, \quad \Upsilon_n = \frac{cE\Gamma\beta - \tilde{c}GJ}{cE\Gamma\beta + \tilde{c}GJ}, \quad \Psi_n = \frac{\tilde{c}GJ}{cE\Gamma I_B},$$

where τ is the ratio of the speeds $\tau = \frac{\tilde{c}}{c}$, and U_b and Φ_b are respectively the axial and torsional bit positions, $U_b(t) = U(L,t)$, $\Phi_b(t) = \Phi(L,t)$. For the sake of simplicity, we consider functions F and $\tilde{F}$ of the form : $z \mapsto p\bar{k}\,z/(\bar{k}^2\,z^2 + \zeta)$ where the parameters p, $\bar{k}$, ζ are positive constants related to the sharpness of the top angle of the friction force, satisfying $0 < \zeta \ll 1$ and $0 < \bar{k} < 1$, and the constant p provides the amplitude of the friction force.

Following the ideas introduced in Chapter 8, the qualitative analysis based on the center manifold theorem [47] and normal forms theory [111] is applied to reduce the model to a singularly perturbed system of ordinary differential equations (ODE) by means of a spectral projection.

9.4   Delayed proportional feedback controller

Setting $x = (x_1, x_2, x_3, x_4)^T$, $x_1 = U_b$, $x_2 = \Phi_b$, $x_3 = \dot{U}_b$, $x_4 = \dot{\Phi}_b$, and defining :

$$\begin{aligned} u_H(t) &= p_H\, U_b(t-1) \\ u_T(t) &= p_\Omega\, \Phi_b(t-\tau), \end{aligned} \tag{9.28}$$

the drilling model can be rewritten as :

$$\begin{cases} \dot{x}(t) = D_1\,\dot{x}(t-2) + D_2\,\dot{x}(t-2\tilde{c}/c) + A_0\,x(t) + A_1\,x(t-2) \\ \qquad + A_2\,x(t-2\tilde{c}/c) + \mathcal{F}(x(t), x(t-2), x(t-2\tilde{c}/c)) \end{cases} \tag{9.29}$$

where $\mathcal{F}$ is the nonlinear part of the system (9.26)-(9.27) and the system matrices are defined below,

$$D_1 = \begin{bmatrix} 0_2 & 0_2 \\ 0_2 & \tilde{d}_1 \end{bmatrix}, \quad D_2 = \begin{bmatrix} 0_2 & 0_2 \\ 0_2 & \tilde{d}_2 \end{bmatrix}, \quad A_0 = \begin{bmatrix} 0_2 & I_2 \\ 0_2 & \tilde{a}_0 \end{bmatrix},$$

$$A_1 = \begin{bmatrix} 0_2 & 0_2 \\ \tilde{p}_H & \tilde{a}_1 \end{bmatrix}, \quad A_2 = \begin{bmatrix} 0_2 & 0_2 \\ \tilde{p}_\Omega & \tilde{a}_2 \end{bmatrix}$$

where 0_2 and I_2 are the zero and the identity 2×2 matrices, and

$$\tilde{d}_1 = \begin{bmatrix} \tilde{\Upsilon}_n & 0 \\ 0 & 0 \end{bmatrix}, \quad \tilde{d}_2 = \begin{bmatrix} 0 & 0 \\ 0 & \Upsilon_n \end{bmatrix}, \quad \tilde{p}_H = \begin{bmatrix} p_H & 0 \\ 0 & 0 \end{bmatrix}, \quad \tilde{p}_\Omega = \begin{bmatrix} 0 & 0 \\ 0 & p_\Omega \end{bmatrix},$$

$$\tilde{a}_0 = \begin{bmatrix} -\frac{\tilde{\Psi}_n(p\bar{k}+\zeta)}{\zeta} & 0 \\ \frac{p\bar{k}}{J\zeta} & -\Psi_n \end{bmatrix}, \quad \tilde{a}_1 = \begin{bmatrix} -\frac{\tilde{\Upsilon}_n\tilde{\Psi}_n(p\bar{k}+\zeta)}{\zeta} & 0 \\ 0 & 0 \end{bmatrix}, \quad \tilde{a}_2 = \begin{bmatrix} 0 & 0 \\ -\frac{\Upsilon_n p\bar{k}}{\zeta I_B} & -\Upsilon_n\Psi_n \end{bmatrix}.$$

Setting the numerical values of the physical parameters given in Table of Appendix 8.5, the following proposition is established.

Proposition 6. *The following properties are established for system (9.29), depending on the values of the gains p_H and p_Ω in (9.28).*
For $p_\Omega = p_H = 0$:
— *Zero is the only eigenvalue with zero real part and the remaining eigenvalues are with negative real parts. Moreover, zero is an eigenvalue of algebraic multiplicity 2 and of geometric multiplicity 1, that is, the zero eigenvalue is non-semisimple and the singularity is of Bogdanov-Takens-type, see [111].*
— *The system (9.29) is formally stable but not asymptotically stable (although there are no characteristic roots with positive real parts).*
For $p_H = -24\delta\, r$ and $p_\Omega = \frac{45\mu r^2}{10}$ for a small enough r :
— *The dynamics of (9.29) are reduced on a cubic center manifold to*

$$\begin{cases} \dot{z}_1 = z_2 \\ \dot{z}_2 = \delta z_1 + \mu z_2 - 3z_2 z_1^2 \end{cases} \tag{9.30}$$

for which the function

$$I(z) = \frac{1}{2} z_1^2 - \frac{1}{2}\frac{z_2^2}{\delta} - \frac{1}{2}\delta z_1^2 z_2^2 + \frac{1}{4}\delta^2 z_1^4 + \frac{1}{4}z_2^4$$

is a Lyapunov function. For $\delta < 0$ and $\mu < 0$, the system is globally asymptotically stable.

Remark 9. When the quasipolynomial function corresponding to a neutral functional equation has no root on the imaginary axis, then one can use the delay-dependent stability criteria based on the definite integral stability method (originated from the Argument Principle) proposed in [220].

Sketch of the proof : The first assertion is obtained by establishing a linear analysis of the system. Indeed, it can be easily verified by computing the associated characteristic equation and substituting the physical values. Numerical tools as the *Quasi-Polynomial Mapping Based Rootfinder QPMR* [215] are useful for locating the spectral values.

Next, we address the second part of the proposition concerning the nonlinear analysis. Following the approach described in [114], which considers a singular delay system linearly dependent on one parameter, and in the same spirit of the decomposition established in [92], with the goal of computing the normal form of delay systems, we extend the scheme of computing the center manifold to the case of NDDE. System (9.29) is regarded as a perturbation of

$$\frac{d}{dt}\mathcal{D}\, x_t = \mathcal{L}_0\, x_t, \quad \text{where} \quad \mathcal{L}_0 = \mathcal{L}|_{\{p_H=0,\, p_\Omega=0\}}, \tag{9.31}$$

Indeed, system (9.29) can be written as

$$\begin{aligned}
\frac{d}{dt}\mathcal{D}\, x_t :&= \mathcal{L}_0\, x_t + \tilde{\mathcal{F}}(x_t) \\
&= \mathcal{L}_0\, x_t + (\mathcal{L} - \mathcal{L}_0)\, x_t + \mathcal{F}(x_t),
\end{aligned} \tag{9.32}$$

such that

$$\mathcal{F}_{\mu,p} = \begin{bmatrix} -0.0405\, x_1^3(t) + 0.0377\, x_3^3(t-2) + p_H\, x_1(t-2) \\ -1.875\, p x_1^3(t) + 1.874998\, p x_1^3(t-1.264911064) \end{bmatrix}.$$

Next, following the theoretical schemes presented in [152], the computations steps for obtaining the evolution equation of system's (9.31) solutions on the center manifold are given.
First, we compute the basis of the generalized eigenspace corresponding to the double eigenvalue $\lambda_0 = 0$.

$$\Phi(\theta)^T = \begin{bmatrix} 1+\theta & 1+2\,\theta & 1 & 2 \\ 1 & 2 & 0 & 0 \end{bmatrix},$$

where $\theta \in [-2, 0]$. Recall that the adjoint linear equation associated to (9.29) is

$$\begin{cases} \dot{u}(t) = D_1 \dot{u}(t+2) + D_2 \dot{u}(t + 2\tilde{c}/c) \\ \qquad - A_0 u(t) - A_1 u(t+2) - A_2 u(t + 2\tilde{c}/c). \end{cases} \tag{9.33}$$

A basis for the generalized eigenspace associated to the double eigenvalue zero can be defined as

$$\Psi(\theta) = \begin{bmatrix} -1 & -3 & -7 & -13 \\ \xi+1 & 3\,\xi+2 & 7\,\xi+3 & 13\,\xi+4 \end{bmatrix}.$$

Let us consider the bilinear form, see [115]

$$
\begin{aligned}
(\psi, \varphi) =& \psi(0)(\varphi(0) - D_1\varphi(-2) - D_2\varphi(-1.264911)) \\
& + \int_{-2}^{0} \psi(\xi + 2)A_1\varphi(\xi)d\xi \\
& + \int_{-1.264911}^{0} \psi(\xi + 1.264911)A_2\varphi(\xi)d\xi \\
& - \int_{-2}^{0} \psi'(\xi + 2)D_1\varphi(\xi)d\xi \\
& - \int_{-1.264911}^{0} \psi'(\xi + 1.264911)D_2\varphi(\xi)d\xi.
\end{aligned}
\tag{9.34}
$$

By using (9.34), we can easily normalize Ψ such that $(\Psi, \Phi) = I_d$, thus the space C can be decomposed as $C = P \bigoplus Q$, where $P = \{\varphi = \Phi z; \; z \in \mathbb{R}^2\}$ and $Q = \{\varphi \in C; \; (\Psi, \varphi) = 0\}$. Recall that each of these subspaces is invariant under the semigroup $T(t)$ and that the matrix B (concerned by the theoretical settings), satisfying $\mathcal{A}\Phi = \Phi B$, is given by

$$
B = \begin{bmatrix} 0 & 0 \\ 1 & 0 \end{bmatrix}.
\tag{9.35}
$$

Let us first set the following decomposition $x_t = \Phi y(t) + z(t)$, where $z(t) \in Q$, $y(t) \in \mathbb{R}^2$, $z(t) = h(y(t))$ and h is some analytic function $h : P \to Q$. Following [152], the explicit solution on the center manifold is given by

$$
\dot{y}(t) = By(t) + \Psi(0)\mathcal{F}[\Phi(\theta)y(t) + h(\theta, y(t))],
\tag{9.36}
$$

$$
\frac{\partial h}{dy}\{By + \Psi(0)\mathcal{F}[\Phi(\theta)y + h]\} + \Phi(\theta)\Psi(0)\mathcal{F}[\Phi(\theta)y + h]
$$
$$
= \begin{cases} \dfrac{\partial h}{d\theta}, & -2 \leqslant \theta \leqslant 0, \\ \mathcal{L}(h(\theta, y)) + \mathcal{F}[\Phi(\theta)y + h(\theta, y)], & \theta = 0, \end{cases}
\tag{9.37}
$$

where $h = h(\theta, y)$ and $\tilde{\mathcal{F}}$ is defined in (9.32).

Since our aim is to establish the parameter values of p_H and p_Ω guaranteeing an asymptotic suppression of the vibrations after some fixed time t_0, we investigate the parameter bifurcations. The computation of the evolution equation on the center manifold of the solutions of system (9.32) is required.

The next step consists in introducing a small scaling parameter r in order to zoom the neighborhood of the singularity. Consider the following change of coordinates :

$$
p_H = -24\delta\, r, \quad p_\Omega = \frac{45\mu r^2}{10}, \quad y_1 = rz_1, \quad y_2 = r^2 z_2.
$$

A time scaling defined by $t_{old} = r\, t_{new}$, leads to the following cubic normal form reduction of (9.29),

$$
\begin{cases} \dot{z}_1 = z_2, \\ \dot{z}_2 = \delta z_1 + \mu z_2 - z_1^3, \end{cases}
$$

for which a normal form is given by (9.30).

If μ is a positive function beyond $(0,0)$ and $\delta < 0$, then,

$$\dot{I}(z_1, z_2) = -\frac{z_2{}^2\mu}{\delta} + 3\,\frac{z_2{}^2 z_1{}^2}{\delta} - \delta\,z_1{}^2 z_2{}^2\mu + 3\,\delta\,z_1{}^4 z_2{}^2 + z_2{}^4\mu - 3\,z_2{}^4 z_1{}^2$$

which is always negative. Thus the system is globally asymptotically stable and the undesired vibrations are suppressed. The proposed scheme offset the computation of a Lyapunov function for a system of PDE with nonlinear boundary conditions.
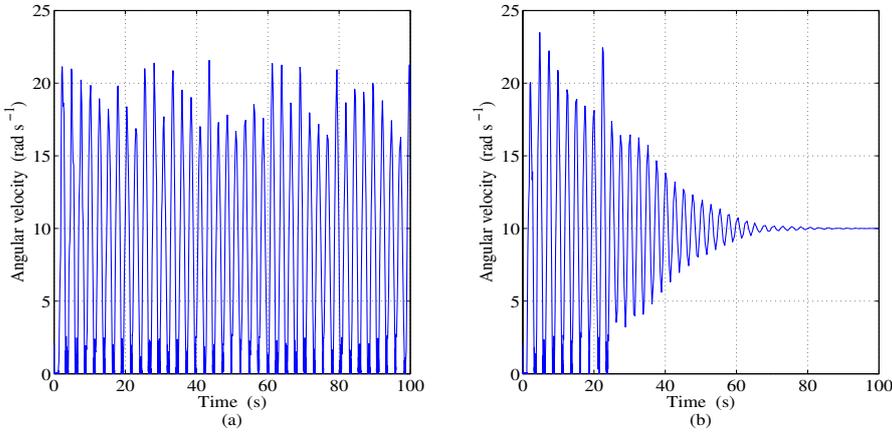
FIGURE 9.8 – Simulation of the coupled torsional-axial model (9.26)-(9.27). Angular velocity at the bottom extremity for a reference velocity of 10rad s^{-1}. (a) Trajectory without control actions (stick-slip). (b) Reduction of stick-slip oscillations by means of the delayed feedback controllers (9.38)-(9.39).

Figures 9.8 and 9.9 show a substantial reduction of drilling vibrations through the delayed feedback controllers :

$$u_H(t) = -24\delta r U_b(t - 1) \tag{9.38}$$

$$u_T(t) = 4.5\mu r^2 \Phi_b(t - \tau) \tag{9.39}$$

for $r = 0.1$, $\delta = -1000$ and $\mu = -10$.

9.5   Delayed PID controller

Setting $x = (x_1, x_2, x_3, x_4, x_5, x_6)^T$, $x_3 = U_b$, $x_4 = \Phi_b$, $x_5 = \dot{U}_b$, $x_6 = \dot{\Phi}_b$, $x_1 = \int_0^t x_3(s)\,ds$ and $x_2 = \int_0^t x_4(s)\,ds$ and considering :

$$\begin{aligned}
u_H(t) &= H_p\,U_b(t - 1) + H_d\,\dot{U}_b(t - 1)\\
u_T(t) &= \Omega_p\Phi_b(t - \tau) + \Omega_i \int_0^{t-\tau} \Phi_b(s)ds,
\end{aligned} \tag{9.40}$$
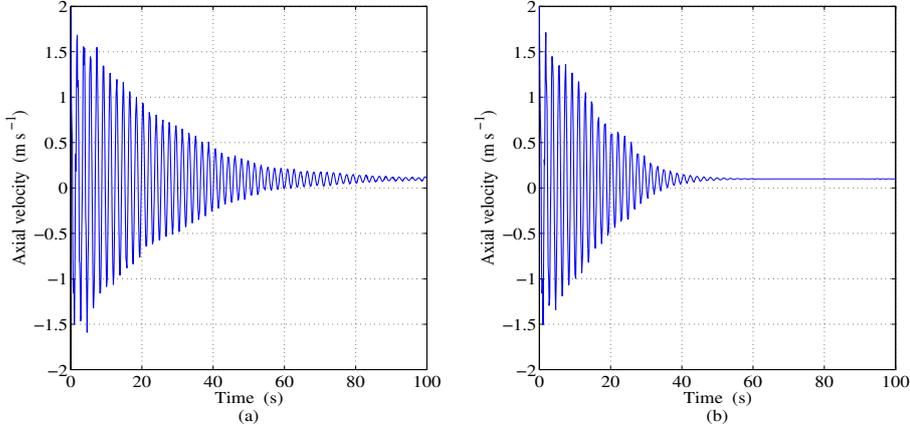
FIGURE 9.9 – Simulation of the coupled torsional-axial model (9.26)-(9.27). Axial velocity at the bottom extremity for a reference velocity of 0.1m s^{-1}. (a) Trajectory without control actions (bit-bounce). (b) Reduction of bit-bounce oscillations by means of the delayed feedback controllers (9.38)-(9.39).

the matrix representation of the system is given by :

$$
\begin{cases}
\dot{x}(t) = \hat{D}_1\,\dot{x}(t-2) + \hat{D}_2\,\dot{x}(t - 2\tilde{c}/c) + \hat{A}_0\,x(t) + \hat{A}_1\,x(t-2) \\
\qquad + \hat{A}_2\,x(t - 2\tilde{c}/c) + \mathcal{F}(x(t), x(t-2), x(t - 2\tilde{c}/c))
\end{cases}
\tag{9.41}
$$

where $\mathcal{F}$ is the nonlinear part of the system (9.26)-(9.27) and the system matrices are defined below,

$$
\hat{D}_1 = \begin{bmatrix} 0_{4\times4} & 0_{4\times2} \\ 0_{2\times4} & \tilde{d}_1 \end{bmatrix}, \quad
\hat{D}_2 = \begin{bmatrix} 0_{4\times4} & 0_{4\times2} \\ 0_{2\times4} & \tilde{d}_2 \end{bmatrix}, \quad
\hat{A}_0 = \begin{bmatrix} 0_2 & I_2 & 0_2 \\ 0_2 & 0_2 & I_2 \\ \tilde{\Omega}_i & \tilde{H}_p & \tilde{a}_0 + \tilde{H}_d \end{bmatrix},
$$

$$
\hat{A}_1 = \begin{bmatrix} 0_{4\times4} & 0_{4\times2} \\ 0_{2\times4} & \tilde{a}_1 \end{bmatrix}, \quad
\hat{A}_2 = \begin{bmatrix} 0_{4\times4} & 0_{4\times2} \\ 0_{2\times4} & \tilde{a}_2 \end{bmatrix},
$$

where $0_{m\times n}$ is the zero matrix of $m \times n$ dimension, and

$$
\tilde{\Omega}_i = \begin{bmatrix} 0 & 0 \\ 0 & \Omega_i \end{bmatrix}, \quad
\tilde{H}_p = \begin{bmatrix} H_p & 0 \\ 0 & \Omega_p \end{bmatrix}, \quad
\tilde{H}_d = \begin{bmatrix} H_d & 0 \\ 0 & 0 \end{bmatrix}.
$$

Proposition 7. *The following properties are established for system (9.41), depending on the values of the gains H_p, H_d, Ω_p and Ω_i in (9.40).*
For $\Omega_p = \Omega_i = H_p = H_d = 0$:
— *Zero is the only eigenvalue with zero real part and the remaining eigenvalues have negative real parts. Moreover, zero is an eigenvalue of algebraic multiplicity 4 and of geometric multiplicity 1, i.e., there is a generalized Bogdanov-Takens singularity, see [111].*

— *The system* (9.41) *is formally stable but not asymptotically stable (although there are no characteristic roots with positive real parts).*

For $H_d = 13.27\,r^{11}\delta_3$, $H_p = 26.55\,r^{12}\delta_2$, $\Omega_i = -11.47\,r^{13}\delta_1$, $\Omega_p = 11.47\,r^{10}\delta_4$ *and a small parameter* r :

— *The dynamics of* (9.41) *reduces on a degree 15 center manifold to*

$$\begin{cases} \dot{z}_1 = z_2,\ \dot{z}_2 = z_3,\ \dot{z}_3 = z_4 \\ \dot{z}_4 = \delta_1 z_1 + \delta_2 z_2 + \delta_3 z_3 + \delta_4 z_4 - z_4^3 \end{cases} \tag{9.42}$$

for which the linear part is written as a companion matrix :

$$A = \begin{bmatrix} 0 & 1 & 0 & 0 \\ 0 & 0 & 1 & 0 \\ 0 & 0 & 0 & 1 \\ \delta_1 & \delta_2 & \delta_3 & \delta_4 \end{bmatrix}$$

thus there exist values for δ_1, δ_2, δ_3, *and* δ_4 *such that* A *is Hurwitz, which guaranteeing local asymptotic stability.*

Sketch of the proof : Similar to the case of the delayed feedback controller, the spectral projection methodology is applied. The singularity here is zero with algebraic multiplicity 4 and geometric multiplicity 1. A basis for the generalized eigenspace $\mathcal{M}_0$ can be defined by

$$\Phi(\theta) = \begin{bmatrix} \frac{1}{6}\theta^3 + \theta^2 + \theta - 1 & \frac{1}{2}\theta^2 + 2\theta + 1 & \theta + 2 & 1 \\ -\frac{1}{6}\theta^3 + \frac{1}{2}\theta^2 - \theta + 2 & -\frac{1}{2}\theta^2 + \theta - 1 & -\theta + 1 & -1 \\ \theta^2 + \theta & 2\theta + 1 & 2 & 0 \\ \theta + 1 & 1 & 0 & 0 \\ 4\theta & 4 & 0 & 0 \\ 1 & 0 & 0 & 0 \end{bmatrix}.$$

The matrix B, satisfying $\mathcal{A}\Phi = B\Phi$, is given by

$$B = \begin{bmatrix} 0 & 1 & 0 & 0 \\ 0 & 0 & 1 & 0 \\ 0 & 0 & 0 & 1 \\ 0 & 0 & 0 & 0 \end{bmatrix}.$$

A basis Ψ of the adjoint space satisfying $(\Psi, \Phi) = I_d$, evaluated at zero is given

by :

$$\Psi(0) = \begin{bmatrix} -0.00082 & -0.00082 & 0.00124 & 0.12511 & 0.01883 & 0.08717 \\ 0.01066 & 0.01066 & -0.016 & -0.14123 & -0.00384 & -0.17785 \\ 0.33261 & 0.33261 & 0.00107 & -0.69201 & -0.7673 & -0.28423 \\ 0.25042 & -0.74957 & 0.12435 & 3.20018 & 0.52271 & 2.56715 \end{bmatrix}$$

The change of coordinates given in the second assertion of Proposition 6 leads to the reduced system (9.42).

Figure 9.10 shows the performance of the delayed PID feedback controllers :

$$u_H(t) = 26.55 \, r^{12}\delta_2 \, U_b(t-1) + 13.27 \, r^{11}\delta_3 \, \dot{U}_b(t-1) \tag{9.43}$$

$$u_T(t) = 11.47 \, r^{10}\delta_4\Phi_b(t-\tau) - 11.47 \, r^{13}\delta_1 \int_0^{t-\tau} \Phi_b(s)ds \tag{9.44}$$

for $r^{10} = 1$, $r^{11} = 0.0001$, $r^{12} = 10$, $r^{13} = 1$, $\delta_1 = -10$, $\delta_2 = -100$, $\delta_3 = -24$ and $\delta_4 = -10$.
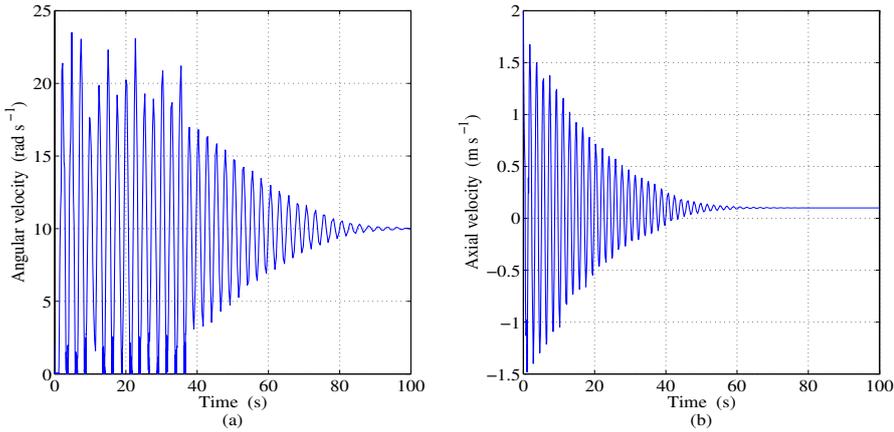
FIGURE 9.10 – Simulation of the coupled axial-torsional model (9.26)-(9.27). Reduction of stick-slip and bit-bounce oscillations by means of the delayed PID feedback controllers (9.43)-(9.44). (a) Angular velocity at the bottom extremity $\dot{\Phi}_b(t)$ for a reference velocity of 10rad s^{-1}. (b) Axial velocity at the bottom extremity $\dot{U}_b(t)$ for a reference velocity of 0.1m s^{-1}.

9.6 Notes and references

The torsional rectification method reviewed in this chapter is based on the identification of both "up" and "down" moving components of the general solution of the wave equation describing torsional drillstring vibrations. A similar approach is proposed in [133] ; the suggested method allows reducing torsional vibrations by exactly

decomposing the drill string dynamics into two traveling waves : those traveling in the direction of the top extremity and those traveling in the direction of the bit. The decomposition is achieved with two sensors that can be placed at the top drive and at a short distance below the top drive. The velocity of the top drive is controlled in order to absorb the wave traveling in the direction of the top drive, thus achieving a reflection coefficient of zero for the frequency range of the undesired torsional vibrations. The performance of the control algorithm was evaluated through a small-scale experimental setup.

The design of low-order controllers presented in Section 9.3 was conducted by an analytic treatment of the NFDE describing the coupled axial-torsional drilling dynamics. Via spectral projection, a finite-dimensional approximation of the PDE model allowing preserving essential dynamics of the original system is obtained ; then, the Lyapunov function guaranteeing the global stability of the reduced model ensures the local stability of the infinite-dimensional system. The model transformation procedure is explained in detail in [36].

Drilling system analysis led to the identification of a local bifurcation of Bogdanov-Takens type (double zero eigenvalues) which has not been studied for NDDE, except for [36], where an analytical study of the uncontrolled drilling vibrations is developed. A similar analysis approach is presented in [114], where a physiological system described by a DDE with double-zero eigenvalue singularity is investigated. In [218], explicit conditions for a Hopf bifurcation to occur are derived ; using center manifold reduction and normal form theory the stability coefficient of the periodic orbit on the center manifold is explicitly determined.

There are some computational techniques to determine center manifolds. For instance, [11] presents an algorithm to establish the center manifold of a neutral functional differential equation ; Bogdanov-Takens and Hopf singularities are considered. In [152], an overview on the theoretical settings for calculating center manifolds is provided ; furthermore, it is shown how the computations may be implemented in the symbolic algebra package *Maple*.

So far we have studied some simple control techniques that help reducing unwanted drilling oscillations. It has been shown that its performance is acceptable, however, it is natural to think that more sophisticated control methods could produce better results. The following chapter concerns the design of a control strategy that exploits an intrinsic characteristic of the system : its flatness property. As will be seen later, this property is useful to solve trajectory tracking problems ; based on this idea, we design a pair of controllers aimed at steering the system trajectories to prescribed paths, achieving in this way the elimination of axial and torsional vibrations.

Characterizing the Codimension of Zero Singularities for Time-Delay Systems : A Link with Vandermonde and Birkhoff incidence Matrices

The analysis of time-delay systems mainly relies on detecting and understanding the spectral values bifurcations when crossing the imaginary axis. This chapter deals with the zero singularity, essentially when the zero spectral value is multiple. The simplest case in such a configuration is characterized by an algebraic multiplicity two and a geometric multiplicity one, known as the Bogdanov-Takens singularity. Moreover, in some cases the codimension of the zero spectral value exceeds the number of the coupled scalar-differential equations. Nevertheless, to the best of our knowledge, the bounds of such a multiplicity have not been deeply investigated in the literature. It is worth mentioning that the knowledge of such an information is crucial for nonlinear analysis purposes since the dimension of the projected state on the center manifold is none other than the sum of the dimensions of the generalized eigenspaces associated with spectral values with zero real parts. Motivated by control-oriented problems, this paper provides an answer to this question for time-delay systems, taking into account the parameters' algebraic constraints that may occur in applications. We emphasize the link between such a problem and the incidence matrices associated with the Birkhoff interpolation problem. In this context, symbolic algorithms are also proposed for LU-factorization for functional confluent Vandermonde as well as some classes of bivariate functional Birkhoff matrices.

Some of the results proposed in this work have been presented in The 13th European Control Conference, June 24-27, 2014, Strasbourg, France [31] and The 21st International Symposium on Mathematical Theory of Networks and Systems July 7-11, 2014, Groningen, The Netherlands [39]. This chapter reproduces the results of an extended version [40] which is not yet available online, the proofs are then presented in the manuscript.

10.1   Introduction

Matrices arising from a wide range of problems in mathematics and engineering typically display a characteristic structure. Exploiting such a structure is the means to the design of efficient algorithms, see for instance [22]. This study is a crossroad between the investigation of a class of such structured matrices originally involved in *Multivariate Interpolation Problems* (namely, the well-known *Birkhoff Interpolation Problem*) and the estimation of the upper bound for the codimension of *spectral values* of linear *Time-Delay Systems* (TDS) (which are the zeros of some characteristic entire function called *characteristic quasipolynomial*). The aim of this paper is three fold : firstly, it emphasizes the link between the above two quoted issues. Secondly, it shows that the codimension of the zero spectral value of a given TDS is characterized by some algebraic properties of an appropriate *functional Birkhoff Matrix*. Finally, it shows the effectiveness of the proposed constructive approach by exploring the generic settings as well as investigating some specific but significant sparsity patterns. In both cases, symbolic algorithms for LU-factorization are established for some novel classes of Birkhoff matrices. It is worth mentioning that such an attempt can be exploited for further classes of Birkhoff matrices and should be of interest in some linear algebra problems involving structured matrices as well as in applications including polynomial interpolation.

The class of systems considered throughout this paper is infinite-dimensional with N discrete (constant) delays. Let $z = (z_1, \ldots, z_n) \in \mathbb{R}^n$ denote the state-vector, then the system reads as follows

$$\dot{z} = \sum_{k=0}^{N} A_k z(t - \tau_k), \tag{10.1}$$

under appropriate initial conditions belonging to the Banach space of continuous functions $\mathcal{C}([-\tau_N, 0], \mathbb{R}^n)$. Here τ_k, $k = 1 \ldots N$ are strictly increasing positive constant delays such that $\tau_0 = 0$ and $\tau = (\tau_1, \ldots, \tau_N)$, and $A_k \in \mathcal{M}_n(\mathbb{R})$ for $k = 0 \ldots N$. It is well known that the exponential stability of the solutions of (12.1) is derived by the location of the spectrum χ, where χ designates the set of roots of the *characteristic function* [75, 20]. Notice that such a function, denoted in the sequel $\Delta(\lambda, \tau)$, is transcendental in the Laplace variable λ. Such a spectrum χ can be split as $\chi = \chi_+ \cup \chi_0 \cup \chi_-$ where $\chi_+ = \{\lambda \in \mathbb{C}, \ \Delta(\lambda, \tau) = 0, \ \Re(\lambda) > 0\}$, $\chi_- = \{\lambda \in \mathbb{C}, \ \Delta(\lambda, \tau) = 0, \ \Re(\lambda) < 0\}$ and $\chi_0 = \{\lambda \in \mathbb{C}, \ \Delta(\lambda, \tau) = 0, \ \Re(\lambda) = 0\}$. More precisely, the characteristic function of system (12.1) $\Delta : \mathbb{C} \times \mathbb{R}^N_+ \to \mathbb{C}$ which reads as

$$\Delta(\lambda, \tau) = \det \left(\lambda I - A_0 - \sum_{k=1}^{N} A_k e^{-\tau_k \lambda} \right), \tag{10.2}$$

One can prove that the quasipolynomial function (12.2) admits an infinite number of zeros, see for instance the references [20, 4, 136]. The study of zeros of an entire function [136] of the form (12.2) plays a crucial role in the analysis of asymptotic stability of the zero solution of some given system (12.1). Indeed, the zero solution

is asymptotically stable if all the zeros of (12.2) are in the open left-half complex plane [151]. Accordingly to this observation, the parameter space which is spanned by the coefficients of the polynomials P_i, can be split into domains, each of them with a constant number of right half-plane characteristic roots (which is nothing but the so-called D-decomposition, see for instance [151, 123] and references therein). These domains are separated by a boundary corresponding to the case when at least one characteristic root belongs to the spectrum. In the stability analysis of TDS, we are particularly interested by the stability domains (all characteristic roots with strictly negative real parts) as well as their boundary. Moreover, under appropriate algebraic restrictions, a given root associated to such a boundary may have high codimension. In this paper, we are concerned with the codimension of the zero spectral value. The typical example for non-simple zero spectral value is the Bogdanov-Takens singularity which is characterized by an algebraic multiplicity two and a geometric multiplicity one. Cases with higher order multiplicities of the zero spectral value are known to us as generalized Bogdanov-Takens singularities. Those types of configurations are not only theoretical and are involved in concrete applications. Indeed, the Bogdanov-Takens singularity is identified in [114] where the case of two coupled scalar delay equations modeling a physiological control problem is studied. In [36] and [146] this type of singularity is also encountered in the study of coupled axial-torsional vibrations of some oilwell rotary drilling system. Moreover, the paper [46] is devoted to the analysis of such type of singularities where codimension two and three are studied, and the associated center manifolds are explicitly computed. It is commonly accepted that the time-delay induces desynchronizing and/or destabilizing effects on the dynamics. However, new theoretical developments in control of finite-dimensional dynamical systems suggest the use of delays in the control laws for stabilization purposes. For instance, [200, 34] are concerned by the stabilization of the inverted pendulum by delayed control laws and provide concrete situations where the codimension of the zero spectral value exceeds the number of the coupled scalar equations modeling the inverted pendulum on cart. In [200], the authors prove that the delayed proportional-derivative (PD) controller stabilizes the inverted pendulum by identifying a codimension three singularity for a system of two coupled delay equations. In [34], the same singularity is characterized by using a particular delay block configuration. It is shown that two delay blocks offset a PD delayed controller.

Although the algebraic multiplicity of each spectral value of a time-delay system is finite (a direct consequence of Rouché Theorem, see [176]), to the best of the author's knowledge, the computation of *the upper bound of the codimension of the zero spectral value* did not receive a complete characterization especially in the case when the physical parameters of a given time-delay model are subject to algebraic constraints. Namely, if the root at the origin is invariant with respect to the delay parameters, however, its multiplicity is strongly dependent on the existing links between the delays and the other parameters of the system.

Furthermore, the knowledge of the codimension of such a spectral value as well as the number of purely imaginary spectral values counting their multiplicities are

valuable information. For instance, such an information allows to estimate the number of unstable roots; **card**(χ_+) where $\chi_+ = \{\lambda \in \mathbb{C},\ \Delta(\lambda, \tau) = 0,\ \Re(\lambda) > 0\}$ for a given time-delay system (12.1). Actually, the main theorem from [119, p. 223], which is reported in the Appendix, emphasizes the link between **card**(χ_+) and **card**(χ_0) (Multiplicity is taken into account). In the light of the quoted result and its potential consequences on designing new approaches for the characterization of the linear stability analysis of time-delay systems, the need of for greater emphasis on the study of the zero singularity and, more generally, the imaginary roots becomes obvious. Finally, it is worth mentioning that such a study is also interesting from a nonlinear analysis viewpoint, which gives another motivation for the present investigation. When the unstable spectrum is an empty set or equivalently $\chi = \chi_- \cup \chi_0$, a complete knowledge of the imaginary roots as well as their multiplicities becomes crucial predominatingly when the center manifold and the normal forms theory are involved for deriving an accurate local qualitative description of the studied dynamical system, see [111]. In particular, in this case, when the zero spectral value is the only spectral value with zero real part; $\chi_0 = \{0\}$, then the center manifold dimension is none other than the codimension of the generalized Bogdanov-Takens singularity [47, 111, 134].

In the context mentioned above, as a first estimation on the bound for the codimension of the zero spectral value for quasipolynomial functions, we emphasize the Pólya-Szegö bound [176, pp. 144], which will be denoted $\sharp_{PS}$ in the sequel. The proof of such a result is based on the Rouché Theorem and Cauchy's argument principle. Recall that $\sharp_{PS}$ bound is nothing but the degree of the considered quasipolynomial function, see also [219] for a modern formulation of the mentioned result. Originally, the Pólya-Szegö result, which is reported in the Appendix, gives a bound for the number of roots of a quasipolynomial function in a horizontal strip $\alpha \leq \mathcal{I}(z) \leq \beta$. Setting $\alpha = \beta = 0$ provides a bound for the number of real spectral values, which is a natural bound for the multiplicity of the zero spectral value. It will be stressed in the sequel that the Pólya-Szegö bound is a sharp bound for the zero spectral value multiplicity in the case of quasipolynomial functions consisting in the so-called *complete* or *dense* polynomials. Nevertheless, it is obvious that the Pólya-Szegö bound remains unchanged when certain coefficients $c_{i,j}$ vanish without affecting the degree of the quasipolynomial function. Such a simple remark allows us claiming that Pólya-Szegö bound does not take into account the algebraic constraints on the parameters. However, such constraints appear naturally in applications. In fact, models issued from applications often consist in *lacunary* ou *sparse* structures [144], illustrative examples will be given in the next section concerned by motivations. Moreover, when one needs conditions insuring a given multiplicity bounded by $\sharp_{PS}$, then computations of the successive differentiations of the quasipolynomial have to be made.

In the sequel, among others, we emphasize a systematic approach allowing to a sharper bound for the zero spectral value multiplicity. Indeed, the proposed approach does not only take into account the algebraic constraints on the coefficients $c_{i,j}$ but it also gives appropriate conditions guaranteeing any admissible multiplicity.

Furthermore, the symbolic approach we adopt in this study underlines the connection between the codimension of the zero singularity problem and *incidence matrices* of the so-called *Confluent Vandermonde Matrix* as well as the *Birkhoff Matrix*, see for instance [23, 102, 103, 106]. To the best of the author's knowledge, the first time the Vandermonde matrix appears in a control problem is reported in [126, p. 121], where the controllability of a finite dimensional dynamical system is guaranteed by the invertibility of such a matrix, see also [113]. Next, in the context of time-delay systems, the use of the standard Vandermonde matrix properties was proposed by [166, 151] when controlling one chain of integrators by delay blocks. Here we further exploit the algebraic properties of such matrices into a different context.

The remaining paper is organized as follows. Section 2 presents some prerequisites and the problem statement. It is concluded by a more focused description of the paper objectives and contributions. Section 3 exhibits some motivating examples including some illustrations of the limitations of the Pólya-Szegö bound $\sharp_{PS}$. Next, the main results are proposed and proved in Section 4 and Section 5. Namely, Section 4 provides some symbolic algorithms for the LU-factorisation associated to some classes of *functional Birkhoff Matrices*. Then, the results of the later section are exploited in Section 5 which provides an adaptive bound for the multiplicity of the zero spectral value for quasipolynomial functions. Various illustrative examples and control-oriented discussions are presented in Section 6. Finally, some concluding remarks end the paper.

10.2   Prerequisites and statement of the problem

Let us start by setting a new parametrization for the quasipolynomial function (12.2) characterizing the time-delay system (12.1) and defining some useful notations adopted through the paper.

Some straightforward computations give the following formal expression of the quasipolynomial function (12.2)

$$\Delta(\lambda, \sigma) = P_0(\lambda) + \sum_{M^k \in S_{N,n}} P_{M^k}(\lambda)\, e^{\sigma_{M^k}\, \lambda}, \tag{10.3}$$

where $\sigma_{M^k} = -M^k \tau^T$ and $S_{N,n}$ is the set of all the possible row vectors $M^k = (M_1^k, \ldots, M_N^k)$ belonging to $\mathbb{N}^N$ such that $1 \le M_1^k + \ldots + M_N^k \le n$. Furthermore, by running the index from 1 to the cardinality $\tilde{N}_{N,n} \triangleq \mathbf{card}(S_{N,n})$ the quasipolynomial (10.3) is written in the following compact form

$$\Delta(\lambda, \sigma) = P_0(\lambda) + \sum_{k=1}^{\tilde{N}_{N,n}} P_k(\lambda)\, e^{\sigma_k\, \lambda}. \tag{10.4}$$

For instance,

$$S_{3,2} = \{(1,0,0),\ (0,1,0),\ (0,0,1),\ (2,0,0),\ (1,1,0),\ (1,0,1),\ (0,2,0),$$
$$(0,1,1),\ (0,0,2)\},$$

is ordered first by increasing sums $(\sum_{i=1}^{N} M_i^k)$ then by lexicographical order. In this case one has :

$$M^2 = (0, 1, 0) \quad \text{and} \quad \tilde{N}_{3,2} = 9.$$

A generical property of retarded systems (12.1) allow considering P_0 as a monic polynomial of degree n in λ and the polynomials P_{M^k} satisfying $\deg(P_{M^k}) = n - \sum_{s=1}^{N} M_s^k \leq (n-1) \ \forall M^k \in S_{N,n}$. In the sequel, $P_0(\lambda)$ will be called the *delay-free polynomial* and the quasipolynomial function $\sum_{k=1}^{\tilde{N}_{N,n}} P_{M^k}(\lambda) \, e^{\sigma_k \lambda}$ will be called the *transcendental part of the quasipolynomial.*

Next, let define $a_{j,k}$ as the coefficient of the monomial λ^k for the polynomial P_{M^j}, $1 \leq j \leq \tilde{N}_{N,n}$, and denote $P_{M^0} = P_0$. Thus, $a_{0,n} = 1$ and $a_{j,k} = 0 \ \forall k \geq d_j = n - \sum_{s=1}^{N} M_s^j$, here $d_j - 1$ is nothing but the degree of P_{M^j}. Furthermore, the following notations are adopted : $a_0 = (a_{0,0}, a_{0,1}, \ldots, a_{0,n-1})^T$ is the vector of the coefficients of the delay-free polynomial and $a_j = (a_{j,0}, a_{j,1}, \ldots, a_{j,d_j-1})^T$ is the vector of the coefficients of the polynomial associated to the auxiliary delay σ_j for $1 \leq j \leq \tilde{N}_{N,n}$. Next, set the delay auxiliary vector $\sigma = (\sigma_1, \sigma_2, \ldots, \sigma_{\tilde{N}_{N,n}})$ and $a = (a_1 / a_2 / \ldots / a_{\tilde{N}_{N,n}})^T$ where

$$(x/y) = (x_1, \ldots, x_{d_x}, y_1, \ldots, y_{d_y})^T$$

for $x = (x_1, \ldots, x_{d_x})^T$ and $y = (y_1, \ldots, y_{d_y})^T$. Let us denote by $\Delta^{(k)}(\lambda, \sigma)$ the k-th derivative of $\Delta(\lambda, \sigma)$ with respect to the variable λ. We say that zero is an eigenvalue of algebraic multiplicity/codimension $m \geq 1$ for (12.1) if $\Delta(0, \sigma^*) = \Delta^{(k)}(0, \sigma^*) = 0$ for all $k = 1, \ldots, m-1$ and $\Delta^{(m)}(0, \sigma^*) \neq 0$. We assume also in what follows that $\sigma_k \neq \sigma_{k'}$ for any $k \neq k'$ where $k, k' \in S_{N,n}$. Indeed, if for some value of the delay vector τ there exists some $k \neq k'$ such that $\sigma_k = \sigma_{k'}$, then the number of auxiliary delays and the number of polynomials is reduced by considering a new family of polynomials $\tilde{P}$ satisfying $\tilde{P}_{M^k} = P_{M^k} + P_{M^{k'}}$. In the sequel, D_q will designate *the degree* of the transcendental part of the quasipolynomial. [1]

Now, to characterize the structure of a given quasipolynomial function one needs to introduce a vector $\mathcal{V}$, which will be called in the sequel *incidence vector*, reproducing the data on the vanishing components of the vector "a" defined above. Thus, $\mathcal{V}$ is a sparsity patterns indicator for the transcendental part of the quasipolynomial. To do so, we introduce the symbol "*star*" ($\star$) to indicate the vanishing of a given coefficient of the transcendental part of the quasipolynomial.

To illustrate the notion of "incidence vector" as well as the symbol "*star*", let consider the following quasipolynomial function :

$$\Delta(\lambda, \sigma) = P_0(\lambda) + (a_{1,0,0,0} + a_{1,0,0,1}\lambda) \, e^{\sigma_{1,0,0}\lambda} + a_{0,1,0,2}\lambda^2 \, e^{\sigma_{0,1,0}\lambda} + a_{0,0,1,1}\lambda \, e^{\sigma_{0,0,1}\lambda}.$$
$$(10.5)$$

---

1. The sum of the degrees of the polynomials involved in the quasi-polynomial plus the number of polynomials involved minus one is called the degree of a given quasi-polynomial. Further discussions on such a notion can be found in [219].

According to the above considerations, P_0 is a polynomial with $\deg(P_0) = n \geq 3$. The transcendental part of (10.5), is characterized by the following incidence vector

$$\mathcal{V} = (x_1, x_1, \star, \star, x_2, \star, x_3). \tag{10.6}$$

Namely, the first two components of $\mathcal{V}$ indicate that P_{M^1} is a *complete* polynomial of degree 1, the three components $\star, \star, x_2$, indicate that $a_{0,1,0,0} = a_{0,1,0,1} = 0$ and P_{M^2} is a *lacunary* polynomial of degree 2 and finally, the last components $\star, x_3$ say that $a_{0,0,1,0}$ and P_{M^3} is lacunary polynomial of degree 1.

Let us better formalize the description of the shape of a given incidence vector. As a matter of fact, the above definition, may help in the sequel, for describing the organisation of the distribution of symbol $\star$ in the components of the incidence vector $\mathcal{V}$.

Definition 2. The symbol $\star$ appearing in a given incidence vector $\mathcal{V}$ is classified as follows :

— If the symbol $\star$ (or a sequence of the symbol $\star$) starts a sequence of an interpolating point x_k in the incidence vector $\mathcal{V}$ then we call it a *starter star*.
— If the symbol $\star$ (or a sequence of the symbol $\star$) is strictly included in a sequence of an interpolating point x_k (the symbol $\star$ is not located at the border of a given sequence x_k) in the incidence vector $\mathcal{V}$ it is called an *intermediate star*.
— The length of a sequence of "stars" is the number of the repetition of symbol $\star$ without interruption.

We recognize that the notion of incidence vectors we introduced above is closely inspired from the notion of the *incidence matrices*. Such matrices are known to be involved in defining the structure of the well known *Birkhoff matrices*. Initially, Birkhoff and Vandermonde matrices are derived from the problem of polynomial interpolation of some unknown function g, this can be presented in a general way by describing the interpolation conditions in terms of *incidence matrices*, see for instance [138]. For given integers $n \geq 1$ and $r \geq 0$, the matrix

$$\mathcal{E} = \begin{pmatrix} e_{1,0} & \cdots & e_{1,r} \\ \vdots & & \vdots \\ e_{n,0} & \cdots & e_{n,r} \end{pmatrix}$$

is called an incidence matrix if $e_{i,j} \in \{0, 1\}$ for every i and j. Such a matrix contains the data providing the known information about the function g. Let $x = (x_1, \ldots, x_n) \in \mathbb{R}^n$ such that $x_1 < \ldots < x_n$, the problem of determining a polynomial $\hat{P} \in \mathbb{R}[x]$ with degree less or equal to ι ($\iota + 1 = \sum_{1 \leq i \leq n,\ 1 \leq j \leq r} e_{i,j}$) that interpolates g at $(x, \mathcal{E})$, i.e. which satisfies the conditions :

$$\hat{P}^{(j)}(x_i) = g^{(j)}(x_i),$$

is known as the *Birkhoff interpolation problem*. Recall that $e_{i,j} = 1$ when $g^{(j)}(x_i)$ is known, otherwise $e_{i,j} = 0$. Furthermore, an incidence matrix $\mathcal{E}$ is said to be *poised* if

such a polynomial $\hat{P}$ is unique. This amounts to saying that, if, $n = \sum_{i=1}^{n} \sum_{j=1}^{r} e_{i,j}$ then the coefficients of the interpolating polynomial $\hat{P}$ are solutions of a linear square system with associated square matrix Υ that we call *Birkhoff matrix* in the sequel. This matrix is parametrized in x and is shaped by $\mathcal{E}$. It turns out that the incidence matrix $\mathcal{E}$ is poised if, and only if, the Birkhoff matrix Υ is non singular for all x such that $x_1 < \ldots < x_n$. The characterization of poised incidence matrices is solved for interpolation problems of low degrees. As a matter of fact, the problem is still unsolved for any degree greater than six, see for instance [106, 190].

Remark 10. Unlike Hermite interpolation problem, for which the knowledge of the value of a given order derivative of the interpolating polynomial at a given interpolating point impose the values of all the lower orders derivatives of the interpolating polynomial at that point, the Birkhoff interpolation problem release such a restriction. Thereby justifying the qualification of "lacunary" to describe the Birkhoff interpolation problem.

The analogy between the introduced incidence vector $\mathcal{V}$ for time-delay system analysis purposes and the incidence matrix $\mathcal{E}$ characterizing multivariate interpolation problems can be interpreted as follows. Each $k-$th row of $\mathcal{E}$ indicate the distribution of the symbol $\star$ in the sequence of x_k corresponding to $\mathcal{V}$. Namely, in that row of $\mathcal{E}$, each "1" corresponds to an x_k of $\mathcal{V}$ and each "0" (situated at the left of at least a "1") corresponds to a symbol $\star$ in $\mathcal{V}$.

Proposition 8. *There exists a one to one mapping between $\mathcal{V}$ and $\mathcal{E}$.*

Now, to illustrate the analogy between the two concepts of incidence vector/matrix, let us consider the reduced example from [190] where the incidence matrix $\mathcal{E}$ is given by

$$\mathcal{E} = \begin{pmatrix} 1 & 1 & 0 & 0 \\ 0 & 0 & 1 & 0 \\ 0 & 1 & 0 & 0 \end{pmatrix}. \tag{10.6'}$$

The first row of $\mathcal{E}$ indicates that $g(x_1)$ and $g'(x_1)$ are known. In terms of time-delay systems purposes, this reproduces the first two components of $\mathcal{V}$, namely, x_1, x_1. The second row of $\mathcal{E}$ says that only $g''(x_2)$ is known, which in terms of $\mathcal{V}$, reproduces the components $\star, \star, x_2$. Finally, the third row says that only $g'(x_3)$ is known, which reproduces the last two components $\star, x_3$ of $\mathcal{V}$. This, shows that the incidence matrix (10.6') and the incidence vector (10.6) reproduce exactly the same information. For the sake of saving space, it is more appropriate to consider $\mathcal{V}$ in the sequel. Recall that one associates to (10.6') (or equivalently to (10.6)) the following Birkhoff matrix

$$\Upsilon = \begin{pmatrix} 1 & 0 & 0 & 0 \\ x_1 & 1 & 0 & 1 \\ x_1^2 & 2x_1 & 2 & 2x_3 \\ x_1^3 & 3x_1^2 & 6x_2 & 3x_3^2 \end{pmatrix}.$$

Accordingly, the interpolation problem is solvable if, and only if,

$$12\, x_3\, x_2 + 6\, x_1^2 - 12\, x_2\, x_1 - 6\, x_3^2$$

does not vanish for all values of x such that $x_1 < x_2 < x_3$.

In the spirit of the definition of functional confluent Vandermonde matrices introduced in [113], we provide a definition for functional Birkhoff matrices.

Definition 3. The square *functional Birkhoff matrix* Υ is associated to a sufficiently regular function ϖ and an incidence matrix $\mathcal{E}$ (or equivalently an incidence vector $\mathcal{V}$) and is defined by :

$$\Upsilon = [\Upsilon^1 \, \Upsilon^2 \, \ldots \, \Upsilon^M] \in \mathcal{M}_\delta(\mathbb{R}) \tag{10.7}$$

where

$$\Upsilon^i = [\kappa^{(k_{i_1})}(x_i) \, \kappa^{(k_{i_2})}(x_i) \, \ldots \, \kappa^{(k_{i_{d_i}})}(x_i)] \tag{10.8}$$

such that $k_{i_l} \geq 0$ for all $(i,l) \in \{1,\ldots,M\} \times \{1,\ldots,d_i\}$ and $\sum_{i=1}^M d_i = \delta$ where

$$\kappa(x_i) = \varpi(x_i)[1 \, \ldots \, x_i^{\delta-1}]^T, \quad \text{for} \quad 1 \leq i \leq M. \tag{10.9}$$

Remark 11. In the sequel, for the time-delay systems analysis purposes, we shall be concerned with square functional Birkhoff matrices such that $\varpi(x_i) = x_i^s$, where s is a given positive integer. Furthermore, in terms of the quasipolynomial function (10.4), the degree of the delay-free polynomial P_0 is fixed thanks to the explicit choice of the function $\varpi(x_i) = x_i^s$. More precisely, $n \triangleq s - 1$. Analogously to the Birkhoff interpolation problem, the non degeneracy of such functional Birkhoff matrices will be a fundamental assumption for investigating the codimension of the zero spectral values for time-delay systems.

Remark 12. When $s = 0$, the matrix Υ is nothing but the standard Birkhoff matrix and thus $\varpi(x_i) = 1$. If, in addition, $\mathcal{V}$ does not contain "stars" then we recover the confluent Vandermonde matrix [113]. The particular case $d_i = 1$ for $i = 1 \ldots M$ corresponds to the standard Vandermonde matrix and in this case $M = \delta$ since Υ is assumed to be a square matrix.

The explicit development of numeric/symbolic algorithms for LU-factorization and inversion of the confluent Vandermonde and Birkhoff matrices [149, 186, 169] is still an attracting topic due to their specific structure and their implications in various applications, see, for instance, [126, 121] and references therein. It is worth mentioning that one of the contributions of this paper is to propose an explicit recursive formula for the LU-factorization for several configurations of the functional Birkhoff matrix defined by (10.7)-(10.9). The proposed formulas are in the spirit of the symbolic expressions established in [169] for the standard Vandermonde case. To the best of the author's knowledge, such an explicit formulas seems to be unavailable in the open literature, see e. g., [106, 169]. In fact, the historical note in [169] emphasizes that rather the extensive numerical literature on practical solutions to Vandermonde systems fails to reveal the explicit factorization formula for the LU-factorization as well as to the symbolic inversion of the standard Vandermonde matrix.

The functional Birkhoff matrix configurations we consider are : the first one, no "stars" in the incidence vector $\mathcal{V}$, that is the functional confluent Vandermonde

matrix. Next, the second configuration is when we deal with *starter "stars"*. Finally, an LU-factorization in the case of *successive intermediate "stars"* is established. We claim that, the characterization we present through the paper yields some new possibilities to get formulae in cases combining the two configurations (starter/intermediate "stars"), but, this needs careful inspection of the implicated polynomials and then by adapting the proposed formula to the specific incidence vector $\mathcal{V}$. Since the formulas depend explicitly on the choice of the specific incidence matrix $\mathcal{E}$, then it makes no sense that one goes further in defining some deeper classification. Furthermore, as a byproduct of the approach, we first propose a different proof for the Pólya-Szegö bound $\sharp_{PS}$ of the origin multiplicity deduced from proposition 14 (presented in the appendix), then, we shall establish a sharper bound for such a multiplicity under the non degeneracy condition of an appropriate Birkhoff matrix.

To summarize, the contribution of the present paper is threefold :

1. In the general case, the Birkhoff interpolation problem may or may not have a unique solution. To the best of the author's knowledge, no general pattern for its determinant is known, and thus no general formula for the interpolating polynomial (when it exists) is known. Moreover, it seems that the problem is still unsolved [106, 190] since such a formula depends directly on the chosen incidence matrix among a multitude of configurations. As an attempt, we propose an explicit recursive formula for the LU-factorization of the functional confluent Vandermonde matrix as well as some classes of the functional Birkhoff matrix.

2. We introduce incidence matrices for describing quasipolynomial functions. Then, we identify the existing link between the multiplicity of the zero singularity of time-delay systems (even in the presence of coupling delays) and an appropriate functional Birkhoff matrix, as defined in Definition 3.

3. Finally, in the generic case (all the polynomials $P_{M_k \, k \geq 0}$ are complete), the Pólya-Szegö bound $\sharp_{PS}$ is completely recovered using an alternative Vandermonde-based method. Moreover, when at least one of the polynomials is lacunary [144] (contains a "star" or a sequence of successive "stars"), then under the non degeneracy of an appropriate functional Birkhoff matrix, we establish a bound for the multiplicity of the zero singularity which is sharper than the Pólya-Szegö bound $\sharp_{PS}$.

In order to increase the readability of the paper, the following notations are adopted. Let ξ stand for the real vector composed from x_i counting their repetition d_i through columns of Υ, that is

$$\xi = (\underbrace{x_1, \ldots, x_1}_{d_1}, \ldots, \underbrace{x_M, \ldots, x_M}_{d_M}).$$

For instance, one has $\xi_1 = x_1$ and $\xi_{d_1+d_2+1} = \xi_{d_1+d_2+d_3} = x_3$. Accordingly and setting $d_0 = 0$, without any loss of generality, we have : $\xi_k = \xi_{d_0+\ldots+d_r+\alpha} = \xi_{\sum_{l=0}^{\varrho(k)-1} d_l + \varkappa(k)}$, where $0 \leq r \leq M - 1$ and $\alpha \leq d_{r+1}$; here $\varrho(k)$ denotes the index of the component of x associated with ξ_k, that is $x_{\varrho(k)} = \xi_k$ and by $\varkappa(k)$ the

order of ξ_k in the sequence of ξ composed only by $x_{\varrho(k)}$. Obviously, $\varrho(k) = r + 1$ and $\varkappa(k) = \alpha$.

10.3   Motivating examples and further observations

10.3.1   A Vector Disease Model

Consider first a simple scalar differential equation with one delay representing some biological model discussed by Cooke in [67] describing the dynamics of some disease. Namely, the infected host population $x(t)$ is governed by :

$$\dot{x}(t) + a_0\, x(t) + a_1\, x(t - \tau) - a_1\, x(t - \tau)\, x(t) = 0, \tag{10.10}$$

where $a_1 > 0$ designates the contact rate between infected and uninfected populations and it is assumed that the infection of the host recovery proceeds exponentially at a rate $-a_0 > 0$; see also [192] for more insights on the modeling and stability results. The linearized system is given by

$$\dot{x}(t) + a_0\, x(t) + a_1\, x(t - \tau) = 0, \tag{10.11}$$

with $(a_0, a_1, \tau) \in \mathbb{R}^2 \times \mathbb{R}_+^*$, then the associated characteristic (transcendental) function Δ becomes

$$\Delta(\lambda, \tau) = \lambda + a_0 + a_1\, e^{-\lambda\tau}, \tag{10.12}$$

for which, the corresponding incidence vector is $\mathcal{V} = (x_1)$.

Zero is a spectral value for (10.11) if, and only if, Δ vanishes at zero which is equivalent to $a_0 + a_1 = 0$. Computations of the first derivatives of (10.12) with respect to λ give, using the notation "$\frac{\partial .}{\partial \lambda} = .'$",

$$\begin{aligned}
\Delta'(\lambda, \tau) &= 1 - \tau\, a_1\, e^{-\lambda\tau}, \\
\Delta''(\lambda, \tau) &= \tau^2\, a_1\, e^{-\lambda\tau}.
\end{aligned} \tag{10.13}$$

The vanishing of the two first derivatives allows us to conclude that the codimension of the zero spectral value is at most two (Bogdanov-Takens singularity) since the algebraic multiplicity two is insured by $\tau = 1/a_1$, $a_0 = -a_1$ and $\Delta''(0) \neq 0$ ($\tau \in \mathbb{R}_+^*$). This provides the simplest example showing that the codimension of the zero spectral value can exceed the number of scalar equations defining a given system. Moreover, this emphasizes that the codimension of the zero singularity is less than the number of the free parameters involved in the associated (quasipolynomial) characteristic function. In this case, the number of free parameters is three and the upper bound of the codimension is two, which is exactly the Pólya-Szegö bound $\sharp_{PS}$.

10.3.2   Furuta Pendulum

Consider now the rotary Furuta inverted pendulum, which consists of a driven arm that rotates in the horizontal plane and a pendulum attached to that arm

which is free to rotate in the vertical plane, see figure 10.1. This device has two rotational degrees of freedom and only one actuator and is thus an under-actuated system. Balancing the pendulum in the vertical unstable equilibrium position requires continuous correction by a control mechanism, see [90]. We focus now on the use of multiple delayed proportional gain as suggested by [34] in controlling the inverted pendulum on cart. Using the Lagrange formalism and adopting the *Quanser*
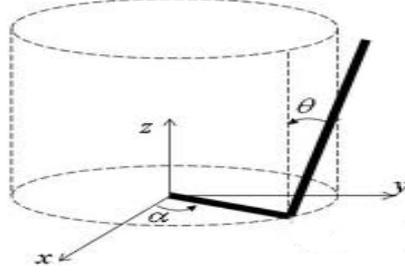
FIGURE 10.1 – Inverted Pendulum on a cart

rotary experiment settings for the physical parameter values [183], we can easily show that the dynamics of the rotary Furuta inverted pendulum in figure 10.1 is governed by the following system of differential equations :

$$\begin{cases} \ddot{\alpha} = -\dfrac{27692}{3} \dfrac{6 \sin(\theta)\dot{\theta}^2 + 265 \cos(\theta)\sin(\theta) - 1806T}{-90601 + 39008 \cos^2(\theta)}, \\ \ddot{\theta} = \dfrac{53}{6} \dfrac{4416 \cos(\theta)\sin(\theta)\dot{\theta}^2 - 1329216 \cos(\theta)T + 453005 \sin(\theta)}{-90601 + 39008 \cos^2(\theta)}, \end{cases}$$

(10.14)

where T is the control law acting on the motor torque. Define

$$\begin{aligned} T(t) = {} & \beta_{1,0}\theta(t) + \gamma_{1,0}\alpha(t) + \beta_{1,1}\theta(t - \tau_1) + \beta_{1,2}\theta(t - \tau_2) \\ & + \gamma_{1,1}\alpha(t - \tau_1) + \gamma_{1,2}\alpha(t - \tau_2). \end{aligned}$$

(10.15)

Recall that it is always possible to normalize one of the delays by a simple scaling of time. Thus, without any loss of generality, $\tau_1 = 1$. With the later remark, when T is defined by (10.15), the linearization around the origin associated with system (10.14) is given by

$$\dot{x} = A_0\,x + A_1\,x(t - 1) + A_2\,x(t - \tau_2),$$

(10.16)

where $A_k = (a_{k,i,j})_{(i,j)\in\{1,\dots,4\}\times\{1,\dots,4\}} \in \mathcal{M}_4(\mathbb{R})$ for $k = 0,\,1,\,2$

$$A_0 = \begin{pmatrix} 0 & 0 & 1 & 0 \\ 0 & 0 & 0 & 1 \\ a_{0,3,1} & a_{0,3,2} & 0 & 0 \\ a_{0,4,1} & a_{0,4,2} & 0 & 0 \end{pmatrix}, \quad A_1 = \begin{pmatrix} 0 & 0 & 0 & 0 \\ 0 & 0 & 0 & 0 \\ a_{1,3,1} & a_{1,3,2} & 0 & 0 \\ a_{1,4,1} & a_{1,4,2} & 0 & 0 \end{pmatrix}, \quad A_2 = \begin{pmatrix} 0 & 0 & 0 & 0 \\ 0 & 0 & 0 & 0 \\ a_{2,3,1} & a_{2,3,2} & 0 & 0 \\ a_{2,4,1} & a_{2,4,2} & 0 & 0 \end{pmatrix}.$$

where

$$a_{0,3,1} = -\frac{16670584}{51593}\gamma_{1,0}, \ a_{0,3,2} = -\frac{16670584}{51593}\beta_{1,0} + \frac{7338380}{154779},$$

$$a_{0,4,1} = \frac{11741408}{51593}\gamma_{1,0}, \ a_{0,4,2} = -\frac{24009265}{309558} + \frac{11741408}{51593}\beta_{1,0},$$

$$a_{1,3,1} = -\frac{16670584}{51593}\gamma_{1,1}, \ a_{1,3,2} = -\frac{16670584}{51593}\beta_{1,1}, \ a_{1,4,1} = \frac{11741408}{51593}\gamma_{1,1},$$

$$a_{1,4,2} = \frac{11741408}{51593}\beta_{1,1}, \ a_{2,3,1} = -\frac{16670584}{51593}\gamma_{1,2}, \ a_{2,3,2} = -\frac{16670584}{51593}\beta_{1,2},$$

$$a_{2,4,1} = \frac{11741408}{51593}\gamma_{1,2}, \ a_{2,4,2} = \frac{11741408}{51593}\beta_{1,2}$$

System (10.16) is characterized by the quasipolynomial function

$$\Delta(\lambda, \tau) = \lambda^4 + \frac{2208852380}{154779}\gamma_{1,0} + \left(\frac{24009265}{309558} - \frac{11741408}{51593}\beta_{1,0} + \frac{16670584}{51593}\gamma_{1,0}\right)\lambda^2$$

$$+ \left((\frac{16670584}{51593}\gamma_{1,1} - \frac{11741408}{51593}\beta_{1,1})\lambda^2 + \frac{2208852380}{154779}\gamma_{1,1}\right)e^{-\lambda}$$

$$+ \left((-\frac{11741408}{51593}\beta_{1,2} + \frac{16670584}{51593}\gamma_{1,2})\lambda^2 + \frac{2208852380}{154779}\gamma_{1,2}\right)e^{-\lambda\tau_2},$$

$$(10.17)$$

for which is associated the incidence vector $\mathcal{V} = (x_1, \star, x_1, x_2, \star, x_2)$. A zero singularity of codimension five is insured by :

$$\beta_{1,0} = \frac{1710742793353}{4582037506368}, \beta_{1,1} = \frac{51593}{2935352}, \beta_{1,2} = -\frac{257965}{10689112}, \ \tau_2 = \frac{72}{265},$$

$$\gamma_{1,0} = \frac{1654329545}{542135726972}, \gamma_{1,1} = \frac{29777931810}{26158048826399}, \ \gamma_{1,2} = -\frac{438397329425}{104632195305596}.$$

$$(10.18)$$

Also, by this example, it is easy to see that, under the delay effect, the codimension of the zero singularity exceeds the dimension of the uncontrolled system (which is free of delays). Moreover, by using the Pólya-Szegö result, one has $\sharp_{PS} = D - 1 = 10$ which is far from the effective sharp bound computationally established. The bound $\sharp_{PS}$ loses its effective value due to the existence of algebraic constraints relating some parameters (with the notations of Proposition 14, $c_{2,1} = c_{2,2} = c_{2,3} = 0$. Such algebraic constraints are not taken into account by the Pólya-Segö approach).

10.3.3 Further insights on the Pólya-Segö bound

As shown in the examples above, $\sharp_{PS}$ bound for the zero root multiplicity of a given quasipolynomial function is still represents a generic bound. To be more precise, consider for instance the following three quasipolynomial functions :

$$\begin{cases} \Delta_1 = \lambda^3 + a_{0,2}\lambda^2 + a_{0,1}\lambda + a_{0,0} + \left(a_{1,2}\lambda^2 + a_{1,1}\lambda + a_{1,0}\right)e^{-\lambda\tau_1} \\ \quad + \left(a_{2,2}\lambda^2 + a_{2,1}\lambda + a_{2,0}\right)e^{-\lambda\tau_2}, \\ \Delta_2 = \lambda^3 + a_{0,2}\lambda^2 + a_{0,1}\lambda + a_{0,0} + \left(a_{1,2}\lambda^2 + a_{1,1}\lambda + a_{1,0}\right)e^{-\lambda\tau_1} \\ \quad + \left(a_{2,2}\lambda^2 + a_{2,0}\right)e^{-\lambda\tau_2}, \\ \Delta_3 = \lambda^3 + a_{1,2}\lambda^2 e^{-\lambda\tau_1} + a_{2,2}\lambda^2 e^{-\lambda\tau_2}. \end{cases} \quad (10.19)$$

It is easy to see that all of them reduce to polynomials of degree three when the delays vanish $\tau_1 = \tau_2 = 0$. The quasipolynomial function Δ_1 characterizes the generic dynamical system consisting in three coupled differential equation with two discrete delays. One easily observes that Δ_1 has complete polynomials with the corresponding incidence vector $\mathcal{V}_1 = (x_1, x_1, x_1, x_2, x_2, x_2)$, which is not the case for the quasipolynomials Δ_2 (characterized by $\mathcal{V}_2 = (x_1, x_1, x_1, x_2, \star, x_2)$) and Δ_3 (characterized by $\mathcal{V}_3 = (\star, \star, x_1, \star, \star, x_2)$).

Indeed, Δ_2 has the so-called intermediate "star" since the polynomial associated with the second delay τ_2 is sparse ; $a_{2,1} = 0$. However, Δ_3 has two connected sequences of starter "stars", since $a_{2,0} = a_{2,1} = 0$ and $a_{1,0} = a_{1,1} = 0$. Moreover, $\sharp_{PS}(\Delta_1) = \sharp_{PS}(\Delta_2) = \sharp_{PS}(\Delta_3)$ because the degree of such quasipolynomials are equal.

Nevertheless, intuitively, the multiplicity of the zero root of Δ_3 is less or equal to the multiplicity of such a root for Δ_1. In addition, the above observation stresses the fact that the zero multiplicity depends on the number of the free parameters as well as on the particular structure of the system rather than on the degree of the quasipolynomial which is a generic bound of the number of free parameters. The next sections provide the main results of the paper. Section 10.4 provides some new LU developments for classes of functional Birkhoff matrices. In Section 10.5 , we first recover the Pólya-Segö bound by an effective computational approach, then we establish a sharper bound for the multiplicity of the zero spectral value taking into account the above observation.

10.4 LU-factorization for some classes of functional Birkhoff matrices

In all generality, the Birkhoff interpolation problem and the "poised"-ness of its incidence matrices are yet open problems [106]. In some reduced cases (two variables), related to our class of systems, we give the explicit LU-factorization of Birkhoff matrices. To the best of the author's knowledge, such formulae seem to be new and then it yields some new possibilities for tackling the Birkhoff interpolation problem.

In this section we intentionally separate the two configurations : the first one, is *the regular case*, that is all the polynomials of the delayed part of the studied quasipolynomial are complete. However, the second configuration occurring when the incidence vector $\mathcal{V}$ contains at least one star.

10.4.1 On functional confluent Vandermonde matrices

It is well known that Vandermonde and confluent Vandermonde matrices V can be factorized into a lower triangular matrix L and an upper triangular matrix U where $V = LU$, see for instance [171, 148]. In what follows, we show that the same applies for the functional confluent Vandermonde matrix (10.7)-(10.9) by establi-

shing explicit formulas for L and U where $\Upsilon = LU$. The factorization is *unique* if no row or column interchanges are made and if it is specified that the diagonal elements of L are unitary. The following theorem concerning (10.7)-(10.9) with $s = n + 1$ will be used in the sequel, but the same arguments can be easily adapted for any positive integer s.

Theorem 33. *Given the functional confluent Vandermonde matrix* (10.7)-(10.9) *with incidence vector $\mathcal{V}$ wanting "stars", the unique LU-factorization with unitary diagonal elements $L_{i,i} = 1$ is given by the formulae :*

$$
\begin{cases}
L_{i,1} = x_1^{i-1} & for \quad 1 \le i \le \delta, \\
U_{1,j} = \Upsilon_{1,j} & for \quad 1 \le j \le \delta, \\
L_{i,j} = L_{i-1,j-1} + L_{i-1,j}\,\xi_j & for \quad 2 \le j \le i, \\
U_{i,j} = (\varkappa(j) - 1)\,U_{i-1,j-1} + U_{i-1,j}\left(x_{\varrho(j)} - \xi_{i-1}\right) & for \quad 2 \le i \le j.
\end{cases}
\tag{10.20}
$$

Proof of Theorem 12. Define a matrix Ω by :

$$
\Omega_{i,j} = \sum_{k=1}^{D} L_{i,k} U_{k,j} = \sum_{k=1}^{i} L_{i,k} U_{k,j} \quad 1 \le i,j \le \delta.
\tag{10.21}
$$

In what follows, we prove that $\Omega_{i,j} = \Upsilon_{i,j}\ \forall (i,j)\ 1 \le i,j \le \delta$. The proof is a total 2D recurrence-based that can be summarized as follows :
— Initialization by proving :
 — $\Omega_{i,j} = \Upsilon_{i,j}$ for $i = 1$ and $1 \le j \le \delta$ that is $\Upsilon_{1,j}$.
 — $\Omega_{i,j} = \Upsilon_{i,j}$ for $j = 1$ and $1 \le i \le \delta$ that is $\Upsilon_{i,1}$.
— Assuming $\Omega_{i,j} = \Upsilon_{i,j}$ holds for any $1 \le i \le i_0 - 1$ and $1 \le j \le j_0 - 1$ and proving :
 — $\Omega_{i_0,j_0-1} = \Upsilon_{i_0,j_0-1}$.
 — $\Omega_{i_0-1,j_0} = \Upsilon_{i_0-1,j_0}$.
 — $\Omega_{i_0,j_0} = \Upsilon_{i_0,j_0}$.
— Conclude that $\Omega_{i,j} = \Upsilon_{i,j}$ for $1 \le i \le \delta$ and $1 \le j \le \delta$
Since L is a lower triangular matrix with a unitary diagonal and U is an upper triangular, using (10.20) one proves $\Omega_{1,j} = U_{1,j} \equiv \Upsilon_{1,j}$ and $\Omega_{i,1} = L_{i,1}U_{1,1} \equiv \Upsilon_{i,1}$ for any $1 \le j \le \delta$ and any $1 \le i \le \delta$. Hence, the initialization assumption holds. Assume now that $\Omega_{i,j} = \Upsilon_{i,j}$ is satisfied for any $1 \le i \le i_0 - 1$ and $1 \le j \le j_0 - 1$. According to (10.20), one gets :

$$
\begin{cases}
L_{i_0,k} = L_{i_0-1,k-1} + L_{i_0-1,k}\,\xi_k, \\
U_{k,j_0-1} = (\varkappa(j_0 - 1) - 1)\,U_{k-1,j_0-2} + U_{k-1,j_0-1}\left(x_{\varrho(j_0-1)} - \xi_{k-1}\right),
\end{cases}
$$

then

$$
\begin{aligned}
L_{i_0,k}U_{k,j_0-1} = {} & (\varkappa(j_0 - 1) - 1)\,L_{i_0-1,k-1}U_{k-1,j_0-2} + x_{\varrho(j_0-1)}\,L_{i_0-1,k-1}U_{k-1,j_0-1} \\
& - \xi_{k-1}\,L_{i_0-1,k-1}U_{k-1,j_0-1} + \xi_k\,L_{i_0-1,k}U_{k,j_0-1}.
\end{aligned}
$$

Thus,

$$
\Omega_{i_0,j_0-1} = x_{\varrho(j_0-1)} \sum_{k=1}^{i_0} L_{i_0-1,k} U_{k,j_0-1} + \sum_{k=1}^{i_0} (\varkappa(j_0-1)-1) L_{i_0-1,k} U_{k,j_0-2}
$$

$$
= x_{\varrho(j_0-1)} \Upsilon_{i_0-1,j_0-1} + (\varkappa(j_0-1)-1) \Upsilon_{i_0-1,j_0-2} \triangleq \Upsilon_{i_0,j_0-1}.
$$

The same argument gives

$$
\begin{cases}
L_{i_0-1,k} = L_{i_0-2,k-1} + L_{i_0-2,k}\, \xi_k, \\
U_{k,j_0} = (\varkappa(j_0)-1) U_{k-1,j_0-1} + U_{k-1,j_0}\left(x_{\varrho(j_0)} - \xi_{k-1}\right),
\end{cases}
$$

then

$$
L_{i_0-1,k} U_{k,j_0} = x_{\varrho(j_0)}\, L_{i_0-2,k-1} U_{k-1,j_0} + (\varkappa(j_0)-1) L_{i_0-2,k-1} U_{k-1,j_0-1}
$$

$$
- \xi_{k-1}\, L_{i_0-2,k-1} U_{k-1,j_0} + \xi_k\, L_{i_0-2,k} U_{k,j_0}.
$$

Thus,

$$
\Omega_{i_0-1,j_0} = x_{\varrho(j_0)} \sum_{k=1}^{i_0} L_{i_0-2,k} U_{k,j_0} + \sum_{k=1}^{i_0} (\varkappa(j_0)-1) L_{i_0-2,k} U_{k,j_0-1}
$$

$$
= x_{\varrho(j_0)} \Upsilon_{i_0-2,j_0} + (\varkappa(j_0)-1) \Upsilon_{i_0-2,j_0-1} \triangleq \Upsilon_{i_0-1,j_0}.
$$

By using again (10.20) one obtains :

$$
\begin{cases}
L_{i_0,k} = L_{i_0-1,k-1} + L_{i_0-1,k}\, \xi_k, \\
U_{k,j_0} = (\varkappa(j_0)-1) U_{k-1,j_0-1} + U_{k-1,j_0}\left(x_{\varrho(j_0)} - \xi_{k-1}\right),
\end{cases}
$$

leading to :

$$
L_{i_0,k} U_{k,j_0} = x_{\varrho(j_0)}\, L_{i_0-1,k-1} U_{k-1,j_0} + (\varkappa(j_0)-1) L_{i_0-1,k-1} U_{k-1,j_0-1}
$$

$$
+ \xi_k\, L_{i_0-1,k} U_{k,j_0} - \xi_{k-1}\, L_{i_0-1,k-1} U_{k-1,j_0}.
$$

Hence, we have :

$$
\Omega_{i_0,j_0} = x_{\varrho(j_0)} \Upsilon_{i_0-1,j_0} + (\varkappa(j_0)-1) \Upsilon_{i_0-1,j_0-1} \triangleq \Upsilon_{i_0,j_0},
$$

which ends the proof.   □

The explicit computation of the determinant of the functional confluent Vandermonde matrix Υ follows directly from (10.20) :

Corollary 2. *The determinant of the functional confluent Vandermonde matrix Υ is given by :*

$$
det(\Upsilon) = \prod_{j=1}^{\delta} (U_{j,j}),
$$

where $U_{j,j}$ for $1 \leq j \leq \delta$ are defined by :

$$
\begin{cases}
U_{1,1} = x_1^{n+1}, \\
U_{j,j} = U_{j-1,j}\left(x_{\varrho(j)} - \xi_{j-1}\right) & \text{if } j>1 \text{ and } \varkappa(j)=1, \\
U_{j,j} = (\varkappa(j)-1) U_{j-1,j-1} & \text{otherwise.}
\end{cases}
$$

Démonstration. Obviously, the determinant of Υ is equal to the determinant of U since $\det(L) = 1$ (triangular with unitary diagonal). The second equation from (10.20) gives : $U_{1,1} = x_1^{n+1}$. Substituting $i = j$ in the last equation from (10.20), and consider $j \equiv 1 \mod (d_0 + \ldots + d_r)$ where $1 \le r \le M$ that is $\varkappa(j) = 1$ then $U_{j,j} = U_{j-1,j} \left(x_{\varrho(j)} - \xi_{j-1} \right)$ otherwise $x_{\varrho(j)} = \xi_{j-1}$ which ends the proof. $\qquad\square$

Corollary 3. *The diagonal elements of the matrix U associated with the functional confluent Vandermonde matrix Υ are obtained as follows :*

$$
\begin{cases}
U_{1,1} = x_1^{n+1}, \\[2mm]
U_{j,j} = x_{k+1}^{n+1} \displaystyle\prod_{l=1}^{k} (x_{k+1} - x_l)^{d_l} & \text{if } j = 1 + d_k \ \text{for } 1 \le k \le M - 1, \\[4mm]
U_{j,j} = (j - 1 - d_k) \, U_{j-1,j-1} & \text{if } d_k + 1 < j \le d_{k+1} \ \text{for } \ 1 \le k \le M - 1,
\end{cases}
$$

Moreover, the functional confluent Vandermonde matrix Υ is non degenerate if, and only if, $\forall \, 1 \le i \ne j \le \delta$ we have $x_i \ne 0$ and $x_i \ne x_j$.

Démonstration. Using (10.20) one easily identifies the induction :

$$
\begin{cases}
U_{1+d_l,1+d_l} = (\varkappa(1 + d_l) - 1) \, U_{d_l,d_l} + U_{d_l,1+d_l} \left(x_{\varrho(1+d_l)} - \xi_{d_l} \right) \\
\qquad\qquad = U_{d_l,1+d_l} \left(x_{l+1} - \xi_{d_l} \right), \\
U_{d_l,1+d_l} = U_{d_l-1,1+d_l} \left(x_{l+1} - \xi_{d_l-1} \right), \\
\qquad\quad \vdots \\
U_{2,1+d_l} = U_{1,1+d_l} \left(x_{l+1} - \xi_1 \right), \\
U_{1,1+d_l} = x_{l+1}^{n+1}.
\end{cases}
$$

This ends the proof. $\qquad\square$

10.4.2 Non degeneracy domain for two classes of 2D-functional Birkhoff matrices : An LU-factorization

Polynomials in nature (e.g. from applications and modeling) are not necessarily generic. They often have some additional structure which we would like to take into account showing what it reflects in the multiplicity bound for the zero spectral value for time-delay systems.

In this section, we consider functional Birkhoff matrices with incidence vector $\mathcal{V}$ containing "stars" . Two configurations are investigated. The first one consists in a sequence of starter "stars" and the second one, involves a sequence of intermediate "stars" in a sequence of x_i, $i > 1$. We claim that if the particular incidence matrix under study contains "stars" in the two configurations (starter/intermediate) one can benefit from the understanding of each situation separately owing the following results.

In what follows, we present an attempt to extend the results of the previous section to the case of Birkhoff matrix (10.7)-(10.9) but with one sequence of x_1 wanting

"stars" and a second x_2 containing "stars" . Explicit formulas for LU-factorization will be given in two subclasses. Such developments can be easily adapted in the study of 2D-Birkhoff interpolation problem.

We consider (10.7)-(10.9) with $\varpi(x) = x^s$ where $s = n + 1$, but the same algorithms can be easily exploited for any functional Birkhoff matrix with the same incidence matrix and a sufficiently regular function ϖ, in particular, for any integer $s \geq 0$. Moreover, such a restriction to the two variables case $x = (x_1, x_2)$ may be extended to higher number of variables.

In terms of zeros of quasipolynomial functions, this amounts to say that all the illustrations we provide are focused on the two-delay case.

Starter stars : Polynomial LU-factorization

In all generality, a functional Birkhoff matrix (10.7)-(10.9) with incidence vector

$$\mathcal{V} = (\underbrace{x_1, \ldots, x_1}_{d_1}, \underbrace{\star, \ldots, \star}_{d_*}, \underbrace{x_2, \ldots, x_2}_{d_2})$$

admits an $LU-$factorization where the associated L and U matrices are with rational coefficients in the variables x_1 and x_2. This claim is illustrated by the following simple example.

Example 1. Let consider the functional Birkhoff matrix $\Upsilon_{\mathcal{E}}$ associated with the incidence vector $\mathcal{V} = (x_1, x_1, \star, x_2, x_2)$, thus, $n = 4$:

$$\Upsilon = \begin{bmatrix} x_1{}^4 & 4\,x_1{}^3 & 4\,x_2{}^3 & 12\,x_2{}^2 \\ x_1{}^5 & 5\,x_1{}^4 & 5\,x_2{}^4 & 20\,x_2{}^3 \\ x_1{}^6 & 6\,x_1{}^5 & 6\,x_2{}^5 & 30\,x_2{}^4 \\ x_1{}^7 & 7\,x_1{}^6 & 7\,x_2{}^6 & 42\,x_2{}^5 \end{bmatrix}$$

for which one can computes the LU factorization that gives :

$$L = \begin{bmatrix} 1 & 0 & 0 & 0 \\ x_1 & 1 & 0 & 0 \\ x_1{}^2 & 2\,x_1 & 1 & 0 \\ x_1{}^3 & 3\,x_1{}^2 & \frac{7\,x_2{}^2 + 7\,x_1 x_2 - 8\,x_1{}^2}{2\,(3\,x_2 - 2\,x_1)} & 1 \end{bmatrix},$$

$$U = \begin{bmatrix} x_1{}^4 & 4\,x_1{}^3 & 4\,x_2{}^3 & 12\,x_2{}^2 \\ 0 & x_1{}^4 & x_2{}^3\,(5\,x_2 - 4\,x_1) & 4\,x_2{}^2\,(5\,x_2 - 3\,x_1) \\ 0 & 0 & 2\,x_2{}^3\,(3\,x_2 - 2\,x_1)\,(-x_1 + x_2) & 2\,x_2{}^2\,(15\,x_2{}^2 + 6\,x_1{}^2 - 20\,x_1 x_2) \\ 0 & 0 & 0 & \frac{x_2{}^3(-x_1 + x_2)(10\,x_1{}^2 - 28\,x_1 x_2 + 21\,x_2{}^2)}{3\,x_2 - 2\,x_1} \end{bmatrix}.$$

Even the coefficients of L and U are rational functions in $x = (x_1, x_2)$, the determinant of $\Upsilon_{\mathcal{E}}$ still have polynomial expression in x as expected. For instance, in the considered example, the denominator of $U_{4,4}$ will be canceled by a factor from $U_{3,3}$.

Nevertheless, there exists a unique configuration in which L and U conserve their polynomial structure (as in the regular case), which occurs when $d_2 = 1$ independently from d_1 and d^*. The following theorem provides an explicit $LU-$factorization for a functional Birkhoff matrix in such a special case :

Theorem 34. *Given the functional Birkhoff matrix* (10.7)-(10.9) *with incidence vector*

$$\mathcal{V} = (\underbrace{x_1, \ldots, x_1}_{d_1}, \underbrace{\star, \ldots, \star}_{d_*}, x_2) \tag{10.22}$$

the unique LU-factorization with unitary diagonal elements $L_{i,i} = 1$ is given by the formulae :

$$
\begin{cases}
L_{i,1} = x_1^{i-1} & for \quad 1 \le i \le d_1 + 1, \\
U_{1,j} = \Upsilon_{1,j} & for \quad 1 \le j \le d_1 + 1, \\
L_{i,j} = L_{i-1,j-1} + L_{i-1,j}\,\xi_j & for \quad 2 \le j \le i \le d_1 + 1, \\
U_{i,j} = (\varkappa(j) - 1)\,U_{i-1,j-1} + U_{i-1,j}\left(x_{\varrho(j)} - \xi_{i-1}\right) & for \quad 2 \le i \le j \le d_1, \\
U_{i,d_1+1} = \Upsilon_{i,j} - (i-1)\displaystyle\int_0^{x_1} U_{i-1,d_1+1}(y, x_2)dy, & for \quad 2 \le i \le d_1 + 1.
\end{cases}
\tag{10.23}
$$

where $\xi = (\underbrace{x_1, \ldots, x_1}_{d_1}, x_2)$.

The proofs of Theorem 34 is provided in the appendix.

Remark 13. The proposed formulas given in Theorem 34 can be easily extended to incidence matrices :

$$\mathcal{V} = (\underbrace{x_1, \ldots, x_1}_{d_1}, \ldots, \underbrace{x_{n-1}, \ldots, x_{n-1}}_{d_{n-1}}, \underbrace{\star, \ldots, \star}_{d_*}, x_n), \tag{10.24}$$

allowing to investigate multiple zero spectral values for the n-delays case.

As a direct consequence of the above Theorem a nondegeneracy condition is given in the following corollary :

Corollary 4. *Let x_1 and x_2 be two distinct nonzero real numbers. The Birkhoff matrix Υ defined by* (10.7)-(10.9) *with incidence vector $\mathcal{V} = (\underbrace{x_1, \ldots, x_1}_{d_1}, \underbrace{\star, \ldots, \star}_{d_*}, x_2)$ is invertible if, and only if, $U_{d_1+1, d_1+1} \ne 0$.*

Intermediate stars : Polynomial LU-factorization

Similarly to the starting "stars" case, a nondegenerate functional Birkhoff matrix (10.7)-(10.9) with incidence vector

$$\mathcal{V} = (\underbrace{x_1, \ldots, x_1}_{d_1}, \underbrace{x_2, \ldots, x_2}_{d_2^-}, \underbrace{\star, \ldots, \star}_{d_*}, \underbrace{x_2, \ldots, x_2}_{d_2^+})$$

admits an $LU-$factorization where the associated L and U matrices are with rational coefficients in the variables x_1 and x_2. Here, we provide an illustrative simple example.

Example 2. Let consider the functional Birkhoff matrix $\Upsilon_{\mathcal{E}}$ associated with the incidence vector $\mathcal{V} = (x_1, x_2, \star, x_2, x_2)$ and $n = 4$:

$$
\Upsilon = \begin{bmatrix}
x_1{}^5 & x_2{}^5 & 20\,x_2{}^3 & 60\,x_2{}^2 \\
x_1{}^6 & x_2{}^6 & 30\,x_2{}^4 & 120\,x_2{}^3 \\
x_1{}^7 & x_2{}^7 & 42\,x_2{}^5 & 210\,x_2{}^4 \\
x_1{}^8 & x_2{}^8 & 56\,x_2{}^6 & 336\,x_2{}^5
\end{bmatrix}.
$$

The corresponding quasipolynomial function is for which one can computes the LU factorization that gives :

$$
L = \begin{pmatrix}
1 & 0 & 0 & 0 \\
x_1 & 1 & 0 & 0 \\
x_1{}^2 & x_2 + x_1 & 1 & 0 \\
x_1{}^3 & x_2{}^2 + x_1 x_2 + x_1{}^2 & \frac{13x_2{}^2 - 5x_1 x_2 - 5x_1{}^2}{6\,x_2 - 5\,x_1} & 1
\end{pmatrix},
$$

$$
U = \begin{pmatrix}
x_1{}^5 & x_2{}^5 & 20\,x_2{}^3 & 60\,x_2{}^2 \\
0 & x_2{}^6 - x_1 x_2{}^5 & 30\,x_2{}^4 - 20\,x_1 x_2{}^3 & 120\,x_2{}^3 - 60\,x_1 x_2{}^2 \\
0 & 0 & 12\,x_2{}^5 - 10\,x_1 x_2{}^4 & 90\,x_2{}^4 - 60\,x_1 x_2{}^3 \\
0 & 0 & 0 & 6\,\frac{x_2{}^4\left(21\,x_2{}^2 - 35\,x_1 x_2 + 15\,x_1{}^2\right)}{6\,x_2 - 5\,x_1}
\end{pmatrix}.
$$

Even the coefficients of L and U are rational functions in $x = (x_1, x_2)$, the determinant of $\Upsilon_{\mathcal{E}}$ still have polynomial expression in x as expected. For instance, in the considered example, the denominator of $U_{4,4}$ will be canceled by a factor from $U_{3,3}$.

The unique configuration in which L and U conserve their polynomial structure (as in the regular case as well the stating "stars" case with $d_2 = 1$), which occurs when $d_2^+ = 1$. The following theorem provides an explicit $LU-$factorization for a functional Birkhoff matrix in such a special case :

Theorem 35. *Given the functional Birkhoff matrix* (10.7)-(10.9) *with incidence vector*

$$
\mathcal{V} = (\underbrace{x_1, \ldots, x_1}_{d_1}, \underbrace{x_2, \ldots, x_2}_{d_2^-}, \underbrace{\star, \ldots, \star}_{d_*}, x_2) \tag{10.25}
$$

the unique LU-factorization with unitary diagonal elements $L_{i,i} = 1$ is given by the

formulae :

$$L_{i,1} = x_1^{i-1} \quad for \quad 1 \le i \le d_1 + d_2^- + 1, \tag{10.26}$$

$$U_{1,j} = \Upsilon_{1,j} \quad for \quad 1 \le j \le d_1 + d_2^- + 1, \tag{10.27}$$

$$L_{i,j} = L_{i-1,j-1} + L_{i-1,j}\, \xi_j \quad for \quad 2 \le j \le i \le d_1 + d_2^- + 1, \tag{10.28}$$

$$U_{i,j} = (\varkappa(j) - 1)\, U_{i-1,j-1} + U_{i-1,j}\, \left(x_{\varrho(j)} - \xi_{i-1}\right) \quad for \quad 2 \le i \le j \le d_1 + d_2^-, \tag{10.29}$$

$$U_{i,j} = \Upsilon_{i,j} - (i-1) \int_0^{x_1} U_{i-1,j}(y, x_2)\, dy \quad for \quad j = d_1 + d_2^- + 1 \ and \ 2 \le i \le d_1 + 1, \tag{10.30}$$

$$U_{i,j} = (j + d^* - (i-1)) \int_0^{x_2} U_{i-1,j}(x_1, y)\, dy \ for \ j = d_1 + d_2^- + 1 \ and \ d_1 + 2 \le i \le j, \tag{10.31}$$

where $\xi = (\underbrace{x_1, \ldots, x_1}_{d_1}, \underbrace{x_2, \ldots, x_2}_{d_2^- + 1}).$

Remark 14. The proposed formulas given in theorem 35 can be easily extended to incidence matrices :

$$\mathcal{V} = (\underbrace{x_1, \ldots, x_1}_{d_1}, \ldots, \underbrace{x_{n-1}, \ldots, x_{n-1}}_{d_{n-1}}, \underbrace{x_n, \ldots, x_n}_{d_n^-}, \underbrace{\star, \ldots, \star}_{d_*}, x_n) \tag{10.32}$$

As a direct consequence of the above Theorem as well as the auxiliary Lemmas 4-6 presented in the appendix, one can compute analytically the determinant of the considered Birkhoff matrix and then easily deduce its nondegeneracy domain. The above Corollary is in the same spirit of Corollary 2 for the functional confluent Vandermonde matrices.

Corollary 5. *Let x_1 and x_2 be two distinct nonzero real numbers. The determinant of the functional Birkhoff matrix Υ defined by* (10.7)-(10.9) *with incidence vector*

$$\mathcal{V} = (\underbrace{x_1, \ldots, x_1}_{d_1}, \underbrace{x_2, \ldots, x_2}_{d_2^-}, \underbrace{\star, \ldots, \star}_{d_*}, x_2)$$

is given by :

$$det(\Upsilon) = \prod_{j=1}^{d_2^- + d_1 + 1} (U_{j,j}),$$

where $U_{j,j}$ for $1 \leq j \leq d_2^- + d_1 + 1$ are defined by :

$$\begin{cases} U_{1,1} = x_1^{n+1}, \\ U_{d_1+1,d_1+1} = x_2^{n+1} \, (x_2 - x_1)^{d_1} \\ U_{d_1+d_2^-+1,d_1+d_2^-+1} = \\ \displaystyle\prod_{\mu=0}^{d^*-1} (d_2^- + d_* - \mu) \sum_{l=0}^{d_1} \binom{d_1}{l} (-1)^l \, x_1^l \underbrace{\int_0^{x_2} \cdots \int_0^{x_2}}_{d_2^-} \Upsilon_{d_1+1-l,d_1+d_2^-+1}(x_1,y) \underbrace{dy \ldots dy}_{d_2^-}, \\ U_{j,j} = (\varkappa(j) - 1) \, U_{j-1,j-1} \quad \textit{otherwise.} \end{cases}$$

Moreover, the functional Birkhoff matrix Υ is invertible if, and only if, $U_{d_1+d_2^-+1,d_1+d_2^-+1} \neq 0$.

We emphasize that the results obtained above can be easily adapted for computing the LU-factorization for any functional Birkhoff matrix (with the same $\mathcal{V}$) with different sufficiently regular function ϖ.

10.5   Codimension of zero Singularities of TDS

This section includes the main contributions of the paper. In its first part, we give an adaptive bound for the zero spectral value taking into account the system structure. The proof of this proposition is constructive and as such underlines and exploit the existing links between the multiplicity of the zero singularity and Birkhoff matrices. Additionally, it gives the values of the system parameters guaranteeing an admissible multiplicity for the zero spectral value. The second part is devoted to recover the Pólya-Szegö generic bound. In this framework, the provided explicit expressions for the LU-factorization of the functional confluent Vandermonde matrices. Finally, the third part, entitled "On beyond of the Pólya-Segö Bound", concerns some classes of functional Birkhoff matrices.

In the light of the above results on LU-factorization of the considered classes of functional Birkhoff matrices, we are now able to establish a sharper bound for the zero multiplicity under the assumption of nondegeneracy of appropriate functional Birkhoff matrices. Indeed, the following result applies even when the delay associated polynomials are sparse.

Proposition 9. *The following assertions hold :*

i) The multiplicity of the zero root for the generic quasipolynomial function (10.4) cannot be larger than $\sharp_{PS} = D + \tilde{N}_{N,n}$, where D is the sum of degrees of the polynomials involved in the quasipolynomial and $\tilde{N}_{N,n}+1$ is the number of the associated polynomials. Moreover, such a bound is reached if, and only if, the parameters of (10.4) satisfy simultaneously :

$$a_{0,k} = - \sum_{i \in S_{N,n}} \left(a_{i,k} + \sum_{l=0}^{k-1} \frac{a_{i,l}\sigma_i^{k-l}}{(k-l)!} \right), \quad for \quad 0 \leq k \leq \sharp_{PS} - 1. \qquad (10.33)$$

ii *Consider a quasipolynomial function* (10.4) *containing at least one incomplete polynomial for which we associate an incidence vector* $\mathcal{V}_{\tilde{\mathcal{E}}}$ *(which is nothing other than* $\mathcal{V}_{\mathcal{E}}$ *given by* (10.34) *where a component associated with a vanishing coefficient is indicated by a "star").*

When the associated functional Birkhoff matrix $\Upsilon_{\tilde{\mathcal{E}}}$ *is nonsingular, then the multiplicity of the zero root for the quasipolynomial function* (10.4) *cannot be larger than "n" plus the number of nonzero coefficients of the polynomial family* $(P_{M^k})_{M^k \in S_{N,n}}$.

Remark 15. In the generic case, the Pólya-Szegö bound $\sharp_{PS}$ is completely recovered by the first assertion of 9. But, its advantage consists in providing the parameter values insuring any admissible multiplicity fo the zero singularity. The proof of Proposition 9 provides a constructive linear algebra alternative for identifying such a bound.

Remark 16. Obviously, the number of non-zero coefficients of a given quasipolynomial function is bounded by its degree plus its number of polynomials. Thus, the bound elaborated in Proposition 9 ii) is sharper than $\sharp_{PS}$, even in the generic case, that is all the parameters of the quasipolynomial are left free, these two bounds are equal. Indeed, in the generic case, that is when the number of the left free parameters is maximal, the Pólya-Szegö bound $\sharp_{PS} = D + \tilde{N}_{N,n} = n + D_q + \tilde{N}_{N,n}$ which is nothing else than n plus the number of parameters of the polynomial family $(P_{M^k})_{M^k \in S_{N,n}}$.

Remark 17. When the matrix $\Upsilon_{\tilde{\mathcal{E}}}$ is singular, one keeps the generic Pólya-Szegö bound $\sharp_{PS}$.

Remark 18. The above proposition can be interpreted as follows. Under the hypothesis :

$$\Delta(i\omega) = 0 \Rightarrow \omega = 0 \tag{H}$$

(that is, all the imaginary roots are located at the origin), the dimension of the projected state on the center manifold associated with zero singularity for equation (10.4) is less or equal to its number of nonzero coefficients minus one. Indeed, under (H), the codimension of the zero spectral value is identically equal to the dimension of the state on the center manifold since, in general, the dimension of the state on the center manifold is none other than the sum of the dimensions of the generalized eigenspaces associated with the spectral values having a zero real part.

Since we are dealing only with the values of $\Delta_k(0)$, we suggest to translate the problem into the parameter space (the space of the coefficients of the P_i). This is more appropriate and consider a parametrization by σ. In the appendix we introduce a lemma that allows to establish an m-set of multivariate algebraic functions (polynomials) vanishing at zero when the multiplicity of the zero root of the transcendental equation $\Delta(\lambda, \tau) = 0$ is equal to m.

Proof of Proposition 9 : The condition (10.33) follows directly from Lemma 2 (see Appendix). Hereafter, we recover the bound $\sharp_{PS}$ by explicit use of functional Vandermonde matrices. Then, assuming that some coefficients of the quasipolynomial

vanish without affecting its degree, we show that a sharper bound can be related to the number of nonzero parameters rather than the degree.

i) More precisely, we shall consider the variety associated with the vanishing of the polynomials ∇_k (defined in Lemma 2 in the appendix) , that is $\nabla_0(0) = \ldots = \nabla_{m-1}(0) = 0$ and $\nabla_m(0) \neq 0$ and we aim to find the maximal m (codimension of the zero singularity).

Let us exhibit the first elements from the family ∇_k

$$
\begin{cases}
\nabla_0(0) = 0 \Leftrightarrow \displaystyle\sum_{s=0}^{\tilde{N}_{N,n}} a_{s,0} = 0, \\[2mm]
\nabla_1(0) = 0 \Leftrightarrow \displaystyle\sum_{s=0}^{\tilde{N}_{N,n}} a_{s,1} + \sum_{s=1}^{\tilde{N}_{N,n}} a_{s,0}\,\sigma_s = 0, \\[2mm]
\nabla_2(0) = 0 \Leftrightarrow 2! \displaystyle\sum_{s=0}^{\tilde{N}_{N,n}} a_{s,2} + 2! \sum_{s=1}^{\tilde{N}_{N,n}} a_{s,1}\,\sigma_s + \sum_{s=1}^{N} a_{s,0}\,\sigma_s^2 = 0.
\end{cases}
$$

If we consider $a_{i,j}$ and σ_k as variables, the derived algebraic system is nonlinear and solving it in all its generality (without attributing values for n and N) becomes a very difficult task. In fact, even the use of Gröbner basis methods [68] seems to be very challenging since the set of variables depends on N and n. However, considering $a_{i,j}$ as variables and σ_k as parameters helps in simplifying the problem to a linear one, as seen in (10.33). Consider the ideal I_1 generated by polynomials $< \nabla_0(0), \nabla_1(0), \ldots, \nabla_{n-1}(0) >$.

As it can be seen from (10.33) and Lemma 2 (see appendix), the variety V_1 associated with the ideal I_1 has the following linear representation $a_0 = \underline{\Upsilon}\,a$ such that $\underline{\Upsilon} \in \mathcal{M}_{n,D_q+\tilde{N}_{N,n}}(\mathbb{R}[\sigma])$ where D_q is the degree of $\sum_{k=1}^{\tilde{N}_{N,n}} P_{M_k}$ and $D_q = D - n$ (D the degree of the quasipolynomial (10.4)). Somehow, in this variety there are no restrictions on the components of a if a_0 is left free. Since $a_{0,k} = 0$ for all $k > n$, the remaining equations consist of an algebraic system only in a and parametrized by σ. Consider now the ideal denoted I_2 and generated by the $D_q + \tilde{N}_{N,n}$ polynomials defined by $I_2 =< \nabla_{n+1}(0), \nabla_{n+2}(0), \ldots, \nabla_{D+\tilde{N}_{N,n}}(0) >$. It can be observed that the variety V_2 associated with I_2 can be written as $\bar{\Upsilon}\,a = 0$ which is nothing but a homogeneous linear system with $\bar{\Upsilon} \in \mathcal{M}_{D_q+\tilde{N}_{N,n}}(\mathbb{R}[\sigma])$. More precisely, $\bar{\Upsilon}$ is a functional confluent Vandermonde matrix (10.7)-(10.9) with $x = \sigma$, $s = n$, $M = \tilde{N}_{N,n}$ and $\delta = D_q + \tilde{N}_{N,n}$ which is associated with some incidence vector :

$$
\mathcal{V} = (\underbrace{\sigma_{M^1}, \ldots, \sigma_{M^1}}_{n-\sum_{s=1}^{N} M_s^1}, \underbrace{\sigma_{M^2}, \ldots, \sigma_{M^2}}_{n-\sum_{s=1}^{N} M_s^2}, \ldots, \sigma_{M^{\tilde{N}_{N,n}}}, \ldots, \sigma_{M^{\tilde{N}_{N,n}}}). \tag{10.34}
$$

Now, using Corollaries 2 and 3 and the assumption that σ_i are distinct non zero auxiliary delays, we can conclude that the determinant of $\bar{\Upsilon}$ cannot

vanish. Thus the only solution for this subsystem is the zero solution, that is, $a = 0$.

Finally, consider the polynomial defined by $\nabla_n(0)$, Lemma 2 states that (see appendix)

$$\nabla_n(0) = 0 \Leftrightarrow 1 = -\sum_{i=1}^{\tilde{N}_{N,n}} \sum_{s=0}^{n-1} \frac{a_{i,s}\sigma_i^{n-s}}{(n-s)!}$$

Now, substituting the unique solution of V_2 into the last equality leads to an incompatibility result. In conclusion, the maximal codimension of the zero singularity is less or equal to $D_q + \tilde{N}_{N,n} + n$ which is exactly the Pólya-Szegö bound $\sharp_{PS} = \underbrace{D_q + (n+1)}_{D+\tilde{N}_{N,n}}$ proving i).

ii) She same arguments apply when z coefficients from the polynomial family $(P_{M^k})_{M^k \in S_{N,n}}$ vanish without affecting the degree of the quasipolynomial, then $a^T \in \mathbb{R}^{D_q + \tilde{N}_{N,n} - z}$ and thus the matrix $\bar{\Upsilon}$ of i) becomes $\Upsilon_{\tilde{\mathcal{E}}} \in \mathcal{M}_{D_q + \tilde{N}_{N,n} - z}(\mathbb{R}[\sigma])$. Thus, the invertibility of the later matrix allows to : the maximal codimension of the zero singularity is less or equal to $D_q + \tilde{N}_{N,n} - z + n < \sharp_{PS}$. Which ends the proof.

$\square$

Remark 19. It is noteworthy that the codimension of the zero singularity may decrease if the vector parameter a_0 is not left free. Indeed, if some parameter component $a_{0,k}$ is fixed for $0 \le k \le n-1$, then the variety associated to the first ideal I_1 may impose additional restrictions on the vector parameter a.

10.6 Illustrative examples : An effective approach vs Pólya-Szegö Bound

A natural consequence of Proposition 9 is to explore the situation when the codimension of zero singularity reaches its upper bound. Starting the section by a generic example, we show the convenience of the proposed approach even in the case of cross-talk between the delays. Then the obtained symbolic results are applied to identify an effective sharp bound in the case of concrete physical system (with constraints on the coefficients). Namely, the stabilization of an inverted pendulum on cart via a multi-delayed feedback. Next, the LU-factorizations are illustrated in the two configurations starter "stars"/intermediate "stars" and then interpreted in terms of the codimension of the zero singularity. This section is ended by a control oriented discussion.

10.6.1 Two scalar equations with two delays : An inverted pendulum on cart with delayed feedback

We associate to the general planar time-delay system with two positive delays $\tau_1 \neq \tau_2$ the quasipolynomial function :

$$\Delta(\lambda, \sigma) = \lambda^2 + a_{0,0,1}\lambda + a_{0,0,0} + (a_{1,0,0} + a_{1,0,1}\lambda)\,\mathrm{e}^{\lambda\,\sigma_{1,0}} + (a_{0,1,0} + a_{0,1,1}\lambda)\,\mathrm{e}^{\lambda\,\sigma_{0,1}}$$
$$+ a_{2,0,0}\mathrm{e}^{\lambda\,\sigma_{2,0}} + a_{1,1,0}\mathrm{e}^{\lambda\,\sigma_{1,1}} + a_{0,2,0}\mathrm{e}^{\lambda\,\sigma_{0,2}}.$$
(10.35)

Generically, the multiplicity of the zero singularity is bounded by $\sharp_{PS} = 9$. However, in what follows, we present two configurations where such a bound cannot be reached. The first, corresponds to the case when $\sigma_i = \sigma_j$ for $i \neq j$ and the second, when some components of the coefficient vector $a = (a_{1,0,0}, a_{1,0,1}, a_{0,1,0}, a_{0,1,1}, a_{2,0,0}, a_{1,1,0}, a_{0,2,0})^T$ vanish.

Formula (10.33) allows us to explicitly computing the confluent Vandermonde matrices $\underline{\Upsilon}$ and $\bar{\Upsilon}$ and the expression of $\nabla_2(0)$ from the proof of Proposition 9 such that $\underline{\Upsilon}\,a = a_0$, $\nabla_2(0) = 0$ and $\bar{\Upsilon}\,a = 0$ where $a_0 = (a_{0,0,0}, a_{0,0,1})^T$:

$$\underline{\Upsilon} = \begin{bmatrix} 1 & 0 & 1 & 0 & 1 & 1 & 1 \\ \sigma_{1,0} & 1 & \sigma_{0,1} & 1 & \sigma_{2,0} & \sigma_{1,1} & \sigma_{0,2} \end{bmatrix},$$

$$\nabla_2(0) - 2 = \begin{bmatrix} \sigma_{1,0}{}^2 & 2\,\sigma_{1,0} & \sigma_{0,1}{}^2 & 2\,\sigma_{0,1} & \sigma_{2,0}{}^2 & \sigma_{1,1}{}^2 & \sigma_{0,2}{}^2 \end{bmatrix}a$$

$$\bar{\Upsilon} = \begin{bmatrix} \sigma_{1,0}{}^3 & 3\,\sigma_{1,0}{}^2 & \sigma_{0,1}{}^3 & 3\,\sigma_{0,1}{}^2 & \sigma_{2,0}{}^3 & \sigma_{1,1}{}^3 & \sigma_{0,2}{}^3 \\ \sigma_{1,0}{}^4 & 4\,\sigma_{1,0}{}^3 & \sigma_{0,1}{}^4 & 4\,\sigma_{0,1}{}^3 & \sigma_{2,0}{}^4 & \sigma_{1,1}{}^4 & \sigma_{0,2}{}^4 \\ \sigma_{1,0}{}^5 & 5\,\sigma_{1,0}{}^4 & \sigma_{0,1}{}^5 & 5\,\sigma_{0,1}{}^4 & \sigma_{2,0}{}^5 & \sigma_{1,1}{}^5 & \sigma_{0,2}{}^5 \\ \sigma_{1,0}{}^6 & 6\,\sigma_{1,0}{}^5 & \sigma_{0,1}{}^6 & 6\,\sigma_{0,1}{}^5 & \sigma_{2,0}{}^6 & \sigma_{1,1}{}^6 & \sigma_{0,2}{}^6 \\ \sigma_{1,0}{}^7 & 7\,\sigma_{1,0}{}^6 & \sigma_{0,1}{}^7 & 7\,\sigma_{0,1}{}^6 & \sigma_{2,0}{}^7 & \sigma_{1,1}{}^7 & \sigma_{0,2}{}^7 \\ \sigma_{1,0}{}^8 & 8\,\sigma_{1,0}{}^7 & \sigma_{0,1}{}^8 & 8\,\sigma_{0,1}{}^7 & \sigma_{2,0}{}^8 & \sigma_{1,1}{}^8 & \sigma_{0,2}{}^8 \\ \sigma_{1,0}{}^9 & 9\,\sigma_{1,0}{}^8 & \sigma_{0,1}{}^9 & 9\,\sigma_{0,1}{}^8 & \sigma_{2,0}{}^9 & \sigma_{1,1}{}^9 & \sigma_{0,2}{}^9 \end{bmatrix}.$$

As shown in the proof of Proposition 9, $\bar{\Upsilon}$ is a singular matrix when $\sigma_i = \sigma_j$ for $i \neq j$. For instance, when $\sigma_{2,0} = \sigma_{0,1}$ that is $2\tau_1 = \tau_2$, then the bound of multiplicity of the zero singularity decrease since the polynomials $P_{2,0}$ and $P_{0,1}$ will be collected $\tilde{P}_{0,1} = P_{0,1} + P_{2,0}$.

Consider now a system of two coupled equations with two delays modeling a friction free inverted pendulum on cart. The adopted model is studied in [10, 200, 201, 34] and in the sequel we keep the same notations. In the dimensionless form, the dynamics of the inverted pendulum on a cart in figure 10.2 is governed by the following second-order differential equation :

$$\left(1 - \frac{3\varepsilon}{4}\cos^2(\theta)\right)\ddot{\theta} + \frac{3\varepsilon}{8}\dot{\theta}^2\sin(2\theta) - \sin(\theta) + U\cos(\theta) = 0, \qquad (10.36)$$
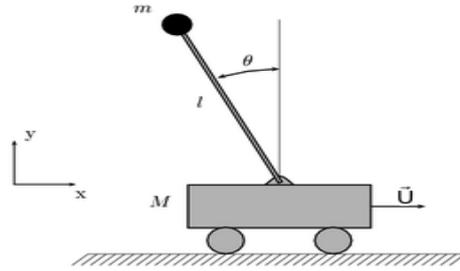
FIGURE 10.2 – Inverted Pendulum on a cart

where $\varepsilon = m/(m + M)$, M the mass of the cart and m the mass of the pendulum and D represents the control law that is the horizontal driving force. A generalized Bogdanov-Takens singularity with codimension three is identified in [200] by using $U = a\,\theta(t-\tau) + b\,\dot{\theta}(t-\tau)$. Motivated by the technological constraints, it is suggested in [34, 35] to avoid the use of the derivative gain that requires the estimation of the angular velocity that can induce harmful errors for real-time simulations and propose a multi-delayed-proportional controller $U = a_{1,0}\,\theta(t - \tau_1) + a_{2,0}\,\theta(t - \tau_2)$, this choice is argued by the accessibility of the delayed state by some simpler sensor. By this last controller choice and by setting $\varepsilon = \frac{3}{4}$, the associated quasipolynomial function Δ becomes :

$$\Delta(\lambda, \tau) = \lambda^2 - \frac{16}{7} + \frac{16\,a_{1,0}}{7}\,\mathrm{e}^{-\lambda\,\tau_1} + \frac{16\,a_{2,0}}{7}\,\mathrm{e}^{-\lambda\,\tau_2}. \tag{10.37}$$

Thus, the associated incidence vector is $\mathcal{V} = (x_1, x_2)$. A zero singularity with codimension three is identified in [34], see Figure 10.3 for the map of local bifurcations in the $(a_{1,0}, a_{2,0})$ plan.
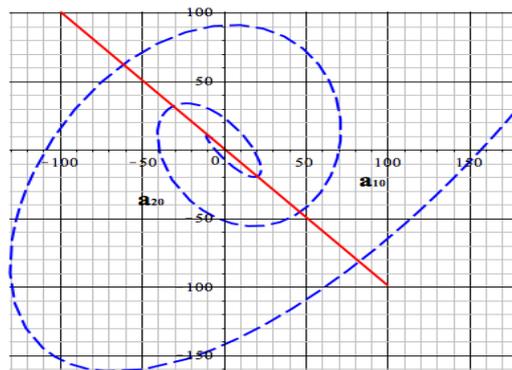
FIGURE 10.3 – Bifurcations curves of (10.37) in the gains $(a_{1,0}, a_{2,0})$ plan (solid red=Pitchfork singularity i.e. the zero singularity, discontinuous blue=Hopf singularity) for the fixed value $\tau_2 = \frac{7}{8}$.

Moreover, it is shown that the upper bound of the codimension for the zero singularity for (10.36) is three (can be easily checked by (10.33)) and this configuration is obtained when the gains and delays satisfy simultaneously :

$$a_{1,0} = -\frac{7}{-7 + 8\,\tau_1}, \quad a_{2,0} = \frac{8\tau_1{}^2}{-7 + 8\,\tau_1{}^2}, \quad \tau_2 = \frac{7}{8\,\tau_1}.$$

However, using Pólya-Szegö result, one has $\sharp_{PS} = D - 1 = (3 + 2 + 2) - 1 = 6$ exceeding the effective bound which is three. This is a further justification for the algebraic constraints on the parameters imposed by the physical model, for instance the sparsity pattern of the delay-free polynomial, namely, the vanishing of $a_{0,1}$.

10.6.2　The nondegeneracy of a 2D-functional Birkhoff matrix : incidence vector with starter stars

As an illustration of the result given in Corollary 4, consider the functional Birkhoff matrix Υ characterized by the incidence vector $\mathcal{V} = (x_1, x_1, x_1, x_1, x_1, \star, \star, x_2)$. Thus, one has

$$\Upsilon = \begin{bmatrix} x_1{}^8 & 8\,x_1{}^7 & 56\,x_1{}^6 & 336\,x_1{}^5 & 1680\,x_1{}^4 & 56\,x_2{}^6 \\ x_1{}^9 & 9\,x_1{}^8 & 72\,x_1{}^7 & 504\,x_1{}^6 & 3024\,x_1{}^5 & 72\,x_2{}^7 \\ x_1{}^{10} & 10\,x_1{}^9 & 90\,x_1{}^8 & 720\,x_1{}^7 & 5040\,x_1{}^6 & 90\,x_2{}^8 \\ x_1{}^{11} & 11\,x_1{}^{10} & 110\,x_1{}^9 & 990\,x_1{}^8 & 7920\,x_1{}^7 & 110\,x_2{}^9 \\ x_1{}^{12} & 12\,x_1{}^{11} & 132\,x_1{}^{10} & 1320\,x_1{}^9 & 11880\,x_1{}^8 & 132\,x_2{}^{10} \\ x_1{}^{13} & 13\,x_1{}^{12} & 156\,x_1{}^{11} & 1716\,x_1{}^{10} & 17160\,x_1{}^9 & 156\,x_2{}^{11} \end{bmatrix}. \qquad (10.38)$$

Under the assumptions $x_1 x_2 \neq 0$ and $x_1 \neq x_2$, the matrix Υ is a non singular matrix if, and only if, the bivariate polynomial $39\,x_2{}^2 - 48\,x_2 x_1 + 14\,x_1{}^2 \neq 0$, see Figure 10.4. Consider, the corresponding quasipolynomial function

$$\Delta(\lambda, \sigma) = \lambda^7 + \sum_{k=0}^{6} a_{0,k}\,\lambda^k + e^{\sigma_{1,0}\lambda} \sum_{k=0}^{4} a_{1,0,k}\,\lambda^k + a_{0,1,2}\lambda^2\,e^{\sigma_{0,1}\lambda}. \qquad (10.39)$$

In terms of time-delay systems analysis purpose, the result above asserts that if the auxiliary non zero distinct delays $\sigma_{1,0}$ and $\sigma_{0,1}$ satisfy $39\,\sigma_{0,1}{}^2 - 48\,\sigma_{0,1}\sigma_{1,0} + 14\,\sigma_{1,0}{}^2 \neq 0$, then, the codimension of the zero singularity is bounded by 13. Furthermore, such a multiplicity bound is reached if, and only if, the parameter vectors a and a_0 satisfy equality (10.33) for $k = 0, \ldots, 12$. Notice that, in this configuration, the Pólya-Segö bound $\sharp_{PS} = 15$.

10.6.3　The nondegeneracy of a 2D-functional Birkhoff matrix : incidence vector with intermediate stars

As an illustration of the result given in Corollary 5, consider the functional Birkhoff matrix Υ characterized by the incidence vector $\mathcal{V} = (x_1, x_1, x_1, x_1, x_2, \star, \star, x_2)$.
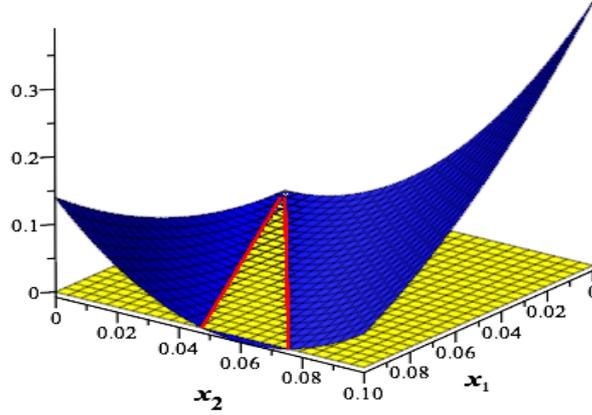
FIGURE 10.4 – In blue, the 3D plot of the surface defined by $39\,x_2{}^2 - 48\,x_2x_1 + 14\,x_1{}^2$. The red curves are associated to the degeneracy domain (in the (x_1, x_2) plane) of the matrix Υ.

Thus, one has

$$
\Upsilon = \begin{bmatrix}
\sigma_{1,0}{}^8 & 8\,\sigma_{1,0}{}^7 & 56\,\sigma_{1,0}{}^6 & 336\,\sigma_{1,0}{}^5 & \sigma_{0,1}{}^8 & 336\,\sigma_{0,1}{}^5 \\
\sigma_{1,0}{}^9 & 9\,\sigma_{1,0}{}^8 & 72\,\sigma_{1,0}{}^7 & 504\,\sigma_{1,0}{}^6 & \sigma_{0,1}{}^9 & 504\,\sigma_{0,1}{}^6 \\
\sigma_{1,0}{}^{10} & 10\,\sigma_{1,0}{}^9 & 90\,\sigma_{1,0}{}^8 & 720\,\sigma_{1,0}{}^7 & \sigma_{0,1}{}^{10} & 720\,\sigma_{0,1}{}^7 \\
\sigma_{1,0}{}^{11} & 11\,\sigma_{1,0}{}^{10} & 110\,\sigma_{1,0}{}^9 & 990\,\sigma_{1,0}{}^8 & \sigma_{0,1}{}^{11} & 990\,\sigma_{0,1}{}^8 \\
\sigma_{1,0}{}^{12} & 12\,\sigma_{1,0}{}^{11} & 132\,\sigma_{1,0}{}^{10} & 1320\,\sigma_{1,0}{}^9 & \sigma_{0,1}{}^{12} & 1320\,\sigma_{0,1}{}^9 \\
\sigma_{1,0}{}^{13} & 13\,\sigma_{1,0}{}^{12} & 156\,\sigma_{1,0}{}^{11} & 1716\,\sigma_{1,0}{}^{10} & \sigma_{0,1}{}^{13} & 1716\,\sigma_{0,1}{}^{10}
\end{bmatrix}.
$$

Under the assumptions $x_1 x_2 \neq 0$ and $x_1 \neq x_2$, the matrix Υ is a non singular matrix if, and only if, the bivariate polynomial $33\,x_2{}^2 - 44\,x_2 x_1 + 14\,x_1{}^2 \neq 0$, see Figure 10.5.

Now, consider the corresponding quasipolynomial function

$$
\Delta(\lambda, \sigma) = \lambda^7 + \sum_{k=0}^{6} a_{0,k}\,\lambda^k + e^{\sigma_{1,0}\lambda} \sum_{k=0}^{4} a_{1,0,k}\,\lambda^k + \left(a_{0,1,0} + + a_{0,1,3}\lambda^3\right) e^{\sigma_{0,1}\lambda}. \quad (10.40)
$$

The result above asserts that if the auxiliary non zero distinct delays $\sigma_{1,0}$ and $\sigma_{0,1}$ satisfy $33\,\sigma_{0,1}{}^2 - 44\,\sigma_{0,1}\sigma_{1,0} + 14\,\sigma_{1,0}{}^2 \neq 0$, then, the codimension of the zero singularity is bounded by 14. Furthermore, such a multiplicity bound is reached if, and only if, the parameter vectors a and a_0 satisfy equality (10.33) for $k = 0, \ldots, 13$. Notice that, in this configuration, the Pólya-Segö bound $\sharp_{PS} = 16$.
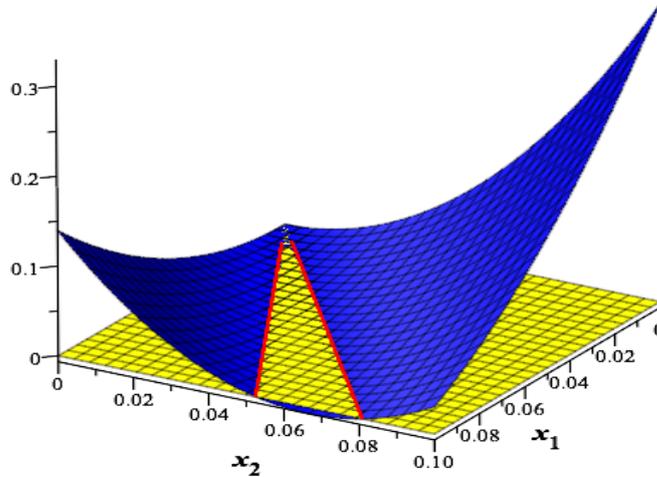
FIGURE 10.5 – In blue, the 3D plot of the surface defined by $33\,x_2{}^2 - 44\,x_2 x_1 + 14\,x_1{}^2$. The red curves are associated to the degeneracy of the matrix Υ.

10.6.4   Controlling Generalized Bogdanov-Takens Singularity

Commonly, the generalized Bogdanov-Takens singularity (typically a chain of integrators) represents an undesired configuration when dealing with stability problems. Our control idea is based on it and it can be summarized as follow : first, we introduce sufficiently many delayed proportional controllers with free gains [166, 129]. Next we identify the appropriate parameters (delays and gains) values allowing to reach the configuration of a spectrum consisting of stable spectrum and a multiple-zero singularity. Hence, we develop the spectral projection in the finite dimensional subspace (the generalized eigenspace) associated with the zero singularity. This suggests the computation of the center manifold and the normal form of the equations governing the dynamics on it for the parameters-perturbed system ; which are known to be powerful tools for the local qualitative study of the dynamics. In other words, this reduces our problem to the control of a finite dimensional dynamical system. It is well known that the stability of the obtained finite dimensional projected dynamics means the stability of the original time-delay system, see [47]. Moreover, the matrix associated with the linear part of the finite dimensional projection of the parameters-perturbed system (associated with the generalized Bogdanov-Takens singularity) is nothing but a companion matrix (depending on the parameters-perturbation). It is always possible to design an appropriate perturbation that makes this matrix Hurwitz, [166, 129]. This approach proved its efficiency particularly in suppressing undesired dynamics of mechanical systems. In [10] it is shown that the only use of a proportional controller is not sufficient in stabilizing the inverted pendulum and it is proved that an additional delay in the control signal is necessary for a successful stabilization. The described approach is emphasized in some recent contribution of

J. Sieber & B. Krauskopf [200] for stabilizing the inverted pendulum by designing a delayed PD controller. Moreover, they established a linearized stability analysis allowing to characterize all the possible local bifurcations additionally to the nonlinear analysis. This analysis involves the center manifold theory and normal forms. The study underlined the existence of a codimension-three triple zero bifurcation. It is also shown that the stabilization of the inverted pendulum in its upright position cannot be achieved by a PD controller when the delay exceeds some critical value τ_c. In [201], the authors investigate some modifications of the delayed PD scheme allowing to extend the range of the permissible delays by introducing an additional parameter. For that, two options were proposed, either to additionally take into account the angular acceleration or to consider an intentional additional delay in the angular position feedback. In [34] the authors introduce a multi-delayed-proportional controller allowing the stabilization of the inverted pendulum without the use of derivative measurements. Usually, the use of PD controller needs the knowledge of the velocity history but in general we are only able to have approximate measurements due to technological constraints. In absence of measurement of the derivative, a classical idea is to use an observer to reconstruct the state, but this task is computationally involved. It is shown in [35] that this type of singularity (triple zero singularity) can be avoided by offsetting the delayed derivative gain by introducing two-delayed-proportional controller. The interest of considering control laws of the form $\sum_{k=1}^{m} \gamma_k \, x(t - \tau_k)$ lies in the simplicity of the controller as well as in its practical implementation facility, suggesting the only use of position sensor. In a similar manner other type of singularities can be avoided. In [135], S.A. Campbell *et. al.* considered a proportional controller to locally maintain the pendulum in the upright position. The authors have shown that when this proportional is delayed and if the time-delay sampling is not too large, the controller still locally stabilizes the system. Among others, using the center manifold theorem and normal forms, they show the loss of stability when the delay exceeds a critical value and a supercritical Andronov-Hopf Bifurcation [134] occurs generating stable limit cycles. Finally, the described approach as well as all the above cited results emphasize the importance of the imaginary roots and motivate investigations making them more understood.

10.7 Concluding remarks and future work

This paper addressed the problem of characterizing the dimension of the generalized eigenspace associated with a zero singularity for time-delay systems (the explicit conditions guaranteeing a given dimension) as well as an effective sharp bound for such a dimension. The existing links between the codimension of the zero singularity and functional Birkhoff matrices are emphasized. It is shown that the codimension bound of the zero singularity relies on the number of nonzero coefficients rather than the degree of the corresponding quasipolynomial. As a matter of fact, for generic quasipolynomials, a linear algebra alternative proof for the Pólya-Segö bound [176] is proposed. In the case of sparse quasipolynomials, a sharper bound

for the codimension of the zero singularity is established under the non degeneracy of an appropriate functional Birkhoff matrix. It is worth noting, that the established LU-developments yields some new possibilities in the study of "poised"- ness of Birkhoff incidence matrices.

Finally, we emphasize that the proposed approach can be extended to wider classes of functional equations, for instance, neutral systems and delay-difference equations. In the next step, the effect of the rational dependency of the delays on the codimension bound of the zero singularity will be explored.

Appendix

In this section, we first summarize the main notations in Table 10.1. Then, for the sake of self-containment, we report some results selected from the literature. Finally, some useful auxiliary lemmas are presented and proved. The proofs of Theorem 34 and Theorem 35 are provided.

<div align="center">

TABLE 10.1 – Table of the Main Notations

</div>

λ	a complexe number.
$\mathcal{R}(\lambda)$	real part of λ.
$\mathcal{I}(\lambda)$	imaginary part of λ.
τ	a delay vector.
σ	an auxiliary delay vector.
z	the vector state of the dynamical system.
n	the number of scalar differential equations defining a system.
N	the number of the delays involved in the dynamical system.
$\Delta(\lambda, \tau)$	a quasipolynomial function.
$P_i(\lambda)$	the quasipolynomial associated polynomials.
$a_{,l}$	coefficient of λ^l of the -th polynomial of Δ.
χ	spectrum associated to a given quasipolynomial.
χ_+	the set of instable spectral values.
χ_-	the set of stable spectral values.
χ_0	the set of critical spectral values i.e. crossing imaginary roots.
$\sharp$	cardinality of a set.
g	unknown function to interpolate.
x_i	interpolating points.
$\hat{P}$	interpolating polynomial.
$\mathcal{E}$	incidence matrix.
$\mathcal{V}$	the corresponding incidence vector.
$e_{i,j}$	entries of the incidence matrix.
Υ	a functional Birkhoff matrix corresponding to a sufficiently regular function ϖ.
$\hat{\Upsilon}$	coalescence matrix associeted to Υ.

Let us start by reporting some useful results from the mentioned literature. When a given quasipolynomial function corresponding to a retarded system has no roots on the imaginary axis, then the main result from [205] gives the exact number of unstable roots, see also [206, Theorem 2.15-2.16]. The proof of such a result is maily based on the argument principle. Motivated by a potential application in bifurcation theory, the main theorem from [119], which is strongly inspired from Stepan's theorem, relaxes the assymption $\mathbf{card}(\chi_0) = \emptyset$. Thus, it emphasizes the link between $\mathbf{card}(\chi_+)$ and $\mathbf{card}(\chi_0)$, both take into account the multiplicity.

Theorem 36 (Hassard, [119], pp. 223). *Consider the quasipolynomial function Δ defined by (10.4). Let $\rho_1, \ldots, \rho_r$ be the positive roots of $\mathcal{R}(y) = \Re(i^n \Delta(i\,y))$, counted by their multiplicities and ordered so that $0 < \rho_1 \leq \ldots \leq \rho_r$. For each $j = 1, \ldots, r$ such that $\Delta(i\,\rho_j) = 0$, assume that the multiplicity of $i\rho_j$ as a zero of $\Delta(\lambda, \tau)$ is the same as the multiplicity of ρ_j as a root of $\mathcal{R}(y)$. Then $\mathbf{card}(\chi_+)$ is given by the formula :*

$$\mathbf{card}(\chi_+) = \frac{n - \mathbf{card}(\chi_0)}{2} + \frac{(-1)^r}{2} sgn\mathcal{I}^{(\mu)}(0) + \sum_{j=1}^{r} sgn\mathcal{I}(\rho_j), \qquad (10.41)$$

where μ designate the multiplicity of the zero spectral value of $\Delta(\lambda, \tau) = 0$ and $\mathcal{I}(y) = \Im(i^{-n}\Delta(iy))$. Furthermore, $\mathbf{card}(\chi_+)$ is odd (respectively, even) if $\Delta^{(\mu)}(0) < 0$ ($\Delta^{(\mu)}(0) > 0$). If $\mathcal{R}(y) = 0$ has no positive zeros, set $r = 0$ and omit the summation term in the expression of $\mathbf{card}(\chi_+)$. If $\lambda = 0$ is not a root of the characteristic equation, set $\mu = 0$ and interpret $\mathcal{I}^{(0)}(0)$ as $\mathcal{I}(0)$ and $\Delta^{(0)}(0)$ as $\Delta(0)$.

The following result from [176] gives a valuable information allowing to have a first estimation on the bound for the codimension of the zero spectral value.

Proposition 10 (Pólya-Szegö, [176], pp. 144). *Let $\tau_1, \ldots, \tau_N$ denote real numbers such that*

$$\tau_1 < \tau_2 < \ldots < \tau_N,$$

and $d_1, \ldots, d_N$ positive integers satisfying

$$d_1 \geq 1, \; d_2 \geq 1 \; \ldots \; d_N \geq 1, \quad d_1 + d_2 + \ldots + d_N = D + N.$$

Let $f_{i,j}(s)$ stands for the function $f_{i,j}(s) = s^{j-1}\,e^{\tau_i\,s}$, for $1 \leq j \leq d_i$ and $1 \leq i \leq N$. Let $\sharp$ be the number of zeros of the function

$$f(s) = \sum_{1 \leq i \leq N, 1 \leq j \leq d_i} c_{i,j}\,f_{i,j}(s),$$

that are contained in the horizontal strip $\alpha \leq \mathcal{I}(z) \leq \beta$. Assuming that

$$\sum_{1 \leq k \leq d_1} |c_{1,k}| > 0, \; \ldots, \; \sum_{1 \leq k \leq d_N} |c_{N,k}| > 0,$$

then

$$\frac{(\tau_N - \tau_1)\,(\beta - \alpha)}{2\,\pi} - D + 1 \leq \sharp \leq \frac{(\tau_N - \tau_1)\,(\beta - \alpha)}{2\,\pi} + D + N - 1.$$

Setting $\alpha = \beta = 0$, the above Proposition allows to $\sharp_{PS} \leq D + N - 1$ where D stands for the sum of the degrees of the polynomials involved in the quasipolynomial function f and N designate the associated number of polynomials. This gives a sharp bound in the case of complete polynomials.

In the sequel, we present some useful lemmas as well as the proofs of the claimed theorems.

Lemma 2. *Zero is a root of $\Delta^{(k)}(\lambda)$ for $k \geq 0$ if, and only if, the coefficients of P_{M^j} for $0 \leq j \leq \tilde{N}_{N,n}$ satisfy the following assertion*

$$a_{0,k} = -\sum_{i \in S_{N,n}} \left[a_{i,k} + \sum_{l=0}^{k-1} \frac{a_{i,l}\sigma_i^{k-l}}{(k-l)!} \right]. \tag{A.1}$$

Démonstration. We define the family ∇_k for all $k \geq 0$ by

$$\nabla_k(\lambda) = \sum_{i=0}^{\tilde{N}_{N,n}} \frac{d^k}{d\lambda^k} P_{M^i}(\lambda) + \sum_{j=0}^{k-1} \left(\binom{k}{j} \sum_{i=1}^{\tilde{N}_{N,n}} \sigma_i^{k-j} \frac{d^j}{d\lambda^j} P_{M^i}(\lambda) \right), \tag{A.2}$$

here, $M^0 \triangleq 0$ and $\frac{d^0}{d\lambda^0} f(\lambda) \triangleq f(\lambda)$. Obviously, the defined family ∇_k is polynomial since P_i and their derivatives are polynomials. Moreover, zero is a root of $\Delta^{(k)}(\lambda)$ for $k \geq 0$ if, and only if, zero is a root of $\nabla_k(\lambda)$. This can be proved by induction. More precisely, differentiating k times $\Delta(\lambda, \tau)$ the following recursive formula is obtained :

$$\Delta^{(k)}(\lambda) = \sum_{i=0}^{\tilde{N}_{N,n}} \frac{d^k}{d\lambda^k} P_{M^i}(\lambda) e^{\sigma_i \lambda} + \sum_{j=0}^{k-1} \left(\binom{k}{j} \sum_{i=1}^{\tilde{N}_{N,n}} \sigma_i^{k-j} \frac{d^j}{d\lambda^j} P_{M^i}(\lambda) e^{\sigma_i \lambda} \right).$$

Since only the zero root is of interest, we can set $e^{\sigma_i \lambda} = 1$ which define the polynomial functions ∇_k. Moreover, careful inspection of the obtained quantities presented in (A.2) and substituting $\frac{d^k}{d\lambda^k} P_i(0) = k! \, a_{i,k}$ leads to the formula (A.1). $\qquad\square$

Here, we prove the results given in section 10.4.2, that is, we consider the incidence vector :

$$\mathcal{V} = (\underbrace{x_1, \ldots, x_1}_{d_1}, \underbrace{\star, \ldots, \star}_{d_*}, x_2).$$

The right hand side of the last equality from (10.23) defining U_{i,d_1+1} for $2 \leq i \leq d_1+1$ can be also written as follows.

Lemma 3. *For $2 \leq i \leq d_1 + 1$ the following equality is satisfied :*

$$\Upsilon_{i,d_1+1} - (i-1) \int_0^{x_1} U_{i-1,d_1+1}(y,x_2) dy = \sum_{k=0}^{i-1} \binom{i-1}{k} (-1)^{i-1-k} x_1^{i-1-k} \Upsilon_{k+1,d_1+1}.$$

Proof of Lemma 3. First, one has $U_{2,d_1+1} = \Upsilon_{2,d_1+1} - x_1 \Upsilon_{1,d_1+1} = \Upsilon_{2,d_1+1} - \int_0^{x_1} U_{1,d1+1}(y,x_2) \, dy$ since $U_{1,d1+1} = \Upsilon_{1,d_1+1}(x_2)$.

Now, let assume that for $2 \leq i \leq p$ where $p < d_1 + 1$ the following equality is satisfied :

$$\sum_{l=0}^{i-1} \binom{i-1}{l} (-1)^{i-1-l} x_1^{i-1-l} \Upsilon_{l+1,d_1+1} = \Upsilon_{i,d_1+1} - (i-1) \int_0^{x_1} U_{i-1,d_1+1}(y, x_2) \, dy.$$

One has to show that for $i = p + 1$:

$$\sum_{l=0}^{p} \binom{p}{l} (-1)^{p-l} x_1^{p-l} \Upsilon_{l+1,d_1+1} = \Upsilon_{p+1,d_1+1} - (p) \int_0^{x_1} U_{p,d_1+1}(y, x_2) \, dy.$$

Indeed,

$$\begin{cases} -\int_0^{x_1} p\, U_{p,d_1+1}(y, x_2) \, dy = -\int_0^{x_1} p \sum_{l=0}^{p-1} \binom{p-1}{l} (-1)^{p-1-l} s^{p-1-l} \Upsilon_{l+1,d_1+1} \, ds, \\[2mm] = -\sum_{l=0}^{p-1} \frac{p!}{l! \, (p-l-1)!} (-1)^{p-1-l} \Upsilon_{l+1,d_1+1} \int_0^{x_1} s^{p-1-l} ds, \\[2mm] = \sum_{l=0}^{p-1} \binom{p}{l} (-1)^{p-l} x_1^{p-l} \Upsilon_{l+1,d_1+1}. \end{cases}$$

$\square$

Proof of Theorem 34. The only difference between algorithms (10.23) and (10.20) lies in definition of the last column of the matrix U. Thus, one has to show that for any $2 \leq i \leq d_1 + 1$ the following equality holds $\Upsilon_{i,d_1+1} = \sum_{k=1}^{i} L_{i,k} U_{k,d_1+1}$. By definition, one has

$$\begin{cases} \Upsilon_{2,d_1+1} = \sum_{k=1}^{2} L_{2,k} U_{k,d_1+1} \\[2mm] \quad\quad = L_{2,1} U_{1,d_1+1} + L_{2,2} U_{2,d_1+1} \\[2mm] \quad\quad = x_1 \Upsilon_{1,d_1+1} + U_{2,d_1+1}. \end{cases} \tag{10.42}$$

Now, let assume that for $2 \leq i \leq p$ where $p < d_1 + 1$ the following equality is satisfied :

$$U_{i,d_1+1} = \Upsilon_{i,d_1+1} - (i-1) \int_0^{x_1} U_{i-1,d_1+1}(y, x_2) \, dy,$$

or equivalently, from Lemma 3

$$U_{i,d_1+1} = \sum_{l=0}^{i-1} \binom{i-1}{l} (-1)^{i-1-l} x_1^{i-1-l} \Upsilon_{l+1,d_1+1}.$$

It stills to show that the last equality from (10.23) holds for U_{p+1,d_1+1} when $p < d_1 + 1$. Indeed, by definition

$$U_{p+1,d_1+1} = \Upsilon_{p+1,d_1+1} - \sum_{k=1}^{p} L_{p+1,k} U_{k,d_1+1}.$$

Moreover, (for same arguments as the ones given in the proof of Lemma 7 presented in the sequel), one has $L_{p+1,k} = \frac{1}{k-1}\frac{\partial L_{p+1,k-1}}{\partial x_1}$. Thus, $L_{p+1,k} = \frac{1}{(k-1)!}\frac{\partial^{k-1}L_{p+1,1}}{\partial x_1^{k-1}} = \frac{1}{(k-1)!}\frac{\partial^{k-1}x_1^p}{\partial x_1^{k-1}} = \frac{p!\,x_1^{p-k+1}}{(p-k+1)!\,(k-1)!}$. So that, one has :

$$L_{p+1,k} = \binom{p}{k-1} x_1^{p-(k-1)}. \tag{10.43}$$

Now, by definition of U_{p+1,d_1+1} and using (10.43) as well as the recurrence assumption, we obtain

$$
\left\{
\begin{aligned}
U_{p+1,d_1+1} &= \Upsilon_{p+1,d_1+1} - \sum_{=1}^{p} L_{p+1,}U_{,d_1+1} \\
&= \Upsilon_{p+1,d_1+1} - \sum_{=1}^{p}\sum_{l=0}^{k-1} \binom{-1}{l}\binom{p}{-1}(-1)^{-l-1}\,x_1^{-l-1}\,x_1^{p-(-1)}\,\Upsilon_{l+1,d_1+1} \\
&= \Upsilon_{p+1,d_1+1} - \sum_{=1}^{p}\sum_{l=0}^{-1} \binom{-1}{l}\binom{p}{-1}(-1)^{-1-l}\,x_1^{p-l}\,\Upsilon_{l+1,d_1+1}
\end{aligned}
\right.
$$

Thus, one has to prove that

$$\sum_{k=0}^{p-1}\binom{p}{k}(-1)^{p-k}\,x_1^{p-k}\,\Upsilon_{k+1,d_1+1} = -\sum_{=1}^{p}\sum_{l=0}^{-1}\binom{-1}{l}\binom{p}{-1}(-1)^{-1-l}\,x_1^{p-l}\,\Upsilon_{l+1,d_1+1}. \tag{10.44}$$

Recall that, the two side expressions of (10.44) are polynomials in x_1 and x_2. The only quantities depending in x_2 are $(\Upsilon_{k,d_1+1})_{1\le k\le p}$. Since, $\deg(\Upsilon_{k,d_1+1}) \ne \deg(\Upsilon_{k',d_1+1})$ for $k \ne k'$, it will be enough to we examine the equality of coefficients of the two side expressions in Υ_{m+1,d_1+1} for arbitrarily chosen $0 \le m \le p-1$. So that, let $m = k_0$ for which corresponds $m = l_0$ in the right hand side quantity from (10.44). Then consider the coefficient of $x_1^{p-m}\Upsilon_{m+1,d_1+1}$ from the two sides of (10.44) . Now, one easily check that $\sum_{=m}^{p}\binom{-1}{m}\binom{p}{-1}(-1)^{-m} = (-1)^{p-m}\binom{p}{m}$ is always satisfied, which ends the proof.

□

In what follow, we propose some lemmas exhibiting some interesting properties of functional Birkhoff matrices. Those will be useful for the analytical proof of Theorem 35.

Lemma 4. *Equation* (10.30) *is equivalent to :*

$$U_{i,j} = \sum_{l=0}^{i-1}\binom{i-1}{l}(-1)^l\,x_1^l\,\Upsilon_{i-l,j} \quad for \quad j = d_1+d_2^-+1 \text{ and } 2 \le i \le d_1+1. \tag{10.45}$$

Proof of Lemma 4. The equality (10.45) follows directly by induction. First, one checks that

$$\Upsilon_{2,d_1+d_2^-+1} = U_{2,d_1+d_2^-+1} + x_1\,\Upsilon_{1,d_1+d_2^-+1}.$$

Indeed,

$$
\begin{cases}
\Upsilon_{2,d_1+d_2^-+1} = \displaystyle\sum_{k=1}^{2} L_{2,k}\, U_{k,d_1+d_2^-+1} \\[2mm]
\qquad = L_{2,1}\, U_{1,d_1+d_2^-+1} + L_{2,2}\, U_{2,d_1+d_2^-+1} \\[2mm]
\qquad = x_1\, \Upsilon_{1,d_1+d_2^-+1} + U_{2,d_1+d_2^-+1},
\end{cases}
\tag{10.46}
$$

since $L_{2,2}=1$. Now, let assume that

$$
U_{i,j} = \sum_{l=0}^{i-1} \binom{i-1}{l} (-1)^l\, x_1^l\, \Upsilon_{i-l,j} \quad \text{for} \quad j = d_1+d_2^-+1 \text{ and } 2 \le i \le p \text{ and } p < d_1+1,
\tag{10.47}
$$

From Equation (10.30) one has

$$
U_{p+1,d_1+d_2^-+1} = \Upsilon_{p+1,d_1+d_2^-+1} - p \int_0^{x_1} U_{p,d_1+d_2^-+1}(y,x_2)dy.
$$

Using (10.47), one has,

$$
\begin{cases}
U_{p+1,d_1+d_2^-+1} \\[2mm]
= \Upsilon_{p+1,d_1+d_2^-+1} \\[2mm]
\quad - p \int_0^{x_1} \left(\Upsilon_{p,d_1+d_2^-+1}(y,x_2) + \sum_{l=1}^{p-1} \binom{p-1}{l}(-1)^l y^l\, \Upsilon_{p-l,d_1+d_2^-+1}(y,x_2) \right) dy \\[2mm]
= \Upsilon_{p+1,d_1+d_2^-+1} - p\, \Upsilon_{p,d_1+d_2^-+1} x_1 + \sum_{l=1}^{p-1} p\binom{p-1}{l}(-1)^l\, \Upsilon_{p-l,d_1+d_2^-+1} \int_0^{x_1} y^l\, dy \\[2mm]
= \sum_{l=0}^{p} \binom{p}{l}(-1)^l\, x_1^l\, \Upsilon_{p+1-l,d_1+d_2^-+1}.
\end{cases}
$$

which ends the proof. $\square$

Lemma 5.

$$
\Upsilon_{i+1,j} = x_2\, \Upsilon_{i,j} + (d_2^- + d^*) \int_0^{x_2} \Upsilon_{i,j}(y)\, dy \quad \text{for} \quad j = d_1 + d_2^- + 1 \text{ and } 1 \le i \le d_1 + d_2^-.
\tag{10.48}
$$

Proof of Lemma 5. Let consider the *coalescence* [139] confluent Vandermonde matrice $\hat{\Upsilon}$ which regularize the considered Birkhoff matrice Υ. That is $\hat{\Upsilon}$ is the rectangular matrix associated with the incidence matrix

$$
\mathcal{V} = (\underbrace{x_1,\ldots,x_1}_{d_1}, \underbrace{x_2,\ldots,x_2}_{d_2^-}, \underbrace{x_2,\ldots,x_2}_{d_*}, x_2).
$$

Here, the "stars" $\star$ in (10.32) are simply replaced by x_2. Thus, Υ and $\hat{\Upsilon}$ have the same number of rows, but the number of columns of $\hat{\Upsilon}$ exceeds the columns number

of Υ by d^*. We point out that $\Upsilon_{i+1,d_1+d_2^-+1}$ is nothing but $\hat{\Upsilon}_{i+1,d_1+d_2^-+1+d^*}$. This means that the term $(d_2^- + d^*) \int_0^{x_2} \Upsilon_{i,j}$ in (10.48) is exactly $\hat{\Upsilon}_{i+1,d_1+d_2^-+d^*}$. Thus, equality (10.48) turns to be

$$\bar{\Upsilon}_{i+1,j} = x_2 \bar{\Upsilon}_{i,j} + \bar{\Upsilon}_{i,j-1} \quad \text{for} \quad j = d_1 + d_2^- + 1 + d^* \text{ and } 1 \leq i \leq d_1 + d_2^-.$$

This last equality can be easily proved by using a 2-D recurrence in terms of $\bar{\Upsilon}$ (regular matrix) as in the proof of Theorem 12 to show that it applies even for $d_1 + 2 \leq j \leq d_1 + d_2^- + 1 + d^*$. $\qquad\square$

The following Lemma provides an other way defining the components of U given by (10.30).

Lemma 6. *for all $i = 1, \ldots, d_1$ and $j = d_1 + d_2^- + 1$ the following equality applies*

$$U_{i+1,j^*} = (x_2 - x_1) U_{i,j^*} + (d_2^- + d^*) \int_0^{x_2} U_{i,j^*}(y) dy. \qquad (10.49)$$

Proof of Lemma 6. Let set

$$\mathcal{I}_k = U_{k+1,j^*} + (x_1 - x_2) U_{k,j^*} - (d_2^- + d^*) \int_0^{x_2} U_{k,j^*}(y) dy.$$

where $j^* = d_1 + d_2^- + 1 + d^*$ and $1 \leq k \leq d_1 + 1$.

Substitute equation (10.45) from lemma 4 in $\mathcal{I}_k$, to obtain

$$\mathcal{I}_k = \sum_{l=0}^{k} \binom{k}{l} (-1)^l x_1^l \Upsilon_{k+1-l,j^*}$$

$$- \sum_{l=0}^{k-1} \binom{k-1}{l} (-1)^l x_1^l \left((x_2 - x_1) \Upsilon_{k-l,j^*} + (d_2^- + d^*) \int_0^{x_2} \Upsilon_{k-l,j^*}(y) dy \right).$$

Using lemma 5, one obtains

$$\mathcal{I}_k = \sum_{l=1}^{k-1} (-1)^l x_1^l \left[\left(\binom{k}{l} - \binom{k-1}{l} \right) \Upsilon_{k+1-l,j^*} + x_1 \binom{k-1}{l} \Upsilon_{k-l,j^*} \right]$$

$$+ (-1)^k x_1^k \Upsilon_{1,j^*} + x_1 \Upsilon_{k,j^*}$$

$$= \sum_{l=1}^{k-1} (-1)^l x_1^l \left(\binom{k-1}{l-1} \Upsilon_{k+1-l,j^*} + x_1 \binom{k-1}{l} \Upsilon_{k-l,j^*} \right) + (-1)^k x_1^k \Upsilon_{1,j^*}$$

$$+ x_1 \Upsilon_{k,j^*}$$

which is as expected identically zero, that ends the proof. $\qquad\square$

The following Lemma provides a differential relation between the coefficients of L matrix.

Lemma 7. *for all $1 \leq k \leq p$ the following equality holds*

$$\frac{\partial L_{d_1+p,d_1+k}}{\partial x_2} = k\, L_{d_1+p,d_1+k+1} \tag{10.50}$$

The following result applies when dealing with $\Upsilon_{i,j}$ and $\Upsilon_{i,j-1}$ are in the same variable block. We emphasize that such a property is inherited by the expressions of L defined in (10.28).

Proof of Lemma 7. The proof is 2-D recurrence-based. First, one easily check that for $p = 2$ then $k = 1$

$$L_{d_1+2,d_1+2} = \frac{\partial L_{d_1+2,d_1+1}}{\partial x_2}$$

since by definition of L one has $L_{d_1+2,d_1+1} = L_{d_1+1,d_1} + x_2\, L_{d_1+1,d_1+1} = L_{d_1+1,d_1} + x_2$ and $\frac{\partial L_{d_1+1,d_1}}{\partial x_2} = 0$. When assuming that

$$L_{d_1+p,d_1+2} = \frac{\partial L_{d_1+p,d_1+1}}{\partial x_2},$$

and again, using the definition of L, one obtains,

$$L_{d_1+p+1,d_1+2} = L_{d_1+p,d_1+1} + x_2 L_{d_1+p,d_1+2},$$
$$L_{d_1+p+1,d_1+1} = L_{d_1+p,d_1} + x_2 L_{d_1+p,d_1+1},$$

which as expected gives :

$$\frac{\partial L_{d_1+p+1,d_1+1}}{\partial x_2} = L_{d_1+p,d_1+1} + x_2 \frac{\partial L_{d_1+p,d_1+1}}{\partial x_2}$$
$$= L_{d_1+p,d_1+1} + x_2 L_{d_1+p,d_1+2} = L_{d_1+p+1,d_1+2}.$$

Let assume that for any $2 < p < d_2^- + 1$ and $k = 1, \ldots, p-1$ one has

$$\frac{\partial L_{d_1+p,d_1+k}}{\partial x_2} = k\, L_{d_1+p,d_1+k+1}.$$

One has to prove the following equalities :

$$\begin{cases} \dfrac{\partial L_{d_1+p+1,d_1+k}}{\partial x_2} = k\, L_{d_1+p+1,d_1+k+1}, \\[2mm] \dfrac{\partial L_{d_1+p,d_1+k+1}}{\partial x_2} = (k+1)\, L_{d_1+p,d_1+k+2}, \\[2mm] \dfrac{\partial L_{d_1+p+1,d_1+k+1}}{\partial x_2} = (k+1)\, L_{d_1+p+1,d_1+k+2}. \end{cases} \tag{10.51}$$

Let us consider the first equality of (10.51), using the definition of L that asserts that

$$L_{d_1+p+1,d_1+k+1} = L_{d_1+p,d_1+k} + x_2 L_{d_1+p,d_1+k+1}$$
$$L_{d_1+p+1,d_1+k} = L_{d_1+p,d_1+k-1} + x_2 L_{d_1+p,d_1+k}.$$

Which gives

$$\frac{\partial L_{d_1+p+1,d_1+k}}{\partial x_2} = \frac{\partial L_{d_1+p,d_1+k-1}}{\partial x_2} + x_2 \frac{\partial L_{d_1+p,d_1+k}}{\partial x_2} + L_{d_1+p,d_1+k}$$

$$= (k-1)L_{d_1+p,d_1+k} + k\, L_{d_1+p,d_1+k+1} + L_{d_1+p,d_1+k}$$

$$= k\, L_{d_1+p+1,d_1+k+1}.$$

By the same way, the remaining two equality from (10.51) are obtained :

$$\frac{\partial L_{d_1+p,d_1+k+1}}{\partial x_2} = \frac{\partial \left(L_{d_1+p-1,d_1+k} + x_2 L_{d_1+p-1,d_1+k+1} \right)}{\partial x_2}$$

$$= \frac{\partial L_{d_1+p-1,d_1+k}}{\partial x_2} + x_2 \frac{\partial L_{d_1+p-1,d_1+k+1}}{\partial x_2} + L_{d_1+p-1,d_1+k+1}$$

$$= kL_{d_1+p-1,d_1+k+1} + (k+1)\, x_2 L_{d_1+p-1,d_1+k+2} + L_{d_1+p-1,d_1+k+1}$$

$$= (k+1)\, L_{d_1+p,d_1+k+2},$$

and

$$\frac{\partial L_{d_1+p+1,d_1+k+1}}{\partial x_2} = \frac{\partial \left(L_{d_1+p,d_1+k} + x_2 L_{d_1+p,d_1+k+1} \right)}{\partial x_2}$$

$$= \frac{\partial L_{d_1+p,d_1+k}}{\partial x_2} + x_2 \frac{\partial L_{d_1+p,d_1+k+1}}{\partial x_2} + L_{d_1+p,d_1+k+1}$$

$$= kL_{d_1+p,d_1+k+1} + (k+1)\, x_2 L_{d_1+p,d_1+k+2} + L_{d_1+p,d_1+k+1}$$

$$= (k+1)\, L_{d_1+p+1,d_1+k+2}.$$

that ends the proof. $\qquad\square$

Proof of Theorem 35. The only change occurring in (10.26)-(10.31) compared with (10.20) is the way in defining the column $d_1 + d_2^- + 1$ of U. Moreover, such a column is only involved in computing the column $d_1 + d_2^- + 1$ of Υ. Thus, it stills to show that the equalities (10.30) and (10.31) ; this will be done by recurrence. Equation (10.30) follow directly by induction from lemma 4.

Let us focus now on (10.31) and denote $j^* = d_1 + d_2^- + 1$. First, let us check that

$$U_{d_1+2,j^*} = (d_2^- + d^*) \int_0^{x_2} U_{d_1+1,j^*}(x_1, y)\, dy.$$

From the one side, using lemma 5 one has

$$\Upsilon_{d+2,j^*} = x_2\, \Upsilon_{d+1,j^*} + (d_2^- + d^*) \int_0^{x_2} \Upsilon_{d+1,j^*}(y)\, dy,$$

$$= x_2 \sum_{k=1}^{d_1+1} L_{d_1+1,k} U_{k,j^*} + (d_2^- + d^*) \int_0^{x_2} \sum_{k=1}^{d_1+1} L_{d_1+1,k} U_{k,j^*}(y)\, dy.$$

Since by definition one has $L_{d_1+1,d_1+1} = 1$ and $L_{d_1+1,k} = L_{d_1+1,k}(x_1)$ for $k \in \{1, \ldots, d_1\}$ then

$$\Upsilon_{d+2,j^*} = x_2 \sum_{k=1}^{d_1+1} L_{d_1+1,k} U_{k,j^*} + (d_2^- + d^*) \sum_{k=1}^{d_1} L_{d_1+1,k} \int_0^{x_2} U_{k,j^*}(y) dy$$
$$+ (d_2^- + d^*) \int_0^{x_2} U_{d_1+1,j^*}(y) dy.$$

From the other side and by definition of Υ,

$$\Upsilon_{d_1+2,j^*} = \sum_{k=1}^{d_1+2} L_{d_1+2,k} U_{k,j^*} = U_{d_1+2,j^*} + \sum_{k=1}^{d_1+1} L_{d_1+2,k} U_{k,j^*}.$$

To prove (10.31) for $i = d_1 + 2$ one has to prove that

$$\sum_{k=1}^{d_1+1} L_{d_1+2,k} U_{k,j^*} = x_2 \sum_{k=1}^{d_1+1} L_{d_1+1,k} U_{k,j^*} + (d_2^- + d^*) \sum_{k=1}^{d_1} L_{d_1+1,k} \int_0^{x_2} U_{k,j^*}(y) dy,$$

or equivalently to prove

$$\sum_{k=1}^{d_1+1} \left(L_{d_1+2,k} - x_2 L_{d_1+1,k} \right) U_{k,j^*} - (d_2^- + d^*) \sum_{k=1}^{d_1} L_{d_1+1,k} \int_0^{x_2} U_{k,j^*}(y) dy = 0. \tag{10.52}$$

Using equation (10.28), one obtain

$$L_{d_1+2,k} - x_2 L_{d_1+1,k} = L_{d_1+1,k-1} + (x_1 - x_2) L_{d_1+1,k}, \quad \text{for } k = 1, \ldots, d_1,$$
$$L_{d_1+2,d_1+1} - x_2 L_{d_1+1,d_1+1} = L_{d_1+1,d_1}.$$

Thus, the right hand side of (10.52) becomes

$$\sum_{k=1}^{d_1} L_{d_1+1,k} U_{k+1,j^*} + (x_1 - x_2) \sum_{k=1}^{d_1} L_{d_1+1,k} U_{k,j^*}$$
$$- (d_2^- + d^*) \sum_{k=1}^{d_1} L_{d_1+1,k} \int_0^{x_2} U_{k,j^*}(y) dy =$$
$$\sum_{k=1}^{d_1} L_{d_1+1,k} \left(U_{k+1,j^*} + (x_1 - x_2) U_{k,j^*} - (d_2^- + d^*) \int_0^{x_2} U_{k,j^*}(y) dy \right).$$

Lemma 6 asserts that for all $i = 1, \ldots, d_1$ and $j = d_1 + d_2^- + 1$ one has

$$U_{k+1,j^*} + (x_1 - x_2) U_{k,j^*} - (d_2^- + d^*) \int_0^{x_2} U_{k,j^*}(y) dy = 0 \tag{10.53}$$

which implies that (10.31) applies for $i = d_1 + 2$.

Let assume now that, (10.31) is satisfied for $i = d_1 + 2, \ldots, d_1 + p$ where $1 < p < d_2^- + d^*$. It stills to prove that (10.31) is satisfied for $i = d_1 + p + 1$.

By the same argument as for $i = d_1 + 2$, one has

$$
\begin{aligned}
\Upsilon_{d_1+p+1,j^*} &= x_2\, \Upsilon_{d+p,j^*} + (d_2^- + d^*) \int_0^{x_2} \Upsilon_{d+p,j^*}(y)\, dy, \\
&= x_2 \sum_{k=1}^{d_1+p} L_{d_1+p,k} U_{k,j^*} (d_2^- + d^*) \sum_{k=1}^{d_1+p-1} \int_0^{x_2} L_{d_1+p,k} U_{k,j^*}(y) dy \\
&\quad + (d_2^- + d^*) \int_0^{x_2} U_{d_1+p,j^*}(y) dy \\
&= x_2 \sum_{k=1}^{d_1+p} L_{d_1+p,k} U_{k,j^*} + (d_2^- + d^*) \sum_{k=1}^{d_1+p-1} \int_0^{x_2} L_{d_1+p,k} U_{k,j^*}(y) dy \\
&\quad + (p-1) \int_0^{x_2} U_{d_1+p,j^*}(y) dy + (d_2^- + d^* - p + 1) \int_0^{x_2} U_{d_1+p,j^*}(y) dy
\end{aligned}
$$

From the other side, we obtain

$$
\Upsilon_{d_1+p+1,j^*} = \sum_{k=1}^{d_1+p} L_{d_1+p+1,k} U_{k,j^*} + U_{d_1+p+1,j^*}.
$$

Hence, we have to prove that

$$
\begin{aligned}
&\sum_{k=1}^{d_1+p} L_{d_1+p+1,k} U_{k,j^*} - x_2 \sum_{k=1}^{d_1+p} L_{d_1+p,k} U_{k,j^*} - (d_2^- + d^*) \sum_{k=1}^{d_1+p-1} \int_0^{x_2} L_{d_1+p,k} U_{k,j^*}(y) dy \\
&= (p-1) \int_0^{x_2} U_{d_1+p,j^*}(y) dy.
\end{aligned}
$$

Now, using the result from Lemma 6, one has to prove that

$$
\sum_{k=d_1+2}^{d_1+p} L_{d_1+p+1,k} U_{k,j^*} - x_2 \sum_{k=d_1+2}^{d_1+p} L_{d_1+p,k} U_{k,j^*} \tag{10.54}
$$

$$
- (d_2^- + d^*) \sum_{k=d_1+1}^{d_1+p-1} \int_0^{x_2} L_{d_1+p,k} U_{k,j^*}(y) dy \tag{10.55}
$$

$$
= (p-1) \int_0^{x_2} U_{d_1+p,j^*}(y) dy. \tag{10.56}
$$

Using equation (10.28), one obtains

$$
L_{d_1+p+1,k} - x_2\, L_{d_1+p,k} = L_{d_1+p,k-1}, \quad \text{for } k = d_1 + 2, \ldots, d_1 + p.
$$

Finally, equation (10.54) becomes

$$E = \sum_{k=1}^{p-1} L_{d_1+p,d_1+k} U_{d_1+k+1,j^*} - (d_2^- + d^*) \sum_{k=1}^{p-1} \int_0^{x_2} L_{d_1+p,d_1+k} U_{d_1+k,j^*}(y) dy$$
$$- (p-1) \int_0^{x_2} U_{d_1+p,j^*}(y) dy = 0.$$
(10.57)

Differentiating E given in (10.57) with respect to the variable x_2 one obtains

$$\frac{\partial E}{\partial x_2} = \sum_{k=1}^{p-1} \left(\frac{\partial L_{d_1+p,d_1+k}}{\partial x_2} U_{d_1+k+1,j^*} + L_{d_1+p,d_1+k} \frac{\partial U_{d_1+k+1,j^*}}{\partial x_2} \right)$$
$$- (d_2^- + d^*) \sum_{k=1}^{p-1} L_{d_1+p,d_1+k} U_{d_1+k,j^*} - (p-1) U_{d_1+p,j^*}$$
$$= \sum_{k=1}^{p-1} \frac{\partial L_{d_1+p,d_1+k}}{\partial x_2} U_{d_1+k+1,j^*}$$
$$+ \sum_{k=1}^{p-1} L_{d_1+p,d_1+k} \left(\frac{\partial U_{d_1+k+1,j^*}}{\partial x_2} - (d_2^- + d^*) U_{d_1+k,j^*} \right) - (p-1) U_{d_1+p,j^*}$$

By using the recurrence assumption, one obtains,

$$\frac{\partial E}{\partial x_2} = \sum_{k=1}^{p-1} \frac{\partial L_{d_1+p,d_1+k}}{\partial x_2} U_{d_1+k+1,j^*} - (p-1) U_{d_1+p,j^*}$$
$$+ \sum_{k=1}^{p-1} L_{d_1+p,d_1+k} \left((d_2^- + d^* - (k-1)) U_{d_1+k,j^*} - (d_2^- + d^*) U_{d_1+k,j^*} \right)$$
$$= \sum_{k=1}^{p-1} \frac{\partial L_{d_1+p,d_1+k}}{\partial x_2} U_{d_1+k+1,j^*} - \sum_{k=2}^{p-1} (k-1) L_{d_1+p,d_1+k} U_{d_1+k,j^*} - (p-1) U_{d_1+p,j^*}$$
$$= \sum_{k=1}^{p-2} \left(\frac{\partial L_{d_1+p,d_1+k}}{\partial x_2} - k L_{d_1+p,d_1+1+k} \right) U_{d_1+1+k,j^*}$$
$$+ \left(\frac{\partial L_{d_1+p,d_1+p-1}}{\partial x_2} - (p-1) \right) U_{d_1+p,j^*} \equiv 0,$$

which is as expected zero since Lemma 7 asserts that each factor is identically zero, that ends the proof. $\qquad\square$

Tracking the Algebraic Multiplicity of Crossing Imaginary Roots for Generic Quasipolynomials : A Vandermonde-Based Approach

A standard approach in analyzing dynamical systems consists in identifying and understanding the eigenvalues bifurcations when crossing the imaginary axis, see for instance [151, 123]. Efficient methods for crossing imaginary roots identification exist. However, to the best of our knowledge, the multiplicity of such roots was not deeply investigated. In recent papers by the authors [37, 31], it is emphasized that the multiplicity of the zero spectral value can exceed the number of the coupled scalar delay-differential equations and a constructive Vandermonde-based approach leading to an adaptive bound for such a multiplicity is provided. Namely, it is shown that the zero spectral value multiplicity depends on the system structure (number of delays and number of non zero coefficients of the associated quasipolynomial) rather than the degree of the associated quasipolynomial [40]. This chapter extends the constructive approach in investigating the multiplicity of crossing imaginary roots $j\,\omega$ where $\omega \neq 0$ and establishes a link with a new class of functional confluent Vandermonde matrices. A symbolic algorithm for computing the LU-factorization for such matrices is provided. As a byproduct of the proposed approach, a bound sharper than the Polya-Szegö generic bound arising from the principle argument is established. This chapter reproduces mainly the results of [41].

11.1 Introduction

Roughly speaking, discretization of nonlinear PDEs in domains with geometrical symmetries arising in fluid mechanics, structural mechanics, reaction-diffusion problems, often display equivariance conditions, rendering symmetry to become an important topic in nonlinear dynamical systems. Typical example for problems with symmetries are networks consisting in identical n-agents reaction problems with diffusion between neighboring agents. For instance, in [73] a network composed from four identical Brusselator chemical reactors is considered, through which it is ob-

served that the existence of multi-dimensional irreducible representations of the symmetry group may force a spectral value to be multiple. In particular, it is emphasized that such underlying symmetries often induce *multiple Hopf bifurcation points* [1]. As another example where multiple Hopf points occur is reported in [204], where the loss of stability of the down hanging equilibrium position of tubes covering fluid is studied. Due to symmetries, it is shown that *Crossing Imaginary Roots* (CIR) (associated with a Multiple Hopf point) are necessarily double. Furthermore, in time-delay systems context, the paper [225] provides a characterization of the 1 :1 resonant Hopf points (double Hopf points with the same frequency ω) in a 6-agents Bidirectional Associative Memory (BAM) neural network. For further discussion about multiple Hopf points and the richness of their induced dynamics one refers the reader to the work [108]. As a matter of fact, it is shown that the Hopf points near a 1 :1 resonant double Hopf point in a general three-dimensional parameter space form a Whitney umbrella, a phenomena which cannot occur near the standard Hopf points (corresponding to a single crossing frequency), see also [214] for further insights about such resonance cases and we refer the reader to [84] which describes a configuration of Hopf point with higher multiplicity, in particular the fourfold 1 :1 resonance (i.e. 1 :1 :1 :1 resonance) with toroidal symmetry.

In this paper, we are interested in characterizing CIRs for the following class of time-delay systems :

$$\dot{x} = \sum_{k=0}^{N} A_k x(t - \tau_k) \tag{11.1}$$

where $x = (x_1, \ldots, x_n) \in \mathbb{R}^n$ denotes the state-vector, under appropriate initial conditions belonging to the Banach space of continuous functions $\mathcal{C}([-\tau_N, 0], \mathbb{R}^n)$. Here τ_j, $j = 1 \ldots N$ are strictly increasing positive constant delays, $\tau_0 = 0$, $\tau = (\tau_1, \ldots, \tau_N)$ and the matrices $A_j \in \mathcal{M}_n(\mathbb{R})$ for $j = 0 \ldots N$. It is well known that the asymptotic behavior of the solutions of (11.1) is determined from the spectrum $\aleph$ designating the set of the roots of the associated characteristic function denoted in the sequel $\Delta(z, \tau)$, often called *quasipolynomial*, that is a transcendental polynomial in the Laplace variable z in which appear exponential terms induced by delays, see for instance [20]. The study of the zeros of such a class of entire functions [136] plays a crucial role especially in the analysis of the asymptotic stability of the zero solution associated with System (11.1). Indeed, the zero solution is asymptotically stable if all the spectral values of (11.1) are in the open left-half complex plane [206, 151]. Accordingly, the parameter space which is spanned by the coefficients of the polynomials P_i (the polynomials associated to Δ), can be split into stability and instability domains (the so-called D-decomposition, see for instance [151] and references therein). These two domains are separated by a boundary corresponding

---

1. An equilibrium point is called a Hopf point if the Jacobian at that point has a conjugate pair of purely imaginary spectral values $\pm i\omega$, $\omega > 0$. If there are two such pairs $\pm i\omega_1, \pm i\omega_2$ then it is called a double Hopf point. If additionally, $\omega_1 = \omega_2$ then it is called a 1 :1 resonant double Hopf point.

to CIRs. Identification of such CIRs may be done for instance by *Rekasius substitution* [168] or *matrix pencil* [151] to mention only a few. However, to the best of the authors' knowledge, the multiplicity of such roots was not deeply investigated. For instance, in [53, 54] the interest in characterizing the algebraic/geometric multiplicities corresponding to such CIR is emphasized. As a matter of fact, such multiplicities characterize the local behavior of CIR under small variation of the system's parameters. Furthermore, the computation of the upper bound of the algebraic multiplicity of CIR is still unsolved.

For linear stability analysis purposes, a complete characterization of CIR allows to estimate the number of the spectral values with positive real part (elements of $\aleph_+ = \{z \in \mathbb{C}, \ \Delta(z,\tau) = 0, \ \Re(z) > 0\}$) for a given Time-delay system (11.1). Indeed, the main theorem from [119] underscores the link between the cardinality **card**$(\aleph_+)$ and $\aleph_0$ (the set of all CIR), both counted by multiplicity. Thus, the quoted result and its potential consequences on the design of a new approach on the linear stability analysis of time-delay systems, underline the importance of studying CIRs. Such an issue is also pointed up from a nonlinear analysis viewpoint, which gives another motivation for the present investigation. Particularly, when the unstable spectrum is an empty set or equivalently the spectrum $\aleph = \aleph_- \cup \aleph_0$ (elements of $\aleph_- = \{z \in \mathbb{C}, \ \Delta(z,\tau) = 0, \ \Re(z) < 0\}$), a complete knowledge of CIR as well as their multiplicities becomes crucial predominatingly when performing a reduction of the infinite dimensional problem to a system of bifurcation equations on the center manifold, the dimension of which is equal to the number of critical spectral values (multiplicities are taken into account). Namely, the center manifold and the normal forms theory are known to provide an accurate local qualitative description of the studied dynamical system.

A stimulating idea from [166], which consists in exploiting the properties of Vandermonde matrices to control one chain of integrators by delay blocks, enticed the authors in [37] and [31] to extend the investigation of such structured matrices. A complete characterization of the root at the origin can be found in [37, 31]. It is shown that the multiplicity of such a root for a generic system is bounded by *the degree of the associated quasipolynomial*, i.e, the sum of the number of its polynomials plus their respective degrees minus one. This bound was already depicted in [176]. Furthermore, in the sparse case, a sharper bound is established in [37] exhibiting the link between the maximal multiplicity and the number of the non vanishing parameters rather than the degree of the quasipolynomial.

The present work is a natural continuation of [37, 31] and [40]. Its aim is four-fold : first, it provides a symbolic algorithm for the LU-decomposition for functional confluent Vandermonde matrices, which generalizes the class considered in [37] (section 11.3). Secondly, it extends the Vandermonde constructive approach established in [37] to characterize CIR with non zero frequencies (section 11.4). Furthermore, to the best of the authors' knowledge, there does not exists any characterization for such multiple CIRs. Finally, as a byproduct of the established approach, it provides a sharp bound of the algebraic multiplicity for a given non zero CIR (section 11.4).

11.2   Prerequisites

11.2.1   Notations and problem formulation

The characteristic function associated with System (11.1) is a quasipolynomial $\Delta : \mathbb{C} \times \mathbb{R}^N_+ \to \mathbb{C}$ of the form :

$$\Delta(z, \tau) = \det \left(z \, I - A_0 - \sum_{k=1}^{N} A_k \, e^{-\tau_k z} \right). \tag{11.2}$$

Without any loss of generality and for the sake of simplicity, the quasipolynomial function can be written

$$\Delta(z, \tau) = P_0(z) + \sum_{k=1}^{\tilde{N}} P_k(z) \, e^{\sigma_k z}, \tag{11.3}$$

where σ_k are admissible combinations of the components of the delay vector $\tau :=$ $(\tau_1, \ldots, \tau_N)$; $\sigma_k := -\sum_{l=1}^{N} \alpha_{k,l} \tau_l$ such that $0 \leq \alpha_{k,l} \leq n$, $\tilde{N}$ the cardinality of all admissible σ_k, which is a positive integer satisfying $\tilde{N} \geq N$. Without any loss of generality, all the σ_k are assumed to be distinct and $\sigma := (\sigma_1, \ldots, \sigma_N)$ is considered as an auxiliary delay vector for the quasipolynomial, see for instance [40]. It is also assumed that $a_{i,j}$ stands for the coefficient of the monomial z^j in P_i, $a_0 :=$ $(a_{0,0}, \ldots, a_{0,n})^\top$ is the vector composed from the coefficients of the polynomial P_0 and $p := \left(a_{1,0}, \ldots, a_{1,n_1-1}, \ldots, a_{\tilde{N},0}, \ldots, a_{\tilde{N},n_{\tilde{N}}-1} \right)^\top$. It follows from (11.2) that P_0 is a monic polynomial of degree n in z and the polynomials P_k are such that $\deg(P_k) := d_k - 1 = n - \sum_{l=1}^{N} \alpha_{k,l} \leq (n-1)$.

A given complex number z_0 is said to be *a spectral value* for (11.1) if $\Delta(z_0, \tau^*) = 0$ for some delay vector τ^*. We denote by $\partial_z^k \Delta(z, \tau)$ the k-th derivative of $\Delta(z, \tau)$ given by (11.3) with respect to the variable z. A spectral value z_0 is of algebraic multiplicity $m \geq 1$ if $\Delta(z_0, \tau^*) = \partial_z \Delta(z_0, \tau^*) = \ldots = \partial_z^{m-1} \Delta(z_0, \tau^*) = 0$ and $\partial_z^m \Delta(z_0, \tau^*) \neq 0$. A generic bound for the multiplicity of a given spectral value is deduced from a complex analysis result by Pólya and Szegö in [176, p. 144]. Their proof is mainly based on Rouché's Theorem and the principal argument. It gives a bound of the number of quasipolynomial roots in any horizontal strip $\beta \leq \mathcal{I}m(z) \leq \alpha$. Setting $\alpha = \beta = \omega$ gives the number of spectral values z with $\mathcal{I}m(z) = \omega$, which is a natural bound for the multiplicity of a given CIR $z = j\omega$, denoted in the sequel **PS**. See also [219] for a modern formulation of the mentioned result.

11.2.2   Integrator+two delay blocks :

For the general linear scalar time-delay systems of arbitrary order with two delays, the geometric criterion from [109] allows to identify all CIRs. Nevertheless, such a criterion doesn't take into account multiple CIRs, which corresponds to the fourth degenerate configuration listed in [109, Sec. 7]. The following result gives the maximum admissible multiplicities for real spectral values as well as for CIRs.

Proposition 11. *For each pair $(\tau_1, \tau_2) \in \mathbb{R}_+^* \times \mathbb{R}_+^*$ $(\tau_1 \neq \tau_2)$, the equation $\dot{x}(t) + a_1 x(t-\tau_1) + a_2 x(t-\tau_2) = 0$ admits a triple spectral value at $z_0 = -(\tau_1 + \tau_2)/(\tau_1 \tau_2)$ if, and only if, $a_1 = \tau_2 \mathrm{e}^{-\tau_1 z_0}/(\tau_2 \tau_1 - \tau_1^2), a_2 = \tau_1 \mathrm{e}^{-\tau_2 z_0}/(\tau_2 \tau_1 - \tau_2^2)$. Moreover, under this configuration, the zero solution is asymptotically stable. However, the maximal multiplicity of a CIR $j\omega_0$ is two and it is reached if, and only if,*

$$a_1 = \frac{\omega_0 \cos(\omega_0 \tau_2)}{\sin(\omega_0 (\tau_1 - \tau_2))}, \quad a_2 = \frac{\omega_0 \cos(\omega_0 \tau_1)}{\sin(\omega_0 (\tau_2 - \tau_1))}, \tag{11.4}$$

where $\omega_0 = \pm\tan(\alpha_0)/\tau_1$, $\tau_2 = -\tau_1 \alpha_0/\tan(\alpha_0)$ and α_0 is a fixed point of $\alpha \mapsto \tan \circ \tan(\alpha)$ (which exists).
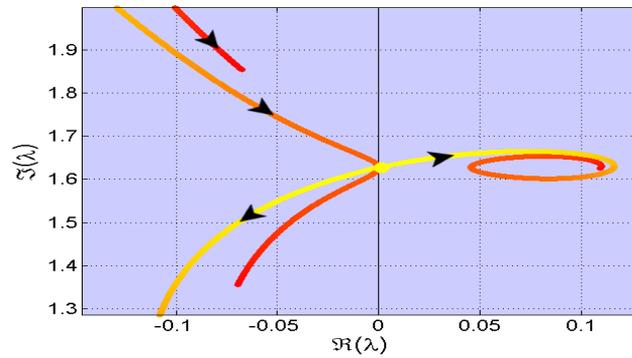
FIGURE 11.1 – Bifurcation of the double imaginary crossing root defined by (11.4) up to the standard normalization $\tau_2^* = 1$, the crossing frequency $\omega_0 = 11.53849769$ and the delay $\tau_1^* = 0.1436275981$ is subject to a positive perturbation ($\varepsilon = 0 \ldots 6$). The evolution of the spectral value from the nominal value $\varepsilon = 0$ (yellow) to the final value $\varepsilon = 6$ (red). Representative bifurcation diagrams have been computed using QPmR [215].

To prove these results, we start by considering the configuration allowing a spectral value z_0 with multiplicity three. Indeed, z_0 is obtained as a solution of the system of equations $\Delta(z_0, \tau) = \ldots = \partial_z^k \Delta(z_0, \tau) = 0$ for $k \in \{1, 2\}$ and $\partial_z^3 \Delta(z_0, \tau) \neq 0$ where the characteristic function is $\Delta(z) = z + a_1 \mathrm{e}^{-z\tau_1} + a_2 \mathrm{e}^{-z\tau_2}$, which can be also written as

$$\Delta(z) = (z - z_0) \left(1 + \frac{\frac{\tau_2 \mathrm{e}^{-(z-z_0)\tau_1}}{\tau_1(\tau_2 - \tau_1)} + \frac{\tau_1 \mathrm{e}^{-(z-z_0)\tau_2}}{\tau_2(\tau_1 - \tau_2)} + z_0}{(z - z_0)} \right).$$

Démonstration. To prove the asymptotic stability of the zero solution, let us assume that there exists $z_1 = \zeta + j\eta$ a root of $\Delta(z) = 0$ such that $\zeta \geq 0$. So that, z_1 is a root of the second factor of Δ, which gives :

$$1 = \sum_{i=1}^{2} \frac{c_i \mathrm{e}^{-(z_1-z_0)\tau_i} - 1}{\tau_i (z_1 - z_0)}, \quad \text{where} \quad c_i = \prod_{\substack{l=1 \\ l \neq i}}^{2} \frac{\tau_l}{(\tau_l - \tau_i)}$$

Hence, $1 = \sum_{i=1}^{2} c_i \int_0^1 cos(\eta\,\tau_i\,t)\,e^{-(\zeta-z_0)\,\tau_i\,t}\,dt$. Without any loss of generality, one assumes that $\tau_1 < \tau_2$ which implies : $1 \leq \int_0^1 e^{-(\zeta-z_0)\,\tau_1\,t}\,dt$, proving the inconsistency of the hypothesis $\zeta > 0$.

Now, let us check that the upper bound of the multiplicity for CIR is two. Such a multiplicity is reached for $j\omega_0$ if, and only if, $\Delta(j\omega_0, \tau) = \partial_z\Delta(j\omega_0, \tau) = 0$. Let us proceed by elimination. The first equation $\Delta(j\omega_0, \tau) = 0$ gives, $a_1 \cos(\omega_0\tau_1) + a_2 \cos(\omega_0\tau_2) + (\omega_0 - a_1 \sin(\omega_0\tau_1) - a_2 \sin(\omega_0\tau_2))\,j = 0$. The vanishing of the real part leads to $a_2 = -a_1 \cos(\omega_0\tau_1)/\cos(\omega_0\tau_2)$, which is substituted in the imaginary part. After equating the resulting expression one has $a_1 = \omega \cos(\omega\,\tau_2)/\sin(\omega\,\tau_1 - \omega\,\tau_2)$. The obtained value for a_1 is then itself substituted in a_2. The final values of a_1 and a_2 are then substituted in the equation $\partial_z\Delta(j\omega, \tau) = 0$, which provides two equations (real and imaginary terms) depending on the three left free parameters ω, τ_1 and τ_2, leading as expected, to the expression of the crossing frequency ω_0 as well as τ_2^* (τ_1 still being free). □

Under such settings, if the delay τ_2 is considered as a bifurcation parameter, then Figure 11.1 provides the local bifurcation scenario ; the double CIR splits into one stable and one unstable spectral values.

Remark 20. For a given quasipolynomial function, the multiplicity of real roots may reach the Polya-Szegö bound, see [31, 37]. However, the multiplicity of an imaginary crossing root may exceed the dimension of the delay-free system but never reach the Polya-Szegö bound.

11.2.3   Rekasius Substitution for a Second Order System

It is well known that *Rekasius substitution* is a way for identifying the crossing roots for a given quasipolynomial, [203]. It consists in offsetting the exponential type transcendental terms in a given quasypolynomial function by the following rational function : $e^{-z\tau} = (1 - Tz)/(1 + Tz)$, where T is some positive real number. This transformation is accompanied with the relation : $\tau = \frac{2}{\omega_c}\left(arctan(\omega_c T) + k\pi\right)$, $k = 0, 1, \dots$ where $\omega_c \in \mathbb{R}_+^*$ and ω_c denotes the crossing frequency. It is worthy to note that such a relation associates each solution of the transformed characteristic function (in the auxiliary variable T) to a $2\pi/\omega_c$-periodic countably infinite set of solutions of the original characteristic quasipolynomial function (in the variable τ), see for instance [168, 156]. However, the question of roots multiplicity-conservation by such a transformation may be more deeply investigated. For instance, in the following example, we show that even for the delay margin [2] τ^0, such a multiplicity is not preserved by the Rekasius substitution. Let us consider the quasipolynomial function :

$$f(z, \tau) = a_{0,0} + a_{0,1}z + z^2 + (a_{1,0} + a_{1,1}z)\,e^{-\tau z} \tag{11.5}$$

---

2. Rekasius substitution asserts that when an imaginary root $j\omega_0$ is associated to a given delay τ^0 then it is also associated to each value of the delay among the family $\{\tau^k\}_{k\in\mathbb{Z}} = \{\tau^0 + k\frac{2\pi}{|\omega_0|}\}_{k\in\mathbb{Z}}$. But, as it was underlined in [124], if $j\,\omega_0$ is a double crossing root associated with the delay $\tau = \tau^0$ then, $j\,\omega_0$ is a simple crossing root for any τ^k.

with $a_{0,0} = \frac{\pi^2+4}{\pi^2-4}$, $a_{0,1} = a_{1,0} = \frac{-4\pi}{\pi^2-4}$, $a_{1,1} = \frac{-8}{\pi^2-4}$.

First, one knows that the CIRs of f are the imaginary roots of the following rational function in the variables z and T :

$$\tilde{f}(z,T) = \frac{\mathcal{P}(z,T)}{\mathcal{Q}(z,T)} \quad \text{where} \quad \mathcal{Q}(z,T) = 1 + T_1 z \quad \text{and}$$

$$\mathcal{P}(z,T) = \left(a_{0,0}z + a_{0,1}z^2 + z^3 - a_{1,0}z - a_{1,1}z^2\right)T$$
$$+ a_{0,0} + a_{0,1}z + z^2 + a_{1,0} + a_{1,1}z.$$

Elementary algebraic manipulations show that $z_0 = j$ is a root of $\tilde{f}$ when $T^* = 1$. Thus, $z_0 = j$ is a root of f where the associated delay $\tau^0 = \pi/2$ is easily deduced. Finally, we check that if $\tau = \tau^0$, then $z_0 = j$ is a double root for f, see Figure 11.2 for the local bifurcation scenario. However, the evaluation of $\partial_z \tilde{f}$ at $(z,T) = (z_0, T^*)$ gives : $\partial_z \tilde{f}(z_0, T^*) = 2(\pi j - 2)/(\pi + 2)$. Thus, $z_0 = j$ is a simple root for $\tilde{f}$ when $T = T^*$, leading us to the following :
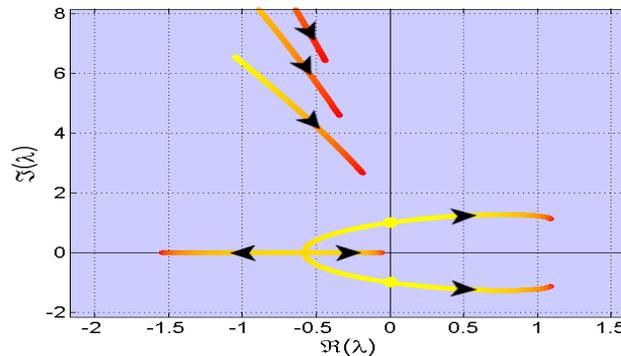
FIGURE 11.2 – Bifurcation of the double imaginary crossing root of (11.5) where the delay τ is subject to a positive perturbation ($\varepsilon = 0\ldots6$). The evolution of the spectral value from the nominal value $\varepsilon = 0$ (yellow) to the final value $\varepsilon = 6$ (red).

Remark 21. For a given quasipolynomial function, Rekasius substitution yields all roots on the imaginary axis but does not necessarily preserve their multiplicity. Furthermore, the other limitations of such a substitution arise when at least one of the polynomials (involved in the considered quasipolynomial) depend on z and τ. This is obviously the case when exploring the multiplicity of CIR.

11.3   Functional Confluent Vandermonde matrices

By *functional confluent Vandermonde matrix* Φ we designate for given positive integers l, δ and M, the matrix defined by :

$$
\begin{cases}
\Phi = [\Phi_1 \, \Phi_2 \, \ldots \, \Phi_M] \in \mathcal{M}_{l,\delta}(\mathbb{R}), \\
\Phi_i = [f(\sigma_i) \, f^{(1)}(\sigma_i) \, \ldots \, f^{(d_i-1)}(\sigma_i)], \\
f(\sigma_i) = g(\sigma_i).[1 \, \ldots \, \sigma_i^{l-1}]^T, \quad \text{for} \quad 1 \le i \le M,
\end{cases} \tag{11.6}
$$

for a sufficiently regular function $g \in \mathcal{C}^k(\mathbb{R})$, see [113]. In the sequel, we are particularly interested by square matrices where it is assumed that $\sum_{i=1}^{M} d_i = \delta = l$. If, $g(x) = 1$ then we are dealing with the so-called confluent Vandermonde matrix, see [113]. If, additionally, $d_i = 1$ for $i = 1 \ldots N$ then we recover the classical Vandermonde matrix and in this case $M = \delta$ since Φ is assumed to be a square matrix, see [169]. The explicit development of numeric/symbolic algorithms for LU-factorization and inversion of the confluent Vandermonde and Birkhoff matrices [186, 169] is still an attracting topic due to their specific structure and their implications in various applications, see [126] and references therein. It is worth mentioning that one of the contributions of this paper is to propose an explicit recursive formula for the LU-factorization for the functional confluent Vandermonde matrix defined by (11.6). The proposed formulas are in the spirit of the symbolic expressions established in [169] for the standard Vandermonde case. To the best of the authors' knowledge, such an explicit formulas seems to be unavailable in the open literature, see e. g., [106, 169]. In fact, the historical note in [169] emphasizes that the rather extensive numerical literature on practical solutions to Vandermonde systems fails to reveal the explicit factorization formula for the LU-factorization as well as the symbolic inversion of Vandermonde matrices. We point out that an explicit recursive formula for the LU-factorization for a class of functional confluent Vandermonde matrices characterized by $g(x) = x^k$ is available in [37] or in its extended version [40]. The following notations are adopted. Let ξ stands for the vector composed by σ_i repeated d_i (nothing but $\deg(P_i) + 1$) times through columns of a given matrix Φ, i.e. $\xi := (\underbrace{\sigma_1, \ldots, \sigma_1}_{d_1}, \ldots, \underbrace{\sigma_{\tilde{N}}, \ldots, \sigma_{\tilde{N}}}_{d_{\tilde{N}}})$ and let $d_0 \equiv 0$, $\nu(k)$ the index of the component of σ corresponding to ξ_k i.e. $\sigma_{\nu(k)} = \xi_k$ and $1 \le \kappa(k) \le d_{\nu(k)}$ the corresponding order in the sequence of $\sigma_{\nu(k)}$.

It is important to note that the vector ξ, called in the sequel the *incidence vector*, is a compact way to depict the *incidence matrix* corresponding to a given functional confluent matrix Φ, see for instance [106]. It characterizes a given square functional confluent matrix Φ defined in (11.6) by specifying its variables as well as their repetitions by indicating the associated orders of derivations through its columns. In terms of the corresponding quasipolynomial, the incidence vector indicates the degree of the polynomials P_k.

In [37], as well as in [40], a particular class of functional confluent Vandermonde matrices with $g(x) = x^s$ is considered and the corresponding LU-factorization is

provided. The following result extends the applicability of the symbolic algorithm
for LU-factorization given in [40] (as well as in [37]) to any functional confluent
Vandermonde matrix with a sufficiently regular function g.

Proposition 12. *For the functional confluent Vandermonde square matrix Φ given
in* (11.6) *the following hold :*

1. *Φ admits the following LU-factorization :*

$$\begin{cases} L_{i,1} = \sigma_1^{i-1} & for \quad 1 \leq i \leq \delta, \\ U_{1,j} = \Phi_{1,j} & for \quad 1 \leq j \leq \delta, \\ L_{i,j} = L_{i-1,j-1} + L_{i-1,j}\,\xi_j & for \quad 2 \leq j \leq i, \\ U_{i,j} = (\varkappa(j) - 1)\,U_{i-1,j-1} + U_{i-1,j}\,\big(\sigma_{\nu(j)} - \xi_{i-1}\big) \\ \qquad for \quad 2 \leq i \leq j. \end{cases} \tag{11.7}$$

2. *The determinant of Φ is given by $\det(\Phi) = \prod_{j=1}^{\delta}(U_{j,j})$ where $U_{j,j}$ for $1 \leq j \leq \delta$ are defined by :*

$$\begin{cases} U_{1,1} = g(\sigma_1), \\ U_{j,j} = g(\sigma_{k+1}) \prod_{l=1}^{k} (\sigma_{k+1} - \sigma_l)^{d_l} \\ \qquad when \quad j = 1 + d_k \ for \ 1 \leq k \leq \tilde{N} - 1, \\ U_{j,j} = (j - 1 - d_k)\,U_{j-1,j-1} \\ \qquad when \quad d_k + 1 < j \leq d_{k+1} \ for \quad 1 \leq k \leq \tilde{N} - 1, \end{cases}$$

Démonstration. Even the functional confluent Vandermonde matrix we consider generalizes the particular one considered in [37, Theorem 3], we follow the same steps
of its proof. Namely, one proceeds by a total 2-D recurrence, which can be summarized as follows. First, one defines a matrix Ω by $\Omega_{i,j} = \sum_{k=1}^{i} L_{i,k}U_{k,j}$ for $1 \leq i, j \leq \delta$
where, $L_{i,k}$ and $U_{k,j}$ are defined in (11.7). Then we prove that $\Omega_{i,j} = \Phi_{i,j}$ $\forall(i,j)$
$1 \leq i, j \leq \delta$. The initialization of the recurrence is done by showing that $\Omega_{1,j} = \Phi_{1,j}$
and $\Omega_{i,1} = \Phi_{i,1}$ for $1 \leq i, j \leq \delta$. Hence, one assumes that $\Omega_{i,j} = \Phi_{i,j}$ holds for
any $1 \leq i \leq i_0 - 1$ and $1 \leq j \leq j_0 - 1$. Finally, proving that $\Omega_{i_0,j_0-1} = \Phi_{i_0,j_0-1}$,
$\Omega_{i_0-1,j_0} = \Phi_{i_0-1,j_0}$, $\Omega_{i_0,j_0} = \Phi_{i_0,j_0}$ allows to conclude that $\Omega_{i,j} = \Phi_{i,j}$ for $1 \leq i \leq \delta$
and $1 \leq j \leq \delta$. The determinant of the functional confluent Vandermonde matrix Φ
follows directly from (11.7) since $L_{i,i} = 1$. $\qquad\qquad\square$

11.4 Characterizing the Multiplicity of CIR : Computational Issues & Links with Functional Vandermonde Matrices

Let us set $c_k = \cos(\sigma_k\omega)$ and $s_k = \sin(\sigma_k\omega)$ and, for a given real positive number
x, we denote by $\lfloor x \rfloor$ the integer part of x or equivalently the floor function at x.

Lemma 8. *An imaginary complex number $z = j\omega$ is a root of $\partial_z^k \Delta(z, \tau) = 0$ for $k \geq 0$ if, and only if, the coefficients of P_i for $0 \leq i \leq \tilde{N}$ satisfy*

$$\alpha_k + \tilde{\alpha}_k = 0 \text{ and } \beta_k + \tilde{\beta}_k = 0, \tag{11.8}$$

where

$$
\begin{cases}
\alpha_0 = \displaystyle\sum_{\substack{i=0, \\ i \text{ even}}}^{n} (-1)^{\lfloor \frac{i}{2} \rfloor} \omega^i a_{0,i} \text{ and } \beta_0 = \sum_{\substack{i=1, \\ i \text{ odd}}}^{n} (-1)^{\lfloor \frac{i}{2} \rfloor} \omega^i a_{0,i}, \\[4mm]
\alpha_k = -\partial_\omega \beta_{k-1} \text{ and } \beta_k = \partial_\omega \alpha_{k-1} \ \forall k \geq 1, \\[4mm]
\tilde{\alpha}_k = \displaystyle\sum_{i=1}^{\tilde{N}} \sum_{l=0}^{d_i} a_{i,l} \frac{\partial^l \left(c_i \sigma_i^{\ k}\right)}{\partial \sigma_i^l} \text{ and } \tilde{\beta}_k = \sum_{i=1}^{\tilde{N}} \sum_{l=0}^{d_i} a_{i,l} \frac{\partial^l \left(s_i \sigma_i^{\ k}\right)}{\partial \sigma_i^l}.
\end{cases}
$$

The proof of Lemma 8 is given in Section 11.7.

Remark 22. If one investigates multiple zero singularities, then (11.8) reduces to

$$a_{0,k} = -\sum_{i=0}^{\tilde{N}} \left[a_{i,k} + \sum_{l=0}^{k-1} \frac{a_{i,l}\sigma_i^{\ k-l}}{(k-l)!} \right], \text{ see for instance [37]}.$$

Let us set $\gamma_k = (\alpha_k + \tilde{\alpha}_k)^2 + (\beta_k + \tilde{\beta}_k)^2$ and for a given positive integer m let α^m, β^m stand for the vectors :

$$
\begin{cases}
V_m(a_0, \omega) = -\left(\alpha_0, \ldots, \alpha_{m-1}\right)^\top, \\
W_m(a_0, \omega) = -\left(\beta_0, \ldots, \beta_{m-1}\right)^\top.
\end{cases} \tag{11.9}
$$

Let $\varrho = \sum_{i=1}^{\tilde{N}} d_i$, we define the functional confluent matrices A_m and B_m belonging to $\mathcal{M}_{m,\varrho}(\mathbb{R})$ and characterized by the incidence vector $\xi = (\underbrace{\sigma_1, \ldots, \sigma_1}_{d_1}, \ldots, \underbrace{\sigma_{\tilde{N}}, \ldots, \sigma_{\tilde{N}}}_{d_{\tilde{N}}})$ as well as the respective functions $g_A(x) = \cos(\omega x)$ and $g_B(x) = \sin(\omega x)$. As a direct consequence of the above Lemma 8, one has :

Proposition 13. *An imaginary crossing root $z = j\omega$ for Eq (11.3) is of multiplicity m if, and only if, one of the following equivalent assertions hold :*

1. *The variety $\mathcal{V}_m$ is non empty and $\gamma_{m+1} \neq 0$, where*

$$
\mathcal{V}_m = \begin{cases}
(\omega, a_{0,0}, \ldots, a_{\tilde{N}, d_{\tilde{N}}}, \sigma_1, \ldots, \sigma_{\tilde{N}}) \in \mathbb{R}^{n+\delta+1} \times \mathbb{R}_+^{\tilde{N}}, \\
\gamma_k = 0 \text{ for } k = 0, \ldots, m-1
\end{cases}.
$$

2. *The frequency ω satisfies the following linear system :*

$$
\begin{cases}
A_m(\omega, \sigma).p = V_m(a_0, \omega), \\
B_m(\omega, \sigma).p = W_m(a_0, \omega).
\end{cases} \tag{11.10}
$$

Remark 23. The first assertion of the above proposition provides a system of trigonometric polynomials to solve. Which characterizes multiple CIRs. A standard

approach in solving such systems of nonlinear trigonometric polynomials consists in considering $\sin(\omega\sigma_i)$ and $\cos(\omega\sigma_i)$ functions as new variables s_i and c_i respectively and then intentionally add some equations expressing $s_i^2 + c_i^2 = 1$. Thus, Groebner basis approaches may be involved to characterize the algebraic *variety* corresponding to the modified problem's solutions, see for instance [68]. However, the added algebraic equations emphasize the links between the variables s_i and c_i but doesn't take into account the link between s_i (as well as c_i) with the variables ω and σ_i (which are involved in the argument of cos and sin functions). Thus, to avoid the possible induced inconsistant solutions one has to consider only the intersection of the obtained algebraic variety with some transcendental relations, for instance $c_i = \arccos(\omega\sigma_i)$. The second assertion of the above proposition provides an effective linear algebra alternative for the above described approach.

Démonstration. Both assertions of the above proposition are direct consequences of Lemma 8. They follow by considering two ideals consisting in the real part $\alpha_k + \tilde{\alpha}_k$, (respectively the imaginary part $\beta_k + \tilde{\beta}_k$) of the successive derivatives of the quasipolynomial function. Namely, a careful inspection of the coefficients $\tilde{\alpha}_k$ and $\tilde{\beta}_k$ from Lemma 8 allows to a linear system where the involved matrices are nothing but the functional confluent Vandermonde matrices A_m and B_m, leading to (11.10). □

Corollary 6. *If the square matrices A_ϱ and B_ϱ are non degenerate then the multiplicity of any imaginary crossing root $z = j\,\omega_0$ for Eq (11.3) is bounded by ϱ.*

Démonstration. For $m = \varrho+1$, the inconsistency of (11.10) follows from the Kronecker-Rouché-Capelli Theorem, see [198]. Indeed, rows of the functional confluent Vandermonde matrix $A_{\varrho+1}$ (respectively $B_{\varrho+1}$) are functionally dependent but linearly independent provided that A_ϱ, (respectively B_ϱ) is non degenerate. Thus, the rank of the augmented matrix $A_{\varrho+1} : V_{\varrho+1}$, $(B_{\varrho+1} : W_{\varrho+1})$, which is equal to $\varrho + 1$ is greater than the rank of the matrix $A_{\varrho+1}$, $(B_{\varrho+1})$. □

Corollary 7. *The functional confluent Vandermonde matrix A_ϱ, respectively B_ϱ, is non degenerate if, and only if, $\forall\, 1 \le i \ne j \le \tilde{N}$, $\omega\sigma_i \ne \pi/2 + k\pi$ and $\sigma_i \ne \sigma_j$, respectively $\omega\sigma_i \ne k\pi$ and $\sigma_i \ne \sigma_j$.*

Remark 24. A necessary and sufficient condition for A_ϱ and B_ϱ to be non degenerate is $\sigma_i \ne \sigma_j \,\forall\, 1 \le i \ne j \le \tilde{N}$ and $\omega\sigma_i \ne k\pi/2$, $k \in \mathbb{N}$. Moreover, a given CIR has the multiplicity ϱ if the linear systems given by (11.10) admit a real solution. The Polya-Szegö bound **PS** is never reached. Indeed, the above multiplicity bound for a given CIR is sharper than **PS** since by definition $\mathbf{PS} = n + \sum_{i=1}^{\tilde{N}} d_i$.

11.5 Illustrative Examples

11.5.1 Scalar equation with two delays

Consider now the scalar delay equation : $\dot{x}(t) + a_{1,0}x(t - \tau_1) + a_{0,1}x(t - \tau_2) + a_{0,0}x(t) = 0$. Here $p = (a_{1,0}, a_{0,1})^\top$ and $\tilde{N} = 2$. According to Corollary 6, the

maximal multiplicity of a given CIR is bounded by $\varrho = 2 < \mathbf{PS} = 3$. Moreover, a necessary condition for a CIR to reach multiplicity two is $\tau_1 \neq \tau_2$ and $\omega \tau_i \neq k\pi/2$. Indeed, in such a configuration, we have $\sigma_{1,0} = -\tau_1$, $\sigma_{0,1} = -\tau_2$ and the functional Vandermonde matrices :

$$
A_2 = \begin{bmatrix} \cos(\sigma_{1,0}\omega) & \cos(\sigma_{0,1}\omega) \\ \sigma_{1,0}\cos(\sigma_{1,0}\omega) & \sigma_{0,1}\cos(\sigma_{0,1}\omega) \end{bmatrix} , \quad V_2 = \begin{bmatrix} -a_{0,0} \\ -1 \end{bmatrix}
$$

$$
B_2 = \begin{bmatrix} \sin(\sigma_{1,0}\omega) & \sin(\sigma_{0,1}\omega) \\ \sigma_{1,0}\sin(\sigma_{1,0}\omega) & \sigma_{0,1}\sin(\sigma_{0,1}\omega) \end{bmatrix} , \quad W_2 = \begin{bmatrix} -\omega \\ 0 \end{bmatrix} .
$$

Using Proposition 12, one proceeds by LU-factorization for each of the matrices given in System (11.10) and obtains a necessary and sufficient condition for a given CIR to reach its maximal multiplicity (two).

$$
\begin{cases} (a_{0,0}\sigma_{0,1} - 1)\sin\left(\omega\,\sigma_{1,0}\right) = \omega\,\sigma_{0,1}\cos\left(\omega\,\sigma_{1,0}\right) \\ (a_{0,0}\sigma_{1,0} - 1)\sin\left(\omega\,\sigma_{0,1}\right) = \omega\,\sigma_{1,0}\cos\left(\omega\,\sigma_{0,1}\right) \end{cases}
$$

When $a_{0,0} = 0$, one recovers example 11.2.2.

11.5.2   D3-equivariant BAM neural network with delay

Let us revisit a generic version of BAM neural network with one constant delay considered in [225], the linearization of which around the origin of $\mathbb{R}^6$ is given by :

$$
\begin{cases} \dot{x}_1 = -a_1 x_1 + b_1 x_4(t - \tau) + c_1 x_5(t - \tau) + d_1 x_6(t - \tau), \\ \dot{x}_2 = -a_2 x_2 + b_2 x_5(t - \tau) + c_2 x_6(t - \tau) + d_2 x_4(t - \tau), \\ \dot{x}_3 = -a_3 x_3 + b_3 x_6(t - \tau) + c_3 x_4(t - \tau) + d_3 x_5(t - \tau), \\ \dot{x}_4 = -a_4 x_4 + b_4 x_1(t - \tau) + c_4 x_2(t - \tau) + d_4 x_3(t - \tau), \\ \dot{x}_5 = -a_5 x_5 + b_5 x_2(t - \tau) + c_5 x_3(t - \tau) + d_5 x_1(t - \tau), \\ \dot{x}_6 = -a_6 x_6 + b_6 x_3(t - \tau) + c_6 x_1(t - \tau) + c_6 x_2(t - \tau), \end{cases} \tag{11.11}
$$

where a_i, b_i, c_i, $d_i \in \mathbb{R}$ such that $a_i > 0$. One easily checks that the corresponding characteristic quasipolynomial associated to (11.11) is given by : $\Delta(z, \tau) = a_{0,0} + a_{0,1}z + a_{0,2}z^2 + a_{0,3}z^3 + a_{0,4}z^4 + a_{0,5}z^5 + z^6 + \left(a_{2,0} + a_{2,1}z + a_{2,2}z^2 + a_{2,3}z^3 + a_{2,4}z^4\right)\mathrm{e}^{-2\tau z} + \left(a_{4,0} + a_{4,1}z + a_{4,2}z^2\right)\mathrm{e}^{-4\tau z} + a_{6,0}\mathrm{e}^{-6\tau z}$

with appropriate values of $a_{i,j}$ as polynomials in the parameters a_k, b_k, c_k, d_k. Let us assume that $a_{i,j} \neq 0$. Then Corollary 7 asserts that the maximum multiplicity of a given CIR is at most 9 if A_9 and B_9 are invertible. However, the Polya-Szegö bound is $\mathbf{PS} = 13$. Furthermore, if, $a_i = a$, $b_i = b$, $c_i = d_i = c$ for $i = 1, \ldots, 6$ then one recovers precisely the BAM network considered in [225] where the 1 :1 resonance Hopf point is studied. It is pointed out that the classical Hopf bifurcation theory cannot be applied to such a system due to its symmetry. Namely, it is shown that the structure of the system (11.11) can be represented by a dihedral group $D3$ of order 6, which is generated by the cyclic subgroup $\mathbb{Z}_3$ together with a flip of order 2. In such a case, the characteristic function of (11.11) reduces to $\Delta(z, \tau) = \left(z + a \pm (2c + b)e^{-z\tau}\right)\left(z + a \pm (b - c)e^{-z\tau}\right)^2$.

Some straightforward numerical computations show that a Hopf point with higher multiplicity than 2 may occur. Indeed, the multiplicity 3 is possible for arbitrarily chosen $(\omega^*, \tau^*) \in \mathbb{R}_+^* \times \mathbb{R}_+^*$ and the remaining parameters satisfy $a = \omega^* \cos(\omega^* \tau^*)/\sin(\omega^* \tau^*), b = \pm \omega^*/3 \sin(\omega^* \tau^*), c = \mp 2\omega^*/3\sin(\omega^* \tau^*)$. In such a case, richer dynamics may occur, see for instance [84].

11.6 Conclusion

In this paper we addressed the question of characterizing multiple CIRs (with non zero frequencies) for time-delay systems as well as their admissible and maximal multiplicities, provided that one is able to explicitly compute the associated characteristic quasipolynomial function. The considered configuration is generic, allowing among others to link such a problem with some Hermite interpolation problem through functional confluent Vandermonde matrices with trigonometric inputs. A general formula for LU-factorization of such matrices is established. To the best of the authors' knowledge, the use of this class of matrices as well as their factorization is new. Finally, we bear down on the immediate extension of our approach to characterize CIRs for neutral systems.

11.7 Proof of Lemma 8

We point out that the coefficient α_k (respectively β_k) is the real part (respectively the imaginary part) of the polynomial $P_0^{(k)}(j\omega)$. Furthermore, α_k and β_k are multivariate polynomials in ω and in the components of a_0 (the coefficients of P_0 in z). It is also important to note that, $\alpha_{s+1} = \beta_{s+1} = 0$ for every integer $s \geq n$. Consider the quasipolynomial given in (11.3). A complex number $j\omega$ is a root of $\Delta(z, \tau) = 0$ if, and only if, $P_0(j\omega) + \sum_{k=1}^{\tilde{N}} P_k(j\omega) e^{j\sigma_k \omega} = 0$ which gives :

$$a_{0,0} + \ldots + a_{0,n}(j\omega)^n + \left(a_{1,0} + \ldots + a_{1,d_1}(j\omega)^{d_1} \right) e^{j\sigma_1 \omega}$$
$$+ \ldots + \left(a_{\tilde{N},0} + \ldots + a_{\tilde{N},d_{\tilde{N}}}(j\omega)^{d_{\tilde{N}}} \right) e^{j\sigma_{\tilde{N}} \omega} = 0.$$

Using Euler formula, one obtains :

$$\alpha_0 + j\beta_0 + \left(a_{1,0} + \ldots + a_{1,d_1}(j\omega)^{d_1} \right) (c_1 + js_1)$$
$$+ \ldots + \left(a_{\tilde{N},0} + \ldots + a_{\tilde{N},d_{\tilde{N}}}(j\omega)^{d_{\tilde{N}}} \right) (c_{\tilde{N}} + js_{\tilde{N}}) = 0.$$

Now, extracting the real and imaginary parts of the above expression allows us to prove (11.8) for $k = 0$:

$$
\begin{cases}
\alpha_0 + c_1 a_{1,0} - \omega s_1 a_{1,1} - \omega^2 c_1 a_{1,2} + \ldots + \omega^{d_1} \dfrac{\partial^{d_1} c_1}{\partial \sigma_1^{d_1}} a_{1,d_1} \\[2ex]
+ \ldots + c_{\tilde{N}} a_{\tilde{N},0} + \ldots + \omega^{d_{\tilde{N}}} \dfrac{\partial^{d_{\tilde{N}}} c_{\tilde{N}}}{\partial \sigma_{\tilde{N}}^{d_{\tilde{N}}}} = 0, \\[2ex]
\beta_0 + s_1 a_{1,0} + \omega c_1 a_{1,1} - \omega^2 s_1 a_{1,2} + \ldots + \omega^{d_1} \dfrac{\partial^{d_1} s_1}{\partial \sigma_1^{d_1}} a_{1,d_1} \\[2ex]
+ \ldots + s_{\tilde{N}} a_{\tilde{N},0} + \ldots + \omega^{d_{\tilde{N}}} \dfrac{\partial^{d_{\tilde{N}}} s_{\tilde{N}}}{\partial \sigma_{\tilde{N}}^{d_{\tilde{N}}}} = 0.
\end{cases}
$$

Consider the first partial derivatives of the quasipolynomial :

$$
\partial_z \Delta(z, \tau) = P_0'(z) + \sum_{i=1}^{\tilde{N}} \left(P_i'(z) + \sigma_i P_i(z) \right) e^{\sigma_i z},
$$

$$
\partial_z^2 \Delta(z, \tau) = P_0''(z) + \sum_{i=1}^{\tilde{N}} \left(P_i''(z) + 2\sigma_i P_i'(z) + \sigma_i^2 P_i(z) \right) e^{\sigma_i z}.
$$

By induction we arrive to :

$$
\partial_z^k \Delta(z, \tau) = P_0^{(k)}(z) + \sum_{i=1}^{\tilde{N}} e^{\sigma_i z} \sum_{m=0}^{k} \binom{m}{k} \sigma_i^{k-m} P_i^{(m)}(z).
$$

Now, assume that $z = j\omega$ is a root of $\partial_z^k \Delta(z, \tau) = 0$ for $k \geq 1$ and let us show that (11.8) is satisfied.

$$
0 = P_0^{(k)}(j\omega) + \sum_{i=1}^{\tilde{N}} \sum_{m=0}^{k} \binom{m}{k} \sigma_i^{k-m} P_i^{(m)}(j\omega) \left(c_i + j s_i \right).
$$

Thus, $\alpha_k = -\mathcal{R}e(\sum_{i=1}^{\tilde{N}} \sum_{m=0}^{k} \binom{m}{k} \sigma_i^{k-m} P_i^{(m)}(j\omega) (c_i + j s_i))$. Obviously, when $k \geq n$ then $P_0^{(k)}(j\omega) = \alpha_k + j\beta_k = 0$. The right-hand side of the above equality is nothing but $\tilde{\alpha}_k$. Indeed,

$$
\mathcal{R}e \left(\sum_{i=1}^{\tilde{N}} \sum_{m=0}^{k} \binom{m}{k} \sigma_i^{k-m} \sum_{l=0}^{d_i} \left[a_{i,l} z^l \right]_{z=j\omega}^{(m)} \left(c_i + j s_i \right) \right) =
$$

$$
\mathcal{R}e \left(\sum_{i=1}^{\tilde{N}} \sum_{l=0}^{d_i} a_{i,l} \sum_{m=0}^{k} \binom{m}{k} \sigma_i^{k-m} \left[z^l \right]_{z=j\omega}^{(m)} \left(c_i + j s_i \right) \right) =
$$

$$
\sum_{i=1}^{\tilde{N}} \sum_{l=0}^{d_i} a_{i,l} \mathcal{R}e \left(\sum_{m=0}^{k} \binom{m}{k} \sigma_i^{k-m} \left[z^l \right]_{z=j\omega}^{(m)} \left(c_i + j s_i \right) \right) = \tilde{\alpha}_k
$$

since one shows by induction w.r.t to l (for a fixed k) that

$$\frac{\partial^l \left(c_i \sigma_i{}^k\right)}{\partial \sigma_i^l} = \mathcal{R}e\left(\sum_{m=0}^{k} \binom{m}{k} \sigma_i^{k-m} \left[z^l\right]^{(m)}_{z=j\omega} \left(c_i + js_i\right)\right).$$

Multiplicity and Stable Varieties of Time-delay Systems : A Missing Link

Multiple spectral values in dynamical systems are often at the origin of complex behaviors as well as unstable solutions. However, in some recent studies, an unexpected property is emphasized. More precisely, an example of real scalar delay system is constructed, where the maximal multiplicity of an appropriate delay-dependant real and negative spectral value leads to a negative spectral abscissa and, as a consequence, the asymptotic stability of the corresponding steady state solution. In algebraic terms (with respect to the parameter space), the variety corresponding to such a multiple root defines a stable variety for the steady state. Furthermore, for the reduced examples we consider, we show that, under mild assumptions, such a multiple spectral value is nothing but the spectral abscissa. To the best of our knowledge, such a property was not deeply investigated. Motivated by the potential implication of such a property in control systems applications, this chapter is devoted to better explore the connetion between those varieties. Finally, the sunflower dynamical equation illustrates the study. The results of this chapter are borrowed from [122].

12.1   Introduction

Symmetries in networked dynamical systems often induce equivariance conditions, which may be associated to multiple spectral values. For instance, it is observed in [73] that the existence of multi-dimensional irreducible representations of the symmetry group may force a spectral value to be multiple. Such multiple roots may induce complex behaviors, for instance, in the case of multiple Hopf points' dynamics one refers the reader to the work [108]. As a matter of fact, it is shown that the Hopf points near a 1 : 1 resonant double Hopf point in a general three-dimensional parameter space form a *Whitney umbrella*, a phenomenon which cannot occur near the standard Hopf points. Furthermore, it is well known the crucial effect of multiplicities (algebraic/geometric) of a given spectral values on the stability of the steady-state of the corresponding dynamical system, see for instance [151]. As an example, the loss of stability of the down hanging equilibrium position of

tubes covering fluid is observed in [204]. It is shown that such an instability is due to a *multiple Hopf point*, which is, itself, due to some symmetries. Recent works by the authors [41, 40, 37] characterized multiple *Crossing Imaginary Roots* (CIR) for time-delay systems using an approach Birkhoff/Vandermonde-based. In [40] it is shown that the admissible multiplicity of the zero spectral value is bounded by the generic *Polya and Szegö bound* denoted PS_B, which is nothing than the *degree* of the corresponding quasipolynomial, see for instance [176]. In [41] it is shown that a given CIR with non vanishing frequency never reach PS_B and a sharper bound for its admissible multiplicities is established. However, even the characterization of the multiplicty of a given complex (non real) spectral value may be carried out by the same approach, it involves hyperbolic/trigonometric *functional confluent Vandemonde matrices*. Furthermore, in such a case the PS_B can never be reached. Furthermore, an example of scalar retarded equation with two delays is studied in [41] where it is shown that the multiplicity of real spectral values may reach the PS_B. The corresponding system has some further interesting properties : (i) it is asymptotically stable, (ii) its spectral abscissa (rightmost root) corresponds to this maximal allowable multiple root located on the imaginary axis. Such observations open the perspective to further explore the exhibiting links between the existence and maximal allowable multiplicity of some negative spectral value reaching PS_B (or the quasipolynomial degree) and the stability of the corresponding dynamical system. In the sequel, the above property is called *multiplicity induced stability*.

Most of the stability analysis in feedback systems is based on the mathematical model of the considered system. However, in practice, it is not possible to find a single fixed model for any physical system such that its behaviour matches with actual system. Therefore, the stability analysis should be done by taking into account the possible perturbations on the parameters of the mathematical model to be considered. In order to find a set of perturbed plants, where the feedback system is stable for all possible plants in this set, the small-gain theorem [223], is widely used.

The present work is a natural continuation of [41] and [40], its aim is to better understand the correspondence between the multiple spectral value variety and the stable variety corresponding to the steady state solution.

The remaining chapter is organized as follows. Section 2 starts by presenting the prerequisite as well as the problem statement. Some motivating example is briefly discussed in section 3. Next, the main results are proposed and proved in Section 4. In Section 5, the multiplicity induced stability is explored for the sunflower equation. Concluding remarks end the chapter.

12.2   Problem Formulation and Prerequisite

In this chapter, we are concerned by the following class of time-delay systems :

$$\dot{x} = \sum_{k=0}^{N} A_k x(t - \tau_k) \tag{12.1}$$

where $x = (x_1, \ldots, x_n) \in \mathbb{R}^n$ denotes the state-vector, under appropriate initial conditions belonging to the Banach space of continuous functions $\mathcal{C}([-\tau_N, 0], \mathbb{R}^n)$. Here τ_j, $j = 1 \ldots N$ are strictly increasing positive constant delays, $\tau_0 = 0$, $\tau = (\tau_1, \ldots, \tau_N)$ and the matrices $A_j \in \mathcal{M}_n(\mathbb{R})$ for $j = 0 \ldots N$. It is well known that the asymptotic behavior of the solutions of (12.1) is determined from the spectrum $\aleph$ designating the set of the roots of the associated characteristic function denoted in the sequel $\Delta(z, \tau)$, often called *quasipolynomial*, that is a transcendental polynomial in the Laplace variable z in which appear exponential terms induced by delays, see for instance [20]. The study of the zeros of such a class of entire functions [136] plays a crucial role especially in the analysis of the asymptotic stability of the zero solution associated with System (12.1). Indeed, the zero solution is asymptotically stable if all the spectral values of (12.1) are in the open left-half complex plane [151].

The characteristic function corresponding to System (12.1) is a quasipolynomial $\Delta : \mathbb{C} \times \mathbb{R}^N_+ \to \mathbb{C}$ of the form :

$$\Delta(z, \tau) = \det\left(z\,I - A_0 - \sum_{k=1}^{N} A_k\, e^{-\tau_k z} \right). \tag{12.2}$$

Without any loss of generality, and for the sake of simplicity, the quasipolynomial function can be written

$$\Delta(z, \tau) = P_0(z) + \sum_{k=1}^{\tilde{N}} P_k(z)\, e^{\sigma_k z}, \tag{12.3}$$

where σ_k are admissible combinations of the components of the delay vector $\tau := (\tau_1, \ldots, \tau_N)$; $\sigma_k := -\sum_{l=1}^{N} \alpha_{k,l} \tau_l$ such that $0 \leq \alpha_{k,l} \leq n$, $\tilde{N}$ the cardinality of all admissible σ_k, which is a positive integer satisfying $\tilde{N} \geq N$. Without any loss of generality, all the σ_k are assumed to be distinct and $\sigma := (\sigma_1, \ldots, \sigma_N)$ is considered as an auxiliary delay vector for the quasipolynomial, see for instance [40]. It is also assumed that $a_{i,j}$ stands for the coefficient of the monomial z^j in P_i, $a_0 := (a_{0,0}, \ldots, a_{0,n})^\top$ is the vector composed from the coefficients of the polynomial P_0 and $p := \left(a_{1,0}, \ldots, a_{1,n_1-1}, \ldots, a_{\tilde{N},0}, \ldots, a_{\tilde{N},n_{\tilde{N}}-1} \right)^\top$. It follows from (12.2) that P_0 is a monic polynomial of degree n in z and the polynomials P_k are such that $\deg(P_k) := d_k - 1 = n - \sum_{l=1}^{N} \alpha_{k,l} \leq (n-1)$.

A given complex number z_0 is said to be *a spectral value* for (12.1) if $\Delta(z_0, \tau^*) = 0$ for some delay vector τ^*. We denote by $\partial_z^k \Delta(z, \tau)$ the k-th derivative of $\Delta(z, \tau)$ given by (12.3) with respect to the variable z. A spectral value z_0 is of algebraic multiplicity $m \geq 1$ if $\Delta(z_0, \tau^*) = \partial_z \Delta(z_0, \tau^*) = \ldots = \partial_z^{m-1} \Delta(z_0, \tau^*) = 0$ and $\partial_z^m \Delta(z_0, \tau^*) \neq 0$. $\mathbb{R}^n$ and $\mathcal{M}_n(\mathbb{R})$ are, respectively, the set of n-dimensional vectors and $n \times n$-dimensional matrices with real numbers denoted as $\mathbb{R}$. For $A \in \mathcal{M}_n(\mathbb{R})$, $z_i(A)$ denotes

its i.th eigenvalue, $i = 1, 2, \ldots, n$. $\mathcal{R}e(\cdot)$ and $\mathcal{I}m(\cdot)$ respectively represent the real and imaginary parts of $(\cdot)$. $j\mathbb{R} := \{j\omega \mid \omega \in \mathbb{R}\}$ is the set of imaginary numbers, where j is the imaginary unit. $\mathbb{C}$ is the set of complex numbers, $\mathbb{R}_+$ is the set positive real numbers. $\mathbb{C}_o := \{s \in \mathbb{C} \mid \mathcal{R}e(s) > 0\}$ is the *open right-half-plane*, $\mathbb{C}_+ := \mathbb{C}_o \cup j\mathbb{R}$ is the *closed right-half-plane*. $\mathcal{H}^\infty$ represents the Hardy space of real functions which are bounded and analytic on $\mathbb{C}_0$. $\mathcal{L}_2^n$ consists of all square integrable and Lebesgue measurable functions. The norm on $\mathcal{H}^\infty$ is $\|G\|_\infty := \sup_{s \in \mathbb{C}_o} \|G(s)\| = \sup_{\omega \in \mathbb{R}} \|G(j\omega)\|$, where $\|\cdot\|$ is the spectral norm. We call G is a stable if $G \in \mathcal{H}^\infty$.

As mentioned in the introduction, the aim of this chapter is to better understand the link between the variety defined by a given multiple (of course stable) root for time-delay systems and the asymptotic stability variety corresponding to steady state solution of the system.

Let us recall some notions and results which will be used in the sequel.

Proposition 14 (Pólya-Szegö, [176], pp. 144). *Let $\hbar_1, \ldots, \hbar_N$ denote real numbers such that $\hbar_1 < \ldots < \hbar_N$, and $d_1, \ldots, d_N$ positive integers satisfying*

$$d_1 \geq 1, \; d_2 \geq 1 \; \ldots \; d_N \geq 1, \quad d_1 + d_2 + \ldots + d_N = D + N.$$

Let $f_{i,j}(s)$ stands for the function $f_{i,j}(s) = s^{j-1} e^{\hbar_i s}$, for $1 \leq j \leq d_i$ and $1 \leq i \leq N$.

Let $\natural$ be the number of zeros of the function

$$f(s) = \sum_{1 \leq i \leq N, 1 \leq j \leq d_i} c_{i,j} \, f_{i,j}(s),$$

that are contained in the horizontal strip $\alpha \leq \mathcal{I}(z) \leq \beta$.
Assuming that

$$\sum_{1 \leq k \leq d_1} |c_{1,k}| > 0, \; \ldots, \; \sum_{1 \leq k \leq d_N} |c_{N,k}| > 0,$$

then

$$\frac{(\hbar_N - \hbar_1)\,(\beta - \alpha)}{2\,\pi} - D + 1 \leq \natural \leq \frac{(\hbar_N - \hbar_1)\,(\beta - \alpha)}{2\,\pi} + D + N - 1.$$

The above result gives a bound on the number of characteristic roots of the quasipolynomial function in the horizontal strip $\alpha \leq \mathcal{I}(z) \leq \beta$. Its proof is based on the argument principal, see also [219] for a modern formulation of the mentioned result.

Now, if one sets $\alpha = \beta$ in the formulation above, then one lets a bound of the number of the quasipolynomial roots such that $\mathcal{I}m(z) = \beta$, which turns to be a bound for the multiplicity of any root z_0 such that $\mathcal{I}m(z_0) = \beta$. This bound is nothing else than the degree of the quasipolynomial i.e. the number of the involved delays including the case where the delay is zero, plus the degrees minus 1. Such a bound is sharp when the corresponding quasipolynomial consists in *complete polynomials* i. e. polynomials having all their terms ordered from the greatest degree up to the independent term.
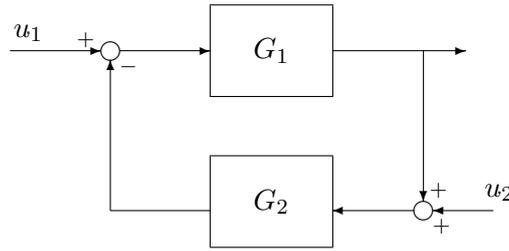
FIGURE 12.1 – Feedback System.

Theorem 37 ([223]). *Let us consider the standard feedback configuration in Figure 12.1, where $u_1 \in \mathcal{L}_2^m, u_2 \in \mathcal{L}_2^n$, and G_1 and G_2 are appropriate dimensional, stable, causal, transfer function matrices. Then, the interconnected system is stable if $\|G_1 G_2\|_\infty < 1$.*

The stability of interconnected system implies $(1 - G_1 G_2)^{-1} \in \mathcal{H}^\infty$, hence, $\Delta(s) = \det(I - G_1(s)G_2(s))$ has no zeros in $\mathbb{C}_+$. By this interpretation of the theorem, if G_1 is a known, stable transfer function, and G_2 represents a set of perturbations, however, its gain is bounded by $\frac{1}{\|G_1\|_\infty}$, then, the interconnected system is stable for all possible poerturbations.

12.3 Motivating example

Let us start with a simple scalar differential equation with one delay representing a biological model discussed by K. L. Cooke in [67] for describing the dynamics of a vector disease model where the infected host population $x(t)$ is governed by :

$$\dot{x}(t) + a_0 \, x(t) + a_1 \, x(t - \tau_1) - a_1 \, x(t - \tau_1) \, x(t) = 0, \tag{12.4}$$

here $a_1 > 0$ designates the contact rate between infected and uninfected populations and it is assumed that the infection of the host recovery proceeds exponentially at a rate $-a_0 > 0$, see also [192] for more insights on the modeling and stability results. Let us focus on the linearized system which is given by :

$$\dot{x}(t) + a_0 \, x(t) + a_1 \, x(t - \tau) = 0. \tag{12.5}$$

Proposition 15. *For a given delay $\tau \in \mathbb{R}_+$, system (12.5) admits a double spectral value at $z = z_0$ if and only if*

$$z_0 = -\frac{a_0 \tau + 1}{\tau} \quad and \quad a_1 = \frac{\mathrm{e}^{-a_0 \tau - 1}}{\tau}. \tag{12.6}$$

If in addition, $a_0 > -\frac{1}{\tau}$ then the zero solution of system (12.5) is asymptotically stable and z_0 is the corresponding rightmost root.
If $a_0 = -\frac{1}{\tau}$ then $z_0 = 0$ is the only double spectral value of (12.5) on the imaginary axis and the set of unstable spectra $\sigma_+ = \emptyset$.

Démonstration. One knows that $z = z_0$ is a spectral value of (12.5) if and only if z_0 is a root of the characteristic equation

$$\Delta(z) = z + a_0 + a_1 e^{-z\tau} = 0. \tag{12.7}$$

Thus, for a fixed delay τ one has $a_1 = -(z_0 + a_0) e^{z_0 \tau}$. Furthermore, z_0 is a double spectral value for (12.5) if and only if $\partial_z \Delta(z_0, \tau) = 0$ and $\partial^2_{zz} \Delta(z_0, \tau) \neq 0$. Hence, one substitute the condition above (guaranteeing that z_0 is a spectral value of (12.5)) in the expression of $\partial_z \Delta(z, \tau)$ one obtains : $1 + z_0 \tau + a_0 \tau = 0$ which gives $z_0 = -\frac{a_0\tau+1}{\tau}$. Now, it can be easily checked that, under the conditions (12.6) we have $\partial^2_{zz} \Delta(z_0, \tau) \neq 0$. Thus, as expected, the maximal multiplicity is two.

Now, when a_1 satisfies (12.6), then one can write the characteristic function (12.7) as :

$$\begin{aligned}
\Delta(z, \tau) &= \left(z + a_0 + \frac{1}{\tau} \right) \left(1 + \frac{e^{-\tau\left(z+a_0+\frac{1}{\tau}\right)} - 1}{\tau \left(z + a_0 + \frac{1}{\tau} \right)} \right) \\
&= \left(z + a_0 + \frac{1}{\tau} \right) \left(1 - \int_0^1 e^{-\tau\left(z+a_0+\frac{1}{\tau}\right)t} \, dt \right)
\end{aligned} \tag{12.8}$$

To prove that $\sigma_+ = \emptyset$, assume that there exists some $z_1 = \zeta_1 + j\, \eta_1$ a root of (12.8) such that $\zeta_1 > 0$. Then ;

$$\begin{aligned}
1 &= \int_0^1 e^{-\tau\left(\zeta_1+j\,\eta_1+a_0+\frac{1}{\tau}\right)t} \, dt \\
&= \Re \left(\int_0^1 e^{-\tau\left(\zeta_1+j\,\eta_1+a_0+\frac{1}{\tau}\right)t} \, dt \right) \\
&\leq \left| \int_0^1 e^{-\tau\left(\zeta_1+j\,\eta_1+a_0+\frac{1}{\tau}\right)t} \, dt \right| \leq \int_0^1 e^{-\tau\left(\zeta_1+a_0+\frac{1}{\tau}\right)t} \, dt.
\end{aligned} \tag{12.9}$$

But, when $a_0 \geq -\frac{1}{\tau}$ for a positive delay τ,

$$\int_0^1 e^{-\tau\left(\zeta_1+a_0+\frac{1}{\tau}\right)t} \, dt < 1 \tag{12.10}$$

which proves the inconsistency of the hypothesis $\zeta_1 > 0$. Furthermore, if one assumes that $\zeta_1 > z_0$, inequality (12.10) leads to the inconsistency of such assumption, which guarantees that z_0 is the corresponding dominant root (rightmost root). $\quad\square$

As an example, consider the linear scalar time-delay systems with two discrete delays. The stability analysis of such a class of systems can be done by using the geometric approach established in [109]. In [41], the following proposition is proved :

Proposition 16 ([41]). *For each pair $(\tau_1, \tau_2) \in \mathbb{R}^*_+ \times \mathbb{R}^*_+$ ($\tau_1 \neq \tau_2$), the equation*

$$\dot{x}(t) + a_1\, x(t - \tau_1) + a_2\, x(t - \tau_2) = 0 \tag{12.11}$$

admits a triple spectral value at $z_0 = -(\tau_1 + \tau_2)/(\tau_1\tau_2)$ if, and only if, $a_1 = \tau_2 e^{\tau_1 z_0}/(\tau_2\tau_1 - \tau_1^2), a_2 = \tau_1 e^{\tau_2 z_0}/(\tau_2\tau_1 - \tau_2^2)$. Moreover, under this configuration, z_0 is the rightmost root and the zero solution is asymptotically stable. When additionally, the system parameters $a_1, a_2 \in \mathbb{R}^+$ then any spectral value is simple.

If the parameters of the system are left free, the above proposition establishes conditions for z_0 to be triple root of (12.11) for any arbitrarily chosen positive delays τ_1 and τ_2. It is important to emphasize that, for an arbitrarily chosen triplet (z_0, τ_1, τ_2) with $z_0 \in \mathbb{C}$, the set of conditions $a_1 = \tau_2 e^{\tau_1 z_0} / (\tau_2 \tau_1 - \tau_1^2), a_2 = \tau_1 e^{\tau_2 z_0} / (\tau_2 \tau_1 - \tau_2^2)$, guarantees that z_0 is a double root for (12.11). That is, the multiplicity three imposes only the negative value of such a root $z_0 = -(\tau_1 + \tau_2)/(\tau_1 \tau_2)$. Furthermore, it is important to recall that no any spectral value can have an algebraic multiplicity greater than three, which is the Polya and Szegö bound PS_B.

From an application point of view, when additional restrictions on the system's parameters are set, then such a multiplicity may not be reached. For instance, a wide range of applications in physics and biology may consider a positivity constraint on the system parameters, see for instance [107]. In such a case, any spectral value z_0 is simple. Indeed, a root to be double for (12.11), demand that $a_1 a_2 < 0$.

Lemma 9. *Let us consider the following delay-differential equation*

$$\dot{x}(t) = Ax(t - \tau), \tag{12.12}$$

where τ is a positive real number, $A \in \mathcal{M}_n(\mathbb{R})$ with real eigenvalues. Then, the characteristic function of (12.12) has at a zero on the imaginary axis if and only if

$$\tau := \begin{cases} \frac{1}{|z_i(A)|}(\frac{\pi}{2} + 2N\pi), & z_i(A) < 0 \\ \frac{1}{|z_i(A)|}(\frac{\pi}{2} + (2N+1)\pi), & z_i(A) > 0 \\ c & z_i(A) = 0 \end{cases},$$

at least for $i = 1, 2, \ldots, n$, N is a non-negative integer, and c is any positive real number.

Démonstration. By the eigenvalue-decomposition of A, there exists a non-singular matrix $V \in \mathcal{M}_n(\mathbb{R})$ such that $V^{-1}AV = z$, where z is a block diagonal matrix, whose non-zero entries are eigenvalues of A. Then, by utilizing the similarity transformation $y := Vx$, the characteristic function of (12.12) can be written as

$$\Delta(z, \tau) := \prod_{i=1}^{\hat{n}} (z - z_i(A)e^{-z\tau})^{m_i}, \tag{12.13}$$

where m_i is the multiplicity of $z_i(A)$, $\sum_{i=1}^{\hat{n}} m_i = n$. From (12.13), $\Delta(j\omega^*, \tau^*) = 0$ for some non-negative (ω^*, τ^*)-pair if and only if

$$rCl\omega^* + z_i(A)\sin(\omega^*\tau^*) = 0 \tag{12.14}$$
$$z_i(A)\cos(\omega^*\tau^*) = 0 \tag{12.15}$$

holds at least for one i, $i = 1, \ldots, n$. Note, (12.15) is satisfied at frequencies $\omega^* = \frac{1}{\tau^*}(\frac{\pi}{2} + N\pi)$, where N is arbitrary but positive integer, if $z_i(A)$ is non-zero. Then, the imaginary axis crossing frequencies are only points, whose magnitudes correspond to the magnitudes of eigenvalues of A. Therefore, (12.14-12.15) is satisfied for $\omega^* = -z_i(A)$ at $\tau^* = \frac{1}{\omega^*}(\frac{\pi}{2} + 2N\pi)$, when $z_i(A) < 0$, and $\omega^* = z_i(A)$ at $\tau^* = \frac{1}{\omega^*}(\frac{\pi}{2} + (2N+1)\pi)$, when $z_i(A) > 0$. $\square$

Corollary 8. *The characteristic function of (12.12) for $A \in \mathcal{M}_n(\mathbb{R})$ with real non-zero eigenvalues has no any zeros in $\mathbb{C}_+$ if and only if*

$$\tau < \min\left\{\frac{\pi}{2z_m}, \frac{3\pi}{2z_p}\right\}, \tag{12.16}$$

where

$$z_m = |\min_{i=1,..,n} z_i(A)|, \tag{12.17}$$

$$z_p = \max_{i=1,..,n} |z_i(A)|. \tag{12.18}$$

Démonstration. Since the imaginary axis crossing frequencies of (12.12) are the magnitudes of eigenvalues of A, the minimum τ^* for which the (12.14–12.15) holds for negative eigenvalues of A, if exists, is $\tau^* = \pi/2|\min_{\{i=1,2,...,n\}} z_i(A)|$. Similarly, the minimum τ^* for which the (12.14–12.15) holds for positive eigenvalues of A, if exists, is $\tau^* = 3\pi/2 \max_{i=1,2,...,n} z_i(A)$.

$\square$

Now, let us consider some more general case :

Proposition 17. *Consider system (12.1). Suppose that for some $k = 0,..,N$, there exists index such that*

$$\tau_k^* < \min\left\{\frac{\pi}{2}\frac{1}{z_{mk^*}}, \frac{3\pi}{2}\frac{1}{z_{pk^*}}\right\}, \tag{12.19}$$

where z_{mk^*}, z_{pk^*}, which are defined in (12.17,12.18) for the corresponding A_k, are non-zero. Then, the characteristic equation of (12.1) has no right-half-plane zeros for all τ_k, $k = \{1,..N\}\backslash\{k^*\}$, if

$$\sum_{k=0, k\neq k^*}^{N} \|A_k\|_2 < \frac{1}{\|(zI - A_k^* e^{-zk^*})^{-1}\|_\infty}, \tag{12.20}$$

Démonstration. Let for some $k = 1,..,N$, say $k = k^*$, there exists τ_k^* satisfying (12.19). Then, since $\Delta(z, \tau_k^*) := \det((zI - A_k^* e^{-z\tau_k}))$ has no zeros in $\mathbb{C}_+$, $G_1(s) := (zI - A_k^* e^{-z\tau_k^*})^{-1} \in \mathcal{H}^\infty$. In addition, since $e^{-\tau z} \in \mathcal{H}^\infty$ for any $\tau > 0$, $G_2 := \sum_{k=0, k\neq k^*}^{N} A_k e^{-zk} \in \mathcal{H}^\infty$. Then, from (12.20), since

$$\|G_1 G_2\|_\infty \leq \|G_1\|_\infty \sum_{k=0, k\neq k^*}^{N} \|A_k\|_2 < 1,$$

by Theorem 37,

$$\left(I - \frac{G_2(z)}{G_1(z)}\right)^{-1} \in \mathcal{H}^\infty, \tag{12.21}$$

which implies that $\det(zI - \sum_{k=0}^{N} A_k e^{-z\tau_k})$ has no zeros in $\mathbb{C}_+$, $\forall \tau_k$, $k = \{1,..N\}\backslash\{k^*\}$.

$\square$

Let us now discuss the robustness of the stability criteria established in Proposition 16. For that, consider System (12.11) with fixed delays $(\tau_1, \tau_2) = (\tau_1^*, \tau_2^*)$ and assume that (a_1^*, a_2^*) are chosen such that the maximal multiplicity is reached. Then, consider a perturbation of the delay vector $(\tau_1, \tau_2) = (\tau_1^* + \varepsilon_1, \tau_2^* + \varepsilon_2)$ (thus z_0^* is no further a triple spectral value for Equation (12.11)). Figure 12.3 gives the stability crossing curves for Equation (12.11).
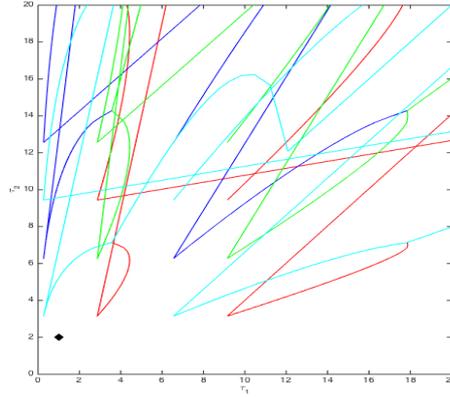

FIGURE 12.2 – Stability crossing curves corresponding to Equation (12.11) in (τ_1, τ_2) plane where $(a_1, a_2) = (a_1^*, a_2^*)$ defined by 16 with $(\tau_1^*, \tau_2^*) = (1, 2)$. Here we use the algorithm from [109].

Lemma 10. *Let us consider* (12.11) *with fixed delays τ_1^* and τ_2^* which admits a maximal multiplicity at $z_0 = z_0^* := -(\tau_1^* + \tau_2^*)/(\tau_1^* \tau_2^*)$, where it is assumed that $\tau_2^* > \tau_1^*$. Then, the characteristic function of* (12.11) *has no $\mathbb{C}_+$ zeros for all $\tau_1 \in [\tau_1^*, \tau_1^* + \varepsilon_1)$ and $\tau_2 \in [\tau_2^*, \infty)$, where*

$$\varepsilon_1 < \pi/2 \left(\frac{1}{a_2^2 - a_1^2 + 2a_1} \right)^{1/2} - \tau_1^* \tag{12.22}$$

Démonstration. By Proposition 16, (12.11) admits the maximal multiplicity at z_0^* if and only if $a_i = \frac{\tau_j^* e^{\tau_i^* z_0^*}}{(\tau_j^* - \tau_i^*)\tau_i^*}$, $i, j = 1, 2$, $i \neq j$. Note, since $\tau_2^* > \tau_1^*$, $a_1 > |a_2|$, where a_2 is negative. In addition, since $|a_i| < 1$, $i = 1, 2$,

$$\frac{1}{a_2^2 - a_1^2 + 2a_1} > 0. \tag{12.23}$$

Then, if $G_1(z) := \frac{1}{z + a_1 e^{-(\tau_1^* + \varepsilon_1)z}} \in \mathcal{H}^\infty$, by utilizing the small-gain theorem and from (12.23), since

$$\sup_{\omega \in \mathbb{R}} \left| \frac{a_2 e^{-j\tau^* \omega}}{(j\omega + a_1 e^{-(\tau_1^* + \varepsilon_1)j\omega})} \right|^2 < \frac{a_2^2}{(\frac{\pi}{2} \frac{1}{\tau_1^* + \varepsilon_1})^2 + a_1^2 - 2a_1} < 1, \tag{12.24}$$

for a positive τ^*, the characteristic function of (12.11) has no $\mathbb{C}_+$ zeros for all $\tau_1 \in [\tau_1^*, \tau_1^* + \varepsilon_1)$ and $\tau_2 \in [\tau_2^*, \infty)$. Note, since $1 > a_1 > |a_2|$, $(\tau_1^* + \varepsilon)a_1^* < \pi/2$, then, by Lemma 9, $G_1(z)$ is stable. $\qquad\square$

As shown in Figure 12.3, the characteristic function of (12.11), where (a_1^*, a_2^*) are chosen such that the maximal multiplicity is reached, has no any zeros in $\mathbb{C}_+$ for sufficiently large τ_2 values, while $\tau_1 a_1^* < \pi/2$.
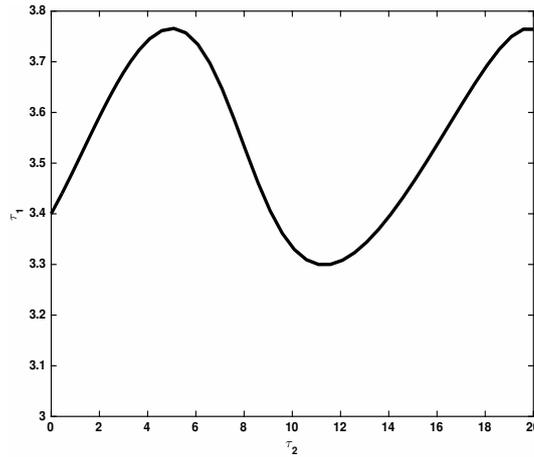

FIGURE 12.3 – Imaginary axis curve seperating the $(\tau_1 - \tau_2)$ delay-parameter space into two regions for the system in (12.11) in (τ_1, τ_2) plane where $(a_1, a_2) = (a_1^*, a_2^*)$ defined by 16 with $(\tau_1^*, \tau_2^*) = (1, 2)$. The plots are obtained by using DDE-BIFTOOL [87, 86]

12.4   Main result

In this section, we shall extend the result of Proposition 16 for two more general classes of systems. The first is nothing than the scalar equation with N delay blocks. The second is the general planar system with two delays.

12.4.1   A scalar equation with N-delay blocks

The following proposition generalizes the result of [41] given in Proposition 16. to linear systems with N constant delays given by :

$$\dot{x}(t) + \sum_{i=0}^{N} a_i\, x(t - \tau_i) = 0. \tag{12.25}$$

where $\tau_0 = 0$ and $\tau_l < \tau_i$ for $l < i$.

Proposition 18. *System* (12.25) *admits a rightmost spectral value at* $z = z_0$ *with multiplicity* $N + 1$ *if and only if*

$$\begin{cases} z_0 = -a_0 - \sum_{i=1}^{N} \frac{1}{\tau_i} & and \\ a_i = \frac{e^{z_0 \tau_i}}{\tau_i} \prod_{\substack{l=1 \\ l \neq i}}^{N} \frac{\tau_l}{(\tau_l - \tau_i)} & for \ i = 1, \dots, N. \end{cases} \tag{12.26}$$

If in addition, $z_0 < 0$ *then the zero solution of system* (12.25) *is asymptotically stable.*

Démonstration. A spectral value z_0 of (12.25) is a root of the characteristic equation

$$\Delta(z) = z + \sum_{i=0}^{N} a_i \, e^{-z \tau_i}. \tag{12.27}$$

Some tedious algebraic computations allow to check that when the system parameters satisfy (12.26) then $\Delta(z_0, \tau) = \dots = \partial_{z,\dots,z}^{N} \Delta(z_0, \tau) = 0$ and $\partial_{z,\dots,z}^{N+1} \Delta(z_0, \tau) \neq 0$.

Now, when a_i satisfy (12.26), then one can write the characteristic equation (12.27) as :

$$\Delta(z) = \left(z + a_0 + \sum_{l=1}^{N} \frac{1}{\tau_l} \right)$$

$$\left(1 + \frac{\sum_{i=1}^{N} \frac{e^{-\left(z + a_0 + \sum_{l=1}^{N} \frac{1}{\tau_l}\right) \tau_i}}{\tau_i} \prod_{\substack{l=1 \\ l \neq i}}^{N} \frac{\tau_l}{(\tau_l - \tau_i)} - \sum_{i=1}^{N} \frac{1}{\tau_i}}{\left(z + a_0 + \sum_{l=1}^{N} \frac{1}{\tau_l} \right)} \right). \tag{12.28}$$

To prove that $\sigma_+ = \emptyset$, let assume that there exists $z_1 = \zeta_1 + j \, \eta_1$ a root of (12.28) such that $\zeta_1 > 0$. Let us set $c_i = \prod_{\substack{l=1 \\ l \neq i}}^{N} \frac{\tau_l}{(\tau_l - \tau_i)}$, then, we have

$$1 = \sum_{i=1}^{N} \frac{c_i \, e^{-(z_1 - z_0) \tau_i}}{\tau_i \, (z_1 - z_0)} - \sum_{i=1}^{N} \frac{1}{\tau_i \, (z_1 - z_0)} \tag{12.29}$$

Interestingly, the following equality which can be easily shown by induction gives considerable simplification on the above expression

$$\sum_{i=1}^{N} \frac{c_i}{\tau_i} = \sum_{i=1}^{N} \frac{1}{\tau_i} \quad and \quad c_i = \prod_{\substack{l=1 \\ l \neq i}}^{N} \frac{\tau_l}{(\tau_l - \tau_i)} \tag{12.30}$$

Thus, (12.29) can be written :

$$1 = \sum_{i=1}^{N} c_i \int_0^1 e^{-(z_1 - z_0) \tau_i t} \, dt, \tag{12.31}$$

which implies :

$$1 = |\sum_{i=1}^{N} c_i \int_0^1 e^{-(\zeta_1 - z_0)\tau_i t}\, dt| \leq \sum_{i=1}^{N} |c_i \int_0^1 e^{-(\zeta_1 - z_0)\tau_i t}|\, dt \qquad (12.32)$$

But, when $a_0 \geq -\frac{1}{\tau}$, for a positive delay τ,

$$\int_0^1 e^{-\tau\left(\gamma_1 + a_0 + \frac{1}{\tau}\right)t}\, dt < 1, \qquad (12.33)$$

which proves the inconsistency of the hypothesis $\zeta_1 > 0$. $\qquad\square$

In the sequel, we will present some sufficient conditions to discuss the stability margins of linear systems defined as in (12.25).

Lemma 11. *The characteristic function of the linear system given in (12.25) has no zeros in $\mathbb{C}_+$ for all positive τ_i values satisfying either*

$$\sum_{i=1,i\neq k}^{N} \frac{1}{\tau_i} < 2a_k(1 - \sin(a_k\tau_k)), \qquad (12.34)$$

where $a_k\tau_k < \pi/2$, and $a_k \neq 0$, or

$$\sum_{i=1}^{N} \frac{1}{\tau_i} < a_0, \qquad (12.35)$$

if $\sum_{i=1}^{N} a_i < a_0$.

Démonstration. Let us assume that a_0 in (12.25) equals to 0 and at least one a_i, $i = 1, \ldots, N$, say a_k, $a_k\tau_2 < \pi/2$. Then, by Corollary 8, $\Delta_k(z, \tau_k) = (z + a_k e^{-s\tau_k})$ has no zeros in $\mathbb{C}_+$, where z is the Laplace variable. Note, since the characteristic function of (12.25) can be written as

$$\Delta(z, \tau) = (z + a_k e^{-z\tau_k})\left(1 - \frac{\sum_{i=1,i\neq k}^{N} a_i e^{-z\tau_i}}{z + a_k e^{-z\tau_k}}\right), \qquad (12.36)$$

by the small-gain theorem, $\Delta(z, \tau)$ has no zeros in $\mathbb{C}_+$ if

$$\left\|\frac{\sum_{i=1,i\neq k}^{N} a_i e^{-z\tau_i}}{z + a_k e^{-z\tau_k}}\right\|_\infty < 1. \qquad (12.37)$$

Now, let $G_1(z) := \frac{1}{z + a_k e^{-z\tau_k}}$ and $G_2(z) := \sum_{i=1,i\neq k}^{N} a_i e^{-z\tau_i}$. Then, since

$$\frac{\partial}{\partial\omega}|G_1(j\omega)|^2 = \frac{2\omega - 2a_k\sin(\omega\tau_k) - 2\omega a_k\tau_k\cos(\omega\tau_k)}{\left(\omega^2 + a_k^2 - 2\omega a_k\sin(\omega\tau_k)\right)^2},$$

$\frac{\partial}{\partial \omega}|G_1(j\omega)|^2 = 0$ for some $\omega = \omega^*$, where ω^* is the solution of

$$\omega^* = \frac{a_k \sin(\omega^* \tau_k)}{1 - a_k \tau_k \cos(\omega^* \tau_k)}.$$

Then, since $G_1 \in \mathcal{H}^\infty$,

$$\|G_1\|_\infty \le \frac{1}{2a_k(1 - \sin(a_k \tau_k))} < \infty. \tag{12.38}$$

In addition, since $G_2 \in \mathcal{H}^\infty$, by (12.30),

$$\|G_2\|_\infty \le \sum_{i=1}^N a_i = \sum_{i=1,N} \frac{1}{\tau_i}.$$

Therefore, by the small-gain theorem, the characteristic functions of (12.25) has no zeros for delay values satisfying (12.34).

For the case of $a_0 \ne 0$, since $a_0 > 0$ and $G_1 : (z) = \frac{1}{z+a_0}$ is in $\mathcal{H}^\infty$ and its $\mathcal{H}^\infty$ norm is bounded by $(1/a_0)$. Then, by the small-gain theorem, the characteristic functions of (12.25) has no zeros for parameters satisfying (12.35). $\qquad\square$

12.4.2 Revisiting sunflower dynamics

In this section we revisit a standard model describing the helical movement of a growing plant, known as the *Sunflower model* :

$$\ddot{x} + \frac{a}{\tau}\dot{x} + \frac{b}{\tau}\sin(x(t - \tau)) = 0 \tag{12.39}$$

Such a model is known to reproduce the dynamics of the upper part of the stem of the plant, which performs a rotating movement. Here the state $x(t)$ designates the angle of the plant with respect to the vertical line and the delay τ corresponds to a geotropic reaction time and a and b some positive parameters, see for instance [226]. In the sequel, we consider the linearized system with $\alpha = a/\tau$ and $\beta = b/\tau$:

$$\ddot{x} + \alpha\dot{x} + \beta x(t - \tau) = 0 \tag{12.40}$$

The following proposition emphasizes again the effect of the multiplicity of a given spectral value on the asymptotic stability of the zero solution of (12.40).

Proposition 19. *System* (12.40) *admits a spectral value at z with multiplicity 2 if and only if $(\alpha, z) = (\alpha_+, z_+)$ or $(\alpha, z) = (\alpha_-, z_-)$ where :*

$$\begin{cases} \alpha_- = -\left(2 + \sqrt{4 + \tau^2\beta^2}\right) e^{1/2\,\tau\left(-\beta - \frac{2+\sqrt{4+\tau^2\beta^2}}{\tau}\right)} \tau^{-2}, \\[2mm] z_- = -\frac{\beta}{2} - \frac{2 + \sqrt{4 + \tau^2\beta^2}}{2\tau} \\[2mm] \alpha_+ = \left(-2 + \sqrt{4 + \tau^2\beta^2}\right) e^{1/2\,\tau\left(-\beta + \frac{-2+\sqrt{4+\tau^2\beta^2}}{\tau}\right)} \tau^{-2}, \\[2mm] z_+ = -\frac{\beta}{2} + \frac{-2 + \sqrt{4 + \tau^2\beta^2}}{2\tau} \end{cases} \tag{12.41}$$

Furthermore, when $(z, \alpha) = (z_+, \alpha_+)$ (respectively (z_-, α_-)) and $\tau\beta > 2\sqrt{3}$ ($\tau\beta < 2\sqrt{3}$) then z_+ (respectively z_-) is a the rightmost root and the corresponding steady state solution is asymptotically stable.

Démonstration. The vanishing of the corresponding quasipolynomial as well as its first derivative gives the two admissible solutions presented in (12.41). Here, the bound of the multiplicity is reached since $PS_B(\Delta) = 2$. Furthermore, for a fixed $(\tau, \beta) \in \mathbb{R}_+^* \times \mathbb{R}_+$ if $\alpha = \alpha_+$ one has $z = z_+$ is a double root of $\Delta_+(z, \tau) = 0$. One can writes the corresponding equation as :

$$\Delta_+(z, \tau) = (z - z_+)^2 \left(1 + \frac{\Delta_+(z, \tau) - (z - z_+)^2}{(z - z_+)^2} \right) = 0. \tag{12.42}$$

Similarly to the proof of Proposition 15, equation (12.42) gives :

$$\Delta_+(z, \tau) = (z - z_+)^2 \left(1 + \int_0^1 \int_0^s \tau \, (2\, z_0 + \beta) \, \mathrm{e}^{-\tau\,(z - z_0)t} dt \, ds \right) = 0. \tag{12.43}$$

Let $z_1 = \gamma_1 + j\omega_1$ be a root of the second factor of Δ_+ such that $\gamma_1 > z_0$ and $\beta\tau > 2\sqrt{3}$ then,

$$1 < \int_0^1 \int_0^s 2\mathrm{e}^{-\tau\,(z_1 - z_0)t} dt \, ds. \tag{12.44}$$

Thus, the assymption is inconsistent and the root z_+ is the rightmost root. Finally, the zero solution is asmptotically stable. The proof for z_- is similar. □

12.4.3 Further remarks : Sensitivity of multiple spectral value

Consider the quasipolynomial

$$\Delta(\lambda, \tau) = \lambda^3 - 1 + b\,\lambda + a\,\mathrm{e}^{-\lambda\tau}. \tag{12.45}$$

The parameter values $\{a^* = 3\,\mathrm{e}^{-1}, b^* = 3/2\,\sqrt[3]{2}, \tau^* = \sqrt[3]{2}\}$ guarantee the existence of a quadruple spectral value at $\lambda_0 = -\frac{2^{2/3}}{2}$. If one considers the particular quasi-polynomial

$$\Delta^*(\lambda, \tau) = \lambda^3 - 1 + b^*\,\lambda + a^*\,\mathrm{e}^{-\lambda\tau}. \tag{12.46}$$

and a delay $\tau \in (\tau^* - \varepsilon, \tau^* + \varepsilon)$ for a sufficiently small positive ε one can observe that the dominant root is the most sensitive to the delay variation see Figure 12.4.3. Furthermore, for $\tau = \tau^* + \varepsilon$ there are always two real roots, see Figure 12.4.3.

12.5 Concluding Remarks

In this note we studied a link between the variety corresponding to a multiple spectral value and the one corresponding to the asymptotic stability of the steady state solution for Time-delay systems. Furthermore, such an emphasized link allows
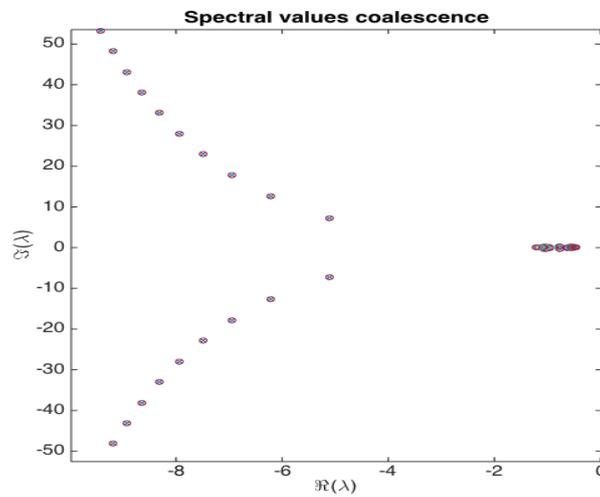
FIGURE 12.4 – Sensitivity of the roots of (12.46) near $\tau = \tau^*$. The dominant root is the most sensitive. Here we use QPMR algorithm from [215].
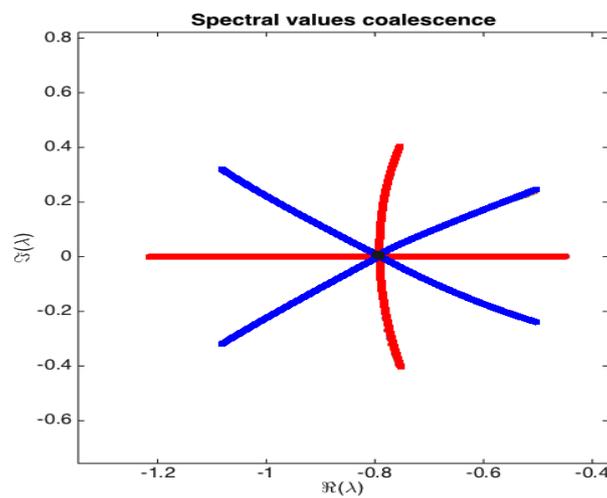

FIGURE 12.5 – Migration of the quadruple root corresponding to (12.46) near $\tau = \tau^*$. Here we use QPMR algorithm from [215].

to drive some simple algebraic criteria for stability based on the explicit analytic identification of the rightmost root. In addition, it is shown that presence of multiple spectral value may allow large perturbations on the delay parameter values of the system. Finally, such a criterion may have a potential implication in control system applications due to its simplicity in design as well as its robustness.

A Spectral Analysis for a class of Lossless Propagation Models

The aim of this chapter is the study of the stability properties of a class of systems expressed by functional differential equations coupled with difference equations. More precisely, the study concerns the spectral theory of Lossless propagation models. First, by introducing an appropriate bilinear form, we extend the spectral projection methodology for simple spectral values for Lossless propagation models. For multiple spectral values an explicit spectral projection formula is provided involving a Dunford calculus. Moreover, a sufficient criteriun for the convergence of series expansions of solutions of Lossless propagation models is established. For the nonlinear case, the center manifold theorem is extended to this class of systems leading to approximate qualitatively the solutions behavior of the infinite dimensional system by the dynamics of a finite dimensional system. Finally, the paper provides illustrative examples for the obtained results.

Part from the provided results was already published in a short conference paper [32]. The proofs of the results given in this chapter can be found in [33].

13.1   Introduction

We are concerned with systems of functional differential equations coupled with difference equations where the elements of interconnection are represented by the delay terms. More precisely, the study concerns the spectral properties of Lossless propagation models called also *Hybrid systems*, see [117]. This class of systems is frequently encountered in control problems where the delay terms come naturally from the feedback. In general by Lossless propagation it is understood the phenomenon associated with long transmission lines for physical signals. In engineering, this problem is strongly related to electric and electronic applications, e.g. circuit structures consisting of multipoles connected through LC transmission lines, this can also be seen in steam and water pipes [165, 99]. The linear and simpler form of such systems can be written

$$\left.\begin{aligned}
\dot{x}(t) &= A\,x(t) + B\,y(t-\tau)\\
y(t) &= C\,x(t) + D\,y(t-\tau)
\end{aligned}\right\} \tag{13.1}$$

where the variables x and y are not necessarily of the same dimension, and the matrix D not necessarily invertible. In [99], the authors establish an efficient matrix

pencil method with high precision in the study of stability.

From another point of view, this type of systems implies but not equivalent to Functional Differential Equations of Neutral type (NFDE)

$$
\left.
\begin{aligned}
\dot{x}(t) &= A\,x(t) + B\,y(t-\tau) \\
\dot{y}(t) - D\,\dot{y}(t-\tau) &= C\,A\,x(t) + C\,B\,y(t-\tau)
\end{aligned}
\right\} .
\tag{13.2}
$$

To the best of our knowledge this treatment by letting $y(t) = \dot{z}(t)$ was suggested first in [1] also applied in [193] and in [116]. This transformation will be called in what follows *Standard Transformation*.

This type of systems is subject to prolific interest due to its frequent use in the modeling for physical and biological phenomenas [185, 151, 91, 107]. In [115] a bilinear form associated to this systems class is defined, which allows [95] to establish an efficient spectral projection procedure. Indeed, [95] is concerned with large time behavior of solutions of linear autonomous NFDE.

We underline the fact that defining such spectral projections represents an important tool to the study of nonlinear systems. Indeed, it permits to restrict the flow to a finite dimensional subspace which is invariant under the solution semigroup. For instance the study of local bifurcations often needs the computation of the center manifold which is characterized by spectral values with zero real part. Unfortunately, spectral projection defined for (13.2) can not be directly invested in the study of the center manifold associated to system (13.1) since the algebraic multiplicity of the zero spectral value increase when using the standard reduction from (13.1) to (13.2) which induces additional dynamics.

Motivated by this fact, we focus this work on establishing a direct way for analyzing such hybrid systems avoiding the use of the standard reduction. To this end, we first introduce a bilinear form associated to (13.1) and then describe a procedure for computing spectral projection associated with simple and multiple spectral values. Then we shall address the question whether the solution of (13.1) can be represented by a series of elementary solutions. This question was tackled for the retarded case [13] and neutral one [128] and [141] but never asked for Lossless systems.

For the sake of self containment, we recall the outlines of the general theory of NFDE at the appendix. We first start by recalling a theorem giving necessary and sufficient conditions for the solution of NFDE to be represented by a series of elementary solutions.

Theorem 38 ([141]). *Let $C = C([-r,0],\mathbb{R}^n)$ denote the Banach space of continuous functions endowed with the supremum norm and let $\mathcal{T}(t) : C \to C$ denote the semigroup of solution operators associated with*

$$
\frac{d}{dt}[x(t) - D_0 x(t-r) - \sum_{k=1}^{\infty} D_k\, x(t-\tau_n)] = \int_0^h d\zeta(\theta)x(t-\theta)
$$

where ζ is an $n \times n$ matrix function of bounded variation, for $j = 1, 2, \ldots, \tau_j < r$ and D_0 is a nonsingular matrix, and $\mid D_j \mid \to 0$ as $j \to \infty$. Let $\lambda_j,\ j = 0, 1, \ldots$ the

associated set of spectral values and P_{λ_j} the associated spectral projection given by

$$P_\lambda = \frac{1}{2\Pi i} \int_{\Gamma_\lambda} (zI - \mathcal{A})^{-1} \, dz. \tag{13.3}$$

where $\mathcal{A}$ is the infinitesimal generator associated with the semigroup $\mathcal{T}(t)$. Then the semigroup $\mathcal{T}(t)$ extends to a group of bounded linear operators and for every $\varphi \in C$, we have

$$\lim_{N \to \infty} \| \mathcal{T}(t)\varphi - \frac{1}{N} \sum_{k=0}^{N-1} \sum_{j=0}^{k} \mathcal{T}(t)P_{\lambda_j}\varphi \| = 0, \qquad t \in \mathbb{R}^+ \tag{13.4}$$

uniformly on compact t-sets.

The invertibility of D_0 ensure that the generator semigroup $\mathcal{T}(t)$ has a complete system of eigenvectors and generalized eigenvectors, see [141] and [128]. Accordingly, the invertibility of D_0 guaranties the exclusion of small solutions, thus, the backward integration is possible via

$$\dot{x}(t) = D_0^{-1}[\dot{x}(t+r) - \sum_{k=1}^{n} A_k \, \dot{x}(t - \tau_n + r) + \int_0^h d\zeta(\theta)x(t-\theta)].$$

For more details about completeness of system of eigenvectors and generalized eigenvectors see [142].

Unfortunately, this theorem can not be directly applied to Lossless systems (13.1) by the only use of the Standard transformation. Indeed, the difference matrix $D_0 = \begin{pmatrix} 0 & 0 \\ 0 & D \end{pmatrix}$ of the transformed system (13.2) is not invertible.

The remaining paper is organized as follow. The second section is devoted to the main results : first, we extend the spectral projection associated with simple spectral values by defining a bilinear form associated with Lossless systems. Next, Dunford calculus is involved for computing the spectral projection associated with arbitrary multiplicity nonzero spectral values. Moreover, some sufficient conditions for series convergence although in some special cases when the matrix D is singular. In the light of these results, in section 3, we extend the center manifold theorem to a class of nonlinear Lossless propagation models, namely,

$$\left. \begin{array}{l} \dot{x}(t) = A\,x(t) + B\,y(t-\tau) + f_1(x(t), y(t), y(t-\tau)) \\ y(t) = C\,x(t) + D\,y(t-\tau) + f_2(x(t), y(t), y(t-\tau)) \end{array} \right\}. \tag{13.5}$$

The section 4 ends the paper by illustrative examples.

13.2 Main Result : Spectral Projection for Lossless propagation model

Consider the system (13.1) where $x \in \mathbb{R}^m$ and $y \in \mathbb{R}^n$ and A, B, C, D are real valued matrices. Thus $A \in \mathcal{M}_{m,m}(\mathbb{R})$, $B \in \mathcal{M}_{m,n}(\mathbb{R})$, $C \in \mathcal{M}_{n,m}(\mathbb{R})$, $D \in \mathcal{M}_{n,n}(\mathbb{R})$.

Analogously, to the well prescribed general theory for functional differential equations [115, 115, 151, 107], the infinitesimal generator associated with the semigroup of the solution operator $\mathcal{T}(t)$ is given by

$$\mathcal{D}om(\mathcal{A}) = \{\varphi = (\varphi_1, \varphi_2)^T \in \mathcal{C}, \text{ s.t. } \frac{d\varphi}{d\theta} \in \mathcal{C}, \mathcal{D}\frac{d\varphi}{d\theta} = \mathcal{L}\,\varphi\},$$

$$\mathcal{A}\varphi = \frac{d\varphi}{d\theta} \text{ and}$$

$$\mathcal{L}\,\varphi = (A\varphi_1(0) + B\varphi_2(-\tau), C\varphi_1(0) - \varphi_2(0) + D\varphi_2(-\tau))^T,$$

$$\mathcal{D}\,\varphi = (\varphi_1(0), 0)^T. \tag{13.6}$$

The associated characteristic matrix is

$$\Delta(z) = \begin{pmatrix} z\,I_n - A & -e^{-z\,\tau}\,B \\ -C & I_m - e^{-z\,\tau}\,D \end{pmatrix}, \tag{13.7}$$

thus λ is said to be a spectral value if $\mathbb{H}(\lambda) = det(\Delta(\lambda)) = 0$.

13.2.1   Bilinear Form for Lossless propagation model

Let us consider φ an $m + n$ column vector and ψ an $m + n$ row vector,

$$\varphi = \begin{pmatrix} v_1 \\ \vdots \\ v_n \\ v_{n+1} \\ \vdots \\ v_{n+m} \end{pmatrix} \text{ and } \psi = (u_1, \ldots, u_n, u_{n+1}, \ldots, u_{n+m}).$$

Moreover, let us set $\psi = \psi_1 + \psi_2 = (u_1, \ldots, u_n, 0, \ldots, 0) + (0, \ldots, 0, u_{n+1}, \ldots, u_{n+m})$.

Analogously, let us set for a block matrix

$$J = \begin{pmatrix} L & M \\ N & Q \end{pmatrix}$$

then $J = \tilde{J}_1 + \tilde{J}_2 = \begin{pmatrix} L & M \\ 0 & 0 \end{pmatrix} + \begin{pmatrix} 0 & 0 \\ N & Q \end{pmatrix}$.

Let denote by $\Gamma(\theta)$ the $m + n$ square matrix where

$$\Gamma(-\tau) = \begin{pmatrix} 0 & \ldots & 0 & 0 & \ldots & 0 \\ \vdots & \ldots & \vdots & \vdots & \ldots & \vdots \\ 0 & \ldots & 0 & 0 & \ldots & 0 \\ 0 & \ldots & 0 & & & \\ \vdots & \ldots & \vdots & & D & \\ 0 & \ldots & 0 & & & \end{pmatrix},$$

and

$$\Gamma(0) = I_d - \tilde{I}_{d1},$$

and for all $s \in [-\tau, 0]$ $\Gamma(s) = \Gamma(0) + \frac{s}{\tau}(\Gamma(0) - \Gamma(-\tau))$ and thus we define the bilinear form $< .,. >: \mathcal{C}^* \times \mathcal{C} \to \mathbb{C}$ by

$$
\begin{aligned}
< \psi, \varphi > = & -\psi_1(0)\varphi(0) - \int_{-\tau}^{0} \frac{d}{d\theta}[\frac{d\psi(\theta)}{d\theta}\,\Gamma(\theta)\,\varphi(\theta)]d\theta \\
& + \int_{-\tau}^{0} \psi_2(\tau + \theta)\varphi(\theta)d\theta.
\end{aligned}
\tag{13.8}
$$

13.2.2 Computing spectral projections using duality : Simple non zero spectral values

By analogy with the theory of NFDE outlined in the appendix, when λ is a simple nonzero eigenvalue of an operator $\mathcal{A}$, then the spectral projection onto the eigenspace $\mathcal{M}_\lambda$ is given by

$$P_\lambda(\varphi) = < \psi_\lambda, \varphi > \; \varphi_\lambda,$$

where

$$
\begin{aligned}
\psi_\lambda(\xi) &= e^{-\lambda \xi}d_\lambda, & 0 \leq \xi \leq r, & \qquad d_\lambda\,\Delta(\lambda) = 0 & (13.9) \\
\varphi_\lambda(\theta) &= e^{\lambda \theta}c_\lambda, & -r \leq \theta \leq 0, & \qquad \Delta(\lambda)\,c_\lambda = 0. & (13.10)
\end{aligned}
$$

13.2.3 Zero characteristic root

Substituting $\lambda = 0$ in the characteristic equation, allows us to say that the stability of the system is delay-independent. Thus, the system (13.1) with zero characteristic root is stable (instable) if the system (13.1)$|_{\tau=0}$ is stable (instable). Then a zero characteristic root can be seen as associated to the system (13.1) without delay. Let us assume for this case that $(I_d - D)$ is invertible, thus

$$
\left.
\begin{aligned}
\dot{x}(t) &= A\,x(t) + B\,y(t) \\
(I_d - D)y(t) &= C\,x(t)
\end{aligned}
\right\}
$$

which gives

$$
\left.
\begin{aligned}
\dot{x}(t) &= \left[A + B(I_d - D)^{-1}C\right]\,x(t) \\
y(t) &= (I_d - D)^{-1}\,C\,x(t)
\end{aligned}
\right\}
$$

this is a homogeneous ODE with an algebraic equation, which can be solved directly by considering the first equation to obtain a solution for x, then by deducing a solution for y by substituting the solution for x in the algebraic equation.

13.2.4   Computing spectral projections using Dunford Calculus : non zero spectral values with arbitrary order

By the standard spectral theory, the spectral projection onto $\mathcal{M}_\lambda$ along $\mathcal{R}((\lambda I - \mathcal{A})^{k_\lambda})$ is associated to a Dunford integral, see [95, 141] and references therein for further details. Indeed,

$$P_\lambda = \frac{1}{2\Pi i} \int_{\Gamma_\lambda} (zI - \mathcal{A})^{-1} \, dz \tag{13.11}$$

where Γ_λ is a small circle containing λ but no other poles of the resolvent $(zI - \mathcal{A})^{-1}$.

Let us first define the following decomposition of a given vector function ξ

$$\begin{cases} \xi = (\xi_1, \xi_2)^T = \tilde{\xi}_1 + \tilde{\xi}_2 & \text{where} \\ \tilde{\xi}_1 = (\xi_1, 0)^T & \text{and} \\ \tilde{\xi}_2 = (0, \xi_2)^T. \end{cases} \tag{13.12}$$

Theorem 39. *The resolvent $(zI_d - \mathcal{A})^{-1}$ of the infinitesimal generator $\mathcal{A}$ defined by (13.6) associated to the system (13.1) is given by*

$$(zI_d - \mathcal{A})^{-1}\varphi = -e^{z\cdot} \int_0^{\cdot} e^{-zt} \tilde{\varphi}_1(t) dt + e^{z\cdot} \Delta(z)^{-1} H(z, \varphi), \tag{13.13}$$

where the characteristic matrix $\Delta(z)$ is defined by (13.41) and $H(z,.) : \mathcal{C} \to \mathbb{C}$ is the operator defined by (13.23).

Moreover, if $\lambda \in \sigma(\mathcal{A})$, then the spectral projection P_λ onto $\mathcal{M}_\lambda$ along $\mathcal{R}((\lambda I - \mathcal{A})^{k_\lambda})$ is given by $P_\lambda \varphi = Res_{z=\lambda}\left(e^{z\cdot} \Delta(z)^{-1} H(z, \varphi)\right)$.

Démonstration. Let us fix φ and define $\psi = (zI - \mathcal{A})^{-1}\varphi$, then $\psi \in \mathcal{D}om(\mathcal{A})$ and $z\psi - \mathcal{A}\psi = \varphi$. From the definition of the infinitesimal generator (13.6), it follows that ψ satisfies the following ODE with boundary condition

$$z\psi - \frac{d\psi}{d\theta} = \varphi \tag{13.14}$$

$$\mathcal{D}\frac{d\psi}{d\theta} = \mathcal{L}\psi \tag{13.15}$$

considering (13.14) and using the variation of constants we obtain

$$\psi(\theta) = e^{z\theta}[\psi(0) - \int_0^\theta e^{-zs}\varphi(s)ds]. \tag{13.16}$$

Moreover, applying $\mathcal{D}$ in (13.14) and using the property of $\psi \in \mathcal{D}om(\mathcal{A})$ leads to

$$z\mathcal{D}\psi - \mathcal{L}\psi = \mathcal{D}\varphi. \tag{13.17}$$

In standard notations we have

$$\mathcal{L}\psi = \begin{pmatrix} A\psi_1(0) + B\psi_2(-\tau) \\ C\psi_1(0) + D\psi_2(-\tau) - \psi_2(0) \end{pmatrix} = \int_0^\tau d\eta(\theta)\psi(-\theta)$$

thus using (13.17) with the decomposition (13.12) allow to

$$0 = z\tilde{\psi}_1(0) - \int_0^\tau d\eta(\theta)(\tilde{\psi}_1(-\theta) + \tilde{\psi}_2(-\theta)) - \mathcal{D}\varphi \tag{13.18}$$

hence, it follows from a substitution of (13.16)

$$0 = z\tilde{\psi}_1(0) - \int_0^\tau d\eta(\theta) \left(e^{-z\theta}[\psi(0) - \int_0^{-\theta} e^{-zs}\varphi(s)ds] \right) - \tilde{\varphi}_1(0) \tag{13.19}$$

and therefore

$$0 = [z\tilde{I}_1 - \int_0^\tau d\eta(\theta)e^{-z\theta}]\psi(0) + \int_0^\tau d\eta(\theta)e^{-z\theta}\int_0^{-\theta} e^{-zs}\varphi(s)ds - \tilde{\varphi}_1(0) \tag{13.20}$$

As in our analysis $z \neq 0$ and from (13.16) we obtain

$$0 = \Delta(z)\,\psi(0) + \int_0^\tau d\eta(\theta)\int_0^{-\theta} e^{-z(s+\theta)}\varphi(s)ds - \tilde{\varphi}_1(0), \tag{13.21}$$

which gives

$$0 = \Delta(z)\,\psi(0) - \int_0^\tau d\eta(\theta)\int_0^\theta e^{-z\theta}\varphi(s-\theta)ds - \tilde{\varphi}_1(0). \tag{13.22}$$

That is $\Delta(z)\,\psi(0) = H(z,\varphi)$ where

$$H(z,\varphi) = \int_0^\tau d\eta(\theta)\int_0^\theta e^{-z\theta}\varphi(s-\theta)ds + \tilde{\varphi}_1(0). \tag{13.23}$$

Thus we obtain explicitly the expression of ψ as a function of Δ and H, then the resolvent that ends the proof. $\qquad\square$

13.2.5 Series Expansion for Lossless Systems

The question whether the solution of retarded systems can be represented by a series of elementary solutions and the deal with the convergence of the series expansion of the solution is studied in [13]. In [141] some convergence results based on the Cesaro sum are given for neutral type system when the matrix associated to the greatest delay (A_n of (13.55)) of the difference equation is nonsingular. A weaker result for the singular case is also established but under the hypothesis that the matrix associated with the greatest delay (B_m of (13.55)) is nonsingular. Those regularity conditions on A_n in [141] ensure that the generator semigroup $\mathcal{T}(t)$ has a complete system of eigenvectors and generalized eigenvectors, see also [128].

A natural question arise : whether the solution of a given Lossless system (13.1) can be represented by a series of elementary solutions and under which conditions the convergence is insured. The main idea is to expand the state into a linear combination of eigenvectors ($\varphi_{\lambda_k}(\theta) = p_k(\theta)e^{\lambda_k\theta}$) and generalized eigenvectors :

$$x_t(\theta) = \sum_{k=0}^\infty p_k(t+\theta)e^{\lambda_k(t+\theta)}, \quad -h \leq \theta \leq 0,\ t \geq 0 \tag{13.24}$$

in other words, in operator language,

$$\mathcal{T}(t)\varphi = \sum_{k=0}^{\infty} \mathcal{T}(t)\,P_{\lambda_k}\varphi, \ t \geq 0. \tag{13.25}$$

The following two theorems give sufficient conditions for convergence of the power series associated with solutions for (13.1).

Theorem 40. *Let $\mathcal{C} = C([-r,0], \mathbb{R}^{n+m})$ and let $\mathcal{T}(t) : \mathcal{C} \to \mathcal{C}$ denote the semigroup of solution operators associated with Lossless system (13.1) such that the matrix $D \in \mathcal{M}_m(\mathbb{R})$ is invertible, $\lambda_j, j = 0, 1, \ldots$ the associated set of eigenvalues and P_{λ_j} the associated spectral projection given by (13.11) . Then the semigroup $\mathcal{T}(t)$ extends to a group of bounded linear operators and for every $\varphi \in \mathcal{C}$, we have*

$$\lim_{N \to \infty} \| \mathcal{T}(t)\varphi - \frac{1}{N} \sum_{k=0}^{N-1} \sum_{j=0}^{k} \mathcal{T}(t)P_{\lambda_j}\varphi \| = 0, \qquad t \in \mathbb{R}^+ \tag{13.26}$$

uniformly on compact t-sets.

The trick here is to identify for (13.1) its system of eigenvalues, and to prove that it is a complete system. In other words, we design an appropriate Neutral system having the same set of eigenvectors as (13.1) (apart from those associated with the zero spectral value), for which we can prove the convergence of its series expansion by using Verduyn-Lunel theorem 38, see [141].

Démonstration. Let us consider system (13.1) and apply the Standard transformation which leads to system (13.2) :

$$\left.\begin{array}{r} \dot{x}(t) = A\,x(t) + B\,y(t-\tau) \\ \dot{y}(t) - D\,\dot{y}(t-\tau) = CA\,x(t) + CB\,y(t-\tau) \end{array}\right\}$$

Here we can not directly apply the result of the theorem 38 since the associated matrix $D_0 = \begin{pmatrix} 0 & 0 \\ 0 & D \end{pmatrix}$, (the matrix of the difference equation associated with the greatest delay) is singular.

However, we write down $y(t-\tau) = D^{-1}y(t) - D^{-1}Cx(t)$ from the second equation of (13.1). We substitute this fact in the first equation, we have

$$\left.\begin{array}{r} \dot{x}(t) = (A + BD^{-1}C)\,x(t) + BD^{-1}\,y(t) \\ y(t) = C\,x(t) + D\,y(t-\tau). \end{array}\right\}$$

A rescaling of time by τ of the first equation gives

$$\dot{x}(t-\tau) = (A + BD^{-1}C)\,x(t-\tau) + BD^{-1}\,y(t-\tau).$$

Subtracting the last equality from the first equation of (13.1) and derivating its second equation lead to

$$\left.\begin{array}{r} \dot{x}(t) - \dot{x}(t-\tau) = (A + BD^{-1}C)\,(x(t) - x(t-\tau)) \\ + BD^{-1}\,(y(t) - y(t-\tau)) \\ \dot{y}(t) - D\,\dot{y}(t-\tau) = CA\,x(t) + CB\,y(t-\tau). \end{array}\right\} \tag{13.27}$$

Then we obtain a neutral system with non-singular matrix $D_0 = \begin{pmatrix} I_d & 0 \\ 0 & D \end{pmatrix}$, thus the theorem 38 can be applied. $\qquad\qquad\qquad\qquad\qquad\qquad\qquad\qquad\square$

Note that the set of the spectral values of the characteristic equation associated with (13.1) belongs to the set of spectral values of the characteristic equation associated with (13.27). Moreover, the only additional spectral value is zero with multiplicity m. Thus the set of eigenvalues associated with (13.27) represents a complete set. But for $\tau \neq 0$, zero is not a spectral value for (13.1), then $P_0\varphi = 0$, $\forall \varphi \in C$.

Let us consider the system (13.1) with a two-block singular matrix $D = \begin{pmatrix} D_{11} & D_{12} \\ D_{21} & D_{22} \end{pmatrix}$ such that D_{11} is a non-singular matrix and $B = (B_1\ B_2)$ and $C = \begin{pmatrix} C_1 \\ C_2 \end{pmatrix}$. Under some restrictions we are able to prove the convergence of the series expansion of the solution.

Theorem 41. *Let $C = C([-r,0], \mathbb{R}^{n+m})$ and let $\mathcal{T}(t) : C \to C$ denote the semigroup of solution operators associated with Lossless system (13.1) such that λ_j, $j = 0, 1, \ldots$ the associated set of eigenvalues and P_{λ_j} the associated spectral projection given by (13.11) and one of the following sets of conditions hold*

    1.

$$\left.\begin{array}{l} B_2 = B_1\, D_{11}^{-1}\, D_{12} \\ D_{22} = D_{21}\, D_{11}^{-1}\, D_{12} \\ C_2 = D_{21}\, D_{11}^{-1}\, C_1 \\ D_{11}^2 = -D_{12}\, D_{21} \end{array}\right\}, \tag{13.28}$$

    2.

$$\left.\begin{array}{l} B_2 = B_1\, D_{11}^{-1}\, D_{12} \\ D_{22} = 0 \\ D_{21} = 0 \end{array}\right\}. \tag{13.29}$$

Then the semigroup $\mathcal{T}(t)$ extends to a group of bounded linear operators and for every $\varphi \in C$, we have

$$\lim_{N \to \infty} \| \mathcal{T}(t)\varphi - \frac{1}{N} \sum_{k=0}^{N-1} \sum_{j=0}^{k} \mathcal{T}(t) P_{\lambda_j} \varphi \| = 0, \qquad t \in \mathbb{R}^+ \tag{13.30}$$

uniformly on compact t-sets.

Démonstration. The same trick as the one used to prove the last theorem is applied here; that is the design of an appropriate Neutral system having the same set of eigenvectors as (13.1) (apart from those associated with the zero spectral value), for which we are able to prove the convergence of its series expansion (invertible matrix D_0).

Let us consider system (13.1)

$$\left.\begin{aligned}\dot{x}(t) &= A\,x(t) + B\,y(t-\tau)\\ y(t) &= C\,x(t) + D\,y(t-\tau)\end{aligned}\right\}$$

and let $y(t) = col(y_1(t), y_2(t))$ which implies

$$\left.\begin{aligned}\dot{x}(t) &= A\,x(t) + B_1\,y_1(t-\tau) + B_2\,y_2(t-\tau)\\ y_1(t) &= C_1\,x(t) + D_{11}\,y_1(t-\tau) + D_{12}\,y_2(t-\tau)\\ y_2(t) &= C_2\,x(t) + D_{21}\,y_1(t-\tau) + D_{22}\,y_2(t-\tau)\end{aligned}\right\} \tag{13.31}$$

then from the second equation of (13.31) and the invertibility of the matrix D_{11} we have

$$y_1(t-\tau) = D_{11}^{-1}\,y_1(t) - D_{11}^{-1}\,C_1\,x(t) - D_{11}^{-1}\,D_{12}\,y_2(t-\tau). \tag{13.32}$$

Substituting this las equality into the first and third equations of (13.31) which gives

$$\left.\begin{aligned}\dot{x}(t) &= (A - B_1\,D_{11}^{-1}\,C_1)\,x(t) + B_1\,D_{11}^{-1}\,y_1(t)\\ &\quad + (B_2 - B_1\,D_{11}^{-1}\,D_{12})\,y_2(t-\tau)\\ y_1(t) &= C_1\,x(t) + D_{11}\,y_1(t-\tau) + D_{12}\,y_2(t-\tau)\\ y_2(t) &= (C_2 - D_{21}\,D_{11}^{-1}\,C_1)\,x(t) + D_{21}\,D_{11}^{-1}\,y_1(t)\\ &\quad + (D_{22} - D_{21}\,D_{11}^{-1}\,D_{12})\,y_2(t-\tau)\end{aligned}\right\}. \tag{13.33}$$

Let us consider separately the two cases.

1. Assume that (13.28) is satisfied, then its first three conditions give

$$\left.\begin{aligned}\dot{x}(t) &= (A - B_1\,D_{11}^{-1}\,C_1)\,x(t) + B_1\,D_{11}^{-1}\,y_1(t)\\ y_1(t) &= C_1\,x(t) + D_{11}\,y_1(t-\tau) + D_{12}\,y_2(t-\tau)\\ y_2(t) &= D_{21}\,D_{11}^{-1}\,y_1(t)\end{aligned}\right\} \tag{13.34}$$

Thus, the third equation gives :

$$y_2(t-\tau) = D_{21}\,D_{11}^{-1}\,y_1(t-\tau)$$

wich leads to

$$\left.\begin{aligned}\dot{x}(t) &= (A - B_1\,D_{11}^{-1}\,C_1)\,x(t) + B_1\,D_{11}^{-1}\,y_1(t)\\ y_1(t) &= C_1\,x(t) + (D_{11} + D_{12}\,D_{21}\,D_{11}^{-1})\,y_1(t-\tau)\\ y_2(t) &= D_{21}\,D_{11}^{-1}\,y_1(t)\end{aligned}\right\} \tag{13.35}$$

hence the fourth and the third equalities of (13.28) lead to

$$\left.\begin{aligned}\dot{x}(t) &= (A - B_1\,D_{11}^{-1}\,C_1)\,x(t) + B_1\,D_{11}^{-1}\,y_1(t)\\ y_1(t) &= C_1\,x(t)\\ y_2(t) &= C_2\,x(t)\end{aligned}\right\} \tag{13.36}$$

which implies

$$
\left.\begin{aligned}
&\dot{x}(t) - \dot{x}(t - \tau) = B_1\, D_{11}^{-1}\, (y_1(t) - y_1(t - \tau)) \\
&\quad + (A - B_1\, D_{11}^{-1}\, C_1)\, (x(t) - x(t - \tau)) \\
&\dot{y}_1(t) - D_{11}\, \dot{y}_1(t - \tau) = C_1\, B_1\, D_{11}^{-1}\, y_1(t) \\
&\quad + C_1\, (A - B_1\, D_{11}^{-1}\, C_1)\, x(t) \\
&\quad - D_{11} C_1 (A - B_1 D_{11}^{-1} C_1) x(t - \tau) \\
&\quad + D_{11}\, C_1\, B_1\, D_{11}^{-1}\, y_1(t - \tau) \\
&\dot{y}_2(t) - \dot{y}_2(t - \tau) = C_2 B_1 D_{11}^{-1}(y_1(t) - y_1(t - \tau)) \\
&\quad + C_2\, (A - B_1\, D_{11}^{-1}\, C_1)\, (x(t) - x(t - \tau))
\end{aligned}\right\} .
\tag{13.37}
$$

Obviously, we obtain a neutral system with non-singular matrix associated with the greatest delay of the difference equation; $D_0 = \begin{pmatrix} I_d & 0 & 0 \\ 0 & D_{11} & 0 \\ 0 & 0 & I_d \end{pmatrix}$, thus the theorem 38 can be applied.

2. Assume that (13.29) is satisfied, then

$$
\left.\begin{aligned}
&\dot{x}(t) = (A - B_1\, D_{11}^{-1}\, C_1)\, x(t) + B_1\, D_{11}^{-1}\, y_1(t) \\
&y_1(t) = C_1\, x(t) + D_{11}\, y_1(t - \tau) + D_{12}\, y_2(t - \tau) \\
&y_2(t) = (C_2 - D_{21}\, D_{11}^{-1}\, C_1)\, x(t)
\end{aligned}\right\} .
\tag{13.38}
$$

which implies

$$
\left.\begin{aligned}
&\dot{x}(t) - \dot{x}(t - \tau) = B_1\, D_{11}^{-1}\, (y_1(t) - y_1(t - \tau)) \\
&\quad + (A - B_1\, D_{11}^{-1}\, C_1)\, (x(t) - x(t - \tau)) \\
&\dot{y}_1(t) - D_{11}\, \dot{y}_1(t - \tau) = C_1\, (A - B_1\, D_{11}^{-1}\, C_1)\, x(t) \\
&\quad + C_1\, B_1\, D_{11}^{-1}\, y_1(t) \\
&\quad + D_{12}(C_2 - D_{21} D_{11}^{-1} C_1)(A - B_1 D_{11}^{-1} C_1) x(t - \tau) \\
&\quad + D_{12}(C_2 - D_{21} D_{11}^{-1} C_1) B_1 D_{11}^{-1} y_1(t - \tau) \\
&\dot{y}_2(t) - \dot{y}_2(t - \tau) = (C_2 - D_{21}\, D_{11}^{-1}\, C_1) \times \\
&(A - B_1\, D_{11}^{-1}\, C_1)\, (x(t) - x(t - \tau)) \\
&\quad + (C_2 - D_{21}\, D_{11}^{-1}\, C_1)\, B_1\, D_{11}^{-1}\, (y_1(t) - y_1(t - \tau))
\end{aligned}\right\} .
\tag{13.39}
$$

Thus, the matrix ($D_0 = \begin{pmatrix} I_d & 0 & 0 \\ 0 & D_{11} & 0 \\ 0 & 0 & I_d \end{pmatrix}$) of the difference equation associated with the greatest delay is non-singular.

$\square$

13.3   Finite dimensional approximation : Center Manifold theorem for Lossless propagation model

As recalled in the first section, using the standard reduction (by letting $y(t) = \dot{z}(t)$) one can transform a Lossless system to a NFDE. Certainly this approach increases the number of spectral values to the system and thus the computation of the center manifold for the NFDE will not be valid for Lossless system but detailed inspection shows that there are only a zero additional spectral value with multiplicity $m = dim(y)$. Thus, by the standard reduction some additional dynamics are induced. When the left eigenvector associated with a given spectral value (other than zero) is the same for both the neutral structure as for the Lossless structure, then one can carefully distinguish the concrete spectral projections and reject the generalized eigenspace associated to the zero value and then compute a center manifold expansion. Finally, one has to translate the obtained result in terms of Lossless system structure. But in the the remaining case (different left eigenvectors) this approach becomes very difficult. In conclusion, even this procedure still possible in some configurations but seems to be a complicated task.

In the light of the obtained results in the previous subsections for Lossless propagation model : the design of an appropriate bilinear form, the definition of the spectral projection and the study of the series expansion for a given solution, we show that the extension of the center manifold theorem to the system (13.5) is possible. Thus, we are able by now to present a direct center manifold computations for Lossless systems (13.5). In what follows, we give the computations schemes that will be illustrated in the last section by an example for the Hopf-bifurcation Like case.

In this section our aim is to reduce the dimension of the system (13.5), namely,

$$\left.\begin{array}{l} \dot{x}(t) = A\,x(t) + B\,y(t-\tau) + f_1(x(t), y(t), y(t-\tau)) \\ y(t) = C\,x(t) + D\,y(t-\tau) + f_2(x(t), y(t), y(t-\tau)) \end{array}\right\}.$$

where $x \in \mathbb{R}^m$ and $y \in \mathbb{R}^n$ and A, B, C, D are real valued matrices. Thus $A \in \mathcal{M}_{m,m}(\mathbb{R})$, $B \in \mathcal{M}_{m,n}(\mathbb{R})$, $C \in \mathcal{M}_{n,m}(\mathbb{R})$, $D \in \mathcal{M}_{n,n}(\mathbb{R})$.

Let us set $z(t) = \begin{bmatrix} x(t) \\ y(t) \end{bmatrix}$ and $\frac{\hat{d}}{dt}w = \frac{\hat{d}}{dt}\begin{bmatrix} w_1 \\ w_2 \end{bmatrix} = \begin{bmatrix} \frac{d}{dt}w_1 \\ 0 \end{bmatrix}$ and consider the linear part of (13.5), namely, (13.1) which can be represented as

$$\frac{\hat{d}}{dt}\mathcal{D}z_t = \mathcal{L}z_t \tag{13.40}$$

where the infinitesimal generator $\mathcal{A}$ and the operators $\mathcal{D}$ and $\mathcal{L}$ are such that

$$\mathcal{D}om(\mathcal{A}) = \{\varphi = (\varphi_1 + \varphi_2) \in \mathcal{C}, \text{ s.t. } \frac{d\varphi}{d\theta} \in \mathcal{C}, \ \mathcal{D}\frac{d\varphi}{d\theta} = \mathcal{L}\,\varphi\}$$

$$\mathcal{A}\varphi = \frac{d\varphi}{d\theta} \text{ and}$$

$$\mathcal{L}\,\varphi = (A\varphi_1(0) + B\varphi_2(-\tau), C\varphi_1(0) - \varphi_2(0) + D\varphi_2(-\tau))^T,$$
$$\mathcal{D}\,\varphi = (\varphi_1(0), 0)^T.$$

The associated characteristic matrix is

$$\Delta(\lambda) = \begin{pmatrix} \lambda I_n - A & -e^{-\lambda\tau} B \\ -C & I_m - e^{-\lambda\tau} D \end{pmatrix} \tag{13.41}$$

and the solution operator $\mathcal{T}(t)$ defined by

$$\mathcal{T}(t)(\phi) = z_t(.,\phi) \tag{13.42}$$

such that $z_t(.,\phi)(\theta) = z(t+\theta,\phi)$ for $\theta \in [-r,0]$ is a strongly continuous semigroup. Obviously, $\sigma(\mathcal{A}) = \sigma_p(\mathcal{A})$ (since the spectrum of a Lossless system is included in the spectrum of delay system of neutral type) and the spectrum of $\mathcal{A}$ consists of complex values $\lambda \in \mathbb{C}$ which satisfy the characteristic equation $p(\lambda) = \det\Delta(\lambda) = 0$.

Let us denote by $\mathcal{M}_\lambda$ the eigenspace associated with $\lambda \in \sigma(\mathcal{A})$. We define $\mathcal{C}^* = C([-r,0],\mathbb{R}^{(n+m)^*})$ where $\mathbb{R}^{(n+m)^*}$ is the space of $(n+m)$-dimensional row vectors and consider the defined bilinear form. Let $\mathcal{A}^T$ be the transposed operator of $\mathcal{A}$, i.e., $< \psi, \mathcal{A}\varphi > = < \mathcal{A}^T\psi, \varphi >$. We underline also the fact that the Banach space decomposition Theorem [115] is extended to lossless propagation model under the prescribed sttings. Thus we obtain a decomposition of the space $\mathcal{C} = P \bigoplus Q$ where $P = span\{\mathcal{M}_\lambda(\mathcal{A}), \lambda \in \Lambda\}$ and Q (the infinite dimensional complementary subspace) are invariant under $\mathcal{T}(t), t \geq 0$. Furthermore, if $\Phi = (\phi_1, \ldots, \phi_m)$ forms a basis of P, $\Psi = col(\psi_1, \ldots, \psi_m)$ is a basis of P^T in $\mathcal{C}^*$ such that $(\Phi,\Psi) = Id$, then

$$\begin{aligned} Q &= \{\phi \in \mathcal{C} \setminus (\Psi,\phi) = 0\} \text{ and} \\ P &= \{\phi \in \mathcal{C} \setminus \exists b \in \mathbb{R}^d : \phi = \Phi b\}. \end{aligned} \tag{13.43}$$

Note also, that such a basis Φ satisfies : $\mathcal{T}(t)\Phi = \Phi e^{Lt}$, where L is a $d \times d$-matrix where the spectrum of L is $\sigma(L) = \Lambda$.

In order to decompose equation (13.40) according to $\mathcal{C} = P \bigoplus Q$, the phase space $\mathcal{C}$ must be extended to the space $\mathcal{BC}$ of functions which are continuous on $[-\tau, 0)$ and may have a finite jump discontinuity at $\theta = 0$. Functions $\xi \in \mathcal{BC}$ can be written as $\xi = \varphi + X_0 \alpha$, where $\varphi \in \mathcal{C}$, $\alpha \in \mathbb{R}^{n+m}$, and $X_0(\theta) = 0$ for $-\tau \leq \theta < 0$ and $X_0(0) = Id_{d \times d}$. Then the bilinear form from Sec. 13.2 can be extended to the space $\mathcal{C}^* \times \mathcal{BC}$ by $< \psi, X_0 > = \psi(0)$ and the infinitesimal generator $\mathcal{A}$ extends to an operator $\tilde{\mathcal{A}}$ (defined in C^1) onto the space $\mathcal{BC}$ as follow

$$\tilde{\mathcal{A}}\phi = \mathcal{A}\phi + X_0[\mathcal{L}\phi - \mathcal{D}\phi'] \tag{13.44}$$

Under the above consideration one can write equation (13.5) as an abstract ODE coupled with an algebraic equation

$$\frac{\hat{d}}{dt}z_t = \tilde{\mathcal{A}}z_t + X_0\mathcal{F}(z_t). \tag{13.45}$$

where $\mathcal{F}$ represents the nonlinear part of the system. Thanks to the projection $\Pi : \mathcal{BC} \to P$ such that $\Pi(\varphi + X_0\alpha) = \Phi[(\Psi,\varphi) + \Psi(0)\alpha]$ we obtain $z_t = \Phi v(t) + w_t$

where $v(t) \in \mathbb{R}^d$ and then equation (13.5) can be split to

$$
\begin{aligned}
\frac{\hat{d}}{dt} v &= Lv + \Psi(0)\mathcal{F}(\Phi v + w) \\
\frac{\hat{d}}{dt} w &= \tilde{\mathcal{A}}_Q w + (I - \Pi) X_0 \mathcal{F}(\Phi v + w),
\end{aligned} \tag{13.46}
$$

The above decomposition theorem can be easily exploited in the aim of computing the the evolution of solutions on the center manifold (the dimensional reduced system) as well as the explicit expression of the center manifold.

Définition 1. *Given a C^1 map h from $\mathbb{R}^d$ into Q. The graph of h is said to be a local manifold if $h(0) = Dh(0) = 0$ and there exists a neighborhood V of $0 \in \mathbb{R}^d$ such that for each $\xi \in V$, there exists $\delta = \delta(\xi) > 0$ and the solution z of (13.40) with initial data $\Phi\xi + h(\xi)$ exists on the interval $]-\delta-r, \delta[$ and it is given by $z_t = \Phi u(t) + h(u(t))$ for $t \in [0, \delta[$ where $u(t)$ is the unique solution of the finite dimensional hybrid system*

$$
\frac{\hat{d}}{dt} u = Lu + \Psi(0)\mathcal{F}(\Phi u + h(u)) \quad where \quad u(0) = \xi. \tag{13.47}
$$

13.3.1   Spectral Projection : Double Semi-simple Characteristic root

Let us consider the system (13.1) with a delay $\tau = \pi$ and matrices

$$
A = \begin{bmatrix} 1 & 0 \\ 0 & 1 \end{bmatrix}, \qquad B = \begin{bmatrix} 1 & 0 & 0 \\ -1 & 0 & 0 \end{bmatrix} \tag{13.48}
$$

$$
C = \begin{bmatrix} 0 & 0 \\ \frac{e^{-\pi}}{4} & 0 \\ \frac{e^{-\pi}}{4} & \frac{e^{-\pi}}{4} \end{bmatrix}, \qquad D = \begin{bmatrix} \frac{1}{2} & 0 & 0 \\ 0 & \frac{1}{4} & 0 \\ 0 & 0 & -\frac{1}{4} \end{bmatrix}. \tag{13.49}
$$

Thus, $\lambda = 1$ is a spectral value with algebraic multiplicity 2 and geometric multiplicity 2, for which the associated right-eigenvectors

$$
\varphi_1^1(\theta) = \begin{bmatrix} 0 \\ 1 \\ 0 \\ 0 \\ (4\,e^\pi + 1)^{-1} \end{bmatrix}, \qquad \varphi_1^2(\theta) = \begin{bmatrix} 1 \\ \frac{-4\,e^\pi + 1}{4\,e^\pi - 1} \\ 0 \\ (4\,e^\pi - 1)^{-1} \\ 0 \end{bmatrix}
$$

and left-eigenvector

$$
\begin{aligned}
\psi_1^1(\xi) &= \begin{bmatrix} 1 & 1 & 0 & 0 & 0 \end{bmatrix}, \\
\psi_1^2(\xi) &= \begin{bmatrix} 1 & 0 & 2\,(2\,e^\pi - 1)^{-1} & 0 & 0 \end{bmatrix}.
\end{aligned}
$$

Simple computations show that

$$\begin{cases} \Delta(\tau = \pi, \lambda_0 = 1)\varphi_1^k = 0, \\ \psi_1^k \Delta(\tau = \pi, \lambda_0 = 1) = 0, \\ \psi_1^k \varphi_1^l = \delta_{k,l}, \ \forall k, \ l \in \{1,2\} \end{cases}$$

The spectral projection of

$$\varphi(\theta) = [\phi_1(\theta), \ \phi_2(\theta), \ \phi_3(\theta), \ \phi_4(\theta), \ \phi_5(\theta)]^T$$

onto $\mathcal{M}_1$ is

$$P_1(\varphi(\theta)) = \begin{bmatrix} \mathrm{e}^\theta \left(\phi_1(0) + \int_0^\pi \mathrm{e}^{-t}\phi_3(t-\pi)\,dt + 2\,\frac{\phi_3(0)-1/2\,\phi_3(-\pi)+1/2\int_0^\pi \mathrm{e}^{-t}\phi_3(t-\pi)dt}{2\,\mathrm{e}^\pi - 1} \right) \\ \mathrm{e}^\theta \left(\phi_2(0) - \int_0^\pi \mathrm{e}^{-t}\phi_3(t-\pi)\,dt - 2\,\frac{\phi_3(0)-1/2\,\phi_3(-\pi)+1/2\int_0^\pi \mathrm{e}^{-t}\phi_3(t-\pi)dt}{2\,\mathrm{e}^\pi - 1} \right) \\ 0 \\ \mathrm{e}^\theta \left(\frac{\phi_1(0)+\int_0^\pi \mathrm{e}^{-t}\phi_3(t-\pi)dt}{4\,\mathrm{e}^\pi - 1} - 2\,\frac{\phi_3(0)-1/2\,\phi_3(-\pi)+1/2\int_0^\pi \mathrm{e}^{-t}\phi_3(t-\pi)dt}{-8\,\mathrm{e}^{2\,\pi}+6\,\mathrm{e}^\pi - 1} \right) \\ \mathrm{e}^\theta \left(\frac{\phi_1(0)+\int_0^\pi \mathrm{e}^{-t}\phi_3(t-\pi)dt}{4\,\mathrm{e}^\pi + 1} + \frac{\phi_2(0)-\int_0^\pi \mathrm{e}^{-t}\phi_3(t-\pi)dt}{4\,\mathrm{e}^\pi + 1} \right) \end{bmatrix}.$$

13.3.2 Spectral Projection : Double non-Semi-simple Characteristic root

Let us consider the system (13.1) with a delay $\tau = \pi$ and matrices

$$A = \begin{bmatrix} \pi^{-1} & 0 \\ 5\pi - 16 & -48 \end{bmatrix}, \qquad B = \begin{bmatrix} -\pi^{-1} & 0 & 0 \\ -16 & -\frac{9}{4}\pi + 9 & 25 \end{bmatrix} \qquad (13.50)$$

$$C = \begin{bmatrix} \frac{1}{2} & 1 \\ 1 & 0 \\ 1 & 4 \end{bmatrix}, \qquad D = \begin{bmatrix} \frac{1}{2} & 0 & 0 \\ 0 & \frac{1}{4} & 0 \\ 0 & 0 & -\frac{1}{4} \end{bmatrix}. \qquad (13.51)$$

Thus, $\lambda = 2\,i$ is a spectral value with algebraic multiplicity 2 and geometric multiplicity 1, for which the associated right-eigenvector

$$\varphi_{2i}(\theta) = \begin{bmatrix} i\mathrm{e}^{2\,i\theta} \\ \mathrm{e}^{2\,i\theta}\pi \\ \frac{\mathrm{e}^{2\,i\theta}\left(-1+6\,i\pi+8\,\pi^2\right)}{i+4\,\pi} \\ \frac{4}{3}\,i\mathrm{e}^{2\,i\theta} \\ \mathrm{e}^{2\,i\theta}\left(\frac{4}{5}\,i + \frac{16}{5}\,\pi\right) \end{bmatrix}$$

and left-eigenvector $\psi_{2i}(\xi) = \begin{bmatrix} -ie^{-2\,i\xi}\pi & e^{-2\,i\xi} & (-32+2\,i)\,e^{-2\,i\xi} & e^{-2\,i\xi}\,(-3\,\pi+12) & 20\,e^{-2\,i\xi} \end{bmatrix}$.

Let us consider φ such that

$$\varphi(\theta) = \begin{bmatrix} \phi_1(\theta) \\ \phi_2(\theta) \\ \phi_3(\theta) \\ \phi_4(\theta) \\ \phi_5(\theta) \end{bmatrix} = \begin{bmatrix} sin(\theta) \\ cos(\theta) \\ sin(\theta) \\ cos(\theta) \\ sin(\theta) \end{bmatrix}.$$

The spectral projection of φ onto $\mathcal{M}_{2i}$ is given by

$$P_{2i}(\varphi(\theta)) = e^{-2\,i\theta}\left(\pi\,\left(-15-896\,\pi-160\,\pi^2+90\,i\pi+2304\,i\pi^2\right)^2\right)\begin{bmatrix} p_1(\theta) \\ p_2(\theta) \\ p_3(\theta) \\ p_4(\theta) \\ p_5(\theta) \end{bmatrix}$$

where

$$p_1(\theta) = 658240\,i\theta\,\pi^2 + \frac{5976146}{3}\,i\pi^2 - \frac{20425}{2} - 4800\,i - \frac{6564224}{3}\,i\pi^3 - 211420\,i\pi$$
$$ - 3600\,\theta - \frac{716026}{3}\,\pi^2 - \frac{1026989}{2}\,\pi^3 + 86976\,\pi^4 + \frac{4588845}{2}\,\theta\,\pi^2 - 123690\,\theta\,\pi$$
$$ - 146880\,\theta\,\pi^3 + 600\,i\pi^4 + 15225\,i\theta - 10200\,i\theta\,\pi^3 - \frac{15089965}{24}\,\pi + \frac{3720335}{4}\,i\theta\,\pi$$

$$p_2(\theta) = -\frac{2835104}{3}\,\pi^4 - 19800\,\pi^5 - 10200\,\theta\,\pi^4 - 6600\,\pi + 123690\,i\theta\,\pi^2 + 15225\,\theta\,\pi$$
$$ + \frac{13211885}{12}\,i\pi^2 + \frac{2445526}{3}\,i\pi^3 + 206784\,i\pi^5 + 658240\,\theta\,\pi^3 + \frac{3720335}{4}\,\theta\,\pi^2$$
$$ + 17825\,i\pi - \frac{8160901}{2}\,i\pi^4 - \frac{4588845}{2}\,i\theta\,\pi^3 + 3600\,i\pi\,\theta + 146880\,i\theta\,\pi^4$$
$$ - 242815\,\pi^2 + \frac{59993129}{12}\,\pi^3$$

$$p_3(\theta) = \frac{15992311}{3}\,\pi^3 - \frac{8918080}{3}\,\pi^4 + 1169600\,\theta\,\pi^3 - \frac{20425}{2} - 4800\,i + 905620\,i\theta\,\pi^2$$
$$ - 3600\,\theta + \frac{13026983}{4}\,i\pi^2 - 1463344\,i\pi^3 + 119808\,i\pi^5 - 190995\,i\pi - 20400\,\theta\,\pi^4$$
$$ + 4154590\,\theta\,\pi^2 - 93240\,\theta\,\pi - 3561256\,i\pi^4 + 15225\,i\theta - 4599045\,i\theta\,\pi^3$$
$$ + \frac{3749135}{4}\,i\theta\,\pi + 293760\,i\theta\,\pi^4 - \frac{15320365}{24}\,\pi - \frac{1893196}{3}\,\pi^2 - 19200\,\pi^5$$

$$p_4(\theta) = -\frac{5113208}{3}\,\pi^3 + 181248\,\pi^4 - 195840\,\theta\,\pi^3 - \frac{40850}{3} - 6400\,i - \frac{2369344}{9}\,\pi^2$$
$$ - 4800\,\theta + \frac{2632960}{3}\,i\theta\,\pi^2 + \frac{6728083}{3}\,i\pi^2 - 3209984\,i\pi^3 + 3059230\,\theta\,\pi^2$$
$$ - 164920\,\theta\,\pi - 288660\,i\pi + \frac{16000}{3}\,i\pi^4 + 20300\,i\theta$$
$$ - 13600\,i\theta\,\pi^3 + \frac{3720335}{3}\,i\theta\,\pi - \frac{15061165}{18}\,\pi$$

$$p_5(\theta) = -69888\,\pi^5 - 32640\,\theta\,\pi^4 + 4811806\,\theta\,\pi^2 - 50232\,\theta\,\pi + 1988864\,\theta\,\pi^3 - \frac{7670272}{3}\,\pi^4$$
$$+ 922400\,i\theta\,\pi^2 + \frac{15803777}{3}\,i\pi^2 + \frac{3127744}{3}\,i\pi^3 + 755712\,i\pi^5 - 109660\,i\pi$$
$$- 8170 - 3840\,i - 14527024\,i\pi^4 - 2880\,\theta - \frac{2933984}{3}\,\pi^2 + \frac{49649200}{3}\,\pi^3$$
$$+ 12180\,i\theta - 7350312\,i\theta\,\pi^3 + 755587\,i\theta\,\pi + 470016\,i\theta\,\pi^4 - \frac{3148169}{6}\,\pi$$

13.3.3   Symbolic computations for center manifolds : Hopf-bifurcation Like case

The aim of this example is not the computations of the center manifold itself but is to provide a finite dimensional approximation of (13.5) in the sense of the convergence criteria based on Cesaro Sum given by (13.26). Thus, for the sake of simplicity, we ask for a finite dimensional approximation up to order three and we select the case where the nonlinearity of (13.5) does not contain quadratic terms, see [152] for more hints about such a choice.

Consider system (13.5) with the delay $\tau = \pi$ and matrices

$$A = 1, \ B = \begin{bmatrix} 1 & -\frac{5}{2} \end{bmatrix}, \ C = \begin{bmatrix} 0 \\ 1 \end{bmatrix}, \ D = \begin{bmatrix} \frac{1}{5} & 0 \\ 0 & -2 \end{bmatrix},$$

and the nonlinear part is defined by $f_1(x(t), y(t), y(t-\tau)) = x^3(t)$ and $f_2(x(t), y(t), y(t-\tau)) = (0, y_2^3(t-\tau))^T$.

By straightforward computations made by $QPMR$-algorithm (Quasi-Polynomial Mapping based Root-finder, developed for computing the spectrum of both Retarded and Neutral Time-Delay Systems) presented in [215] show that $\lambda_0 = \pm\frac{i}{2}$ are the only spectral values with zero real part and are of algebraic and geometric multiplicity 1. Moreover, all remaining spectral values are of negative real part. Thus the phase space can be split into an invariant center variety of dimension 2 and a stable variety. Here we compute some important elements for describing the solutions dynamics on the center manifold. For $\lambda_0 = \pm\frac{i}{2}$, the associated right-eigenvector is

$$\varphi_{\frac{i}{2}}(\theta) = \begin{bmatrix} \mathrm{e}^{\frac{i\theta}{2}} \\ 0 \\ \frac{1}{5}(1+2\,i)\,\mathrm{e}^{\frac{i\theta}{2}} \end{bmatrix}$$

Thus we consider the real part and the imaginary part separately :

$$\varphi_{\frac{1}{\frac{i}{2}}}(\theta) = \begin{bmatrix} \cos(\frac{\theta}{2}) \\ 0 \\ \frac{1}{5}\cos(\frac{\theta}{2}) - \frac{2}{5}\sin(\frac{\theta}{2}) \end{bmatrix}$$

and

$$\varphi^2_{\frac{i}{2}}(\theta) = \begin{bmatrix} \sin(\frac{\theta}{2}) \\ 0 \\ \frac{2}{5}\,\cos(\frac{\theta}{2}) + \frac{1}{5}\,\sin(\frac{\theta}{2}) \end{bmatrix}.$$

then the centre eigenspace of this steady state $(0,0,0)$ can be written in the form $X = a_1\,\varphi^1_{\frac{i}{2}}(\theta) + a_2\,\varphi^2_{\frac{i}{2}}(\theta)$. Working through it in details allows to

$$X = \begin{bmatrix} x \\ y_1 \\ y_2 \end{bmatrix} = \begin{bmatrix} a_1\cos(\frac{\theta}{2}) + a_2\sin(\frac{\theta}{2}) \\ 0 \\ \frac{a_1}{5}\left(\cos(\frac{\theta}{2}) - 2\,\sin(\frac{\theta}{2})\right) + \frac{a_2}{5}\left(2\,\cos(\frac{\theta}{2}) + \sin(\frac{\theta}{2})\right) \end{bmatrix},$$

which proves that $y_1 = 0$ in the center variety.

Thus, approximating (13.5) on the two-dimensional center variety turns to approximate $(13.5)|_{y_1=0}$ to obtain after renaming y_2 by y

$$\left.\begin{array}{l} \dot{x}(t) = x(t) - \dfrac{5}{2}\,y(t-\pi) + x^3(t) \\[2mm] y(t) = x(t) - 2\,y(t-\pi) + y^3(t-\pi) \end{array}\right\}, \tag{13.52}$$

and $\pm\frac{i}{2}$ are two simple spectral values characterizing the center variety, with left-eigenvectors

$$\varphi^1_{\frac{i}{2}}(\theta) = \begin{bmatrix} \cos(\frac{\theta}{2}) \\ \frac{1}{5}\,\cos(\frac{\theta}{2}) - \frac{2}{5}\,\sin(\frac{\theta}{2}) \end{bmatrix}$$

$$\varphi^2_{\frac{i}{2}}(\theta) = \begin{bmatrix} \sin(\frac{\theta}{2}) \\ \frac{2}{5}\,\cos(\frac{\theta}{2}) + \frac{1}{5}\,\sin(\frac{\theta}{2}) \end{bmatrix}.$$

then the centre eigenspace of this steady state $(0,0)$ can be written in the form $X = a_1\,\varphi^1_{\frac{i}{2}}(\theta) + a_2\,\varphi^2_{\frac{i}{2}}(\theta)$.

The basis of the generalized eigenspace P associated with $\pm\frac{i}{2}$ is

$$\Phi = \begin{bmatrix} \cos(\frac{\theta}{2}) & \sin(\frac{\theta}{2}) \\ \frac{1}{5}\,\cos(\frac{\theta}{2}) - \frac{2}{5}\,\sin(\frac{\theta}{2}) & \frac{2}{5}\,\cos(\frac{\theta}{2}) + \frac{1}{5}\,\sin(\frac{\theta}{2}) \end{bmatrix}.$$

The computation of the left-eigenvectors allows us to

$$\psi_{\frac{i}{2}}(\xi) = \begin{bmatrix} -(4+2\,i)\,e^{-\frac{i\xi}{2}} & 5\,e^{-\frac{i\xi}{2}} \end{bmatrix}.$$

Analogously to the prescribed FDE theory described in the first section, this leads to a basis for the complementary space Q, which is given by

$$\tilde{\Psi} = \begin{bmatrix} -4\,\cos\left(\frac{\xi}{2}\right) - 2\,\sin\left(\frac{\xi}{2}\right) & 5\,\cos\left(\frac{\xi}{2}\right) \\ 4\,\sin\left(\frac{\xi}{2}\right) - 2\,\cos\left(\frac{\xi}{2}\right) & -5\,\sin\left(\frac{\xi}{2}\right) \end{bmatrix}.$$

The normalized basis of Q denoted Ψ is obtained by using the defined bilinear form (13.8) such that $< \Psi, \Phi >= I_d$, thus we have

$$\Psi = \begin{bmatrix} \psi_{1,1} & \psi_{1,2} \\ \psi_{2,1} & \psi_{2,2} \end{bmatrix}.$$

such that :

$$\psi_{1,1} = \frac{-256 \cos\left(\frac{\xi}{2}\right)+272 \sin\left(\frac{\xi}{2}\right)+104\,\pi \cos\left(\frac{\xi}{2}\right)-128\,\pi \sin\left(\frac{\xi}{2}\right)}{-876+184\,\pi+85\,\pi^2}$$

$$\psi_{1,2} = \frac{120 \cos\left(\frac{\xi}{2}\right)-40\,\pi \cos\left(\frac{\xi}{2}\right)-400 \sin\left(\frac{\xi}{2}\right)+180\,\pi \sin\left(\frac{\xi}{2}\right)}{-876+184\,\pi+85\,\pi^2}$$

$$\psi_{2,1} = \frac{368 \cos\left(\frac{\xi}{2}\right)+704 \sin\left(\frac{\xi}{2}\right)+128\,\pi \cos(1/2\,\xi)+104\,\pi \sin\left(\frac{\xi}{2}\right)}{-876+184\,\pi+85\,\pi^2}$$

$$\psi_{2,2} = \frac{-720 \cos\left(\frac{\xi}{2}\right)-180\,\pi \cos\left(\frac{\xi}{2}\right)-520 \sin\left(\frac{\xi}{2}\right)-40\,\pi \sin\left(\frac{\xi}{2}\right)}{-876+184\,\pi+85\,\pi^2}.$$

Hence, the dynamics of (13.5) in the center manifold is given by the top equation of (13.47) which can be written

$$\begin{bmatrix} \frac{du_1}{dt} \\ \frac{du_2}{dt} \end{bmatrix} = L \begin{bmatrix} u_1 \\ u_2 \end{bmatrix} + \Psi(0)F(\Phi u + h(u)). \tag{13.53}$$

where the matrix L characterizing the linear part of the approximation is given by

$$L = \begin{bmatrix} 0 & \frac{1}{2} \\ -\frac{1}{2} & 0 \end{bmatrix}.$$

Thus using (13.53), straightforward computations allows us to the following finite dimensional approximation

$$\begin{aligned}
\frac{d\,u_1}{dt} &= \frac{u_2}{2} + \frac{8}{25}\frac{(-776+317\,\pi)\,u_1{}^3}{-876+184\,\pi+85\,\pi^2} + \frac{96}{25}\frac{(-3+\pi)\,u_2\,u_1{}^2}{-876+184\,\pi+85\,\pi^2} \\
&\quad - \frac{48}{25}\frac{(-3+\pi)\,u_2{}^2 u_1}{-876+184\,\pi+85\,\pi^2} + \frac{8}{25}\frac{(-3+\pi)\,u_2{}^3}{-876+184\,\pi+85\,\pi^2} \\
\frac{d\,u_2}{dt} &= -\frac{u_1}{2} + \frac{16}{25}\frac{(503+182\,\pi)\,u_1{}^3}{-876+184\,\pi+85\,\pi^2} + \frac{432}{25}\frac{(4+\pi)\,u_2\,u_1{}^2}{-876+184\,\pi+85\,\pi^2} \\
&\quad - \frac{216}{25}\frac{(4+\pi)\,u_2{}^2 u_1}{-876+184\,\pi+85\,\pi^2} + \frac{36}{25}\frac{(4+\pi)\,u_2{}^3}{-876+184\,\pi+85\,\pi^2}
\end{aligned} \tag{13.54}$$

13.4   Outlines of the General Theory of NFDE

Let us consider the general discretely delayed autonomous first order nonlinear system NFDE where we separate its linear and nonlinear quantities as follow

$$\frac{d}{dt}[x(t) + \sum_{k=1}^{n} A_k\, x(t-\tau_k)] = \sum_{k=0}^{m} B_k\, x(t-\tau_k) + \mathcal{F}(x(t), \dots, x(t-\tau_n)) \tag{13.55}$$

where A_i, B_j are $n \times n$ real valued matrix and the delays τ_k are ordered such that $\tau_j < \tau_j$ when $i < j$ and let $\tau_n = r$.

The latter system can be written

$$\frac{d}{dt}\mathcal{D}x_t = \mathcal{L}x_t + \mathcal{F}(x_t) \tag{13.56}$$

where $x_t \in \mathcal{C} = C([-r,0],\mathbb{R}^n)$, $x_t(\theta) = x(t+\theta)$, $\mathcal{D}$, $\mathcal{L}$ are bounded linear operators such that $\mathcal{L}\phi = \sum_{k=0}^n B_k\,\phi(-\tau_k)$, $\mathcal{D}\phi = \phi(0) + \sum_{k=1}^n A_k\,\phi(-\tau_k)$ and $\mathcal{F}$ is sufficiently smooth function mapping $\mathcal{C}$ into $\mathbb{R}^n$ with $\mathcal{F}(0) = D\mathcal{F}(0) = 0$. We point out that the linear operators $\mathcal{D}$ and $\mathcal{L}$ can be written in the integral form by $\mathcal{L}\phi = \int_{-r}^0 d\eta(\theta)\phi(\theta)$ and $\mathcal{D}\phi = \phi(0) + \int_{-r}^0 d\mu(\theta)\phi(\theta)$, where μ and η are two real valued $n \times n$ matrix.

The linearized equation of (13.56) is given by

$$\frac{d}{dt}\mathcal{D}x_t = \mathcal{L}x_t \tag{13.57}$$

for which the solution operator $\mathcal{T}(t)$ defined by

$$\mathcal{T}(t)(\phi) = x_t(.,\phi) \tag{13.58}$$

such that $x_t(.,\phi)(\theta) = x(t+\theta,\phi)$ for $\theta \in [-r,0]$ is a strongly continuous semigroup with the infinitesimal generator $\mathcal{A}$ which has the domain

$$\mathcal{D}om(\mathcal{A}) = \{\phi \in \mathcal{C} : \frac{d\phi}{d\theta} \in \mathcal{C}, \mathcal{D}\frac{d\phi}{d\theta} = \mathcal{L}\phi\} \text{ and is given by } \mathcal{A}\phi = \frac{d\phi}{d\theta}.$$

It is also known that $\sigma(\mathcal{A}) = \sigma_p(\mathcal{A})$ and the spectrum of $\mathcal{A}$ consists of complex values $\lambda \in \mathbb{C}$ which satisfy the characteristic equation $p(\lambda) = \det\Delta(\lambda)$, see [151] for further details on spectral properties of linear functional differential equations.

Let us denote by $\mathcal{M}_\lambda$ the eigenspace associated with $\lambda \in \sigma(\mathcal{A})$. We define $\mathcal{C}^* = C([-r,0],\mathbb{R}^{n*})$ where $\mathbb{R}^{n*}$ is the space of n-dimensional row vectors and consider the bilinear form on $\mathcal{C}^* \times \mathcal{C}$ which is proposed in [115]

$$(\psi,\varphi) = \psi(0)\,\varphi(0) - \int_{-r}^0 d[\int_0^\theta \psi(\tau-\theta)d\mu(\tau)] + \int_{-r}^0 \int_0^\theta \psi(\tau-\theta)d\eta(\theta)\phi(\tau)d\tau$$

and let $\mathcal{A}^T$ be the transposed operator of $\mathcal{A}$, i.e., $(\psi,\mathcal{A}\varphi) = (\mathcal{A}^T\psi,\varphi)$.

Note that in the particular case, when $\mathcal{D} = I_d$ then the bilinear form reduces to

$$(\psi,\varphi) = \psi(0)\,\varphi(0) + \int_{-r}^0 \int_0^\theta \psi(\tau-\theta)d\eta(\theta)\phi(\tau)d\tau$$

In [152], the author give a procedure based on the above bilinear form allowing to the the explicit computation of the center variety for delay systems. The following Theorem [115] permits the decomposition of the space $\mathcal{C}$.

Theorem 42. *Let Λ be a nonempty finite set of eigenvalues of $\mathcal{A}$ and let $P = \text{span}\{\mathcal{M}_\lambda(\mathcal{A}), \lambda \in \Lambda\}$ and $P^T = \text{span}\{\mathcal{M}_\lambda(\mathcal{A}^T), \lambda \in \Lambda\}$. Then P is invariant under $\mathcal{T}(t), t \geq 0$ and there exists a space $\mathcal{Q}$, also invariant under $\mathcal{T}(t)$ such that $\mathcal{C} =$*

$P \bigoplus Q$. *Furthermore, if* $\Phi = (\phi_1, \ldots, \phi_m)$ *forms a basis of* P, $\Psi = col(\psi_1, \ldots, \psi_m)$ *is a basis of* P^T *in* $\mathcal{C}^*$ *such that* $(\Phi, \Psi) = Id$, *then*

$$Q = \{\phi \in \mathcal{C} \setminus (\Psi, \phi) = 0\} \text{ and}$$
$$P = \{\phi \in \mathcal{C} \setminus \exists b \in \mathbb{R}^m : \phi = \Phi b\}. \tag{13.59}$$

Also, $\mathcal{T}(t)\Phi = \Phi e^{Bt}$, *where* B *is an* $m \times m$ *matrix such that* $\sigma(B) = \Lambda$.

Let us consider the extension of the space $\mathcal{C}$ that contains continuous functions on $[-r, 0)$ with possible jump discontinuity at 0, we denote this space $\mathcal{BC}$. A given function $\xi \in \mathcal{BC}$ can be written $\xi = \varphi + X_0 \alpha$, where $\varphi \in \mathcal{C}$, $\alpha \in \mathbb{R}^n$ and X_0 is defined by $X_0(\theta) = 0$ for $-r \leq \theta < 0$ and $X_0(0) = Id_{n \times n}$. Then Hale-Verduyn Lunel bilinear form [115] can be extended to the space $\mathcal{C}^* \times \mathcal{BC}$ by $(\psi, X_0) = \psi(0)$ and the infinitesimal generator $\mathcal{A}$ extends to an operator $\tilde{\mathcal{A}}$ (defined in C^1) onto the space $\mathcal{BC}$ as follow

$$\tilde{\mathcal{A}}\phi = \mathcal{A}\phi + X_0[\mathcal{L}\phi - \mathcal{D}\phi'] \tag{13.60}$$

Under the above consideration one can write equation (13.56) as an abstract ODE

$$\dot{x}_t = \tilde{\mathcal{A}}x_t + X_0\mathcal{F}(x_t), \tag{13.61}$$

see [91]. Thanks to the projection $\Pi : \mathcal{BC} \to P$ such that $\Pi(\varphi + X_0\alpha) = \Phi[(\Psi, \varphi) + \Psi(0)\alpha]$ hence $x_t = \Phi y(t) + z_t$ where $y(t) \in \mathbb{R}^m$ and then equation (13.56) can be split to

$$\dot{y} = By + \Psi(0)F(\Phi y + z)$$
$$\dot{z} = \tilde{\mathcal{A}}_Q + (I - \Pi)X_0\mathcal{F}(\Phi y + z), \tag{13.62}$$

and the interest turns to be focused only on the first equation after writing z as a function of y; that is the flow restriction on the finite dimensional subspace P.

Conclusion et perspectives

Cette partie comporte une description succinte des travaux en cours ainsi que les développements futurs. Elle présente la suite à donner aux travaux de ce manuscrit ainsi que les nouvelles thématiques auxquelles je m'intéresse. Ces perspectives s'articulent essentiellement autour de trois sujets : les deux premiers concernent deux questions théoriques (la linéarisation explicite au voisinage de points de Hopf et l'étude des propriétés et de la distribution des zéros de fonctions analytiques et notamment les quasipolynômes) et le troisième sujet consiste à explorer les applications en sciences du vivant et exploiter les outils de la théorie qualitative dans l'analyse et le contrôle de leurs dynamiques.

14.1 Linéarisation explicite au voisinage d'un point d'équilibre non hyoperbolique

Plusieurs perspectives sont envisagées dans ce contexte ; l'exploration de la *profondeur d'isochronie*, l'élaboration de formules de linéarisation explicite au voisinage d'un centre isochrone, l'adaptation de l'approche de synchronisation de fréquences aux systèmes couplés et enfin la caractérisation de centres isochrones pour des systèmes à retard.

14.1.1 Profondeur d'isochronie

Considérons la forme normale à l'ordre $2N + 1$ en coordonnées polaires d'un centre linéaire non-linéairement perturbé :

$$\dot{r} = \sum_{j=1}^{N} \alpha_{2j+1} r^{2j+1} + O(r^{2N+3}), \ \dot{\theta} = 1 + \sum_{j=1}^{N} \beta_{2j+1} r^{2j} + O(r^{2N+2}). \qquad (14.1)$$

Les coefficients α_k sont appelés *coefficients de Lyapunov*. Les coefficients β_k ne sont autres que les *coefficients du développement de la fonction période*. Le calcul des coefficients de Lyapunov permet de résoudre le problème du *Foyer-Centre*. En effet, la non nullité d'un coefficient de Lyapunov implique l'existence d'un foyer. Dans ce cas, le signe (positif/négatif) du coefficient (non nul) du monôme de plus bas degré (en r) décide de l'instabilité/stabilité du foyer. Le problème de profondeur du centre consiste à déterminer k, le nombre des premiers coefficients de Lyapunov, dont la nullité implique la nullité de tous les cofficients de Lyapunov (conséquence du théorème de Hilbert). D'une manière analogue, le problème de *profondeur d'isochronie*

consiste à déterminer k, le nombre des premiers coefficients de la fonction période, dont la nullité implique la nullité de tous les cofficients de la fonction période. A titre d'exemple, pour la famille des systèmes de type Liénard (2.21) de degré arbitraire n, nous arrivons à identifier une formule explicite pour la profondeur d'isochronie (sachant que l'existence d'un centre à l'origine est assurée dans cette classe), cette conjecture est vérifiée pour les systèmes de degré $n \leqslant 20$, voir [30]. Travailler sur l'élaboration d'une preuve de cette formule déterminant la profondeur en fonction du degré, est une des perspectives envisagées (sachant qu'on dispose d'un ensemble de relations de recurrences explicites entre les coefficients de la fonction période). L'idée est de démontrer que les k premiers coefficients forment une base pour les coefficients suivants.

14.1.2 Linéarisation explicite

D'après le Théorème de H. Poincaré (linéarisation au voisinage d'un centre), un centre est isochrone s'il admet un changement de variables analytique linéarisant. Les méthodes classiques utilisées dans la caractérisation des conditions d'isochronie, telle que la méthode des formes normales et l'établissement d'un commutateur transversal (s'il est de plus analytique mais non polynomial) ne fournissent pas d'information sur la linéarisation explicite. L'avantage de notre approche, basée sur le critère d'Urabe est de lier cette propriété d'isochronie à l'identification d'une fonction impaire, dite la fonction d'Urabe, qui satisfait un certain nombre de conditions. Dans [15], une formule explicite de linéarisation est établie dans le cas où la fonction d'Urabe est constante. Dans [30] une forme spécifique de fonction d'Urabe (appelée forme standard) a été identifiée $h(\xi) = \frac{a\,\xi^{2n+1}}{\sqrt{b+c\,\xi^{4n+2}}}$ avec a, b, $c \in \mathbb{R}$, $b > 0$ et $n \in \mathbb{N}^*$ pour la majorité des centres isochrones décelés. Puis dans [14, 15] il a été démontré que cette forme standard même si elle est aussi fréquente n'est pas la seule possible mais des formes plus complexes peuvent exister (pour des systèmes d'ordres supérieurs). Il est important d'établir le lien entre les formules de linéarisation et la fonction d'Urabe non constante. Un point de départ envisagé est celui de commencer par les fonctions sous forme standard.

14.1.3 Synchronisation de fréquence par couplage non linéaire d'oscillateurs

Etant donné un système d'EDO n'ayant pas la propriété d'isochronie ni dans le plan (x, y) ni dans le plan (w, z) :

$$
\begin{cases}
\dot{x} = -y + f_1(x, y) \\
\dot{y} = x + f_2(x, y) \\
\dot{w} = -z + f_3(w, z) \\
\dot{y} = w + f_4(w, z)
\end{cases}
$$

où $f_1, f_2 \in \mathbb{R}[x, y]$ et $f_3, f_4 \in \mathbb{R}[w, z]$ représentent la nonlinéarité du système. Sous quelles conditions existe-il $g_1, g_2, g_3, g_4 \in \mathbb{R}[x, y, w, z]$ tel que le système

$$
\begin{cases}
\dot{x} = -y + f_1(x, y) + g_1(x, y, z, w) \\
\dot{y} = x + f_2(x, y) + g_2(x, y, z, w) \\
\dot{w} = -z + f_3(w, z) + g_3(x, y, z, w) \\
\dot{y} = w + f_4(w, z) + g_4(x, y, z, w)
\end{cases}
$$

admet un centre isochrone dans le plan (x, y). Ce problème est en cours d'exploration, il est fortement lié aux problèmes de platitude.

14.1.4   Centres isochrones pour des systèmes à retard

L'investigation des centres isochrones d'un système à retard se ramène à la caractérisation de tels centres pour un système plan d'équations différentielles ordinaires correspondants. En effet, étant donné un système à retard $\dot{x} = f(x_t)$ $(x_t \in \mathcal{C} = C([-r, 0], \mathbb{R}^n), x_t(\theta) = x(t + \theta))$, dont le linéarisé autour d'un point de Hopf (point d'équilibre non hyperbolique admettant une unique fréquence de coupure ω_0) n'admet que des valeurs spectrales telles que $\Re(\sigma) \leq 0$. Ainsi, grâce à la décomposition spectrale x_t s'écrit $x_t = \Phi y(t) + z_t$ avec $y(t) \in \mathbb{R}^2$ et Φ une base de l'espace propre $\mathcal{M}_{j\omega_0}$. Puis, en se basant sur le théorème de la variété du centre, (dans la variété du centre $z_t = h(y)$) on sait que les dynamiques dominantes du système initial seront gouvernées par $\dot{y} = By + \Psi(0)F(\Phi y + h(y))$.
L'exploration de cette propriété d'isochronie pour de tels systèmes n'a jamais été étudiée et fera partie des perspectives envisagées.

14.2   Localisation des zéros de quasipolynômes

La stabilité d'un quasipolynôme $\Delta(\lambda, \tau)$ se traduit par la mise en évidence d'un réel $\sigma > 0$ tel que toutes les racines λ_k de $\Delta(\lambda, \tau)$ soient à partie réelle strictement inférieure à $-\sigma$. Ainsi, tester la stabilité pour un systéme à retard revient à vérifier l'absence de racines à partie réelle positive de son quasipolynôme caractéristique.

14.2.1   Caractérisation des fréquences de coupures d'un quasipolynôme

La variété du centre joue un rôle important dans l'analyse qualitative des systèmes à retard non linéaires. La dimension du projeté de l'état dans cette variété n'est autre que la dimension de l'espace propre généralisé associé aux valeurs spectrales imaginaires pures. Il existe différentes approches pour identifier ces valeurs spectrales pour les quasipolynômes de la forme $\Delta(\lambda, \tau) = \sum_{k=0}^{N} P_k(\lambda)e^{-\lambda \tau_k}$ avec $\tau_0 = 0$, $0 < \tau_1 < \tau_2 < \ldots < \tau_N$ et $\tau = (\tau_1, \tau_2, \ldots, \tau_N)$. D'autre part, différentes applications issues de la biologie (équations structurées en âge) ou même de l'astrophysique (dynamique de satellites) sont modélisés par des systèmes à retard dont les

paramètres dépendent également du retard. Ce qui suggère l'intérêt de considérer les quasipolynômes de la forme $\Delta(\lambda, \tau) = \sum_{k=0}^{N} P_k(\lambda, \tau) e^{-\lambda \tau_k}$. Cette dépendance paramétrique en le retard s'avère être une limitation pour les approches classiques dans l'identification des fréquences de coupure. A titre d'exemple, la transformation de Rekasius ne permet pas d'explorer la multiplicité d'une valeur spectrale imaginaire pure. Ce problème s'inscrit dans les perspectives envisagées ; des questions auxiliaires ont été abordées dans ce manuscrit. L'exploration de cette classe est une problèmatique adressée dans la thèse en cours (2015-2018) de Chi Jin.

14.2.2   Comportement des valeurs spectrales d'un système à retard en présence de perturbations

Une technique standard dans la stabilisation de systèmes à retard consiste à établir les fréquences de coupure puis à identifier le vecteur perturbation permettant de migrer ces valeurs spectrales vers le demi-plan complexe gauche. Toutefois, cette migration dépend fortement des multiplicités (algébrique/géométrique) de ces valeurs spectrales. L'idée consiste à considérer que la valeur spectrale et les vecteurs propres correspondants comme fonctions en la perturbation et de considérer leur développement en série (de Taylor dans le cas d'une racine semi-simple) comme suit : (dans le cas non semi-simple, les puissances deviennent des fractions rationnelles, car il s'agit d'un developpement en série de Puiseux)

$$\lambda = \lambda_0 + \sum_{i=1}^{r} \varepsilon^i \, \lambda_i + \dots,$$

$$u = u_0 + \sum_{i=1}^{r} \varepsilon^i \, u_i + \dots.$$

Nous abordons actuellement deux directions. La première dans le cadre de la thèse en cours (2014-2017) de Dina Irofti, où la perturbation est due à une incertitude sur la valeur du vecteur retard. La seconde, dans le cadre de la thèse de Chi Jin, où on considère des incertitudes sur les coefficients du quasipolynôome qui à leur tour dépendent du retard. Dans une collaboration en cours avec Wim Michiels (UC Leuven), nous étudions la migration des racines multiples correspondant au problèmesaux valeurs propres non linéaire :

$$M(\lambda, \varepsilon)u = 0, \; \lambda \in \mathbb{C}, \; u \neq 0.$$

où M est un opérateur dépendant de la variable λ et du paramétre ε.

14.2.3   Interpolation de Birkhoff

Le lien explicite entre le problème d'interpolation de Birkhoff et la multiplicité des zéros de quasipolynôme a été souligné dans ce manuscrit. Exploiter ce type de matrices structurées dans des problèmes de stabilisation est à notre connaissance un usage nouveau qui nous fera bénéficier de leurs propriétés. Ce sujet est envisagé dans mes perspectives.

14.3 Applications en biologie/biochimie

Le monde du vivant est très représentatif d'un domaine où les dynamiques à retard se manifestent. Par exemple, les célébre modèle de croissance du tournesol [226] (sunflower equation) ou celui décrivant le processus physiologique de production des cellules sanguines [143, 170] ou bien les éléments figurés du sang, aux comportements dynamiques nombreux et variés, sont apparus comme des modèles mathématiques à la fois simples et fidèles aux désordres des phénomènes observés. Le retard engendré par ces phénomènes de transport dans un milieu biologique complexe, s'observe également dans le monde du vivant lors du transport des influx nerveux dans les réseaux de neurones, et dans les communications internes du cerveau (vitesse finie, relativement lente, de propagation de l'influx nerveux). Voir aussi des application en concérologie, en particulier l'analyse de modèles de leucémie aigue myéloblastique dans [97, 26]. Dans cette thématique deux problèmes sont envisagés dans mes perspectives.

14.3.1 Dynamiques des populations impliquant retard et termes stochastiques

Dans le cadre d'une collaboration en cours avec Paul Reynaud de Fitte (LMRS, Université de Rouen) nous nous intéressons à l'analyse des dynamiques prédateur/proie avec refuge dont une modèle mathématique (normalisé) est donné par :

$$\begin{cases} \dot{x} = x\left(1 - x\right) - \dfrac{ay\left(x - m\right)_{+}}{k_1 + \left(x - m\right)_{+}}, \\ \dot{y} = by\left(1 - \dfrac{y}{k_2 + \left(x - m\right)_{+}}\right), \end{cases}$$

où $x \geq 0$ est la densité de proie, $y \geq 0$ est la densité de prédateur, $m \geq 0$ modélise le refuge pour la proie i.e. la quantité $\left(x - m\right)_{+} := \max\left(x - m, 0\right)$ désigne la densité de proie accessible au prédateur et les paramétres physiques $a, b, k_1, k_2 \in \mathbb{R}_{+}^{*}$. Le premier objectif est d'établir une analyse qualitative paramétrique des solutions de ce modèle (positivité, bornitude, stabilité, périodicité). L'étape suivante consiste à considérer le retard qui existe naturellement dans les interconnexions en plus d'éventuels termes stochastiques.

14.3.2 Analyse des réseaux en chimie/biochimie

Motivé par une classe de systèmes à retards étudiée dans la théorie des réseaux de réactions biochimiques (systèmes provenant du principe d'action de masse retardée), et à l'aide de techniques du calcul formel et de la théorie des graphes, le but de cette collaboration avec Silviu Niculescu, Alban Quadrat, Yacine Bouzidi (Inria, Lille) et Marc Roussel (Leithbridge University, Canada) est de développer une analyse générale de la stabilité des systèmes interconnectés définis par des équations

différentielles polynomiales à retards et de leurs sensibilités aux variations des retards et des paramètres du système (existence de points d'équilibre positifs, stabilité, comportement oscillatoire, bifurcations de Hopf, ...).

En particulier, nous abordons un modèle décrivant le mécanisme irreversible de la réaction de Belousov-Zhabotinskii, le modèle Oregonator donné par les equations cinétiques :

$$A + Y \xrightarrow{k_1} X + P$$
$$X + Y \xrightarrow{k_2} 2P$$
$$B + X \xrightarrow{k_3} 2X + Z$$
$$2X \xrightarrow{k_4} A + P$$
$$Z \xrightarrow{k_5} fY$$
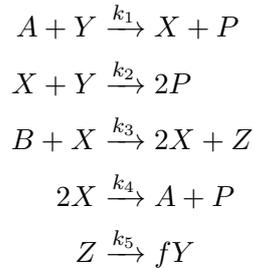
où A l'ion Bromate et B un composé organique, Y l'ion bromure, X l'acide bromique et Z le cérium sont les variables chimiques, P un produit, les k_i, $i = 1, 2, \ldots, 5$,sont des constantes positives représentant les constantes de vitesse/cinétiques et f un coefficient stoichiométrique. Etant donné que la loi d'action de masse suggère que la vitesse de réaction est proportionnelle au produit des concentrations des réactants, l'Oregonator est décrit par le système dynamique :

$$\dot{X}(t) = k_1 A Y(t) - k_2 X(t) Y(t) + k_3 B X(t) - 2k_4 X(t)^2$$
$$\dot{Y}(t) = -k_1 A Y(t) - k_2 X(t) Y(t) + f k_5 Z(t) \qquad (*)$$
$$\dot{Z}(t) = k_3 B X(t) - k_5 Z(t).$$

Nous exploitons une idée de modélisation, proposée dans [191], qui consiste à généraliser la loi d'action de masse en prenant en considération (dans un sous ensemble des réactions) le temps nécessaire pour l'apparition de produits (composés chimiques intermédiare) résultant de la transformation des réactants. Cette approche permet d'agréger ces modèles en introduisant des retard et en éliminant les variables intermédiaires dans l'équation dynamique. Concrètement, dans le cadre de l'analyse de l'Oregonator, cette idée permet de se focaliser uniquement sur les deux premières équations et considérer que la variable $Z(t)$ (variable intermédiaire) est proportionnelle à $X(t - \tau)$ où τ est le temps de la réaction pour obtenir :

$$\dot{X}(t) = k_1 A Y(t) - k_2 X(t) Y(t) + k_3 B X(t) - 2k_4 X(t)^2$$
$$\dot{Y}(t) = -k_1 A Y(t) - k_2 X(t) Y(t) + \alpha f k_5 X(t - \tau) \qquad (**)$$

Il a été démontré dans [191] que les solutions respectives de $(*)$ et de $(**)$ ont les mêmes propriétés qualitatives (point d'equilibre, oscillations, points de Hopf de fréquences respectives ω_* et ω_{**}), voir aussi [88]. Une des problèmatiques que nous considérons est d'établir le lien entre ces fréquences d'une part et le retard de modélisation τ et les paramétres du système (interconnections) d'autre part.

Bibliographie

[1] V.E. Abolinia and A. D. Myshkis. Mixed problem for an almost linear hyperbolic system in the plane. *Mat. Sb.*, 350 :423–442, 1960. (Cité en pages 9 et 248.)

[2] R. Abraham and J. E. Marsden. *Foundations of Mechanics*. The Benjamin/Commings Publishing, 1978. (Cité en page 123.)

[3] S.A. Abramov and M.A. Barkatou. D'alembertian series solutions at ordinary points of lode with polynomial coefficients. *Journal of Symbolic Computation*, 44(1) :48 – 59, 2009. (Cité en page 1.)

[4] L. V. Ahlfors. *Complex Analysis*. McGraw-Hill, Inc., 1979. (Cité en pages 99 et 172.)

[5] A. Algaba, E. Freire, and E. Gamero. Isochronicity via normal form. *Qualitative Theory of Dynamical Systems*, 1(2) :133–156, 2000. (Cité en pages 64 et 71.)

[6] A. Algaba, M. Merino, E. Freire, E. Gamero, and A. J. Rodrigues-Luis. Some results on chua's equation near a triple-zero linear degeneracy. *International Journal of Bifurcation and Chaos*, 13(03) :583–608, 2003. (Cité en page 107.)

[7] V. V. Amel'kin, N. A. Lukashevich, and A. P. Sadovskiĭ. *Nonlinear oscillations in second-order systems*. Beloruss. Gos. Univ., 1982. (in Russian). (Cité en pages 16 et 40.)

[8] D. Angeli, J.E. Ferrell, and E.D. Sontag. Detection of multistability, bifurcations, and hysteresis in a large class of biological positive-feedback systems. In *Proceedings of the National Academy of Sciences of the United States of America*, pages 1822–1827, 2004. (Cité en page 145.)

[9] S. Antman. volume 107 of *Applied Mathematical Sciences*. Springer-Verlag, Berlin, 1991. (Cité en page 158.)

[10] F. M. Atay. Balancing the inverted pendulum using position feedback. *Appl. Math. Lett.*, 12(5) :51–56, 1999. (Cité en pages 5, 93, 94, 95, 114, 196 et 200.)

[11] M. Ait Babram, O. O. Arino, and M-L. Hbid. Computational scheme of a center manifold for neutral functional differential equations. *J. Math. Anal. Appl.*, 258(2) :396–414, 2001. (Cité en pages 105, 141 et 170.)

[12] A.G. Balanov, N. B. Janson, P.V.E. McClintock, and C. H. T. Wang. Bifurcation analysis of a neutral delay differential equation modelling the torsional motion of a driven drill-string. *Chaos, Solitons and Fractals*, 15 :381–394, 2002. (Cité en pages 118, 119 et 125.)

[13] H.T Banks and A. Manitius. Projection series for retarded functional differential equations with applications to optimal control problems. *Journal of Differential Equations*, 18(2) :296 – 332, 1975. (Cité en pages 248 et 253.)

[14] M. Bardet and I. Boussaada. Complexity reduction of c-algorithm. *Applied Mathematics and Computation*, 217(17) :7318 – 7323, 2011. (Cité en pages 3, 41, 61, 62 et 270.)

[15] M. Bardet, I. Boussaada, A.R. Chouikha, and J-M. Strelcyn. Isochronicity conditions for some planar polynomial systems {II}. *Bulletin des Sciences Mathématiques*, 135(2) :230 – 249, 2011. (Cité en pages 2, 3, 39, 61, 62 et 270.)

[16] M. A. Barkatou. On rational solutions of systems of linear differential equations. *Journal of Symbolic Computation*, 28(4) :547 – 567, 1999. (Cité en page 1.)

[17] M.A. Barkatou and A. Duval. Sur les séries formelles solutions d'équations aux différences polynomiales. *Ann. Inst. Fourier*, 44(2) :495–524, July 1994. (Cité en page 1.)

[18] G. Bastin, J-M. Coron, and S. O. Tamasoiu. Stability of linear density-flow hyperbolic systems under {PI} boundary control. *Automatica*, 53 :37 – 42, 2015. (Cité en page 135.)

[19] T. Becker and V. Weispfenning. *Gröbner bases*. Springer-Verlag, 1993. (Cité en pages 36 et 65.)

[20] R. Bellman and K. Cooke. *Differential-difference equations*. Academic Press, New York, 1963. (Cité en pages 99, 172, 216 et 233.)

[21] L. Besnard, Y.B. Shtessel, and B. Landrum. Control of a quadrotor vehicle using sliding mode disturbance observer. In *American Control Conference, 2007. ACC '07*, pages 5230–5235, July 2007. (Cité en page 79.)

[22] D.A. Bini and P. Boito. A fast algorithm for approximate polynomial gcd based on structured matrix computations. In D.A. Bini, V. Mehrmann, V. Olshevsky, E. Tyrtyshnikov, and M. van Barel, editors, *Numerical Methods for Structured Matrices and Applications*, volume 199 of *Operator Theory : Advances and Applications*, pages 155–173. Birkhäuser Basel, 2010. (Cité en page 172.)

[23] A. Björck and T. Elfving. Algorithms for confluent Vandermonde systems. *Numer. Math.*, 21 :130–137, 1973. (Cité en page 175.)

[24] I. I. Blekhman. *Synchronisation in Science and Technology*. ASME press, 1988. (Cité en pages 61 et 62.)

[25] B. Bonnard, L. Faubourg, and E. Trélat. *Mécanique céleste et contrôle des véhicules spatiaux*. Mathématiques et Applications. Springer-Verlag Berlin Heidelberg, 2006. (Cité en page 1.)

[26] C. Bonnet, J. L. Avila Alonso, H. Ozbay, J. Clairambault, S-I. Niculescu, and P. Hirsch. A Discrete-Maturity Interconnected Model of Healthy and Cancer Cell Dynamics in Acute Myeloid Leukemia. In *The 10th AIMS Conference on Dynamical Systems, Differential Equations and Applications*, Madrid, Spain, 2014. (Cité en page 273.)

[27] S. Bouabdallah and R. Siegwart. Backstepping and sliding-mode techniques applied to an indoor micro quadrotor. In *Robotics and Automation, 2005.*

ICRA 2005. Proceedings of the 2005 IEEE International Conference on, pages 2247–2252, April 2005. (Cité en page 79.)

[28] I. Boussaada. Amplitude independent frequency synchroniser for a cubic planar polynomial system. *J. Comput. Nonlinear Dynam.*, 7(2) :021009–021009, 2012. (Cité en pages 3 et 61.)

[29] I. Boussaada, A. Cela, H. Mounier, and S-I. Niculescu. Control of drilling vibrations : A time-delay system-based approach. In *Proceedings of The 11th IFAC Workshop on Time Delay Systems*, pages 1–5, 2013. (Cité en pages 5 et 122.)

[30] I. Boussaada, A.R. Chouikha, and J-M. Strelcyn. Isochronicity conditions for some planar polynomial systems. *Bulletin des Sciences Mathématiques*, 135(1) :89–112, 2011. (Cité en pages 2, 15, 40, 41, 43, 44, 46, 48, 49, 50, 58, 59, 61, 62, 63 et 270.)

[31] I. Boussaada, D. Irofti, and S-I. Niculescu. Computing the codimension of the singularity at the origin for time-delay systems in the regular case : A Vandermonde-based approach. *13th European Control Conference*, pages 1–6, 2014. (Cité en pages 7, 171, 215, 217 et 220.)

[32] I. Boussaada, W. Michiels, and S-I. Niculescu. Spectral analysis for delay differential-algebraic systems. In *Proceedings of the 10th IFAC Workshop on Time Delay Systems, Boston, USA*, pages 1–6, 2012. (Cité en pages 8, 9 et 247.)

[33] I. Boussaada, W. Michiels, and S-I. Niculescu. Further remarks on spectral analysis of delay differential-algebraic systems. *Preprint*, pages 1–12, 2015. (Cité en page 247.)

[34] I. Boussaada, I-C. Morarescu, and S-I. Niculescu. Inverted pendulum stabilization : Characterization of codimension-three triple zero bifurcation via multiple delayed proportional gains. *Systems and Control Letters*, 82 :1 – 9, 2015. (Cité en pages 5, 93, 173, 182, 196, 197 et 201.)

[35] I. Boussaada, I-C. Morarescu, and S-I. Niculescu. Inverted pendulum stabilization via a pyragas-type controller : Revisiting the triple zero singularity. *Proceedings of the 19th IFAC World Congress, 2014*, Cape Town :6806–6811, 2015. (Cité en pages 5, 93, 197 et 201.)

[36] I. Boussaada, H. Mounier, S-I. Niculescu, and A. Cela. Analysis of drilling vibrations : A time-delay system approach. In *Proceedings of The 20th Mediterranean Conference on Control and Automation*, pages 1–5, 2012. (Cité en pages 5, 122, 137, 147, 170 et 173.)

[37] I. Boussaada and S-I. Niculescu. Computing the codimension of the singularity at the origin for delay systems : The missing link with Birkhoff incidence matrices. *21st International Symposium on Mathematical Theory of Networks and Systems*, pages 1 – 8, 2014. (Cité en pages 7, 215, 217, 220, 222, 223, 224 et 232.)

[38] I. Boussaada and S-I. Niculescu. Computing the codimension of the singularity at the origin for delay systems : The missing link with birkhoff incidence matrices. *21st International Symposium on Mathematical Theory of Networks and Systems July 7-11, 2014, Groningen, The Netherlands*, pages 1–6, 2014. (Cité en pages 99, 100, 107 et 114.)

[39] I. Boussaada and S-I. Niculescu. Computing the codimension of the singularity at the origin for delay systems : The missing link with birkhoff incidence matrices. *21st International Symposium on Mathematical Theory of Networks and Systems July 7-11, 2014. Groningen, The Netherlands*, pages 1699–1706, 2014. (Cité en page 171.)

[40] I. Boussaada and S-I. Niculescu. Characterizing the codimension of zero singularities for time-delay systems : A link with Vandermonde and Birkhoff incidence matrices. *To appear in : Acta Applicandae Mathematicae*, pages 1–46, 2016. (Cité en pages 7, 8, 171, 215, 217, 218, 222, 223, 232 et 233.)

[41] I. Boussaada and S-I. Niculescu. Tracking the algebraic multiplicity of crossing imaginary roots for generic quasipolynomials : A vandermonde-based approach. *To appear in : IEEE Transactions on Automatic Control*, page 6pp, 2016. (Cité en pages 7, 8, 215, 232, 236 et 240.)

[42] I. Boussaada, M-B. Saldivar, H. Mounier, A. Cela S-I. Niculescu, and S. Mondié. Delay system modeling of rotary drilling vibrations. In E. Witrant, E. Fridman, O. Sename, and L. Dugard, editors, *Recent Results on Time-Delay Systems : Analysis and Control*, volume 5, pages 277–287. Birkhäuser Basel, 2015. (Cité en pages 5, 115 et 160.)

[43] C. Califano, S. Monaco, and D. Normand-Cyrot. On the problem of feedback linearization. *Systems & Control Letters*, 36(1) :61 – 67, 1999. (Cité en page 1.)

[44] F. Calogero. Oxford University Press, Oxford, 2012. (Cité en page 15.)

[45] S.A. Campbell. Calculating centre manifolds for delay differential equations using maple. In *In Delay Differential Equations : Recent Advances and New Directions*. Springer-Verlag, 2009. (Cité en page 105.)

[46] S.A. Campbell and Y. Yuan. Zero singularities of codimension two and three in delay differential equations. *Nonlinearity*, 22(11) :2671, 2008. (Cité en page 173.)

[47] J. Carr. *Application of Center Manifold Theory*. Springer, 1981. (Cité en pages 1, 80, 135, 162, 174 et 200.)

[48] O.A. Chalykh and A.P. Veselov. A remark on rational isochronous potentials. *J. Nonlinear Math. Phys.*, 12(suppl. 1) :179–183, 2005. (Cité en page 56.)

[49] J. Chavarriga, I.A. García, and J. Giné. Isochronicity into a family of time-reversible cubic vector fields. *Appl. Math. Comput.*, 121(2-3) :129–145, 2001. (Cité en page 44.)

[50] J. Chavarriga, J. Gine, and I.A. Garcia. Isochronous centers of a linear center perturbed by fourth degree homogeneous polynomial. *Bulletin des Sciences Mathématiques*, 123(2) :77 – 96, 1999. (Cité en page 37.)

[51] J. Chavarriga, J. Gine, and I.A. Garcia. Isochronous centers of a linear center perturbed by fifth degree homogeneous polynomials. *Journal of Computational and Applied Mathematics*, 126 :351 – 368, 2000. (Cité en page 37.)

[52] J. Chavarriga and M. Sabatini. A survey of isochronous centers. *Qualitative Theory of Dynamical Systems*, 1(1) :1–70, 1999. (Cité en pages 16, 40, 44, 62, 66, 70, 71, 72 et 77.)

[53] J. Chen, P. Fu, S-I. Niculescu, and Z. Guan. An eigenvalue perturbation approach to stability analysis, part i : Eigenvalue series of matrix operators. *SIAM J. Cont. and Optim.*, 48(8) :5564–5582, 2010. (Cité en page 217.)

[54] J. Chen, P. Fu, S-I. Niculescu, and Z. Guan. An eigenvalue perturbation approach to stability analysis, part ii : When will zeros of time-delay systems cross imaginary axis ? *SIAM J. Cont. and Optim.*, 48(8) :5583–5605, 2010. (Cité en page 217.)

[55] X. Chen, V.G. Romanovksi, and W. Zhang. Linearizability conditions of time-reversible quartic systems having homogeneous nonlinearities. *Nonlinear Anal.*, 69(5-6) :1525–1539, 2008. (Cité en pages 26 et 44.)

[56] X. Chen and V.G. Romanovski. Linearizability conditions of time-reversible cubic systems. *J. Math. Anal. Appl.*, 362(2) :438–449, 2010. (Cité en pages 44, 61, 66 et 77.)

[57] Y. Chitour, G. Mazanti, and M. Sigalotti. Stability of non-autonomous difference equations with applications to transport and wave propagation on networks. preprint, 2015. (Cité en page 135.)

[58] Y. Chitour, G. Mazanti, and M. Sigalotti. Stability of non-autonomous difference equations with applications to transport and wave propagation on networks. *Netw. Heterog. Media*, to appear. Preprint arXiv :1504.01116. (Cité en page 135.)

[59] A.G. Choudhury and P. Guha. On isochronous cases of the Cherkas system and Jacobi's last multiplier. *Journal of Physics A : Mathematical and Theoretical*, 43 :125202, 12 pp, 2010. (Cité en pages 42 et 55.)

[60] A.R. Chouikha. Monotonicity of the period function for some planar differential systems. I. Conservative and quadratic systems. *Appl. Math. (Warsaw)*, 32(3) :305–325, 2005. (Cité en pages 16, 37 et 40.)

[61] A.R. Chouikha. Monotonicity of the period function for some planar differential systems. II. Liénard and related systems. *Appl. Math. (Warsaw)*, 32(4) :405–424, 2005. (Cité en page 71.)

[62] A.R. Chouikha. Isochronous centers of Lienard type equations and applications. *J. Math. Anal. Appl.*, 331(1) :358–376, 2007. (Cité en pages 2, 17, 18, 22, 33, 35, 37, 40, 41, 43, 44, 46, 59, 61, 62, 63, 66, 69 et 77.)

[63] A.R. Chouikha, V.G. Romanovski, and X. Chen. Isochronicity of analytic systems via Urabe's criterion. *J. Phys. A, Math. Theor.*, 40(10) :2313–2327, 2007. (Cité en pages 17, 18, 33, 35, 41, 43, 44, 46, 49, 57, 59, 61, 63, 66 et 77.)

[64] C. Christopher and J. Devlin. On the classification of liÃ©nard systems with amplitude-independent periods. *Journal of Differential Equations*, 200(1) :1 – 17, 2004. (Cité en pages 71 et 77.)

[65] F. Clayer, H. Heneusse, and J. Sancho. Procédé de transmission acoustique de données de forage d'un puits. *In World Intellectual Property Organization, (In French)*, 92/04644 :235–254, 1992. (Cité en page 130.)

[66] J-P. Françoise. Isochronous systems and perturbation theory. *Journal of Nonlinear Mathematical Physics*, 12 :315 – 326, 2005. (Cité en page 62.)

[67] K. L. Cooke. Stability analysis for a vector disease model. *Rocky Mountain J. Math.*, 9 :31–42, 1979. (Cité en pages 181 et 235.)

[68] D. Cox, J. Little, and D. O'Shea. *Ideals, varieties, and algorithms. An introduction to computational algebraic geometry and commutative algebra.* Springer, 2007. (Cité en pages 45, 46, 194 et 225.)

[69] B. d'Andréa Novel, J.-M. Coron, B. Fabre, and T. Hélie. Wind instruments as time delay systems. part i : modeling*. *Proceedings of the 8th IFAC Workshop on Time-Delay Systems*, 42(14) :284 – 289, 2009. (Cité en page 135.)

[70] B. d'Andréa Novel, J.-M. Coron, B. Fabre, and T. Hélie. Wind instruments as time delay systems. part ii : control and estimation*. *Proceedings of the 8th IFAC Workshop on Time-Delay Systems*, 42(14) :290 – 295, 2009. (Cité en page 135.)

[71] C. Canudas de Wit, F. Rubio, and M. Corchero. D-oskil : A new mechanism for controlling stick-slip oscillations in oil well drillstrings. *IEEE Transactions on Control Systems Tech.*, 16 :1177–1191, 2008. (Cité en pages 117, 149 et 150.)

[72] C. Canudas de Wit, B. Siciliano, and G. Bastin. *Theory of robot control.* Springer, New York, 1996. (Cité en pages 149 et 150.)

[73] M. Dellnitz and B. Werner. Computational methods for bifurcation problems with symmetries-with special attention to steady state and hopf bifurcation points. *Journal of Computational and Applied Mathematics*, 26(1-2) :97 – 123, 1989. (Cité en pages 215 et 231.)

[74] R.L. Devaney. Reversible diffeomorphisms and flows. *Trans. Amer. Math. Soc.*, 218 :89–113, 1976. (Cité en page 44.)

[75] O. Diekmann, S.A. Van Gils, S.M. Verduyn Lunel, and H.O. Walther. *Delay equations*, volume 110 of *Applied Mathematical Sciences, Functional, complex, and nonlinear analysis.* Springer-Verlag, New York, 1995. (Cité en pages 97 et 172.)

[76] D. Dolicanin, G.V. Milovanovic, and V. G. Romanovski. Linearizability conditions for a cubic system. *Applied Mathematics and Computation*, 190(1) :937 – 945, 2007. (Non cité.)

[77] D. Drumheller. Acoustical properties of drill strings. *J. Acous. Soc. of Amer.*, 85 :1048–1064, 1989. (Cité en page 130.)

[78] D. Drumheller. An overview of acoustic telemetry. *Sandia Research Report*, Sand-92-0677c :1048–1064, 1992. (Cité en page 130.)

[79] D. Drumheller and S. Knudsen. The propagation of sound waves in drill strings. *J. Acous. Soc. of Amer.*, 97 :2116–2125, 1995. (Cité en page 130.)

[80] F. Dumortier and S. Ibanez. Nilpotent singularities in generic 4-parameter families of 3-dimensional vector fields. *Journal of Differential Equations*, 127(2) :590 – 647, 1996. (Cité en page 107.)

[81] F. Dumortier, S. Ibanez, and H. Kokubu. New aspects in the unfolding of the nilpotent singularity of codimension three. *Dynamical Systems*, 16(1) :63 – 95, 2001. (Cité en page 107.)

[82] F. Dumortier, J. Llibre, and J.C. Artés. *Qualitative theory of planar differential systems.* Universitext. Springer-Verlag, Berlin, 2006. (Non cité.)

[83] V. V. Ivanov E. P. Volokitin. Isochronicity and commutation of polynomial vector fields. *Siberian Math. Journal*, 40 :23–38, 1999. (Cité en pages 19 et 31.)

[84] J. Egea, S. Ferrer, and J.C. van der Meer. Bifurcations of the hamiltonian fourfold 1 :1 resonance with toroidal symmetry. *Journal of Nonlinear Science*, 21(6) :835–874, 2011. (Cité en pages 216 et 227.)

[85] J. Eker and K.J. Aström. A nonlinear observer for the inverted pendulum. *The 8th IEEE Conference on Control Application, Dearborn, USA, September 15-18*, page 7pp, 1996. (Cité en page 93.)

[86] K. Engelborghs, T. Luzyanina, and D. Roose. Numerical bifurcation analysis of delay differential equations using dde-biftool. *ACM Transactions on Mathematical Software (TOMS)*, 28(1) :1–21, 2002. (Cité en page 240.)

[87] K. Engelborghs, T. Luzyanina, and G. Samaey. DDE-BIFTOOL v.2.00 : a Matlab package for bifurcation analysis of delay differential equations. TW Report No.330, Department of Computer Science, Katholieke Universiteit Leuven, 2001. (Cité en page 240.)

[88] I. R. Epstein and Y. Luo. Differential delay equations in chemical kinetics. nonlinear models : The cross-shaped phase diagram and the oregonator. *The Journal of Chemical Physics*, 95(1) :244–254, 1991. (Cité en page 274.)

[89] F. W. J. Olver et. al. (Editors). *NIST Handbook of Mathematical Functions.* Cambridge Univ. Press, Cambridge, 2010. (Cité en page 48.)

[90] I. Fantoni and R. Lozano. *Non-Linear Control for Underactuated Mechanical Systems.* Springer, 2001. (Cité en page 182.)

[91] I. Fantoni and R. Lozano. *Topics in functional differential and difference equations.* Amer. Math. Soc., Fields Inst. Commun, 2001. (Cité en pages 140, 248 et 267.)

[92] T. Faria and L.T. Magalhes. Normal forms for retarded functional-differential equations with parameters and applications to Hopf bifurcation. *J. Differential Equations*, 122(2) :181–200, 1995. (Cité en pages 98, 142 et 164.)

[93] J-C. Faugère. Fgb salsa software. (Cité en pages 18, 37, 45, 61, 65 et 66.)

[94] J-C. Faugère. A new efficient algorithm for computing Gröbner bases (F_4). *Journal of Pure and Applied Algebra*, 139(1-3) :61–88, 1999. Effective methods in algebraic geometry (Saint-Malo, 1998). (Cité en page 45.)

[95] M. V. S. Frasson. *Large Time Behavior of Neutral Delay Systems*. Ph.D Thesis of the University of Leiden, 2005. (Cité en pages 248 et 252.)

[96] E. Freire, E. Gamero, A.J. Rodrigues-Luis, and A. Algaba. A note on the triple-zero linear degeneracy : Normal forms, dynamical and bifurcation behaviors of an unfolding. *International Journal of Bifurcation and Chaos*, 12(12) :2799–2820, 2002. (Cité en page 107.)

[97] E. Fridman, C. Bonnet, F. Mazenc, and W. Djema. Stability of the cell dynamics in acute myeloid leukemia. *Systems and Control Letters*, 2016. (Cité en page 273.)

[98] E. Fridman, S. Mondié, and B. Saldivar. Bounds on the response of a drilling pipe model. *IMA Journal of Mathematical Control and Information*, pages 1–14, 2010. (Cité en page 120.)

[99] P. Fu, S-I. Niculescu, and J. Chen. On the Stability of Linear Delay-Differential Algebraic Systems : Exact Conditions via Matrix Pencil Solutions. *IEEE Transaction on Automatic Control*, 51 :1063–1069, 2006. (Cité en page 247.)

[100] I. Garcia. *Contribution to the qualitative study of planar vector fields*. Ph.D Thesis, Dept. de Matematica. University of Lleida, 2000. (Cité en pages 66 et 77.)

[101] I. A. Garcia and S. Maza. Linearization of analytic isochronous centers from a given commutator. *Journal of Mathematical Analysis and Applications*, 339(1) :740 – 745, 2008. (Cité en page 32.)

[102] W. Gautshi. On inverses of Vandermonde and confluent Vandermonde matrices. *Numer. Math.*, 4 :117–123, 1963. (Cité en page 175.)

[103] W. Gautshi. On inverses of Vandermonde and confluent Vandermonde matrices ii. *Numer. Math.*, 5 :425–430, 1963. (Cité en page 175.)

[104] C. Germay. Modeling and analysis of self-excited drill bit vibrations. *PhD dissertation, University of Liege*, page 121, 2009. (Cité en pages 118, 123, 125, 126 et 127.)

[105] C. Germay, N. Van De Wouw, H. Nijmeijer, and R. Sepulchre. Nonlinear drilling dynamics analysis. *SIAM J. Dynamical Systems*, 8(2) :527–553, 2005. (Cité en page 120.)

[106] L. Gonzalez-Vega. Applying quantifier elimination to the Birkhoff interpolation problem. *J. Symbolic. Comp.*, 22(1) :83–104, 1996. (Cité en pages 175, 178, 179, 180, 184 et 222.)

[107] K. Gopalsamy. *Stability and Oscillations in Delay Differential Equations of Population Dynamics*. Kluwer Academic Publishers, 1992. (Cité en pages 237, 248 et 250.)

[108] W. Govaerts, J. Guckenheimer, and A. Khibnik. Defining functions for multiple hopf bifurcations. *SIAM Journal on Numerical Analysis*, 34(3) :1269–1288, 1997. (Cité en pages 216 et 231.)

[109] K. Gu, S-I. Niculescu, and J. Chen. On stability crossing curves for general systems with two delays. *Journal of Mathematical Analysis and Applications*, 311(1) :231 – 253, 2005. (Cité en pages 218, 236 et 239.)

[110] K. Gu, S.-I. Niculescu, and J. Chen. On stability of crossing curves for general systems with two delays. *J. Math. Anal. Appl.*, 311 :231–253, 2005. (Cité en pages 95, 101 et 109.)

[111] J. Guckenheimer and P. Holmes. *Nonlinear oscillations, dynamical systems, and bifurcation of vector fields.* Springer, 2002. (Cité en pages 1, 64, 84, 135, 142, 145, 162, 163, 167 et 174.)

[112] P. Guha and A.G. Choudhury. Symplectic rectification and isochronous Hamiltonian systems. *J. Phys. A*, 42(19) :192001, 6, 2009. (Cité en page 55.)

[113] T.T. Ha and J.A. Gibson. A note on the determinant of a functional confluent Vandermonde matrix and controllability. *Linear Algebra and its Applications*, 30(0) :69 – 75, 1980. (Cité en pages 175, 179 et 222.)

[114] J. K. Hale and W. Huang. Period doubling in singularly perturbed delay equations. *J. of Diff. Eq.*, 114 :1–23, 1994. (Cité en pages 142, 145, 164, 170 et 173.)

[115] J. K. Hale and S. M. Verduyn Lunel. *Introduction to functional differential equations*, volume 99 of *Applied Mathematics Sciences*. Springer Verlag, New York, 1993. (Cité en pages 97, 98, 140, 165, 248, 250, 259, 266 et 267.)

[116] J. K. Hale and P. Martinez-Amores. Stability in neutral equations. *J. Nonlinear Anal. Theor. Meth. Appl.*, 1 :161–172, 1977. (Cité en page 248.)

[117] J.K. Hale and W. Huang. Variation of constants for hybrid systems of functional differential equations. *Proceedings of the Royal Society of Edinburgh, Section : A Mathematics*, 125 :1–12, 1 1995. (Cité en page 247.)

[118] G.W. Halsey, A. Kyllingstad, and A. Kylling. Torque feedback used to cure slip-stick motion. In *Proceedings of the 63rd Society of Petroleum Engineers Drilling Engineering*, volume 29, pages 277–282. Annual Technical Conference and Exhibition, Houston, TX, 1988. (Cité en page 155.)

[119] B.D. Hassard. Counting roots of the characteristic equation for linear delay-differential systems. *Journal of Differential Equations*, 136(2) :222 – 235, 1997. (Cité en pages 174, 203 et 217.)

[120] G. Hoffmann, S. Waslander, and C. Tomlin. Distributed cooperative search using information-theoretic costs for particle filters with quadrotor applications. *Proceedings of the AIAA Guidance, Navigation, and Control Conference*, Aug 2006. (Cité en page 79.)

[121] S-H. Hou and W-K. Pang. Inversion of confluent Vandermonde matrices. *Computers and Mathematics with Applications*, 43(12) :1539 – 1547, 2002. (Cité en page 179.)

[122] S-I. Niculescu I. Boussaada, H. Unal. Multiplicity and stable varieties of time-delay systems : A missing link. In *Submitted to : The 22nd International Symposium on Mathematical Theory of Networks and Systems*, page 1, 2016. (Cité en pages 8 et 231.)

[123] T. Insperger and G. Stepan. *Semi-Discretization for Time-Delay Systems : Stability and Engineering Applications*. Applied Mathematics Sciences. Springer, 2011. (Cité en pages 95, 97, 173 et 215.)

[124] E. Jarlebring and W. Michiels. Invariance properties in the root sensitivity of time-delay systems with double imaginary roots. *Automatica*, 46(6) :1112 – 1115, 2010. (Cité en page 220.)

[125] R. Barreto Jijon, C. Canudas de Wit, S.-I. Niculescu, and J. Dumon. Adaptive observer design under low data rate transmission with applications to oil well drill-string. In *Proceedings of IEEE American Control Conference*, 2010. (Cité en pages 116 et 131.)

[126] T. Kailath. *Linear Systems*. Prentice-Hall information and system sciences series. Prentice Hall International, 1998. (Cité en pages 175, 179 et 222.)

[127] W. Kang. Extended controller form and invariants of nonlinear control systems with a single input. *Journal of Mathematical Systems Estimation and control*, 6 :27–51, 1996. (Cité en pages 79 et 80.)

[128] F. Kappel. Linear autonomous functional differential equations. In O. Arino, M.L. Hbid, and E.A. Dads, editors, *Delay Differential Equations and Applications*, volume 205 of *NATO Science Series*, pages 41–139. Springer Netherlands, 2006. (Cité en pages 248, 249 et 253.)

[129] V.L. Kharitonov, S-I. Niculescu, J. Moreno, and W. Michiels. Static output feedback stabilization : necessary conditions for multiple delay controllers. *IEEE Trans. on Aut. Cont.*, 50(1) :82–86, 2005. (Cité en pages 95, 96, 114 et 200.)

[130] O.N. Kirillov and D.E. Pelinovsky. *Nonlinear physical systems : spectral analysis, stability and bifurcations*. John Wiley & Sons, Inc, 2013. (Cité en page 145.)

[131] A.J. Krener, W. Kang, and E.C. Dong. Control bifurcations. *Automatic Control, IEEE Transactions on*, 49(8) :1231–1246, 2004. (Cité en page 80.)

[132] A.J. Krener, S. Karahan, M. Hubbard, and R. Frezza. Higher order linear approximations to nonlinear control systems. In *Decision and Control, 1987. 26th IEEE Conference on*, volume 26, pages 519–523, Dec 1987. (Cité en page 82.)

[133] E. Kreuzer and M. Steidl. Controlling torsional vibrations of drill strings via decomposition of traveling waves. *Archive of Applied Mechanics*, 82 :515–531, 2012. (Cité en page 169.)

[134] Y. Kuznetsov. *Elements of applied bifurcation theory ; Second edition*, volume 112 of *Applied Mathematics Sciences*. Springer, New York, 1998. (Cité en pages 1, 79, 94, 139, 141, 145, 174 et 201.)

[135] M. Landry, S.A. Campbell, K. Morris, and C.O. Aguilar. Dynamics of an inverted pendulum with delayed feedback control. *SIAM J. Appl. Dyn. Syst.*, 4(2) :333–351, 2005. (Cité en pages 93, 94, 95 et 201.)

[136] B.J. Levin. *Distribution of zeros of entire functions*. Translations of Mathematical Monographs. AMS, Providence, Rhode Island, 1964. (Cité en pages 172, 216 et 233.)

[137] X. Liu, B. Li, and Y. Yue. Transmission behavior of mud-pressure pulse along well bore. *Journal of Hydrodinamics*, 19 :236–240, 2007. (Cité en page 130.)

[138] G.G. Lorentz and K.L. Zeller. Birkhoff interpolation. *SIAM Journal on Numerical Analysis*, 8(1) :pp. 43–48, 1971. (Cité en page 177.)

[139] R.A. Lorentz. *Multivariate Birkhoff Interpolation*. Lecture notes in Mathematics. Springer-Verlag, 1992. (Cité en page 207.)

[140] W.S. Loud. The behavior of the period of solutions of certain plane autonomous systems near centers. *Contributions to Diff. Eq*, 3, 1964. (Cité en pages 22 et 37.)

[141] S.M. Verduyn Lunel. Series expansions for functional differential equations. *Integral Equations and Operator Theory*, 22(1) :93–122, 1995. (Cité en pages 248, 249, 252, 253 et 254.)

[142] S.M.V. Lunel. About completeness for a class of unbounded operators. *Journal of Differential Equations*, 120(1) :108 – 132, 1995. (Cité en page 249.)

[143] M. Mackey. Unified hypothesis for the origin of aplastic anemia and periodic hematopoiesis. *Blood*, 51(5) :941 – 956, 1978. (Cité en page 273.)

[144] M. Marden. *Geometry of Polynomials*. American Mathematical Society Mathematical Surveys, 1966. (Cité en pages 174 et 180.)

[145] P. Mardesic, C. Rousseau, and B. Toni. Linearization of isochronous centers. *Journal of Differential Equations*, 121(1) :67 – 108, 1995. (Cité en pages 16, 70, 71, 72 et 77.)

[146] M.B. Saldivar Marquez, I. Boussaada, H. Mounier, and S-I. Niculescu. *Analysis and Control of Oilwell Drilling Vibrations*. Advances in Industrial Control. Springer, 2015. (Cité en pages 5, 7, 115, 135, 137, 138, 145, 149, 150, 151, 154, 157, 160 et 173.)

[147] F. Mazenc and D. Normand-Cyrot. Reduction model approach for linear systems with sampled delayed inputs. *IEEE Transactions on Automatic Control*, 58(5) :1263–1268, 2013. (Cité en page 4.)

[148] L. Melkemi. Confluent Vandermonde matrices using Sylvester's structures. *Research Report of the Ecole Normale Supérieure de Lyon*, 98-16 :1–14, 1998. (Cité en page 184.)

[149] L. Melkemi and F. Rajeh. Block lu-factorization of confluent Vandermonde matrices. *Applied Mathematics Letters*, 23(7) :747 – 750, 2010. (Cité en page 179.)

[150] C. Mendez-Barrios, S.-I. Niculescu, C.-I. Morarescu, and K. Gu. On the fragility of pi controllers for time-delay siso systems. *Control and Automation, 2008 16th Mediterranean Conference on*, pages 529–534, June 2008. (Cité en page 96.)

[151] W. Michiels and S-I. Niculescu. *Stability and stabilization of time-delay systems*, volume 12 of *Advances in Design and Control*. Society for Industrial and Applied Mathematics (SIAM), 2007. (Cité en pages 9, 97, 140, 173, 175, 215, 216, 217, 231, 233, 248, 250 et 266.)

[152] J. Milton, J-L. Cabrera, T. Ohira, S. Tajima, Y. Tonosaki, C.W. Eurich, and Sue Ann Campbell. The time-delayed inverted pendulum : Implications for human balance control. *Chaos*, 19 :12pp, 2009. (Cité en pages 94, 141, 143, 144, 164, 165, 170, 263 et 266.)

[153] I.-C. Morărescu, W. Michiels, and M. Jungers. Synchronization of coupled nonlinear oscillators with gamma-distributed delays. In *Proceedings of IEEE American Control Conference*, 2013. (Cité en page 94.)

[154] I.-C. Morărescu, S.-I. Niculescu, and K.Gu. On the geometry of stability regions of smith predictors subject to delay uncertainty. *IMA Journal of Mathematical Control and Information*, 24(3) :411–423, 2007. (Cité en page 95.)

[155] I.-C. Morărescu, S.-I. Niculescu, and K.Gu. Stability crossing curves of shifted gamma-distributed delay systems. *SIAM Journal on Applied Dynamical Systems*, 6(2) :475–493, 2007. (Cité en pages 95 et 101.)

[156] U. Munz, C. Ebenbauer, T. Haag, and F. Allgower. Stability analysis of time-delay systems with incommensurate delays using positive polynomials. *Automatic Control, IEEE Transactions on*, 54(5) :1019–1024, 2009. (Cité en page 220.)

[157] N. Muskinja and B. Tovornik. Swinging up and stabilisation of a real inverted pendulum. *IEEE Transaction on Industrial Electronics*, 53(2) :631–639, 2006. (Cité en page 93.)

[158] K. Nandakumar and M. Wiercigroch. Stability analysis of a state dependent delayed, coupled two dof model of drill-string vibration. *Journal of Sound and Vibration*, 332 :2575–2592, 2013. (Cité en page 145.)

[159] N.A.Rahman, A. Mohaideen, F.H. Bakar, K.H. Tang, R. Maury, P. Cox, P. Le, H. Donald, E. Brahmanto, and B. Subroto. Solving stickslip dilemma : dynamic modeling system significantly reduces vibration, increases rop by 54%. In *Proceedings of the Abu Dhabi International Petroleum Exhibition and Conference*, pages 948–963, 2012. (Cité en page 146.)

[160] E. M. Navarro-López and D. Cortés. Avoiding harmful oscillations in a drill-string through dynamical analysis. *Journal of Sound and Vibrations*, 307 :152–171, 2007. (Cité en page 145.)

[161] E. M. Navarro-López and D. Cortés. Sliding-mode control of a multi-dof oilwell drillstring with stick-slip oscillations. *Proceeding of the 2007 American Control Conference*, pages 3837 – 3842, 2007. (Cité en pages 117 et 118.)

[162] E. M. Navarro-López and R. Suárez. Modelling and analysis of stick-slip behavior in a drillstring under dry friction. *Congreso anual de la AMCA 2004*, pages 330 – 335, 2004. (Cité en pages 117 et 118.)

[163] E. M. Navarro-López and R. Suárez. Practical approach to modelling and controlling stick-slip oscillations in oilwell drillstring. *Proceeding of the 2004 IEEE, International Conference on Control Applications*, 10(5) :3162 – 3174, 2004. (Cité en pages 117 et 118.)

[164] E.M. Navarro-López. An alternative characterization of bit-sticking phenomena in a multi-degree-of-freedom controlled drillstring. *Nonlinear Analysis : Real World Applications*, 10(5) :3162 – 3174, 2009. (Cité en pages 117 et 118.)

[165] S-I. Niculescu. Delay Effects on Stability, A Robust Control Approach. *Springer, Lecture Notes in Control And Information Sciences*, 2001. (Cité en page 247.)

[166] S-I. Niculescu and W. Michiels. Stabilizing a chain of integrators using multiple delays. *IEEE Trans. on Aut. Cont.*, 49(5) :802–807, 2004. (Cité en pages 95, 96, 114, 175, 200 et 217.)

[167] N. Olgac and R. Sipahi. An exact method for the stability analysis of time delayed linear time-invariant (lti) systems. *IEEE Transactions on Automatic Control*, 47(5) :793–797, 2002. (Cité en page 101.)

[168] N. Olgac and R. Sipahi. An exact method for the stability analysis of time-delayed lti systems. *IEEE Trans. Automat. Contr.*, 47 :793–797, 2002. (Cité en pages 217 et 220.)

[169] P.J. Olver. On multivariate interpolation. *Stud. Appl. Math.*, 116 :201–240, 2006. (Cité en pages 179 et 222.)

[170] S. Cunha Orfao, G. Jank, K. Mottaghy, S. Walcher, and E. Zerz. Qualitative properties and stabilizability of a model for blood thrombin formation. *Journal of Mathematical Analysis and Applications*, 346(1) :218 – 226, 2008. (Cité en page 273.)

[171] H. Oruc. factorization of the Vandermonde matrix and its applications. *Applied Mathematics Letters*, 20(9) :982 – 987, 2007. (Cité en page 184.)

[172] S. Parfitt, R. W. Tucker, and C. Wang. Drilling guidlines from the cosserat dynamics of a drill-rig assembly. *preprint*, 2000. (Cité en page 127.)

[173] D. Pavone and J.P. Desplans. Analyse et modélisation du comportement dynamique d'un rig de forage. *IFP report*, 42208, 1996. (Cité en page 125.)

[174] A. Pikovsky, M. Rosenblum, and J. Kurths. *Synchronization : A Universal Concept in Nonlinear Sciences*. Cambridge Nonlinear Science Series, 2003. (Cité en pages 61 et 62.)

[175] I. I. Pleshkan. A new method of investigating the isochronicity of a system of two differential equations. *Differential Equations*, 5 :796 – 802, 1969. (Cité en pages 64, 66, 70, 71 et 72.)

[176] G. Polya and G. Szegö. *Problems and Theorems in Analysis, Vol. I : Series, Integral Calculus, Theory of Functions.* Springer-Verlag, New York, Heidelberg, and Berlin, 1972. (Cité en pages 7, 95, 99, 173, 174, 201, 203, 217, 218, 232 et 234.)

[177] K. Pyragas. Continuous control of chaos by self-controlling feedback. *Phys. Lett. A*, 170 :421–428, 1992. (Cité en page 108.)

[178] K. Pyragas. Control of chaos via an unstable delayed feedback controller. *Phys. Rev. Lett.*, 86 :2265–2268, 2001. (Cité en page 108.)

[179] B. Qinsheng and Y. Pei. Symbolic computation of normal forms for semi-simple cases. *Journal of Computational and Applied Mathematics*, 102(2) :195 – 220, 1999. (Cité en page 65.)

[180] A. Quadrat. A constructive algebraic analysis approach to Artstein's reduction of linear time-delay systems. In *12th IFAC Workshop on Time Delay Systems*, Proceedings of 12th IFAC Workshop on Time Delay Systems, Ann Arbor, United States, 2016. University of Michigan. (Cité en page 1.)

[181] A. Quadrat and D. Robertz. A constructive study of the module structure of rings of partial differential operators. *Acta Applicandae Mathematicae*, 133 :187–243, 2014. (Cité en page 1.)

[182] A. Quadrat, E. Zerz, and G. Regensberger. *Algebraic and Symbolic Computation Methods in Dynamical Systems.* Submitted to Springer ser. Adv. in Delays and Dynamics, 2016. (Cité en page 1.)

[183] Quanser. Control rotary challlenges. (Cité en page 182.)

[184] Tucker R. W. and Wang C. On the effective control of torsional vibrations in drilling systems. *Journal of Sound and Vibration*, 224(1) :101–122, 1999. (Cité en pages 153, 154, 155, 157 et 159.)

[185] V. Rasvan and S-I. Niculescu. Oscillations in lossless propagation models : a liapunov-krasovskii approach. *IMA J. of Math. Contr. and Info.*, 19 :157–172, 2002. (Cité en page 248.)

[186] J. S. Respondek. On the confluent Vandermonde matrix calculation algorithm. *App. Math. Letters*, 24(2) :103 – 106, 2011. (Cité en pages 179 et 222.)

[187] T. Richard, C. Germay, and E. Detournay. A simplified model to explore the root cause of stick-slip vibrations in drilling system with drag bits. *Appl. Math. Comput.*, 305 :432–456, 2007. (Cité en pages 118 et 120.)

[188] V.G. Romanovski and D.S. Shafer. *The center and cyclicity problems : a computational algebra approach.* Birkhäuser Boston Inc., Boston, MA, 2009. (Cité en pages 15, 16, 40 et 44.)

[189] P. Rouchon. Flatness and stick-slip stabilization. *Technical Report*, 492 :1–9, 1998. (Cité en pages 118 et 120.)

[190] F. Rouillier, M.S. Din, and E. Schost. Solving the Birkhoff interpolation problem via the critical point method : An experimental study. In J. Richter-Gebert and D. Wang, editors, *Automated Deduction in Geom.*, volume 2061

of *LNCS*, pages 26–40. Springer Berlin Heidelberg, 2001. (Cité en pages 178 et 180.)

[191] M. R. Roussel. The use of delay differential equations in chemical kinetics. *The Journal of Physical Chemistry*, 100(20) :8323–8330, 1996. (Cité en page 274.)

[192] S. Ruan. Delay differential equations in single species dynamics. In *Delay Differential Equations and Applications*, volume 29 of *Fields Inst. Commun.*, pages 477–517. Springer, Berlin, 2006. (Cité en pages 181 et 235.)

[193] V. Răsvan. Absolute stability of time lag control systems. *Bucharest : Academiei (in Romanian)*, 1975. (Cité en page 248.)

[194] M. Sabatini. On the period function of $x'' + f(x)x'^2 + g(x) = 0$. *J. Differ. Equations*, 196(1) :151–168, 2004. (Cité en pages 17, 40 et 62.)

[195] B. Saldivar and S. Mondié. Drilling vibration reduction via attractive ellipsoid method. *Journal of the Franklin Institute*, 350 :485–502, 2013. (Cité en page 118.)

[196] B. Saldivar, S. Mondié, J-J. Loiseau, and V. Rasvan. Suppressing axial torsional coupled vibrations in oilwell drillstrings. *Journal of Control Engineering and Applied Informatics*, 15 :3–10, 2013. (Cité en page 118.)

[197] A. Seuret, C. Edwards, S.K. Spurgeon, and E. Fridman. Static output feedback sliding mode control design via an artificial stabilizing delay. *Automatic Control, IEEE Transactions on*, 54(2) :256–265, Feb 2009. (Cité en page 94.)

[198] I. Shafarevich and A. Remizov. Matrices and determinants. In *Linear Algebra and Geometry*, pages 25–77. Springer Berlin Heidelberg, 2013. (Cité en page 225.)

[199] A. Shiriaev, A. Pogromsky, H. Ludvigsen, and O. Egeland. On global properties of passivity-based control of an inverted pendulum. *Int. J. of Robust Nonlinear Control*, 10 :283–300, 2000. (Cité en page 93.)

[200] J. Sieber and B. Krauskopf. Bifurcation analysis of an inverted pendulum with delayed feedback control near a triple-zero eigenvalue singularity. *Nonlinearity*, 17 :85–103, 2004. (Cité en pages 93, 94, 95, 96, 103, 104, 105, 107, 114, 144, 173, 196, 197 et 201.)

[201] J. Sieber and B. Krauskopf. Extending the permissible control loop latency for the controlled inverted pendulum. *Dynamical Systems*, 20(2) :189–199, 2005. (Cité en pages 94, 96, 103, 196 et 201.)

[202] R. Sipahi and N. Olgac. Complete robustness of third-order lti multiple time-delay systems. *Automatica*, 41 :1413–1422, 2005. (Cité en pages 95 et 101.)

[203] R. Sipahi and N. Olgac. Complete stability robustness of third-order {LTI} multiple time-delay systems. *Automatica*, 41(8) :1413 – 1422, 2005. (Cité en page 220.)

[204] A. Steindl and H. Troger. Bifurcations of the equilibrium of a spherical double pendulum at a multiple eigenvalue. In T. Küpper, R. Seydel, and H. Troger,

editors, *Bifurcation : Analysis, Algorithms, Applications*, volume 79 of *ISNM 79*, pages 277–287. Birkhäuser Basel, 1987. (Cité en pages 216 et 232.)

[205] G. Stepan. On the stability of linear differential equations with delay. In *Qualitative Theory of Differential Equations, Colloquia Mathematica Societas Janos Bolyai*, pages 971–984, 1979. (Cité en page 203.)

[206] G. Stepan. *Retarded Dynamical Systems : Stability and Characteristic Functions*. Pitman research notes in mathematics series. Longman Scientific & Technical, 1989. (Cité en pages 97, 140, 203 et 216.)

[207] I.H. Suh and Z. Bien. Proportional minus delay controller. *IEEE Trans. on Aut. Cont.*, 24 :370–372, 1979. (Cité en page 94.)

[208] I.A. Tall and W. Respondek. Normal forms for two-inputs nonlinear control systems. In *Decision and Control, 2002, Proceedings of the 41st IEEE Conference on*, volume 3, pages 2732–2737, Dec 2002. (Cité en page 79.)

[209] P. Tubei, C. Bergeron, and S. Bell. Mud-pulser telemetry system for down hole measurement-while-drilling. *IEEE 9th Proc. Instrument and Measurement Tech. Conf.*, pages 219–223, 1992. (Cité en page 130.)

[210] R. W. Tucker and C. Wang. L'équilibre d'une masse fluide animée d'un mouvement de rotation. *Acta Mathematica*, pages 259–380, 1885. (Cité en page 135.)

[211] R. W. Tucker and C. Wang. On the effective control of torsional vibrations in drilling systems. *Journal of Sound and Vibration*, 224 :101–122, 1999. (Cité en pages 116 et 121.)

[212] R. W. Tucker and C. Wang. The excitation and control of torsional slip-stick in the presence of axial vibrations. *preprint*, 2000. (Cité en page 127.)

[213] M. Urabe. The potential force yielding a periodic motion whose period is an arbitrary continuous function of the amplitude of the velocity. *Arch. Ration. Mech. Anal.*, 11 :27–33, 1962. (Cité en page 44.)

[214] S-A. van Gils, M. Krupa, and W-F. Langford. Hopf bifurcation with non-semisimple 1 :1 resonance. *Nonlinearity*, 3(3) :825, 1990. (Cité en page 216.)

[215] T. Vyhlidal and P. Zitek. Mapping based algorithm for large-scale computation of quasi-polynomial zeros. *IEEE Transactions on Automatic Control*, 54(1) :171–177, 2009. (Cité en pages 164, 219, 245 et 263.)

[216] J. Wang, I. Boussaada, A. Cela, H. Mounier, and S.I. Niculescu. Analysis and control of quadrotor via a normal form approach. In *21st International Symposium on Mathematical Theory of Networks and Systems*, pages 1–8, 2012. (Cité en pages 3 et 79.)

[217] J. Wang, H. Mounier, A. Cela, and S.I. Niculescu. Event driven intelligent pid controllers with applications to motion control. In *18th IFAC World Congress, Milan, Aug. 2011*, pages 10080–10085, 2011. (Cité en page 79.)

[218] M. Weedermann. Hopf Bifurcation calculations for scalar delay differential equations. *Nonlinearity*, 19 :2091–2102, 2006. (Cité en pages 138 et 170.)

[219] F. Wielonsky. A Rolle's theorem for real exponential polynomials in the complex domain. *J. Math. Pures Appl.*, 4 :389–408, 2001. (Cité en pages 174, 176, 218 et 234.)

[220] Q. Xu, G. Stepan, and Z. Wang. Delay-dependent stability analysis by using delay-independent integral evaluation. *Automatica*, 70 :153 – 157, 2016. (Cité en page 163.)

[221] P. Yu. Computation of normal forms via a perturbation technique. *Journal of Sound and Vibration*, 211(1) :19 – 38, 1998. (Cité en page 65.)

[222] P. Yu and A.Y.T. Leung. Normal forms of vector fields with perturbation parameters and their application. *Chaos, Solitons & Fractals*, 34(2) :564 – 579, 2007. (Cité en page 65.)

[223] G. Zames. On the input-output stability of time-varying nonlinear feedback systems part one : Conditions derived using concepts of loop gain, conicity, and positivity. *Automatic Control, IEEE Transactions on*, 11(2) :228–238, 1966. (Cité en pages 232 et 235.)

[224] E. Zerz. Multidimensional behaviours : an algebraic approach to control theory for pde. *International Journal of Control*, 77(9) :812–820, 2004. (Cité en page 1.)

[225] C. Zhang, B. Zheng, and L. Wang. Multiple hopf bifurcations of symmetric BAM neural network model with delay. *Applied Mathematics Letters*, 22(4) :616 – 622, 2009. (Cité en pages 216 et 226.)

[226] S. Zhao and T. Kalmar-Nagy. Center manifold analysis of the delayed lienard equation. In *Delay Differential Equations*, pages 1–17. Springer US, 2009. (Cité en pages 243 et 273.)

Résumé :

Les travaux présentés s'inscrivent dans le domaine des systèmes dynamiques de dimensions finie et infinie. Ils portent plus particulièrement sur l'application de la théorie qualitative des systèmes dynamiques aux problèmes de stabilité (asymptotique) et de contrôle. Ces travaux s'articulent essentiellement autour de différentes versions du théorème de la variété du centre et de différentes théories des formes normales pour les équations différentielles fonctionnelles. L'objectif commun à ces recherches est, d'une part, de prouver l'efficacité de ces méthodes dans des applications émanant des problèmes de contrôle, et d'autre part, d'étendre leur applicabilité à des systèmes algébro-différentiels non-linéaires à retard et dépendant de paramètres. En particulier, des liens entre différents concepts ont été établis et ont, notamment, permis de mettre en évidence une nouvelle approche de stabilisation utilisant la commande retardée basée sur la multiplicité des valeurs spectrales. Ce paradigme a été appliqué successivement à la stabilisation du pendule inversé, la stabilisation du quadrotor en présence de rafale de vent, le contrôle des vibrations se propageant le long d'un système de forage, le contrôle d'un modèle de transmission de maladie et l'analyse de croissance du tournesol.